Environmental assessment of chemical contamination from abandoned coal and mineral mines

A Thesis Submitted for the Degree of Doctor of Philosophy

By

Ushemegbe Rita Ekhareafo

Department of Civil and Environmental Engineering,

Brunel University
London

2025

Declaration

I, Rita Ekhareafo, hereby declare that this thesis is my original work and has not been submitted, either in whole or in part, for any other degree or qualification at any other institution. Where information has been acquired from other sources, this has been duly acknowledged.

Signanture

Date: 06/11/2025

Abstract

Abandoned mine lands (AMLs) are enduring sources of environmental pollution due to the release of toxic substances like metals, metalloids, organic and organometallic pollutants into the environment. These substances are transported through various processes such as acid mine drainage that aid the movement of pollutants across compartments and are driven by the pollutants' physicochemical properties, environmental conditions and the physical state of the abandoned mine. Chemicals released can be toxic, bioaccumulate, and persist; hence, highly polluted mine lands may pose significant ecological and human health risks. Worldwide, it is estimated that there are over a million abandoned mines. Nigeria is no exception, with over 1500 abandoned mines identified to date across many states, and so far, only a few have been reclaimed due to the high cost of restoration.

This research focused on the environmental assessment of chemical contamination from abandoned coal and mineral mines in Nigeria. A systematic evidence map protocol was developed to evaluate current methods for assessing chemical contamination risks from abandoned coal and lead-zinc mines. The protocol was applied to review the evidence, which revealed that current AML risk assessment methods use contaminated land risk indices to evaluate chemical risk. Furthermore, the review identified evolving data-driven and probabilistic risk assessment methods, including logistic and linear regression models, which are emerging risk assessment approaches in AML chemical risk assessment. At the same time, Bayesian Kernel Machine Regression (BKMR), cumulative probability distribution analyses for HI, and Incremental Lifetime Cancer Risk (ILCR) have been reported for mixture risk assessment, and the study showed the relevance of bioindicator-based assessments for validating predictions from chemical-based assessments.

A major aim of the project was to assess the chemical contamination and associated ecological and human health risks at coal and lead-zinc mines in Nigeria. In this phase of the research, environmental samples were collected from two abandoned lead-zinc mines at the Gimbi/Rikaya site in Plateau and the Abakaliki site in Ebonyi. The case study on abandoned coal mines was undertaken in Enugu, Nigeria. Site-specific contamination and ecological risk assessment at the Abakaliki and Gimbi/Rikaya sites revealed that both sites were heavily contaminated with Pb, Zn, and Cd, with higher concentrations at Abakaliki. Spatial distributions followed the pattern tailings > sediment > soil, with tailings as the primary contamination source. Sequential extraction confirmed that Pb, Cd, and Zn occur mainly in the exchangeable and reducible fractions, indicating high mobility and bioavailability, particularly in Abakaliki soils, where >34% of Pb occurred in mobile forms. In contrast, Pb mobility was lower at Gimbi, with only about 6% of F1 in the soil. Dissolved metals, Pb, Zn, Ni, Cu, and Mn in surface water at Abakaliki exceeded the environmental quality standards (EQS) and also the Biotic Ligand Model (BLM) bioavailability values. In contrast, only Zn exceeded EQS and bioavailability values at Gimbi. Ecological risk indices (Er, RI) and cumulative risk scores (CRS) indicated very high risk at Abakaliki and considerable risk at Gimbi, with Cd, Pb, and Zn as the dominant risk drivers.

Chemical contamination and human health risk assessment (HHRA) at the Onyeama abandoned coal mine revealed the presence of both heavy metals and polycyclic aromatic hydrocarbons in soil, tailings, and water at varying concentrations. Fe, Mn, Zn, and Pb were the dominant metals of concern, reflecting inputs from historical mining residues and secondary weathering. The ∑BaPeq value (0.86 mg TEQ/kg) exceeded the Canadian Soil Quality Guideline (0.6 mg TEQ/kg), with BaP and DBA contributing substantially to the toxic load. The HHRA indicated ingestion and dermal contact as the dominant exposure pathways. Waterborne exposure contributed the highest non-carcinogenic and carcinogenic risk, with cumulative HI and CR values exceeding acceptable thresholds, particularly for children, highlighting their vulnerability. In contrast, soil and tailings contamination presented relatively lower cumulative HI and CCR. Overall, these findings confirm that abandoned Pb/Zn and coal mines pose both ecological and human health risks to inhabitants living on or near abandoned mines, pointing to the need for targeted management measures, including the containment of tailings, remediation of contaminated sediments, and monitoring of surface and groundwater pathways, to mitigate long-term ecological and human health impacts.

Acknowledgements

First and foremost, I give all glory and praise to God, my source of life, for beginning and completing this PhD. I have enjoyed His grace and mercy through thick and thin. Lord, I am deeply grateful.

I want to express my sincere gratitude to The London NERC Doctoral Training Programme for funding my PhD project (NE/S007229/1) my PhD project and for providing invaluable training opportunities that helped me develop essential research skills. I am especially thankful for their assistance during my visa replacement issues and for all the support provided throughout my studentship. My heartfelt appreciation goes to my first supervisor, Prof. Rakesh Kanda, for his unwavering support, guidance, and patience, and for the technical and professional advice he offered throughout this research. I am deeply grateful for the opportunity to develop my research and laboratory skills under your supervision. I extend my sincere gratitude to my second supervisor, Dr Olwenn Martins, for her guidance, encouragement, and thoughtful feedback throughout this journey. Her persistent push and valuable insights have been instrumental in shaping my research skills. I would also like to thank my Research Development Advisor, Dr Thomas Miller, for his consistent support and valuable advice whenever needed. My appreciation also goes to my progression panel, Dr Alice Baynes, Dr Ovokeroye Abafe, and Dr Daniel Perkins, for their constructive feedback and encouragement during the review stages. I am grateful to the technical team of the Environmental Science Division, Dr Nicolas Beresford, Marta Straszkiewicz, and Jolene Jalota, for their training, technical support, and feedback during my chemical analyses. Working with the APHA License was a great deal! I sincerely appreciate all the help received. My sincere appreciation goes to the Ministry of Solid Mineral Development (MSMD) for providing information resources on mining in Nigeria, and to the Nigeria Geological Survey Agency (NGSA) for granting me access to their pXRF instrument at no cost. I also thank Dr Raymond Daspan (HOD) of the Department of Geology, University of Jos, for providing technical support during sampling. Thank you to Mr Ajol Fube for his help in the field. Thanks to Mr Umar for the field guide. Special thanks to Mr Nas and Mr Justine Anumnu for their field assistance and technical support, and to Mrs Tosin for her help with XRF measurements. I also appreciate Prof. Michael Oladunjoye for his guidance and support during fieldwork planning and execution, and Mr Afolabi for providing GIS training and assisting with map generation. I am thankful to my office colleagues, Jasmine, Gideon, Konstantinos, Mourice, and Ekuwa, for their friendship and for the experiences we shared throughout this journey. My thanks also go to my IFCS family for always being a blessing. I also appreciate Living Seed Europe and the London family for their prayers and encouragement. I am grateful to my friend Moses Apata for his support and encouragement, and to my dear sister and friend, Mrs Oby Nwosu, for her kindness and prayers. My heartfelt appreciation also goes to Mr and Mrs Ilozavbi for their spiritual cover and prayers, and to Mr and Mrs Akpa for their prayers and encouragement. I am grateful to Uncle Akin MacSunny for his encouragement and prayers. Finally, to my family back home in Nigeria and France, thank you for your constant love, prayers, and support. I appreciate everything you have done for me.

Dissemination of Thesis

Publications

Ekhareafo U. R. et al., (2025) Current methods for the evaluation of chemical contamination risks from abandoned coal and lead-zinc mine lands: Protocol for a systematic evidence map. *Evidence-Based Toxicology*. https://doi.org/10.5281/zenodo.14246187

Conferences/Seminars

Brunel Graduate School
Research Showcase, June 2025
Poster presentation: Tracing Hidden Risks: Fieldwork Snapshots from Nigerian Abandoned Mine Lands

UCL Arts and Sciences
Festival of Research, May 2025
Fieldwork Photo exhibition

The BRUPOD
Research Podcast, May 2025
Podcast: Water contamination in Nigeria
https://shorturl.at/JBGIZ

UKRI/NERC DTP Conference
Micro to Macro, Changing Environment on every scale, Sept 2024
Oral presentation: Abandoned mineral mines: A chemical pollution case study in Nigeria

UKRI/NERC DTP Conference
Earth and Beyond, Communicating Science for our Environment, Sept 2023
Poster presentation: Impacts of Abandoned Mine Tailings and Water on the Environment: A Review

Wageningen & Brunel University London
Research Collaboration, June 2023
Oral presentation: Assessment of Chemical Contamination from Abandoned Mine Lands and their impact on Human and Ecological Receptors

SETAC Europe 33rd Annual Meeting
Data-driven environmental decision-making, May 2023
Poster presentation: Protocol for a Systematic Evidence Map of the State-Of-The-Art Assessment of Risks related to Chemical Contamination from Abandoned Mine Lands

RSDO-Research
Funder Seminar Series, May 2023
Oral presentation: Assessment of Chemical Contamination from Abandoned Coal and Mineral Mines in Nigeria

CHMLS 8th PGR Conference, March 2023
Poster presentation: Assessment of Chemical Contamination from Abandoned Mines in Nigeria

Contents

List of Figures **Page**

List of Tables **Page**

Chapter 1: General Introduction

1.1 Background

Historically, the mining of natural resources did not always adequately consider impacts on health and the environment (Gallart, 2017; Macklin et al., 2023). Mining activities vary greatly in method and scale, including artisanal and industrial mining at small, medium or larger scales, and open-pit, surface, and underground methods. Many past mining operations lacked planning and were conducted haphazardly, leaving behind a legacy of contaminated mine lands (Hasheela et al., 2015). Mine closure, the planned or unplanned cessation of a mining operation, is a critical phase in the mining life cycle that ought to be designed and included in the mine operation plan (De Gaff, 2018). Properly designed closure aims to restore land for ecological or alternative uses, ensure ecological and human safety, and reduce environmental and social damage (De Gaff, 2018; ICMM, 2019, 2021; Laurence, 2006). The costs of mine closure are significant and as a result, mine lands are often left unattended when mineral resources are exhausted (ICMM, 2019, 2021).

An abandoned mine refers to a former mine where extraction and processing occurred that is no longer in operation, and for which there is no responsible entity to finance the cost of remediation or restoration (Ziemkiewicz et al., 2021). By contrast, abandoned mine lands (AMLs) include waste repository sites, water bodies and surrounding watersheds where extraction, beneficiation, or processing of mineral resources has occurred. AMLs are also defined by the absence of responsible parties to oversee their management or restoration (Holmes & Stewart, 2011; UK EA, 2008; US EPA, 2024c). The difference is in their scope and structure, both characterised by a range of landscape features that may include stagnant pond water, mine water, waste rocks, tailings impoundments, areas impacted by smelter plumes, abandoned equipment, and structures. Many mining companies ceased operations before environmental regulations governing mine management came into force in their jurisdictions. Hence, governments are often left with the legacies of abandoned mines and responsibility for their rehabilitation (Coelho et al., 2011; Hasheela et al., 2015). Globally, over a million abandoned mines; 550,000 in the US (BML, 2017), about 100, 000 in China (Ashby & van-Etten, 2021), 10,000 in Sweden, 17260 in Slovakia, 26, 000 in the Czech Republic (EEA, 2004), 8,500 in the UK (Hughes, 2024a), 6,000 in France (Martínez-López et al., 2021), 50,000 in Australia (Tyson, 2020), 3,092 in Indonesia (Hans, 2021), 1,500 in Nigeria (MECD, 2022), and 6,150 in South Africa (Venkateswarlu et al., 2016), have been identified, including shafts, adits, and alluvial surface mines (Coelho et al., 2011). These sites can pose severe and persistent environmental hazards, releasing harmful substances into the surrounding environment and exposing nearby communities to health risks.

Abandoned mines are a global issue, found on every continent (Coelho et al., 2011). In Africa, for instance, many of these mines are artisanal and small-scale, where mining was previously unregulated,

unskilled, and irresponsible (Dales & Ramasamy, 2019); similar situations exist in the Philippines (Domingo et al., 2024). Artisanal mining employs approximately 40 million people, compared with 7 million in large-scale mines (IGF, 2017). Nevertheless, many of these artisanal sites are likely to be abandoned, as there is little incentive for remediation once resources are depleted. Artisanal mining sites are often located near or within abandoned large-scale mines, meaning that both types of mines pose environmental risks, even if some remediation efforts have been attempted at industrial sites (Otamonga & Poté, 2020). In 2022, it was estimated that over 14 billion tonnes of tailings were generated annually from mining activities (Cacciuttolo & Cano, 2022). These vast quantities of mine waste, often stored in tailings dams or discarded across landscapes, pose significant ecological and human health risks. The scale of this impact is underscored by recent research, which shows that at least 23 million people globally live on floodplains contaminated with potentially hazardous levels of toxic waste from metal mining (Macklin et al., 2023). Additionally, stagnant pond water, mine water, abandoned equipment (such as diesel tanks and vehicles), dilapidated buildings, abandoned processing facilities, discarded chemical drums, and unsecured mine shafts and adits also characterise these sites (ICMM, 2025; Mhlongo & Amponsah-Dacosta, 2016). These remnants reflect an effort to avoid taking responsibility and highlight the absence of, or inadequate, legislation to enforce site rehabilitation (Bennett, 2016).

Physiochemically, AML components such as tailings, waste rocks, and mine water are characterised by low pH, except in sites where they are basic due to the buffer effect caused by local geology, carbonate dissolution, or bacterial sulphate reduction, all enhanced by natural events (Qin et al., 2021), and have high salinity/electrical conductivity (EC) (i.e. high dissolved salts and inorganic ions in solution), are low in oxygen content, have low water retention capacity (due to the high permeability of the waste materials), poor soil organic matter and fertility (because of the loss of soil profiles, nutrients, and microbial activity), affecting the ecological communities associated with them (Sanliyuksel Yucel et al., 2016).

Abandoned mines are significant sources of persistent contamination, due to the presence of heavy metals (HMs), polycyclic aromatic hydrocarbons (PAHs), natural radionuclides and other contaminants (Gopinathan et al., 2023). These pollutants are released through mine waste, tailings, acid mine drainage (AMD), circum-neutral mine drainage (CNMD) and other environmental processes (Iatan, 2021; Nordstrom, 2011). Heavy metals such as lead are potent neurotoxins that can result in reduced IQ, learning disabilities, and behavioural issues in children. In adults, exposure to lead is associated with high blood pressure, heart disease, and kidney damage (Chukwu & Obiora, 2023; Y. Han et al., 2023; Morgan, 2024; Sartorius et al., 2022; Wani et al., 2021). PAHs are carcinogenic and mutagenic, partially persistent in anaerobic or low-oxygen conditions, and bind strongly to sediments and soil (Bukowska et al., 2022; C. Li et al., 2019; Venkatraman et al., 2024). Natural radionuclides, including uranium, thorium, and radon, pose radiotoxic risks through inhalation or ingestion, depending on the

environmental conditions (Momčilović et al., 2013; Paul et al., 2022). These contaminants migrate through soil, water, and air, influencing surrounding ecosystems and necessitating detailed environmental and health assessments to guide remediation efforts.

AMD is a significant source of contamination, affecting watercourses globally. Several specific sites have been described in the literature, for example, the Tinto-Odiel rivers in southern Spain. (Grande et al., 2003), surface waters of the Gujiao and Gyama valley in China (X. Huang et al., 2010; Ping et al., 2017), and the Blyde River catchment in South Africa (Selebalo et al., 2021). Over 23,000 km of contaminated rivers have been recorded in the United States (Cravotta III et al., 2010; Gammons et al., 2010). It is estimated that over 5,000 km of watercourses in 15 EU member states have been polluted by abandoned coal and metal/mineral mines (Johnston & Rolley, 2008). Additionally, the release of heavy metals and PAHs into surrounding soils and sediments can cause extensive pollution, with high contamination levels recorded in rivers and soils (W. Han et al., 2023; Hughes, 2024a; Sartorius, 2024; Wolkersdorfer & Mugova, 2022). In coal AMLs, PAHs contribute to environmental and health risks, with severe implications for aquatic ecosystems (C. Li et al., 2019). Moreover, the dispersion of pollutants through surface runoff, groundwater leaching, and sediment transport exacerbates the contamination of water and soil resources (Candeias et al., 2015; Patel et al., 2024).

Consequently, assessing chemical contamination from abandoned mines is critical for evaluating the extent of environmental pollution and its potential impacts on living organisms (Dash et al., 2019; Kumar et al., 2019). Understanding the nature and scale of the problem is the foundation for developing effective remediation strategies. Mine rehabilitation or remediation forms an integral part of the mine life cycle; however, inadequate legislative frameworks and the absence of appropriate financial instruments have allowed many mine legacies to persist. In many cases, limited funding makes remediation of abandoned mine lands a challenging task, necessitating the prioritisation of sites that require immediate intervention(Fallis, 2013; Mavrommatis & Menegaki, 2017).

Nigeria was a major exporter of tin, columbite, and coal before the oil boom of the 1970s. However, with the shift to oil production, many mines were abandoned, leaving behind extensive environmental legacies, including waste dumps, open pits, and acid mine drainage (Merem et al., 2017; Omotehinse & Ako, 2019). These AMLs now pose serious ecological and health risks that remain largely unaddressed. Over 1500 abandoned mines have been identified nationwide (MECD, 2022), including more than 1,100 tin and columbite sites in Plateau State alone (Alao & Ibrahim, 2014). Although government initiatives aimed to reclaim 100 sites annually between 2007 and 2020, only 44 sites had been rehabilitated by 2022 due to limited funding and institutional capacity (Vanguard, 2017). Reclamation efforts have focused mainly on physical restoration, neglecting the chemical

contamination and associated human health risks, despite the continued use of mine lands, including ponds, for domestic and agricultural purposes.

Following the 2014 oil price collapse and the economic impacts of the COVID-19 pandemic, Nigeria renewed its commitment to diversifying its economy through the solid minerals sector (KPMG, 2017; MRC, 2020). However, this renewed mining drive is occurring amid inadequate remediation and environmental management frameworks for existing AMLs. These gaps underscore the need for research to assess chemical contamination and risk in Nigeria's abandoned mine lands to inform sustainable remediation strategies.

Most existing studies on AMLs in Nigeria have focused on landscape degradation and heavy metal pollution in soil and water, with limited attention to contamination of water resources and exposure risks. The absence of proper water management has led to the uncontrolled discharge of untreated mine water into ponds, streams, and rivers. Research and remediation efforts in the country remain insufficient, with little progress in inventorying, characterising, prioritising, or restoring AMLs (Ahmed & Oruonye, 2018; Edun & Davou, 2013). In contrast, countries such as the UK, the US, Australia, and Canada have implemented comprehensive frameworks for the assessment and management of AMLs. These include systematic contaminant characterisation, environmental quality standards, and long-term monitoring programmes supported by robust legislation and remediation technologies. Such initiatives have enabled effective identification, prioritisation, and rehabilitation of contaminated sites. However, similar holistic evaluations are yet to be undertaken in Nigeria, where efforts remain fragmented and largely focused on physical reclamation rather than contaminant risk assessment.

This research addresses these gaps by focusing on legacy mining areas to identify pollutants, understand their fate and interactions, and assess associated ecological and human health risks. The findings will provide evidence to guide policy decisions and support effective remediation of abandoned mine lands in Nigeria.

1.2 Aims and Objectives

The project aims to undertake an environmental assessment of chemical contamination from abandoned coal and mineral mines in Nigeria through case studies. The study also identifies and quantifies chemical contaminants; examines their interactions across various environmental media, and determines the fate, mobility, and impacts of contaminants on receptors.
The following specific objectives were articulated:

- Review the legal framework for mining and the management of abandoned mines in Nigeria.
- Develop a systematic evidence map protocol for the evaluation of chemical contamination risks from

abandoned coal and lead-zinc mine lands.

- Undertake a narrative evidence review of current methods in assessing risk from abandoned coal and lead-zinc mine lands.
- Evaluate chemical contamination associated with the sites
- Assess exposure pathways, including transport, mobility, bioavailability, and bioaccumulation of identified contaminants.
- Conduct ecological and human health risk assessment for key contaminants from case studies.
- Develop policy recommendations for chemical contamination from abandoned mine lands in Nigeria.

1.3 Case Studies

Globally, the most mined minerals by volume are coal, iron ore, aluminium (bauxite), copper, chromium, zinc, titanium, and lead (Casey, 2018; LePan, 2020; Venditti, 2023), with over 7 billion tonnes of coal (IEA News, 2023) and 17 million tonnes of lead-zinc mined each year (Venditti, 2023). Among these, coal and lead mines are of particular concern due to the significant and well-documented severe health risks, especially those linked to exposure associated with legacy contamination from AMLs (Hughes, 2024b; J. Li & McDonald-Gillespie, 2020; Sartorius, 2023). Hence, given their substantial toxic legacies, environmental persistence, widespread and extensive documentation of their health and ecological impacts of their associated metals, lead-zinc mines are valuable case studies within the broader global context of AMLs contamination (Morgan, 2024; Rouhani et al., 2023; Sartorius, 2023, 2024; Tozsin et al., 2022; Wani et al., 2021).

Building on this global perspective, the present study focuses on three case studies of abandoned mines in Nigeria: one coal mine and two lead–zinc mines. These sites were selected because they represent regions of intensive mining activity during the early 20th century, where most AMLs remain unremediated due to high reclamation costs and weak institutional frameworks for mine closure and post-mining land management. Further details of these case studies are provided in subsequent chapters.

1.4 Justification of Study

- Knowledge gaps in Nigeria: The study location, Nigeria, is particularly important due to substantial knowledge gaps regarding contamination from abandoned mine lands (AMLs), especially when compared with regions where more extensive assessments have been conducted.
- Relevance of coal and lead/zinc mining: Coal and lead/zinc are among the most extensively mined minerals worldwide, leaving behind a legacy of contamination that poses significant environmental and chemical risks. Lead/zinc mines are of particular concern due to their well-

documented and severe health impacts, especially those arising from legacy contamination associated with AMLs.

- Limited attention to organic contaminants: Although the environmental impacts of heavy metals and acid mine drainage from abandoned coal mines have been widely documented, potential human health risks associated with organic contaminants, particularly polycyclic aromatic hydrocarbons (PAHs), have received limited attention.
- Gap in risk assessment synthesis: There remains a knowledge gap in the synthesis of current risk assessment approaches addressing chemical contamination from abandoned coal and lead/zinc mine lands.
- Integrated analytical framework: This study adopts an integrated approach to investigating AML-related chemical risks by combining analytical, toxicological, and environmental data. This comprehensive framework aims to enhance understanding of contamination patterns and exposure pathways, thereby supporting more effective and evidence-based management strategies for AMLs.

Chapter 2: Literature Review and Legal Framework of Nigeria

2.1 Background

Mining is the process of extraction of naturally occurring coal, minerals, and metals of high economic value. Mineral and metal mining dates to the Bronze Age. Many mines were exploited in ancient Greece and the Roman Empire for iron, copper, gold, lead and other minerals. Technological advancement with explosives and machinery expanded mining for industrial minerals in the 19th century, rose rapidly in the 20th century, and growth in the industry has continued (Carvalho, 2017; Fernández-Lozano et al., 2015). Coal is the most abundant fossil fuel on Earth and is used for electricity generation, as fuel in cement production, where it provides the high temperatures required for clinker production and in the steel industry for extracting iron from iron ore. An increase in world population and industrialisation has increased demand for fossil fuels, minerals, and metals as raw materials (Dales & Ramasamy, 2019). The mining sector plays a key role in economic and infrastructural development, employment, and the provision of raw materials for industrial use. Coal, mineral and metal extraction are essential for building materials for commercial and private use, and to produce asphalt, medicines, household and electronic products, thereby supporting the economic development of nations rich in natural resources and improving human quality of life (Kibria, 2014).

Mining is also one of the most hazardous occupations and can have widespread detrimental effects on the environment, including the biosphere, land, climate, surface water, and groundwater (Coelho et al., 2011). Past mining activities have left huge imprints on the environment. Abandoned mines across different regions of the world represent significant sources of soluble metals and highly contaminated anthropogenic sediment to rivers and streams (Kincey et al., 2018; UK EA, 2008) and their impact is expected to continue to rise if strict regulations are not enforced (Nakazawa et al., 2016).

Most historic abandoned metal and mineral mines predate the inception of environmental legislation and a better understanding of the environmental implications of mining. Similarly, in the early years of coal mining, exploitation was carried out without consideration for its environmental implications and with no environmental regulations in place. Often, when most of the coal had been mined from a particular site, miners relocated to a new site, abandoning the old one. In Nigeria, during the oil boom, the shift from coal to oil as an energy source contributed to the abandonment of many coal mines. Local political instability and civil unrest can also result in unplanned mine closures. For example, operations at the Kilembe copper mine in Uganda ceased in 1982 following a period of political instability and economic decline (UPPC, 2025), while the Panguna copper-gold mine on Bougainville Island, Papua New Guinea, was abandoned in 1989 following civil conflict linked to mining-related grievances (Regan, 2017). Illegal or artisanal mining is another cause of abandoned mine sites (Van Zyl et al., 2002). Mine owners were either not identified or could not afford the resources required and the prohibitive costs of reclamation and remediation, leaving governments responsible for environmental

damage (Coelho et al., 2011; Van Zyl et al., 2002).

2.2 Mining Lifecycle

There are different stages in mining operations (Figure 2.1), including:

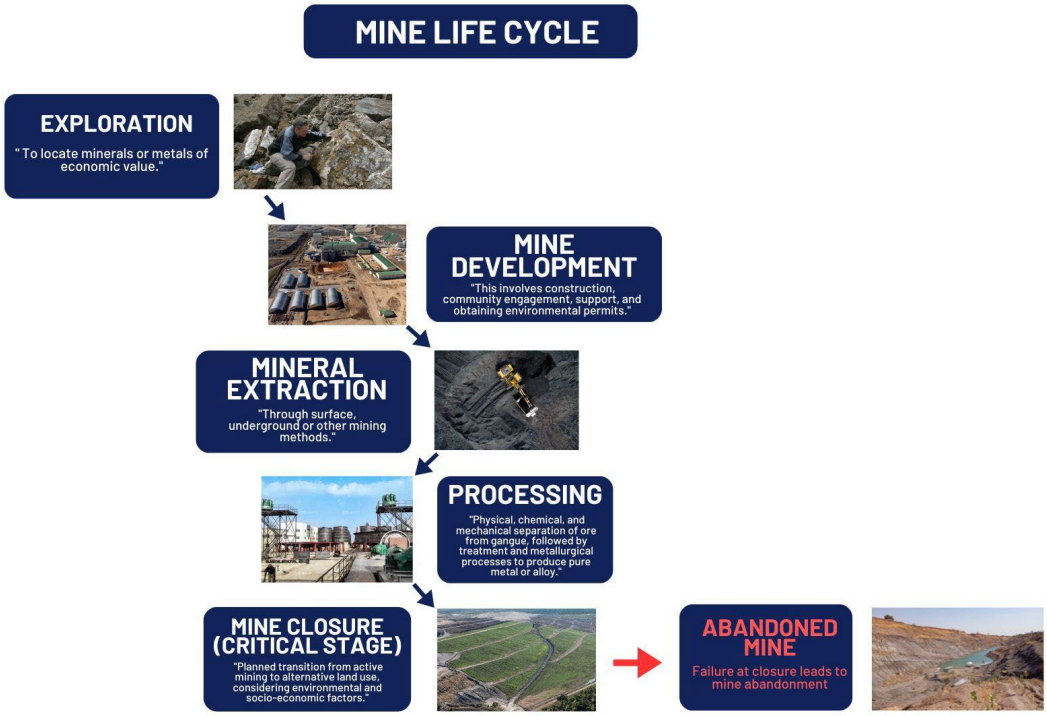

Figure 2.1: The typical lifecycle of LSM, illustrating the sequential stages from exploration through development, operation, and closure. Characterised by formal planning, regulatory oversight, and the implementation of environmental management practices at each stage.

- E*xploration and prospecting* to locate minerals or metals of economic value.
- *Development of the site and planning, which involves construction, community engagement, support and obtaining an* environmental permit.
- *Extraction of the mineral:* surface and underground mining are the two major methods employed in mining; Surface mining by opencast or open pit is created through excavation to assess ore close to the surface, while underground mining assesses ore in buried bedrock through the construction of shafts and tunnels. Other types include soluble and placer mining, in-situ leach mining and heap leaching mining (Balasubramanian, 2017).
- *Processing or production* of the mineral includes all the physical, chemical, and mechanical methods employed to separate the ore from the gangue (the undesirable materials), and then the treatment. Finally, metallurgical processes are used to produce pure metals or alloys. These processes generate waste and release harmful chemicals to the environment with short- and long-term impacts (Kibria, 2014; Lottermoser, 2010; Wood, 2020).
- *Mine closure* is the final and important stage of the mining life cycle (Figure 1). Because

minerals are not renewable, the life of a mine is finite. Once factors such as low prices, technical issues, and security threats are set in, mining ceases. Mine closure is the process of transitioning from active mining to another land use, taking into account environmental and socio-economic factors. This requires implementing reclamation plans established before mining begins to remove or reduce hazards and associated risks to humans and the environment. However, this is often neglected and mined lands become abandoned (Dales & Ramasamy, 2019; Fields, 2003; Mclemore & Frey, 2018).

It is important to note that Artisanal and small-scale mining (ASM), characterised by limited regulation, dangerous and informal practices, poses acute risks to workers and nearby communities through unsafe conditions and direct exposure to contaminants. As a result, the lifecycle of ASM differs markedly from that of LSM, which is typically regulated and supported by advanced technologies and formal management systems (Figure 2.1). The following section outlines the key stages of the ASM lifecycle (Figure 2.2) and their associated environmental and health implications.

Figure 2.2: Simplified lifecycle of ASM, illustrating key stages from site selection to abandonment. The informal and unregulated nature of ASM contributes to unmanaged waste generation and long-term environmental contamination.

Artisanal mining is mostly informal and illegal, with no formal approval from licencing authority. It typically begins with informal *site selection*, driven by local knowledge or visible mineralisation, rather than systematic geological assessment. Once a site is chosen, it is *prepared* by miners who clear vegetation, strip topsoil, and open shallow pits or shafts, causing immediate land degradation, habitat loss, and increased erosion. The removal of protective surface layers also enhances the mobilisation of potentially contaminated materials. *Extraction* relies on manual labour and rudimentary tools, often resulting in unstable shafts and unsafe working conditions. As sulphide-bearing materials are unearthed and exposed to air and water, geochemical reactions may mobilise contaminants. *Processing* involves simple crushing and separation techniques, and in some cases, the use of mercury for gold recovery. This stage is a major source of direct environmental discharge, with metals and metalloids frequently released into surrounding ecosystems without treatment.

Waste materials (tailings and waste rock) are typically dumped without containment, leaving them vulnerable to weathering and leaching. This unmanaged waste can generate polluted drainage, including

AMD, CNMD, and other metal-rich effluents. When operations cease, sites are commonly *abandoned* without closure, resulting in long-term contamination of soil, water, and sediments. These degraded landscapes continue to expose nearby communities and ecosystems to persistent chemical hazards through multiple pathways.

Collectively, the ASM life cycle demonstrates how informal, unregulated mining practices create sustained environmental impacts and complex exposure risks, particularly in abandoned mine land settings.

2.3 Abandoned Mine Lands (AMLs)

Abandoned mines are sites where intensive mineral exploration, operation and production ceased without reclamation or rehabilitation. Also, the situation where there are no identifiable owners or operators for the facilities is regarded as AMLs (Van Zyl et al., 2002). They constitute a serious global concern due to inherent health and environmental hazards (Coelho et al., 2007, 2011; Peplow & Edmonds, 2005).

AMLs are characterised by waste rock piles made of unprocessed sub-grade mined rock, tailings of mined rocks processed to remove desired mineral or metal, roads or paths no longer in use, storage tanks for diesel and fuel, drainage diversions, adits, mills, dilapidated buildings and structures like tramways, mine shafts, abandoned heavy equipment (Hufty, 2019; Klawans, 2024; NPS, 2020), left unclaimed as license owners failed to take legal responsibility for reclamation (Mclemore & Frey, 2018). Tunnelling, digging, and manual extraction of coal, minerals, and metals using carts to large open-cut and long wall mining lead to dangerous impoundments, slides and piles, clogged streams, gases from hazardous explosives, waters polluted with dissolved metals and other hazardous substances (DEP, 2015; Johnston & Rolley, 2008).

AMLs create changes to the original system where the topography, stream network, fauna and flora are affected, as well as alterations to the physical and chemical properties of soil, surface water, groundwater, and the biological communities due to exposure to pollutants (Martínez-López et al., 2021).

AMLs are difficult to manage. Orphaned areas, especially in regions with no defined legal framework, where mine operators do not have the legal obligation to deal with the consequences of abandonment (Fields, 2003). The exact locations of most legacy mines are not traceable because some AMLs are out of sight, and relevant data that could help identify them has been lost due to unscheduled closures or natural disasters, leaving no measurable information available to achieve this. Most developed countries have established rehabilitation programs involving communities to identify AMLs (Alonzo et al., 2024; IGF, 2025).

Many abandoned mines are used alternatively for household and commercial waste disposal, which adds to the existing problem, causing danger from unsanitary conditions, and exposure to old waste

disposal may lead to adverse health effects on communities close to such sites (Coelho et al., 2011). For example, in the USA, 5.5 million people live within a mile of abandoned mine lands (Grist, 2021) and in the UK, it is estimated that one quarter of homes sit above abandoned coal mines (Lane, 2021).

2.4 Sources of Contamination

The environment is integrated, and its components are linked by dynamic processes; affecting one part affects other parts (Mbaya, 2013). The natural geology consists of mutually related subsystems, and the destruction of one of the subsystems leads to the modification of the entire system (Lenton, 2016). Main changes to the environmental balance generally come from digging a part of the land surface, as well as from deposits of different kinds of wastes and tailings and from the chemical products used in ore separation or purification (Younger & Robins, 2002). All these modifications cause hydrological and hydrogeological impacts (on surface and groundwater, respectively), geochemical impacts (on water, sediment, soil, and alluvium) and biological impacts (on living things) (Ashley et al., 2003). These impacts vary with the timing of their production and can cause sporadic and/or diffuse pollution. Sporadic pollution may occur when the mine is active, through accidental releases or operational failures, although if a control system is in place to monitor the process, the pollution can be restricted or contained from spreading. Diffuse pollution mostly occurs with abandoned mines, where the absence of active management allows contaminants to be released continuously or intermittently from multiple sources across the site.

Contamination or pollution sources are typically categorised as point and non-point (diffuse) sources. Point source pollution originates from specific, identifiable sources that release pollutants into the environment at clearly defined locations (US EPA, 2025). For example, mine water may be discharged from mine adits or drainage tunnels (Figure 2.3), which eventually enter surface and groundwater systems (UK EA, 2019).

In contrast, diffuse sources are contamination sources that originate over a broad area rather than from a single identifiable discharge point, unlike point sources. These sources release contaminants gradually and intermittently through chemical and physical processes such as rainfall, surface runoff, sediment transport, leaching, and atmospheric deposition (Stuart et al., 2012; US EPA, 2025). Diffuse pollution occurs when contaminants are mobilised from exposed mine wastes, tailings, waste rock piles, contaminated soils, and abandoned workings over large areas (Figure 2.4) through infiltrating water, runoff, wind dispersion, and sediment transport, making them difficult to monitor and control due to their spatial and temporal variability (Byrne et al., 2021; US EPA, 2025). These contaminants are subsequently transported into surrounding ecosystems, including water resources, thereby causing contamination. AML is the cause of poor water quality in most regions of the world (Aroh, 2021; NPS, 2020; Van Zyl et al., 2002) and among the most contentious aspects of mining (Bebbington & Williams, 2008).

Figure 2.3: Point source pollution from the Onyeama abandoned mine adit discharging into the Ekulu River tributary

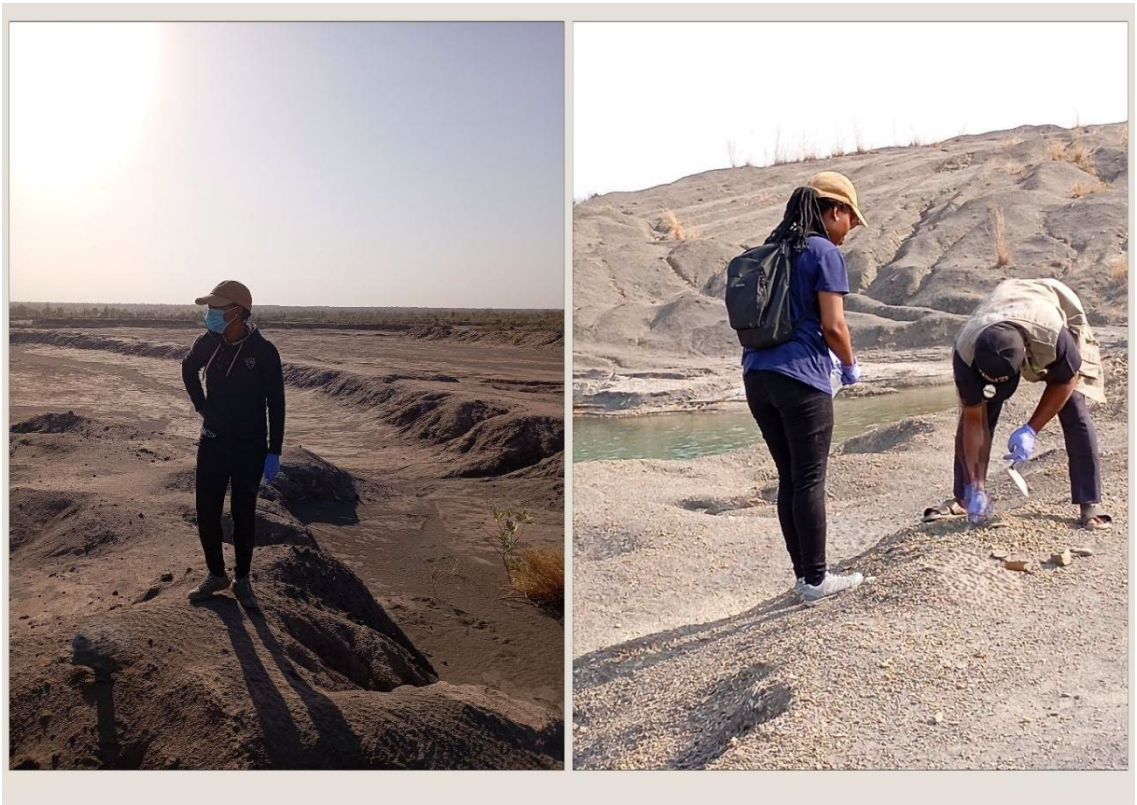

Figure 2.4: Gimbi and Abakaliki tailings impoundments; sources of diffuse pollution

2.4.1 Mine Water

Mine water is water influenced by a mine (Wolkersdorfer & Mugova, 2022). It settles in a mine and is usually managed or pumped during mining operations to keep the mine dry. The source of this water is typically from surface and groundwater that enters mine workings, water used for mining processes and water from post-closure drainage due to abandonment (911Metallurgist, 2020). Mine water could be acid mine drainage formed by the oxidation of sulfidic minerals like pyrite, neutral and alkaline mine drainage predominantly in carbonate-rich geologic environments, pit lakes and seepage water in open pits or from tailings (Banks et al., 1997; Johnston & Rolley, 2008; Mindat, 2025; UK EA, 2021).

Primarily, mine water chemistry varies because of the heterogeneity of the geologic environment and the influence of chemical and biological processes. Sulphide oxidation occurs in iron pyrite-rich coal seams and mineral veins exposed to air, releasing sulphate and dissolved metal ions. This is facilitated when water is actively pumped out of the mine (Patel et al., 2024; UK EA, 2008). However, when mining ceases and pumping is turned off, the mine becomes flooded, and the oxidation of sulphide minerals stops, which enables the reaction of sulphate with metal ions in the water to form sulphuric acid. This can cause metal mobilisation or immobilisation, depending on the surrounding rock types (Nordstrom, 2011; Ukhan et al., 2022). So, carbonate buffering and secondary mineral formation reactions influence the chemical composition. In most cases, sulphuric acid causes the dissolution of metal compounds, which leads to their elevated concentrations. Mine water, in general, has a range of chemical constituents depending on the mine type. Heavy metals such as Fe, Mn, Zn, Pb and major ions Cl^-, HCO^{3-}, $SO_4^{2-,}$ Na^+, Mg^+ (Abiye, 2014; Patel et al., 2024; UK EA, 2008; Ukhan et al., 2022).

pH is a measure of the acidity or alkalinity of water, reflecting the concentration of hydrogen ions (H^+) in a solution. It is a crucial parameter in mining-influenced waters because it influences the mobility of metals and the extent of chemical reactions, such as pyrite oxidation. The pH of mine water ranges from acidic to alkaline, depending on mineral interactions and environmental conditions. For example, the oxidation of sulphide minerals such as pyrite generates acidity, leading to low pH conditions, whereas the presence of buffering minerals such as carbonates can neutralise acidity and result in circum-neutral to alkaline mine waters (Ukhan et al., 2022). It could be as low as <3 in AMD (Bigham & Cravotta, 2016) and >=7 for neutral to alkaline due to water interactions with carbonate rocks such as calcite (Nordstrom, 2011; Ukhan et al., 2022); for instance, the abandoned mine water in Zhangqiu District exhibits weakly alkaline pH, with dominant cations being Ca^{2+} and anions HCO^{3-} and $SO4^{2-}$ (Y. Liu et al., 2023). Neutral to semi-neutral pH (buffering) has little or no effect on watercourses because of reduced metal mobility. However, when the buffer capacity is exhausted, influenced by dilution effect, the mine water can become acidic (low pH), which leads to increased toxicity and ecological disturbance. Ore type, host rock, mine depth, climate and time of closure influence the chemistry

(Johnston & Rolley, 2008; Masindi et al., 2017; Perry et al., 2016; Ukhan et al., 2022; Wolkersdorfer & Mugova, 2022).

The salinity of mine water is depth-dependent (Mugova & Wolkersdorfer, 2025; UK EA, 2008). Seasonal variations influence mine water geochemistry and oxidation rate, primarily attributed to changes in environmental parameters such as temperature, pH, dissolved oxygen and carbon dioxide levels. Higher pH values are observed during the summer because of reduced CO_2 and increased bicarbonate, resulting in enhanced oxidation rates. Conversely, in the winter, lower pH values and higher dissolved CO_2 levels slow oxidation rates to nearly zero, even if the water is saturated with oxygen (Banks et al., 1997; UK EA, 2021).

Water in flooded mines rises to the surface and discharges through old mine adits, springs, ground seepage or riverbeds, thus introducing pollutants (Beane et al., 2016; Johnston & Rolley, 2008; Y. Liu et al., 2023; Ukhan et al., 2022). In deeper mines, the water may not rise; instead, it connects to groundwater aquifers, where the predominant problem will be sulphate and chloride pollution. Mine water discharge, leachate and runoff from waste disposal structures are sources of pollution to water bodies (Beane et al., 2016). Mine water also serves as a pathway for the movement of potential contaminant loads from the vicinity of AML to a new environment, making the problem widespread and more complex to resolve.

2.4.1.1 Acid Mine Drainage (AMD)

AMD occurs geochemically during the oxidation of pyrite (FeS_2), a sulphide mineral associated with coal and metal mines (Bigham & Cravotta, 2016; Blowes et al., 2014; Kefeni et al., 2017; Simate & Ndlovu, 2014). When it comes into contact with water and air during and after mining, pyrite undergoes a series of oxidative reactions that release acid and metal-rich drainage into the environment. AMD from abandoned mine lands is a major concern (Z. Wang et al., 2021) because of their consequences on biological activity in streams and rivers (D. Chen et al., 2021; Oyetibo et al., 2021; Ushakova et al., 2022).

Metals such as gold, copper, lead, zinc, silver, and molybdenum are often found in rocks with sulphide minerals and iron sulphide minerals like pyrite and pyrrhotite; they are also commonly associated with coal beds or strata (Jiao, Zhang, et al., 2023). During mining, when these sulphide-bearing rocks are excavated and exposed to air and water, they form sulfuric acid. This acidic water dissolves other toxic metals in the surrounding rock, which eventually run off into streams, rivers, and lakes or leach into groundwater. Hence, AMD is acidic drainage with high concentrations of sulphide oxidation products and associated metals. AMD typically occurs when iron sulphide minerals, especially pyrite, or “fool’s gold”, are abundant and there is insufficient neutralising material to counteract the acid formation (Popham, 2019). AMD are also released from waste rock piles, tailings, open pits, underground tunnels,

and leach pads (Anawar, 2015; Parbhakar-Fox, 2016).

This is what happens geochemically during the oxidation of pyrites, resulting in the production of ferrous ions and ferric ions – a complex reaction that has hindered effective treatment options:

$$2FeS_2 + 7O_2 + 2H_2O \rightarrow 2Fe^{2+} + 4SO_4^{2-} + 4H^+ \quad (1)$$

The oxidation of sulphide to sulphate solubilises ferrous iron (Fe2+), which is subsequently oxidised to ferric iron (Fe3+):

$$4Fe^{2+} + O_2 + 4H^+ \rightarrow 4Fe^{3+} + 2H_2O \quad (2)$$

Either of these reactions can occur spontaneously or can be catalysed by microorganisms that derive energy from the oxidation process. The ferric iron produced can further oxidise additional pyrite:

$$FeS_2 + 14Fe^{3+} + 8H_2O \rightarrow 15Fe^{2+} + 2SO4^{2-} + 16H^+ \quad (3)$$

The net effect of these reactions is the release of H^+ ions, which lowers the pH and maintains the solubility of the ferric ion, thereby contributing to the characteristic orange colour observed in AMD discharges.

In lead-zinc mine tailings containing sulphide minerals such as sphalerite (ZnS) and galena (PbS), oxidation occurs upon exposure to air and water, generating AMD laden with zinc, lead, and sulphuric acid:

For sphalerite:

$$ZnS + 2O_2 \rightarrow Zn^{2+} + SO_4^{2-} \quad (4)$$

$$ZnS + 2O_2 + H_2O \rightarrow Zn^{2+} + SO_4^{2-} + 2H^+ \quad (5)$$

For Galena:

$$PbS + 2O_2 \rightarrow Pb^{2+} + SO_4^{2-} \quad (6)$$

$$PbS + 2O_2 + H_2O \rightarrow Pb^{2+} + SO_4^{2-} + 2H^+ \quad (7)$$

When pyrite is present alongside sphalerite and galena, the primary acid generator is pyrite (equation 3), while galena or sphalerite act as anodes in galvanic reactions, rapidly accelerating overall dissolution of metal sulphides into the environment, lowering the surrounding pH, often to 4 or less (Qian et al., 2018).

AMD represents a critical environmental issue associated with both active and inactive mines. In active mining operations, although water treatment and controlled discharge may reduce immediate impacts, continuous dewatering and pumping can create aerated conditions within mine workings, thereby enhancing sulphide oxidation and acid generation. In contrast, when mines are abandoned, and workings become flooded following cessation of pumping, oxidation rates generally decrease under reducing conditions. However, the initial flooding phase may result in the flushing of accumulated or "vestigial" acidity from exposed mine materials (Mugova et al., 2024; Younger et al., 2002). Furthermore, seasonal fluctuations in the water table can expose previously unreacted sulphide minerals, leading to the generation of "juvenile acidity," which may subsequently be mobilised during periods of increased recharge and groundwater rise (Mugova et al., 2024; Younger et al., 2002).

AMD have been found to be associated with the continuous pollution of the Tinto-Odiel rivers in the mining region of southern Spain (Grande et al., 2003; Guerrero et al., 2021). In the US, AMD generated from abandoned coal mines constitutes a major source of contaminated rivers, with a total of about 23,000 km (Cravotta III et al., 2010; Gammons et al., 2010). Many water courses in the UK and Africa, for example, have been polluted by discharges from abandoned coal mines (Edwards et al., 2014; Merem et al., 2017; UK EA, 2008)Discharges from AMLs have been identified as a source of pollution to over 1500km of rivers in England (UK EA, 2019) and in many waters of China and Australia (Lei et al., 2010; X. Li et al., 2021; Zhu et al., 2022).

2.4.2 Heavy Metal Contamination

Abandoned metal and coal mines have been traced to be responsible for over half of the heavy metals found in rivers (Mayes et al., 2013; Tran et al., 2020). The process of metal extraction requires crushing and grinding the orebody into fine grains to liberate valuable minerals from the surrounding gangue material. This process generates a large volume of waste known as tailings, which are fine-grained residue commonly discharged as slurries following mineral processing (BAM, 2004). They are either dumped at the perimeters of the mine sites or stored in engineered containment facilities such as tailings ponds or impoundments (Johnson et al., 2000; Kossoff et al., 2014; Schoenberger, 2016). During rainfall and snowmelt, water flows over and interacts with tailings impoundments, which are rich in quantities of harmful and toxic substances such as arsenic, lead, cadmium, chromium, zinc, and cyanide (if cyanide leaching is used for extraction) (Ashim Sikdar et al., 2020). These toxic metals leach and percolate through the ground, contaminating surface water and groundwater, especially when the bottoms of facilities are not lined with impermeable liners (W. Li, Deng, et al., 2024; Randelovic et al., 2020). Impacts of wet tailings impoundments, waste rock, heap leach, and dump leach facilities on water quality are usually severe, leading to the death of aquatic plants and animals (Bes et al., 2014; Johnson et al., 2000; Kossoff et al., 2014; Martín-Crespo et al., 2015; Ngole-Jeme & Fantke, 2017).

Soil contamination resulting from AML occurs over a large area, such that agricultural activities near such sites become particularly affected (Horasan, 2020; Yu et al., 2025). Moreover, spills and leaks of hazardous materials, as well as deposition of contaminated windblown dust, lead to soil contamination (Del Rio-Salas et al., 2019; Djebbi et al., 2017). This could cause potential risk to human health, aquatic life, and plants if the level of pollutants present is high (Kuter, 2013). The risk is greatest if the windblown dust is characterised by high levels of arsenic, cadmium, lead, and PAHs (Coelho et al., 2007, 2011; S. Kim et al., 2008; Pless-Mulloli et al., 2000).

2.4.3 Erosion and Sedimentation

Disturbed land and unprotected slopes create opportunities for land erosion (Sengupta, 1993). Short-duration and high-intensity storms trigger erosion of exposed soils, open pit areas, tailings waste, heap and dump leach piles, waste rock and overburden piles, resulting in substantial sediment loading to surface waters and drainage ways (Fallis, 2013; Kuter, 2013; Richard et al., 2021). It may also be the erosion of contaminated floodplain material and/or remobilisation of contaminated in-channel sediments. These constitute classic diffuse sources of contamination (Ciszewski & Aleksander-Kwaterczak, 2020; Domingo et al., 2023).

The effect of erosion and sedimentation is the transport of particulate matter from disturbed land to surrounding environmental media, particularly surface water bodies, where they act as a key pathway for the mobilisation and redistribution of contaminants (Domingo et al., 2023; Downham, 2022). These particulates often carry adsorbed metals and metalloids, facilitating their redistribution within aquatic systems and increasing exposure risks to biota (Kincey et al., 2018; Luís et al., 2011). The build-up of thick fine mineral layers and sediments in the vicinity of regional floodplains affects aquatic life through habitat alteration and heavy metal pollution (Ayari et al., 2021; B. Huang et al., 2018; Pinto et al., 2004). Such changes may smother benthic habitats, reduce water quality, and contribute to long-term contamination of sediments, which can act as secondary sources of pollution

2.5 Ecological Impacts and Human Health

The impacts of AMLs on soil, surface water, and groundwater affect human health through different pathways. Inhalation of and skin contact with heavy metals and organic contaminants, drinking polluted water and consumption of food produced from contaminated environments (Passariello et al., 2002; Wani et al., 2021) cause impacts which are toxic to ecological and human health. Details of their occurrences in mine lands and other environments, and their effects, are provided in Tables 2.1 and 2.2.

Eye irritation and respiratory symptoms have been observed among people living near abandoned mines (Coelho et al., 2007). Widespread, acute lead poisoning in Zamfara State, Nigeria, has led to the deaths

of about 400 children since 2010 and is considered the worst outbreak of lead poisoning in modern history; more than 3,500 children required urgent, lifesaving treatment, and high rates of infertility and miscarriage were reported among adults (Burton, 2012; Dooyema et al., 2012; Human Rights Watch, 2011; Tirima et al., 2018). Similarly, extremely elevated blood lead levels have been reported in children living near the former Pb–Zn mining area of Kabwe, Zambia, highlighting the long-term risks associated with abandoned mine contamination (Yabe et al., 2015; Yohannes et al., 2021). In coal mining regions, recent studies have shown that communities living near mining activities are at increased risk of chronic respiratory and cardiovascular diseases due to exposure to coal dust and associated pollutants (Cortes-Ramirez et al., 2024; Mahlangeni et al., 2024). Prolonged exposure to coal-derived particulate matter has also been linked to respiratory conditions such as coal workers' pneumoconiosis and other chronic illnesses (Akbar & Kallawicha, 2024; Pless-Mulloli et al., 2000). These findings demonstrate that contamination from abandoned and legacy mining sites can pose significant ecological and human health risks through multiple exposure pathways.

Continued exposure of residents in the vicinity of an abandoned mercury (Hg) mine in the Philippines, where Hg levels exceeded recommended values in sediments, fish, and residents' blood, led to reports of bleeding gums, anaemia, and neurologic effects (Gong et al., 2018; Maramba et al., 2006). Daily intake of rice by the local community around the Myungbong Au-Ag abandoned mine in Korea was found to increase the potential risk of cancer due to a long period of exposure (Lee et al., 2008). High Cd blood levels were reported in residents living in the vicinity of an abandoned Cu mine in Korea (S. Kim et al., 2008). Residents of Palu City were reported to be at serious health risk from exposure to high levels of atmospheric Hg in connection with mining (Nakazawa et al., 2016).

The ecological impacts of abandoned mines are diverse, affecting both terrestrial and aquatic ecosystems (Peplow & Edmonds, 2005). The process of mining strips away vegetation and topsoil, resulting in biodiversity loss and forest degradation (Palmer et al., 2010). Mine wastes and tailings are dumped on the surrounding land, which is unstable, easily erodible, and prone to being carried into streams and rivers. The eroded sediments clog stream channels and disrupt the natural flow pattern. These disturbances affect ecological communities (Venkateswarlu et al., 2016). Continuous exposure to heavy metals can potentially lead to bioaccumulation and biomagnification through trophic levels (Bonnail et al., 2016; Calabro et al., 2022), leading to adverse effects in wildlife as well as humans who depend on these environments (Sartorius, 2024).

Table 2.1: Toxic metals associated with mining and other environments; sources, environmental and human health effects (Adapted and modified) from (Coelho et al., 2011; Kibria, 2014)

Toxic metals	Environmental sources	Environmental/Ecological effects	Human Effects*	Occurrences of metals in abandoned mines in Nigeria.
Arsenic (As)	Natural (Parental rock material), naturally found in association with coal, gold, iron, lead, silver, zinc ores; mining (mine tailings) & smelting, volcanoes, pesticides fertilisers, treated wood/wood treatment sites, industrial effluents, sewage sludge, tanneries, coal (fly & bottom ash), animal farms, incineration and incineration ash, detergents, petroleum combustion, air, land and water can be contaminated via windblown dust, water runoff; natural contamination (groundwater) reported from Bangladesh, West Bengal,	Soil and water close to mines can be contaminated with As. Terrestrial plants can absorb As via root or adsorption of air borne arsenic deposited on the leaves; As is phytotoxic to plants (bean, soybean, rice, are highly sensitive to As), rice and vegetables grown in contaminated soil & irrigation water can contain elevated levels of As; As toxicity on rice includes delayed seedling emergence, reduced plant growth, yellowing, wilting of leaves, reduced grain yields; freshwater fish can bio-accumulate As in different organs; phytoplankton are	As can cause cancer in humans from the consumption of elevated levels of As via drinking water and food or exposure to air, soil or water. IARC group 1 (Anzecc & Armcanz, 2000; Coelho et al., 2011; Kibria et al., 2010).	Reported in abandoned lead–zinc and barite mining communities of Abakaliki, Southeast Nigeria, as well Abandoned tin mines in Jos, plateau (Bwede et al., 2021; Chukwu & Obiora, 2023; Gospel et al., 2020; Necula et al., 2021; Obasi & Akudinobi, 2020; Obiora et al., 2016, 2019; Ozobialu et al., 2020; Waida et al., 2022).

Toxic metals	Environmental sources	Environmental/Ecological effects	Human Effects*	Occurrences of metals in abandoned mines in Nigeria.
	Vietnam, China, and Taiwan (Kabata-Pendias, 2010; Smedley & Kinniburgh, 2002).	among the most sensitive organisms to arsenic (Coelho et al., 2011; Kibria et al., 2010).		
Cadmium (Cd)	Parental rock material, phosphate fertilizers, farmyard manures, sewage sludge, mine tailings, batteries, industrial processes (electroplating, non-ferrous metal, iron and steel production), burning of fossil fuel and waste combustion, minor component in most zinc ores (by product of Zn), coal contain significant amounts of cadmium (flue dust), discharge from refineries, lead and zinc smelting, pigments for plastics and paint residues,	Acidified soils enhance cadmium uptake by plants, which may cause a threat to animals which feed on them and to the rest of the food chain. Earthworms and other essential soil organisms are extremely susceptible to cadmium poisoning. Cadmium may bioaccumulate in freshwater aquatic organisms (mussels, oysters, shrimps, lobsters, and fish) and is highly toxic to plants and animals. Cd toxicity can damage the nervous and reproductive systems and can	Human uptake of cadmium can occur through food ingestion (liver, mushrooms, shellfish, mussels, cocoa powder, dried seaweed), inhalation of fine dust and fumes; people can be exposed from highly soluble cadmium compounds, tobacco smoke, living near the hazardous waste sites or factories; Cd can damage the lungs, kidney, liver, and may cause reproductive failure and infertility; Cd is also carcinogenic to humans, IARC group 1; an endocrine	Reported in abandoned lead–zinc mining communities of Abakaliki, Southeast Nigeria, and an abandoned gold mine in southwest Nigeria (Bwede et al., 2021; Chukwu & Obiora, 2023; Eludoyin et al., 2017; Gospel et al., 2020; Obasi & Akudinobi, 2020; Obiora et al., 2016, 2019; Ozobialu et al., 2020; Waida et al., 2022).

Toxic metals	Environmental sources	Environmental/Ecological effects	Human Effects*	Occurrences of metals in abandoned mines in Nigeria.
	plastic stabilizers (Kabata-Pendias, 2010; Kibria et al., 2010; Marcotullio, 2007; Wikipedia, 2014a).	reduce the ability of aquatic organisms to osmoregulate. (Coelho et al., 2011; Kibria et al., 2010).	disrupting chemicals (EDCs) (Coelho et al., 2011; Kibria, 2012; Kibria et al., 2010).	
Copper (Cu)	Parental rock material, copper fungicide, algicides, copper mining (mine tailings), fertilisers, farmyard manures, sewage sludge, copper dust, drinking water pipes, antifouling paints, coal and wood combustion, iron and steel production, industrial processes, incineration ash (Kabata-Pendias, 2010; Kibria et al., 2010; Marcotullio, 2007; Wikipedia, 2014b).	Cu can accumulate in plants and animals. Cu is more toxic to freshwater fish and invertebrates than any other heavy metal except mercury. Cu can cause gill damage, reduced growth, and kidney damage in aquatic organisms (Coelho et al., 2011; Kibria et al., 2010).	Cu is essential to all living organisms as a trace dietary mineral; it is not classified as carcinogenic to humans. High uptake of copper may cause liver and kidney damage. IARC group 3 (Coelho et al., 2011; Kibria, 2012; Kibria et al., 2010).	Reported in abandoned Abakaliki lead-zinc, Enugu coal, and Jos Plateau tin and lead-zinc mines (Akpan et al., 2021; Bwede et al., 2021; Chukwu & Obiora, 2023; Eludoyin et al., 2017; Gospel et al., 2020; Obasi & Akudinobi, 2020; Obiora et al., 2016, 2019; Omotehinse & Ako, 2019; Ozobialu et al., 2020).
Lead (Pb)	Natural (parental rock material), farmyard manures; mining; sewage sludge,	High lead levels can damage the gill epithelium of fish, and affected fish may die	Lead is poisonous to animals and humans; it damages the nervous, kidney and brain	Reported in Abakaliki, Enugu, and Jos Plateau abandoned mine districts

Toxic metals	Environmental sources	Environmental/Ecological effects	Human Effects*	Occurrences of metals in abandoned mines in Nigeria.
	batteries, lead ore mine wastes, lead smelters, sewage discharge, storm water runoff, lead pipes, fossil fuel combustion (lead petrol), corrosion of household plumbing usually found in ore with zinc, silver and (most abundantly) copper, pesticides, batteries, paint pigment, steel mill residues (Kabata-Pendias, 2010; Kibria et al., 2010; Marcotullio, 2007).	from suffocation (Coelho et al., 2011; Kibria et al., 2010).	systems and can cause brain disorders; excessive lead also causes blood disorders in mammals; may decline fertility of men through sperm damage; probably carcinogenic to humans; IARC group 2A and 2B (inorganic), IARC group 3 (organic); EDCs (Coelho et al., 2011; Kibria, 2012; Kibria et al., 2010).	(Akpan et al., 2021; Bwede et al., 2021; Chukwu & Obiora, 2023; Gospel et al., 2020; Obasi & Akudinobi, 2020; Obiora et al., 2016, 2019; Omotehinse & Ako, 2019; Ozobialu et al., 2020; Waida et al., 2022).
Mercury (Hg)	Parental rock material, fertilisers, pesticides, lime, manures, sewage sludge, mercury used in gold production/gold separation may enter water bodies via mine tailings; barometers,	Mercury bio-accumulates in fish and can enter the human food chain in the form of methyl mercury, etc.; mercury compounds can damage vital tissues and organs (gills, liver, kidney,	Hg exposure can occur via inhalation of mercury vapour or ingestion of mercury-contaminated seafood. Mercury poisoning in humans causes incurable severe retardation of brain functions,	Reported in Abakaliki lead/zinc mine (Obasi & Akudinobi, 2020)

Toxic metals	Environmental sources	Environmental/Ecological effects	Human Effects*	Occurrences of metals in abandoned mines in Nigeria.
	thermometers and fluorescent light bulbs, coal combustion, metallurgy. Mercury occurs in deposits throughout the world mostly as cinnabar (mercuric sulphide) (Kabata-Pendias, 2010; Wikipedia, 2014c).	brain and skin) of fish and may reduce reproductive success (Kibria et al., 2010).	disruption of the nervous system, DNA, chromosomal, sperm damage, birth defects and miscarriages, possibly carcinogenic to humans; IARC group 3, biomagnify up the food chain, EDCs (Coelho et al., 2011; Kibria, 2012; Kibria et al., 2010; Wikipedia, 2014c)	
Nickel (Ni)	Parent rock material, fertilisers, fuel and residual oil combustion, alloy manufacture, nickel mining and smelting, sewage sludge, incineration and incineration ash, electroplating, batteries (Kabata-Pendias, 2010; Marcotullio, 2007).	Released into the air by power plants and trash incinerators, most nickel released is adsorbed by sediment or soil particles, in acid soils, it becomes more mobile and often runs off to groundwater, high concentrations of Ni on sandy soils can severely damage plants, can reduce the growth	Humans can be exposed by breathing contaminated air, drinking contaminated water, eating contaminated food, or smoking cigarettes or dermal exposure via contaminated soils and waters or eating chocolate and fats, Ni is an essential element in small amounts but too high uptake can cause lung, nose, larynx,	Reported in Abakaliki lead-zinc, Enugu coal, and Jos-Plateau tin and lead-zinc AMLs (Akpan et al., 2021; Bwede et al., 2021; Chukwu & Obiora, 2023; Gospel et al., 2020; Obasi & Akudinobi, 2020; Obiora et al., 2016, 2019; Omotehinse & Ako, 2019; Ozobialu et al., 2020; Waida et al., 2022)

Toxic metals	Environmental sources	Environmental/Ecological effects	Human Effects*	Occurrences of metals in abandoned mines in Nigeria.
		rates of algae in waterways, though Ni is an essential element for animals at low concentrations but extremely harmful when the maximum tolerable amount is exceeded (can cause different kinds of cancer, in those organisms living near refineries) (Coelho et al., 2011)	and prostate cancer, lung embolism, respiratory failure, birth defects, asthma and chronic bronchitis, and heart disorders, Ni exposure through breathing can cause pneumonitis; IARC group 1 (Coelho et al., 2011)	
Uranium (U) Persistent for many years (half-life): U-238: 47 billion years; U-235: 704 million years.	Found naturally (U-238: 99.28%, U-235: 0.72%, U-234:.006%) in very small amounts in all rock, soil, and water, erosion of tailing from mines and mills could be main source in the environment, exist as dust that falls into surface water, plants and soils through rainfall, uranium compounds	Plants absorb uranium through their roots; therefore, root vegetables may contain higher amounts of this element, but washing can remove uranium (Lottermoser, 2010).	People can be exposed to uranium (or radioactive daughters such as radon) by inhaling dust in air or by ingesting contaminated water and food, and working in the phosphate fertilizers industry and living or working near a coal-fired power plant; uranium can affect the kidney, brain, liver, heart, and	Not reported

Toxic metals	Environmental sources	Environmental/Ecological effects	Human Effects*	Occurrences of metals in abandoned mines in Nigeria.
	in soil combine with other compounds and persist in soil for many years (Kabata-Pendias, 2010; Lottermoser, 2010; Wikipedia, 2014d). .		other systems; radon gas can cause lung cancer and deaths from inhalation; IARC group 1 (Radon 222) (Coelho et al., 2011; Kibria, 2011).	
Zinc (Zn)	Parental rock, fertilisers, pesticides, coal and fossil fuel combustion, non-ferrous metal smelting, galvanised iron and steel, alloys, brass, rubber manufacture, oil tyres, sewage sludge, batteries, brass, rubber production, mine tailings, urban run-off, waste incineration (Kabata-Pendias, 2010; Kibria et al., 2010; Marcotullio, 2007)	Zinc has significant implications for both terrestrial and marine ecosystems. Research highlights both direct and indirect toxicological effects on various organisms, ranging from intestinal microbiota in piglets to phytoplankton in marine environments. Zn can cause gill damage, reduced growth and kidney damage in fish. At high concentrations, it disrupts the intestinal	Zinc is an essential mineral for humans, but excessive intake can cause health problems such as stomach cramps, skin irritations, pancreatic damage, and respiratory disorders (Kibria et al., 2010).	Reported in Abakaliki, Enugu, and Jos Plateau abandoned mining districts (Akpan et al., 2021; Bwede et al., 2021; Chukwu & Obiora, 2023; Ezeigbo & Ezeanyim, 1993; Gospel et al., 2020; Obasi & Akudinobi, 2020; Obiora et al., 2016, 2019; Ogbonna et al., 2015; Omotehinse & Ako, 2019; Ozobialu et al., 2020; Ozoko, 2015; Waida et al., 2022)

Toxic metals	Environmental sources	Environmental/Ecological effects	Human Effects*	Occurrences of metals in abandoned mines in Nigeria.
		microbiota in weaned piglets, showing lasting effects on specific bacterial populations and metabolic activities (Kibria et al., 2010; Ma et al., 2009; Starke et al., 2014).		
*Cerium (Ce)	A rare earth element, mined primarily from Bastnäsite and Monazite ores, alongside other rare earth elements (REEs). Cerium is one of the rare chemicals found in household equipment such as colour televisions, fluorescent lamps, energy-saving lamps, and glasses. All rare chemicals have comparable properties. Gets to the environment through petrol-producing industries and disposed household	Cerium will gradually accumulate in soils and water sediments, which eventually lead to increasing concentrations in soil particles, humans, and animals. In aquatic organisms, it damages cell membranes, which has several negative effects on reproduction and nervous system functions (Abdelnour et al., 2019; He et al., 2021; Rawlins et al., 1998; Su et al., 2021).	Cerium is mostly dangerous in the work environment because damp dust and gases can be inhaled with the air. This can cause lung embolisms, especially during long-term exposure. Cerium can be a threat to the liver when it accumulates in the human body. Cerium has no known biological role, but cerium salts have been reported to stimulate metabolism (Abdelnour et al., 2019; He et	Not reported

Toxic metals	Environmental sources	Environmental/Ecological effects	Human Effects*	Occurrences of metals in abandoned mines in Nigeria.
	equipment (Abdelnour et al., 2019; Kabata-Pendias, 2010; Lenntech, 2025; MMTA, 2016).		al., 2021; Rawlins et al., 1998; Su et al., 2021).	
*Zirconium (Zr) Zirconium is generally considered low in toxicity in its bulk or mineral form; however, toxicity arises from its soluble compounds and nanoparticulate forms. The most toxic forms are zirconium nanoparticles (Zr-NPs) and certain salts (e.g., zirconium chloride, zirconium nitrate), while natural zircon and metallic zirconium are largely inert (Health	Zirconium is primarily extracted from zircon mineral, often found in the sands of coastal waters. Anthropogenic activities such as industrial use and nuclear reactors are increasing atmospheric Zr emissions (Kabata-Pendias, 2010; Shahid et al., 2013; Shirani et al., 2023; USGS, 2017; Vlasov, 2023).	Zirconium, due to its various uses, has contributed to soil and water pollution. While its effects are generally minimal, at certain concentrations or geochemical conditions, it can cause phytotoxicity by affecting plant chlorophyll and enzyme activity and may trigger antioxidant responses. It slightly alters soil chemistry, potentially affecting microbial communities and nutrient cycling. Zirconium is mainly absorbed by plant roots and accumulates there, with	ZrO_2-NPs are likely to have negative impacts on various organs and exhibit potential disease risks. Intravenous administration of ZrO_2-NPs can lead to oxidative stress and histopathological changes in organs such as the spleen, kidney, heart, brain, and lungs (T. Sun et al., 2019). Overall, Zr is considered toxic and disrupts various tissues and cells when exposure is prolonged (Shirin et al., 2022). Cases of pulmonary fibrosis and pneumoconiosis have been	Not reported

Toxic metals	Environmental sources	Environmental/Ecological effects	Human Effects*	Occurrences of metals in abandoned mines in Nigeria.
Council of the Netherlands, 2002; Y. Yang et al., 2019).		limited movement to above-ground parts, reducing its risk of entering the food chain (Montes et al., 2021; Shahid et al., 2013).	reported among workers exposed to zirconium dust, although establishing a direct causal relationship remains challenging due to concurrent exposures to other substances (Atik et al., 2022).	

* International Agency for Research on Cancer (IARC): group 1= carcinogenic to humans; IARC group 2A = probably carcinogenic to humans; IARC group 2B = possibly carcinogenic to humans; IARC group 3= Not classifiable as to its carcinogenicity to humans; IARC group 4= probably not carcinogenic to humans. * (Anzecc & Armcanz, 2000)

Table 2:2 Organic contaminants associated with mining and other environments; sources, environmental and human health effects

Toxic Organic Compounds	Environmental sources	Environmental/Ecological effects	Human Effects*	Occurrence in abandoned Coal mines in Nigeria.
Polycyclic Aromatic Hydrocarbons (PAH)	Natural sources like forest fires, volcanic eruptions and through anthropogenic activities like incomplete combustion of fossil fuels, wood, and waste incineration, oil refining, coke and asphalt production,	Adverse effects on aquatic and terrestrial ecosystems. Impacts plant growth and soil microbial community dynamics. Bioaccumulate in food webs, disrupt reproduction in fish	Carcinogenic and mutagenic, benzo[a]pyrene is known to have the highest cancer risk among the 16 PAHs, respiratory issues, and immune suppression (Bukowska et al., 2022; K. H. Kim et al., 2013).	PAHs from runoff originating from automotive workshops and abandoned coal mines are suspected contributors to contamination in parts of the Onyeama abandoned coal mine drainage, which is

Toxic Organic Compounds	Environmental sources	Environmental/Ecological effects	Human Effects*	Occurrence in abandoned Coal mines in Nigeria.
	and aluminium production. Tobacco smoking, charbroiling of food, heavy traffic and industrial zones. They are abundant in air, water, soil, and sediment (Srogi, 2007; Venkatraman et al., 2024).	(Montuori et al., 2022; Odinga et al., 2021)		thought to be responsible for benzo[a]pyrene concentrations reaching up to 1.266 mg/kg in some areas of the Ekulu River, as reported (Ugochukwu et al., 2021). In 2023, Umeh conducted a similar study and found PAHs and heavy metals in surface waters, particularly in the Ekulu River, which drains the Onyeama abandoned coal mine (Umeh et al., 2023).
Petroleum Hydrocarbons (TPH, diesel, oils)	Originally from crude oil, through oil seeps or diffusion during drilling and transportation processes. Accidental spills and leaks, industrial emissions from industries that use petroleum	Contamination of soil, sediment, and groundwater causes stress for benthic macroinvertebrates, shellfish, and bottom-feeding fish, smothers aquatic life, reduces	Respiratory distress, skin disorders, and neurotoxicity. Acute effects from immediate exposure include headaches, dizziness, and nausea, while chronic effects of exposure include	Not Reported

Toxic Organic Compounds	Environmental sources	Environmental/Ecological effects	Human Effects*	Occurrence in abandoned Coal mines in Nigeria.
	products in various processes and waste discharge. General fuel storage in fuelling stations and mining sites. These reach water sources through various pathways (ATSDR, 1999; Sahoo et al., 2024).	microbial activity in soils, and causes problems for plant roots (ATSDR, 1999; Khan et al., 2018; LSRCA, 2025).	carcinogenic, developmental, and endocrine toxicities in humans and other species (ATSDR, 1999; Sahoo et al., 2024).	
Volatile Organic Compounds (VOCs) (e.g., BTEX, Styrene)	Originates from the exploitation and use of fossil fuels; that is, the incomplete combustion and evaporation release them into the environment. They are found in closed and open spaces, including industrial processes, transportation, consumer products (paints, cleaners, adhesives, aerosol sprays), stored fuel & automobile products,	VOCs contribute to the formation of ground-level ozone, a major component of smog, and can negatively impact air quality (David & Niculescu, 2021); cause water pollution, negatively affecting aquatic life and compromising the overall health of ecosystems (Wietse Bandstra, 2024); and damage plant tissues	Most VOCs are known to be carcinogenic, teratogenic, mutagenic, genetic toxicant and neurotoxicant. VOCs exposure leads to short-term (eyes, nose, and throat irritation, headaches, loss of coordination and nausea) and long-term effects, increases the risk of respiratory diseases, neurological disorders, birth defects, leukaemia, and	Not reported

Toxic Organic Compounds	Environmental sources	Environmental/Ecological effects	Human Effects*	Occurrence in abandoned Coal mines in Nigeria.
	pesticides, use of biofuels, forest fires, incineration and natural sources like vegetation. They are abundant in the air (David & Niculescu, 2021; Lim et al., 2014; Medunić et al., 2018; Polzin et al., 2007; US EPA, 2024b).	and affect growth (Lim et al., 2014; PDH, 2023).	endothelial injury (ATSDR, 2024; Lim et al., 2014; Riggs et al., 2021; US EPA, 2024b; K. Zhang et al., 2021).	
Polychlorinated Biphenyls (PCBs)	PCBs were man-made organic chemicals known as chlorinated hydrocarbons that were domestically manufactured from 1929 until manufacturing was banned in 1979 (US EPA, 2024a). They were widely used as industrial chemicals due to their advantageous properties until their harmful effects were recognised.	PCBs are highly persistent in the environment, leading to long-term contamination of soil, water, and air. They bioaccumulate in the food chain, affecting various trophic levels, including plants, microorganisms, birds, and mammals (Beyer & Biziuk, 2009). Disrupts ecological balance, leading to ecosystem damage and	PCBs are carcinogenic, developmental, and neurotoxic. They are recognised by the International Agency for Research on Cancer (IARC) as Group 1 carcinogens or cancer-causing substances (ATSDR, 2000; Breivik et al., 2002). There is a significant non-carcinogenic risk, particularly for	Not reported

Toxic Organic Compounds	Environmental sources	Environmental/Ecological effects	Human Effects*	Occurrence in abandoned Coal mines in Nigeria.
	Mining equipment (older transformers, capacitors), industrial discharges, and mine water effluents (ATSDR, 2000; Breivik et al., 2002).	affecting biodiversity, toxic to fish and birds and cause neurological damage (Melymuk et al., 2022).	vulnerable populations like children (Martínez-López et al., 2021)	
Explosives Residues (e.g TNT-(2,4,6-trinitrotoluene) and RDX (hexahydro-1,3,5-trinitro-1,3,5-triazine)	They primarily originate from military, industrial, and mining activities. Manufacturing of ammunition, live-fire and training exercises, and unexploded ordnance leave behind contamination in soil and water. Explosives used for blasting in mineral extraction and improper waste disposal make them environmentally available. TNT and RDX are highly persistent, with slow	Slow degradation rates make them persist in soil and groundwater, where they contaminate and migrate into groundwater, affecting drinking water supplies and aquatic ecosystems. They bioaccumulate in plants and microorganisms, disrupting food chains. toxic to fish and invertebrates, causing developmental and reproductive issues. alter microbial communities in soil, affecting nutrient	Classified as possible human carcinogens, linked to liver and bladder cancer; neurotoxicity; exposure can lead to headaches, dizziness, and cognitive impairments; interfere with hormone regulation, causing thyroid and endocrine disruption. Respiratory and skin effects through inhalation and skin contact (Hoek, 2008; Juhasz & Naidu, 2007; Pennington & Brannon, 2002).	Reported

Toxic Organic Compounds	Environmental sources	Environmental/Ecological effects	Human Effects*	Occurrence in abandoned Coal mines in Nigeria.
	degradation rates, leading to long-term contamination. They dissolve and migrate into groundwater, affecting drinking water supplies and aquatic ecosystems. Blasting and demolition in open-pit and underground mining (Ariyarathna et al., 2016; Beyer & Biziuk, 2009; Juhasz & Naidu, 2007).	cycling and ecosystem stability (Hoek, 2008; Juhasz & Naidu, 2007; Pennington & Brannon, 2002).		

2.6 Abandoned Mines in Africa

Africa hosts 30% of global mineral resources. The mining sector represents an area of critical environmental governance, and mineral development forms the basis of national resource policies and regional development plans, which include the Africa Mining Vision (Dales & Ramasamy, 2019).

Several countries in Africa engage in coal mining, with South Africa leading and generating significant revenue for the continent, followed by Zimbabwe, Botswana, Mozambique, and more than 10 other countries in sub-Saharan Africa (Ericsson, 1991). Over 6,000 abandoned coal and mineral mines have been identified in South Africa, and the situation is similar in other countries (Edwards et al., 2014; Festin et al., 2019; Mhlongo & Amponsah-Dacosta, 2016; Olalde, 2017). Coal mining in Nigeria was an important part of the economy during its operation, and coal production peaked between 1958 and 1959 (Nwaobi, 2005). However, its mechanisation failed after the Second World War in 1972, alongside technical issues, declining demand, etc., which led to the abandonment of the coal mines (Aroh, 2021; Ezemokwe & Madubuike, 2015; Omotehinse & Ako, 2019; Sikakwe et al., 2015).

Mineral resources such as copper, diamonds, gold, and tin provide great revenues for low- and middle-income countries (LMICs) and serve to alleviate poverty (Kibria, 2014). Many key mineral commodities, such as gold, bauxite, iron ore, copper, cobalt, and diamonds, have been produced across the continent for centuries and remain attractive to foreign investors due to the continent's vast mineral reserves. However, these activities have left a legacy on the environment across the continent, partly due to artisanal and small-scale mining (ASM).

ASM has served as a means of livelihood and economic opportunity for local communities and has also contributed to the gross domestic product (GDP) of many of these African countries (Worlanyo & Jiangfeng, 2021). Active mining is ongoing amid numerous abandoned mines, and the majority of AMLs in Africa are attributable to ASM and medium-scale mining (MSM). This is because ASM is a defining characteristic of the rural economy and provides more employment opportunities than the large-scale mining sector (Dales & Ramasamy, 2019). The lack of funds, skills, and incentives is a major reason ASM miners fail to meet regulatory requirements for mine rehabilitation. United Nations Educational, Scientific and Cultural Organisation (UNESCO) mapped abandoned mines between 2013 and 2018 and found that environmental legacies of abandoned mines were widespread in sub-Saharan Africa and pose a serious threat to human and ecosystem health, especially in areas where heavy metals and hazardous chemicals are prevalent (Basu et al., 2015; Dales & Ramasamy, 2019).

The findings also highlighted that 'pollution hazards from gold mines, especially mercury and hazardous chemical compounds, are local problems capable of causing regional impacts' (Dales & Ramasamy, 2019). Hence, the need for this study.

2.7 The Realities of AMLs in Nigeria

To address the realities of AMLs in Nigeria, this section reviews the country's mining history, legal framework, and current mining practices, with particular attention to the legislation that has shaped the present state of AMLs.

Nigeria is among the countries in sub-Saharan Africa where mining was a source of exports before the oil boom of the 1970s (Ericsson, 1991). Nigeria is endowed with abundant mineral resources, which have contributed to gross national income and socio-economic growth. Industrial and commercial mining in Nigeria dates back to 1905 and continued through the 1970s, with major production of coal, tin, and columbites in the 1940s. Tin and Columbite were mined intensively in the Jos Plateau region, leaving a devastating legacy in terms of impacts on human lives and the environment (Calvert, 1977).

The solid minerals in Nigeria made up some of the known largest deposits of precious metals and stones, as well as industrial minerals such as gold, sapphire, marble, tin and others (Merem et al., 2017). Nigeria is endowed with over 40 solid minerals identified in almost 450 locations in the country (Olade, 2019). Some of the metallic and industrial minerals include gold, iron ore, cassiterite, columbite, wolframite, pyrochlore, monazite, marble, coal, limestone, clays, barites, lead-zinc, and many others occur in the different metallogenic provinces of Nigeria (Figure 2.5), The government has classified seven of these minerals as strategic minerals namely bitumen, gold, coal, iron ore, limestone, lead/zinc ores, and barites. Other minerals with good economic prospects include tin, tantalite, niobium, gypsum, gemstones, kaolin, etc. (Lar, 2018). The deposits currently being exploited are Cassiterite (tin), Columbite, Tantalite, Wolframite, Lead/zinc, Gold, Silver, Coal, Barytes, Gypsum, laterite, and others (Figure 2.6). These were exploited on a large scale in the early 19th century, thus contributing to the nation's wealth (Aigbedion & Iyayi, 2007). Solid minerals represented 100% of Nigeria's total mineral exports between 1950 and 1958. It fell to 50% in 1959, and by 1969, petroleum had overtaken it, accounting for 90% of total mineral exports. The ratio of solid minerals to total export has continued to decline geometrically since then.

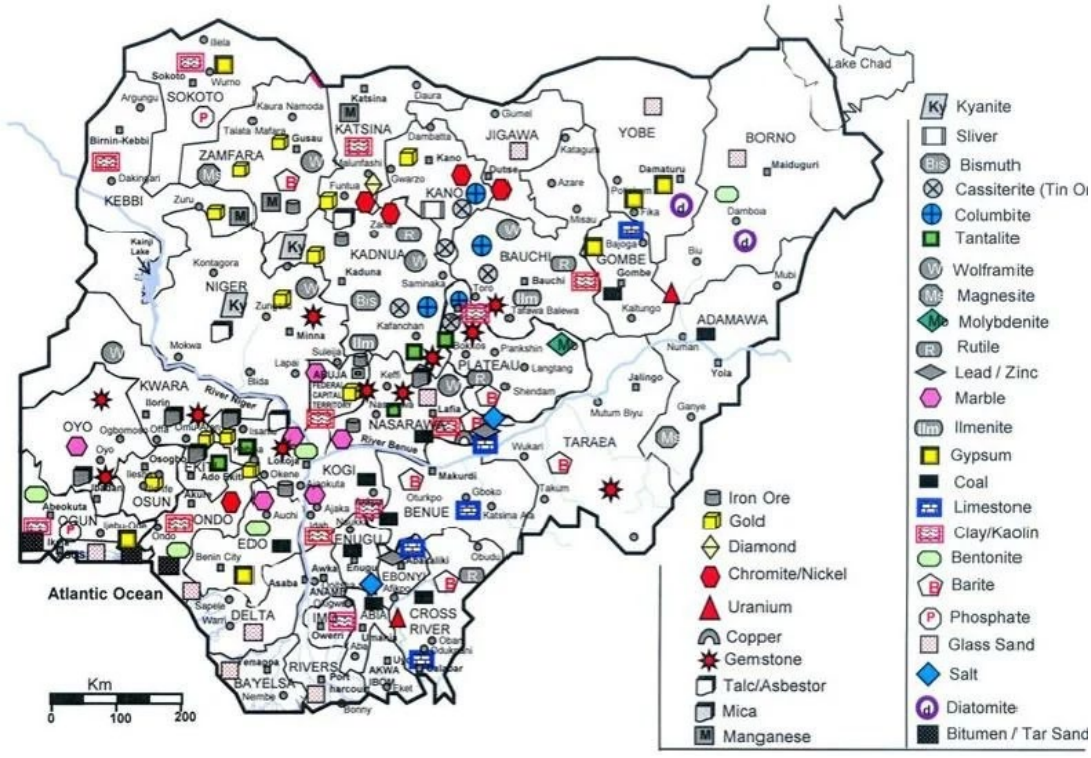

Figure 2.5: Mineral Resources Map of Nigeria (Nigeria Vision 2020, 2009)

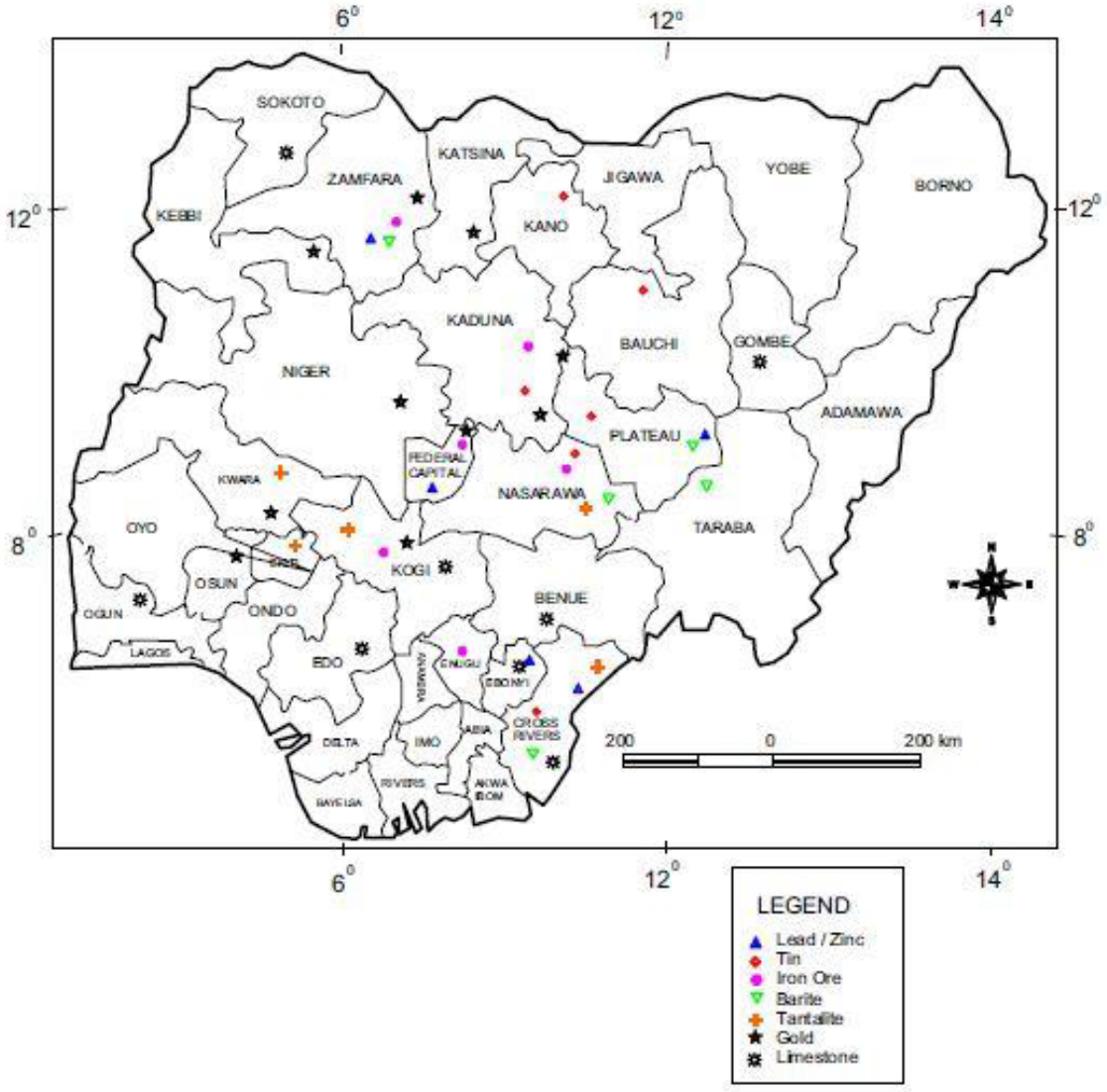

Figure 2.6: Map of Nigeria showing the locations of active mining sites for various mineral commodities (Lar et al., 2015)

The need to diversify Nigeria's economy has been widely discussed over the past decade (KPMG, 2017), given its overreliance on the oil sector as a major source of income. The essence of the diversification is to create an enabling, competitive, and strategic environment for development. To this end, one major focus is to build the solid mineral sector, which contributed only 1% of GDP in 2015 (NBS, 2015). To demonstrate government commitment to this aim, the Ministry of Mines and Steel Development issued a revised sector growth and development roadmap (KPMG, 2017) with the key objectives of addressing challenges, outlining strategies for the development and utilisation of key minerals and metals, and targeting a contribution of about 10% to Nigeria's GDP by 2026. To further strengthen this, a ₦30 billion intervention fund was launched by the Federal Government to open up the sector to multinational companies (KPMG, 2017). Thus, the current drive for issuing mining licences in the country.

How the impending effects of these exploitations will be managed effectively and efficiently remains unanswered, as there is no way to extract minerals without distorting the natural equilibrium of the geologic system. Over 1500 mine sites have been identified as abandoned (MECD, 2022) with no substantial remediation implementation plans in place to address the legacy of these mines. Yet the number of licences being issued is increasing. If this is the case, how can the current licence drive be harnessed to increase economic growth while addressing post-mining challenges and protecting the surrounding environments for communities living within and around the affected areas?

2.7.1 Mining in Pre-colonial Period

Nigeria is blessed with large deposits of various minerals, and precolonial Nigerian communities were aware of their occurrences and measurably exploited tin, gold, and iron.

Mining in Nigeria dates back over 2,400 years. It initially took the form of artisanal mining practised by communities seeking natural resources for social and economic benefits within their environment. This is clearly seen in the Nok Culture (340 BC) and the Igbo Ukwu Bronze civilisation (705 AD). Ife and Benin Bronze work flourished respectively between 1163-1200 AD and 1630-1648 AD, using basic clays, base metals, and gold, among others. Hence, mining existed long before colonial rule (NBS, 2015).

Mineral extraction was carried out locally by Nigerian communities to meet their immediate needs. Gold was mined and processed for ornamental uses, iron and tin were extracted and smelted to make weapons of war, farming implements and household equipment (NEITI, 2011).

Mining was carried out crudely and organised into household units, known as *gida* in Hausa and *ebi* in Yoruba. Mineral production was generally localised, or at best regionalised. For example, tin straw produced in the Plateau region remained essentially within this region, while iron ore remained in the Yoruba axis. Wages were paid to labourers in kind, and miners formed a guild association to protect members and regulate standards and methods of production and output; they equally regulated prices and rules for admitting new members. This guild system was famously practised among smiths, ironworkers, carvers, etc., in the Tiv, Hausa, Yoruba, Benin, and Nupe peoples. There was exclusive reliance on the minerals locally available; there was no attempt to learn about the mining and processing of other minerals not available in the locality (Calvert, 1977; Ekundare, 1973; NEITI, 2011).

2.7.2 Mining in Colonial Period

During the colonial period in Nigeria, greater attention was paid to agriculture, though the government also exploited a few minerals. Organised mining began in 1903, following the commissioning of the mineral survey of the Southern and Northern protectorates. Actual mining activities began in 1905 when the Royal Niger Company (RNC) started operations on the Jos Plateau region, while coal exploration and mining commenced in Enugu in 1906 (NBS, 2015; NEITI, 2011).

Among the mineral deposits of Nigeria, tin was the first to receive any commercial interest. According to historical records, William Wallace discovered in 1885 that tin mining was being carried out by the people of Bauchi. The development of the tin mining industry was slow and took several years. A stable government had not been assured, and foreign investors interested in tin exploitation were worried about the risk of losing their capital in a new industry. There was no commercial production of tin throughout the 19th century (Bridge & Fredriksen, 2012; Ekundare, 1973).

At the close of the 19th century, tin was bought from the local communities in Plateau and the northern region and traded by the Royal Niger Company (RNC). This was driven by global demand for tin. To encourage production, the conditions needed to change. This led to the mechanisation of tin mining in the early 20th century, and Nigeria stood among the major producers (Ekundare, 1973).

Coal was discovered in 1909 at Udi, close to Enugu. During the same period, companies were exploiting tin in the northern part of the country. Coal exploitation began in 1915, while exports began in the 1930s. It was used as a source of energy and also served as a raw material for the manufacture of tar and synthetic fertiliser. The Nigerian Railway system was dependent on coal production to run the train engines and consequently controlled production. The poor coking quality of the coal probably explains the late exportation of the product, as it was not able to compete with industrial coal from other regions of the world. During the colonial period, Nigeria was the only coal-producing country among the West African nations. She became the major source of coal on the West African coastline, and the nations that could not export from other parts of the world because of the Second World War (Ekundare, 1973; NBS, 2015; NEITI, 2011).

The introduction of diesel engines to railway operations led to a decline in coal demand, which rendered the operation uneconomical. It is important to note that the Obwetti, Iva and Onyeama coal mines were fully operational in Enugu before the decline in production.

Columbite, a by-product of tin, was also exploited. It was sourced during the Second World War for manufacturing gas turbines and jet engines, and for welding chromium nickel and steel. High demand encouraged in-depth exploitation, and 85% of the total world supply of Columbite then came from Nigeria, with support from the United States Defence Materials Procurement Agency in 1953 (Ekundare, 1973; Freeman et al., 1953). The decline in its mining came from a reduction in US use in manufacturing spacecraft engines, which was the largest consumer of the product.

Mining operations of the Jos tin and cassiterite during the colonial period were mainly medium- to large-scale open pit and hydraulic placers (Bridge & Fredriksen, 2012), while coal mining in Enugu was underground surface mining. Lead-zinc-barite veins were mined on a small scale by open-cast mining.

This account explains why most legacy mines in Nigeria are located in areas where tin, coal, and columbite were heavily mined during the colonial and early post-colonial eras. The environmental

implications of these activities were not well researched at the time, and strong environmental laws were not in place to enforce best mining practices. Most mining activities took place with the mindset of generating revenue, income, and competing with other nations.

Illegal mining activities were among the motivations for the establishment of the legal framework. They aimed to curtail and monitor their activities as well as implement best mining practices and generate revenue for the government.

2.7.3 The Legal Framework of Mining and Post-Mining in Nigeria

Mining regulation known as the Mineral Act was established in 1946. It represented the government's policy and national aspiration, promulgated to allow the colonial government to mine its mineral resources unfettered and undistracted by co-colonialists. Nonetheless, the Mineral Ordinance established in 1902 was the enabling legal instrument for mining prior to the Mineral Act of 1946. The Coal Ordinance in 1950, the Explosives Act in 1964 and the Explosives Regulations in 1967 were all established to provide the legal framework for solid mineral development in Nigeria (Ekundare, 1973; Freeman et al., 1953).

In 1919, the Geological Survey of Nigeria (GNS) was established during the administration of Dr J.D. Falconer in the colonial era to complete the minerals survey initiated in 1903 to evaluate the mineral potentials of the nation (NGSA, 2017). Mining activities were dominated by the private sector because the colonial government gave rights of mineral exploitation to foreign companies with expatriates who operated and lived close to the Jos Plateau tin fields (Alao & Ibrahim, 2014; Ekundare, 1973). In 1950, the government established the Nigeria Coal Corporation (NCC) to manage coal exploration and extraction while the Nigerian Mining Corporation (NMC) was set up under Decree no 39, Gazette No. 59 in 1972, to explore, acquire, and process for different kinds of minerals occurring in the nation with the exception of petroleum and coal, as well as to import ores, products, and by-products of minerals not available in Nigeria. The National Iron Ore Mining Company (NIOMCO) Itakpe was established in 1979 to produce Iron for the Ajaokuta and Aladja Steel plants in Nigeria. At present, the government have scrapped the NCC and NMC with the privatisation of most of its subsidiary companies, while the NIOMCO is currently not producing, and its fate is to be determined by the government (NEITI, 2011; Nwaobi, 2005; Punch, 2022).

Nigeria was once the largest exporter of columbite and the eighth-largest producer of tin in the world. Mineral mining, especially Tin production, was mainly carried out by the private sector before the establishment of the NMC in 1972. Notwithstanding, the government was responsible for the provision of infrastructure in mine fields and for the collection of royalties, rents, and other payments from mine operators. Many foreign companies' owners left the mining sector in the early 70s because of the nationalisation policy, leading to a sharp decline in solid mineral production. The discovery of

petroleum in 1958 and the global energy crisis of 1973 also contributed to the shifting of the government's attention from solid mineral production to the petroleum sector (NEITI, 2011).

Currently, the legal framework for the development of the solid minerals in Nigeria is the Nigerian Minerals and Mining Act 2007, which replaced the Minerals and Mining Act, No 34 of 1999, and the Mining Act of 1946. The Act was established with the aim of regulating all aspects of exploration and exploitation of the nation's solid minerals and other related purposes. The Nigerian Minerals and Mining Regulations of 2011 were established to guide the interpretation and implementation of the Mining Act of 2007. The Act, aside from vesting the ownership of all mineral resources to the Federal Government, also makes provision for licensing rights to explore and produce minerals, mining incentives to license holders, as well as their obligations and duties.

The Ministry of Solid Minerals Development (MSMD), was created in 1985 to focus on research and exploration of the solid minerals and encourage the rapid and beneficial development of the nation's solid mineral resources through the formulation of policy, regulation of mining operations and generation revenue for government as well as providing information on mining potential and production subject to the Mining Act of 2007 and the mineral and mining regulation of 2011.
The government has increased attention and development to the solid mineral sector through the creation of the Nigerian Minerals and Mining Act 2007, National Minerals and Metals Policy 2008 and the Nigerian Minerals and Mining Regulation of 2011, which regulates mineral exploration and exploitation in a transparent format and, importantly, the decision to extend the Extractive Industries Transparency Initiative (EITI) principles to the solid mineral sector. These initiatives were also devised to attract and encourage foreign investors to the solid mineral sector. Since then, there has been an increase in productive activities in the sector.

2.7.3.1 Organisational Structure of The Ministry of Solid Minerals Development (MSMD)

A brief overview of some of the arms and functions of the MSMD as directly related to the subject under discussion is presented here, and the structure of the ministry is shown in Figure 2.7.
The Minister, subject to the provisions of the 2007 Mining Act, performs the administrative duties set out in the Act to ensure the orderly and sustainable development of Nigeria's mineral resources.
The Ministry is the primary source of information, policy, regulation, and oversight for Nigeria's solid mineral sector. The aim of the government in establishing the MMSD is to accelerate the development of the nation's solid mineral resources by unlocking the economic potential of the solid minerals sub-sector.
As a knowledge-based organisation, it plays an important role in providing reliable baseline geoscience data, as well as in the administration and regulation of the sector. The structure places greater emphasis

on strengthening its information and enforcement responsibilities, and also represents the market-facing department of the federal government.

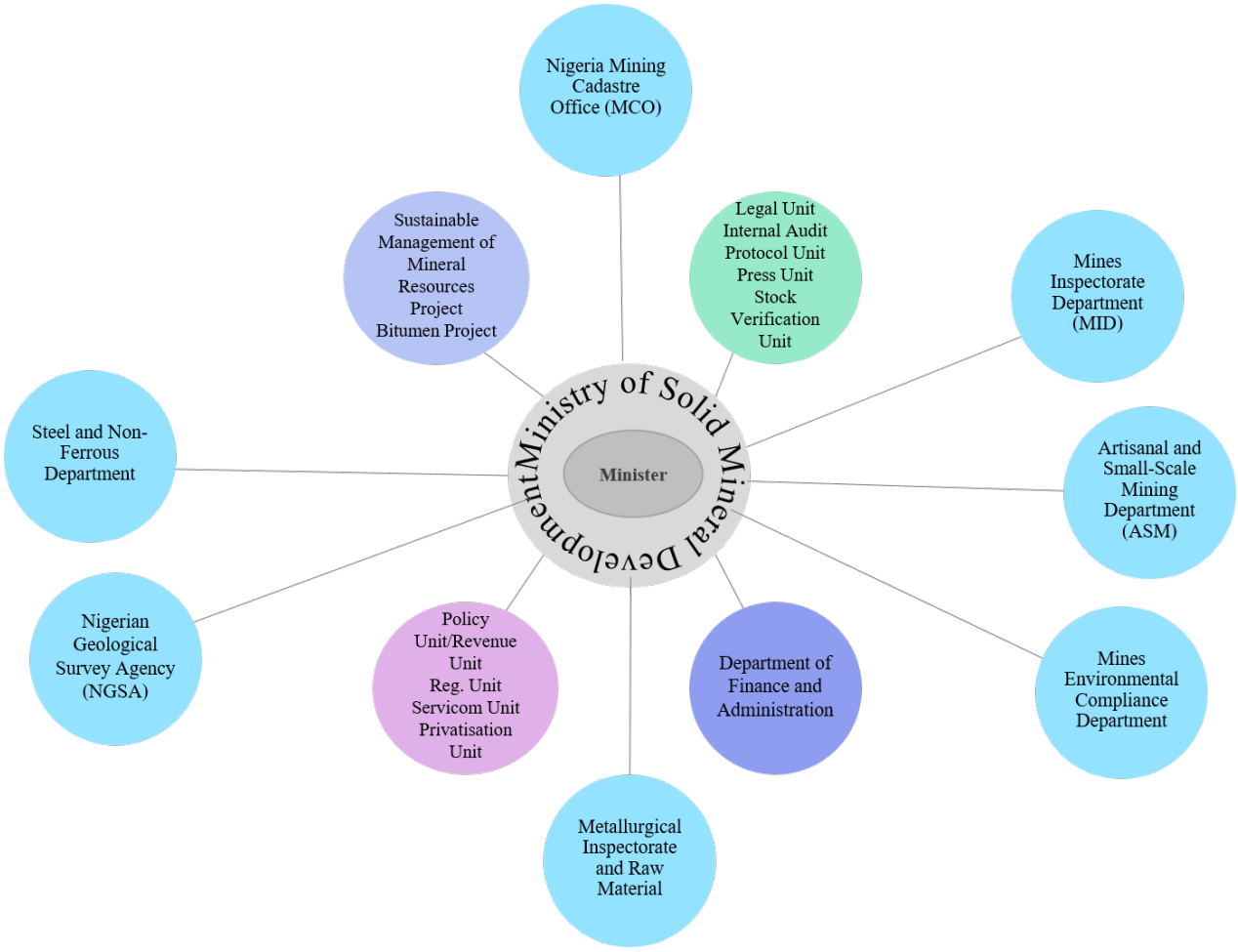

Figure 2.7: Organisation structure/chart of the Ministry of Solid Minerals Development

2.7.3.1.1 Sustainable Management of Mineral Resources Project (SMMRP)

Serves to increase the capacity of the staff in the ministry and that of the Artisanal Small-scale Mining (ASM) to carry out designated functions and mining in a sustainable way.

2.7.3.1.2 The Nigeria Geological Survey Agency (NGSA)

The NGSA is a government parastatal under the MSMD with the statutory role of conducting relevant, up-to-date geoscience research to provide information important for the development of the nation's economy and for protection against natural hazards. The NGSA operation is supported by an act of parliament established in 2006, which has since been carried out successfully, the geophysical survey of the country to evaluate its mineral resource potentials (NGSA, 2017).

2.7.3.1.3 The Nigeria Mining Cadastre Office (MCO)

The MCO administers and manages all mineral titles in Nigeria transparently, in accordance with the statutory guidelines detailed in the Minerals and Mining Act, 2007, and the Minerals and Mining Regulation, 2011. The Reconnaissance Permit, Exploration Licence, Small Scale mining lease, Mining Lease, Quarry Lease, and Water Use Permit are titles conferred by the MCO. Figure 2.8 details the valid mineral titles of Nigeria.

Figure 2.8: Map of valid mineral titles of Nigeria, December 2021 (source: Nigeria Mining Cadastre Office - Research, Development and Sustainability Unit)

2.7.3.1.4 The Mines Inspectorate Department (MID)

The MID is responsible for supervising the overall reconnaissance, exploration and exploitation activities in the solid mineral sector. The department also collects royalties and operational fees on behalf of the government. Records of functional and active mines (Figure 2.6) are established from approved, valid mineral titles during field inspections. Inactive mines and abandoned mines are reported to the minister. The database system set up for this purpose has not been very effective, as most activity records are carried out manually.

2.7.3.1.5 Mines Environmental and Compliance Department (MEC)

The MEC, among other functions, monitors and enforces compliance by holders of mineral titles with all environmental requirements and obligations, as required by the law and completes regular environmental audits to ensure the adoption of environmentally sound practices in all mining operations (KPMG, 2017). License holders have a duty and obligation, among other things, to submit an Environmental Impact Assessment (EIA) statement, which is approved by the federal Ministry of the Environment, prior to commencing mining operations. This is to ensure that mining is conducted sustainably and that mines are properly closed. An EIA statement is also required for environmental protection and rehabilitation programs, Reclamation of mined-out areas, etc.

2.7.3.1.6 The Artisanal and Small-Scale Mining Department (ASMD)

The department, among other duties, is responsible for organising, supporting, and assisting small-scale mining operations, as well as registering and administering ASM operators and mineral buying centres. Figure 2.9 shows that SSML (Small Scale Mining Lease) have the highest number of titles in the nation.

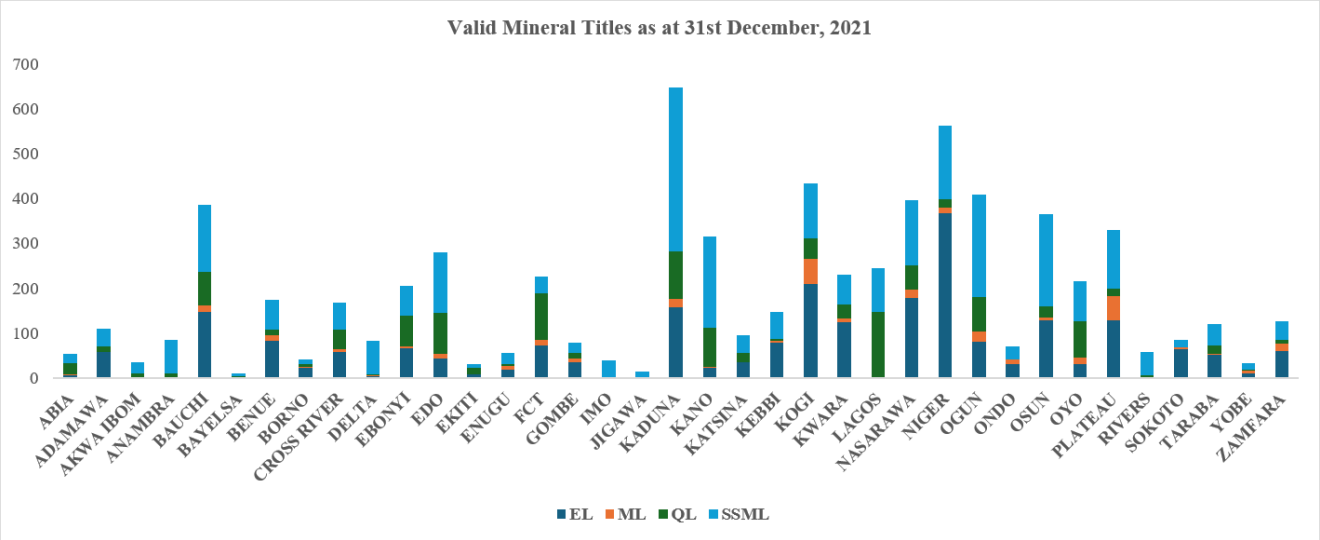

Figure 2.9: Summary of valid mineral titles of Nigeria. EL- Exploration License, ML – Mining Lease, QL - Quarry Lease, SSML - Small Scale Mining Lease (Data sourced from: Nigeria Mining Cadastre Office - Research, Development and Sustainability Unit)

The establishment of the ministry (MSMD) and government parastatals has helped stabilise the system to encourage development of the sector. The ministry's activities have been instrumental in the recent growth recorded in the sector.

The National Environmental Standards and Regulations Enforcement Agency (NESREA), along with the National Contaminated Land Management Framework under the Federal Ministry of Environment, plays a role in managing abandoned mines nationwide.

2.7.4 Current Mining and Post-Mining Practices in Nigeria

The discovery of oil in 1956 marked a turning point for Nigeria's mining sector, as national focus shifted from solid mineral extraction to petroleum exploitation. This shift led to a steady decline in formal mining operations and a subsequent rise in artisanal mining activities targeting economically valuable deposits (Edwards et al., 2014). These unregulated practices have contributed to the proliferation of newly abandoned mines, adding to the country's existing legacy mine sites.

ASMs constitute over 90% of mining activities in the nation, 75% of which are illegal. The mining sector is considered unguided, unregulated, and pressured by inadequate policies and untrained miners (Adebayo, 2015). Most of these activities occur in rural areas where those involved do not have any legal mineral titles or mining experience. More so, many carry out these hazardous and crude mining operations because local communities depend on them for their livelihoods. The lack of concern about the environmental and health implications is largely due to ignorance and a lack of awareness (Tychsen et al., 2011).

Initially, the solid mineral sector accounted for up to 50% of GDP until its decline in the 1960s. The sector accounted for less than 5% in the 70s, less than 1% in the 90s, and less than 0.5% in 2007 (Figure 2.10). The civil war in Nigeria also led to a mass exodus of foreign investors and expatriates, further impacting the sector.

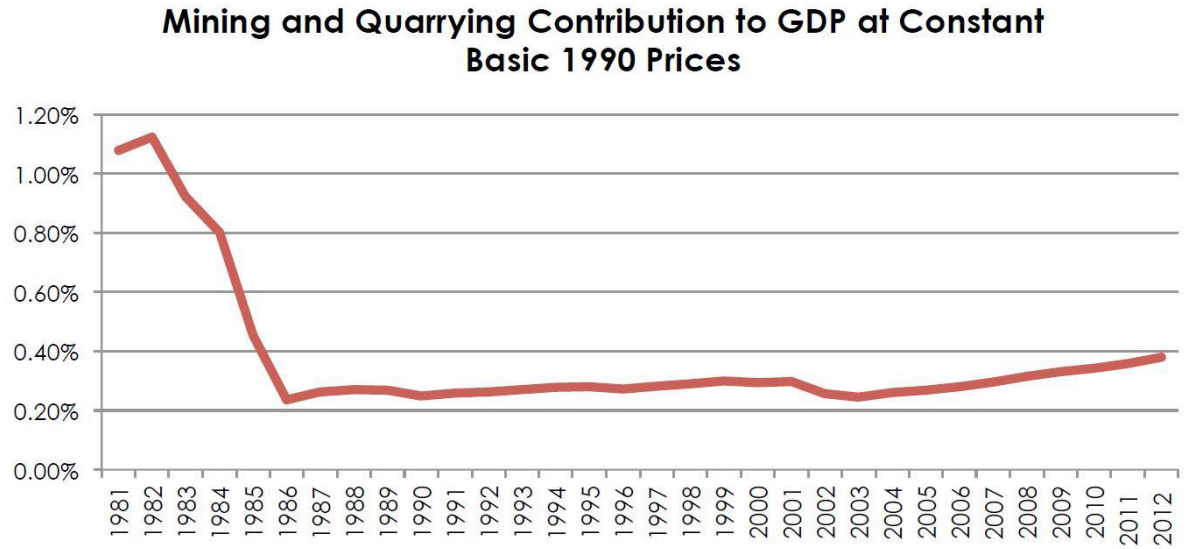

Figure 2.10: Change in mining and quarrying contribution to GDP (NBS, 2015)

Fluctuations in oil prices led the nation to consider economic diversification. A private sector-led economic revival program was launched in 1994 with a view to developing the mineral sector, agriculture and the manufacturing industry (Azubuike et al., 2022; NBS, 2015; Olade, 2019).

While the global oil price declined further in the mid-year of 2014 (Marc et al., 2018; Mead & Stiger, 2015), the solid mineral sector began to pick up (MRC, 2020) because of the efforts put in place by the government to develop the sector and the nation's economy.

Nigeria has not exploited its potential for industrial development largely because of the lack of infrastructure needed for the extraction, processing and transportation of products. Nonetheless, support from the International Development Association (IDA) and the World Bank initiated the economic diversification project aimed at implementing the objectives of the roadmap for the sustainable development of the sector, which was inaugurated in 2016 (KPMG, 2017; MRC, 2020). Seven strategic minerals, namely limestone, iron ore, barite, zinc, gold, coal, and bitumen, have been identified for priority development to restore the sector (Table 2.3).

Table 2:3: Strategic minerals identified by the Ministry of Solid Mineral Development (Ojo, 2015)

Mineral Name (7 strategic Minerals)		Approximate Mineral Reserve
1	Coal	2.7 billion tonnes
2	Bitumen	27 billion barrels
3	Limestone	3 trillion tonnes
4	Iron Ore	10 billion tonnes
5	Barites	15 million tonnes
6	Zinc	5 million tonnes
7	Gold	200 million ounces

2.7.4.1 Coal Mining

Commercial Coal mining was operated by the Nigerian Coal Corporation (NCC), which was commissioned in the 1950s to explore, develop, and exploit the resources. The NCC, between 1950 and 1959, steadily and successfully operated the Okpara and Onyeama underground mines and the Oruka and Okaba surface mines at the eastern edge of the Anambra Coal Basin, now Enugu State (MSMD, 2010). A decline in production began to set in from the 70s through to the 90s; many factors, including the civil war, influenced production operations at some point, and the failure of mechanisation in the industry, probably due to the nature of the geologic setting. Moreover, the NCC's joint ventures with several external establishments failed to yield the expected results, which may have contributed to the abandonment. The agency has not been in operation for several years.

Currently, coal production is ongoing, but not at a commercial scale sufficient for export. It serves as a source of fuel for industrial plants such as Dangote Cement Company in Kogi State, Ashaka Cement in Gombe State, and others.

The federal government plans to revive the coal mining industry for domestic use and electricity generation, aiming for a 30% share of coal in the country's energy mix. This has involved issuing coal mining licenses for a substantial amount of production capacity. The advantage lies in the fact that the characteristics of the Nigerian sub-bituminous coals are low in sulphur, ash content, and thermoplastic properties, which is good for coal-fired electric power plants, according to the research conducted by the Behre Dolbear & Company (USA), Inc., as reported by the ministry (MMSD, 2016).

While the government has promoted coal mining and power generation, its plans are in line with the Paris Agreement's 1.5°C goal; scientific analyses recommend that coal power be phased out across Africa by 2034 to remain within safe climate limits (Climate Analytics, 2022). Also, at COP26, Nigeria announced a commitment to net-zero emissions by 2060 and a new climate bill with five-year emission budgets, according to the UNFCCC. The country also updated its Nationally Determined Contributions (NDCs) in 2021, setting ambitious targets for reducing emissions (DCC_FMEN, 2021). So, the Nigerian government's stance on coal is complex, reflecting both a desire to revive the domestic coal sector and a commitment to climate action. Notably, the abandoned coal mines have yet to be reclaimed or remediated due to cost implications.

2.7.4.2 Mineral and Metal mining

Quarrying accounts for 90% of the mining sector's production and is responsible for most open-pits that have shaped the current landscape of Nigeria (Olade, 2019). Limestone production is very steady because cement factories demand the product as a raw material for their production. Granite, on the other hand, experiences minor fluctuations in its exploitation but is still in high demand for construction purposes.

Metallic and non-metallic minerals contribute the least to mineral production (Figure 10); 8 % and 3% by value in the year 2016, as reported by (Olade, 2019). Due to increasing demand for exports, the private sector delves more into exploration and exploitation. A three-year review shows a steady increase in mineral production from 54.5 Mt, 64.3 Mt and 89.5 MT by tonnage from 2019 to 2021, with the contribution of the mining sector to GDP from 0.26% to 0.63% (Dennis, 2022).

2.7.4.3 Scale of Mining

Current mining practices in Nigeria vary in scale, with many sites operated by licensed corporate bodies or individuals who hold titles. However, the sector is predominantly dominated by ASM operations, which account for 90% of mining activities in the country (Tychsen et al., 2011). While some small-

scale mining operations utilise basic mechanisation, artisanal mining remains largely manual and is carried out by unskilled or semi-skilled workers (Adebayo, 2015). ASM operations are mainly informal and characterised by rudimentary methods, limited technical expertise, minimal social infrastructure, and insufficient consideration for environmental impacts. These operations are widespread across all 36 states and the Federal Capital Territory (Tychsen et al., 2011), reflecting their importance as a livelihood strategy and a means of poverty alleviation, particularly in rural communities.

Artisanal miners are especially active in extracting gold, gemstones, and tin-tantalite in regions or rural communities where these resources occur. As of 31st of December 2021, a total of 2,989 valid SSML were approved in the 36 states, including the federal capital territory of Nigeria. However, this number does not account for the many illegal mining operations currently active across the country, which significantly contribute to the proliferation of undocumented and abandoned mine sites. It is estimated that over 200,000 individuals are directly involved in ASM activities in Nigeria (Tychsen et al., 2011). There are currently no active medium-scale mining operations in the country. Arguably, the Agbaja and Itakpe iron ore projects in Kogi State, though fitting the medium-scale classification, are not operational (Olade, 2019). Some quarrying operations, however, may be considered medium-scale based on their output and operational structure.

The Segilola Gold Project in Itagunmodi, Osun State, is presently the only large-scale commercial gold mining operation in Nigeria. With an estimated reserve of about 3 million tonnes, the company commenced feasibility studies in 2017, completed them in 2019, concluded construction in 2020, and commenced full operations in 2021 (Burger & Taylor, 2021).

2.7.4.4 Common Mining Methods

Consideration of the mining method employed in any operation is crucial, as different methods have varying impacts on human health and the environment. Understanding these differences is essential for selecting appropriate environmental assessment techniques and designing effective remediation plans.

In the early stages of coal mining in Nigeria, extraction was done manually using basic tools such as pickaxes, head pans, and baskets to transport the coal to the surface. Over time, mining practices were mechanised to improve productivity and meet growing demand. In the Orukpa and Okaba coalfields, surface mining methods such as open-cast (strip mining), drift, slope, contour, and auger mining were employed. In contrast, underground mining methods, particularly adit and drift systems, were used in the Okpara and Onyeama mines. The first formal coal mining operation in Nigeria began at the Ogbete mine in Enugu in 1915, where vegetation and topsoil were cleared to expose the coal seams before extraction (Maina et al., 2016; Nwaobi, 2005).

Tin mining, by contrast, was largely associated with surface-based activities such as open-pit digging and the washing of alluvial gravels to extract tin. In the early 20th century, this process was relatively low in technological intensity and heavily reliant on manual labour (Bridge & Fredriksen, 2012; Freeman et al., 1953). Today, the Segilola Gold Mine in Itagunmodi, Osun State, represents Nigeria's most advanced mining operation. It is a highly mechanised facility that uses a combination of conventional open-pit and underground mining techniques. The process involves drilling, blasting, loading, and hauling, all conducted with strict adherence to environmental and human safety standards (Burger & Taylor, 2021)

2.7.4.5 Mine Clean Up

The subject of mine clean-up was largely overlooked during the early days of organised and commercial mining, mainly because environmental regulations were either weak or non-existent in the early 20th century. At that time, the focus of mine design and operations was primarily on maximising the economic deposit with little or no consideration for worker safety or environmental protection. As a result, the concept of sustainable mining was not integrated into mining practices.

Subsequent developments in mining laws and environmental regulations have made mine closure and site rehabilitation formal requirements for obtaining mineral titles or licences. However, implementing these requirements has proven difficult, particularly because a significant portion of mining activity in the country is conducted by artisanal and ASM, many of whom operate informally or illegally. According to a personal discussion with the Director of ASM, the widespread nature of unregulated mining has made clean-up efforts highly challenging.

Even among licenced mining companies, there are frequent attempts to evade responsibility for mine site rehabilitation. Some companies abandon their sites or transfer ownership to third parties, while others leave equipment on-site to create the impression that operations are ongoing. As confirmed by the Director of the Environmental Compliance Department, this tactic leads regulators to classify such sites as "inactive" rather than "abandoned" during inspections, despite the absence of actual activity or reclamation plans. This pattern contributes significantly to the deterioration of mined lands.

Furthermore, regulatory bodies often fail to consistently monitor and enforce compliance, with their engagement typically centred around revenue collection rather than environmental oversight. To address the growing environmental impacts from both active and abandoned mines, particularly those linked to poorly regulated artisanal operations, greater emphasis must be placed on human and environmental health. Incorporating mine closure planning and clean-up into the core of mining operations is essential for promoting truly sustainable mining practices (Aigbedion & Iyayi, 2007; Eludoyin et al., 2017; Ndinwa & Ohwona, 2014).

The legacy of poor mine closure practices in Nigeria is not only a result of inadequate environmental regulations in the early stages of mining development but is also deeply tied to historical, economic, and socio-political factors that disrupted mining activities. Understanding the root causes of mine abandonment is essential for framing the current challenges with site rehabilitation, regulatory enforcement, and sustainable mining practices.

Several factors have contributed to the cessation of mining operations in Nigeria, leading to the proliferation of abandoned mine sites. Key reasons include:

- The discovery of oil and gas in the 1960s, which shifted the national economic focus away from solid minerals.
- The departure of foreign companies, expatriates, and investors during and after the Nigerian Civil War in the late 1960s.
- Political instability, which discouraged continued investment by indigenous entrepreneurs.
- Persistent insecurity in mining regions.
- The rise of illegal mining, which operates outside regulatory frameworks and often leads to unrehabilitated sites.

These factors have resulted in numerous legacy mines that remain unreclaimed. For example, over 80 years of tin mining in Plateau State have led to approximately 316 square kilometres of degraded land, around 4% of the state's surface area. This degradation is heavily concentrated along the Jos-Ropp axis, the central part of the tin field. Recognising the severity of the damage, the Plateau State Government declared this area a 'disaster zone' in 1982 in a bid to secure funding for rehabilitation efforts (Bridge & Fredriksen, 2012).

The Department of MEC Inventory of abandoned (legacy) mines statistics shows a total of 1500 AMLs, out of which 975 were revalidated as of 2022 and are categorised from high to small in terms of risks, and a total of 700 in number are at high risk (MECD, 2022). Aside from this, the many degraded and abandoned mines left by illegal miners are not considered here and will be significant when inventorised.

2.7.4.6 Reclamation and Remediation Practices

Mineral deposits often span large land areas, and as a result, mining activities significantly disrupt the lives of communities where these deposits are located. In many cases, the affected lands are left degraded, impacted through deforestation, the exhaustion of mined-out areas, soil erosion, and the disruption of aquifer systems. These impacts contribute to increased aridity and soil infertility, driven by nutrient depletion and exposure to harsh environmental conditions that impede ecosystem recovery. Furthermore, these processes enhance chemical contamination.

According to the MECD, of the over 1,500 identified legacy mine sites across the country, only 44 have been reclaimed as of 2022. Six of these were reclaimed in 2021, and another six in 2022 (MECD, 2022). The director further noted that, due to the high cost and wide distribution of these sites, reclamation efforts are prioritised by risk level and are implemented across different geopolitical zones, depending on the availability of funds. Consequently, due to limited funding and the scale of degradation, reclamation efforts are typically limited to six sites per year, distributed across the various geopolitical zones.

It was noted that most current reclamation efforts are concentrated on physical rehabilitation, particularly at sites that pose immediate physical hazards to surrounding communities, such as deep open pits spanning large areas, unstable mine shafts, and eroded landscapes. These efforts often involve backfilling, fencing off dangerous areas, grading uneven land, and stabilising slopes to prevent accidents. However, less attention is given to environmental restoration, such as soil remediation, revegetation, and water quality restoration, which are also crucial for long-term ecosystem recovery and the safe return of land to productive use. This challenge, as emphasised, has been the limitation of funds.

2.8 Assessment of Chemical Contamination of AMLs

To effectively propose and implement a remediation strategy for any AML, it is essential to first conduct a detailed, site-specific environmental assessment. This assessment should evaluate the site's physical and chemical conditions, including any existing contamination, and focus on interactions between various environmental media such as mine tailings, soil, vegetation, aquatic life, surface water, and groundwater. The purpose of this assessment is to define the environmental problems present, identify potential contaminant types, and quantify their concentrations, distributions, extents, mobilities, and fates within the AML environment. These data are critical for designing appropriate strategies to minimise or eliminate contaminants.

An exhaustive environmental characterisation of AML sites is necessary to fully understand the nature of the contaminants and their interactions with human and ecological receptors. This process also provides insight into the geologic, hydrologic, hydrogeologic, and engineering properties of the site, such as soil and rock composition and surface and groundwater behaviour, which influence contamination patterns and the feasibility of remediation. Furthermore, it involves spatial and temporal analysis of contaminants when they are present. Understanding contaminant types and pathways is key to evaluating the health risks they pose to both humans and ecological receptors. A thorough site assessment is therefore a prerequisite for identifying site conditions, defining environmental issues, and selecting appropriate tools and techniques to develop a suitable remediation and rehabilitation plan (Benson et al., 2003).

When designing an environmental assessment program, multiple considerations must be addressed to ensure that sufficient and relevant data are collected. These data are essential for identifying the physical, chemical, and toxicological characteristics of pollutants. To achieve this, a multidisciplinary approach is often required to integrate diverse data sets and generate accurate results that support evidence-based remediation recommendations. Among the many approaches, chemical and geochemical techniques are particularly effective in identifying and quantifying environmental contamination, offering robust scientific data on contaminant types and concentrations across the site.

The MECD in Nigeria conducts environmental assessments and monitoring to promote sustainable mining practices. Its responsibilities include reviewing Environmental Impact Assessments (EIAs), conducting site verifications, monitoring mitigation efforts, and inspecting environmental performance using tools such as gas detectors and air quality testers. The department also oversees environmental rehabilitation, reclamation of abandoned sites, and the review of annual environmental protection reports. However, there is limited focus on the chemical assessment of abandoned mines (required for remediation and restoration), which is critical to understanding and mitigating long-term environmental risks, largely because efforts so far have been on AML rehabilitation and reclamation.

2.9 Conclusion

This review highlights the historical, environmental, and regulatory dimensions of AMLs in Nigeria, with emphasis on the legacy of environmental degradation, gaps in sustainable mining practices, and the challenges of remediation. One of the key findings is that the absence of environmental laws during the early stages of organised mining in Nigeria contributed significantly to widespread land degradation and poor mine closure practices. The transition to oil and gas in the 1960s, civil unrest, insecurity, and the proliferation of illegal artisanal mining further compounded the abandonment of mines without proper remediation.

Despite efforts by MSMD through its MECD to address the situation, progress remains limited. Of the over 1,500 identified legacy mine sites, only a small fraction have been reclaimed, largely due to funding constraints and the sites' vast geographic spread. Remediation efforts so far have focused primarily on physical hazards, with less attention to long-term environmental and health risks posed by chemical contamination.

The findings also emphasise the importance of comprehensive, site-specific environmental assessments as a basis for effective remediation. These assessments must account for physical, chemical, geological, and biological factors, as well as human and ecological health risks. Yet implementation remains slow and resource-limited. Furthermore, weak regulatory enforcement and poor monitoring, particularly in ASM, undermine environmental protection goals. The delay in institutional response, except during

revenue collection, and the tendency of some license holders to abandon responsibilities further worsen the situation.

Overall, there is an urgent need for a more integrated and multidisciplinary approach to mine reclamation and remediation in Nigeria, one that prioritises environmental sustainability, community safety, and public health. Stronger enforcement, increased funding, improved data collection, and consistent monitoring are critical to reversing environmental damage and preventing future degradation caused by both legal and illegal mining operations.

Building on the findings of this review, the next stage of this research will focus on enhancing the understanding of chemical risk characterisation methods, specifically in the context of AMLs. This will help identify and refine site-specific practices and approaches for exposure assessment, hazard identification, and risk quantification, with particular attention to how contaminant fate, transport, and bioavailability are modelled across environmental compartments such as soil, groundwater, and biota.

To validate the applicability and reliability of these methods, the research will include comparative case studies conducted across AMLs with diverse geologic and environmental settings/conditions. These case studies will serve as a critical step in testing risk characterisation tools and developing evidence-based practices for remediation planning and implementation. By grounding the research in real-world contexts, this stage will improve the accuracy of chemical risk evaluations and contribute to broader national goals such as sustainable land use, pollution prevention, and the ecological restoration of degraded environments, particularly in Nigeria.

Chapter 3: Current Methods for The Evaluation of Chemical Contamination Risks from Abandoned Coal and Lead-Zinc Mine Lands: Protocol for a Systematic Evidence Map

3.1. Background

Abandoned mines present unique challenges due to their diverse contaminant sources, multiple pathways, diffuse pollution, and persistent environmental legacies. The complex interactions of physical, chemical and environmental hazards (BML, 2017; DEP, 2015; Fields, 2003; Lottermoser, 2010; Venkateswarlu et al., 2016) are associated with the nature of mining operations, the type of mine structures, and long-term legacy impacts (Hufty, 2019; Jain et al., 2016), which amplify overall risk. Consequently, the risk assessment (RA) method for AMLs goes beyond a narrow focus on soil or water contamination typical of contaminated land (CL) scenarios. As recognised by ICMM, traditional RA and guidance fail to consider the specificities of metals, a significant problem in AMLs (ICMM, 2007b). They require additional layers of considerations, such as mine infrastructure, waste repositories, geotechnical instability of hillslopes and tailings dams, river mobility, and the chronic effects of AMD. Furthermore, the scope of contaminants studied, the sampling strategies, analytical methods, exposure models, specific sources, multiple pathways, contaminant fate and transport models, and specific receptors typically considered in AMLs RA context, which may have been omitted from some established guidance that applies to contaminated land more generally.

Furthermore, risk assessment methods for AMLs need to be able to cope with increased complexity resulting from climate change and increased anthropogenic pressures. Accounting for multiple chemical stressors, mixture risk assessment, and considering the effects of changing magnitude and/or frequency of extreme events, sea-level rise and other consequences of climate change, is required as these factors may modify exposure and therefore risks (Marras et al., 2022). For instance, extreme rainfall and rising temperatures can accelerate AMD formation, enhance contaminant mobility, and widen pollutant dispersion (Anawar, 2013; W. Li, Deng, et al., 2024; Richard et al., 2021). Additionally, climate-driven impacts, including erosion, permafrost thaw, altered hydrology, and land instability (Bulovic et al., 2024; Palma et al., 2019; T. B. dos Santos et al., 2019), threaten ecosystems and human health (Grajal-Puche et al., 2024; Hughes, 2024a). A case from Kam Kotia AML in Canada highlights that in 2012, rapid snowmelt caused a tailings dam breach, releasing contaminated water and sediment into the surrounding environment (MacMillan et al., 2021).

Some regulatory updates now reflect these emerging concerns. For example, the UK's updated guidance (UK EA, 2020) mandates that climate change impacts be considered from project inception through long-term monitoring of CL.

Although many national and international guidelines are available, e.g. (CCME, 2016; ICMM, 2007, 2016; ISO, 2017; NEPM, 2014; UK EA, 2020; US EPA, 2000a; WHO, 2010), most are general (for contaminated lands overall) and not tailored to AML-specific complexities. In contrast, academic research frequently applies more tailored and nuanced, site-specific assessments. This chapter describes the development of a protocol for a systematic evidence map (SEM) aiming to identify and synthesise methods used to assess and evaluate chemical risks from AMLs. This published protocol is designed to identify current practices reported in peer-reviewed literature.

A bibliographic search for literature reviews synthesising methods of risk assessment specific to chemical contamination from AMLs yielded no comprehensive results. This highlights a notable gap in efforts to consolidate guidance in relation to risk from legacy mine contamination. Addressing this gap would be valuable for developing more universally applicable frameworks and informing risk-based decision-making in diverse contexts. A SEM can help synthesise current methods, highlight where guidance is lacking, and how current practice deviates from established guidance.

This work is novel in developing a SEM protocol specifically to map methods for assessing chemical contamination risks in AMLs. As noted by the handling editor, such synthesis efforts are rare in this research domain (https://doi.org/10.5281/zenodo.14246187), underscoring the originality and relevance of this contribution.

3.1.1 Systematic Evidence Map (SEM)

Evidence maps follow transparent and replicable methods, including the formulation of structured research questions, comprehensive and reproducible literature searches, and standardised data extraction procedures (James et al., 2016; Wolffe et al., 2020). This ensures consistency and reliability, making evidence maps particularly valuable for informing environmental policy, prioritising future research, and guiding mitigation strategies (James et al., 2016; Miake-Lye et al., 2016).

They are used to systematically catalogue and visualise the breadth and characteristics of research in any field (Miake-Lye et al., 2016). In the context of environmental risk assessment, particularly in complex domains such as chemical contamination from abandoned mines, evidence maps help organise diverse sources of information across geographic regions, contaminant types, pathways and receptors, amongst other factors (James et al., 2016). Unlike traditional systematic reviews that aim to synthesise outcomes, evidence maps focus on providing a high-level overview of the existing evidence, its areas of concentration, and significant gaps (Snilstveit et al., 2016). They do not necessarily include or necessitate a critical appraisal of individual studies, and such a step has not been included in the proposed work.

3.1.2 Scope and Objective

The scope of this SEM is limited to abandoned coal and lead-zinc mines, although an initial attempt was made to include other types of abandoned mineral mines, e.g., gold, mercury, arsenic, etc. However, expanding the review to all mine types would not be manageable within the time and resource constraints of a PhD project.

While metals differ in mobility, oxidation states, bioavailability, and toxicity, Pb/Zn AMLs may not fully capture the impacts of other abandoned metal and mineral mines, such as abandoned gold mines. This limitation is acknowledged, as reviewing all abandoned minerals/metal mines is impractical due to time and resource constraints. This protocol has been carefully designed and may be adaptable to other types of AMLs, with a focus on evaluating risk assessment. However, given the varying behaviour of potentially toxic elements (PTEs) across environmental media, particularly in terms of mobility and bioavailability, it can also be adapted for use in assessing other inorganic contaminant sources. When applying the protocol to different contaminant types, it is essential to consider compartment-specific processes and exposure pathways. These factors influence the selection of risk assessment methods both for ecological and human health contexts. Furthermore, not all methods may be fully captured by focusing on Pb/Zn metals and coal mines. For example, because of the complex transformation processes of mercury (Alpers et al., 2005), abandoned mercury mines may require specific risk assessment methods that our approach may miss.

The specific objectives of this SEM protocol were articulated as follows:

- Identify approaches for evaluating chemical risks from abandoned lead-zinc and coal mines.
- Extract relevant information about the different procedures above.
- Establish current methods related to chemical risk assessment of AMLs.

This SEM was designed to answer the following question: *What are the current methods for evaluating chemical risks from abandoned coal and lead-zinc mines?* To support this, a Population, Intervention, and Outcome (PIO) statement was developed (Table 3.1). Here, the Population refers to the types of AMLs being assessed, the Intervention refers to the chemical risk assessment methods applied, and the Outcome refers to the types of risks or effects identified as impacting ecological and/or human receptors.

Table 3.1: Population, Intervention and Outcome (PIO) statement of assessment practices relating to chemical risk from Abandoned Mine Lands

What are the current methods for evaluating chemical risks from abandoned coal and lead-zinc mines?

Population (types of AMLs)	Abandoned mine lands (mines that are no longer active, have been shut down, closed, forgotten, or have ceased operation). Only coal and lead-zinc mines; all other former mining activities are out of scope.
Intervention (methods of chemical risk assessment)	Chemical risk assessment practices: studies must include an evaluation of the chemical risks. Intermediary interventions include exposure assessment and/or modelling, and risk assessment and characterisation. Studies in which actual effects (realised risks) are monitored are within scope, while studies limited to exposure or hazard assessment or characterisation will not be considered.
Outcome (types of risk and effects identified for ecological and human receptors)	Risks and effects of chemicals associated with AMLs on ecological and human receptors
Time Frame	Peer-reviewed studies or grey literature published between 2000 and 2024.

3.2. Materials and Methods

This protocol was developed with due consideration given to the recommendations from the Conduct of Systematic Reviews in Toxicology and Environmental Health Research (COSTER) (Whaley et al., 2020). Deviations from the COSTER recommendations are documented in the published protocol's supplementary material 2.1. This is reported following the Preferred Reporting Items for Systematic Review and Meta-Analysis Protocols (PRISMA-P) guidelines (Moher et al., 2015; Shamseer et al., 2015). The checklist is provided in supplementary material 2.2 (PRISMA-P Checklist).

3.2.1 Eligibility Criteria

The PIO statement in Table 3.1 was used to further develop the eligibility criteria (Table 3.2) for the inclusion of studies in the evidence synthesis, with the following considerations:

Population: The focus is on abandoned coal and lead-zinc mines, as they represent an enduring toxic legacy with significant environmental and public health risks. Studies on other types of mines will be excluded, although the protocol may be adaptable for application to other abandoned mine types.

Intervention: This refers to the chemical risk assessment methods applied to evaluate risk. Initial pilot activities revealed that there is a large body of literature documenting chemical contamination in AMLs, but many studies stop short of conducting a chemical risk assessment. Including these studies, which primarily focus on analytical methods reporting concentrations of chemical contaminants, would add little value as they have already been extensively researched and reported over the years, and the effort required would exceed the resources available for this project. The scope was therefore refined to studies that report or conduct chemical risk assessments. Consequently, studies focusing solely on exposure or hazard assessments will be excluded. However, studies that evaluate actual impacts or harm, i.e., realised risks from exposure to toxic chemicals from AMLs, will be considered eligible while not specifically targeted by our search strategy.

Outcome: Types of risks and impacts identified for ecological and human receptors. Studies investigating quantitatively measurable toxicological effects on reproduction, growth, behaviour, or development on ecological and human receptors at the community, population, or individual level will be included. Studies focusing on physical injury from engineering failures, hazards due to subsidence, or structural failures of tailings dams will be excluded. Studies focusing solely on exposure measurement, contaminant fate, transport, bioavailability, and bioaccumulation, as well as reviews and meta-analyses, will also be excluded.

Timeframe: To comprehensively capture advances, applications, and persistent gaps in chemical risk assessment methods for AMLs, studies published between 2000 and 2024 will be included. This timeframe reflects a period of significant methodological development across international contexts.

Table 3.2: Eligibility criteria

Element	Statement	Inclusion	Exclusion
Population (types of AMLs)	Abandoned mine lands	Coal and lead-zinc mines. Abandoned open-pit or surface mines. Abandoned underwater and underground mines	Other types of AMLs, such as mercury and arsenic. Active mines, surface, open pit, underground, or underwater mines undergoing reclamation, rehabilitation,

Element	Statement	Inclusion	Exclusion
			remediation, or restoration Other types of activities, such as active or abandoned quarries and smelting sites.
Intervention (Methods of chemical risk assessment)	Chemical risk assessment practices	Process: evaluation of the actual effects or potential impacts due to chemical exposures Agents: organic and inorganic chemicals Exposure via water, sediment, soil, dust, air, biota (including food) Receptors: living organisms (humans and non-humans, including micro-organisms, plants, vertebrate and invertebrate animals), and their systems (populations, communities, ecosystems)	Process: Studies focusing on inventory, prioritisation of sites, and chemical contamination without assessing the risk of such contamination. Agents: Studies focusing on nanominerals, macrominerals, microplastics, radionuclides or organometallics Receptors: studies focusing on environmental media as endpoints without assessing associated risks to humans and non-human organisms.

Element	Statement	Inclusion	Exclusion
Outcome (types of risk and effects identified for ecological and human receptors)	Chemical risks and effects on ecological and human receptors	Evaluation of chemical/toxicological risks and impacts on reproduction, growth, behaviour, survival, or development in ecological and human receptors.	Physical injury due to natural or engineering hazards (subsidence), structural failure of tailings dams, hydrogeochemical behaviour, and rock-water interaction.
Time Frame	Peer-reviewed studies and grey literature	Studies published between 2000 and 2024	Studies published before the year 2000

3.2.2 Information Sources

The following six bibliographic databases were selected to search for peer-reviewed articles using search algorithms adequate for each database;

- Web of Science
- PubMed
- Academic Search Complete and Business Source Premier (via EBSCOhost)
- ScienceDirect
- Scopus

In addition, manual searches of grey literature not indexed in the selected databases were conducted, targeting specific websites of government agencies, institutes, and other platforms, including:

- International Council on Mining and Metals (ICMM)
- US Environmental Protection Agency (US EPA)
- UK Environment Agency (UK EA)
- The International Organisation for Standardisation (ISO)
- Canadian Council of Ministers of the Environment (CCME)

3.2.3 Search Strategy

Pilot searches were conducted to iteratively develop the search strategy, with assistance from an information specialist and insights drawn from other systematic evidence maps related to environmental studies. Initially, we planned to include all types of mines in our mapping. However, after conducting preliminary searches, we realised this approach was unmanageable. We refined our focus to coal and lead-zinc mines. During the piloting phase, we noticed many studies reported chemical concentrations without contributing significantly to the research question. As a result, we decided to specify our focus on studies assessing risk.

This approach addressed the challenge of identifying manuscripts explicitly related to chemical risk assessment methods from AMLs, as vague terms like "assessment" and "risk" often yielded irrelevant research. The number of hits for synonyms related to the elements of the PIO statement was recorded and combined using Boolean operators to ensure the search strategy maintained sensitivity while achieving some level of specificity.

A general approach is shown in Table 3.3. This was tested across all listed databases, adjusting the search strings to ensure appropriate retrieval of relevant literature, except for ScienceDirect, which only supports eight Boolean operators, restricting long, complex search algorithms. Truncation of words was used with care. Proximity searches were run to find combined forms of terms. For example, Web of Science uses the proximity operator NEAR/3 while Scopus's is w/3. A simplified search algorithm was developed for ScienceDirect as follows:

(Abandoned OR inactive) AND (coal OR lead OR zinc) AND Mine AND (Contaminant OR Pollution) AND "Risk Assessment"

The use of adequate filters, such as article type and publication year, was also explored and applied. The results from piloting the search strategy, the complete search algorithms for each database, the compiled search strings, and the number of articles retrieved from each database are included in the supplementary materials 2.3 (search strategy). The sensitivity of the search strategy was assessed using a set of relevant articles identified during an initial review of the impacts of abandoned coal and lead-zinc mines. All selected articles were successfully retrieved using Web of Science, while 90% were also captured by Scopus and PubMed. This confirmed that our core search terms would be effective in retrieving key literature relevant to the evidence mapping.

The first round of open peer review of the protocol revealed (https://doi.org/10.5281/zenodo.14246187) that the term "historic" had been omitted from the pilot search. To ensure that relevant articles were not missed, this term was later searched separately in combination with other key terms, as shown below:

(Historic) NEAR/3 (Coal OR Lead OR Zinc OR mine OR exploitation OR site OR land) AND (Pollut* OR contamin* OR chemical) AND (Risk)*

Details of this additional pilot search and database-specific retrieval are provided in Section 2.3 of the supplementary materials. A summary table of pilot searches and a flow diagram of the literature search results are presented in Table 3.4 and Figures 3.1, respectively.

Table 3.3: General search strategy combined with Boolean operators

S/N	Keywords	Synonym
#1	Abandoned mines	(inactive OR historic OR orphan OR derelict OR forgotten OR disused OR deserted OR abandoned) NEAR/3 (Coal OR Lead OR Zinc OR mine* OR exploitation OR site OR land)
#2	Contamination	Pollut* OR contamin* OR chemical
#3	Risk	Risk
Total	#1 AND #2 And #3	(inactive OR historic OR orphan OR derelict OR forgotten OR disused OR deserted OR abandoned) NEAR/3 (Coal OR Lead OR Zinc OR mine* OR exploitation OR site OR land) AND (Pollut* OR contamin* OR chemical) AND (Risk)

Table 3.4: Search strings from pilot search, including the databases searched and the number of articles identified from the initial search on 26/07/2024, and the additional search on 13/05/2025

No	Search String	Indexes searched	Number of articles (Initial)	Number of articles (additional)
1	(inactive OR orphan OR derelict OR forgotten OR disused OR deserted OR abandoned) NEAR/3 (Coal OR Lead OR Zinc OR mine* OR exploitation OR site OR land) (Topic) and Pollut* OR contamin* OR chemical (Topic) and Risk (Topic) and 1981 or 1982 or 1987 or 1991 or 1992 or 1993 or 1995 or 1996 or 1997 or 1998 or 1999 (Exclude – Publication Years)			
	((TS=((historic) NEAR/3 (Coal OR Lead OR Zinc OR mine* OR exploitation OR site OR land))) AND TS=(Pollut* OR contamin* OR chemical)) AND TS=(Risk)	Web Of Science	886	80

2	(TITLE-ABS-KEY((inactive OR orphan OR derelict OR forgotten OR disused OR deserted OR abandoned) W/3 (coal OR lead OR zinc OR mine* OR exploitation OR site OR land)) AND TITLE-ABS-KEY(pollut* OR contamin* OR chemical) AND TITLE-ABS-KEY(Risk)) AND PUBYEAR > 1999 AND PUBYEAR < 2025			
	(historic) W/3 (Coal OR Lead OR Zinc OR mine* OR exploitation OR site OR land)	Scopus	1049	90
3	(Abandoned OR inactive) AND (coal OR lead OR zinc) AND Mine AND (Contaminant OR Pollution) AND "Risk Assessment"			
	(Historic) AND (coal OR lead OR zinc) AND Mine AND (Contaminant OR Pollution) AND "Risk Assessment"	Science Direct	966	205
4	(("inactive"[Title/Abstract] OR "orphan"[Title/Abstract] OR "derelict"[Title/Abstract] OR "forgotten"[Title/Abstract] OR "disused"[Title/Abstract] OR "deserted"[Title/Abstract] OR "abandoned"[Title/Abstract]) AND ("Coal"[Title/Abstract] OR "Lead"[Title/Abstract] OR "Zinc"[Title/Abstract] OR "mine*"[Title/Abstract] OR "exploitation"[Title/Abstract] OR "site"[Title/Abstract] OR "land"[Title/Abstract]) AND ("pollut*"[All Fields] OR "contamin*"[All Fields] OR ("chemical"[All Fields] OR "chemical s"[All Fields] OR "chemically"[All Fields] OR "chemicals"[All Fields])) AND ("risk"[MeSH Terms] OR "risk"[All Fields])) AND (2000:2024[pdat])			
	(((Historic[Title/Abstract]) AND (Coal[Title/Abstract] OR Lead[Title/Abstract] OR Zinc[Title/Abstract] OR mine*[Title/Abstract] OR exploitation[Title/Abstract] OR site[Title/Abstract] OR land[Title/Abstract])) AND (Pollut*[Title/Abstract] OR contamin*[Title/Abstract] OR chemical[Title/Abstract])) AND (Risk[Title/Abstract])	PubMed	565	114
5	AB (Inactive OR orphan OR derelict OR forgotten OR disused OR deserted OR abandoned) N3 (Coal OR Lead OR Zinc) AND (mine* OR exploitation OR site OR land AND (Pollut* OR contamin* OR chemical) AND (Risk))			
	AB ((Historic) N3 (Coal OR Lead OR Zinc) AND (mine* OR exploitation OR site OR land)) AND AB (Pollut* OR contamin* OR chemical) AND AB Risk	Academic Search Complete and Business Source Premier (via EBSCOhost)	392	6

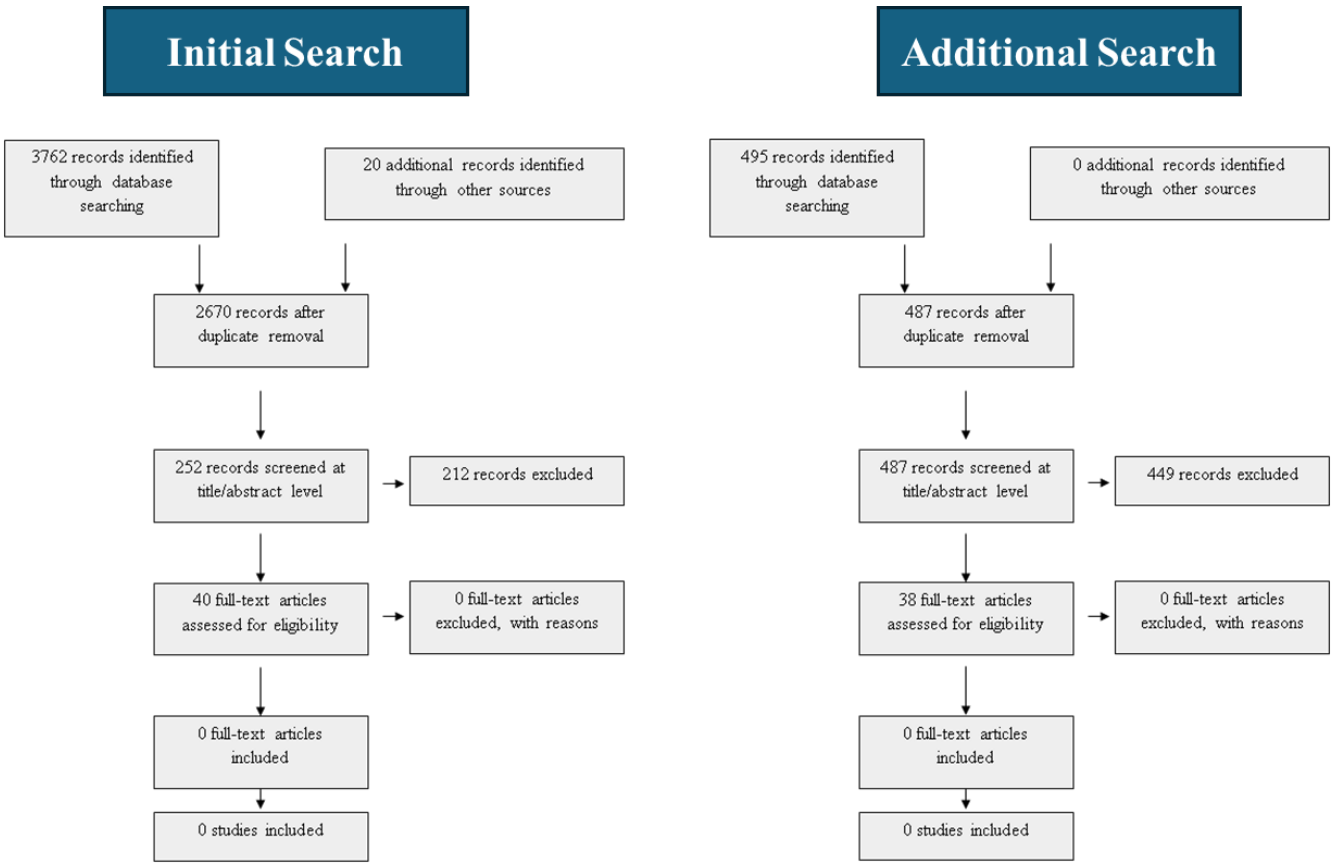

Figure 3.1: Flow diagram for literature search results for initial searches before protocol revision and additional searches after the first revision.

3.2.4 Data Management

The screening of the literature is being managed using CADIMA, a user-friendly, free online tool established by the Julius Kühn Institut and the Collaboration for Environmental Evidence (Julius Kühn Institut, 2017). The Mendeley Reference Manager (Elsevier, 2013) was used to manage manual searches, while Citavi (Swiss Academic Software GmbH, 2024) was used for the automatic retrieval of full-texts that were accessible.

3.2.5 Selection Process/Screening

The defined eligibility criteria are applied to screen the merged list of references retrieved from each literature source after the duplicates have been removed. Screening is carried out in two stages. In the first stage, titles and abstracts are examined for relevance to the formulated question, with studies deemed irrelevant excluded. In the second stage, the full texts of the remaining studies from the first stage will be assessed for inclusion. The reasons for excluding studies at the full-text stage will be documented.

CADIMA facilitates a consistency check as a method of piloting the screening stage. Any disagreements between screeners were resolved through discussion and used to revise and clarify the eligibility criteria and ensure a consensus on their interpretation was reached between all parties. Prior to the pilot screening, we had not specified abandoned coal and Pb/Zn mines as the population or chemical risk assessment as the intervention. Instead, we included various types of abandoned metal and mineral mines (e.g., Cu, Ag, Hg, Ni, etc.) in the population. After conducting a pilot screening of 15% of the 8,427 articles retrieved (after removing duplicates), we found that most studies focused on chemical contamination assessment rather than risk assessment. Consequently, we refined our eligibility criteria to focus on abandoned coal and Pb/Zn mines as the Population and chemical risk assessment as the Intervention. When we reran the search and applied the refined criteria, the retrieved articles were streamlined to those addressing chemical risk assessment of abandoned coal and Pb/Zn mines. The eligibility criteria were applied to 15% (automatically generated by CADIMA) of the merged reference list at the title and abstract level by two reviewers; the outcome was poor, mainly due to stricter interpretation of the exclusion criteria leading to some articles being marked as "excluded" when they should have been rated "unclear". A common example was when the title or abstract referred to AML without specifying the type of mine. The discrepancies were resolved through discussion.

One reviewer will screen the remaining articles independently, with an overlap of 10% of retrieved articles screened independently in duplicate by a second reviewer as a quality control step. Any disagreements will be discussed as soon as they arise and resolved by consensus to ensure a consistent interpretation of eligibility criteria and avoid drift. If the rate of discrepancies in inclusion-exclusion decisions became too high (>1%), this would trigger duplicate screening of previously screened literature. (Discrepancies between ‘included’ and ‘unclear’ decisions at the title–abstract screening stage are also recorded, though they do not materially affect the selection process).

3.2.6 Data Extraction

A data extraction template was developed and piloted to ensure consistency in the data extraction process. The pilot extraction was conducted independently by two reviewers. Discrepancies in the extraction process were resolved through discussion and used to refine the data extraction template and ensure that a consensus understanding of the process was reached. The piloted data extraction sheet is available in supplementary materials 2.5 (Data Extraction Sheet-Pilot 1 and 2). The data will be extracted from all included studies by a single reviewer, and a sample of 25% of the extracted data will be independently checked by a second reviewer, as a quality control step. The data extraction template is designed to facilitate identification, documentation, and validation by a second reviewer. The finalised data extraction template is included in supplementary materials 2.6 (Finalised data extraction template). A coding strategy combining both deductive and inductive approaches was developed to guide the data extraction process and is provided in supplementary material 2.7 (Code Book for Data

Extraction). This dual approach was selected to ensure both consistency and flexibility in capturing relevant information across studies. The deductive component involved the predefined categorisation of commonly encountered data types to standardise data recording. In parallel, the inductive component was designed to allow for the identification and categorisation of emerging terms or concepts, both before and during the extraction process.

In brief, the following data will be extracted from all studies included during the full-text screening stage:

- Bibliographic metadata: Author(s), year, journal name, journal details (volume, issue, page), article title and abstract, and source of funding.
- Abandoned mined land details: study location (country, state, or county where the study was carried out), mine name, information about the type of mine, method of mining, duration of operation, and year of abandonment.
- Exposure measurement (if relevant): Sample medium, sampling strategy, sample storage and preparation, sample volume (unit), method of chemical analysis, the limit of detection (including unit), precision, accuracy, contaminant or pollutant name, CAS number, information about the reported concentrations, including the unit in the article, and other contextual measurements.
- Exposure modelling (if relevant): Source medium, pathway, target media, modelling method and reference used to model the exposure, chemical name, CAS number, and outcome.
- Effect monitoring (if relevant): Taxonomic group, species, sampling strategy/method, sample storage and preparation, sample size (unit), type and level of observed effect, measurement methods, statistical significance, statistical methods, reported outcomes.
- Risk characterisation: source, exposure pathway, receptor, risk characterisation method, reference for the method used, the source of reference dose used, uncertainty factors, risk category, outcome, and consideration of mixtures.

This data extraction process is designed to systematically capture key components relevant to chemical risk assessment at AMLs. This approach is structured to ensure that all necessary information is included to assess risk accurately and comprehensively.

First, bibliographic metadata will be extracted to organise and classify the studies included in this evidence map. This information helps establish the context of each study, including its authorship, funding source, publication details, abstract, and DOI, all of which are essential for understanding the scope of the research and its applicability to the overall mapping process.

The details of the abandoned mine lands, such as the location, type of mine, mining method, and duration of abandonment, are crucial for evaluating environmental impacts. These factors influence the

pollution pathways and long-term risks associated with AMLs. Information about the mining history, waste characteristics, and local geology is fundamental to predicting and assessing site-specific environmental risks. The data from this section will help evaluate the applicability of different risk assessment methods across specific contexts and support subset analyses of methodological differences.

Exposure assessment methods include details on the sampling strategy, sample storage and preparation, and the chemical analysis techniques used. Parameters such as the exposure medium, contaminant(s), and limit of detection data will help inform the applicability and performance of the methods described. Exposure modelling is often essential for extrapolating measured concentrations of contaminants in environmental media to concentrations in relevant exposure pathways. Information such as exposure pathways, target media, and modelling methods helps document the current methods used to predict human and ecological receptor exposure to chemical contaminants from AMLs.

Effect monitoring data, such as the taxonomic group, species involved, and the type and level of effects observed, provide crucial evidence of the actual risks faced by receptors exposed to AML contaminants. These data are particularly important for identifying realised risks and understanding the ecological and human health consequences of chemical exposure. These data can be used to compare observed risks with those predicted by chemical risk assessments.

Finally, data from risk characterisation methods, including references to the guidelines or method used, and the incorporation of uncertainty factors, will help document the range of risk assessment methods and applications across various exposure sources and routes. Also, information on whether mixture risks are considered, along with the range of methods used, will be recorded.

The extraction of these data types will ensure that the evidence map captures a comprehensive overview of current practices, which will allow us to query and document advancements, applications, and any gaps in methods related to risk from AMLs. Piloting the data extraction has helped to establish guidelines for maintaining a consistent format to extract data from included studies. The use of drop-down menus also allows for categorisation, which will facilitate the data analyses. Following the extraction process, the data will be cleaned, such as removing irrelevant symbols, units, or numbers, before analysis.

3.2.7 Data Analysis and Reporting

The outcome will address our objectives: identifying procedures, extracting relevant information for evaluating chemical risks, and establishing current best practices related to chemical risk assessment of AMLs.

The key characteristics of mines that have undergone risk assessment will be summarised in tabular format, accompanied by a map visualising their geographic locations. Information related to exposure

measurement, exposure modelling, effect monitoring, and risk characterisation will also be summarised in tables. This analysis aims to provide insights into both the diversity and frequency of various methodologies and practices used to characterise chemical risks from AMLs. This will be complemented by a critical narrative synthesis of what researchers identified as necessary in the included studies.

The visualisation tool Tableau (Salesforce Inc., 2025) allows the creation of interactive dashboards, enabling users to select subsets of data and easily view all relevant references and sources. Tableau will be used to illustrate quantitative datasets for each risk assessment process category and to generate reports that summarise findings and highlight key insights.

We will address the "current method" question for each of the four categories through narrative analysis and trend evaluation from the database. Tableau will help track changes over time, illustrating how evidence has evolved. Part of this process will involve reviewing the methods used, compiling a list of those considered current, and establishing criteria for this distinction. Additionally, we will examine guidance documents from organisations such as the US EPA, UK EA, ICMM, and ISO to understand the recommended approaches to risk characterisation related to AMLs. The collated methods will be compared with currently available guidance to assess alignment and deviations. Through the data analysis, we aim to identify scientific advancements in AML risk characterisation within the study timeframe and highlight improvements made over the years. Identified gaps and limitations will also be documented.

3.3. Discussion (Reflection)

This method development followed a rigorous and systematic process, beginning with the conceptualisation of the study and the identification of knowledge gaps in the area of chemical risk assessment of AMLs. Building on this foundation, a comprehensive literature search strategy was designed and piloted to ensure relevance and coverage. The piloting stage also included study selection and preliminary data extraction, which helped to refine the approach. From this iterative process, a structured data extraction template and codebook were developed to promote consistency, transparency, and replicability throughout the evidence mapping.

While this structured process provided a strong methodological foundation, the peer review and evaluation process played a critical role in further refining the approach, ensuring both scientific rigour and clarity.

The evaluation of this protocol by the editor and reviewers highlighted both the novelty and the rigour of the proposed approach while identifying areas that required substantial improvement. The central

objective, which is to develop a systematic evidence map describing current methods for the evaluation of chemical contamination risks from abandoned coal and lead-zinc mine lands, was recognised as an interesting and valuable contribution, particularly given that evidence mapping has rarely been applied in this domain. This validation affirms the originality of the study design and reinforces its potential to fill a critical gap in synthesising methodological practices rather than outcomes alone.

At the same time, the review process demanded a high degree of methodological refinement. In the first round of review, substantial revisions were recommended, including improving the conciseness and structure of the manuscript, clarifying objectives from the outset, and providing greater detail on data abstraction and coding procedures. These comments required rethinking the content and organisation of the manuscript to ensure transparency, reproducibility, and accessibility, even for non-specialist readers. The process of responding to these critiques strengthened the protocol by sharpening its focus, reducing redundancy, and establishing a more rigorous framework for data management, including piloting, coding, and the use of a codebook for consistency.

The second round of review acknowledged the significant improvements made, noting that all substantive methodological issues had been satisfactorily addressed. At this stage, only minor revisions were required, mainly concerning clarity of expression, grammar, and style. This stage of feedback was equally important, as it reinforced the value of presenting methods not only with scientific rigour but also with readability and accessibility. A final careful review for grammar and clarity, as suggested by the editor, further enhanced the overall quality of the manuscript and ensured it could be readily understood by both subject experts and non-native English speakers.

The review also underscored the distinctive nature of the Registered Reports format, where methods are evaluated prior to data collection. The editor emphasised this structure as a means of improving the quality of planned methods, reducing research bias, and ensuring that methodological rigour rather than results determines publication. Engaging with this process not only enhanced the robustness of the protocol but also provided a reflective opportunity to position the work within broader debates on transparency and research integrity.

Beyond its methodological advantages, the open science framework, especially the open peer review process, transformed this experience into a form of collaborative knowledge development. The transparent exchange of feedback between author, editor, and reviewers fostered a sense of shared inquiry and mutual learning, demonstrating how scientific progress can emerge through dialogue rather than one-directional critique. This process provided valuable insight into how open peer review supports accountability, inclusivity, and collective refinement of ideas (Fecher et al., 2014; Ross-Hellauer, 2017; Tennant et al., 2017).

The entire review and revision process extended over nearly a year, reflecting both the depth of engagement required and the iterative nature of open peer review. As a doctoral researcher, this was both highly rewarding and demanding: the exposure to open science practices provided me with robust training in research transparency and communication, yet it also introduced challenges in managing my time and maintaining project momentum within the fixed PhD timeline. This experience justifies why Chapter 4 presents only partial preliminary results, as much of the effort was devoted to ensuring methodological rigour and transparency before advancing to complete data synthesis.

Overall, the two-stage evaluation process was constructive and iterative. By balancing recognition of the study's novelty with calls for greater clarity, justification, and refinement, it provided a pathway to strengthen both the scientific foundation and the protocol's presentation. This reflection highlights that the rigour of peer review, when constructively applied, can be a key component of method development, ensuring that the final protocol is both innovative and methodologically sound. This experience has strengthened my research capacity and provided an opportunity to appreciate the role of peer review as a catalyst for producing research that is both scientifically robust and broadly useful.

3.3.1 Implications for Abandoned Mine Lands in Nigeria

The development of this SEM protocol has important implications for the assessment and management of AMLs in Nigeria and other mining-impacted regions with similar legacy mining histories. Nigeria hosts numerous abandoned coal and lead–zinc mines, many of which remain poorly characterised and inadequately monitored despite growing concerns regarding contamination of soils, sediments, surface water, groundwater, and ecological systems. The absence of a consolidated framework for evaluating chemical risks from these sites poses significant challenges for environmental management, regulatory decision-making, and remediation prioritisation.

This protocol provides a structured framework that may support future environmental risk assessment practices in Nigeria. The methodological approach may assist regulators, researchers, and environmental practitioners in identifying suitable methods for exposure assessment, effect monitoring, exposure modelling, and risk characterisation in mining-impacted environments. By promoting methodological consistency, the protocol will help to improve the assessment of ecological and human health risks associated with abandoned mines.

Summarily, this SEM protocol provides a foundation for strengthening evidence-based environmental management and supporting the development of more context-specific risk assessment and remediation strategies for abandoned mine lands in Nigeria.

3.4. Conclusion

This chapter has outlined the development of a SEM protocol designed to synthesise existing methods for assessing chemical contamination risks associated with AMLs. The rationale emphasises the complexities of AMLs, which distinguish them from traditional CL. Eligibility criteria were clearly defined to facilitate the retrieval of relevant articles for the synthesis. A detailed search strategy, study selection process, and a structured data extraction template with a coding framework were developed to ensure consistency and transparency.

The protocol development process, refined through iterative piloting and open peer review, established a robust methodological foundation that aligns with principles of open science and research transparency. By systematising the mapping of methodological practices rather than outcomes, the SEM protocol contributes to improving how evidence on chemical risk assessment in AMLs is organised and interpreted. This method development also underscores the value of reflective and collaborative practices in enhancing research quality and reproducibility.

The next chapter applies this validated protocol to generate preliminary findings from the identified literature. These results illustrate how the developed framework functions in practice and provide insights into current trends, gaps, and methodological diversity in the assessment of chemical risks from AMLs.

The protocol was submitted to the Journal of Evidence-Based Toxicology and underwent two rounds of peer review. It has been accepted for publication. Details of the manuscript, supplementary materials, and all documents associated with the peer review process can be accessed via: https://doi.org/10.5281/zenodo.14246187

Chapter 4: Current Methods for The Evaluation of Chemical Contamination Risks from Abandoned Coal and Lead-Zinc Mine Lands: A Narrative Evidence Review

4.1 Introduction

Chemical risk assessment (CRA) of AMLs typically begins with site characterisation, involving a desk study to review historical data, including Earth Observation (EO) data, and a walkover survey. A key output of this initial phase is the development of a Conceptual Site Model (CSM), which systematically identifies potential contaminant sources, exposure pathways and receptors at risk. Internationally recognised guidance, like the US EPA, UK Environment Agency, and Australia's NEPM, all mandate the use of a CSM as a foundational step in site assessment, ensuring that risk evaluations are based on a comprehensive understanding of site-specific conditions (NEPM, 2014; UK EA, 2020; US EPA, 2000a). This may be followed by field sampling, sample preparation and laboratory analysis to identify and quantify contaminants in line with established standards and procedures (ISO, 2018; UK EA, 2020; US EPA, 2000a).

CRA for AMLs essentially aligns with frameworks used in contaminated land assessment and follows a structured four-step evaluation involving hazard identification, hazard assessment, exposure assessment, and risk characterisation (ISO, 2017; OECD, 2021; UK EA, 2020; US EPA, 2022; WHO, 2010). The hazardous properties of a chemical, such as mobility, toxicity, persistence, and bioaccumulation, are intrinsic and independent of specific sites and are therefore considered consistent and measurable across contexts. AML assessment utilises toxicological benchmarks from existing hazard evaluations. As a result, detailed hazard characterisation to identify specific adverse effects or mechanisms of action is not usually undertaken. For this SEM, the sources and references for the hazard thresholds and characterisation are collated rather than attempting to document or retrieve detailed information about the hazard evaluation of individual substances. Conversely, the specifics of exposure assessment methods in the AML context are captured. Risk characterisation is conducted by comparing estimated exposure levels with toxicological thresholds, such as the Reference Dose (RfD) or Acceptable Daily Intake (ADI), to determine whether a significant risk exists. (ISO, 2017; OECD, 2021; UK EA, 2020; US EPA, 2022; WHO, 2010). The Outcome informs mitigation strategies, such as site remediation, which is the final stage of risk assessment and is not considered in this SEM.

Risk characterisation of AMLs is essential for evaluating individual sites, prioritising those requiring remediation, and developing sustainable, site-specific mitigation plans to protect affected receptors. The effectiveness of these outcomes largely depends on the approach or method employed, making method selection a critical step in the risk assessment process.

4.1.1 Scope and Objective

In the preceding chapter, an evidence map protocol was developed to systematically capture the range of methods used in assessing chemical contamination risks from abandoned coal and lead-zinc mines. The Protocol set out a structured approach to identify, extract, and synthesise data from the literature to provide a comprehensive overview (an evidence map) of methods used in assessing AML risks, and to draw on current practices from the pull. However, due to the extended peer-review process for publishing the Protocol and the time constraints of thesis submission, it was not feasible to complete data extraction for all studies within this timeframe.

To ensure that methodological insights from the identified literature are incorporated into this thesis, some data were extracted from the included studies (a total of 159), following the steps outlined in Section 3.2.6. These studies form the basis of the current chapter, which aims to present a narrative review of methods applied in the site-specific assessment of chemical contamination risks from abandoned coal and lead–zinc mine lands. The emphasis here is on synthesising methodological approaches across key stages of the risk assessment process, including abandoned mine details, exposure measurement (environmental sampling and analysis), exposure modelling, risk characterisation, and effect monitoring as found in research articles.

This narrative review should be understood as an interim application of the evidence map protocol, providing a focused methodological synthesis from a subset of studies while highlighting current practices, strengths, gaps, and limitations in AML risk assessments. In doing so, it offers immediate value and lays the foundation for the full evidence map, which will be completed and disseminated as a separate publication.

4.2 Summary of Methods

The methods applied in this chapter followed the Protocol developed in Chapter 3. This was prepared in accordance with the Preferred Reporting Items for Systematic Reviews and Meta-Analysis Protocols (PRISMA-P) and the PRISMA flowchart (Shamseer et al., 2015), in consideration of the Conduct of Systematic Reviews in Toxicology and Environmental Health Research (COSTER) recommendations (Whaley et al., 2020). The Protocol was submitted to the Journal of Evidence-Based Toxicology and underwent two rounds of peer review. It has been accepted for publication. Details of the manuscript, supplementary materials and all documents associated with the review process can be accessed via: https://doi.org/10.5281/zenodo.14246187.

A structured narrative synthesis format is being adopted for the narrative review. This approach enabled the integration of qualitative interpretation with descriptive quantitative summaries, allowing for systematic organisation of findings while maintaining the interpretive depth characteristic of narrative

reviews. The synthesis combined tabular and graphical representations of extracted data with thematic analysis to identify methodological trends, research patterns, and knowledge gaps in the evaluation of current methods.

Problem formulation was based on the aim and scope of the SEM, which was to identify current methods for assessing chemical risks from abandoned coal, lead, and zinc mine lands; therefore, the Population, Intervention, and Outcome (PIO) statement was adopted, with a timeframe from 2000 to 2024. This statement helped to address the research question, ‘‘What are current practices in the evaluation of chemical risks from abandoned coal and lead-zinc mines?’’ The key PIO elements of the question are summarised in Table 3.1 of the Protocol in Chapter 3. The Population was defined as the types of AML assessed, including Pb, Zn, Pb/Zn, and coal mines. The Intervention was defined as the chemical risk assessment methods applied in the study. The Outcome was defined as the risks or effects identified as impacting ecological and/or human receptors. We observed that studies conducting risk assessments inherently examined the receptors at risk. The PIO statement was used to develop the eligibility criteria presented in Table 3.2 of Chapter 3, which served as criteria for study inclusion.

4. 3 Results

4.3.1 Search Strategy, Data Management, Screening and Study Selection

The searches were conducted across the five bibliographic databases using the Boolean operations defined for each database, in accordance with Section 3.2.3 of Chapter 3, as of July 2024. Additional searches were conducted using the term “historic” following recommendations from one of the reviewers during the peer review process. Figures 4.1 and 4.2 show the number of hits retrieved from each database for the initial and additional searches, respectively. The two search phases yielded 3,762 records (Figure 4.1) and 495 records (Figure 4.2). The captured studies were retrieved as RIS files and subsequently uploaded to CADIMA, a data management software. They were merged, and CADIMA facilitated the identification of duplicate entries; some were automatically removed, while others were manually removed. After duplicates were removed, 2,670 and 487 records from the two search phases were screened at the title and abstract levels according to predefined eligibility criteria in Section 3.2.1 of Chapter 3. Following title and abstract screening, 495 and 38 studies were deemed eligible for full-text screening. The full texts of the eligible studies were downloaded. CADIMA automatically downloaded those it could access; others were downloaded using CITAVI, while the remaining articles were downloaded manually during the full-text screening. Articles written in languages other than English, such as Chinese, that could not be translated, were excluded. Articles that evaluated multiple mines and conducted a risk assessment, and specified the different mines to include either lead, zinc, or lead-zinc, were included, ensuring that the method used for the risk assessment was captured. This process facilitated the selection of eligible studies for the review. After full-text assessment, 149 and

10 articles were retained for inclusion in the data extraction inventory, while a total of 346 and 28 non-eligible studies were excluded. The reasons for exclusion are provided in Figures 4.1 and 2. The screening process was conducted by the evaluator, with 15% of the records independently verified by a second reviewer in parallel using CADIMA to ensure consistency. In cases of discrepancy, reviewers discussed and resolved differences through consensus at both stages. The primary discrepancies encountered during the title and abstract screening stage were associated with studies that did not specify whether the mine was abandoned or active, or failed to indicate whether the mines investigated were among those of interest. Such studies were initially excluded, as were those that did not explicitly state whether risk assessment was conducted. However, reviewers agreed that these studies should be retained for verification during full-text screening. At the full-text screening stage, the main discrepancies arose from studies that assessed multiple mines. Reviewers agreed that if any of the mines studied were abandoned and included those within our scope, the study should be included to ensure that risk assessment methods were not missed.

4.3.2 Data Extraction and Analysis

The evaluator carried out the data extraction. PDFs of all eligible studies were downloaded from CADIMA, along with an accompanying Excel file containing their bibliographic information. The bibliographic data were imported into the developed data extraction template (see Section 3.2.6, Chapter). Before commencing extraction, the codebook (Section 3.2.6, Chapter 3) was reviewed to ensure consistency in data handling. Each article was systematically examined, and information relevant to the research aim, as highlighted in the data extraction sheet, was extracted from the appropriate sections of the studies.

Data were extracted from 41 of the 149 included studies and organised and analysed descriptively. The findings were summarised in a figure and tabular form, accompanied by a narrative review describing the key characteristics of the investigated AMLs. The review focused on site-specific details of coal and lead/zinc mines, exposure measurement, exposure modelling, effect monitoring, and risk characterisation approaches. This descriptive approach highlights the range and frequency of methodologies employed in AML risk assessments, as well as the aspects identified by researchers as important within the included studies.

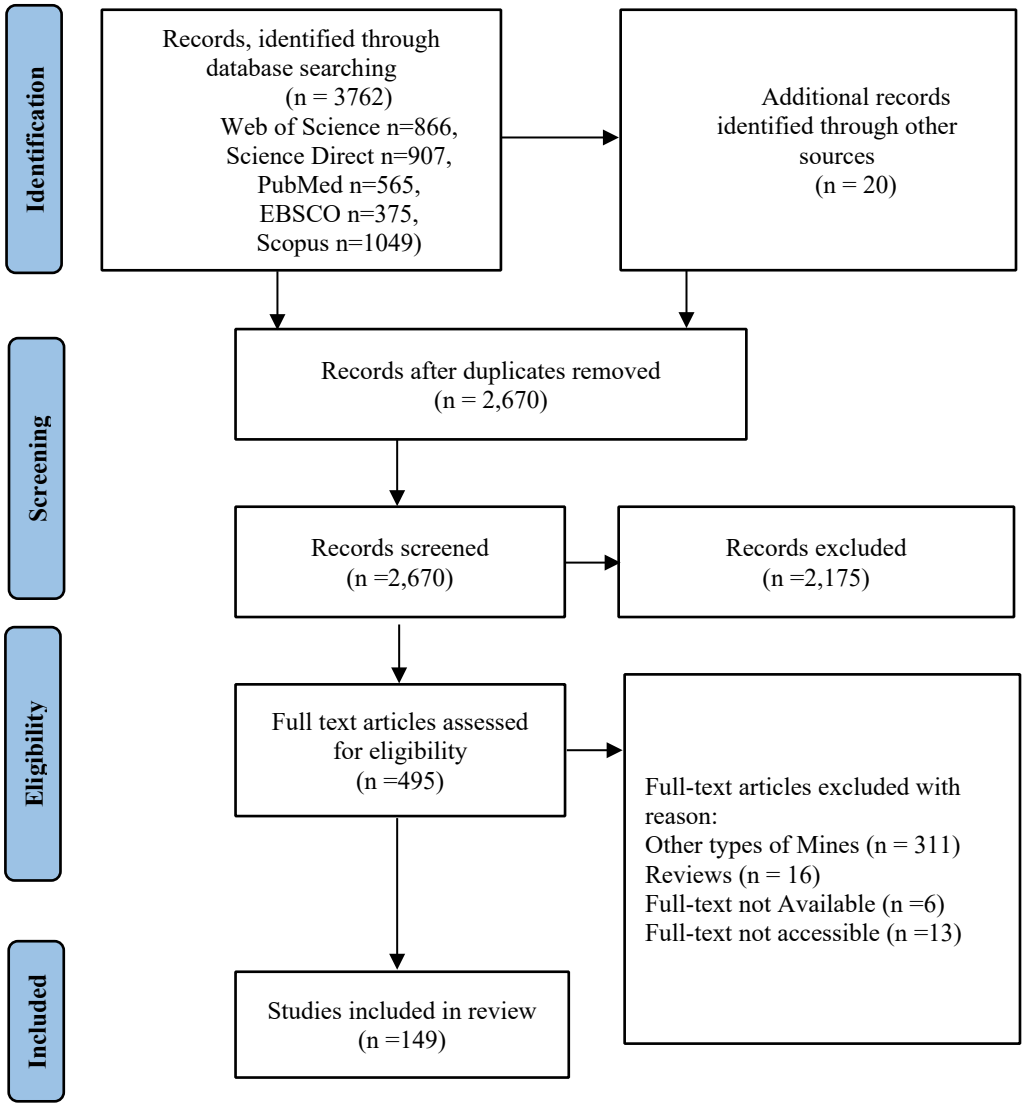

Figure 4.1: PRISMA flowchart (Moher et al., 2015) for the selection of studies, highlighting the searched databases, identified, screened, excluded and included studies.

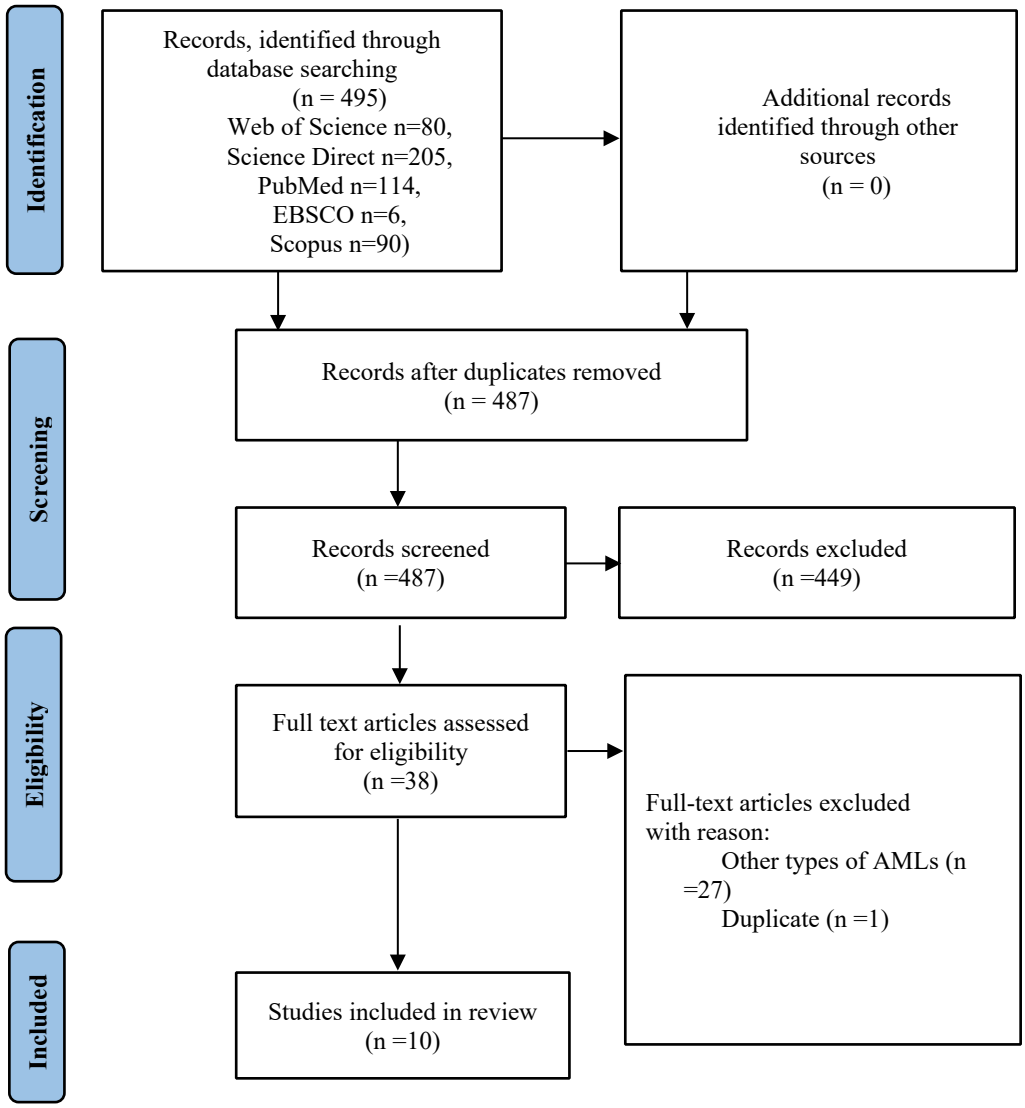

Figure 4.2: PRISMA flowchart (Moher et al., 2015) for the selection of studies from the updated search, highlighting the searched databases, identified, screened, excluded and included studies.

4.3.3 Reviewed Articles

The number and publication dates of the reviewed articles are shown in Figure 4.3. A steady increase in the number of publications is observed from 2002, with a notable surge after 2018 and a peak in 2021. Although the number of articles is not as large, this trend suggests a growing research focus on understanding and managing risks associated with contamination from legacy mine sites. The geographic distribution of the studies shows that most of the studies are from Asia, particularly China(n=12) and Korea (n=6), followed by Africa, Morocco (n=4) and Tunisia (n=3), with contributions from Europe and North America. China, emerging as the primary contributor to the body

of reviewed literature, is consistent with its extensive mining history, which has led to the expansion of environmental research programs.

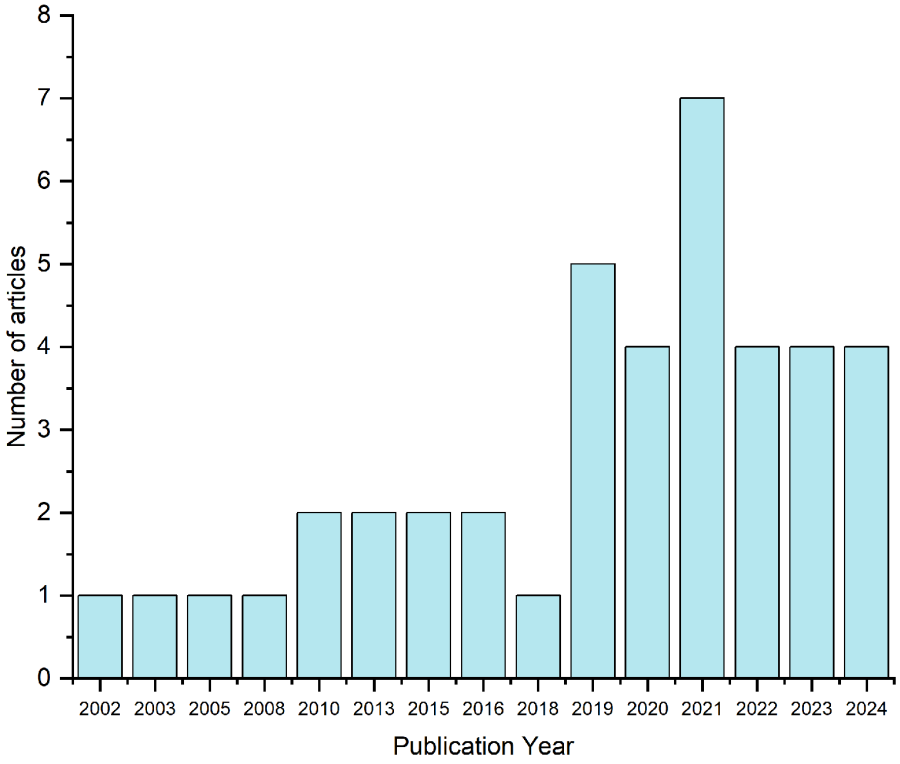

Figure 4.3: Publication years of the articles focusing on evaluating chemical contamination risks from abandoned coal and Pb/Zn mine lands.

Funding sources revealed predominance of publicly funded research (Figure 4.4). Over half of the studies (n=26) acknowledged support from national or government agencies, while a significant proportion of studies (n=11) did not report funding information. The predominance of publicly funded studies highlights strong governmental involvement in addressing mine-related contamination. Unreported funding records were more common in older studies (J. Y. Kim et al., 2005; Milton & Johnson, 2002), suggesting that disclosure of research funding sources was not consistently required or prioritised in earlier publications.

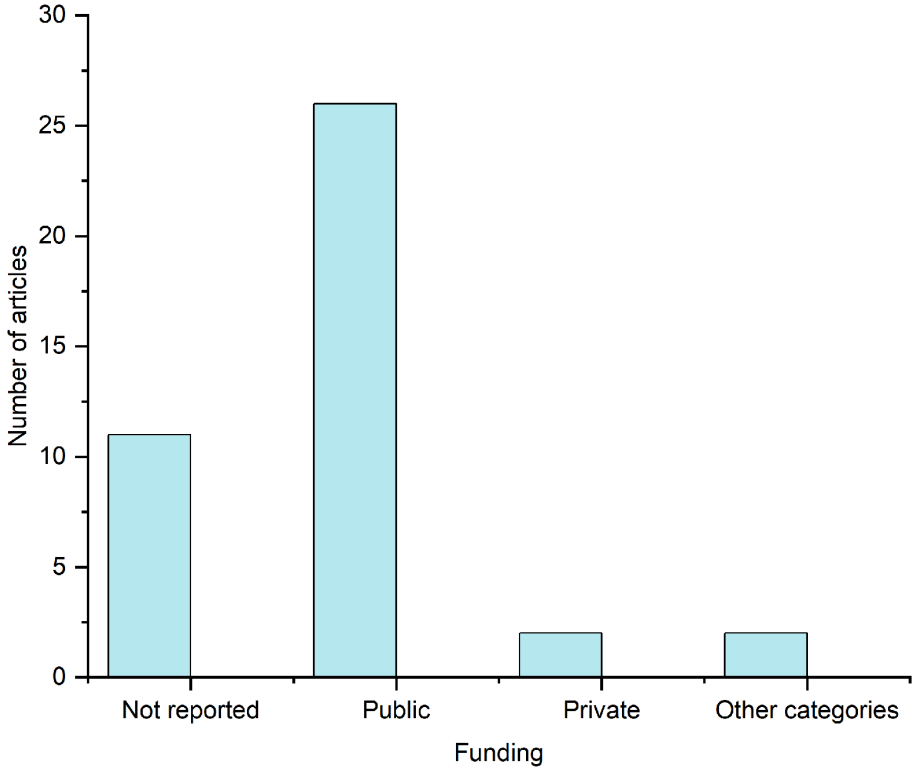

Figure 4.4: Research funding sources from reviewed articles showing the different categories of sources, with public funding the most reported.

4.3.4 Abandoned Coal and Lead-Zinc Mines Identified

Across the reviewed studies, the mine types (Figure 4.5) investigated showed that lead–zinc abandoned mines (58.5%) were the most frequently examined, followed by coal mines (22%), whereas lead-only and zinc-only sites appeared less often. The predominance of Pb–Zn AMLs reflects their complex contamination profiles, as these sites are often associated with the release of multiple toxic metals like Pb, Zn, Cd, and As (Gutiérrez et al., 2016), which pose significant ecological and human health risks. In contrast, coal-related studies, though fewer, focus on acid mine drainage and associated trace metal mobility after abandonment. The comparatively limited attention to single-metal (lead or zinc) mines results from their smaller geographical footprint, as geological mineralisation of these metals is commonly associated with each other (Koski & Mosier, 2012; Yu et al., 2025).

The mining methods (Figure 4.6) practised during mine operations were commonly not documented. A small number of articles identified open-cast (n=8) and underground (n=7) mining operations, which reveal historical importance in both coal and Pb/Zn extraction, each associated with distinct contamination pathways, such as acid mine drainage and subsurface leaching in underground workings (D. Chen et al., 2021; F. Wang et al., 2024) versus surface runoff and tailings dispersion in open-cast systems (Prathap & Chakraborty, 2019). Meanwhile, over half of the studies did not report the mining method (n=23). This may be due to insufficient site documentation or a secondary focus on contamination outcomes rather than the mining context. Given that mining methods strongly influence

contaminant behaviour and exposure potential, consistent reporting of this parameter is essential for improving the accuracy and comparability of risk assessments across AMLs.

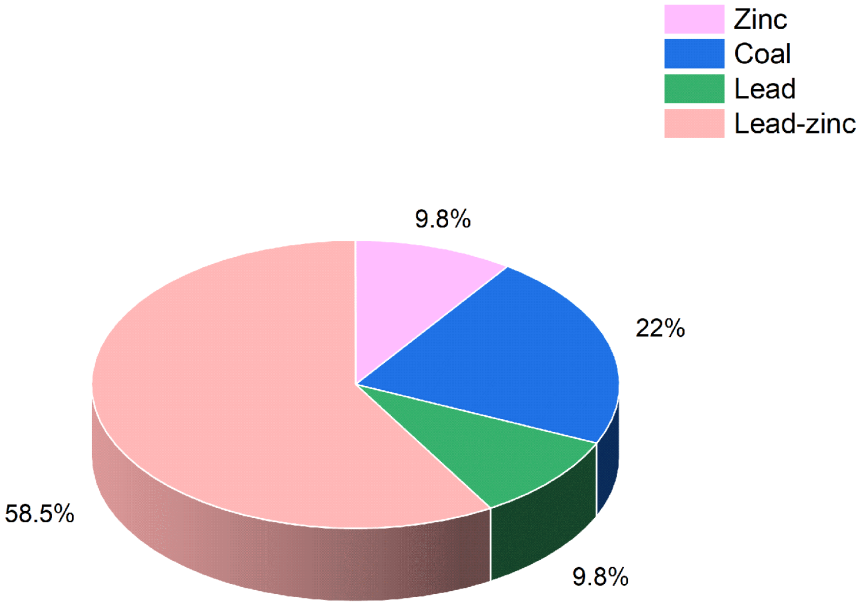

Figure 4.5: Abandoned mine land types identified across the reviewed articles

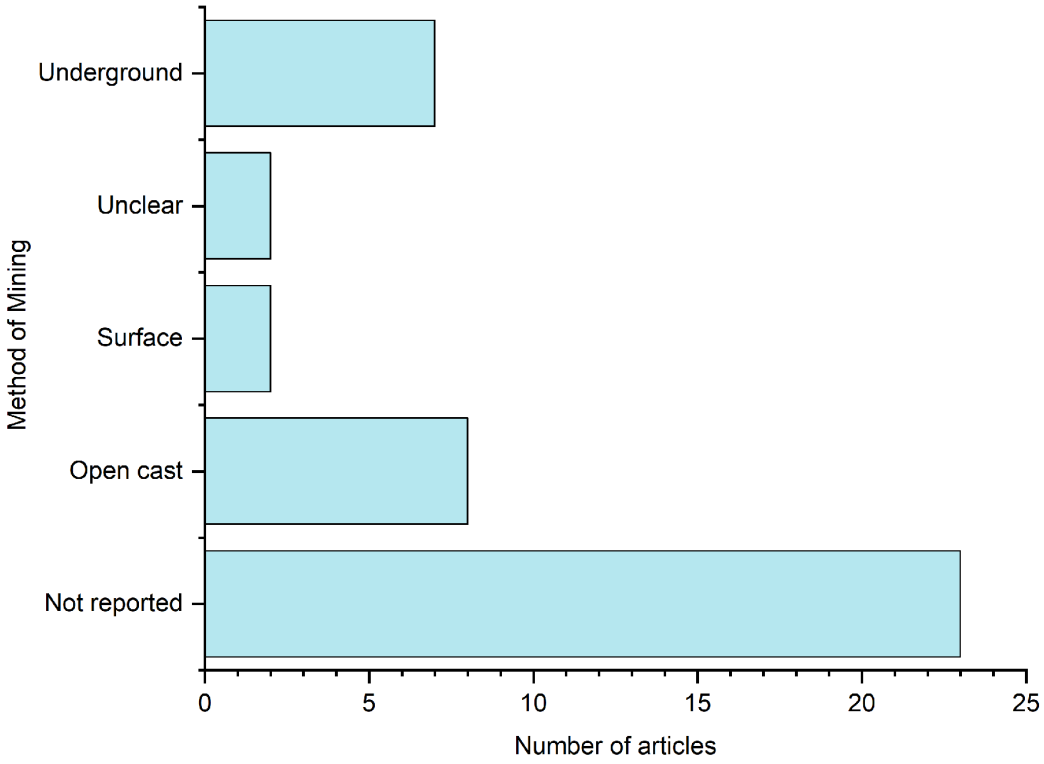

Figure 4.6: Methods of mining recorded

We examined the years the mines were abandoned to determine their operational duration and gained insight into their level of impact from the studies. Figure 4.7 shows articles reporting the details. Most articles (n=28) provided the year of abandonment, while a substantial number did not report it (n=7); others either did not specify, or the information was unclear. Among studies that reported the year of mine abandonment, most sites were closed in the 1980s and 1990s, with a noticeable peak between 1985 and 1992 (Figure 4.8). Fewer sites were abandoned before 1970 and after 2000, possibly due to limited historical data for older sites and the relatively recent nature of mine closure for newer ones. This pattern aligns with the global decline in small- and medium-scale mining operations, driven by resource depletion (B. Huang et al., 2018; Son et al., 2019), economic shifts, and evolving environmental regulations. Fewer studies are concentrated on mines abandoned before 1970 or after 2000, possibly due to limited historical data for older sites and the relatively recent nature of closure for newer ones. The temporal concentration of reported abandonment years underscores how mid-to-late 20th-century mining activities continue to shape current contamination legacies and motivate ongoing risk evaluations.

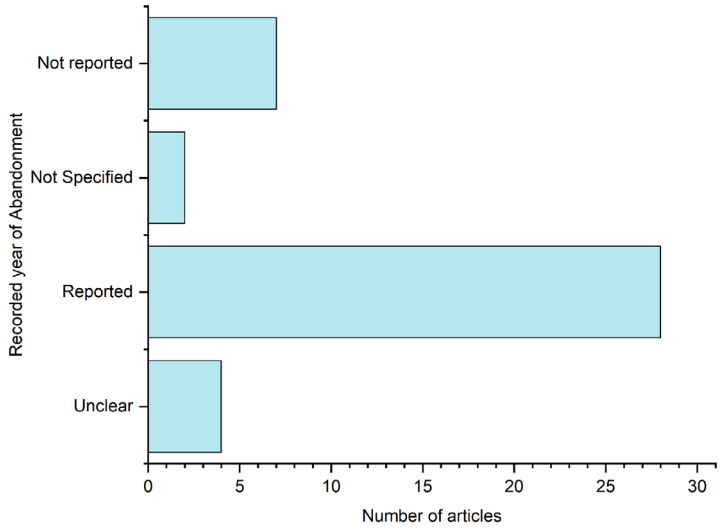

Figure 4.7: Number of articles reporting year of abandonment. Over 50% of the reviewed articles reported the year the mines were abandoned, while others either did not report the year at all or provided unclear and nonspecific information.

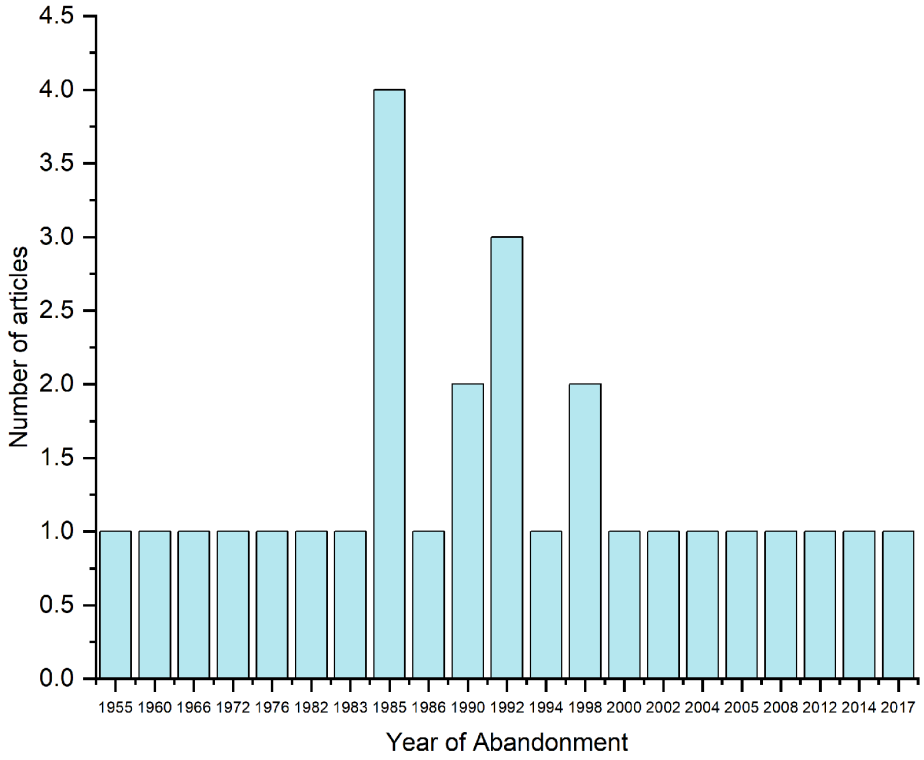

Figure 4.8: The year of abandonment reported for coal, lead-zinc, lead and zinc abandoned mines considered across the reviewed studies. Abandonment peaked from 1985 to 1992. There was a slight increase before and after this period, except in 1998.

4.3.5 Exposure Measurements

Exposure measurements accounted for the different media, sampling strategies, sample preparation, storage, analytical methods conducted and the types of contaminants being measured prior to risk assessments. The evaluation of exposure media across the reviewed studies revealed a predominant focus on soil (Figure 4.9), which accounted for most of the contamination and risk measurement sources (n = 78). Sediment (n = 43) and tailings (n = 33) were also frequently assessed. Additionally, water (n = 31) and other samples (n = 31) were commonly assessed. The category "others" primarily comprised plant and animal matrices, including animal tissues, human biomarkers (such as blood samples), and vegetables and grains. Dust and rock were the least studied (n = 3 each). The dominance of soil, sediment, tailings, and biological matrices highlights surface contamination processes and chronic exposure routes. At the same time, the relatively few studies that report on airborne and geologically related pathways point to emerging gaps for future research in exposure characterisation at abandoned coal and Pb/Zn mine sites.

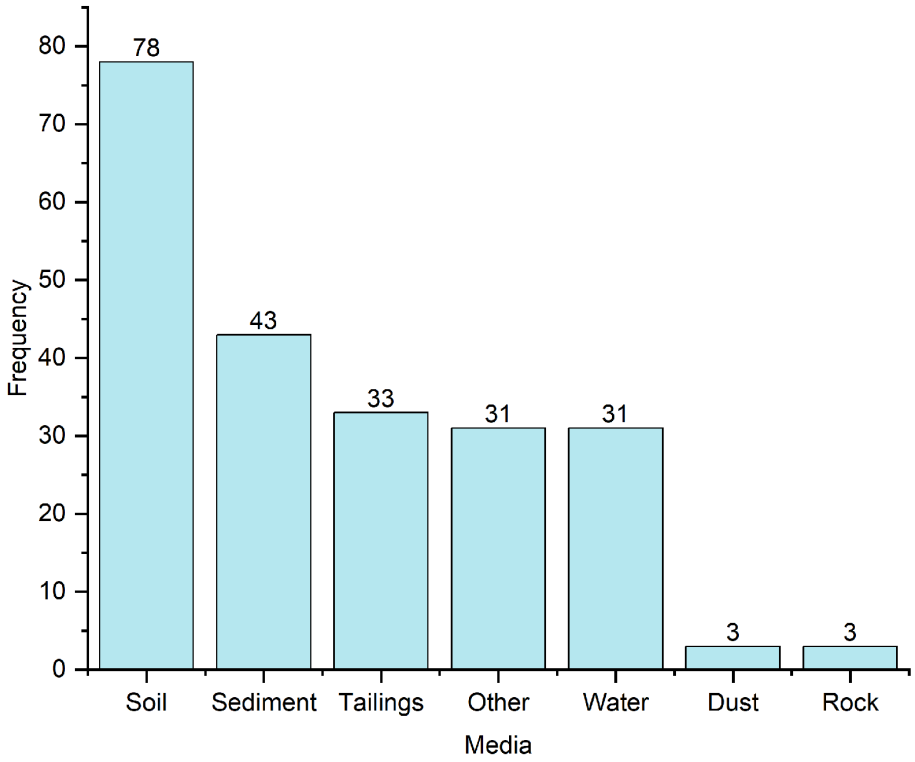

Figure 4.9: The different types of environmental media, with frequency representing the exposure measurements across the media in the reviewed studies. Soil was the most frequently assessed media, followed by sediment, tailings, and water. Other categories primarily included plant and animal matrices such as vegetables, grains, plant and animal tissues, and blood samples.

A range of sampling strategies, storage methods, and preparation procedures were reported in the reviewed studies. The most applied sampling strategies included depth profiling, spatial (upstream/downstream), grab, random, temporal (seasonal, periodic, proximity, and gradient), systematic grid, and transect designs (Chanpiwat & Numprasanthai, 2024; Del Rio-Salas et al., 2019; Nobuntou et al., 2010). Most samples were transported on ice and then refrigerated (~4 °C) or frozen (−20 °C) until processing to prevent transformation (D. Chen et al., 2021). Water samples were commonly acidified with nitric acid (HNO_3) to pH < 2, sometimes with hydrochloric acid (HCl) to stabilise analytes (Nassiri et al., 2021). Storage containers were primarily polyethylene (PE), high-density polyethylene (HDPE), or polypropylene (PP) for soils and waters metal analyses, with glass or amber glass used unless there was a risk that the chemicals could stick to the plastic or break down in light (Alvarenga et al., 2013; Qin et al., 2021). These approaches align closely with international standards for trace-metal preservation, and the frequent specification of holding times (<24 h) and pre-cleaned, acid-washed bottles indicates general regulatory compliance (US EPA, 2000a). While polyethylene and polypropylene containers are suitable for sample storage for metal analyses, they may

not be ideal for organic compounds, as certain organics can leach from plastic surfaces. In such cases, glass or amber glass containers are preferred to avoid contamination.

Sample preparation protocols were broadly consistent but tailored to each study's aim and matrices evaluated. Most studies focused on metals, while only one study considered organics, that is, total petroleum hydrocarbons (Rodriguez-Ruiz et al., 2015) alongside metals. Solid samples were typically dried (either in air or an oven), then sieved to a particle size of ≤2 mm (with some studies targeting finer fractions, specifically <63–150 μm), and homogenised/ground before analysis. Water samples and prepared extracts were commonly filtered with (0.45/0.22 μm) filters. For quantifying total metal(loid)s, studies predominantly used microwave-assisted acid digestion using Aqua regia (HNO_3 and HCl), sometimes with hydrofluoric acid (HF) and hydrogen peroxide (H_2O_2) (Z. Sun et al., 2020). Four studies applied sequential extraction using the European Community Bureau of Reference (BCR) schemes (Nassiri et al., 2022), while other studies used single-extractant tests, including ethylenediaminetetraacetic acid (EDTA), calcium chloride (Son et al., 2019), and ammonium acetate to characterise chemical forms, bioavailability, and potential mobility. Other studies assessed human-relevant availability using in-vitro bioaccessibility assays with the Unified BARGE Method (UBM) and the Solubility/Bioaccessibility Research Consortium method (SBRC) (Pérez-Sirvent et al., 2016). At the same time, waste leachability was evaluated via the toxicity characteristic leaching procedure (TCLP) and the synthetic precipitation leaching procedure (SPLP) using EPA Methods 1311 and 1312, respectively.

A variety of analytical techniques were employed to determine contaminants across the different samples in the reviewed studies (Figure 4.10). Among these, Inductively Coupled Plasma–Mass Spectrometry (ICP-MS) was the most frequently used method (31.7%) to measure metals/melloids, predominantly for biological samples and solid or liquid samples collected far from contaminant sources, its use reflects not only its superior precision and multi-element detection capability, but also its selectivity and effectiveness in complex or organic-rich matrices where interferences are common (Sartorius et al., 2022; Q. Xu et al., 2024; J. Yang et al., 2015). Inductively Coupled Plasma–Atomic Emission Spectroscopy (ICP-AES)/Inductively Coupled Plasma–Optical Emission Spectroscopy (ICP-OES) (27%) are interchangeable terms used for the same technique and were also widely used, valued for their robustness and accuracy in quantifying metals in soil, sediment, and water samples. Atomic Absorption Spectroscopy (AAS) (7.9%), Atomic Fluorescence Spectroscopy (AFS) (6.3%) and X-ray Fluorescence (XRF) (6.3%) were also employed less frequently for metal determination. Other techniques, including Gas Chromatography–Mass Spectrometry (GC-MS), Liquid Chromatography–Mass Spectrometry (LC-MS), and High Performance Liquid Chromatography (HPLC) (1.6%), were occasionally used to determine organics and metabolites (Rodriguez-Ruiz et al., 2015; Ushakova et al.,

2022). X-ray Diffraction (XRD) (6.3%) and Scanning Electron Microscopy (SEM) (4.8%) were primarily used for mineralogical and microstructural characterisation of solid samples.

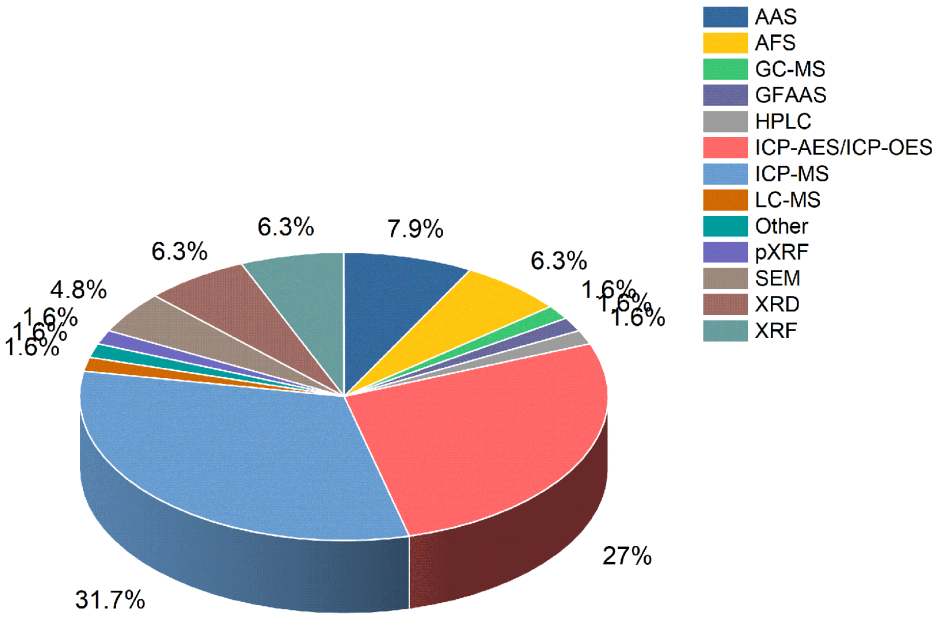

Figure 4.10: Analytical techniques used for contaminant quantification and mineralogical characterisation in reviewed studies. ICP-MS was the most frequently used, followed by ICP-AES/ICP-OES. Other techniques, such as AAS, AFS, and XRF, were used less often. pXRF was used as a field-based tool for rapid contaminant measurement, while SEM and XRD were primarily used for mineralogical and structural characterisation of contaminated materials.

The reviewed studies also showed that Pb and Zn were the most frequently measured contaminants (Figure 4.11). Followed closely by Cd, Cu, and As. Other commonly reported contaminants included Cr, Ni, Mn, and Fe. Trace elements such as Hg, Co, Sb, Se, and V were reported less frequently. Elements including Be, Th, Al, Mo, Ba, Zr, Ti, and Sr were rarely analysed in the studies. Only one study analysed TPH (C_{10}–C_{40}) (Rodriguez-Ruiz et al., 2015), indicating occasional consideration of hydrocarbon residues at coal-related sites. The measured contaminants were reported across various environmental samples (soil, water, tailings, sediments, and biota), and some studies evaluated multiple media (J. Y. Kim et al., 2005; Mehta et al., 2020; Nikolaidis et al., 2010). Therefore, the frequency does not represent the exact number of studies reviewed.

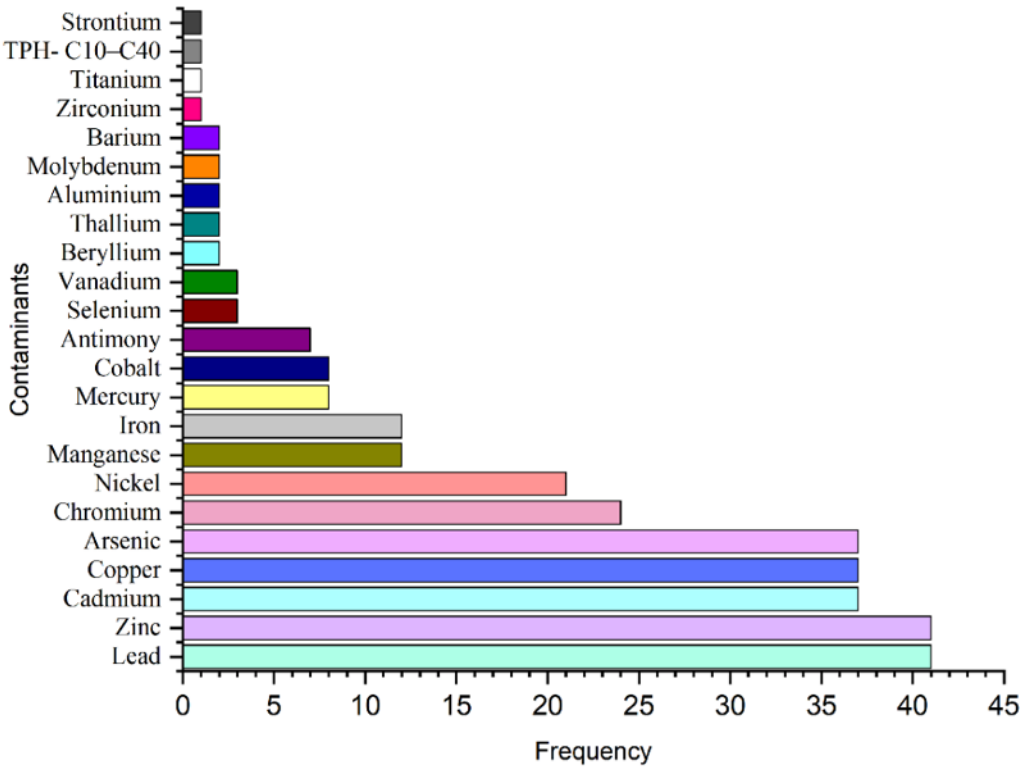

Figure 4.11: Frequency of contaminants measured in the reviewed articles. Pb and Zn were the most commonly assessed contaminants, followed by Cd, Cu, and As. Other frequently analysed metals included Cr, Ni, Mn, and Fe, while trace elements such as Hg, Co, Sb, Se, and V were measured less frequently. The reported frequencies reflect that many studies analysed multiple environmental media (e.g., soil, water, sediment, and biota), leading to repeated contaminant measurements across different matrices.

4.3.6 Exposure Modelling

In the reviewed studies, various exposure modelling approaches (Table 4.1) were used to estimate exposure and further assess potential health risks linked to the investigated sites.

Table 4.1: Summary of exposure modelling methods used, and contaminants considered in the reviewed studies. Most models were based on US EPA frameworks for estimating human exposure and health risks.

Method	Contaminant	Reference	Number of articles
Average daily dose (ADD)	Zinc, lead, copper, nickel, cadmium, arsenic, cobalt and chromium	US EPA, 1991 and APAT-ISPRA, 2008	4
Chronic Daily Intake (CDI)	Arsenic, cadmium, chromium and lead	US EPA 1989, 2011a, 2011b, 2009, 2013; US EPA, 2001	2
Estimated daily intake (ADD)	Cadmium	MHWK 2007, Jang et al. 2007 and US EPA 1997	1

Predicted average daily dose	Arsenic, cadmium, chromium, copper, mercury, nickel, lead, zinc, manganese and antimony	US EPA 2001 and 2002	1
Risk Based Corrective Action (RBCA) tool kit	Arsenic	ASTM 1998	1
Estimated mean daily zinc intake	Zinc	Hunter al. 1987	1
Average daily metal intake (ADI)	Arsenic, cadmium, chromium, nickel, lead	US EPA, 2001; Ghouma et al., 2022	2
Estimated dietary intake (EDI)	Cadmium, lead, and cadmium	MHWK 2007, Jang et al. 2007 and US EPA 1997; US EPA 2007	2

Among the reviewed articles, 13 studies conducted exposure modelling to estimate contaminant exposure. The most frequently employed approaches included ADD and CDI models, as shown in Table 4.1, to estimate metal exposure through ingestion, inhalation, and dermal contact. The reference list showed that most of the methods were adapted from the US EPA guidance on human health risk assessments (US EPA, 2001, 2007). Other models used were the Average Daily Metal Intake (ADI), Estimated Dietary Intake (EDI) and Predicted Average Daily Dose; these appear to be author-modified terms, as the authors cite US EPA guidance.

The Risk-Based Corrective Action (RBCA) toolkit and estimated mean daily zinc intake methods appeared less frequently. One study (J. Y. Kim et al., 2005) considered tailings as source media and leaching as a pathway for contaminant transport to target media (groundwater), utilising the RBCA toolkit. However, for the estimated mean daily zinc intake method (Milton & Johnson, 2002). It was unclear whether pathway and target media were considered, except that the model outcomes were compared with reference values from a non-contaminated AML site to infer risk.

Notably, some studies focused on exposure to a single contaminant, such as cadmium, arsenic, and zinc. In contrast, others considered multiple contaminant exposures, such as the combinations of arsenic, cadmium, and lead.

4.3.7 Risk Characterisation

This section explains how risk characterisation in the reviewed studies combined exposure measurements and estimates with established toxicity benchmarks. It covers various sources and pathways of contamination considered when evaluating potential adverse effects on both human and ecological receptors. The primary sources of contamination (Figure 4:12) identified across the literature were contaminated soils (n = 20), contaminated water (n = 14), and contaminated sediments (n = 10), which were the most frequently reported. These three media represent the main environmental compartments where contaminants are concentrated, mobilised, and made bioavailable. Food crops (n = 8), which were also reported as a source of contamination, reflect the transfer of metals such as Pb,

Cd, Zn, and As from soil to edible plant parts through root uptake and foliar deposition (Lee & Chon, 2003; J. Yang et al., 2015). Contaminated tailings (n=5) were assessed in some studies, while others examined contaminated waste dumps (n=3) and tailings and waste dumps (n=3) together. These were identified as major sources of contamination, contributing to secondary pollution in surrounding soils, water bodies, and food systems. Only two studies reported animal products (n=2) (Alvarenga et al., 2013; Sartorius et al., 2022). As a source of contamination, it signified bioaccumulation and trophic transfer through the food chain. Airborne particulates ($PM_{2.5}$ and PM_{10}) and contaminated dust (n=1 each) were the least considered sources, suggesting that airborne pathways are comparatively underexplored despite their potential importance for human inhalation exposure. Other (n=1) represents the study that considered multiple sources for risk characterisation (Nouairi et al., 2019). Several studies considered multiple contamination sources at the same site; hence, the number of articles is not mutually exclusive.

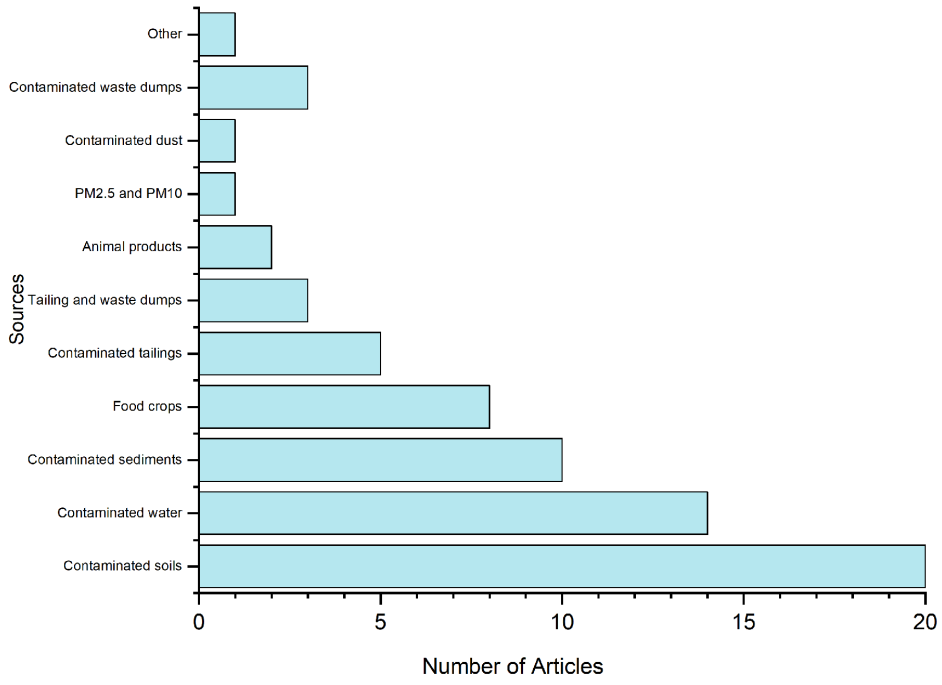

Figure 4.12: Main sources of contamination identified in the reviewed articles. Contaminated soils, water, and sediments were most frequently reported, followed by food crops, tailings and waste dumps. Airborne particulates ($PM_{2.5}$ and PM_{10}) and contaminated dust were the least studied.

Recorded exposure pathways (Figure 4.13) revealed that ingestion (n = 20) was the most frequently assessed exposure pathway, emphasising the predominance of exposure through consumption of contaminated soil, water, or food. Furthermore, this pathway reflects the significant contribution of oral intake to total metal exposure, particularly for communities living near abandoned mine lands (Q. Xu et al., 2024; J. Yang et al., 2015). Dermal contact (n = 5) and inhalation (n = 3) followed, although both

represent important secondary exposure routes, especially in areas affected by dust resuspension (P. Santos et al., 2023; Yahyaoui & Ben Amor, 2024). One study considered root uptake as a pathway for contaminant transfer from contaminated waste dumps to plants (Milton & Johnson, 2002). Many studies did not explicitly state the exposure pathway; these were categorised as unclear (n = 22) or not reported (n = 6), indicating that the exposure pathway was either insufficiently described or embedded within generalised risk estimates without explicit specification. This lack of clarity limits comparability across studies and reduces the precision of cumulative exposure assessments (Bouzekri et al., 2020; Zineb et al., 2024). A few studies described other (n = 3) pathways, which included combined or indirect exposure routes.

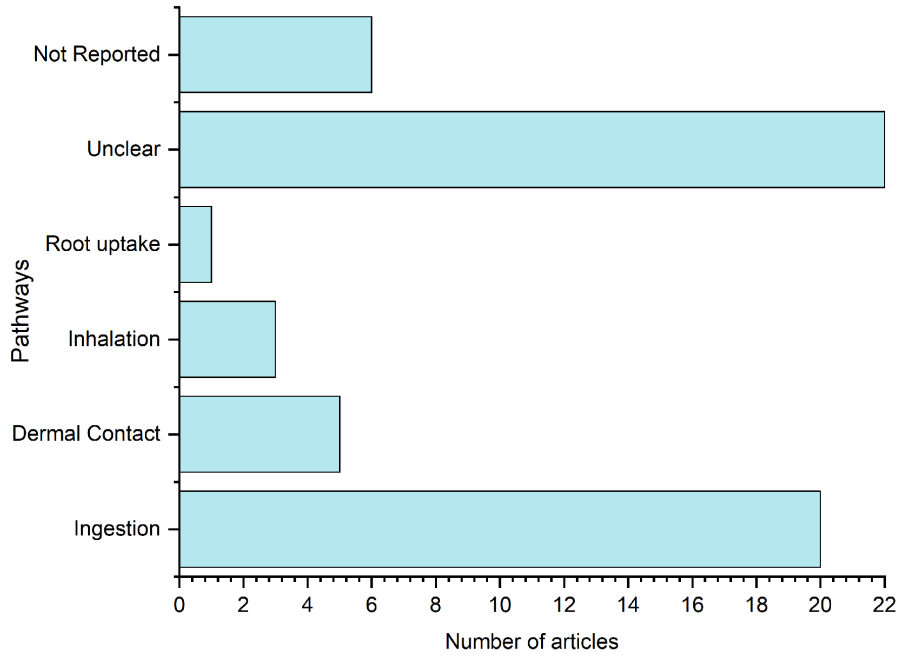

Figure 4.13: Exposure pathways considered across studies. Ingestion was the most frequently assessed pathway, followed by dermal contact and inhalation. Many studies did not specify or clearly report the exposure route; they are categorised as unclear and not reported. Several studies considered multiple contamination pathways within the same site. Hence, the number of articles is not exact in some cases.

Among the receptors identified to be potentially exposed to contaminants (Figure 4.14), humans (n = 20) were the most frequently assessed receptors, reflecting a strong emphasis on human health risk assessments, particularly those estimating non-carcinogenic and carcinogenic risks associated with exposure to metals such as Pb, Cd, As, and Zn through soil, water, and food (Sartorius, 2024; Yohannes et al., 2021). Animals (n=7) appeared in fewer studies, and plants (n=2) were the least frequently assessed despite their critical roles as both receptors and mediators of contaminant uptake in terrestrial ecosystems. In several cases, receptor categories were classified as unclear (n = 17) or not reported (n = 4) because the articles did not specify them. This implies that receptors were assumed implicitly,

limiting the interpretation of which receptors are actually at risk. Summarising the source–pathway–receptor findings reveals that the high number of unclear or unreported pathways and receptors is mainly due to the use of risk-assessment indices that do not require explicit source–pathway–receptor inputs to estimate potential risk.

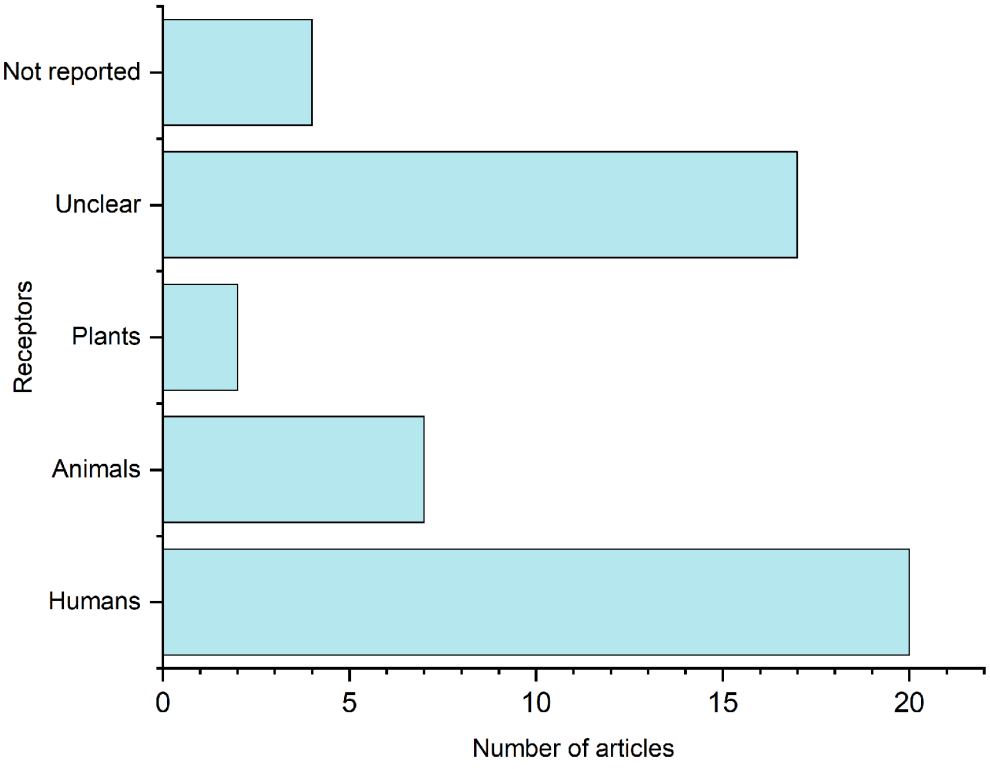

Figure 4.14: Receptors considered in the articles. Humans, followed by animals and plants, were the most frequently reported receptors. Several studies did not specify or clearly report the category of receptors being assessed.

4.3.7.1 Risk Assessment (RA) Methods

Several risk assessment methods (n = 54) were identified in the reviewed studies, reflecting variations in approach and application. Some studies adopted standard frameworks such as those developed by the US EPA, WHO, EU, and CCME to quantify risk. In contrast, others employed modified versions of existing methods or developed site-specific approaches to evaluate potential risks. Table 4.2 presents a summary of the most and least frequently used risk assessment methods from the body of literature, while each of the methods and corresponding references as recorded from each article reviewed are provided in Appendix 4.1.

As shown in the table, the Geoaccumulation Index (Igeo) was the most frequently applied method (n = 13), followed by the Hazard Quotient (HQ) (n = 12) and the Potential Ecological Risk Index (Er) (n =

10). Other methods, including the Contamination Factor (Cf) (n = 7), Sediment Quality Guidelines (SQGs) (n = 6), Carcinogenic Risk (CR) (n = 6), and Enrichment Factor (EF) (n = 6), were also commonly used, and Background values (n = 2) appeared in two studies (L. M. Huang et al., 2013; Nouairi et al., 2019). Other methods were used as a single approach to evaluate risk for one contaminant source among several methods considered for the same site. The combination of quantitative indices and model-based frameworks highlights both traditional and emerging practices in AML risk assessment.

Table 4.2: Summary of the most to least frequently used risk assessment methods reported in the reviewed literature.

Risk Assessment Method	Frequency
Geoaccumulation Index (Igeo)	13
Hazard Quotient (HQ)	12
Potential Ecological Risk (Er)	10
Contamination factor (Cf)	7
Sediment Quality Guidelines (SQGs)	6
Carcinogenic Risk (CR)	6
Enrichment Factor (EF)	6
Background values	2
Single-factor pollution index (Wi)	1
CESQ & Background values	1
National Food Safety Standard of China and General Standard for Contaminants in Food	1
Soil Environmental Quality Standards	1
Single-factor pollution index	1
Evaluation criteria limits	1
Drinking Water Guideline	1
Heavy Metal Evaluation Index (HEI)	1
Mean ERM Quotient (M-ERM-Q)	1
Sediment Pollution Index (SPI)	1
China Standards for Drinking Water Quality	1
Bioconcentration Factor (BCF)	1
Heavy metal pollution index (HPI)	1
Geochemical background values	1
Guidelines for drinking water quality	1
Potential leaching risk	1
Benchmark dose levels (BMDLs)	1
Single-Factor Pollution Index (PI)	1
Carcinogenic Health Risk	1
Noncarcinogenic Health Risk	1
Incremental Lifetime Carcinogenic Risk (ILCR)	1
Hazard Average Quotient (HAQ)	1
Integrated Risk	1
Soil Threshold and Guideline values	1

Cancer Risks	1
Degree of contamination (Cd)	1
EU drinking water guidelines	1
Maximum Allowable Concentration (MAC)	1
Crustal Enrichment Factors (EFc)	1
National background	1
USEPA Eco-SSLs	1
USEPA HHB-SSLs	1
Background values of soil elements in China	1
Enrichment factor (EF)	1
Biological Exposure Indices	1
Environmental standards for water quality	1
Food Safety Standard	1
Worrisome levels of soil contamination in Korea	1
Maximum Tolerable Value in Irrigation Water	1
Translocation factor (Tf)	1
Contamination index (CI)	1
World Average Natural Soils	1
Maximum Allowable Limit	1
Reference values from control sites	1
Logistic regression models and linear regression models	1

The studies were categorised (Figure 4.15) according to the type of risk assessment performed. Human health risk assessments were the most frequent, accounting for 39.7% of the studies. Ecological risk assessments accounted for 27.6%, while studies evaluating both human and ecological risks accounted for a smaller share (1.7%). An equal proportion of studies (1.7% each) were classified as not reported or other categories, and 27.6% of the studies were deemed unclear when the risk category was not explicitly specified.

Collectively, these findings depict a research landscape that remains rooted in traditional risk assessment indices while gradually evolving towards more integrated, data-driven, and probabilistic methods of risk characterisation.

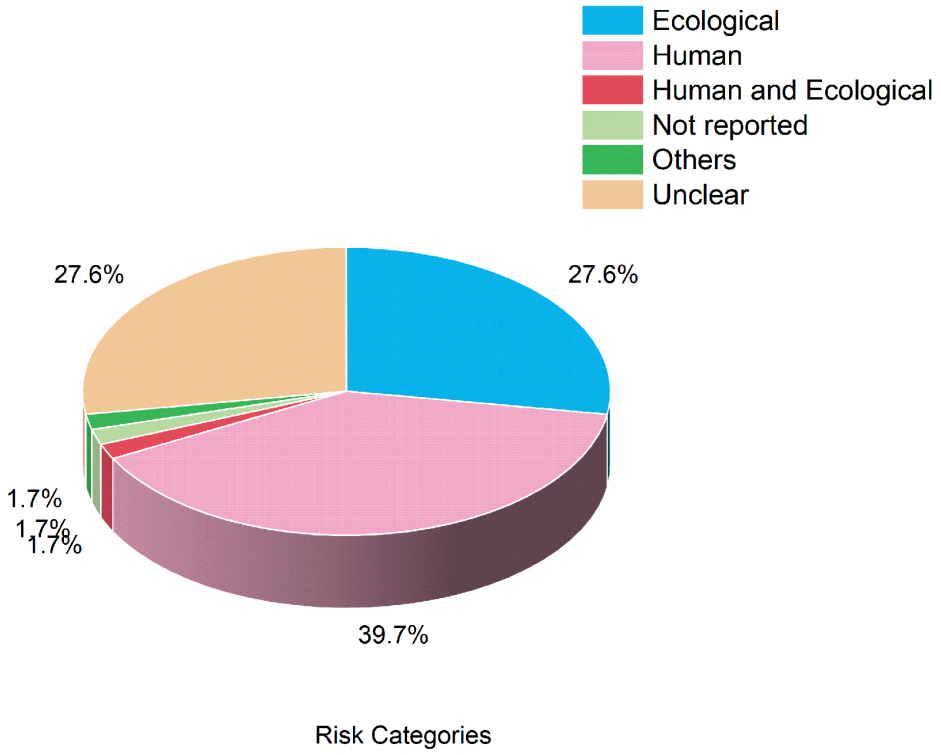

Figure 4.15: Distribution of risk categories among studies. In increasing order, Human, ecological and both human and ecological risk were assessed.

4.3.7.2 Mixture Risk Assessment (MRA)

Some studies considered MRA methods, reflecting efforts to evaluate the combined effects of multiple contaminants rather than individual ones. These approaches integrate various exposure and toxicity metrics to assess the cumulative or interactive risks posed by complex contaminant mixtures identified at the AML sites. The methods identified varied in complexity, ranging from traditional indices to more advanced statistical and probabilistic models. The methods and their respective references are presented in Appendix 4.2.

A total of 14 mixture risk assessment methods were identified across the reviewed studies. The Potential Ecological Risk Index (RI) was the most frequently used (n = 10), followed by the Hazard Index (HI) (n = 8). Other commonly employed methods included the Pollution Load Index (PLI) (n = 3), Heavy Metal Pollution Index (HPI) (n = 2), and Total Carcinogenic Risk (TCR) (n = 2). Several additional indices were reported only once, such as the Nemerow Comprehensive Pollution Index (Pn and PC), the Comprehensive Pollution Index (Wn), the Degree of Contamination (Cd), and the Modified Contamination Degree (MCd). More complex approaches were also utilised, including Bayesian Kernel Machine Regression (BKMR) and cumulative probability distribution analyses for the Hazard Index (HI) and Incremental Lifetime Cancer Risk (ILCR). These results indicate that most mixture assessments relied on conventional additive indices (Qin et al., 2021), whereas a few recent studies have

incorporated probabilistic and machine learning approaches (Z. Sun et al., 2020; Q. Xu et al., 2024). Of the 33 studies that conducted a risk assessment, 20 accounted for MRA, while the rest did not.

Table 4.3: Mixture risk assessment (MRA) methods identified and their frequency of use in the research studies.

MRA Method	Frequency
Potential Ecological Risk Index (RI)	10
Hazard Index (HI)	8
Pollution load Index (PLI)	3
Heavy metal Pollution Index (HPI)	2
Nemerow Comprehensive Pollution Index (Pn)	1
Total Carcinogenic Risk (TCR)	2
Bayesian Kernel Machine Regression (BKMR)	1
Cancer Risk (CRtotal)	1
Comprehensive Pollution Index (Wn)	1
Cumulative probability distribution of HI of toxic metal(loid)s	1
Cumulative probability distribution of ILCR of Pb and i-As	1
Degree of contamination (Cd)	1
Modified Contamination degree (MCd)	1
Total Cancer Risk (TCR)	1
Total Health Risk (RZ)	1
Nemerow Comprehensive Pollution Index (PC)	1

4.3.8 Effects Monitoring

While risk characterisation provides quantitative estimates of potential hazards, a few studies have conducted actual effect studies to examine the realised effects of contamination within biological systems. These investigations offer critical validation of risk predictions by linking contaminant concentrations to observable biological responses or ecological alterations. This section summarises seven studies in the reviewed literature that evaluated these effects, highlighting the types of species used, the endpoint used to assess contaminant impact, and the broader significance of these findings within AML environments. Six studies used plant and animal species, while one study analysed human blood samples.

Figures 4.16 and 4.17 show the varieties of bioindicator species that were used to assess the realised effects of chemical contamination. The organisms were selected for their sensitivity to metal stress and their ecological relevance in soil, aquatic, and sediment environments. The most frequently employed test organisms were the earthworm *Eisenia fetida* and the aquatic crustacean *Daphnia magna* (Figure 4.16), each accounting for 13.3% of the studies. They were used to evaluate endpoints including

mortality, reproduction, developmental inhibition, and acute toxicity. Significant effects within the population were observed, with a significant effect on mortality for *D.magna* (Alvarenga et al., 2013; D. Kim et al., 2022; Ushakova et al., 2022).

Soil-dwelling invertebrates *Folsomia candida* and Eisenia andrei, the nematode *Caenorhabditis elegans*, and the microbial model Escherichia coli (DH5α) all 6.7%, showed a significant effect on mortality and reproduction inhibition, while Algal species such as *Chlamydomonas reinhardtii* and *Chlorococcum infusionum* were applied to evaluate contaminant effects on primary producers; no significant effect on growth was observed (D. Kim et al., 2022). *Danio rerio (embryo)* toxicity testing focused on hatching delay and abnormal development; significant effects were observed, as well as in *Vibrio fischeri* (D. Kim et al., 2022; Rodriguez-Ruiz et al., 2015). Two of the studies utilised mixed species assemblages and microbial communities, including iron-reducing and acidophilic bacteria such as *Ferrovum, Acidithiobacillus, Gallionella, and Leptospirillum.* Microbial diversity and changes in microbial interactions were significant within the population and community composition, and microbial community function was significant (D. Chen et al., 2021; D. Kim et al., 2022).

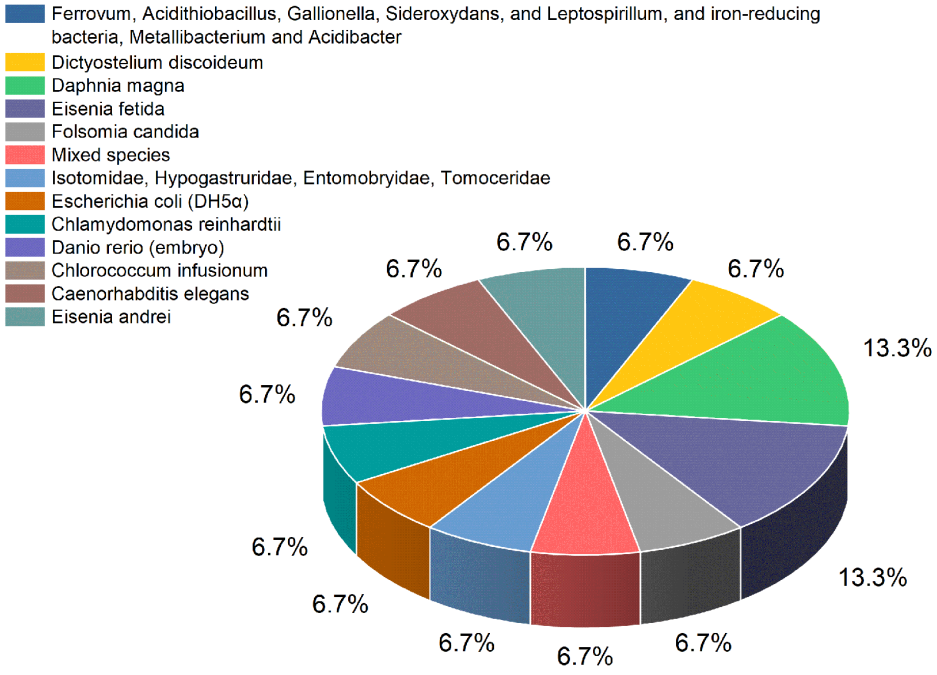

Figure 4.16: Shows the microbial and invertebrate species that were used to monitor contaminant effects in the articles; Eisenia fetida and Daphnia magna were the most frequently used.

Plant-based monitoring studies employed a range of species to evaluate the phytotoxic effects (Figure 4.17). The most frequently used species was *Lactuca sativa* (37.5%), followed by *Oryza sativa* (25%), which were primarily assessed for seed germination, root elongation, and shoot growth inhibition under

metal exposure (Alvarenga et al., 2013; Chanpiwat & Numprasanthai, 2024; Rodriguez-Ruiz et al., 2015). Significant effects were observed. Other plants, including *Vigna radiata* (12.5%) and *Scenedesmus quadricauda* (12.5%), were used to assess growth reduction, biomass decline, and changes in chlorophyll content; all outcomes were significant (D. Kim et al., 2022). Mixed taxa (12.5%), combining multiple plant species to evaluate differential tolerance and contaminant uptake, also showed significant effects. Together, these studies highlight the application of standardised bioassays and ecologically relevant plant species in assessing vegetation-level responses to mine-derived contaminants.

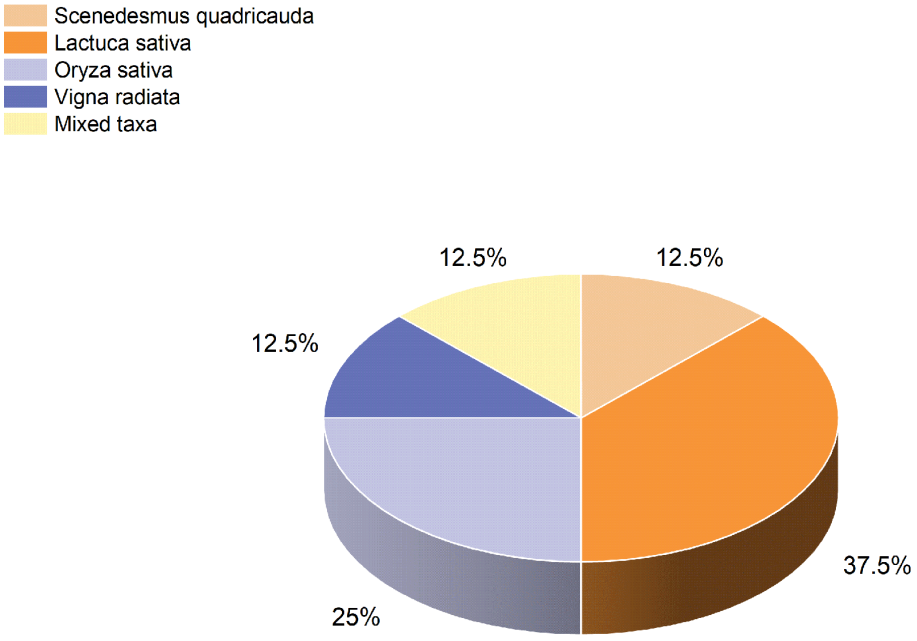

Figure 4.17 shows the plant species used. Lactuca sativa and Oryza sativa were the most common, while Vigna radiata, Scenedesmus quadricauda, and mixed taxa were used less frequently to assess phytotoxic and growth-related effects.

The significant differences recorded across the studies that conducted effect monitoring are shown in Figure 4.18. The majority (75.8%) reported statistically significant differences in at least one measured endpoint between contaminated and control samples. These outcomes included significant alterations in growth, reproduction, enzyme activity, or survival across various test species. In contrast, 24.2% of the studies found no significant difference. The predominance of significant outcomes suggests that contaminants from abandoned coal and Pb/Zn mine lands exert measurable biological and ecological effects across multiple environmental compartments.

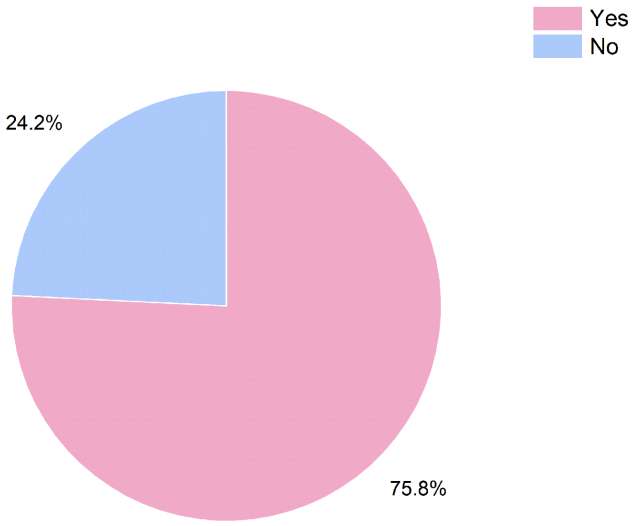

Figure 4.18: Proportion of studies reporting statistically significant differences in measured endpoints between contaminated and control conditions. 75.8% of the studies reported significant effects, while 24.2% found no significant difference.

4.4 Discussion

This study reviewed current practices for chemical contamination risk assessment associated with abandoned coal and Pb/Zn mine lands. The findings reveal an uneven research landscape, characterised by the spatial concentration of studies, diverse analytical approaches, varying risk assessment methods, and inconsistent reporting practices. Most research emphasises integrating site-specific geochemical data with risk modelling frameworks, primarily for human health risk assessment. In contrast, some studies focus on contamination as the basis for characterising both ecological and human health risks, with considerable variation in the parameters considered. These findings prompt critical reflection on the strengths and limitations of existing assessment practices and highlight the long-term environmental and health implications of abandoned mines.

4.4.1 Characteristics of Abandoned Mines and Approaches to Exposure Assessment

A comprehensive understanding of the characteristics of abandoned mine sites is essential for interpreting contaminant persistence, transport pathways, and risk patterns (US EPA, 2000a). The reviewed studies demonstrated that mine type, mining method, operational duration, and abandonment period critically shape contamination profiles and how contaminants spread through the environment and reach living organisms. Most of the studies focused on abandoned Pb/Zn mines, consistent with

their extensive historical exploitation and well-documented association with persistent metals such as Pb, Zn, Cd, Cu, and As (El Azhari et al., 2016; Z. Li et al., 2020; Mehta et al., 2020; P. Santos et al., 2023; Yahyaoui & Ben Amor, 2024). Whereas abandoned coal mines were less examined, they were relevant to understanding their distinct contamination mechanisms, notably AMD and associated metal mobilisation reported in (D. Chen et al., 2021; Pan et al., 2021; Ushakova et al., 2022).

Over half of the studies explicitly stated the year or duration of abandonment, while others provided relative temporal descriptions or no record at all. This inconsistent reporting of mine age, operational duration, and abandonment timelines deviates from best practice guidance, such as the US EPA CSM outlined in the Risk Assessment Guidance for Superfund (RAGS), Volume I, Part D (US EPA, 2001) and the Department for Environment, Food and Rural Affairs (DEFRA) and Environment Agency (EA) Contaminated Land Exposure Assessment (CLEA) Model (UK EA, 2020). These frameworks require explicit documentation of contaminant sources, release mechanisms, and spatial and temporal context. The omission of such information restricts the interpretation of contaminant persistence and natural attenuation processes. Where data were available, sites abandoned for more extended periods often exhibited greater contamination, suggesting the cumulative influence of weathering, leaching, and inadequate post-closure management. These site-specific attributes directly influence the nature and persistence of contaminants in environmental media, shaping the pathways through which receptors are exposed. This was observed in some of the studies that were abandoned for decades, such as the Boudoukha mining field (Zineb et al., 2024), Chungcheong Bukdo mine (J. Yang et al., 2015), Agios Philippos mine (Nikolaidis et al., 2010), and lead–zinc mine in Gyongyosoroszi (Sipter et al., 2008).

Sampling strategy, storage, and preparation are critical steps that underpin the accuracy of analytical data and risk interpretation. Across studies, sampling approaches varied, but most provided bases for the chosen design and the reference protocol used (L. M. Huang et al., 2013; Sartorius et al., 2022; J. Yang et al., 2015). This variation aligns broadly with the recommendations of (ISO, 2017; US EPA, 2000a), which permits methodological flexibility when site heterogeneity is high. Sample preparation protocols, storage and preservation practices were generally consistent with trace-metal standard protocols. Among the reported contaminants, Pb > Zn > Cd > Cu > As were the most reported. This is common in Pb-zinc AMLs, and Cr, Ni, Mn, and Fe have also been reported, though not in all reviewed studies.

In terms of analytical practice, the frequent use of ICP-MS, ICP-AES/OES, and AAS demonstrates general alignment with analytical quality standards such as the US EPA's SW-846 methods for metals in environmental matrices (US EPA, 2018). Complementary use of XRD and SEM supports mineralogical analyses that helped clarify how metals were bound within or on mineral particles, which are relevant to understanding and interpreting contaminant mobility and bioavailability (Del Rio-Salas et al., 2019; El Azhari et al., 2016; Zineb et al., 2024). While pXRF enabled quick in situ mapping of

contaminant hotspots, which informed targeted sampling for laboratory quantification of identified contaminants (Del Rio-Salas et al., 2019). Several studies demonstrated good analytical accuracy using certified reference materials, reporting recoveries and precisions within acceptable ranges, consistent with OECD quality assurance guidelines (OECD, 2017). However, other studies did not report these, which makes it difficult to assess data accuracy and precision.

4.4.2 Evaluation of Risk Characterisation Practices

The reviewed studies consistently identified soils, tailings, sediments, and surface waters as sources of contamination, with soils being the most prominent. This aligns with established guidelines that advocate a multimedia approach to exposure assessment. Ingestion through contaminated soil, water, crops, or animal products was the most frequently assessed exposure pathway, reflecting regulatory emphasis in human health risk models. In contrast, dermal and inhalation pathways were less often quantified. Additionally, 22 studies reported unclear information, and six did not specify exposure pathways, highlighting ongoing gaps in pathway definition and transparency. This pattern suggests that, while most studies focused on the dominant exposure route (ingestion) recognised by frameworks, incomplete documentation limits comparability and comprehensive risk quantification. Regarding receptors, most studies concentrated on human health, consistent with frameworks. However, ecological receptors were less represented, partly because many studies did not clearly define the receptors being assessed, especially those relying on contamination indices to infer risk instead of structured risk assessment models. This underscores the importance of applying established risk assessment frameworks, which require the explicit definition of source–pathway–receptor (S–P–R) relationships at the beginning of the assessment. These frameworks not only enhance transparency and reproducibility but also ensure systematic evaluation of both human and ecological endpoints.

The current review shows that risk characterisation across studies is mainly carried out using quantitative indices and frameworks developed by international regulatory agencies. Igeo, Er, HQ and CR are the most commonly used methods, reflecting their standardisation, ease of calculation, and comparability across contaminants and locations. Their widespread application demonstrates practical usefulness for quickly screening contamination severity and prioritising areas for remediation. Other frequently employed methods include Cf, SQGs, and EF, while BAF and BV are used less often.

However, indices such as Igeo, EF, Cf, and RI are fundamentally concentration-driven, relying on background normalisation or toxicity coefficients, particularly in the case of Igeo and RI, rather than direct exposure models. While these indices are suitable for initial screening to determine contamination intensity and potential ecological concern, they lack the mechanistic depth to capture site-specific exposure pathways, bioavailability, receptor sensitivity, or cumulative effects (Gutiérrez et al., 2016; US EPA, 2001). This limitation is especially significant in dynamic systems like abandoned mine sites,

where the fate and transport of contaminants are particularly complex (ICMM, 2007) and are influenced by several factors such as weathering, climate change, hydrology, and land use (Anawar, 2013; W. Li, Deng, et al., 2024; Richard et al., 2021). Although not regulatory or standardised risk assessment tools, these indices align with the tiered assessment philosophy described in frameworks such as (CCME, 2006; UK EA, 2020; US EPA, 1989b). Preliminary evaluations guide the need for more detailed quantitative analysis. For example, high Igeo or Er values at a mine site may prompt a follow-up human health risk assessment using formal regulatory methods such as the Hazard Quotient (HQ) or Carcinogenic Risk (CR). In this review, several studies (Nouairi et al., 2019; P. Santos et al., 2023; Z. Sun et al., 2020; Yahyaoui & Ben Amor, 2024) adopted this approach, initially applying contamination indices and subsequently conducting HQ and CR assessments in line with established standards.

In contrast, HQ and CR are regulatory tools formally defined by the US EPA (US EPA, 1989b, 2001) and adopted in related international frameworks such as (CCME, 2006; WHO, 2021). Additional relevant agencies and frameworks are listed in Appendix 4.3. A substantial subset of the reviewed studies applied these regulatory approaches (see Table 4.3), particularly the US EPA human health risk assessment framework. These methodologies first require estimating exposure through ADD, CDI, or EDI, which involves quantifying the amount of contaminant that individuals or populations may take in via ingestion, inhalation, or dermal contact under specific exposure scenarios. Only after establishing these exposure levels are the toxicity potential (HI and CR) for individual contaminants calculated for receptors using contaminant reference doses and the cancer slope factor; this was the procedure most commonly followed in the reviewed literature. However, some studies used their national frameworks but relied on US EPA exposure factors to inform their assessments (Y. Han et al., 2023; J. Yang et al., 2015).

While these single-contaminant approaches provide valuable insight into individual metal risks, real-world exposures in abandoned mine environments often involve complex mixtures of contaminants that may interact additively, antagonistically or synergistically, necessitating cumulative or mixture risk assessment approaches.

Considerations for MRA were applied across the reviewed studies (n = 19). Among the most frequently employed methods were RI, PLI, HPI, and Pn, which were integrated indices used to quantify combined contamination levels across multiple metals. These indices offer an aggregated measure of contamination intensity at a screening level (Ayari et al., 2023; Mehta et al., 2020; Prathap & Chakraborty, 2019; P. Santos et al., 2023), and BKMR (Z. Sun et al., 2020; Q. Xu et al., 2024) represented the established frameworks considered for estimating the cumulative health and ecological risks arising from multi-contaminant exposure. In the assessments, HI and TCR typically assume additive effects to estimate cumulative risk. In contrast, BKMR and other probabilistic models enable the assessment of non-linear and interactive effects among contaminants.

Although additive indices such as RI, HPI, and PLI employed in the studies provide an initial indication of cumulative impact, they often underestimate interactive effects, which is a deviation from the USEPA's Cumulative Risk Assessment Guidance (US EPA, 2000b) and OECD's recommendations for assessing the risk of exposure to multiple chemicals (OECD, 2018).

The recent applications of advanced statistical tools such as BKMR and cumulative probability models mark progress toward capturing these complexities and better align with contemporary mixture risk frameworks. Integrating chemical analyses with biological validation further strengthens the link between predicted and realised risk (Q. Xu et al., 2024).

The review also identified a strong emphasis on human health risk assessments (39.7%), consistent with the widespread adoption of US EPA-derived protocols. In contrast, ecological risk assessments were less common (27.6%), and only 1.7% of studies addressed both domains concurrently. A notable proportion of studies were categorised as unclear or not reported, indicating that risk type was embedded within generalised contamination evaluations. This results from the absence of source-pathway-receptor linkages in many studies that were using Igeo or CF methods, which constrains holistic risk evaluation.

In summary, the reviewed studies indicate a continued reliance on concentration-based RA methods such as Igeo, Ef, and Er for AML risk assessments, which limits the comprehensiveness of risk evaluation. Similarly, indices such as PLI, RI, and HPI were frequently applied for multi-contaminant or cumulative assessments, but generally lack integration of cumulative and mixture toxicity considerations. Nonetheless, there is adherence to internationally recognised methods for chemical risk characterisation, such as the HQ, CR, HI and TCR, particularly in human health assessments.

4.4.3 Effects Monitoring outcomes Effect Monitoring and Realised Risk

A subset of the reviewed literature (n = 8) focused on the effects (realised risk) of contamination from abandoned coal and Pb/Zn mine lands. The methodology adopted mainly established guidelines (OECD, 2010, 2018; US EPA, 1998) which emphasise the importance of field observations, laboratory bioassays, and ecological effects data to characterise ecological risk. The use of test organisms across multiple trophic levels, including *Eisenia fetida, Daphnia magna*, *Chlamydomonas reinhardtii*, and *Lactuca sativa* (Alvarenga et al., 2013; D. Kim et al., 2022; Rodriguez-Ruiz et al., 2015), provided direct measures of contaminant bioavailability and biological response. Endpoints such as growth and reproduction inhibition, mortality, effects on seed germination and growth, root elongation, and inhibition of fruiting activity reflect both acute and sublethal ecological effects (Ushakova et al., 2022; Yohannes et al., 2021), capturing dimensions of risk that chemical indices alone cannot. This approach strengthens the causal link between contaminant levels and ecological impairment, providing essential validation for risk predictions.

These practices demonstrate strong alignment with the stressor-response and risk characterisation phases outlined in the US EPA and similar frameworks (CCME, 2006; EEA, 2020; US EPA, 1998). These studies demonstrate the importance of incorporating biological studies to help validate or complement chemically inferred risks. The use of receptor and endpoint-specific assessments, alongside the deliberate selection of ecologically relevant and sensitive species, enhances the ecological realism of risk evaluation and supports more meaningful interpretation of contaminant effects within mine-impacted environments.

Across all the studies, 75.8% reported statistically significant impacts, suggesting that legacy mine contaminants frequently exceed biological thresholds of concern. Overall, this group of studies represents a significant methodological advancement over risk evaluations that rely exclusively on contamination indices. By capturing the realised ecological consequences of contamination, they help bridge the gap between chemical presence and ecological harm. However, a persistent mismatch between conventional risk assessment and biological effect monitoring continues to hamper the validation of risk assessment methods. While chemical data provide predicted risks, biomonitoring reveals actual biological responses, and the two often diverge due to differences in bioavailability, mixture effects, and tolerance levels. Integrating effect-based tools and biomarkers into risk frameworks is therefore crucial for aligning predicted risks with observed ecological outcomes (Moulinec et al., 2025).

4.4.4 Advances, Gaps, Limitations, and Future Research

Evaluating how chemical contamination risks are characterised is essential to understanding the strengths and weaknesses of current assessment practices for abandoned coal and Pb/Zn mine lands. The reviewed studies showed a wide range of methods from traditional indices to advanced mixture and probabilistic models, revealing both progress and inconsistency in how risk is defined and applied. The following synthesis summarises key advances, gaps, and limitations, and outlines future directions for developing more integrated frameworks that address both ecological and human health risks in mine-impacted environments.

The gradual inclusion of advanced models such as Bayesian Kernel Machine Regression (BKMR), Cumulative Probability Distribution of Incremental Lifetime Carcinogenic Risk, and Cumulative Probability Distribution of Hazard Index methods in AML risk assessments represents a methodological shift from traditional indices like Igeo, Er, and RI toward recognising cumulative and interactive contaminant effects. In parallel, studies employing effect monitoring for risk quantification provide a more holistic understanding of realised risk, bridging the gap between chemical quantification and ecological outcomes.

Despite these advances, significant methodological and conceptual gaps persist. Many studies continue to rely on simplified contamination indices, which limit the incorporation of mixture toxicity, speciation, and bioavailability assessments. Most assessments also assume contaminant independence, overlooking potential synergistic, antagonistic, or interactive effects that are particularly relevant in multi-metal exposure contexts such as AMLs. These omissions collectively highlight the persistent gap in addressing mixture toxicity within current risk assessment practices. The dominance of human health risk assessments over ecological evaluations further reflects an imbalance that constrains understanding of risks within mine-impacted environments. In addition, the absence of standardised reporting on AML characteristics, exposure pathways, receptors, and risk categories continues to limit comparability and reproducibility across studies.

Conceptually, most risk assessments remain compartmentalised, focusing on isolated contaminants or single exposure routes and, consequently, overlooking the complex interactions among metals, biological systems, and environmental processes. The limited application of MRA methods reinforces this reductionist tendency, underscoring the need for more integrated approaches. Likewise, while human health risks dominate the literature, ecological and multi-receptor assessments remain scarce, despite evidence that ecosystem degradation can indirectly exacerbate human exposure. Although approaches such as the ISO 19204:2017 Triad framework (ISO, 2017) provide a robust model for ecological integration, they do not encompass human exposure and health endpoints, highlighting the need for a unified eco-human assessment framework. Bridging this gap will require integrated risk assessment models that combine chemical monitoring, biological testing, and ecological modelling under a single evaluative structure.

Future risk assessment practices would benefit from stronger integration of exposure sources, pathways, and receptor specificity, broader adoption of mixture risk models that reflect real-world contaminant complexity, and greater emphasis on combined human–ecological risk frameworks. More transparent reporting and consistent categorisation of risk types would also facilitate synthesis across studies and enhance the comparability of risk characterisation outcomes.

4.4.5 Implications of Current Risk Assessment Approaches to Nigerian AMLs

The findings are particularly relevant to Nigeria, where abandoned mine sites are often located near agricultural lands and rural communities that may depend on contaminated soils and water resources for farming and domestic use. The limited consideration of airborne particulates and inhalation pathways across the reviewed studies also highlights an important knowledge gap, especially in regions affected by artisanal mining and dry-season dust generation. Methodologically, the review reveals growing integration of bioaccessibility testing, sequential extraction procedures, and mixture risk assessment approaches, which may provide more realistic evaluations of contaminant mobility,

bioavailability, and cumulative risk. These approaches may be particularly valuable in Nigerian AML settings where multiple contaminants coexist, and exposure pathways are complex.

Furthermore, the relatively limited use of effect monitoring and ecological bioassays suggests that many AML assessments continue to rely primarily on contaminant concentrations and predictive indices without adequately validating actual biological effects. Expanding effect-based monitoring approaches within Nigerian AML investigations could improve understanding of realised ecological impacts and strengthen site-specific risk characterisation.

In addition to providing a broader overview of current practices in AML risk assessment, the methodological approaches synthesised in this chapter informed aspects of the analytical framework applied in the subsequent practical chapters of this thesis, which use Nigerian lead-zinc mines as case studies. In particular, the reviewed literature provided methodological context for selecting exposure media, contaminant characterisation approaches, contamination indices, and risk assessment techniques used to evaluate contamination risks within the study area. This integration strengthens the alignment between the present review and the site-specific investigations undertaken in later chapters.

Generally, this narrative synthesis highlights both current practices and existing methodological gaps in the assessment of abandoned coal and lead–zinc mine lands. The findings provide a useful framework for guiding future contamination assessments, environmental monitoring, and remediation planning within mining-impacted environments in Nigeria.

4.5 Conclusion

This study highlights both the progress and persistent limitations within the body of research evaluated. Although the field has expanded considerably in recent years, driven by growing awareness of the environmental legacies of mining, its evolution remains uneven, with substantial variation in methodological sophistication, analytical capacity, and geographical representation. Risk assessment differs markedly between metals and organic contaminants due to their contrasting environmental behaviours. Metals are persistent and non-degradable, with risk driven by factors such as speciation, pH, redox potential, and dissolved organic carbon, all of which influence bioavailability. In contrast, organic contaminants such as PAHs are degradable but vary widely in persistence and toxicity. For metals, risk is best assessed through bioavailable fractions rather than total concentrations, while for organics, focus lies on toxicity profiles, degradation potential, and dominant exposure pathways.

Across the reviewed literature, contamination was dominated by potentially toxic metals (Pb, Zn, Cd, Cu, As), with soils, sediments, water, and tailings serving as the primary media for contamination storage and transport, highlighting a gap in the assessment of organic contamination risk at abandoned

coal mines. Risk assessments relied heavily on traditional indices such as Igeo, Cf, and RI, and established methods such as HQ and CR, mainly from the US EPA and others from WHO, EU, and CCME. While traditional methods provide a consistent basis for estimating potential risks, they are limited in their ability to address mixture toxicity and site-specific variability. More recent advances incorporating models such as BKMR and cumulative probability-based approaches indicate a gradual methodological transition toward integrative and grounded assessments.

The evaluation of biological effect monitoring in studies focusing solely on effects revealed that approximately three-quarters of tests reported significant adverse outcomes, validating the ecological relevance of observed contamination. Test species, including *Eisenia fetida, Daphnia magna, Lactuca sativa,* and *Oryza sativa*, proved effective for detecting both sublethal and acute responses across soil and sediments. These findings underscore the potential of bioindicator-based assessments to complement chemical data and strengthen the evidence base for risk characterisation.

Nevertheless, substantial challenges remain. Key gaps include inconsistent reporting of mine characteristics. While the gradual adoption of advanced models reflects a shift toward recognising mixture and cumulative effects, most studies still rely on simplified indices such as Igeo, Er, and RI. These conventional tools, although useful for preliminary screening, do not adequately address mixture toxicity, bioavailability, or site-specific complexity. Furthermore, the dominance of human health-focused assessments over ecological evaluations, combined with inconsistent reporting of mine characteristics, pathways, and receptors, continues to limit comparability and integrative understanding. Current approaches remain largely compartmentalised, overlooking the interconnected nature of human and ecological risks. Advancing risk assessment of mine-impacted environments will require unified frameworks that integrate chemical, biological, and ecological evidence, supported by standardised reporting and broader application of mixture and probabilistic models.

Chapter 5: Chemical Contamination and Ecological Risk Assessment of Abandoned Lead-Zinc Mines in Nigeria

5.1 Introduction

Mining continues to be one of the earliest human endeavours for essential survival and sustenance, from making simple tools from rocks to trading extracted metals. The exploitation and trading of metals and minerals such as Pb, Zn, Ag, Cu and Ni enhance society and improve lives. Countries like Brazil, Bolivia, China, Burkina Faso, Congo, Ghana, Colombia, Ecuador, India, Indonesia, Tanzania, Madagascar, Thailand, Ethiopia, and Nigeria have large populations sustained by mining activities (Schwartz et al., 2021). Mining plays a pivotal role in global economies throughout history, providing essential raw materials for various industries and contributing significantly to economic and infrastructural development (Lottermoser, 2010, 2016). However, it is crucial to acknowledge that the exploitation of mineral resources has long-lasting, serious environmental consequences and socio-economic impacts, including habitat disruption, deforestation, soil erosion, and water pollution and the human health and well-being of host communities and beyond can endure for decades without adequate mitigation measures (Chukwu & Obiora, 2023; Obiora et al., 2016).

Lead–zinc mining in Nigeria and globally is notorious for its adverse effects. Globally, approximately 0.357 to 0.857 Mt of lead and 0.462 to 1.380 Mt of zinc are discharged into the environment annually through mining and processing (Buckley et al., 2017; IGF, 2017). These metals permeate soils, dust, air, water, plants, and animals, causing degradation to agricultural soils, soil pollution and socio-economic destabilisation.

5.1.1 Geology and Mineralisation of Lead-Zinc in Nigeria

Lead-Zinc occurs in the Cretaceous rocks of the Nigerian Benue Trough, a rift basin in Central West Africa stretching NNE-SSW for about 800 km with a width ranging between 100 and 150 km (Bute et al., 2024; Oladele, 2016). The trough is said to contain up to 6000 m of Cretaceous to Tertiary sediment, of which those predating the mid-Santonian have been folded, faulted, and compressed in several places by compressional events (Fatoye et al., 2014; Oladele, 2016). Based on tectonic, geographical, and stratigraphical features (Nwajide, 2013), the Trough has been subdivided into (Figure 5.1) Northern, Central and Southern segments, which are also arbitrarily referred to as the Upper, Middle, and Lower Benue Trough, respectively (Fatoye et al., 2014).

The Lower Benue Trough is a linear, intracratonic graben basin trending NE-SW. The Southern Benue Trough is made up of Nkalagu and Abakaliki; the Central Benue Trough comprises Makurdi through Lafia to Wukari; while the Northern Benue Trough is made up of Pindigi, Gombe, and Ashaka, with Jessu and Numan in the Yola arm. The study areas fall within the Central (Wase-Gimbi) and lower

(Abakaliki) Benue Trough, and the mineralisation and occurrence of lead-zinc are vein-type and hosted in the sandstone and shale beds. The trough is also endowed with limestone, coal, barytes, salt, fluorspar, etc., (Yusuf et al., 2022). Specifically, the middle or central Benue Trough is around Wase–Bashar–Zurak, with structurally controlled (fractures and faults) mineralisation commonly associated with barite and carbonate veins within Cretaceous sedimentary sequences (Fatoye et al., 2014; Ogundipe & Obasi, 2017; Yusuf et al., 2022). While the Abakaliki is known as the Abakaliki Anticlinorium with lodes, it is hosted by the Albian Asu River Group, composed of black shales/siltstones of the Lower Cretaceous.

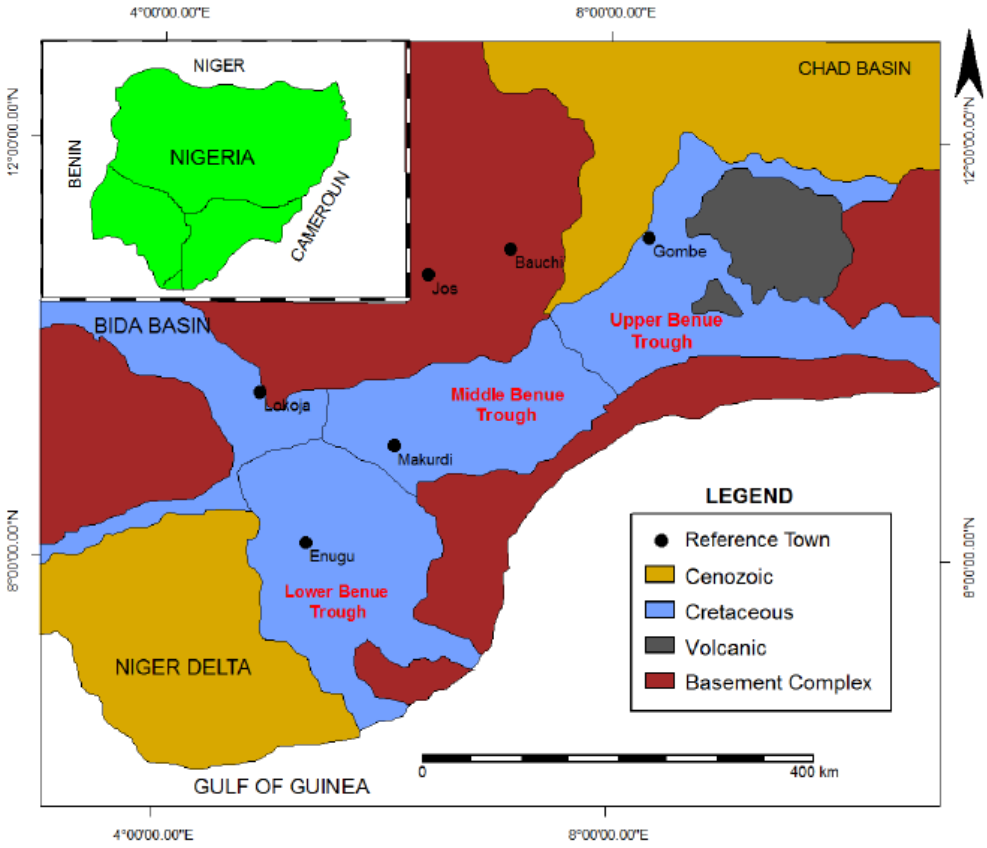

Figure 5.1: Geologic map of Nigeria (Fatoye et al., 2014)

Geochemically, galena–sphalerite with barite/fluorite and carbonate gangue are typical in the central Benue trough/district (Wase–Bashar–Zurak) and sphalerite + galena ± chalcopyrite, with barite, fluorite, calcite/dolomite gangue, are common in the Lower Benue Trough (Akande & Mücke, 1993; Arinze et al., 2019). Lead stands out as a soft, malleable, blue-grey heavy metal and is likely the earliest metal discovered that doesn't naturally occur in a pure state. When melted, lead exhibits a shiny chrome-silver lustre. The primary ore mineral of lead is galena (PbS), which is commonly found alongside sphalerite (ZnS) and barytes ($BaSO_4$). Galena frequently contains inclusions of silver and serves as a significant source of this metal (Fatoye et al., 2014).

Zinc, on the other hand, is a crystalline, bluish-white metal that is brittle at most temperatures. It transforms into a malleable state between 100 and 1500°C, yet above 2100°C, it regains brittleness and can be pulverised through beating. The main source of zinc is the primary sulphide sphalerite (ZnS), typically occurring in conjunction with galena and barytes. Sphalerite, containing 67% Zn, often carries traces of simple sulphides such as cadmium, gallium, germanium, and indium in solution (Fatoye et al., 2014).

5.1.2 History of Lead-Zinc Mining

Mining in earlier times was carried out by local inhabitants who worked on the outcrop sections of the deposits, which were alluded to as being influenced by early Portuguese traders in the southern region of Nigeria, where the deposits occurred in Zurak, Arufu and Abakaliki district, as found by the Mineral Survey of Nigeria between 1904 and 1909 (Farrington, 1952; Obiora et al., 2016, 2019).

The production of Lead-Zinc was first recorded in 1925 and continued on a small scale until 1937, but ceased due to low metal prices, particularly for lead. It was later picked up again in 1947 (Farrington, 1952) and continued until they were abandoned during the Nigerian Civil War between 1966 and 1970. Some of the abandoned mines were later reactivated by artisanal miners, which grew from small-scale to large-scale mining that is still ongoing (Chukwu & Obiora, 2023; Obiora et al., 2019).

The mining of allied metals in the Jos Plateau region has continued for over a century, with the exploitation of economic minerals dating back to 1902, as documented by Calvert (Calvert, 1977). The extraction and commercialisation of tin and salt in the upper Plateau, as well as lead-zinc in the lower Plateau and parts of Nasarawa State, began during the pre-colonial era (News Tower Magazine, 2011; Vanguard, 2018).

In the Zurak area of the Wase Local Government Council, lead-zinc deposits were mined and later abandoned. Currently, small- to medium-scale lead-zinc mining is ongoing in this region, alongside artisanal mining by local communities.

5.1.3 Environmental pollution of Lead-Zinc

The extraction of lead, zinc, and copper during the 18th to 19th centuries relied on rudimentary, inefficient ore-processing tools and methods (Farrington, 1952; Gandhi, 2014). As a result, substantial quantities of copper, lead, zinc, and other mineral compounds were unintentionally released into the environment and became integrated into sediments and soils. Table 5.1 shows the Pb-Zn concentrations in soils around AMLs. This has led to persistent local and regional pollution, with ongoing risks stemming from drainage from these abandoned mines and the mobilisation of mine tailings.

Lead and zinc contamination significantly affect environmental quality and ecosystem functioning. Elevated concentrations of these metals in soils and sediments can alter physicochemical properties, reduce microbial activity, and impair nutrient cycling processes essential for ecosystem stability. In plants, Pb and Zn toxicity may reduce seed germination, inhibit root elongation, suppress photosynthesis, induce oxidative stress, and decrease biomass productivity (Jain et al., 2016). Such effects can reduce vegetation cover and contribute to habitat degradation around abandoned mine sites.

Aquatic and terrestrial organisms are also vulnerable to metal contamination due to the persistence, bioavailability, and bioaccumulative nature of Pb and Zn (M. Sun et al., 2024). Metals mobilised from mine wastes can enter surface water and sediments, where they may accumulate in benthic organisms, fish, and other ecological receptors (Ciszewski & Aleksander-Kwaterczak, 2020). Chronic exposure has been associated with impaired reproduction, behavioural alterations, reduced growth, and disruption of food web dynamics (Milton & Johnson, 2002). Furthermore, trophic transfer of metals through the food chain can increase ecological risks to higher organisms and reduce biodiversity within affected ecosystems.

Although ecological impacts remain the primary concern in environmental risk assessments of AMLs, prolonged exposure to Pb and Zn contamination may also pose indirect risks to human populations through contaminated water, soil, crops, and aquatic resources (Wani et al., 2021).

Table 5.1: Reported concentrations (mg/kg) of heavy metals in soils in the vicinity of lead–zinc mining areas by countries

Country	Mine name/site	Pb	Zn	Cd	As	Cr	Other HMs	Source/References
China	Taolin Pb/Zn mine	188.4	415.5	2.18	30.15	38.43	Co, Cu, Mn, Mo, Ni, Sb, V, & Fe	(B. Huang et al., 2018)
Mexico	Sonoran Desert	536.5	576.5	Nd	47.2	Na	Cu, Sb, Fe, Mn & Ti	(Del Rio-Salas et al., 2019)
Greece	Agios Philippos mine	80.4	345.1	3.2	8.9	NC	Cu, Fe & Mn	(Nikolaidis et al., 2010)
Italy	Gorno mining district	255	14 730	17.2	107	60.1	Be, Co, Cu, Ni, Sb, Ti, & V	(Mehta et al., 2020)
Spain	Alcudia Valley Mining District	34.46	99.89	0.14	18.59	NC	Cu, Sb & Hg	(Higueras et al., 2017)
Tunisia	Lakhouat abandoned Pb–Zn mine	355.2	1101	2.42	17.38	27.29	Co, Cu, Hg, Ni & Zr	(Ayari et al., 2023)
Korea	Not Specified	10756	10545	117	36982	10.7	Ni & Cu	(D. Kim et al., 2022)
Algeria	Boudoukha mining field	408.4	244.1	1.9	13.3	NC	Fe	(Zineb et al., 2024)
Korea	Dongil and Okdong mines	38	81	3. 4	40	NC	Cu	(Lee & Chon, 2003)
Hungary	lead–zinc mine in Gyongyosoroszi	27.8	142	0.43	31.4	NC	Hg	(Sipter et al., 2008)
Morocco	abandoned Zeïda Pb mining district	213.1	75	0.1	84.6	64.7	Cu & Ni	(Nassiri et al., 2021)
Spain	Lanestosa Pb–Zn mining district	3,353	11,841	16.7	1.2	8.3	Cu, Mo, Sb, Co, Mn, Ni, Ba, Co & Al	(Rodriguez-Ruiz et al., 2015))
Spain	Abandoned mine of Sierra Minera of Cartagena-La Unión,	4056	3826	5	295	NC	Cu & Fe	(Pérez-Sirvent et al., 2016)
China	Yaoposhan polymetallic mine	265	214	0.648	47.9	71.9	Ni, Cu & Hg	(Z. Sun et al., 2020)
China	Abandoned Pb–Zn mine in Guangxi Zhuang Autonomous Region	157	753	5.3	36.5	197.6	Cu, Ni, & Hg	(L. M. Huang et al., 2013)
Nigeria	Abakaliki Pb/Zn AML	799.0	465.9	2.0	Nd	129.8	Mn, Ni, Cu, Ti, Zr, Ce, Sr, Ba, Al & Fe	This study
Nigeria	Gimbi Pb/Zn AML	63.0	485.6	0.5	Nd	48.6	Mn, Ni, Cu, Ti, Zr, Ce, Sr, Ba, Al & Fe	This study

Nd – Not detected, NC – Not considered, Na – Not available.

5.1.4 Abakaliki AMLs

The Abakaliki lead-zinc mining area in Ebonyi State encompasses an area of about 21.8 sq. km and consists of three Local Government Areas: Abakaliki, Ezza, and Ikwo (Obiora et al., 2016). The site of consideration lies within latitude 06^0 18' 00''N to 06^0 18' 18''N and longitude 08^0 04'26''E to 08^0 4'42''E, situated in Echara-Onuphu community, Mkaliki part of Abakaliki local government area of Ebonyi State (Figure 5.2).

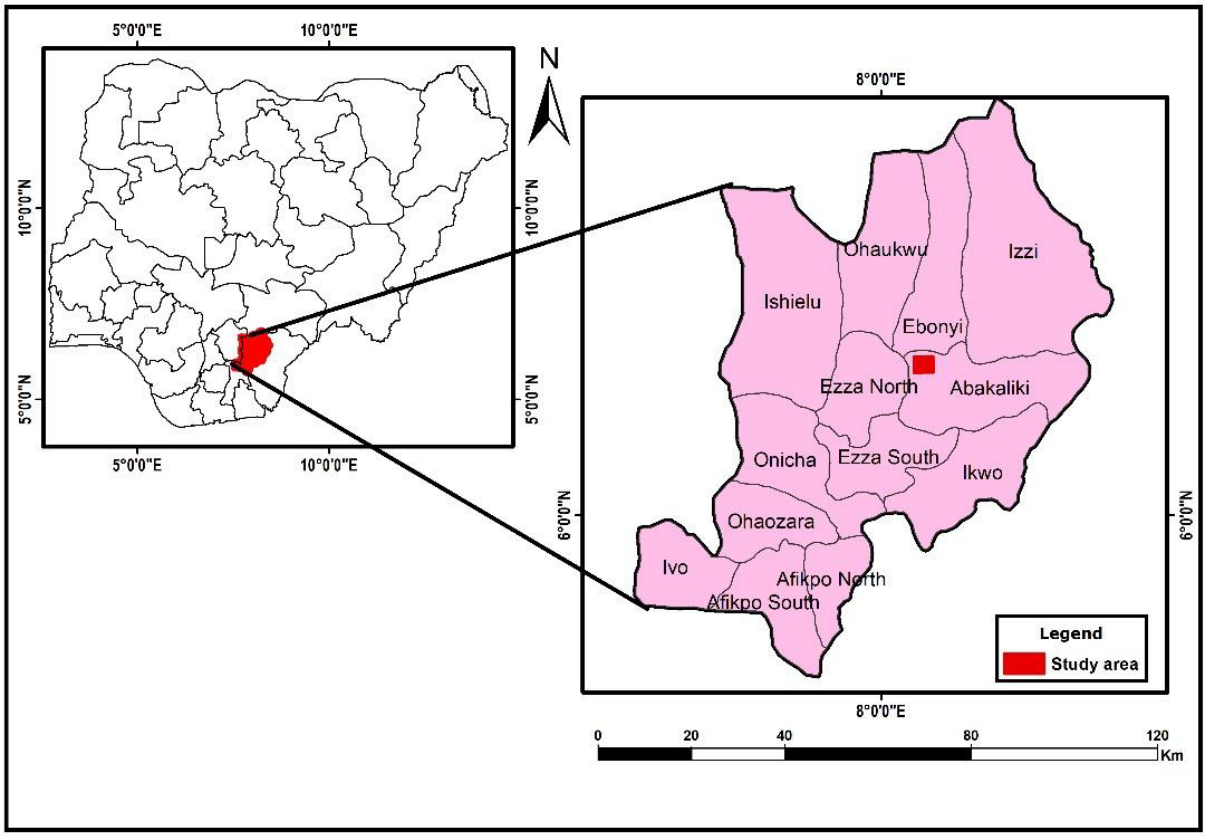

Figure 5.2: Location Map of Study Area (Abakaliki)

Mining at the site was carried out through the surface mining method. The mine was abandoned due to the frequent collapse of mining tunnels, which tragically resulted in the deaths of miners on an almost weekly basis. One contributing factor may have been the continuous inflow of groundwater into the pit, which likely weakened the tunnel walls. The current state of the mine (Figure 3A) is a large open pit filled with mine water, surrounded by waste piles and tailings.

5.1.5 Wase-Gimbi AML Sites

Gimbi is located within the lead-zinc mining district of Wase Local Government Area in Plateau State (Figure 5.3), spanning between latitudes 08°55′00″N and 09°02′00″N, and longitudes 10°09′00″E and 10°20′00″E. The area is well known for its abundant lead-zinc mineralisation, which has been exploited

for several decades. Key companies that have held mining licenses in the region include the Tongyi Group, Zurak Lead-Zinc Mine, Jawanda Zinc Mine, and Unique El-Mao Nig. Ltd.

Unfortunately, some of the mine pits, along with ponds formed through artisanal mining, have been abandoned, posing significant environmental challenges. Moreover, local communities live near these sites. Three abandoned mine pits previously operated by the Tongyi Group were visited during this study: the Gimbi pit (Figure 5.4B) and the Rikaya pits (Figures 5.4C and 3D), which are located a few hundred meters apart.

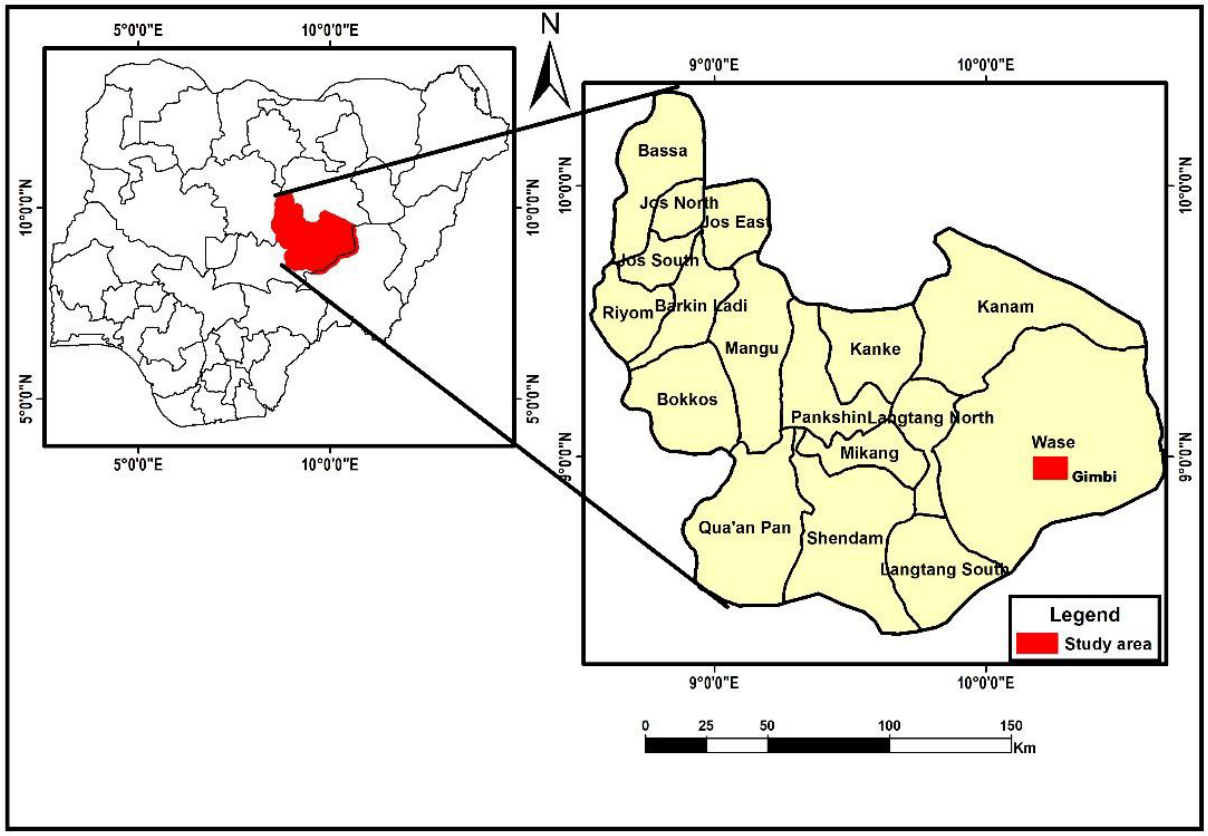

Figure 5.3: Location map of Study Area (Wase-Gimbi)

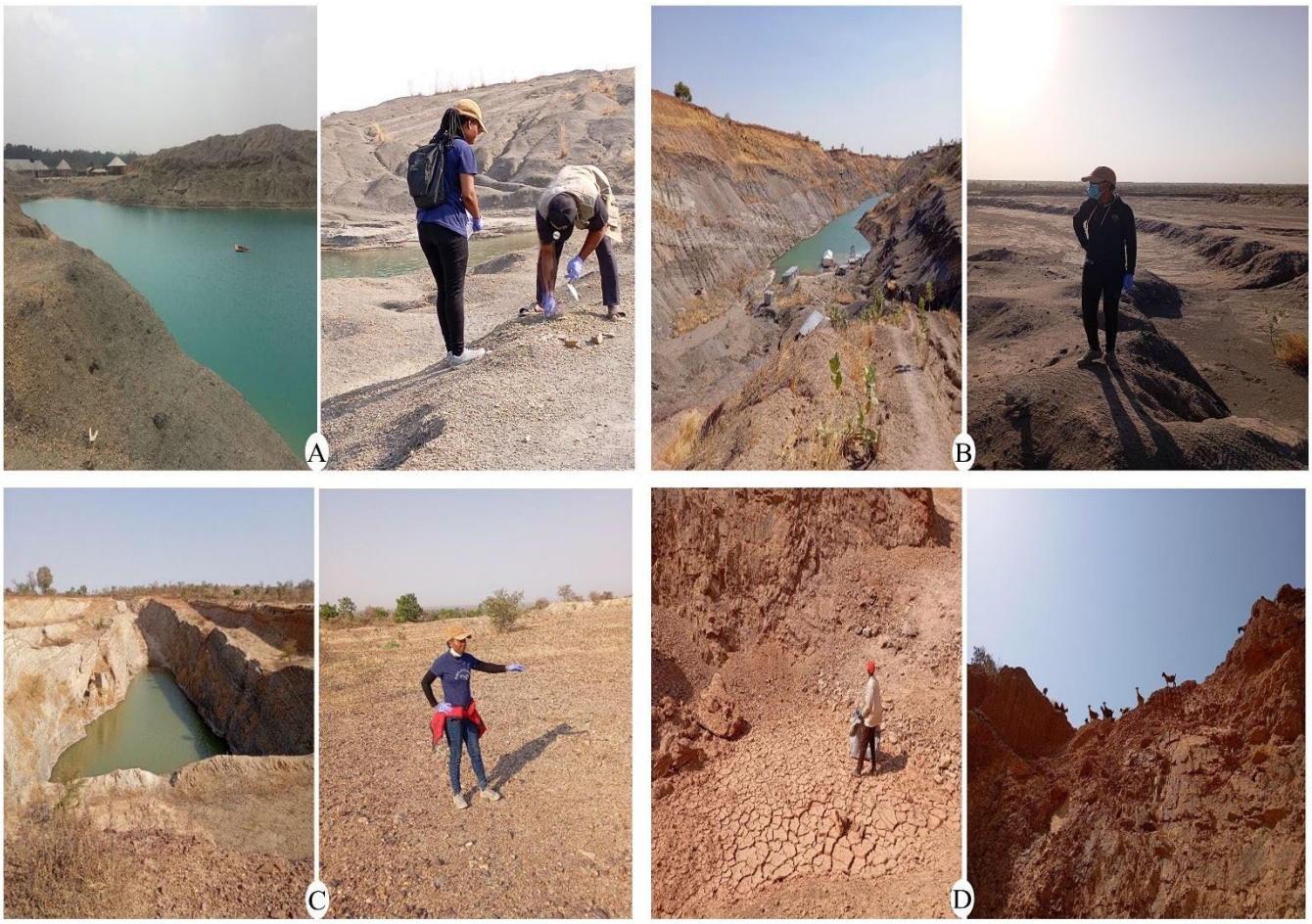

Figure 5.4: Abandoned Lead-Zinc mine at (A) Echara-Onuphu community, Abakaliki, (B) Gimbi environ – Pit 1, (C) Gimbi environ – Rikaya Pit 1 and (D) Gimbi environ – Rikaya Dry Pit 2

5.1.6 Chapter Aim and Objectives

This chapter aims to assess the risk of metal contamination in environmental media from abandoned lead–zinc mines on ecological receptors. Through chemical characterisation, metal speciation, and bioavailability-based ecological risk evaluation. Specific objectives are to:

- Determine the concentrations of potentially toxic metals in soil, tailings, sediment, and water samples collected at abandoned lead–zinc mine sites.
- Compare the measured metal concentrations with established international environmental quality standards to evaluate contamination levels.
- Evaluate chemical contamination using Pollution Indices.
- Characterise the chemical speciation of metals in solid matrices (soil, sediment, and tailings) to assess their mobility and potential bioavailability.
- Estimate the bioavailability of dissolved metals in water samples using the Biotic Ligand Model (BLM).

- Evaluate the ecological risk posed by the potentially toxic elements and establish exposure pathways.

5.2 Materials and Methods

The methods include sample collection, sample processing, and data analysis techniques designed to achieve this chapter's objectives. Prior to sampling, a Field Sampling Plan (FSP) for the environmental assessment of chemical contamination from abandoned coal and mineral mines was developed to provide structure and guidance for sampling activities. Additionally, a protocol for sample collection from abandoned coal and mineral mines was produced to outline site-specific procedures. Standard Operating Procedures (SOPs) for sediment, soil, and water sampling were also prepared to support comprehensive fieldwork.

5.2.1 Study Area

The study was conducted in the north-central and southwestern regions of Nigeria, as described in Sections 4.1.3 and 4.1.4. One AML pit was sampled in Abakaliki, Southeastern Nigeria, and three AML pits in Wase, the North Central part of Nigeria. The pits in Gimbi and Rikaya are within the Wase mining district. Soil samples were collected from arable and grazing land areas surrounding the AML sites. Tailings samples were obtained from impoundments and waste piles, while water and sediment samples were collected from AML ponds and river channels where accessible. Borehole water samples were also collected from the Gimbi community, located approximately 3 km from the AML site, from which the AML derives its name. Maps of the sampling locations are shown in Figures 5.5 and 5.6a-b.

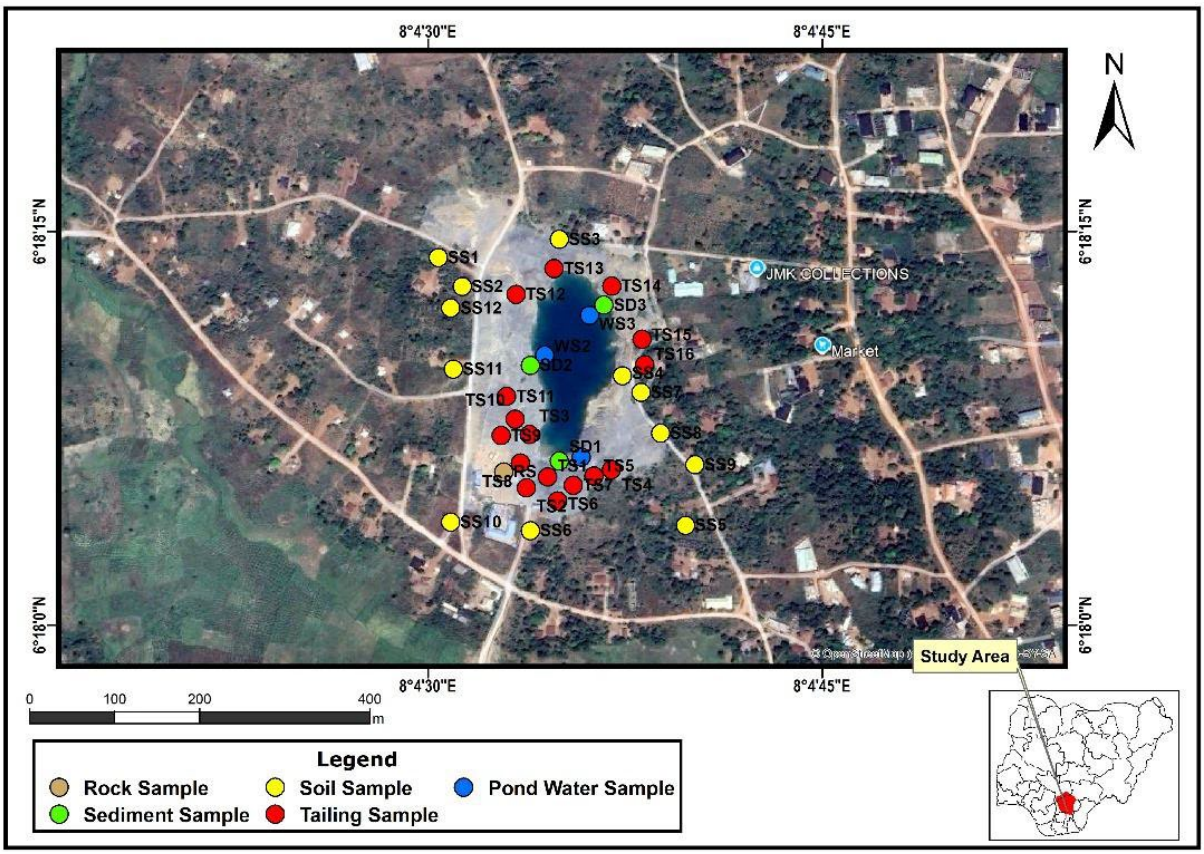

Figure 5.5: Sampling location map (Abakaliki)

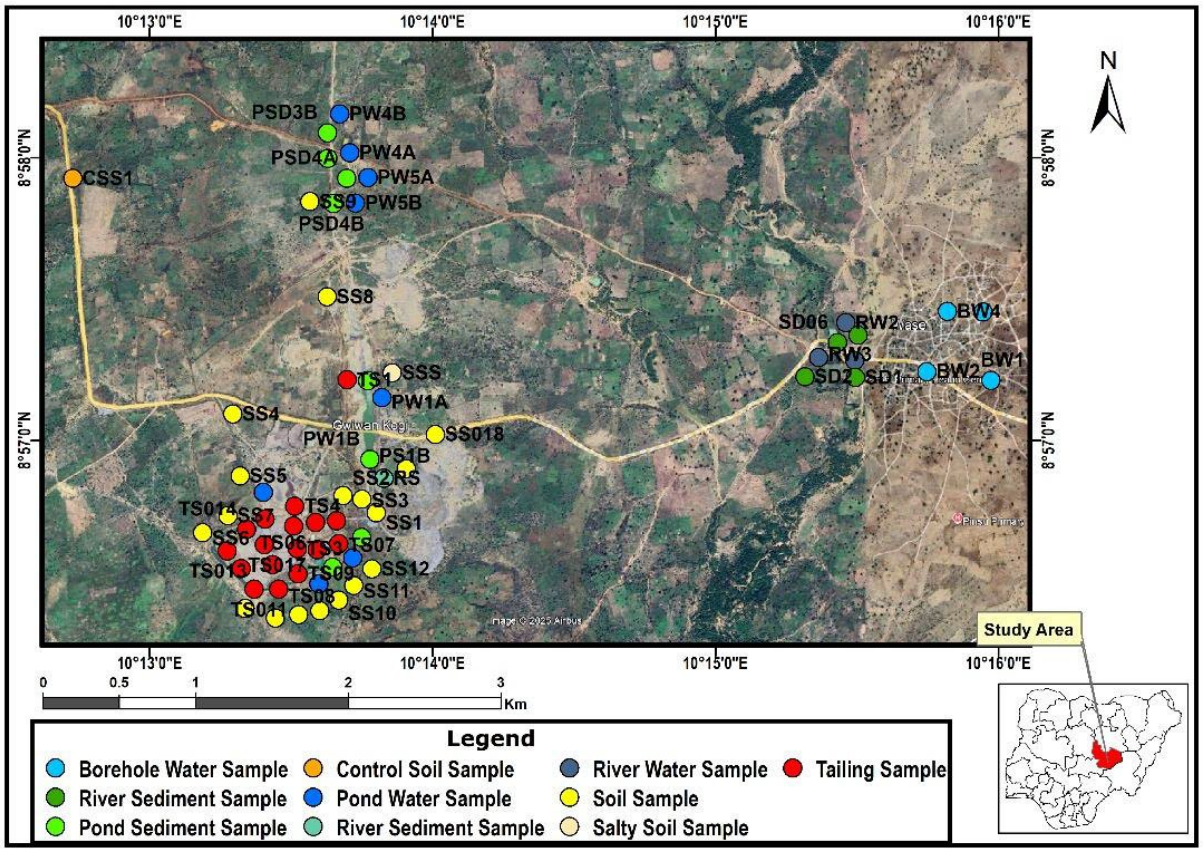

Figure 5.6a: Sampling location Map (Wase-Gimbi)

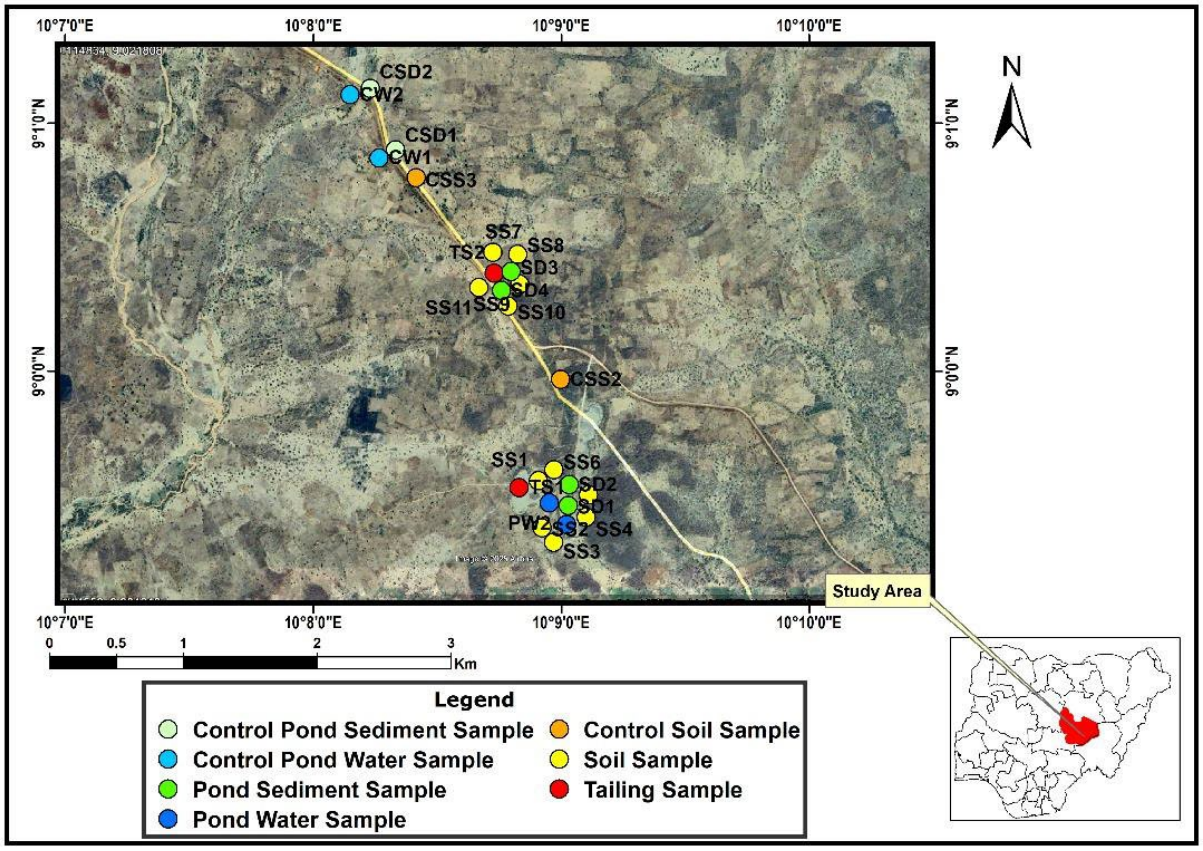

Figure 5.6b: Sampling location Map (Wase-Gimbi-Rikaya)

5.2.2 Field Measurements

A portable X-ray fluorescence (pXRF) analyser (S1 Titan by Bruker Nano Analytics, Germany) was used for in-situ, simultaneous multi-element analysis of soil and tailings at the Abakaliki abandoned lead-zinc site. In-situ measurements could not be conducted at the Wase-Gimbi sites because the equipment was unavailable due to security concerns in the region.

Field measurements were conducted after calibration with the instrument's certified reference material to ensure consistency with established element concentrations. Triplicate readings were automatically taken over 60 seconds, and the mean values are displayed as the result. Before each measurement, the probe was placed directly on the soil surface, ensuring the area was free from debris, stones, or vegetation. Sampling details, including elevation and GPS coordinates, were recorded at each location. Detailed information is provided in Appendices 5.1-5.4.

5.2.3 Sample Collection

Water samples were collected from mine ponds, isolated ponds around the AMLs, and the river channel. One-litre water samples were collected from each sampling point. A 50 mL sub-sample was transferred unfiltered into a 50 mL plastic tube for analysis of total metals and acidified to pH <2 with ICP-MS-

grade nitric acid. For stream and river water samples, a second sub-sample was filtered through a 0.2 μm PES syringe filter, transferred to another 50 mL plastic tube for analysis of dissolved metals, and similarly acidified to pH <2 with ICP-MS-grade nitric acid.

Sediment samples were collected in 250 mL plastic bottles from the same sampling points as the water samples. Due to the dry season, most river channels were dry; therefore, samples could not be collected from the upstream, midstream, and downstream locations as planned in the sampling protocol. Instead, samples were collected from local ponds dug by community members along river channels to access water for domestic use (Figure 5.7).

Soil and tailings samples were also collected in 250 mL plastic bottles. A random sampling strategy was adopted due to the uneven and disturbed nature of the abandoned mine site. Samples were collected from a depth of 0–5 cm below the topsoil using a stainless-steel trowel and plastic tools.

In total, 128 samples were collected from the three locations. The breakdown of sample types and their distribution is presented in Figures 5.5 and 5.6a–b:

- Abakaliki AML site: 3 water, 3 sediment, 14 soil, 16 tailings, and 1 rock sample.
- Gimbi AML site: 15 water, 12 sediment, 20 soil, 17 tailings, and 1 rock sample.
- Gimbi-Rikaya AML site: 4 water, 6 sediment, 13 soil, and 2 tailings samples.

Water samples included borehole water as the control, while sediment samples comprised pond and river sediments, with control samples collected outside the sampling AML site. The soil samples included control samples.

All samples were packed in polystyrene boxes with ice packs and shipped via FedEx courier from Nigeria to the Environmental Science Division Laboratory at Brunel University. Sample details are provided in Appendices 5.1-5.4.

Figure 5.7: a and b - Dry river channels due to the dry season, and c and d sample collection in the dry channel. The river channel is about 2 km from Wase-Gimbi AMLs

5.2.4 Reagents and Materials

The following reagents and materials were used for metal analysis: Analytical grade reagents including, high purity water obtained from Milli-Q® water purification system (Millipore, 18.2MΩ cm^{-1} at 25 °C) used to prepare all solutions, Whatman Polyethersulfone (PES) syringe filter (0.2 & 0.45 µm, 68% Nitric acid, 37% HCL, stock solutions of zinc, lead, copper, arsenic, nickel, titanium, cadmium, chromium, cerium, strontium, zirconium, manganese, mercury, iron, barium and aluminium. Calcium nitrate tetrahydrate ($Ca(NO_3)_2 \cdot 4H_2O$), sodium chloride (NaCl), magnesium sulphate ($MgSO_4$), potassium chloride (KCl), and iron(II) sulphate heptahydrate ($FeSO_4 \cdot 7H_2O$) were used to prepare

standard solutions for macro-element analysis. Solutions of 0.11 M acetic acid (CH_3COOH), 1 M nitric acid (HNO_3), 0.1 M hydroxyl ammonium chloride ($NH_2OH \cdot HCl$) and 1 M ammonium acetate (CH_3COONH_4) were prepared for sequential analysis. Potassium hydrogen phthalate ($KHC_8H_4O_4$), sodium bicarbonate ($NaHCO_3$) and sodium carbonate (Na_2CO_3) compounds for DOC analysis. All plastic and glassware were rinsed thoroughly with Milli-Q water before sample preparation. SOPs were developed and incorporated strictly to ensure a quality control programme.

5.2.5 General Parameter Analysis

pH Measurement

A 20 mL subsample was pipetted from each water sample bottle into a labelled 50 mL tube. The 450 pH/ion meter electrode was rinsed with Milli-Q water and carefully dried with Kim wipes. The electrode tip was then placed in the water sample and gently swirled for a few seconds. The "READ" button was pressed to start the measurement using the auto-read function, and the results were displayed automatically once a stable endpoint was reached.

Dissolved Organic Carbon (DOC)

DOC was measured using the TOC-V CPN analyser (Shimadzu, Japan). The instrument oxidises organic carbon to CO_2 via high-temperature catalytic combustion (680°C), and the resulting CO_2 is quantified using a non-dispersive infrared (NDIR) detector.

Calibration standards were prepared using sodium bicarbonate ($NaHCO_3$) for Inorganic Carbon (IC) and potassium hydrogen phthalate ($KHC_8H_4O_4$) for Total Carbon (TC). TC standards (1, 10, 100, 250, 500, and 1000 mg/L) were used to generate calibration curves for the Non-Purgeable Organic Carbon (NPOC) method. Method validation was performed after calibration using two replicates of mixed TC/IC concentrations (1, 10, 20, 50, 100, and 250 mg/L). The mean recovery ranged from 83% to 95% at concentrations between 1 and 100 mg/L, while the 250 mg/L concentration exceeded 120%. The validation data are presented in Appendix 5.5.

A 10 mL subsample was withdrawn from each filtered water sample using a 10 mL pipette and dispensed through a 0.45 µm Polytetrafluoroethylene (PTFE) syringe filter into a clean 50 mL tube, which was then tightly capped. The NPOC method was used to measure DOC in the samples. Prior to analysis, the samples were pretreated with 3 drops of 2.0 M HCl to convert inorganic carbon (IC) to carbon dioxide (CO_2), then sparged for 2 min to remove CO_2 and total inorganic carbon (TIC). The samples were then quantified using a non-dispersive infrared detector (NDIR).

5.2.6 Sample Preparation for Metal Quantification

Surface Water Samples

Collected water samples were prepared to measure both the dissolved fraction (metals in solution) and the total fraction (metals in both solution and suspended particles).

The dissolved and total water samples were digested in accordance with the US EPA 3051 method using microwave-assisted acid digestion with a MARS6 instrument. A 45 mL water sample was withdrawn from each sample, transferred to labelled MARS vessels, 5 mL of 68% nitric acid was added, and the vessels were then placed in the instrument for digestion. All digested samples were allowed to cool, then filtered through a 0.45 µm PES filter into labelled 50 mL tubes, and stored at room temperature for ICP-OES analysis to determine the elemental concentrations of dissolved and total metals. Note that the dissolved samples were initially filtered through a 0.2 µm filter in the field, and both the total and dissolved samples were then filtered through a 0.45 µm filter to prevent blockage of the analytical instrument during analysis. Additionally, Quality control and blank samples were included in all sample batches.

Soil, Tailings and Sediment

Solid samples were prepared using 0.5 g of each soil, sediment, and tailings sample, which was weighed and transferred into labelled microwave vessels, then digested with 68% Nitric acid and 37% hydrochloric acid (4:1; i.e., 8 mL of HNO3 and 2 mL of HCl were added to each sample). A 15-minute pre-digestion period was allowed before transferring the samples to the MARS 6 instrument for microwave-assisted acid digestion. The temperature was ramped to 175 °C within 5 minutes and maintained at that temperature for an additional 4.5 minutes, in accordance with the US EPA Method 3051A. Quality Control standards of known concentration (spiked and unspiked) were included in each sample batch. After digestion, the samples were allowed to cool to room temperature and transferred into labelled 50 mL centrifuge tubes. They were then centrifuged at 3000 rpm for 10 minutes using a Heraeus MegaFuge 16R (Thermo Scientific) to separate the solid residues from the liquid phase. The supernatant (liquid extract) was carefully decanted into labelled 15 mL centrifuge tubes and brought to a final volume of 15 mL with deionised water. The resulting extracts were stored at room temperature prior to ICP–OES analysis.

Sequential Chemical Extraction (SCE)

A three-step sequential chemical extraction (SCE) was conducted to partition trace metals in soil/sediment samples into operationally defined geochemical fractions: exchangeable/acid-soluble (EA), reducible (RF), and oxidisable (OF). This method, as applied in this study, was a modified version

of the protocols first developed by Tessier (Tessier et al., 1979) and then modified by the Community Bureau of Reference (BCR) scheme (Rauret et al., 1999) and the procedure described by Beane (Beane et al., 2016). The modified approach was used to assess the speciation and relative bioavailability of trace metals in solid matrices by determining the distribution of total metal concentrations among specific solid-phase fractions within the environmental media that are potentially bioavailable and ecologically relevant.

Approximately 0.5 g of homogenised soil/sediment was accurately weighed in a flow cabinet and transferred into a 50 mL polypropylene centrifuge tube to assess the exchangeable/acid fraction (F1). To each tube, 20 mL of 0.11 M acetic acid was added, and the tube was securely capped. Samples were agitated using a Model R100 Rotatest shaker overnight for 16 hours at room temperature (~22°C). After shaking, samples were centrifuged at 3000 rpm for 20 minutes to separate the extract from the solid phase. The supernatant was decanted into labelled 40 mL glass tubes, evaporated to dryness using a Fisher Stirring Hotplate, and reconstituted with 15 mL of 1 M nitric acid. The reconstituted solution was centrifuged again at 3000 rpm for 10 minutes and transferred to a labelled and dated 15 mL polypropylene centrifuge tube, stored at room temperature, and analysed within 24 hours. Residual solids were washed with 20 mL of Milli-Q water, shaken for 15 minutes, and centrifuged (3000 rpm, 20 minutes). Wash solutions were discarded in waste containers, while the residues were stored.

To assess the reducible fraction (F2), the residue from the exchangeable fraction was treated with 20 mL of 0.1 M hydroxylammonium chloride (adjusted to pH 2 with HCl) to release metals associated with iron and manganese oxides. Immediate shaking was performed for 16 hours at room temperature using the same shaker. Post-extraction, the mixture was centrifuged (3000 rpm, 20 minutes), and the supernatant was collected in fresh labelled glass tubes, evaporated to dryness, reconstituted in 15 mL of 1 M nitric acid, centrifuged (3000 rpm, 10 minutes), and stored for ICP-OES analysis within 24 hours. The residue was rinsed with Milli-Q water, shaken, centrifuged, and the waste was disposed of as previously described.

To isolate metals associated with organic matter and sulphides fraction (F3), the residue from the reducible step was transferred to 40 mL glass tubes and treated in two stages with 10 mL aliquots of 30% hydrogen peroxide. The first addition was digested at 85°C for 1 hour using the Fisher Stirring Hotplate. After cooling and volume reduction (<3 mL), a second 10 mL aliquot was added, followed by another 1-hour digestion at 85 ℃ to reduce the volume to ~1 mL. The remaining digest was transferred into 50 mL centrifuge tubes and extracted with 25 mL of 1 M ammonium acetate (pH 2, adjusted with HCl) by shaking overnight for 16 hours. The extract was centrifuged (3000 rpm, 20 minutes), decanted, evaporated, and reconstituted with 15 mL of 1 M nitric acid. Final solutions were stored and analysed within 24 hours. The residue was rinsed with Milli-Q water, shaken, centrifuged, and the waste was disposed of as previously described.

The residual fraction was not measured; instead, total metal concentrations from a single nitric/hydrochloric acid (aqua regia) digestion were used as the basis for calculating percentage partitioning; details are provided in the subsequent section.

5.2.7 Instrumental Analysis

Quantification of prepared aqueous extracts and digested solid samples was performed using ICP-OES on a PerkinElmer Optima 5000 series instrument. This technique enabled the quantification of cationic metal elements and a limited range of non-metal elements in liquid samples.

Prior to analysis, the instrument was calibrated using a series of multi-element standard solutions of known concentrations. The established calibration range was 0, 0.1, 0.5, 1, 2.5, 5, and 10 mg/L. Calibration curves were generated to establish a reliable linear relationship between the instrument response and the concentration of each target element.

5.2.8 Data and Statistical Analysis

All data analyses were processed using Microsoft Excel (Microsoft Corporation, 2023) and data visualisation and graphing were performed using OriginPro 2022b (OriginLab Corporation, 2022).

5.2.8.1 Method Validation

Method validation was carried out using both water and soil matrices to assess the method's accuracy, reproducibility, and detection limits under the study conditions. Quality control procedures, including the analysis of blanks and duplicates where applicable, were implemented to ensure data integrity.

Method accuracy and matrix performance were evaluated using known concentrations of each analyte, which were spiked into blank MQ water, river water, soil, and sediment samples at two levels: low (2 mg/L) and high (8 mg/L). These spike levels were selected from the established calibration range (0, 0.1, 0.5, 1, 2.5, 5, and 10 mg/L) to reflect environmentally relevant concentrations and method sensitivity. Recoveries (%) were calculated by deducting spiked samples from unspiked samples, dividing by the spiked concentration added, and multiplying by one hundred. Recoveries within the range of 80–120% were considered acceptable for method accuracy.

The Limits of Detection (LOD) for each analyte were determined using blank-based calculations; all samples, blanks, and standards were prepared using the same digestion and dilution protocols to ensure matrix consistency. Blank replicates (n=10) were analysed for each element to estimate the baseline signal variability. The LOD was calculated as the mean blank signal (μ) plus three times the standard deviation (σ).

Replicate analyses from each spike level for each matrix type were used to assess method precision, expressed as relative standard deviation (%RSD), which is the standard deviation of the replicates divided by the replicates' mean multiplied by 100. The %RSD values ≤10% were considered acceptable at higher concentrations.

The calibration and validation results, including regression equations, coefficients of determination (R^2), LOD, precision, and accuracy, are summarised in Appendices 5.6 and 7 for soil and water, respectively.

5.2.8.2 Linear Regression and Correlation Analysis

Linear regression analysis was employed to compare field XRF and ICP-OES data and assess the relationship between the two methods. Additionally, a correlation analysis utilising the Pearson Correlation matrix was conducted to examine relationships among the metals and the sampled media, and between the two study sites.

5.2.8.3 Surface Water Quality

Environmental Quality Standard (EQS) for water was assessed first by comparing the dissolved concentrations with EQS standard values, while the Biotic Ligand Model principle was applied to the water data using the BioMet Bioavailability tool v5.1 (Bio-Met, 2022) to determine site-specific EQS that are bioavailable for key metals available in the tool, including Ni, Pb, Zn and Cu. Dissolved oxygen content (DOC), pH and Ca data were used for the assessment. For Mn, the Metal Bioavailability Assessment Tool (M-BAT) by the Water Framework Directive–United Kingdom Technical Advisory Group WFD-UKTAG was used for the assessment (WFD-UKTAG, 2014). The US EPA National Recommendation for Water Quality Criteria – Aquatic Life Criteria (Buchman, 2008) were used to assess other metals not covered by the BioMet Bioavailability tool. The Bio-Met tools incorporate the following variables, with their definitions and derivations presented below:

HC5 (Hazardous Concentration for 5%) represents the concentration of a contaminant predicted to adversely affect the most sensitive 5% of species within a species sensitivity distribution (SSD).

Local HC5 (dissolved) (µg/L) is a bioavailability-corrected value, which is derived from ecotoxicological data based on SSD. It aims to protect at least 95% of local species, taking into account site-specific conditions. This is referred to as the Site-specific Predicted No Effect Concentration (PNEC) dissolved in the M-BAT tool. This concentration is derived from the ecotoxicological data and site-specific water quality data using the BLM.

BioF is the Bioavailability Factor. This is a correction factor that accounts for site-specific differences in metal bioavailability resulting from local water chemistry conditions. It is calculated as the ratio of

the reference HC5 value, derived under standard high-bioavailability conditions, to the local HC5 value, derived using site-specific water chemistry parameters. The BioF enables adjustment of measured metal concentrations while maintaining a constant environmental quality standard (EQS-bioavailable).

$$BioF = \frac{Reference\ HC5}{Local\ HC5} \quad \text{Eq. 1}$$

Bioavailable Concentration (µg/L): Is the concentration of metal that is bioavailable at the site or water body. This value is calculated by multiplying the dissolved metal concentration for the site by the BioF.

$$\text{Bioavailable metal concentration} = Dissolved\ metal\ concentration \times BioF \quad \text{Eq. 2}$$

Risk Characterisation Ratio (RCR): This is the risk characterisation ratio for the site or water body under consideration. A value of 1 or greater identifies a potential risk.

$$RCF = \frac{Bioavailable\ metal\ concentration}{EQSbioavailable} \quad \text{Eq. 3}$$

5.2.8.4 Soil and Sediment Quality

To evaluate metal contamination, the measured concentrations in soil and sediment were compared with established quality guideline values. Since Nigeria does not have officially established national soil and sediment quality guidelines, internationally recognised standards were adopted. Specifically, threshold values from the Canadian Council of Ministers of the Environment (CCME, 2016) were employed for comparative assessment to determine the levels of toxic metals in the sampled site.

5.2.8.5 Environmental Contamination and Risk Assessment

Environmental risk assessment was assessed using different pollution indices for measured Heavy Metals (HMs). The enrichment factor (EF), geo-accumulation (Igeo), contamination factor (CF), degree of contamination (Cd), and Ecological risk index (RI) were evaluated. Details are in Table 5.2.

Table 5.2: Degree of trace metal contamination based on different indices

Index	References	Value	Degree of contamination and level of risk	Interpretation/Comment
EF	(Buat-Menard & Chesselet, 1979)	<2	Depletion to minimal enrichment	
		2–5	Moderate enrichment	
		5–20	Significant enrichment	
		20–40	Very high enrichment	
		>40	Extremely high enrichment	
Igeo	(Muller, 1969)	<0	Uncontaminated	
		0–1	Uncontaminated to moderately contaminated	
		1–2	Moderately contaminated	
		2–3	Moderately to strongly contaminated	
		3–4	Strongly contaminated	

		4–5	Strongly to extremely contaminated	
		>5	Extremely contaminated	
CF	(Hakanson, 1980)	< 1	low contamination	
		1 ≤ CF < 3	moderate contamination	
		3 ≤ CF < 6	considerable contamination	
		CF ≥ 6	very high contamination	
C_d	(Hakanson, 1980)	Cd < 8	Low degree of contamination	
		8 ≤ Cd <16	Moderate degree of contamination	
		16 ≤ C< 32	Considerable degree of contamination	
		Cd ≥ 32	Very high degree of contamination	Indicating serious anthropogenic pollution
ER	(Hakanson, 1980)	<40	Low ecological risk	
		40–80	Moderate ecological risk	
		80–160	Considerable ecological risk	
		160–320	High-risk ecological risk	
		>320	Very high-risk ecological risk	
RI	(Hakanson, 1980)	<150	Low ecological risk	
		150–300	Moderate ecological risk	
		300–600	Considerable ecological risk	
		>600	Very high ecological risk	
RAC	(Perin et al., 1985)	< 1%	No risk	Metals tightly bound, not mobile
		1–10%	Low risk	Small portion is bioavailable
		11–30%	Medium risk	Moderate mobility/bioavailability
		31–50%	High risk	High potential for release
		> 50%	Very high risk	Very easily mobilised and toxic
CRS	(L. Jiang et al., 2021)	0	None	
		1	Low	
		2	Moderate	
		3	Considerable	
		4	High	
		5	Very High	
		6	Extremely Serious	

Enrichment Factor (EF)

The Enrichment Factor (EF) is commonly used to distinguish between natural and anthropogenic sources of trace metals and to evaluate the degree of contamination (e.g., spatial assessment and source identification). This was calculated by comparing the concentration of target elements with that of a reference element (Buat-Menard & Chesselet, 1979), expressed as:

$$EF = \frac{(Ci|Cr)_{sample}}{(Ci|Cr)_{background}} \quad \text{Eq. 4}$$

Where:

Ci = Concentration of the element of interest

Cr = Concentration of the reference element

Sample refers to the examined environment or media.

Background refers to a reference (uncontaminated) environment.

Commonly used reference elements include Sc, Mn, Ti, Al, and Fe due to their typically crustal origin and relatively low geochemical variability (W. H. Liu et al., 2005). Iron was used as the reference element in this study due to its relative stability and its common use as a conservative normalising element in contamination assessments. Background values for both the reference element and all other elements were sourced from established literature (Buchman, 2008; S. R. Taylor & McLennan, 1985). These reference data have been widely used to evaluate the influence of anthropogenic activities on metal enrichment, particularly in polluted environments associated with abandoned lead-zinc mine sites (Domingo et al., 2023).

Geoaccumulation Index (Igeo)

The Geoaccumulation Index (Igeo) was used to assess the level of trace metal contamination by comparing measured concentrations with pre-industrial levels (Muller, 1969). It was calculated using equation 2:

$$Igeo = Log_2\left(\frac{C_n}{1.5 \times Bn}\right) \quad \text{Eq. 5}$$

Where:

Cn = Measured concentration of the element n in the sample

Bn = background value of element n.

The constant 1.5 is a correction factor to account for natural variations in background values due to lithological effects.

The background values used in this study were sourced from Taylor and McLennan's report of upper continental crust values (S. R. Taylor & McLennan, 1985).

Contamination Factor (CF)

The Contamination Factor (C_f) was introduced by Hakanson to quantify the level of contamination by individual trace metals (Hakanson, 1980). The C_f was evaluated using the expression:

$$C_f = \frac{Cmetal}{Cbackground} \quad \text{Eq. 6}$$

Where:

C_{metal} = Measured concentration of the metal in the sample

$C_{background}$ = Background or reference concentration of the same metal

Hakanson recommends using defined, standardised preindustrial reference values to estimate contamination levels at contaminated sites. However, preindustrial reference values related to pre-mining databases for metal concentration are mostly not available globally (Zapico et al., 2017). Therefore, Taylor and McLennan's upper continental crust values (S. R. Taylor & McLennan, 1985) were used.

Degree of Contamination (C_d)

The Degree of Contamination (C_d) was used to assess overall heavy metal pollution in tailings, soils, and sediments. The C_d was calculated (Equation 4) as the sum of the Contamination Factors (Cf) for all studied metals (Hakanson, 1980):

$$C_d = \sum C_f^i \quad \text{Eq. 7}$$

Where:

C^i_f is the ratio of the measured concentration of a metal to its background/reference value.

Ecological Risk Index (RI)

The Potential Ecological Risk Index (RI), also developed by Hakanson, was used to evaluate the potential risk of trace metals to the environment (Hakanson, 1980). Taking into account both contamination levels and metal toxicity. The overall RI is the sum of the ecological risk factors (Er_i) for each metal:

$$RI = \sum Er_i \quad \text{Eq. 8}$$

Where:

$$Er_i = C_f^i \times T_r \quad \text{Eq. 9}$$

C^i_f = Contamination factor of metal i

T_r = Toxic-response factor, a metal-specific constant representing its ecological hazard.

Toxic-response factors (Tr) were assigned following (Hakanson, 1980). Table 5.3 presents commonly reported metals. For elements not included in the original framework, such as manganese (Mn) and barium (Ba), a conservative Tr value of 1 was adopted, based on literature precedent (W. Li, Cao, et al., 2024), reflecting their relatively low ecological toxicity.

Table 5.3: Toxic-response factors (Tr) by (Hakanson, 1980).

Metal	T_r
Cd	30
Pb	5
Cu	5
Ni	5
Cr	2
Zn	1
Hg	40
As	10
V	2

Risk Assessment Code (RAC)

Risk Assessment Code (RAC) is defined as the exchangeable and carbonate-bound fraction (F1) expressed as a percentage. In this study, RAC was calculated as the percentage of F1 relative to the total metal concentration obtained from the single nitric/hydrochloric acid digest. This fraction is considered the most mobile and bioavailable, hence posing the greatest environmental risk. For the BCR method, it is the percentage of F1. RAC was determined for the studied heavy metals, and the results were interpreted based on RAC classifications (Table 5.2) described by (Perin et al., 1985), and it's expressed as:

$$RAC = \left(\frac{F1}{Total_{metal}}\right) \times 100 \qquad \text{Eq.10}$$

Where:

F1 is the exchangeable fraction

$Total_{metal}$ is the total metal concentration.

Comprehensive Pollution Risk Score (CRS)

The Comprehensive Pollution Risk score described by Jiang and Liang (W. Jiang & Liang, 2023) uses the points-weighing methods that is, the sum of all pollution and risk indices evaluated or assessed:

$$CRS_i = S_i(Igeo) + S_i(EF) + S_i\left(E_r^i\right) \qquad \text{Eq. 11}$$

Where:

CRS_i is the comprehensive pollution risk score; S_i (Igeo) is the score of the Igeo pollution level of metal i; S_i(EF) is the score of the EF pollution level of metal i; S_i (E^i_r) is the score of the E^i_r pollution level of metal i. The method considers factors such as concentration, occurrence fraction of Igeo, EF, and Er to

summarise the risk assessment into a comprehensive conclusion, assuming that these factors contribute equally to the degree of heavy metal pollution.

5.3 Results

Field X-ray fluorescence (XRF) measurements, laboratory-determined metal concentrations, and sequential extraction results from the two study sites, Abakaliki and Plateau State (Sections 5.1.4–5.1.5 and 5.2.1), are presented.

Field XRF analysis was used to identify the potentially toxic metals (PTMs) present at the Abakaliki site and to provide semi-quantitative estimates of their concentrations. The study compared laboratory-determined total metal concentrations with field XRF data to evaluate the correlation and reliability of the two analytical approaches. The total metal concentrations data were subsequently used to calculate the contamination indices, the results of which are presented in a later section.

Total metal concentrations in soil, tailings, and sediment samples from each study site are presented, and metal contents across media were compared with guideline values to assess contamination levels. Water samples, including dissolved and total metal concentrations, are presented and compared with guideline values and BLM results.

Additionally, results from the sequential extraction analysis are presented to assess the potential bioavailability and partitioning of metals among solid-phase fractions. All raw datasets (pXRF, ICP–OES, and sequential extraction analyses) are provided in Appendices 5.8-5.10, 5.12-5.13 and 5.15-5.16 for all the sites.

5.3.1 Portable X-Ray Fluorescence (pXRF) Field Results

Field-based X-ray fluorescence (XRF) analysis was conducted on soil and tailings samples (Table 5.4) from the study sites to identify and quantify the presence of major and trace elements. The data reflect semi-quantitative values due to the environmental variability and limitations associated with in-field measurements.

Concentrations of elements such as Fe, Mn, Cr, Zn, Pb, and Cd were notable across both media, with generally higher variability observed in tailings samples. For instance, Pb concentrations in tailings ranged from 116.0 to 2,645.0 mg/kg, with a mean of 1,144.3 mg/kg, while in soil, the range was 201.0 to 1,811.0 mg/kg, averaging 977.8 mg/kg. Similarly, Zn levels were significantly elevated in tailings (mean: 2,228.7 mg/kg) compared to soil (mean: 483.3 mg/kg). In general, as shown in Figure 5.8, Ti, Pb, Zn, Mn, Ba, Zr, and Ce were the most abundant metals. These results suggest substantial contamination, particularly in tailings.

Cerium, a light rare earth element (LREE), was detected in both soil and tailings samples, with maximum and mean concentrations of 504.0 and 292.0 mg/kg and 476 and 220.0 mg/kg, for soil and tailings, respectively. This is a significant observation, as cerium has not previously been reported in AML or related studies in Nigeria, suggesting either a previously unrecognised geochemical feature or a potential indicator of rare earth element (REE) enrichment in the area.

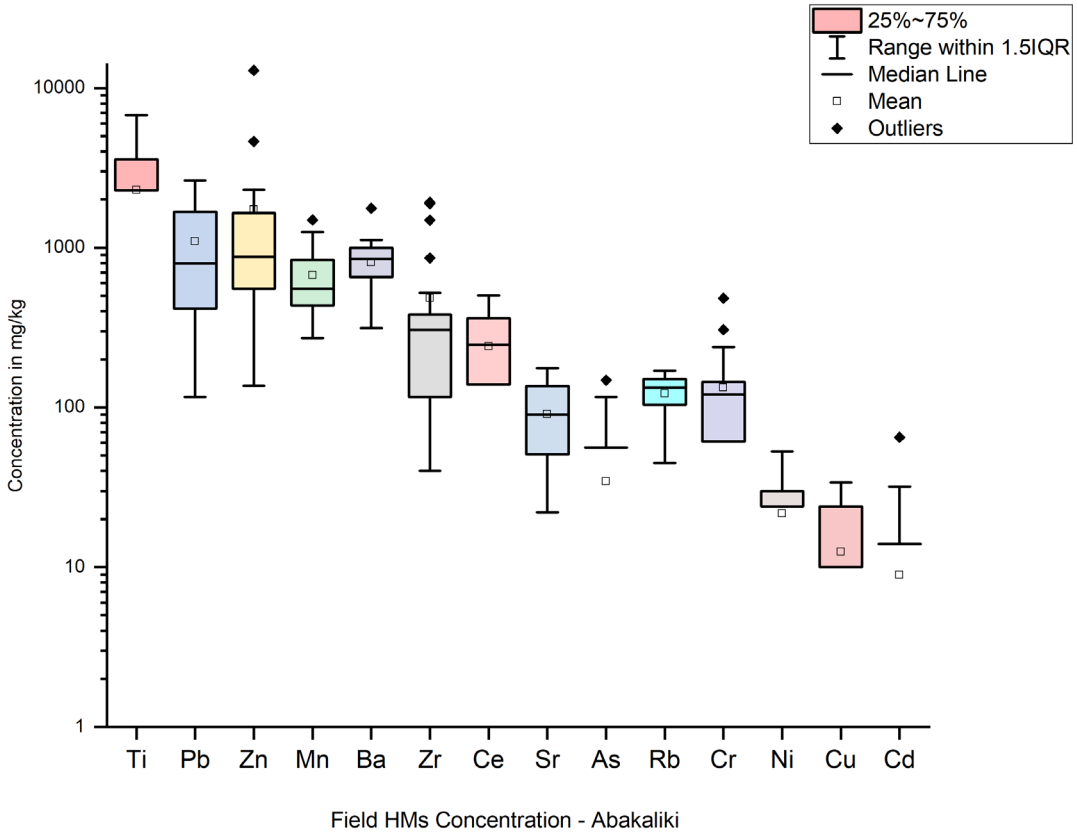

Figure 5.8: Heavy Metal (HM) concentrations at Abakaliki Pb/Zn AML and surrounding soils.

Table 5.4: Descriptive statistics for pXRF results (mg/kg)

Statistical Parameter	Mg	Al	Si	K	Ca	Ti	Cr	Mn	Fe	Ni	Cu	Zn	As	Rb	Sr	Zr	Cd	Sn	Ba	La	Ce	Pb
Tailings n=15																						
Mean	159.5	66.6	725	172.9	0	1764.9	107.4	515.7	51814	22.1	10	2228.7	29.5	143.1	108.3	224.3	11.4	69.9	959.1	91.5	220	1144.3
Minimum	0	0	158.4	15.2	0	0	0	271	19659	0	0	274	0	104	22	40	0	0	655	0	0	116
Maximum	386.6	178.5	1250.3	268.1	0	3905	306	972	106054	50	30	12858	148	170	176	381	65	344	1761	426	476	2645
Median	189.9	62.8	706.2	197.6	0	1970	99	479	53954	24	0	1420	0	147	124	277	0	0	919	0	247	796
Standard Error	37.3	14.7	80.7	20.1	0	390.8	18.2	46.3	5715.6	4.4	3.2	808.9	11.4	4.4	12.3	33.5	4.6	27.5	66.2	31.5	40.8	212.6
Standard Deviation	144.5	57	312.7	77.8	0	1513.7	70.3	179.4	22136	16.9	12.4	3132.9	44.3	17	47.6	129.6	17.8	106.6	256.4	121.8	158	823.4
Sample Variance	20872	3248	97798	6052	0	2.00E+06	4946	32199	5.00E+08	285	154	1.00E+07	1959	287	2264	16808	315	11371	65747	14843	24954	677998
Kurtosis	-1.7	-0.1	0	-0.4	0	-1.6	4	1.9	1.3	-1	-1.5	10.9	2.4	0.5	-0.8	-1.5	5.7	2.2	7.1	2.8	-1	-1.1
Skewness	0	0.7	0.1	-0.6	0	0	1.5	1.3	0.7	0	0.7	3.2	1.6	-0.7	-0.7	-0.5	2.2	1.7	2.3	1.5	-0.3	0.5
Range	386.6	178.5	1092	252.9	0	3905	306	701	86395	50	30	12584	148	66	154	341	65	344	1106	426	476	2529
Soil n=6																						
Mean	132.9	52.8	1081.2	63.1	155.8	3613.2	196.8	1065.8	79306	20.5	18.7	483.3	46.8	70.7	46.3	1131.3	2.8	129.8	434.7	84.5	292	977.8
Minimum	0	0	360.2	42.1	0	0	0	837	28318	0	0	137	0	45	29	108	0	0	0	0	0	201
Maximum	332.9	135.4	1784.4	87.4	352	6775	482	1491	116599	53	34	922	116	114	61	1922	17	426	691	201	504	1811
Median	88.2	39.9	1021.5	63.3	159	4021.5	169	987	83474	21.5	18	516.5	38.5	62.5	52	1175	0	71	477.5	66.5	302	900.5
Standard Error	63	19.8	226.8	7.1	61	1042.2	66.3	105.3	11735	8.1	5.1	113.5	19.2	10.4	5.5	306.2	2.8	69.5	108.4	38.8	74.4	273.6
Standard Deviation	154.2	48.4	555.4	17.4	149.3	2552.9	162.4	257.9	28745	19.9	12.4	278.1	46.9	25.5	13.5	750.1	6.9	170.3	265.6	95.1	182.1	670.3
Sample Variance	23791	2343	308513	301	22293	7.00E+06	26360	66516	8.00E+08	396	153	77315	2201	652	181	562585	48	29004	70565	9035	33171	449303
Kurtosis	-2.4	0.9	-1.8	-1.1	-2.2	-1.3	2	0	2.7	0.3	-0.4	0.2	-1.1	0.6	-1.7	-1.9	6	0.9	-0.2	-2.8	0	-2.2
Skewness	0.4	1	0	0.1	0.1	-0.3	1	1	-1	0.7	-0.3	0.4	0.6	1.1	-0.7	-0.2	2.4	1.2	-0.8	0.2	-0.6	0.2
Range	332.9	135.4	1424.2	45.3	352	6775	482	654	88281	53	34	785	116	69	32	1814	17	426	691	201	504	1610

5.3.2 General Physicochemical Characterisation

The pH and DOC levels for the study sites indicate strong to alkaline conditions and vary from low to high, respectively. The mean pH of surface water at the Abakaliki site was 3.61, with a range of 3.56–3.72, indicating strongly acidic conditions. In contrast, the mean pH values at Gimbi and Rikaya were 7.46, ranging from 5.30 to 8.66, suggesting near-neutral to slightly alkaline conditions. The mean DOC concentration at Abakaliki was 2.23 mg/L (range: 1.12–4.44 mg/L), indicating low to moderate DOC, while Gimbi recorded a higher mean DOC of 7.28 mg/L, with a broader range of 0.66–49.14 mg/L, exhibiting a higher and more variable DOC. These results are presented in Table 5.5

Table 5.5: pH and DOC results of water from the sampled sites

AML Site	Sample ID	pH	DOC (mg/L)
Abakaliki	WS1	3.56	4.44
	WS2	3.56	1.15
	WS3	3.72	1.12
Plateau-Gimbi	PWS1A	7.27	2.91
	PWS1B	8.09	2.8
	PWS2A	6.01	2.64
	PWS2B	5.3	1.3
	PWS3	7.25	1.96
	PWS4B	7.77	4.1
	PWS5A	8.15	10.46
	PWS5B	7.45	14.43
	BHW1	8.05	0.7
	BHW2	7.94	1.73
	BHW3	8.24	0.91
	BHW4	8.66	0.74
	RW1	8.23	4.55
	RW2	6.83	0.66
	RW3	6.59	16.82
Plateau-Rikaya	PWS1	7.71	3.81
	PWS2	7.76	6.87
	PCW1	7.24	49.14
	PCW2	7.16	11.87

5.3.3 Total Metal Concentration

Total metal concentrations were determined in soil, sediment, tailings, and water samples to assess the extent of contamination in the selected case studies. These results served as a reference for evaluating the outcome of field XRF data and for identifying metals of environmental concern, including Pb, Zn, Mn, Cd, Cu, Ni, Ba, Al, and Fe. Although total concentrations alone do not reveal the environmental mobility or biological impact of metals, they provide an essential foundation for further analyses such as sequential extraction, bioaccessibility, or geochemical modelling that inform ecological risk assessments (John & Leventhal, 2004).

The data sets for tailings, soil, and sediment samples for the Abakaliki, Gimbi, and Gimbi-Rikaya sites are in Appendices 5.9, 5.12, and 5.15, respectively, while those for water samples are in Appendices 5.18 and 5.19.

The descriptive statistics for the total metal concentration for the two case studies are presented in Tables 5.6-8 for tailings, soils and sediments, while Tables 5.9-10 are for water samples. Descriptions of the concentration levels of each sampled media are provided for each site in the subsequent sessions.

Table 5.6: Descriptive statistics of the Total metal concentrations (mg/kg) for Abakaliki AML

Statistical Parameter	*Mn*	*Zn*	*Pb*	*Ni*	*Cr*	*Cu*	*Ti*	*Zr*	*Ce*	*Sr*	*Ba*	*Cd*	*Al*	*Fe*	*Mg*	*Ca*	*Na*	*K*
Tailings (n=18)																		
Minimum	203.6	345.7	107	21.9	29.4	16.5	4.8	0	6.3	9.4	21.7	0.1	0	27278.2	13618	881.4	434.7	3386.7
Maximum	479.9	14059.1	3291.2	42.6	47.3	147.8	8.7	5.6	14.7	18.5	57.7	76.9	28220.8	37149.8	34781.6	6109.5	1358.6	7695.7
Mean	282.3	4462	1103	30.4	39.5	54.4	6.4	2.7	9.4	12.8	33	20.2	17516.6	31175.4	26923.9	3096.8	843.8	5335.3
Median	274.9	3982.7	829.8	28.8	38.8	42.5	6	2.6	8.8	12	29.1	12.9	22182.4	30537.4	27661.1	2489.6	884.6	5041.9
Standard Error	15.5	880.5	218.3	1.3	1.1	8.5	0.3	0.4	0.6	0.7	2.2	5	2330.8	692.4	1168.2	380.4	66.3	297.7
Standard Deviation	65.7	3735.5	926.2	5.7	4.6	36.1	1.1	1.6	2.4	2.8	9.3	21	9888.6	2937.7	4956.3	1614	281.1	1263
Sample Variance	4317	13954228	857878	33	21	1304	1	3	6	8	87	442	97784498	8630226	24564822	2605049	79011	1595046
Kurtosis	4	0.9	0.4	0.1	0.1	2	-0.1	0.2	0.6	-0.4	1.4	1.5	-0.1	-0.6	2	-0.6	-1	-0.5
Skewness	1.7	1	1.1	0.7	-0.1	1.6	0.9	-0.2	1	0.8	1.1	1.3	-1.3	0.6	-0.8	0.8	0	0.5
Range	276.3	13713.4	3184.2	20.8	17.9	131.3	3.9	5.6	8.4	9.1	36	76.8	28220.8	9871.6	21163.6	5228	923.8	4309
Soil (n=12)																		
Minimum	485	116.7	187.5	4.9	56.7	13.6	10.5	0	20	9.5	15.7	0.1	11431.1	34622.6	950.5	1073.9	452	2137
Maximum	2185	945.6	1848.5	29.5	226	56.4	51.8	11.6	56.2	17.9	49.8	5	24802	45466.8	17585.8	5210.6	1306.2	6034.8
Mean	966.3	465.9	799	13.3	129.8	27.5	27.5	4.7	36.9	13.6	31.3	2	16688.8	40505.8	5385.8	2823.4	714	3353.6
Median	828.8	439	574.8	13.5	123.7	22.9	25.5	3.8	35.6	13.6	29.3	2	15290	39436.8	3235.6	2501	589.4	2895.9
Standard Error	137.7	81.1	162.1	2.1	14.4	4	3.2	1.3	3.2	0.7	3.7	0.5	1217.7	1187.3	1468.1	411.5	82.6	340.8
Standard Deviation	477.2	281	561.4	7.2	49.9	13.8	11.2	4.5	11	2.5	12.6	1.7	4218.2	4112.9	5085.8	1425.5	286.3	1180.4
Sample Variance	227673	78982	315195	52	2495	191	126	20	120	6	160	3	17793299	16915828	25865416	2032018	81955.8	1393457
Kurtosis	3.5	-1	-0.9	1	0.1	-0.1	1	-1.5	-0.8	-0.1	-1.3	-0.7	0.5	-1.9	1.7	-0.6	0.4	1.5
Skewness	1.9	0.4	0.7	0.9	0.6	1	0.6	0.4	0.2	0.4	0.3	0.6	1.1	0.1	1.5	0.8	1.2	1.5
Range	1700	828.9	1661	24.6	169.3	42.8	41.3	11.6	36.2	8.4	34.1	5	13370.9	10844.2	16635.3	4136.8	854.3	3897.8
Sediment (n=3)																		
Minimum	255.2	705.6	265.9	20.4	29.5	21.6	4.9	0	5.9	12.6	28.1	2.2	0	32897.7	29987.4	3783	630.3	4171
Maximum	339.3	1640	1472.6	38	45.9	51.2	8.1	0	12.1	18.6	41.2	4.8	23420.7	37449.1	39673.1	4234.2	1084.2	6828.2
Mean	307	1272.9	1023	31.2	39.7	39.8	6.7	0	9.5	15.9	35.9	3.8	7806.9	35748.6	35844.4	3975.8	904	5716.6

Statistical Parameter	*Mn*	*Zn*	*Pb*	*Ni*	*Cr*	*Cu*	*Ti*	*Zr*	*Ce*	*Sr*	*Ba*	*Cd*	*Al*	*Fe*	*Mg*	*Ca*	*Na*	*K*
Median	326.3	1473.1	1330.6	35.2	43.6	46.6	7.2	0	10.6	16.5	38.5	4.3	0	36899.1	37872.7	3910.3	997.5	6150.6
Standard Error	26.1	287.7	380.8	5.5	5.1	9.2	0.9	0	1.9	1.7	4	0.8	7806.9	1434.3	2974.3	134.3	139.1	797.2
Standard Deviation	45.3	498.3	659.5	9.5	8.9	15.9	1.6	0	3.2	3	6.9	1.4	13521.9	2484.3	5151.6	232.7	240.9	1380.7
Sample Variance	2048	248309	434946	89	79	253	3	0	11	9	48	2	1.83E+08	6171512	26538774	54132.3	58055.4	1906463
Kurtosis	0	0	0	0	0	0	0	0	0	0	0	0	0	0	0	0	0	0
Skewness	-1.6	-1.5	-1.6	-1.6	-1.6	-1.6	-1.1	0	-1.3	-0.9	-1.4	-1.5	1.7	-1.6	-1.5	1.2	-1.5	-1.3
Range	84.1	934.4	1206.7	17.6	16.4	29.5	3.2	0	6.2	5.9	13.1	2.6	23420.7	4551.4	9685.7	451.3	453.9	2657.2
Reference/Control soil (n=2)																		
RSS1	530.6	94.6	67.5	18.7	66.6	22.8	17.8	8.7	29	39.3	74	0	17608.8	37568.7	5744.9	21076.1	833.6	3884.8
RSS2	461.6	62.4	27.2	14.2	43	16.3	11.4	10.8	33.8	19.6	43.9	0.1	17402.5	35341.7	1956.4	7690.9	1039.8	5279.9
Rock Sample	1030.4	429.5	905.3	4.3	16.9	22.1	7.7	0.1	38.9	6.3	9.2	2.8	6964.9	23203.7	1932.4	1880.5	1861.5	4307

Table 5.7: Descriptive statistics of the Total metal concentrations (mg/kg) for Gimbi AML

Statistical Parameter	*Mn*	*Zn*	*Pb*	*Ni*	*Cr*	*Cu*	*Ti*	*Zr*	*Ce*	*Sr*	*Ba*	*Cd*	*Hg*	*Al*	*Fe*	*Mg*	*Ca*	*Na*	*K*
Tailings (n=17)																			
Minimum	787.3	111.2	21.6	15.3	3.8	24.7	0	0	4.7	17.8	23.7	0	0	624.6	20720.4	1346.3	5815.1	818	2182.4
Maximum	7533	17769.1	2544.3	39.1	23.6	181.8	12.6	9.5	26.1	215.7	314.3	33.4	0	9261.4	40403.1	26541.1	46649.3	3031.3	8122.8
Mean	3829.3	7720.6	1030.5	23.5	13	78.8	2	4.2	14.7	47.7	94.8	18.2	0	4653.7	29885.2	15691.8	18479.4	1741.1	5218.6
Median	4183	8596.2	1065	22.6	14.1	78.8	0	4	12.9	35.1	72.4	20.2	0	4327.6	31549.8	16715.7	17422.4	1624.8	5371.4
Standard Error	546.5	1250.4	192.8	1.5	1.3	10.4	0.8	0.6	1.4	11	17.8	2.9	0	678.1	1463.6	1522.7	2278.7	144	356.5
Standard Deviation	2253.1	5155.6	794.7	6.4	5.3	42.9	3.4	2.7	6	45.2	73.5	12.1	0	2796	6034.6	6278.3	9395.2	593.6	1469.7
Sample Variance	5076371	26580594	631594	41	28	1837	12	7	36	2042	5395	146	0	7817404	36416074	39417404	88270604	352310	2160147
Kurtosis	-1.4	-0.6	-0.5	0.8	0.1	0.7	5.1	0.6	-0.1	13.8	4.4	-1.3	0	-0.9	-1.2	0.3	4.4	0.4	0.5

Statistical Parameter	*Mn*	*Zn*	*Pb*	*Ni*	*Cr*	*Cu*	*Ti*	*Zr*	*Ce*	*Sr*	*Ba*	*Cd*	*Hg*	*Al*	*Fe*	*Mg*	*Ca*	*Na*	*K*
Skewness	0.2	0	0.4	1	-0.1	0.8	2.1	0.5	0.6	3.6	2	-0.4	0	0.4	0	-0.5	1.7	0.8	-0.2
Range	6745.7	17657.8	2522.7	23.8	19.8	157.1	12.6	9.5	21.3	197.8	290.6	33.4	0	8636.8	19682.7	25194.8	40834.2	2213.4	5940.4
Soil (n=19)																			
Minimum	31.9	21.5	7.4	0	3.4	5.1	0	2.3	3.3	5.5	19.5	0	0	2249.8	8389.8	734	3325.8	383.3	2590.3
Maximum	1791.3	6239.2	706.9	12.7	137.8	39.6	139.5	15.9	52.5	39.1	149.3	9.5	0	17647.3	41548.4	58720.1	15444.6	8680.8	8760.8
Mean	623.4	485.6	63	6.3	48.6	11.3	44	6	29.6	18.8	82.5	0.5	0	6639.2	22636.4	5179.1	8477.7	1234.3	4061.2
Median	594.7	49.1	27.9	6.3	33.1	9.9	27.2	4.9	27.6	18.6	77.6	0	0	5299.9	20070.2	2235.7	7554.1	836.1	3865.6
Standard Error	93.8	325.7	35.9	0.8	7.8	1.8	8.5	0.8	2.9	1.9	8	0.5	0	891.1	2600.3	2983.9	821.3	418.6	382.3
Standard Deviation	408.7	1419.8	156.3	3.5	34	7.9	37.3	3.4	12.5	8.1	34.8	2.2	0	3884.1	11334.5	13006.7	3580	1824.6	1666.3
Sample Variance	167054	2015872	24440	12	1156	62	1388	12	155	66	1209	5	0	15086041	128471737	169174999	12816730	3329072	2776568
Kurtosis	2.5	17.4	18.8	-0.5	1.2	9.8	1.3	2.9	-0.2	0.7	-0.6	19	0	2.7	-1.1	18.7	-1.1	18	3.6
Skewness	1.1	4.1	4.3	-0.1	1.2	2.8	1.3	1.6	0	0.6	0.1	4.4	0	1.6	0.5	4.3	0.3	4.2	1.9
Range	1759.4	6217.8	699.5	12.7	134.4	34.5	139.5	13.6	49.2	33.6	129.8	9.5	0	15397.4	33158.6	57986.1	12118.8	8297.5	6170.5
Sediment (n=12)																			
Minimum	245.8	9.6	16.8	0	5.1	6.2	3.8	0.4	7.8	6.8	34.1	0	0	1294.8	6227.1	1270	3763.4	568.1	1663.5
Maximum	3850.1	2634.7	448.1	39.5	81.3	99.1	27.4	8.5	74.4	260.9	377.4	3.3	1.3	29793	40401.5	30731.3	188458.4	2890.8	13949
Mean	1239.8	559.8	158.2	17.9	26.6	32.1	10.5	3.5	39	52.7	158.1	0.3	0.1	11724.1	24739.7	9347	32632.2	1769.6	6950.2
Median	1085.9	397.8	113.4	14.3	18.1	22.9	9.1	3.5	39.5	33	98.4	0	0	10892.1	27084.4	6478.3	10905.5	1885.3	6167.1
Standard Error	303.6	209.1	41.9	3.8	6.7	7.5	1.8	0.8	6.6	19.8	35	0.3	0.1	2419.8	3097.8	2258.9	15918.8	193.1	1032.5
Standard Deviation	1051.6	724.4	145.3	13.2	23.1	25.8	6.3	2.7	22.8	68.5	121.2	0.9	0.4	8382.4	10731.1	7825.2	55144.5	668.9	3576.8
Sample Variance	1105856	524744	21116	175	532	667	40	7	519	4699	14694	1	0	70264961	115156356	61233197	3040917256	447493	12793727
Kurtosis	2.5	6.8	-0.2	-0.7	2.2	3.6	4.5	-0.8	-1.3	9.5	-0.8	12	12	0.7	-0.9	5.1	6.4	-0.1	-0.2
Skewness	1.5	2.4	1	0.6	1.7	1.8	1.9	0.5	-0.1	3	0.9	3.5	3.5	1	-0.3	2.1	2.6	-0.2	0.5
Range	3604.3	2625.1	431.3	39.5	76.2	92.9	23.6	8.1	66.5	254.1	343.3	3.3	1.3	28498.1	34174.5	29461.3	184695	2322.8	12285.5

Control/Reference soil (n=1)

Statistical Parameter	*Mn*	*Zn*	*Pb*	*Ni*	*Cr*	*Cu*	*Ti*	*Zr*	*Ce*	*Sr*	*Ba*	*Cd*	*Hg*	*Al*	*Fe*	*Mg*	*Ca*	*Na*	*K*
Control Soil Sample	195.5	7.2	8.3	0	33.1	7.3	26.6	5.4	34.6	7.9	52.3	0	0	5916.3	12597.9	1025.3	3657.8	891.2	2639.6
Rock Sample	8987.5	6258.1	939.9	22.6	20.5	1517.9	3.6	8.9	9.3	22	0	20.4	0	75.1	36426.5	1688.4	1705.5	2657.7	5295.4

Table 5.8: Table: Descriptive statistics of the Total metal concentrations (mg/kg) for Gimbi-Rikaya AML

Statistical Parameter	*Mn*	*Zn*	*Pb*	*Ni*	*Cr*	*Cu*	*Ti*	*Zr*	*Ce*	*Sr*	*Ba*	*Cd*	*Al*	*Fe*	*Mg*	*Ca*	*Na*	*K*
Tailings (n=2)																		
Minimum	809.4	421.7	10.9	11.8	3.5	13.8	4	1.1	9.4	18.5	20.5	0	6921.9	14798.4	2084.7	4852.9	934.9	3597.4
Maximum	1206.8	452.5	546.8	15.6	22.8	109.7	17	4.2	65	20.5	116.6	0	9842.4	25680.7	7105.4	4991	1475.6	4891.2
Mean	1008.1	437.1	278.9	13.7	13.2	61.8	10.5	2.7	37.2	19.5	68.6	0	8382.2	20239.6	4595.1	4922.0	1205.3	4244.3
Standard Deviation	281.0	21.8	378.9	2.7	13.6	67.8	9.2	2.2	39.3	1.4	68.0	0.0	2065.1	7694.9	3550.2	97.7	382.3	914.9
Soil (n=11)																		
Minimum	154.6	13.4	4.3	0	5.9	3.5	11	1.4	23.9	6.7	25.5	0	2065.3	6416	633.3	1988.1	325.5	1490.6
Maximum	1898.7	198.2	118.8	19.5	66.5	18.2	53.6	6.8	119.2	31	205.4	0	8971.5	33994.7	4012	12922.9	1929	5385.2
Mean	904.1	48.9	33.4	7.1	23.7	10.2	33.7	3.3	47.4	14.2	96.2	0	4934.5	19838.7	1675.5	5904.9	776.2	3126.9
Median	816.3	30.4	34.3	4.9	21.9	10.4	38.9	2.6	41.4	11.4	84.7	0	4943.3	21228.1	1519.3	5761.9	511.9	3107.1
Standard Error	195.5	15.5	10.5	1.9	5.6	1.6	4.8	0.5	8.5	2.2	19.8	0	646.4	2848.3	266.7	964.5	157.4	401.1
Standard Deviation	648.3	51.4	34.7	6.4	18.5	5.2	15.9	1.8	28.3	7.2	65.6	0	2143.8	9446.8	884.4	3198.9	522.2	1330.2
Sample Variance	420263	2640	1201	40	342	27	252	3	802	52	4300	0	4595820	89241882	782151	10232663	272680	1769466
Kurtosis	-1.8	9	3.1	-0.4	1.6	-1.2	-1.8	-0.1	3.7	1.9	-0.8	0	-0.3	-1.2	5.2	1.1	1.1	-0.6
Skewness	0.3	2.9	1.6	0.5	1.3	0.1	-0.3	0.8	1.9	1.4	0.7	0	0.4	-0.1	2	1.2	1.4	0.6
Range	1744.1	184.8	114.6	19.5	60.7	14.6	42.6	5.4	95.3	24.3	179.8	0	6906.2	27578.8	3378.8	10934.8	1603.5	3894.6
Sediment (n=4)																		
Minimum	959.2	85.5	7.8	7.8	0	23.7	3.6	0	6.7	**13.7**	30.9	0	3057.5	23907	1965.6	6058.3	864.1	2644.9
Maximum	2574.9	4270	588.1	19.8	27.2	70.2	21.4	4.3	73.9	39.9	178.4	8.4	8258.9	36711.4	6336.2	9090	1612.7	5893.3

Statistical Parameter	*Mn*	*Zn*	*Pb*	*Ni*	*Cr*	*Cu*	*Ti*	*Zr*	*Ce*	*Sr*	*Ba*	*Cd*	*Al*	*Fe*	*Mg*	*Ca*	*Na*	*K*
Mean	1529.7	1516.4	181.8	13.9	8.5	39.4	9.3	1.4	24.6	23.6	75.2	3.5	5171.8	29897.0	3965.0	7226.8	1256.2	4785.1
Median	1292.4	855	65.6	14	3.5	31.9	6.1	0.8	8.8	20.4	45.8	2.7	4685.4	29484.9	3779.2	6879.4	1273.9	5301.1
Standard Error	362	965.5	137.1	2.7	6.3	10.4	4.1	1	16.5	6	34.6	2.1	1164	2957.2	1155.8	655	153.4	743.9
Standard Deviation	724	1931	274.2	5.4	12.5	20.9	8.2	1.9	32.9	11.9	69.2	4.2	2328	5914.4	2311.6	1310	306.7	1487.8
Sample Variance	524226	3728687	75163	29	157	436	68	4	1084	143	4786	18	5419459	34980382	5343577	1716181	94083	2213648
Kurtosis	2.5	1.9	3.5	-2.8	3.7	3.4	3	3.3	4	0.3	3.8	-3.6	-0.4	-3.4	-5.4	2.3	1.5	2.3
Skewness	1.6	1.5	1.9	-0.1	1.9	1.8	1.7	1.8	2	1.1	1.9	0.4	0.9	0.2	0.1	1.4	-0.3	-1.6
Range	1615.7	4184.4	580.3	12	27.2	46.5	17.8	4.3	67.2	26.2	147.5	8.4	5201.4	12804.5	4370.6	3031.7	748.7	3248.4
Control Soil Sample (n=2)																		
CSS1	640	17.4	15.2	4.8	21.6	8.7	74.8	4	27.2	26.4	88.9	0	6483.7	15583.9	2817.6	15593.5	1228.1	5764
CSS2	763.5	190.4	24.1	4.9	9.9	14.7	28.3	0.9	35.5	55.4	59	0	4097.8	21848.5	2458.2	33426.9	817	4315.2
Control Sediment (n=2)																		
SD1 Control	621.3	12.3	24.7	10.3	95.4	13.6	44.7	*2.6*	47.9	9	60.7	0	6969.2	39787.8	795	3202.8	1763.8	4874.6
SD2 Control	252.3	7.6	9	5.8	23.4	6.2	70.1	7.3	39.6	11.1	80.6	0	12200.7	11064.1	2626.7	3449.3	1643.8	7380.8

Control soil and sediment were collected outside of the AML-impacted areas.

5.3.3.1 Total Metal Concentrations – Abakaliki

The metal concentrations at the Abakaliki Pb/Zn site varied across the different environmental samples, as detailed in Table 5.6 of the descriptive statistics. An overview of the heavy metal concentrations at the site is illustrated in the box plot in Figure 5.9, which shows that Zn, Pb, and Mn are the most abundant metals, with Zn up to 14,000 mg/kg.

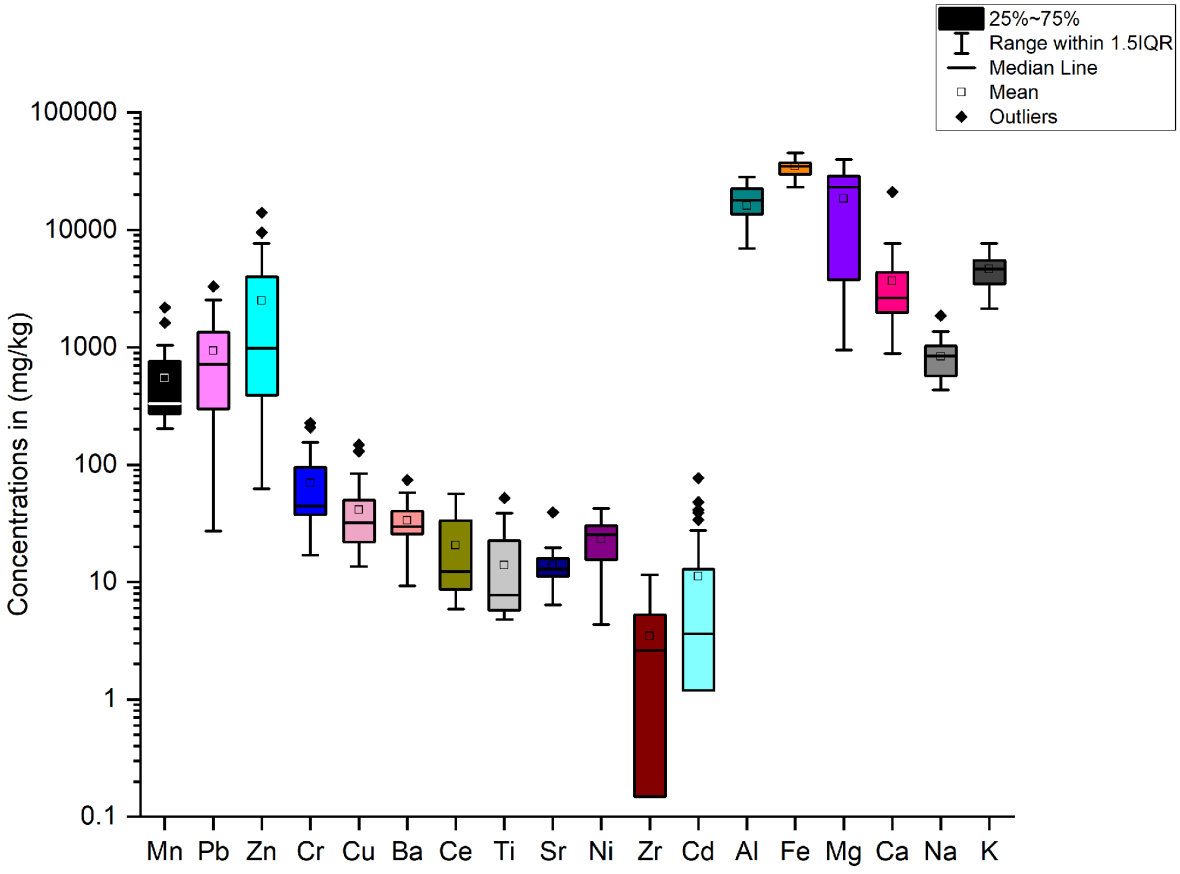

Figure 5.9: Distribution of metal concentrations at Abakaliki Pb/Zn AML.

The rock and the two reference (control) soil samples (RSS1 and RSS2) revealed notable differences in metal concentrations (Table 5.6). The rock sample showed high concentrations of Pb (905.3 mg/kg) and Zn (429.5 mg/kg), while Cu (22.1 mg/kg), Cd (2.8 mg/kg), and Ni (4.3 mg/kg) were present at moderate to low concentrations. As the sample was collected from exposed weathered shaly sandstone rather than directly from a mineralised Pb–Zn ore vein, this explains why Pb and Zn concentrations were lower than might be expected from ore material. In contrast, Pb and Zn concentrations were lower in RSS1 (67.5 mg/kg and 94.6 mg/kg, respectively) and RSS2 (27.2 mg/kg and 62.4 mg/kg, respectively). Cadmium was undetectable in RSS1 and measured at 0.1 mg/kg in RSS2. Macro elements such as Fe, Al, and K were generally higher in the reference/control soils, while Ca, Mg, and Na varied across the three samples. Cerium was relatively high in the rock (38.9 mg/kg), with comparable values observed in RSS1 (29.0 mg/kg) and RSS2 (33.8 mg/kg). Zirconium levels were low in all three samples, ranging from 0.1 to 10.8 mg/kg.

5.3.3.1.1 Tailings Metal Concentration

Tailings samples were collected at the base, on top of the heaps, and close to the mine pit filled with water (Figure 5.4A). The tailings heaps in the site were a mixture of mine waste and spoils (Figure 5.4A). The distribution of heavy metals and major elements in the tailings samples is shown in Figure 5.10. The most prominent contributors to total metal concentrations across all samples (Table 5.6) were Zn, Pb, and Mn. Zinc was the dominant heavy metal in nearly all samples, with concentrations reaching up to 14,059.1 mg/kg and a mean of 4,462.0 mg/kg) far exceeding the value recorded for soil reference samples of 94.6 mg/kg. The concentrations of Pb were also elevated, ranging from 107.0 to 3,291.2 mg/kg and a mean of 1,103.0 mg/kg, well above the measured value in the reference soil of 27.2 mg/kg. Mn levels were generally lower than Zn and Pb but still showed notable variation compared to other metals, with a mean of 282.3 mg/kg and a maximum value of 479.9 mg/kg.

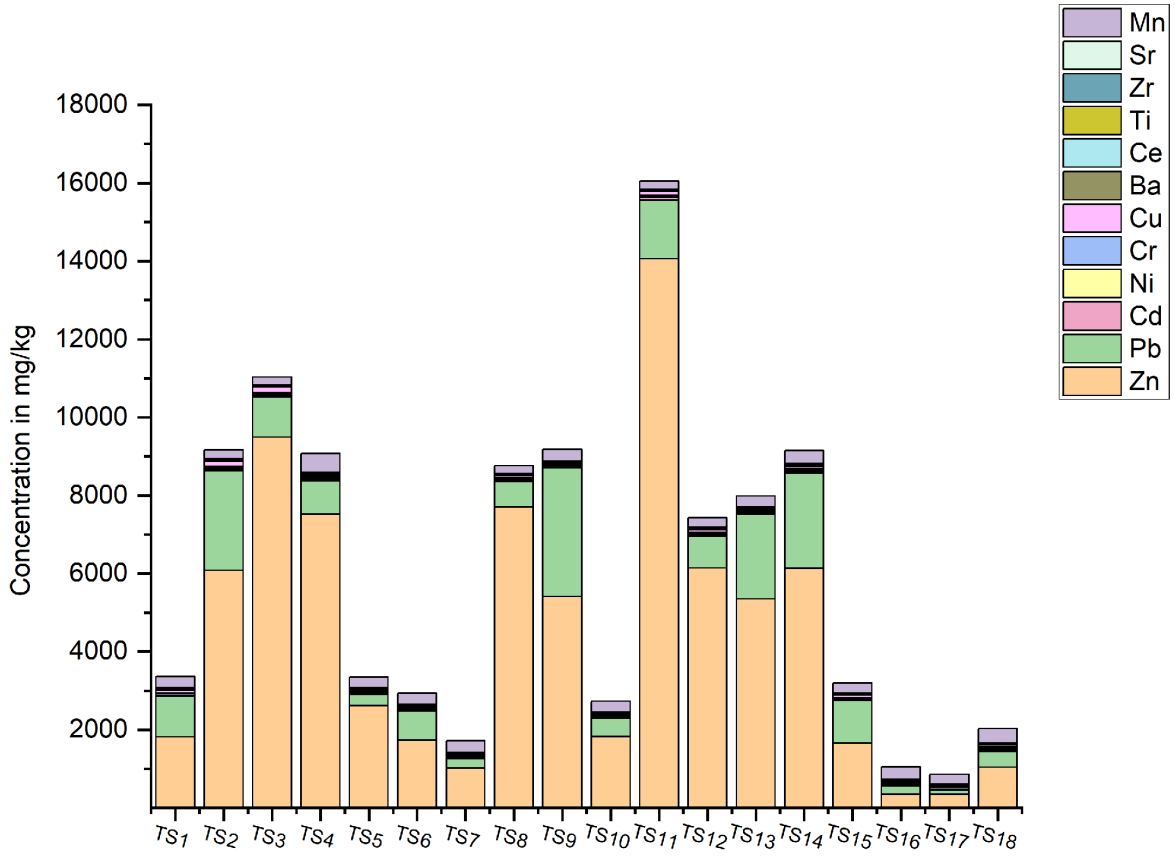

Figure 5.10: Heavy Metal (HM) concentrations of tailings samples at the Abakaliki AML

Sample TS11 displayed the highest overall metal load, with Zn alone accounting for more than 14,000 mg/kg. Other samples with cumulative concentrations exceeding 9,000 mg/kg included TS2, TS3, TS4, TS8, TS9, TS11, and TS14. Other heavy metals such as Cr, Cu, Ni, Cd, Ba, Ce, Ti, Sr, and Zr were also detected but contributed less significantly to total concentrations. However, cadmium concentration is significant as it was not detected in the reference soil samples, with a maximum of

76.9 mg/kg and a mean of 20.0 mg/kg. Mean and maximum values of Cu and Ni were 54.4 and 147.8 mg/kg and 30.4 and 42.6 mg/kg, respectively. These results reflect the high level of contamination in the tailings material and suggest a high potential for environmental mobility and toxicity, particularly for Zn, Pb, and Cd.

5.3.3.1.2 Soil Metal Concentration

The analysis of heavy metal distribution reveals significant variability in total metal concentrations across the 12 soil samples. The control soil samples (RSS1 and RSS2) shown in the statistical table and figure were collected approximately 2 km from the mine pit, and help verify the concentration levels in soils closer to the pit.

The mean concentrations of the most dominant metals were Mn (899.1 mg/kg), Pb (691.6 mg/kg), and Zn (410.6 mg/kg), all of which exceeded the mean values (Mn, 530.6 mg/kg, Zn, 94.6 mg/kg and Pb, 67.5 mg/kg) of the local reference samples. Manganese showed the highest mean and maximum values (up to 2,185.0 mg/kg), and the maximum value for Pb was 1,848.5 mg/kg, followed by Zn (945.6 mg/kg), indicating significant enrichment likely linked to the previous mining activity. Sample SS11 (Figure 5.11) exhibited the highest cumulative metal burden, exceeding 4,500 mg/kg in total.

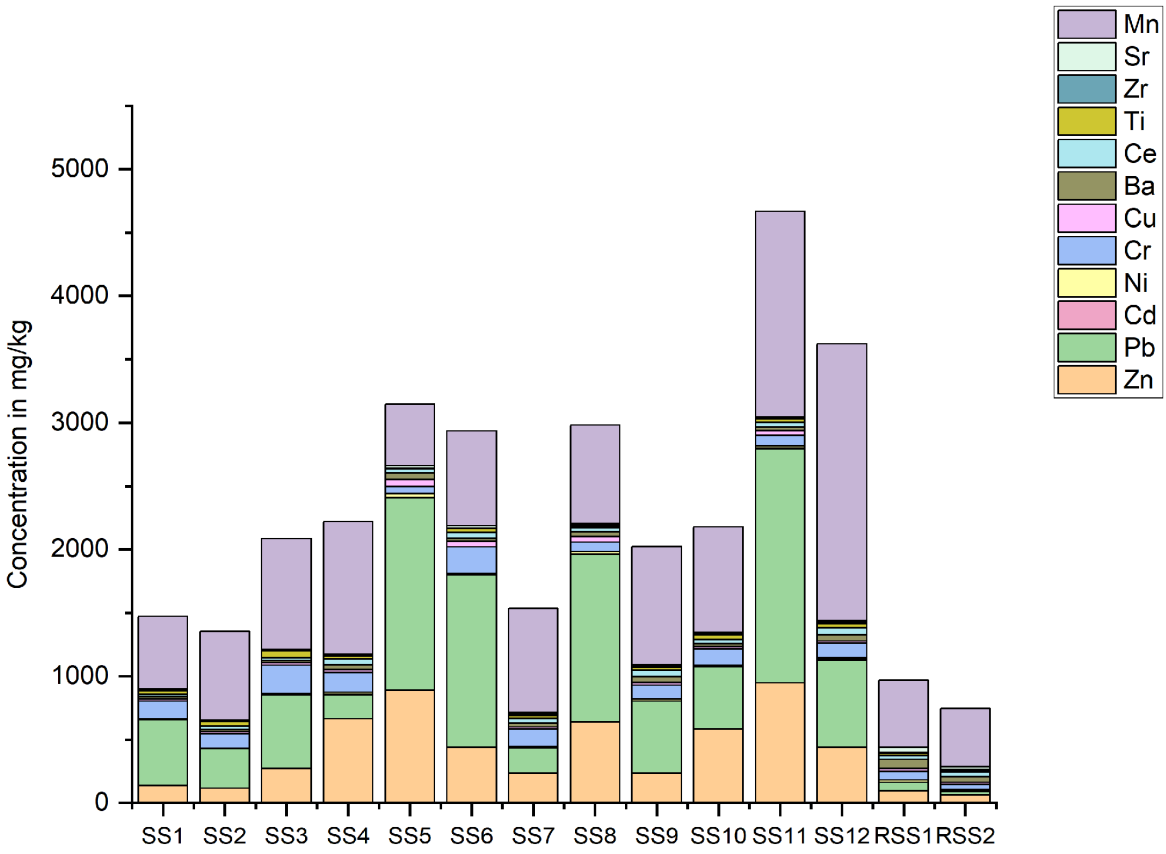

Figure 5.11: Soil Heavy Metal (HM) concentrations at Abakaliki Pb/Zn AML.

Lower mean concentrations were observed for Cr (119.1 mg/kg), Cu, (26.3 mg/kg), Ba (35.2 mg/kg), Ce (36.1 mg/kg), Ti (25.7 mg/kg), and Sr (15.9 mg/kg), despite these lower levels, they were still consistently detected with elevated concentration recorded in the field XRF data. Ni, Cd, and Zr were present at trace levels, with Cd having a mean concentration of only 1.3 mg/kg.

5.3.3.1.3 Sediment Metal Concentration

Sediment samples were collected at the same spot as the mine pond water samples. Due to the instability of the tailing/waste materials heaps, it was difficult to collect samples; only 3 samples were collected. Figure 5.12 illustrates the concentration of heavy metals in the sediment samples (SD1–SD3) of the Pb/Zn AML pit. The most abundant metals in all three samples were Zn and Pb, which together accounted for the largest proportion of the total metal load. Zn concentrations ranged from 705.6 to 1,640.0 mg/kg, with a mean of 1,272.9 mg/kg (Table 5.6). The concentrations of Pb were also elevated, ranging from 265.9 to 1,472.6 mg/kg, with a mean of 1,023.0 mg/kg, and both Zn and Pb concentrations exceeded the soil reference values in every sample.

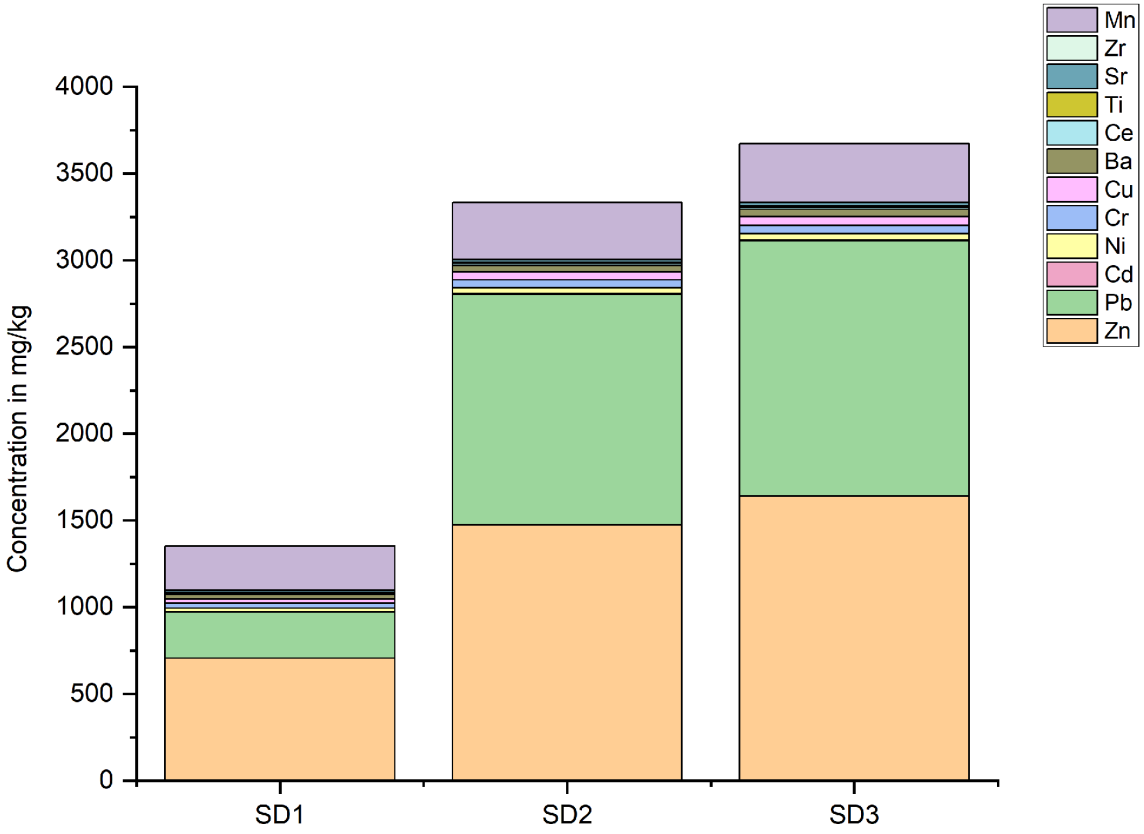

Figure 5.12: Sediment Heavy Metal (HM) concentrations at Abakaliki Pb/Zn AML

Manganese was the next most abundant metal, with concentrations ranging from 255.2 to 339.3 mg/kg and a mean of 307.0 mg/kg. Other metals were present in lower concentrations but consistently detected across the sample points, mean values of Cr (39.7 mg/kg), Cu (39.8 mg/kg), Ba (35.9 mg/kg), Ce

(9.5 mg/kg), Ti (6.7 mg/kg), Sr (15.9 mg/kg), and Ni (31.2 mg/kg). Cadmium, although present in trace amounts, is still significant across all samples, with a minimum and maximum of 2.2-4.8 mg/kg. Overall, the sediments showed clear evidence of metal enrichment, particularly for Zn and Pb.

The concentrations of major elements, including Al, Fe, Mg, Ca, Na, and K, varied across the three environmental media: soil, tailings, and sediment. Aluminium concentrations were highest in Tailings samples, reaching up to 28220.8 mg/kg, followed by soil at 24802.0 mg/kg, with a mean of 17516.6 mg/kg and 16688.8 mg/kg for Tailings and sediment, respectively. The highest mean concentration in soil was Fe (40505.8 mg/kg), while Mg levels were markedly elevated in tailings (mean: 26,693.9 mg/kg) and sediments (mean: 35,844.4 mg/kg), whereas soils and control soils had considerably lower concentrations. Calcium followed a different pattern, with the highest levels in control soil samples (21076.1 mg/kg), followed by tailings (6109.5 mg/kg), soil (5210.6 mg/kg), and sediments (4234.2 mg/kg). Na concentrations were relatively low across all media but were highest in tailings (1358.6 mg/kg), with a mean of 843.8 mg/kg and a sediment mean of 904.0 mg/kg. K concentrations were also highest in tailings, with a mean of 5,331.3 mg/kg, and showed notable variation across all media types. Overall, tailings and sediment samples consistently exhibited higher concentrations of major elements compared to soils and reference soils, except for Ca.

The heavy metal concentrations across soil, tailings, and sediment samples from the AML reveal distinct spatial patterns and contamination intensities associated with past mining activities. Overall, the standard deviation across tailings and soil media was higher, suggesting a greater variability in contamination. Lead is highly variable in soil and tailings, indicating hotspots of contamination. The data indicate a contamination gradient: tailings > sediment > soil, with Zn, Pb, and Cd posing the greatest environmental concern.

5.3.3.2 Total Metal Concentration – Gimbi

The metal concentration at the Gimbi site is shown in Figure 5.13 and the descriptive statistics (Table 5.8). The metal concentrations vary across the different sampled media. Manganese, Zn and Pb were the most abundant heavy metals observed, above 2000 mg/kg, while Cd, Ni, and Cu were below 1000 mg/kg. The control soil sample showed low concentrations for most heavy metals, supporting its use as a baseline for natural background levels. Notably, control soil contained 195.5 mg/kg Mn, 7.2 mg/kg Zn, 8.3 mg/kg Pb, and non-detectable levels of Ni and Cd. In contrast, the rock sample exhibited significantly elevated concentrations of Mn (8987.5 mg/kg), Zn (6258.1 mg/kg), Pb (939.9 mg/kg), Ni (22.6 mg/kg), Cu (1517.9 mg/kg), Fe (36426.5 mg/kg), and Cd (20.4 mg/kg). Interestingly, the control soil samples showed higher levels of some elements than the rock, such as Cr (33.1 vs 20.5 mg/kg), Ce (34.6 vs 9.3 mg/kg), Ba (52.3 vs 0.0 mg/kg), and Al (5916.3 vs 75.1 mg/kg), suggesting differing mineralogical compositions or surface accumulation effects. Additionally, titanium (Ti: 26.6 mg/kg)

was higher in the control soil than in the rock (3.6 mg/kg), indicating its likely natural origin in the soil matrix.

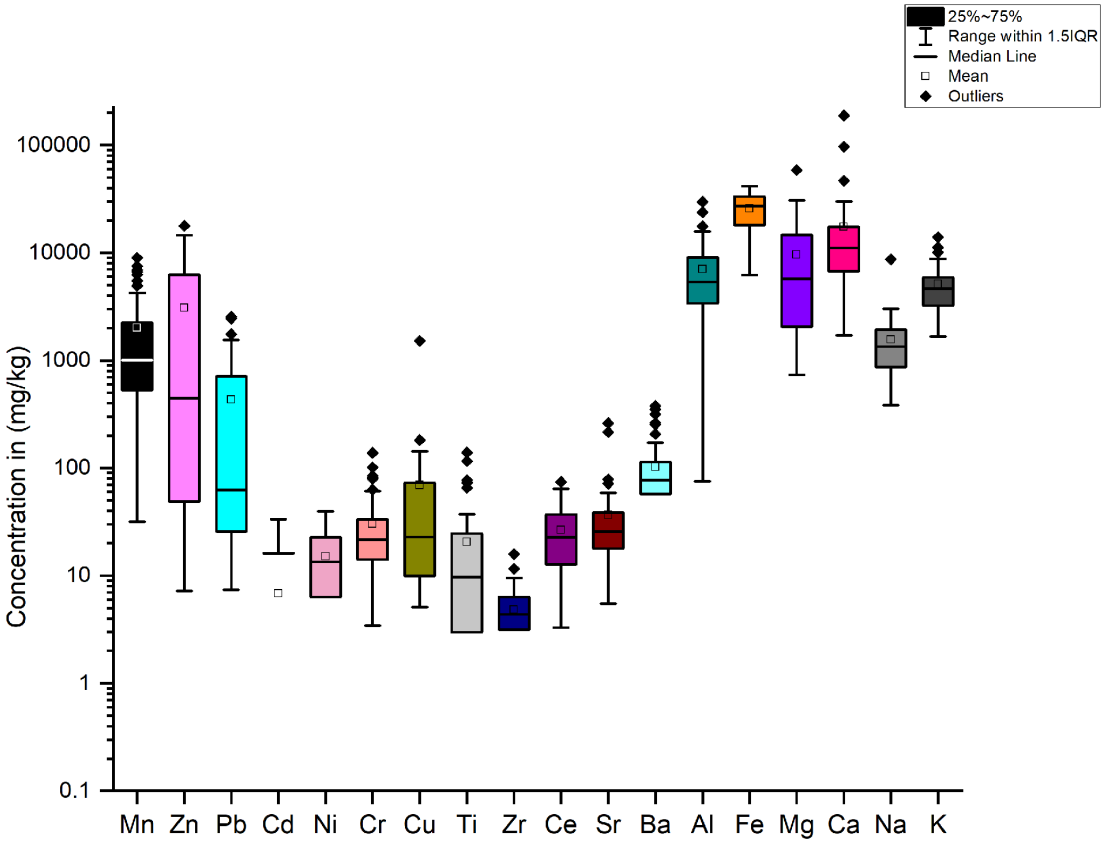

Figure 5.13: Heavy Metal (HM) concentrations at Gimbi Pb/Zn AML

5.3.3.2.1 Tailings Metal Concentration

The Gimbi abandoned mine site contains extensive tailings deposits and impounded mine wastes from Pb–Zn mining activities, from which tailings samples were collected for this study. Tailings impoundments are commonly used to store waste materials generated during ore processing and may remain important sources of environmental contamination long after mine closure. Weathering and seepage from these deposits (Kossoff et al., 2014) can mobilise metals and metalloids into surrounding soils, sediments, surface waters, and groundwater, potentially contributing to long-term environmental impacts (Lyu et al., 2019).

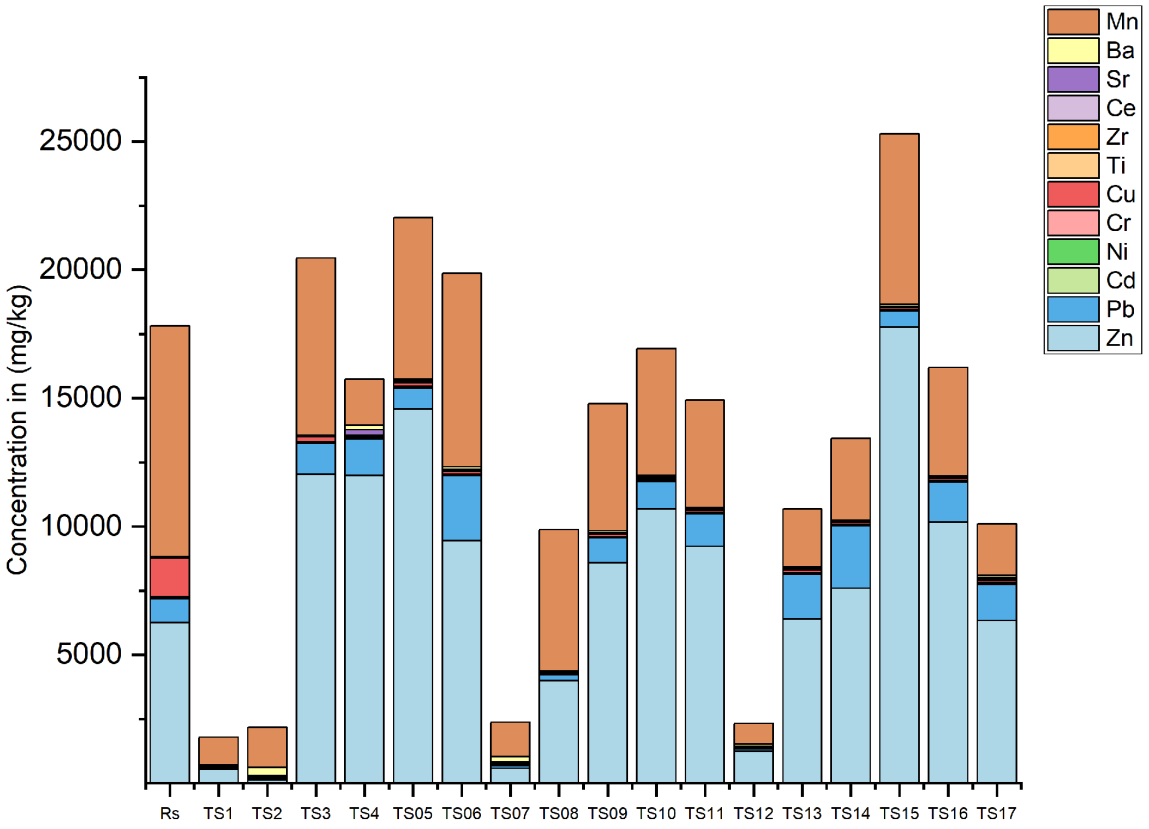

Figure 5.14: Gimbi Pb/Zn AML Heavy Metal (HM) concentrations in tailings samples

Tailings samples were collected from the waste piles near the mine pit and from the tailings impoundment adjacent to the mine pit. However, it was not possible to access and sample the entire impoundment due to a barrier created by the dam structure. The site was characterised by a non-draining tailings impoundment, where a channel had been excavated around a central tailings deposit. This design lacked a surface outlet, allowing accumulated water to infiltrate into the subsurface, thereby increasing the potential for contaminant leaching into surface and groundwater resources (Tomiyama & Igarashi, 2022; Zhu et al., 2022). Hence, the concentrated sampling (Figure 5.6a) was conducted to evaluate the concentration of metals within the impoundment.

The distribution of heavy metal concentrations in the site is presented in Figure 5.14 with the descriptive statistics in Table 5.7. The samples exhibit notably elevated levels of Zn, Mn, and Pb, which dominate the metal contents across most tailings samples. The concentrations of Zn were particularly high, reaching over 11,000 mg/kg in several samples (e.g., TS3, TS4, TS5, TS6, TS9, TS10, TS11, TS14, TS15, and TS16), with a maximum of 17,769 mg/kg. Manganese was also prominent, with values ranging from 787 to 7,533 mg/kg and a mean of 3,829 mg/kg.

Lead concentrations varied widely, with a mean of 1,030.5 mg/kg and a maximum of 2,544.3 mg/kg. Other metals, such as Ni, Cr, and Cu, were present at lower concentrations, with maximum values of

39.1, 23.6, and 181.8, respectively, but were far exceeding the values measured in the control soil sample in all samples except for Cr. Cadmium, although at lower concentrations, reached up to 33.4 mg/kg, with several samples exceeding the control value of 0.0 mg/kg. Trace elements such as Ba, Ce, and Sr were present at minor concentrations, with maximum values of 314.3 mg/kg, 26.1 mg/kg, and 215.7 mg/kg, respectively, while Ti, Cr, and Zr were detected consistently but at low levels.

Major elements enrichment was also observed in the tailings samples. Fe showed the highest concentration among all tailings samples (29,885.2 mg/kg), consistent with residual ore material. Mg was also high (15,691.8 mg/kg), likely reflecting processing residues, while Ca had a moderate mean value of 18,479.4 mg/kg, and Al (4,653.7 mg/kg) was lower than it was in soils and sediments, possibly due to removal during ore processing. Both Na (1,741.1 mg/kg) and K (5,218.6 mg/kg) were moderately elevated.

Overall, the distribution pattern of HMs indicates significant contamination by mine-derived materials, with multiple tailings samples exceeding critical ecological screening levels for several metals, especially Zn, Pb, and Mn. The elevated concentrations suggest that the tailings pose a potential risk to the surrounding environments, especially through leaching processes associated with the dam structure.

5.3.3.2.2 Soil Metal Concentration

The soils in Gimbi were generally sandy and arkosic and easily friable. Table 5.7 shows the descriptive statistics, and Figure 5.15 represents the distribution of heavy metal concentrations in soil samples from the Gimbi Pb/Zn AML. Across 19 samples, Mn and Zn dominate the profiles, with Mn ranging from 31.9 to 1791.3 mg/kg with a mean of 623.4 mg/kg and Zn ranging from 21.5 to 6239.2 mg/kg with a mean of 485.6 mg/kg.

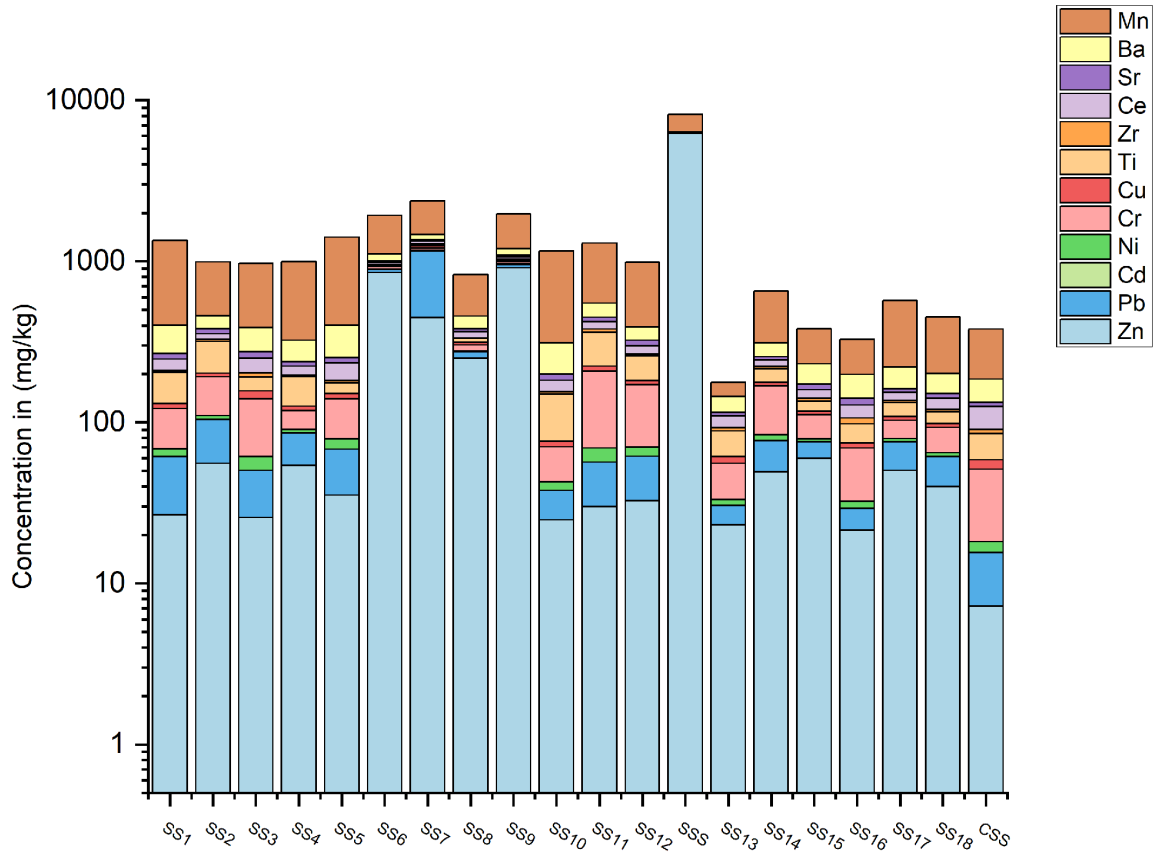

Figure 5.15: Gimbi Pb/Zn AML soil Heavy Metal (HM) concentrations

One sample (SSS) showed exceptionally high Zn concentration, contributing to the right-skewed distribution (Skewness = 4.2). This sample was collected from the mine pit, where white crystalline precipitates were observed on the surface of the soil and along the pit's edge (Figure 5.16), indicative of salt crusts left behind by evaporated mine water. These salt-encrusted residues are typically associated with the evaporation of metal-rich and potentially saline drainage. Consistent with the visible salt accumulation, the sample recorded the highest total metal concentration among all soil samples, with highly elevated levels of Zn (6239.2 mg/kg) and Mn (1791.2 mg/kg), well above both the local background values (7.2 and 195.5 mg/kg, respectively), that is, the CSS sample in the figure. These elevated concentrations suggest significant accumulation of metals through evaporative concentration processes. The presence of salts also indicates the likelihood of alkaline or saline conditions, which is confirmed by the pH of the sampled mine pond water at both the downstream and upstream locations, ranging from 7.27 to 8.09. This condition can influence metal mobility and bioavailability.

Moderate levels of Pb were observed, ranging from 7.4–706.9 mg/kg and a mean of 63.0 mg/kg, exceeding the local background value (8.3 mg/kg) in several samples. Trace levels of Cd, Ni, and Cr were also detected, with Cd generally near or below detection limits in most samples but peaking at 9.5 mg/kg. Elements such as Ce, Zr, Ti, Sr, and Ba were consistently low.

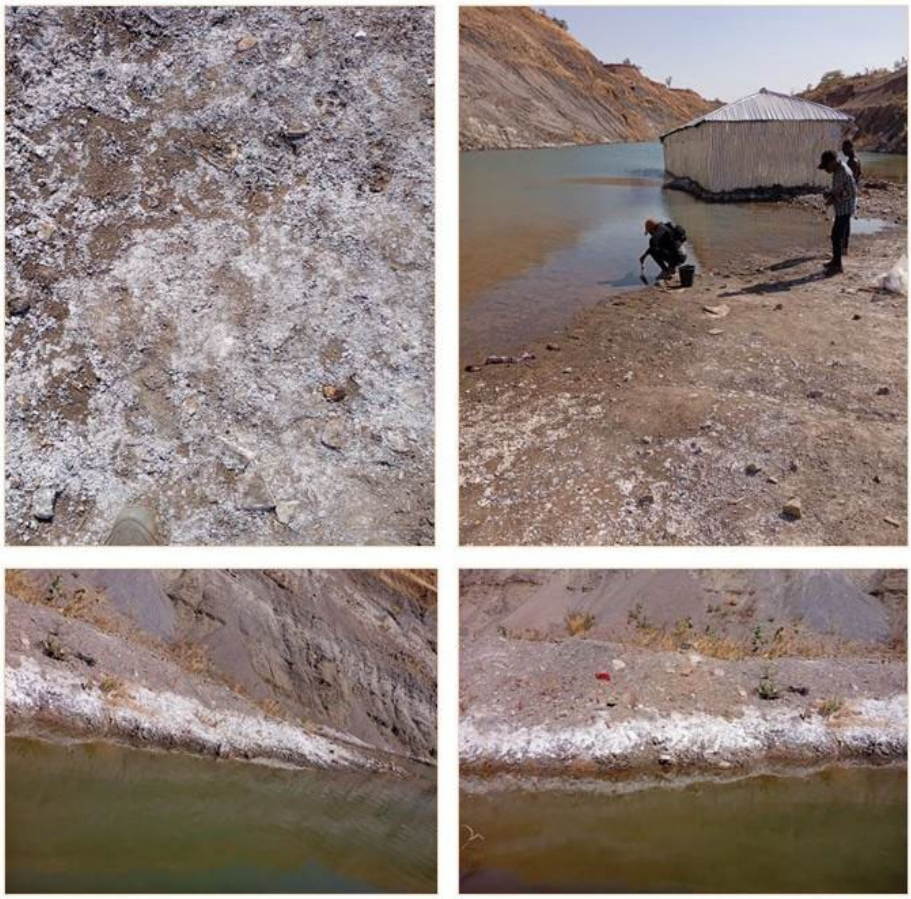

Figure 5.16: Gimbi Pb/Zn AML Pit with salt precipitate around the pit.

These results reflect spatial variability and localised enrichment likely linked to the AML, with Zn showing particularly elevated levels near the AML pit.

The samples also exhibited moderate concentrations of major elements. Aluminium had a mean concentration of 6,639.2 mg/kg, reflecting the presence of aluminosilicate minerals. The mean for Fe was relatively high, 22,636.4 mg/kg, suggesting contributions from iron-bearing lithologies. Across all soil samples, Mg had a mean of 5,179.1 mg/kg, with 8,477.7 mg/kg mean for Ca, both indicating limited carbonate input, while Na had the lowest mean concentration (1,234.3 mg/kg), and K was moderate (4,061.2 mg/kg), likely derived from feldspars and clay minerals.

5.3.3.2.3 Sediment Metal Concentration

Figure 5.17 illustrates the concentration of HMs in sediment samples collected from the AML site (PSD1A, PSD1B, PSD2A, and PSD2B), and PSD4A, PSD4B, PSD5A and PSD5B were collected at the isolated ponds around the mines, approximately 1 km from the AML pit, while SD3 to SD5 were collected from the river channel approximately 1.8 Km from the mine. A total of twelve sediment samples were analysed, revealing spatial variability in HM distribution.

The dominant metals across the sediment samples were Mn, Zn, and Pb, with mean concentrations of 1239.8 mg/kg, 559.8 mg/kg, and 158.2 mg/kg, respectively. These values indicate elevated concentrations, particularly for Mn and Zn, in several samples, exceeding those in the control soil sample.

High levels of Mn and Zn were especially pronounced in samples PSD1B, PSD4B, PSD5B, and SD3, as the stacked bar plot shows a clear dominance of these metals. This suggests significant deposition of mine-derived particulates in the mine pit and mobilised metals in the river channel.

Moderate concentrations of Ba, Cu, Ce, Cr, and Ni were also observed, with some samples (e.g., PSD2A, PSD4B, PSD5B and SD3) exhibiting visible enrichment in these elements. The relatively high standard deviations and skewed distributions of Zn and Mn further highlight the heterogeneous contamination across the sediment samples, likely influenced by proximity to tailings and sedimentation dynamics.

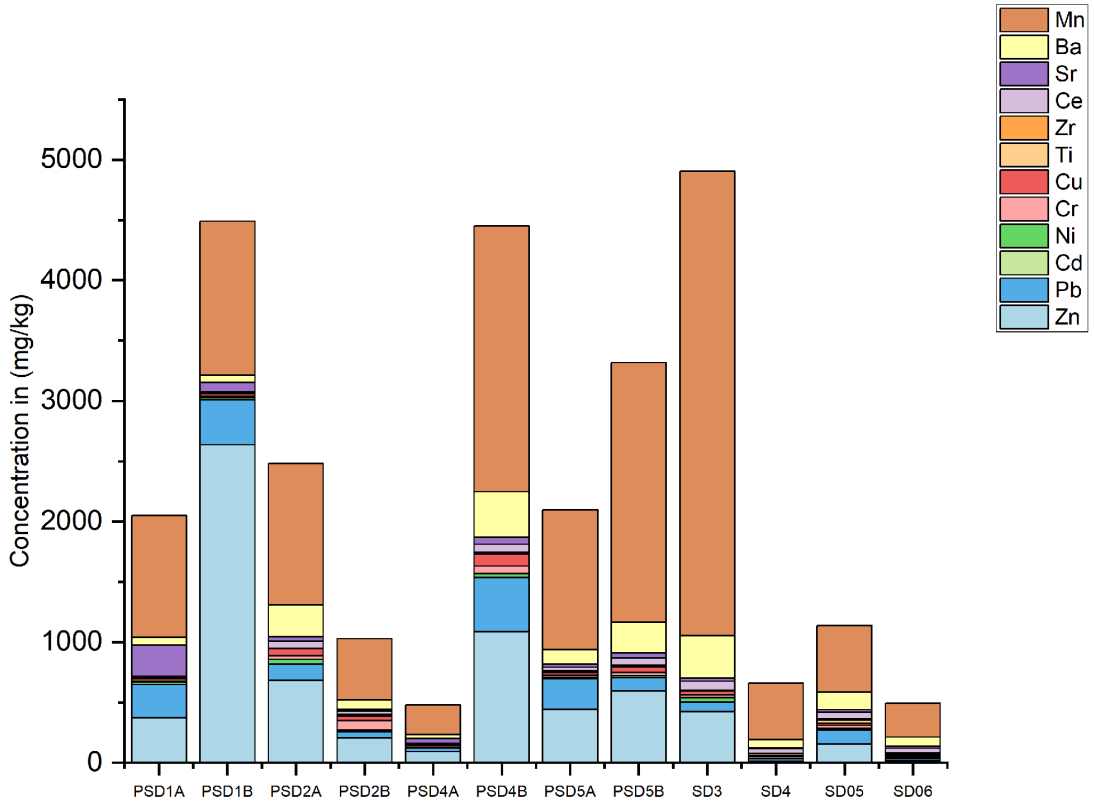

Figure 5.17: Gimbi Pb/Zn ALM sediment HMs concentrations

Metal concentrations at the site follow a clear gradient: Tailings > Sediment > Soil, indicating mine-derived contamination. The main contaminants of concern, in decreasing order, are Zn > Mn > Fe > Pb > Cu > Cr > Ni > Cd. These patterns suggest an ongoing dispersion of metals from tailings into surrounding environments, with sediments acting as secondary sinks. The soils may not have been greatly influenced by the tailings materials because of the impoundment.

5.3.3.3 Total Metal Concentration - Gimbi-Rikaya

The collected samples from the Gimbi-Rikaya site include soil, sediment, and mine tailings; the descriptive statistics are shown in Table 5.8. The distribution of major and trace metal concentrations is illustrated in Figure 5.18, showing major elements (Al, Fe, Mg, Ca, Na, K) occurring at much higher concentrations (10^3–10^4 mg/kg), while trace metals (Mn, Zn, Pb, Cd, Ni, Cr, Cu, etc.) are generally lower, ranging from sub-mg/kg to 10^3 mg/kg. Notably, Mn, Zn, and Pb exhibit the highest variability and outliers among trace metals, indicating localised enrichment.

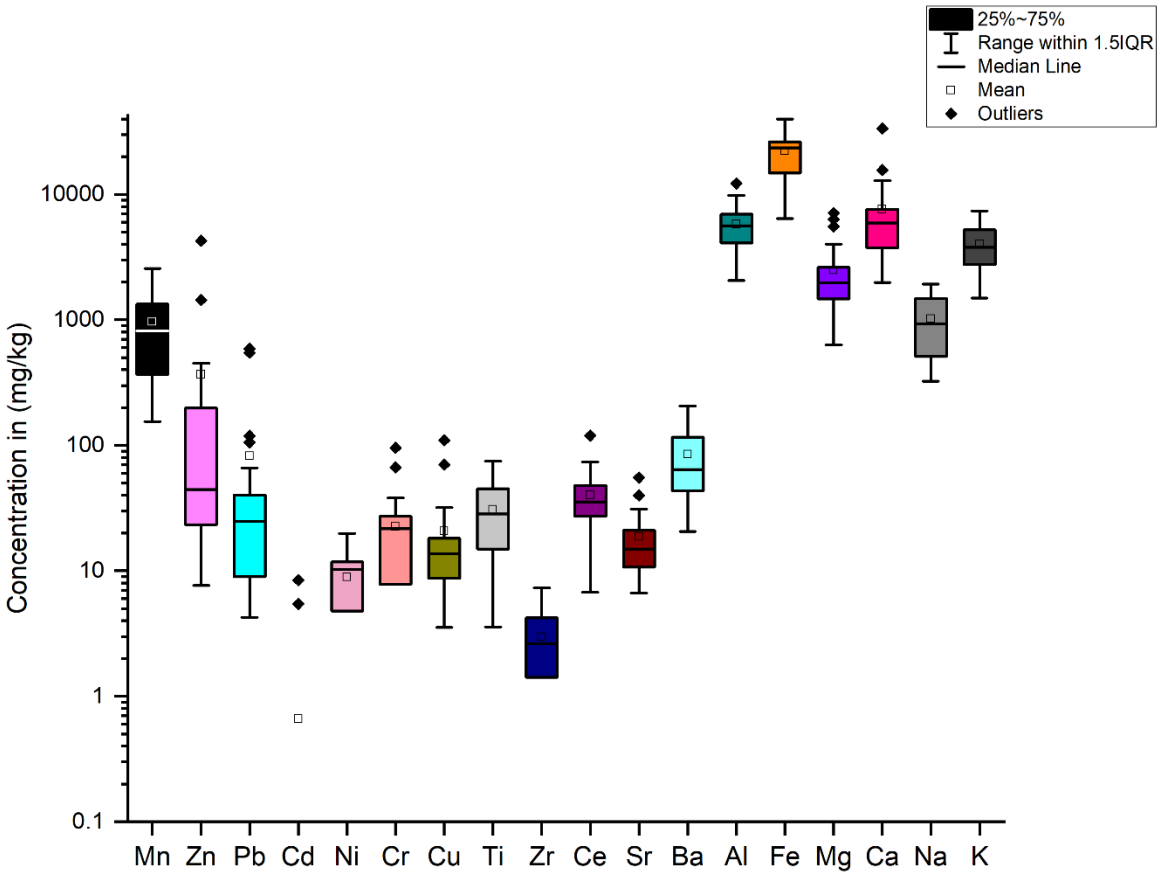

Figure 5.18: Distribution of metal concentrations across samples at the Gimbi Rikaya AML site

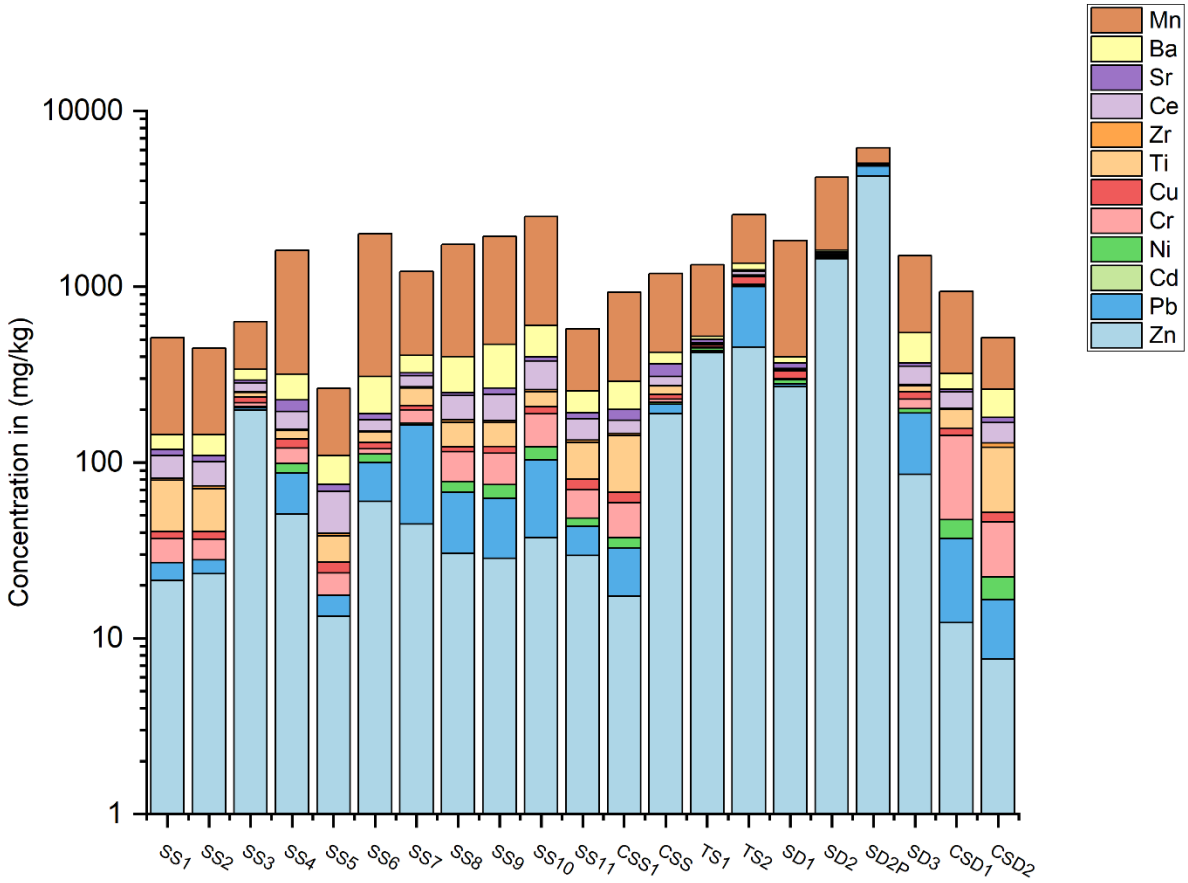

Figure 5.19: Gimbi-Rikaya Tailings Soil, & Sediment Heavy Metal (HM) concentrations

Tailings showed significantly elevated concentrations of Zn, with a mean of 437.1 mg/kg and 278.9 mg/kg for Pb (Figure 5.19). TS2 shows a sharp spike in Pb concentration, aligning with the statistical mean, while Cu concentrations were also moderately elevated in some samples, with a mean of 61.7 mg/kg and a maximum value of 109.7 mg/kg. Due to the small sample size (n=2), variability measures are limited, but concentrations highlight these as primary sources of contamination. Aluminium and Fe showed higher concentrations, with means of 8,382.2 mg/kg and 20,239.6 mg/kg, reflecting the enrichment of these elements in processed materials. The mean of Mg was 4,595.0 mg/kg, and Ca was comparable to soil at 4,921.9 mg/kg, while Na and K mean values were 1,205.3 mg/kg and 4,244.3 mg/kg, respectively, suggesting higher salt and alkali content in tailings.

Soil samples generally exhibited low to moderate total metal concentrations (Figure 5.19), dominated by Mn with a mean of 904.1 mg/kg. Zinc and Pb concentrations reached up to 198.2 mg/kg and 118.8 mg/kg, respectively, below typical risk thresholds but with positively skewed distributions indicating localised hotspots. Aluminium and Fe recorded mean concentrations of 4,934.5 mg/kg and 19,838.7 mg/kg, respectively, indicating the presence of alumino-silicate and iron-bearing minerals. Magnesium averaged 1,675.5 mg/kg, while Ca showed a relatively high mean of 5904.9 mg/kg, likely due to

weathering or evaporite deposits. Also present at moderate levels were Na and K with mean values of 776.2 mg/kg and 3,126.9 mg/kg, respectively.

Sediment samples (Figure 5.19) revealed extreme variability in Zn and Pb, with Zn ranging from 85.5–4270 mg/kg and Pb from 7.8–588.1 mg/kg, with several samples exceeding control values. Particularly, SD2 and SD2P had visibly high cumulative concentrations; these samples were taken from the dry mine pit pond shown in Figure 5.3D. High standard deviations reflect spatial heterogeneity and suggest dispersion of contaminants from tailings and soil erosion. The sediments' Al and Fe remained high, with mean values of 5171.8 mg/kg and 29,897.0 mg/kg, respectively. On the other hand, Mg averaged 3,965.0 mg/kg, and Ca rose to 7,226.8 mg/kg, possibly influenced by runoff from mine materials. The mean values of Na and K were 1,256.2 mg/kg and 4,785.1 mg/kg, respectively, indicating transport and accumulation of soluble ions. Across the three sampled media, Mn was consistently dominant, with mean values of 1008.1 mg/kg, 904.1 mg/kg, and 1529.7 mg/kg for tailings, soil, and sediment, respectively.

The data from these sites collectively underscore the role of mine tailings as a significant source of contamination, with accumulation of contaminants in surrounding soils and sediments. Concentration levels indicate potential ecological risks, particularly from Pb and Zn. These patterns provide essential insight for source-pathway-receptor modelling and environmental risk assessment.

Overall, the Total metal concentration at Abakaliki far exceeded that of Gimbi and Gimbi-Rikaya, suggesting that metal mobility is higher at the site than at the Gimbi sites.

5.3.4 Total and Dissolved Metal Concentrations in Water Samples

5.3.4.1 Abakaliki

Water samples collected from the Abakaliki site exhibited elevated concentrations of both dissolved and total metals (Table 5.9). The water samples showed comparable levels between total and dissolved forms, suggesting high metal solubility and mobility in the aquatic environment.

For the dissolved metals, notably high mean concentrations were observed for Zn, Pb, Cd, Ni, Mn, and Al, at 105,855.3 µg/L, 995.7 µg/L, 618 µg/L, 342.3 µg/L, 12,651.8 µg/L, and 8,904.5 µg/L, respectively. The total metal concentrations followed similar trends, with Zn, Pb, Cd, Mn, and Al again displaying high values. Zn had extremely high concentrations in both forms, with a mean of 106,779.7 µg/L total and 105,855.3 µg/L dissolved, indicating that almost all Zn present is in the dissolved phase. This suggests that Zn is highly soluble under prevailing pH or redox conditions, which is likely due to acid mine drainage or complexation with dissolved organic matter. Similar patterns were observed for Mn (total: 12,453.8 µg/L; dissolved: 12,651.8 µg/L) and Al (total: 8,681.6 µg/L; dissolved: 8,904.5

µg/L), further supporting a high degree of metal dissolution, possibly influenced by mine water chemistry or weathering of tailings and mine walls.

The total and dissolved concentrations of Pb, Cd, Ni, Cr, and Cu also showed similar ranges, indicating they are predominantly soluble rather than particulate-bound. The slight differences in total Pb concentrations (1,014.3 µg/L) and dissolved Pb (995.7 µg/L) could reflect minimal association with suspended solids, suggesting limited adsorption or precipitation under current conditions. Titanium was consistently reported at 0 µg/L in both forms, likely due to its negligible presence in the water phase. The rare earth element Ce also showed similar values in both forms, supporting the idea that even less mobile elements may remain in solution in such disturbed environments. Other metals, even at low concentrations, may still contribute to synergistic toxic effects alongside elevated toxic metal levels.

Major elements were dominated by Ca, Mg, Na, and K in both dissolved and total metal fractions, with mean concentrations of 677,179.5, 380,449.0, 47,556.9, and 19,321.2 mg/kg, respectively, for dissolved metals and 637,363.1, 383,050.2, 41,538.4, and 18,335.7 mg/kg, respectively, for total metals reflecting the strong influence of mineral weathering and water-rock interactions within the study area.

Overall, the behaviour of dissolved fractions of metals such as Ni, Cd, Pb, and Zn is often comparable to or exceeds their total concentrations, indicating a high proportion of bioavailable or mobile forms, which is an environmental and public health concern.

Table 5.9: Total and dissolved metal concentrations (µg/L) for water samples - Abakaliki

Statistic Parameters	*As*	*Zn*	*Pb*	*Cd*	*Ni*	*Cr*	*Cu*	*Ti*	*Zr*	*Ce*	*Sr*	*Ba*	*Mn*	*Fe*	*Al*	*Mg*	*Ca*	*Na*	*K*
Dissolved Metals (n=3)																			
Min	13.1	88028.4	981.6	518.9	264.5	6.6	121	0	19.9	50.5	451.1	440.3	10632.2	188.7	7377	314373	625124	34660.1	15001.8
Max	20.1	115050	1013.8	669	383.9	20.6	189.8	0	34.4	60.3	487.9	575.1	14511.5	439.5	10039.6	415922	734143	55223.3	21661.5
Mean	17.7	105855	995.7	618	342.3	12.7	161.1	0	24.9	54.2	474.2	523.9	12651.8	339	8904.5	380449	677180	47556.9	19321.2
SD	4	15441.1	16.5	85.8	67.5	7.2	35.8	0	8.2	5.4	20.1	73	1944.6	132.6	1374	57275.1	54675	11235.2	3745
Total Metals (n=3)																			
Min	0	89592.2	985.1	442.2	210.2	5.1	111.6	0	0	7.8	375.6	349.1	10705.2	169.4	7299.1	320546	612347	34774.2	15176.8
Max	14.6	121728	1065.4	629.5	346.6	16.2	172.4	0	20.1	50.5	436.3	580.2	15008.1	509.9	10355.6	430455	667239	46330.4	20913.3
Mean	4.9	106780	1014.3	558.8	294	12.3	151.1	0	6.7	25.3	408.8	501.9	12453.8	374.9	8681.6	383050	637363	41538.4	18335.7
SD	8.4	16184.3	44.4	101.7	73.4	6.2	34.3	0	11.6	22.3	30.7	132.4	2261.7	180.8	1548.9	56488.7	27767.2	6025.2	2912.1

Table 5.10: Total and dissolved metal concentrations (µg/L) for water samples – Gimbi/Rikaya

Statistical Parameter	*As*	*Zn*	*Pb*	*Cd*	*Ni*	*Fe*	*Cr*	*Cu*	*Ti*	*Zr*	*Ce*	*Sr*	*Ba*	*Hg*	*Mn*	*Al*	*Mg*	*Ca*	*Na*	*K*
Dissolved Metals (n=15)																				
Min	0	176.8	0	0	0	0	1	1.4	0	0	0	166.2	568.7	0	0	139	0	20716.61	28212.1	13646.4
Max	23.9	26393.1	461.6	141.5	39.9	3050.5	8	49.6	0	32.8	17.5	2217	1088.1	16.4	5750.9	2819.5	829000.1	674749.3	254990.6	151090.1
Mean	10.5	4315.8	86.9	18.8	5.8	291.9	3.8	18	0	16.3	8.9	679	717.4	5.9	1160	421.3	204000.6	288089.3	135370.9	44367.9
SD	7.5	8979.7	157.2	41.5	13.8	776.1	2.1	14.6	0	11.1	6.3	650.3	169.7	5.6	1946.2	704.4	273464.5	231704.65	78258.733	36589.9
BHW Mean (n=4)	11.1	456.8	3.1	0.4	0	29.9	4.7	17.4	0	21.4	8.1	2255.8	710.6	55.2	7.3	199.9	248654.3	192900.4	342103	21329.4
Total Metals (n=15)																				
Min	0	311.3	0	0	0	0	1.6	3.8	0	0	0	161.7	549.6	0	0	140	5287.9	48890.7	28882.6	16567.9
Max	17.1	26622	1298	79.6	19.6	22452	23.1	101.1	0	32.9	92.3	1974	1026.1	108.9	5937.7	16659.2	831495.3	665341.1	276412.5	159550.1
Mean	4.3	4418.6	163.3	7.3	1.8	2392.6	5.3	23.8	0	7.7	15.1	643.3	740.3	15.6	1566.6	2076.9	207085.8	290625.7	140117.5	46030.6
SD	6.4	9000.8	350.4	20.3	5.1	5921.8	5.4	25.6	0	11.7	29.2	575.8	175.7	27.5	1989.4	4558.5	271495.4	218914.4	80147.5	37843.8
BHW Mean (n=4)	13.1	412.2	1.5	0.5	0	37.5	4	19.1	0	21.6	9.2	2348	620.7	8.3	11	180.9	259612.5	203328.9	143011.7	21282.1

BHW- Borehole Water

5.3.4.2 Gimbi and Rikaya

Data on the analysed water samples for dissolved and total metal concentrations at the Gimbi/Rikaya sites are shown in Table 5.10. The results reveal significant contamination and substantial variability across several analytes, indicating heterogeneous pollution sources or geochemical controls at the sites.

Total concentrations of Fe, Pb, Al, Cr, and Cd were substantially higher than their corresponding dissolved fractions. For example, Fe recorded a mean total concentration of 2,392.6 µg/L, compared to 291.9 µg/L in the dissolved phase, while Pb averaged 163.3 µg/L in the total fraction and 86.9 µg/L in the dissolved fraction. Similarly, Al showed a significant difference, with mean concentrations of 2,076.9 µg/L (total) and 421.3 µg/L (dissolved), suggesting a considerable proportion of these metals is associated with particulate matter or present in insoluble forms.

In contrast, elements such as Zn, Sr, Ba, and Mn exhibited relatively similar mean concentrations in both total and dissolved fractions. Zn averaged 4,418.6 µg/L (total) and 4,315.8 µg/L (dissolved); Sr was 643.3 µg/L (total) and 679.0 µg/L (dissolved); and Ba was 740.3 µg/L (total) and 717.4 µg/L (dissolved). These results indicate that the elements are predominantly present in soluble or colloidal forms under the prevailing water chemistry conditions. Mn also showed a relatively even distribution between phases (1,566.6 µg/L total vs 1,160.0 µg/L dissolved).

Among the major elements, Ca, Na, and K recorded the highest dissolved concentrations, with mean values of 288,089.3 µg/L, 135,370.9 µg/L, and 44,367.9 µg/L, respectively. Mg was also elevated (204,000.6 µg/L), while Al and Fe showed significantly higher concentrations in the total fraction (2,076.9 µg/L and 2,392.6 µg/L, respectively), indicating a strong association with particulates. The dominance of Ca, Na, K, and Mg in the dissolved phase reflects their high solubility and likely geogenic origin.

Borehole Water (BHW) samples served as controls to establish background water chemistry for comparison with mine-impacted waters. The mean (4) BHW generally exhibited substantially lower concentrations of contamination-associated metals such as Zn, Pb, Cd, Fe, and Mn, for both dissolved and total metal concentrations, indicating limited influence from mining activities; however, relatively elevated Sr, Mg, Ca, and Na concentrations reflect the natural geochemical signature of the groundwater system.

In summary, the data indicate that both dissolved and total fractions of several toxic metals are present at levels that may pose a potential risk to the environment. The high concentrations of Zn, Cd, Mn, and Al, especially in their dissolved forms, underscore the likelihood of elevated bioavailability and mobility. The pronounced variability across samples suggests complex geochemical dynamics influenced by factors such as pH, redox potential, and historical mining in the area.

5.3.5 Soil and Sediment Quality

Due to the absence of national soil and sediment quality guidelines (SQGs) in Nigeria, soil and sediment samples were compared with various international SQGs instead, which provide a simple way to evaluate the degree to which the contaminant-bearing sediments might adversely affect the aquatic ecosystem within the media (MacDonald et al., 2000). The Canadian Soil and Sediment Quality guidelines were used in this evaluation.

Mean concentrations of soils in several metals exceeded background and soil quality guideline values across the AML sites (Table 5.11). At Abakaliki, Pb (799 mg/kg), Zn (466 mg/kg), and Cd (2.0 mg/kg) in soils were markedly enriched above background and guideline limits. In Gimbi, soils contained elevated Mn (623 mg/kg) and Zn (486 mg/kg), while tailings showed extreme enrichments, particularly Zn (4462–7721 mg/kg), Pb (939–1031 mg/kg), and Cd (18–20 mg/kg), far above both background and soil quality thresholds. At Gimbi-Rikaya, soils also had high Mn (904 mg/kg) and moderately elevated Zn, while tailings contained notable Pb (279 mg/kg) and Zn (437 mg/kg). Overall, Pb and Cd consistently exceeded guideline values, particularly in tailings, underscoring their roles as major sources of contamination. In contrast, Ni, Cr, Cu, Ba, and most major elements (Al, Fe, Mg, Ca, Na, K) generally remained within guideline limits despite localised enrichments.

The reference soils showed concentrations closer to background levels, whereas the rock sample contained elevated concentrations of Mn, Pb, and Zn, confirming it as a potential geogenic source of contamination.

The mean concentration of each metal in the sediment samples at each site was compared with the corresponding soil and sediment quality guideline value for that metal. According to MacDonald, sediment samples were predicted to be non-toxic if the measured concentrations were below the corresponding Threshold Effect Concentration (TEC). Similarly, samples were predicted to be toxic if the corresponding Probable Effect Concentration (PEC) was exceeded in sediment samples collected in the field (MacDonald et al., 2000).

Generally, mean concentrations of several metals in the sediments across the sites (Table 5.12) exceeded background levels and, for some elements, surpassed sediment quality guideline thresholds. Zinc and Pb were markedly elevated at all sites compared with background values. Zn at Abakaliki (1272.9 mg/kg) and Gimbi-Rikaya (1516.4 mg/kg) far exceeded the TEL (123 mg/kg) and PEL (315 mg/kg), while Zn at Gimbi (559.8 mg/kg) also exceeded both thresholds. At Abakaliki, Pb (1023 mg/kg) was substantially higher than the PEL (91.3 mg/kg), whereas Gimbi (158.2 mg/kg) and Gimbi-Rikaya (181.8 mg/kg) also exceeded the TEL but remained below the PEL.

At all sites, Cu concentrations (32–40 mg/kg) were above background and close to or slightly above the TEL (35.7 mg/kg), but well below the PEL (197 mg/kg). At the Abakaliki site, Cr (39.7 mg/kg) exceeded the TEL (37.3 mg/kg) but remained below the PEL (90 mg/kg), whereas Gimbi and Gimbi-Rikaya values were lower (26.6 and 8.5 mg/kg, respectively). Nickel levels (13.9–31.2 mg/kg) were above background; only the Abakaliki site slightly exceeded the TEL (18 mg/kg), and none exceeded the PEL (36 mg/kg). Cadmium was elevated at Abakaliki (3.8 mg/kg) and Gimbi-Rikaya (3.5 mg/kg), surpassing both the TEL (0.6 mg/kg) and PEL (3.5 mg/kg), while Gimbi (0.3 mg/kg) remained below guideline thresholds.

Control sediments showed generally low metal concentrations, with most analytes well within or below background ranges and SQGs values. Zn (9.9 mg/kg), Pb (16.9 mg/kg), Ni (8.0 mg/kg), Cr (59.4 mg/kg), Cu (9.9 mg/kg), and Cd (0.0 mg/kg) were markedly lower than in AML-impacted sites, with only Cr slightly exceeding the TEL (37.3 mg/kg) but remaining below the PEL (90 mg/kg). These values indicate minimal anthropogenic influence in the control sediments and support their suitability as a local reference baseline for comparative assessment.

In summary, sediments from the Abakaliki and Gimbi-Rikaya sites showed the most frequent exceedances of PEL values, particularly for Zn, Pb, and Cd, suggesting a higher ecological risk compared with Gimbi.

Table 5.11: Soil Mean Metal Concentrations for Abakaliki, Gimbi and Gimbi Rikaya AMLs with Background values and Canadian Soil Quality Standards for Agricultural and Residential/parkland; all in (mg/kg).

	Abakaliki AML			Gimbi AML				Gimbi-Rikaya AML			*Background values	**Soil Quality Guideline Values	
Analyte	Tailings (n=18)	Soil (n=12)	Reference soil (n=2)	Tailings (n=17)	Soil (n=19)	Control Soil Sample	Rock Sample	Tailings (n=2)	Soil (n=11)	Control soil (n=2)	Mean	Agricultural	Residential /parkland
Mn	282.3	966.3	496.1	3829.3	623.4	195.5	8987.5	1008.1	904.1	701.8	330	-	-
Zn	4462	465.9	78.5	7720.6	485.6	7.2	6258.1	437.1	48.9	103.9	48	200	200
Pb	1103	799	47.3	1030.5	63	8.3	939.9	278.9	33.4	19.6	16	70	140
Ni	30.4	13.3	16.5	23.5	6.3	0	22.6	13.7	7.1	4.9	13	50	50
Cr	39.5	129.8	54.8	13	48.6	33.1	20.5	13.1	23.7	15.8	<37	64	64
Cu	54.4	27.5	19.5	78.8	11.3	7.3	1517.9	61.7	10.2	11.7	17	63	63
Ti	6.4	27.5	14.6	2	44	26.6	3.6	10.5	33.7	51.6	2,200	-	-
Zr	2.7	4.7	9.7	4.2	6	5.4	8.9	2.7	3.3	2.5	190	-	-
Ce	9.4	36.9	31.4	14.7	29.6	34.6	9.3	37.2	47.4	31.4	64	-	-
Sr	12.8	13.6	29.5	47.7	18.8	7.9	22	19.5	14.2	40.9	120	-	-
Ba	33	31.3	59	94.8	82.5	52.3	0	68.6	96.2	74	440	750	500
Cd	20.2	2	0	18.2	0.5	0	20.4	0	0	0	0.098	1.4	10
Al	17516.6	16688.8	17505.6	4653.7	6639.2	5916.3	75.1	8382.2	4934.5	5290.7	47,000	-	-
Fe	31175.4	40505.8	36455.2	29885.2	22636.4	12597.9	36426.5	20239.6	19838.7	18716.2	18,000	-	-
Mg	26923.9	5385.8	3850.7	15691.8	5179.1	1025.3	1688.4	4595	1675.5	2637.9	13,300	-	-
Ca	3096.8	2823.4	14383.5	18479.4	8477.7	3657.8	1705.5	4921.9	5904.9	24510.2	30,000	-	-
Na	843.8	714	936.7	1741.1	1234.3	891.2	2657.7	1205.3	776.2	1022.5	28,900	-	-
K	5335.3	3353.6	4582.4	5218.6	4061.2	2639.6	5295.4	4244.3	3126.9	5039.6	28,000	-	-

*(Buchman, 2008; S. R. Taylor & McLennan, 1985) sources for the values in bold

** (CCME, 1999): Canadian Council of Ministers of the Environment soil quality guidelines

Table 5.12: Sediment Mean Metal Concentrations for Abakaliki, Gimbi and Gimbi Rikaya AMLs with Background values and Sediment Quality Guideline for the protection of aquatic life; all in (mg/kg)

	Abakaliki AML	Gimbi AML	Gimbi-Rikaya AML		Sediment Background values	*Sediment Quality Guidelines Values					
Analyte	Sediment (n=3)	Sediment (n=12)	Sediment (n=4)	Control sediment (n=2)	Mean (mg/kg)	TEC	ISQGs (TEL)	LEL	PEC	PEL	SEL
Mn	307	1239.8	1529.7	436.8	400						
Zn	1272.9	559.8	1516.4	9.9	7 – 38	121	123	–	120	315	820
Pb	1023	158.2	181.8	16.9	4 – 17	35.8	35	31	128	91.3	250
Ni	31.2	17.9	13.9	8	9.9	22.7	18	16	48.6	36	75
Cr	39.7	26.6	8.5	59.4	7 – 13	43.4	37.3	26	111	90	110
Cu	39.8	32.1	39.4	9.9	10 – 25	31.6	35.7	16	149	197	110
Ti	6.7	10.5	9.3	57.4	_	–	–	–	–	–	–
Zr	0	3.5	1.4	5	_	–	–	–	–	–	–
Ce	9.5	39	24.6	43.8	_	–	–	–	–	–	–
Sr	15.9	52.7	23.6	10.1	49	–	–	–	–	–	–
Ba	35.9	158.1	75.2	70.7	0.7	–	–	–	–	–	–
Cd	3.8	0.3	3.5	0	0.1 – 0.3	0.99	0.6	–	4.98	3.5	–
Al	7806.9	11724.1	5171.8	9584.9	2,600	–	–	–	–	–	–
Fe	35748.6	24739.7	29897	25425.9	9,900 – 18,000	–	–	20,000	–	–	40,000
Mg	35844.4	9347	3965	1710.8	–	–	–	–	–	–	–
Ca	3975.8	32632.2	7226.8	3326	–	–	–	–	–	–	–
Na	904	1769.6	1256.2	1703.8	–	–	–	–	–	–	–
K	5716.6	6950.2	4785.1	6127.7	–	–	–	–	–	–	–

(Buchman, 2008), Threshold effect concentration (PEC), Interim sediment quality guidelines (ISQGs) or Threshold effect levels (TEL), Lowest effect levels (LEL), Probable effect concentration (PEC), Probable effect levels (PEL), Severe effect levels (SEL) (Buchman, 2008; CCME, 2002).

5.3.6 Surface Water Quality

European and UK Environmental Quality Standards (EQS) for surface water were compared with the mean concentrations at Abakaliki and Gimbi sites. They showed distinct patterns of compliance and exceedance (Table 5:13). At Abakaliki, most trace metals exceeded their respective thresholds, while fewer exceedances were observed at Gimbi/Rikaya.

At both sites, dissolved As concentrations remained below the average concentration (AC) of 50 µg/L. In contrast, Zn was present at extremely high levels, at 105,855 µg/L in Abakaliki and 4,315.8 µg/L in Gimbi/Rikaya, far above the AC of 10.9 µg/L. At both sites, Pb concentrations also surpassed both the AC (1.2 µg/L) and Maximum Allowable Concentration (MAC) (14 µg/L), reaching 995.7 µg/L and 86.9 µg/L, respectively.

Cadmium showed severe exceedance of EQS at both locations, with 618.0 µg/L at Abakaliki and 18.8 µg/L at Gimbi/Rikaya, higher than the EQS thresholds across all water hardness categories. For Ni, concentrations at both sites were greater than the AC of 4 µg/L, although only the Abakaliki value (342.3 µg/L) exceeded the MAC of 34 µg/L. Dissolved Fe remained within the AC threshold of 1,000 µg/L (339.0 µg/L and 291.9 µg/L, respectively), though total Fe was markedly elevated, particularly at Abakaliki (380,449.0 µg/L). With respect to Cr, trivalent and Hexavalent chromium (4.7 and 3.4 µg/L, respectively) were exceeded at Abakaliki (12.7 µg/L) and at Gimbi/Rikaya (3.8 µg/L); in both cases, concentrations were below the MAC of 32 µg/L, although no EQS value was available for comparison.

Copper concentrations at both sites (161.1 µg/L and 18.0 µg/L) were greater than the AC of 1 µg/L, while Mn showed pronounced exceedance of the AC value of 123 µg/L at both sites, with 12,651.8 µg/L at Abakaliki and 1,160.0 µg/L at Gimbi/Rikaya. For other analytes, including Ti, Zr, Ce, Sr, Ba, Hg, Al, Mg, Ca, and Na, no EQS thresholds were available. Nonetheless, several occurred at elevated levels, most notably Al, Sr, Ba, and Hg.

Table 5.13: Hardness-based Environmental Quality Standards (EQS) and the European and UK river water EQS for dissolved metals using the BLM. All concentrations are µg/L as dissolved metal.

Pollutant	Abakaliki Mean (ug/L)	Gimbi/Rikaya (ug/L)	Average concentrations (AC) µg/l	Maximum Allowable Conc. (MAC) µg/l	Category of environmental quality standard*	Source
Arsenic (As)	17.7	10.5	50	Not applicable	SP	b
Zinc (Zn)	105855.3	4315.8	10.9 (bioavailable)	Not applicable	SP	b
Lead (Pb)	995.7	86.9	1.2 (bioavailable)	14	PS	a
			≤0.08 = <40mg $CaCO_3$/l	≤0.45 = <40mg $CaCO_3$/l	PHS	a
			0.08 = 40 to <50	0.45 = 40 to <50	PHS	a
			0.09 = 50 to <100	0.6 = 50 to <100	PHS	a
Cadmium (Cd)	618	18.8	0.15 =100 to <200	0.9 =100 to <200	PHS	a

Pollutant	Abakaliki Mean (ug/L)	Gimbi/Rikaya (ug/L)	Average concentrations (AC) µg/l	Maximum Allowable Conc. (MAC) µg/l	Category of environmental quality standard*	Source
			0.25 = ≥ 200	1.5 = ≥ 200	PHS	a
Nickel (Ni)	342.3	5.8	4 (bioavailable)	34	PS	b
Iron (Fe)	339	291.9	1000	Not applicable	SP	b
*Chromium (III) ($Cr3^{+}$)			4.7	32 (95th percentile)	SP	b
*Chromium (VI) ($Cr6^{+}$)	12.7	3.8	3.4	Not applicable	SP	b
Copper (Cu)	161.1	18	1 (bioavailable)		SP	
Titanium (Ti)	0		_	_	_	
Zirconium (Zr)	24.9	16.3	_	_	_	
Cerium (Ce)	54.2	8.9	_	_	_	
Strontium (Sr)	474.2	679	_	_	_	
Barium (Ba)	523.9	717.4	_	_	_	
Mercury (Hg)	30.7	5.9	_	_	_	
Manganese (Mn)	12651.8	1160	123 (bioavailable)	Not applicable	SP	b
Aluminum (Al)	8904.5	421.3	_	_	_	
Iron (Fe)	380449	204000.6	_	_	_	
Magnesium (Mg)	677179.5	288089.3	_	_	_	
Calcium (Ca)	47556.9	135370.9	_	_	_	
Sodium (Na)	19321.2	44367.9	_	_	_	

*PHS is priority hazardous substance, PS is priority substance, OP is other pollutant
a - https://www.gov.uk/guidance/surface-water-pollution-risk-assessment-for-your-environmental-permit
b - https://www.gov.uk/guidance/surface-water-pollution-risk-assessment-for-your-environmental-permit

Biotic Ligand Model (BLM) Derived EQS

To assess whether elevated trace element concentrations in dissolved water samples exceeding the EQS values for surface water were bioavailable, the BLM model was applied to Mn, Cu, Zn, Ni, and Pb. Definitions of the BLM variables and their derivation methods used in the following tables are provided in Section 5.2.8.3.

The BLM-derived bioavailable concentrations indicated consistent exceedances of $EQS_{bioavailable}$ thresholds for Ni, Cu, Pb, Zn and Mn across all sampling points at Abakaliki (Table 5:15). Ni (EQS 4 µg/L) ranged from 55 to 80 µg/L, exceeding the threshold by more than an order of magnitude. Cu (EQS 1 µg/L) showed bioavailable concentrations between 39 and 179 µg/L, while Pb (EQS 1.2 µg/L) ranged from 140 to 548 µg/L, both reflecting substantial exceedances. The most pronounced results were observed for Zn (EQS 10.9 µg/L), where bioavailable concentrations reached 42,873–55,759 µg/L, surpassing the threshold by several thousand-fold. Manganese (Table 5.17) showed consistent

and pronounced exceedance, with bioavailable concentrations ranging from 275 to 375 µg/L, representing approximately 2–3 times the $EQS_{bioavailable}$.

Table 5.14: BLM. Derived EQS for Cu, Zn, Ni, and Pb concentrations in µg/L at Abakaliki

Abakaliki Sample ID	Local HC5 (dissolved) [µg/L]	BioF	Bioavailable Concentration [µg/L]	Risk Characterisation Ratio (RCR)	Measured Dissolved Concentration [µg/L]
Ni - EQSbioavailable 4 ug/L					
WS1	23	0.17	65	16	379
WS2	19	0.21	80	20	384
WS3	19	0.21	55	14	264
Cu - EQSbioavailable 1 ug/L					
WS1	4	0.23	39	39	173
WS2	1	0.94	179	179	190
WS3	1	1.00	121	121	121
Pb - EQSbioavailable 1.2 ug/L					
WS1	9	0.14	140	116	992
WS2	2	0.51	500	417	982
WS3	2	0.54	548	457	1014
Zn - EQSbioavailable 10.9ug/L					
WS1	26	0.42	48673	4465	115050
WS2	22	0.49	55759	5115	114487
WS3	22	0.49	42873	3933	88028

Note: The measured dissolved concentration (µg/L) is not among the calculated variables in the Bio-Met tool; it refers to the site-specific concentration of dissolved metals measured in water samples collected in the field.

The bioavailability-adjusted assessment for Gimbi-Rikaya indicated variable exceedance of $EQS_{bioavailable}$ thresholds across metals. Ni (EQS 4 µg/L) was generally below the threshold, with exceedances only at PWS2A and PWS2B (8 µg/L). Cu (EQS 1 µg/L) showed consistent exceedances, ranging from 1–32 µg/L across several sampling points, with the highest values recorded at PWS2A and PWS2B. Pb (EQS 1.2 µg/L) displayed particularly strong exceedances in some samples, with bioavailable concentrations up to 193 µg/L (PWS2B) and 104 µg/L (PWS2A). Zn (EQS 10.9 µg/L) showed the greatest exceedances, with values ranging from 60 to 8,459 µg/L, particularly elevated at PWS2A and PWS2B. Overall, Zn and Pb showed the highest relative exceedance, while Cu was moderately elevated at multiple sites and Ni rarely exceeded the threshold (Table 5.16). For Mn (Table 5:17), exceedances of the EQSbioavailable (123 µg/L) were limited to specific sampling points; most waters were below the threshold, with only PWS2A (142 µg/L) and PWS2B (149 µg/L) exceeding the standard. All other samples, including controls, were within safe limits.

Table 5.15: BLM. Derived EQS for Cu, Zn, Ni, and Pb concentrations in µg/L at Gimbi-Rikaya

Gimbi-Rikaya Sample ID	Local HC5 (dissolved) [µg/L]	BioF	Bioavailable Concentration [µg/L]	Risk Characterisation Ratio (RCR)	Measured Dissolved Concentration [µg/L]
Ni – $EQS_{bioavailable}$ 4 ug/L					
RW1-F	9	0.46	0	0	0
RW2-F	16	0.26	0	0	0

Gimbi-Rikaya Sample ID	Local HC5 (dissolved) [µg/L]	BioF	Bioavailable Concentration [µg/L]	Risk Characterisation Ratio (RCR)	Measured Dissolved Concentration [µg/L]
RW3-F	35	0.12	0	0	3
CW1-F	49	0.08	0	0	2
CW2-F	25	0.16	0	0	0
PWS1A-F	13	0.31	1	0	2
PWS1B-F	6	0.62	0	0	0
PWS2A-F	21	0.19	8	2	40
PWS2B-F	19	0.21	8	2	39
PWS3-F	13	0.30	0	0	0
PWS4B-F	10	0.41	0	0	0
PWS5A-F	14	0.28	0	0	0
PWS5B-F	27	0.15	0	0	0
PWS1-R-F	8	0.53	0	0	0
PWS2-R-F	14	0.29	0	0	0
BHW1-F	4	0.93	0	0	0
BHW2-F	6	0.66	0	0	0
BHW3-F	4	1.00	0	0	0
BHW4-F	4	1.00	0	0	0
Cu – $EQS_{bioavailable}$ 1 ug/L					
RW1-F	11	0.09	1	1	8
RW2-F	2	0.50	11	11	23
RW3-F	48	0.02	1	1	29
CW1-F	118	0.01	0	0	24
CW2-F	61	0.02	0	0	12
PWS1A-F	18	0.06	0	0	9
PWS1B-F	10	0.10	1	1	7
PWS2A-F	3	0.31	15	15	48
PWS2B-F	2	0.65	32	32	50
PWS3-F	10	0.10	1	1	8
PWS4B-F	15	0.07	1	1	12
PWS5A-F	31	0.03	1	1	17
PWS5B-F	74	0.01	0	0	14
PWS1-R-F	10	0.10	0	0	1
PWS2-R-F	30	0.03	0	0	7
BHW1-F	2	0.55	14	14	26
BHW2-F	6	0.18	3	3	17
BHW3-F	2	0.47	8	8	17
BHW4-F	1	0.79	8	8	10
Pb - $EQS_{bioavailable}$ 1.2 ug/L					
RW1-F	10	0.12	0	0	0
RW2-F	1	0.98	7	6	7
RW3-F	30	0.04	7	6	172
CW1-F	55	0.02	0	0	4
CW2-F	29	0.04	0	0	0
PWS1A-F	5	0.22	0	0	1
PWS1B-F	6	0.19	0	0	1
PWS2A-F	5	0.22	104	86	462
PWS2B-F	3	0.45	193	161	426

Gimbi-Rikaya Sample ID	Local HC5 (dissolved) [µg/L]	BioF	Bioavailable Concentration [µg/L]	Risk Characterisation Ratio (RCR)	Measured Dissolved Concentration [µg/L]
PWS3-F	4	0.34	62	52	185
PWS4B-F	9	0.14	0	0	3
PWS5A-F	24	0.05	2	1	33
PWS5B-F	28	0.04	0	0	9
PWS1-R-F	9	0.14	0	0	1
PWS2-R-F	14	0.08	0	0	0
BHW1-F	1	0.81	0	0	0
BHW2-F	4	0.32	1	1	4
BHW3-F	2	0.62	5	4	8
BHW4-F	2	0.77	1	1	1
Zn – $EQS_{bioavailable}$ 10.9 ug/L					
RW1-F	46	0.24	89	8	375
RW2-F	21	0.52	252	23	489
RW3-F	58	0.19	159	15	844
CW1-F	113	0.10	41	4	430
CW2-F	56	0.19	78	7	399
PWS1A-F	26	0.43	426	39	996
PWS1B-F	25	0.43	239	22	557
PWS2A-F	34	0.32	8459	776	26393
PWS2B-F	34	0.32	8295	761	25729
PWS3-F	22	0.50	3425	314	6806
PWS4B-F	29	0.37	66	6	177
PWS5A-F	70	0.16	65	6	417
PWS5B-F	82	0.13	60	6	454
PWS1-R-F	30	0.36	120	11	335
PWS2-R-F	45	0.24	81	7	336
BHW1-F	14	0.79	325	30	410
BHW2-F	19	0.57	311	29	544
BHW3-F	21	0.38	173	16	456
BHW4-F	16	0.68	282	26	417

Table 5.16: BLM. Derived EQS for Mn concentrations in µg/L at Gimbi-Rikaya and Abakaliki

Gimbi-Rikaya Sample ID	Site-specific PNEC Dissolved [µg/L]	BioF	Bioavailable Concentration [µg/L]	Risk Characterisation Ratio (RCR)	Measured Dissolved Concentration [µg/L]
Mn – $EQS_{bioavailable}$ 123 ug/L					
RW1-F	142	0.87	0	0	0
RW2-F	2110	0.06	144	1	2474
RW3-F	2297	0.05	90	1	1679
CW1-F	951	0.13	66	1	514
CW2-F	650	0.19	40	0	212
PWS1A-F	895	0.14	101	1	734
PWS1B-F	184	0.67	97	1	144
PWS2A-F	4744	0.03	142	1	5493

Gimbi-Rikaya Sample ID	Site-specific PNEC Dissolved [µg/L]	BioF	Bioavailable Concentration [µg/L]	Risk Characterisation Ratio (RCR)	Measured Dissolved Concentration [µg/L]
PWS2B-F	4760	0.03	149	1	5751
PWS3-F	947	0.13	52	0	400
PWS4B-F	189	0.65	0	0	0
PWS5A-F	165	0.75	0	0	0
PWS5B-F	633	0.19	0	0	0
PWS1-R-F	184	0.67	0	0	0
PWS2-R-F	349	0.35	0	0	0
BHW1-F	199	0.62	0	0	0
BHW2-F	245	0.50	15	0	29
BHW3-F	138	0.89	0	0	0
BHW4-F	123	1.00	0	0	0
Abakaliki Sample ID					
WS1	4705	0.03	335	3	12812
WS2	4762	0.03	375	3	14512
WS3	4763	0.03	275	2	10632

Note: The measured dissolved concentration (µg/L) is not part of the calculated variables in the Bio-Met or M-Bat tools but refers to the site-specific concentration of dissolved metals measured in water samples collected from the field.

5.3.7 Speciation of Metals in Environmental Samples

The results of the sequential chemical extraction in the exchangeable/acid-soluble (F1), reducible (F2), and oxidisable (F3) fractions for soils, tailings, and sediments are presented in Appendices 5.10, 5.13, and 5.16 for Abakaliki, Gimbi and Gimbi Rikaya sites, respectively. Also, summary tables of the percentage (%) partitioning, with the minimum, mean, and maximum values for each element across all three sites, are provided in Appendices 5.11, 5.14, and 5.17.

Abakaliki AML Site

Metal speciation analysis at the Abakaliki site revealed clear differences in metal partitioning among geochemical fractions across the three sampled media.

The tailings samples revealed a different partitioning pattern compared to soils (Figure 5.20). Zn, Cd, and Ni showed significant contributions from both the F1 and F3 fractions, indicating that while part of their content is readily available, a considerable portion is also bound to organic matter or sulphides. For Pb, it was predominantly associated with the F2, with additional contributions from the F3, particularly in RS, TS2-4, TS8-9, and TS13–14, suggesting strong binding to Fe–Mn oxides and sensitivity to redox changes, while Mn was largely distributed across all three fractions, with dominance in the F2, suggesting sensitivity to redox changes. Other elements, Cr and Cu, were predominantly associated with the F3, reflecting strong binding to more stable phases.

Aluminium and Fe were also enriched in the F2 and F3, with Fe showing particularly high levels in the F3, highlighting the strong retention of these metals within organic and sulphide complexes. Barium was distributed across F1 and F2, suggesting moderate mobility with partial stabilisation. Overall, tailings contained a higher share of metals in the exchangeable and oxidisable fractions than soils, suggesting both higher potential mobility and long-term retention depending on environmental conditions.

Soil samples showed distinct partitioning patterns among the metals Mn, Zn, Pb, Cd, Ni, Cu, Cr, Fe, Ba, and Al (Figure 5.21). The metals Cd, Zn, and Ni were predominantly associated with the F1, indicating high mobility and potential bioavailability, particularly at sampling points SS3–SS6. Pb, Mn and Ba were mainly present in the F2, suggesting susceptibility to release under reducing conditions. Chromium, Cu, Al, and Fe were enriched in the F3, reflecting stronger binding to organic matter or sulphides and lower in immediate mobility. These results indicate that while Cd, Zn, and Ni represent the most labile and environmentally available metals in soils, Cr, Cu, Al, and Fe are more stable, with Pb, Mn and Ba being sensitive to redox changes (when the environment becomes reducing due to waterlogging, organic matter decomposition, or low oxygen, the oxides dissolve).

Sediment samples revealed mixed partitioning of metals across the three fractions (Figure 5.22). Cadmium was mainly present in the F1, indicating high mobility, with some contributions from F3, while Zn was distributed across all three fractions, with higher proportions in F1 and F3, suggesting partial mobility and partial stabilisation. Pb was dominated by the F2, particularly in SD2, indicating a strong association with Fe–Mn oxides and redox sensitivity. Natural environmental processes such as seasonal wetting–drying cycles, flooding, and fluctuating water tables can alter sediment redox conditions. Under reducing conditions, Fe–Mn oxides may dissolve, releasing and remobilising previously adsorbed Pb into pore water and surrounding aquatic systems, thereby increasing its potential mobility and bioavailability. But under oxidising conditions, Pb associated with Fe–Mn oxides tends to remain relatively immobilised and retained within sediments.

Manganese was also mainly F2, with smaller shares in F1, again reflecting redox sensitivity. Ni showed contributions from both F1 and F3, highlighting a mix of mobile and more stable forms. Chromium and Cu were predominantly associated with F3, indicating binding to organic matter and sulphides. Barium was more evenly distributed across F2 and F3, suggesting moderate mobility and binding, while Fe and Al were strongly enriched in F3, with smaller proportions in F2, indicating retention in organic/sulfidic phases but with partial redox sensitivity reflected in F2. Results show a combination of mobile (Cd, Zn, and Ni) and redox-sensitive (Pb and Mn) metals, alongside more stable forms (Cr, Cu, Fe and Al), suggesting that environmental conditions strongly influence their potential release.

Overall, soils were more enriched in labile fractions, tailings showed both enhanced mobility and retention, and sediments reflected stronger redox control on metal partitioning.

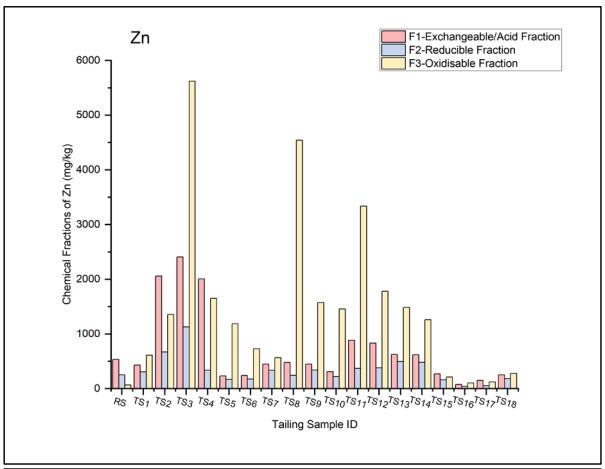
Zn
F1-Exchangeable/Acid Fraction
F2-Reducible Fraction
F3-Oxidisable Fraction
Chemical Fractions of Zn (mg/kg)
Tailing Sample ID

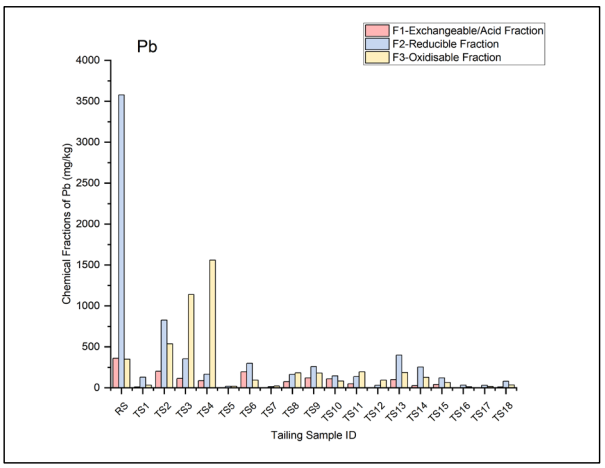
Pb
F1-Exchangeable/Acid Fraction
F2-Reducible Fraction
F3-Oxidisable Fraction
Chemical Fractions of Pb (mg/kg)
Tailing Sample ID

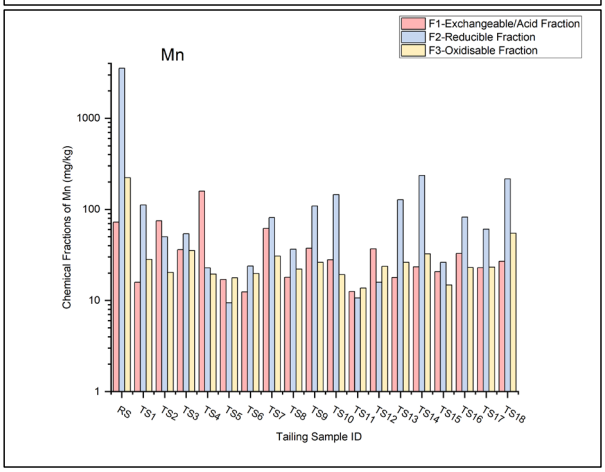
Mn
F1-Exchangeable/Acid Fraction
F2-Reducible Fraction
F3-Oxidisable Fraction
Chemical Fractions of Mn (mg/kg)
Tailing Sample ID

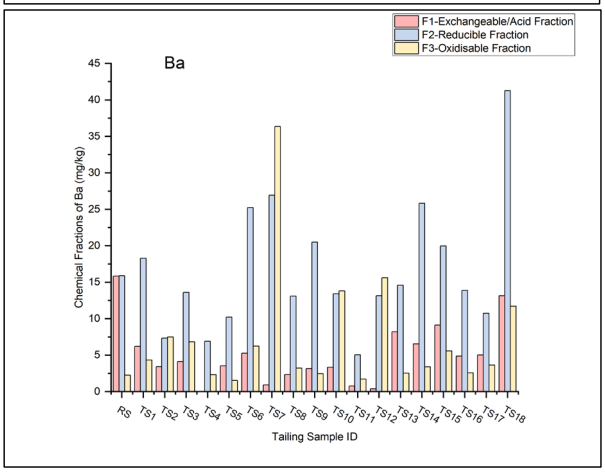
Ba
F1-Exchangeable/Acid Fraction
F2-Reducible Fraction
F3-Oxidisable Fraction
Chemical Fractions of Ba (mg/kg)
Tailing Sample ID

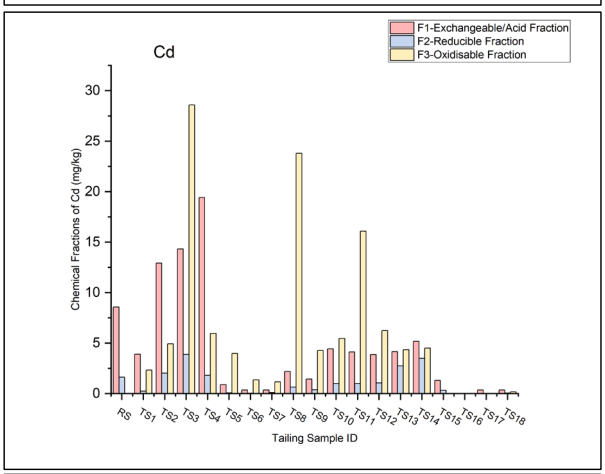
Cd
F1-Exchangeable/Acid Fraction
F2-Reducible Fraction
F3-Oxidisable Fraction
Chemical Fractions of Cd (mg/kg)
Tailing Sample ID

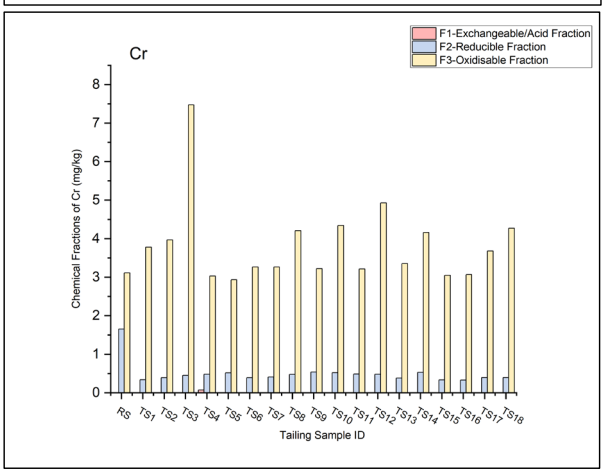
Cr
F1-Exchangeable/Acid Fraction
F2-Reducible Fraction
F3-Oxidisable Fraction
Chemical Fractions of Cr (mg/kg)
Tailing Sample ID

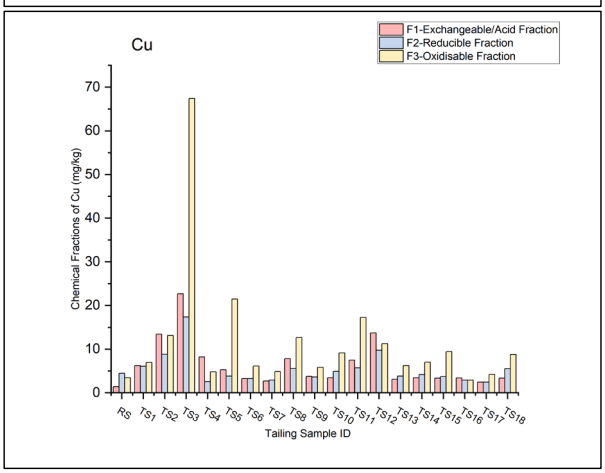
Cu
F1-Exchangeable/Acid Fraction
F2-Reducible Fraction
F3-Oxidisable Fraction
Chemical Fractions of Cu (mg/kg)
Tailing Sample ID

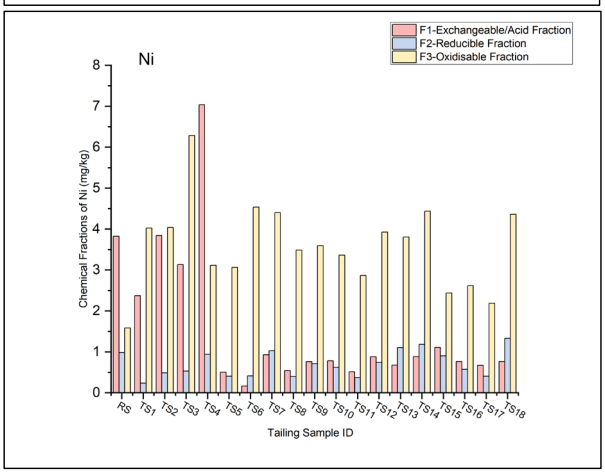
Ni
F1-Exchangeable/Acid Fraction
F2-Reducible Fraction
F3-Oxidisable Fraction
Chemical Fractions of Ni (mg/kg)
Tailing Sample ID

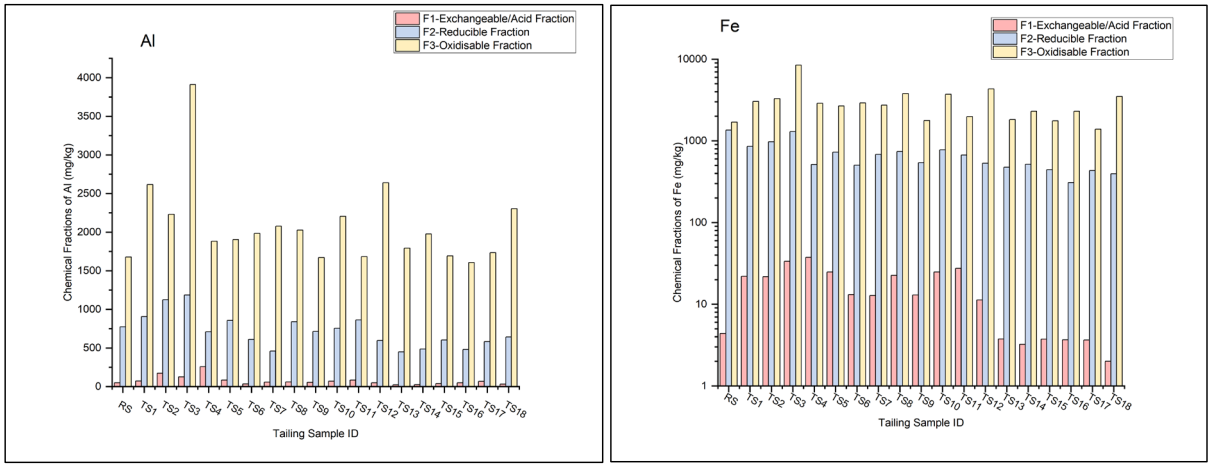

Figure 5.20: Chemical Fractions (F1, F2 and F3) for Mn, Zn, Pb, Cd, Ni, Cu, Cr, Fe, Ba, and Al in the Tailing samples collected at the Abakaliki Pb/Zn AML

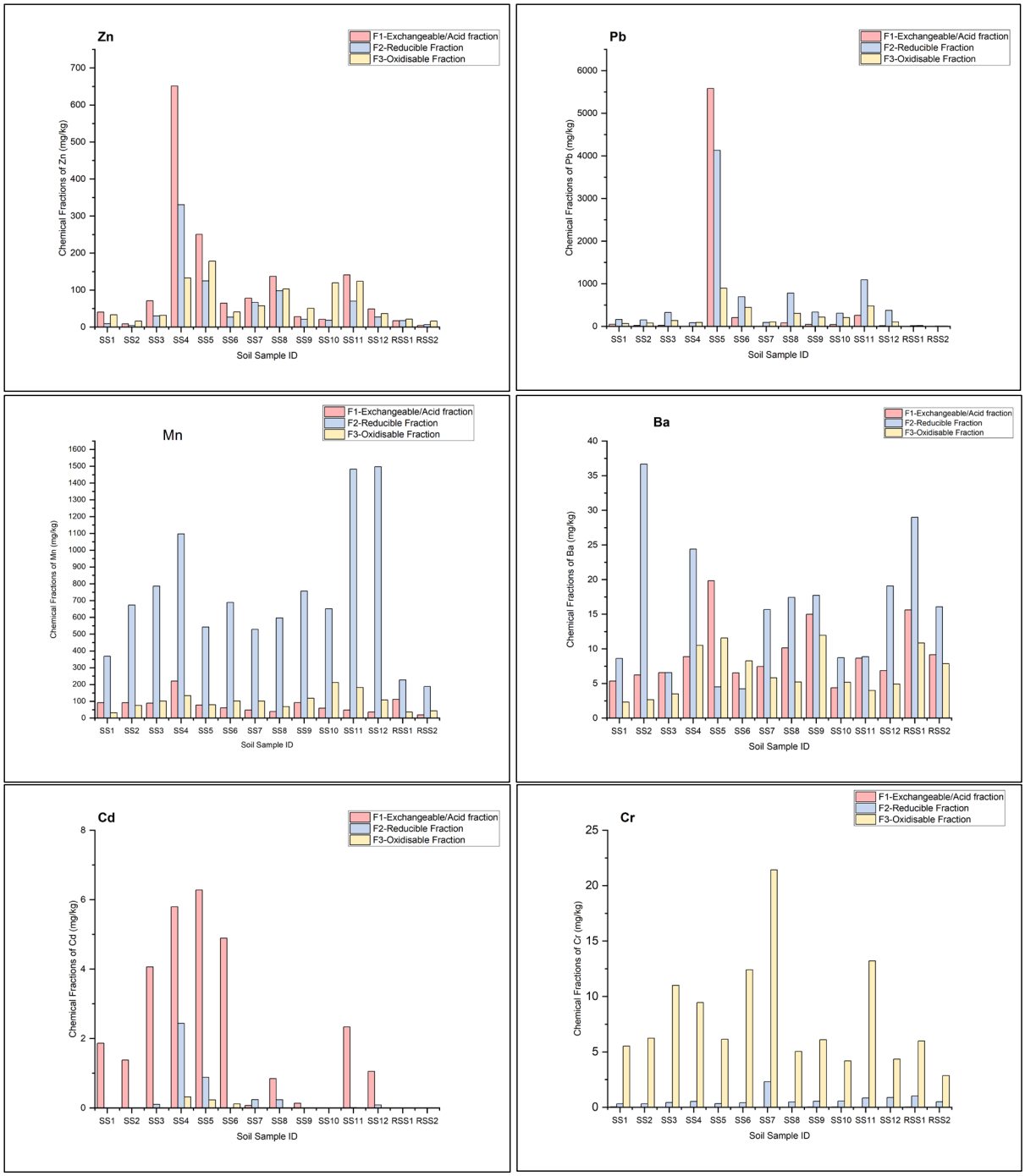

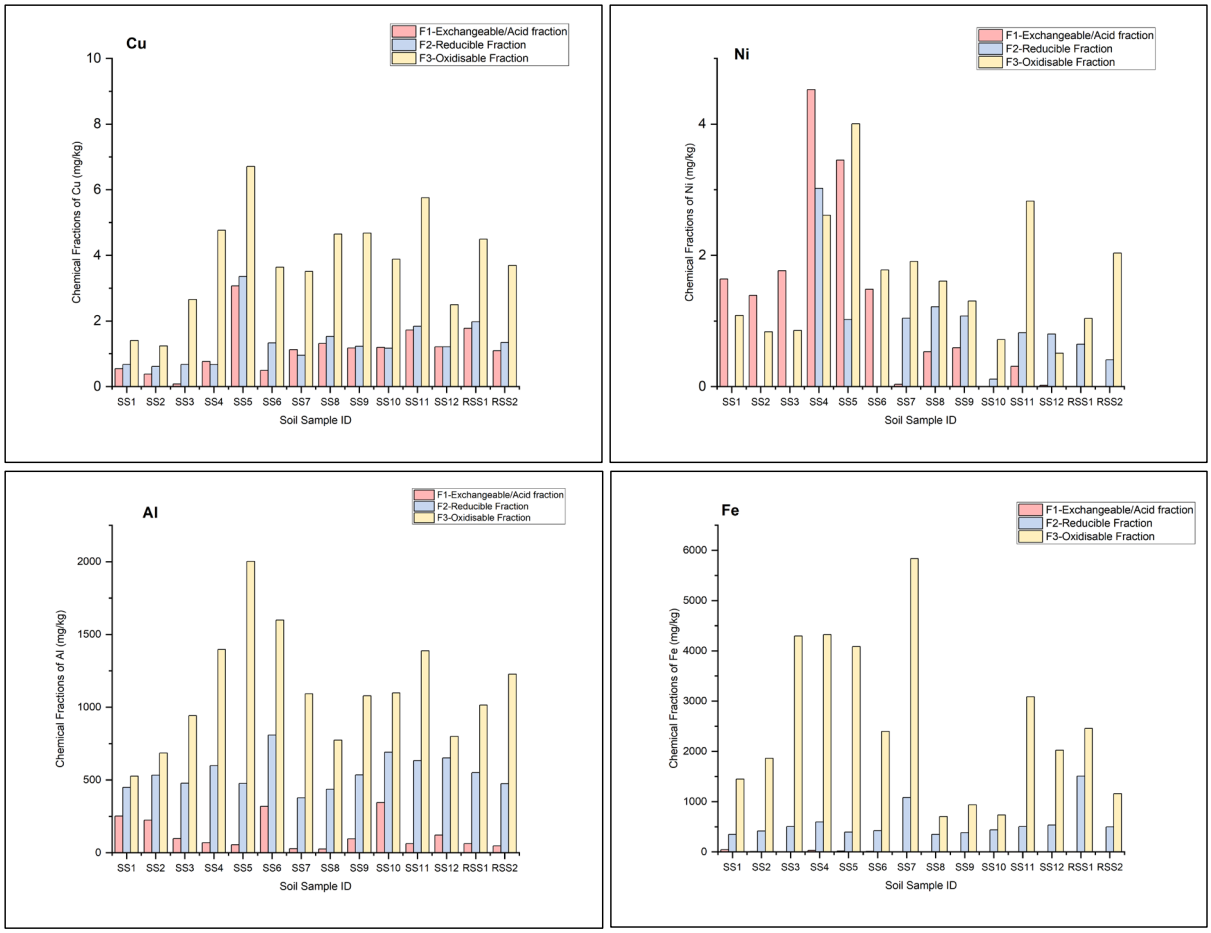

Figure 5.21: Chemical Fractions (F1, F2 and F3) for Mn, Zn, Pb, Cd, Ni, Cu, Cr, Fe, Ba, and Al in the soil samples collected at the Abakaliki Pb/Zn AML

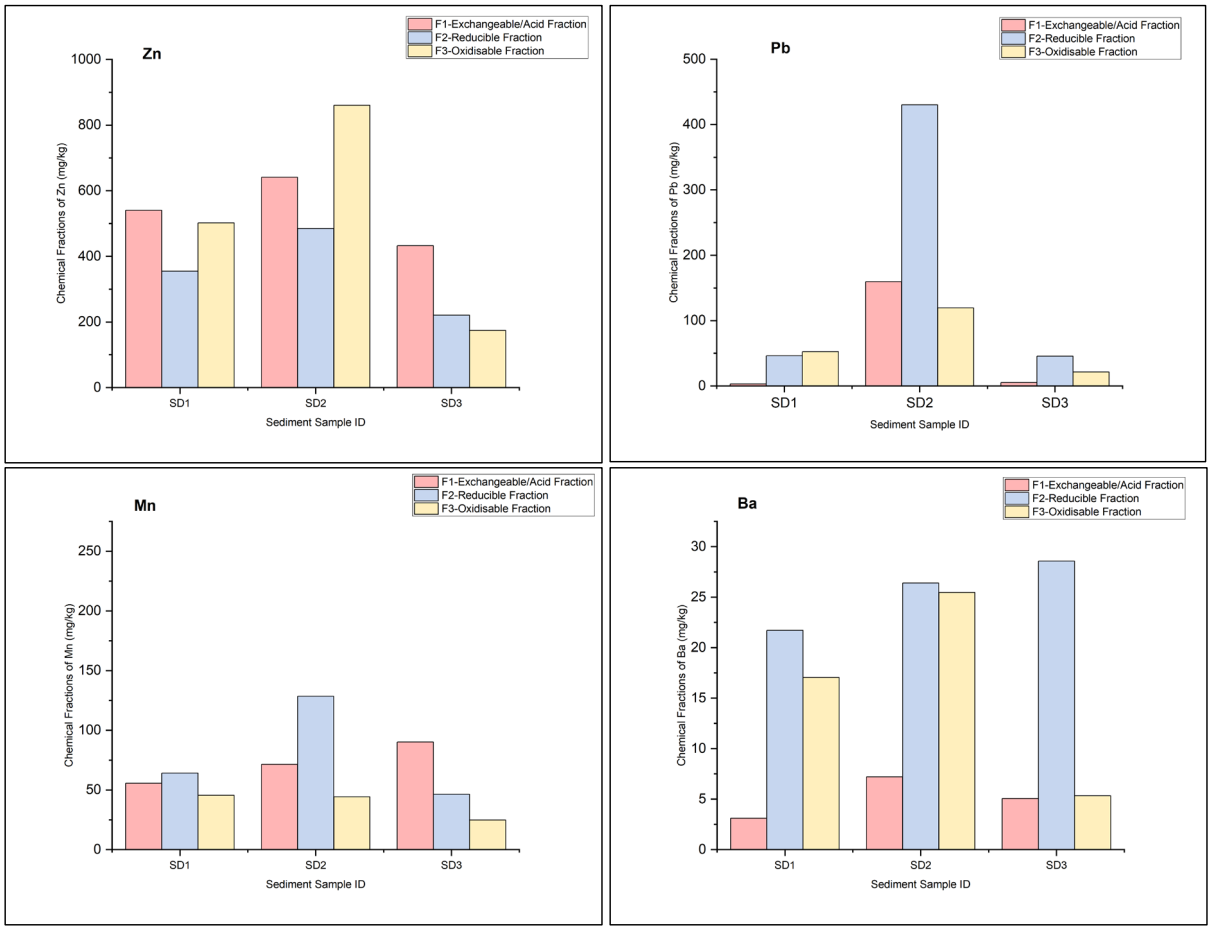

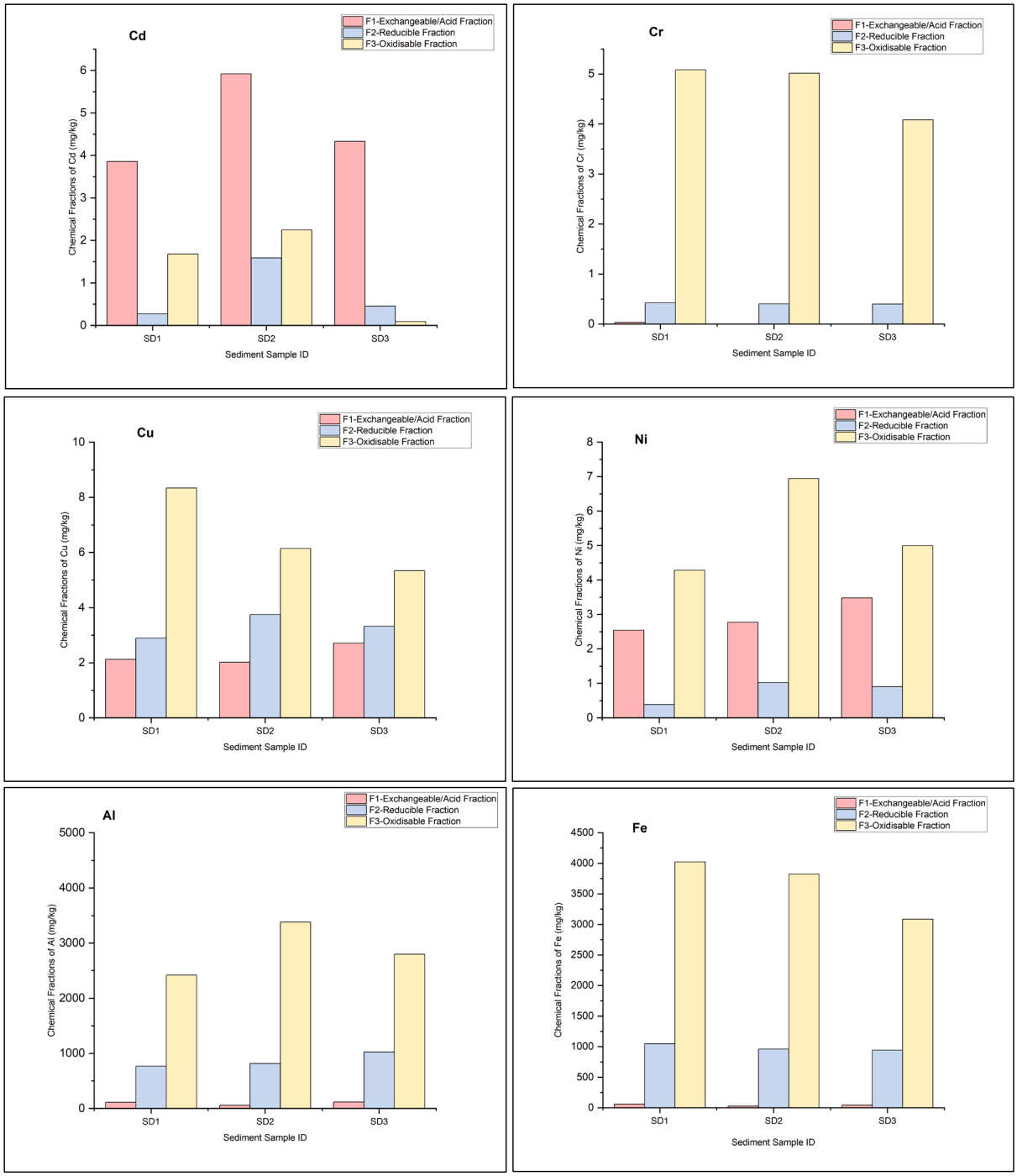

Figure 5.22: Chemical Fractions (F1, F2 and F3) for Mn, Zn, Pb, Cd, Ni, Cu, Cr, Fe, Ba, and Al in the Tailing samples collected at the Abakaliki Pb/Zn AML.

Gimbi AML Site

The Gimbi site speciation results revealed distinct differences in the distribution of metals across F1, F2, and F3 fractions. In tailings samples (Figure 5.23), metals showed distinct partitioning patterns compared to soils. Zinc occurred at very high concentrations and was distributed relatively evenly across F1, F2, and F3, indicating both high total loads and substantial potential mobility. In the case of Pb, it was most abundant in F1 and F2 in some samples, but also showed strong representation in F3, suggesting partial stabilisation, yet with a large exchangeable component. Manganese was dominated by F2, with considerable amounts also present in F1 and F3, reflecting its strong cycling with Fe/Mn

oxides but with higher mobility than in soils, while Ba was mainly associated with F2, with smaller contributions from F1 and F3.

In several samples, Cd was concentrated in F1, with elevated levels, highlighting its high lability. However, Cr occurred predominantly in F3, indicating strong binding within organic/sulfidic or mineral-associated phases. Similarly, Cu showed a close pattern, with F3 being dominant, although F1 and F2 contributions were more evident than in soils. For Ni, it was distributed across all fractions, but F3 remained the main reservoir, consistent with strong mineral or organic associations. However, Al and Fe were overwhelmingly concentrated in F3, pointing to their incorporation into stable mineral phases. Furthermore, the samples also showed a greater relative contribution of Al and Fe to F2 compared with soils, suggesting enhanced association with secondary oxide phases.

Broadly, tailings were characterised by high total metal concentrations, particularly Zn, Pb, Mn, and Fe, with more balanced distributions across F1–F3 compared to soils. This implies that while some metals (e.g., Cd, Zn) remain highly labile, others (e.g., Cr, Cu, Al, Fe) are largely stabilised but could become mobilised under changing redox conditions.

In soils (Figure 5.24), Zn was widely distributed among the three fractions, with relatively higher concentrations in F1 and F2, suggesting greater mobility and potential bioavailability, while Pb was consistently enriched in F3, with contribution from F2, indicating strong association with organic matter and sulphides, and thus lower immediate mobility. Manganese was dominated by F2, reflecting its strong affinity for Fe/Mn oxides. Similarly, Ba was also predominantly reducible, though substantial proportions occurred in F1 and F3, pointing to intermediate stability.

Cadmium was concentrated almost entirely in F1, highlighting its high lability and environmental risk, while Cr and Cu were mainly associated with F3, suggesting strong binding to organic matter or sulphide phases. In the case of Ni, it showed a relatively even distribution across fractions but tended to favour F3. Al and Fe were overwhelmingly associated with F3, reflecting their incorporation within stable mineral phases (e.g., aluminosilicates, iron oxides). This indicates that they are largely immobile under natural conditions compared to other metals in the soil samples.

Collectively, soil samples displayed a clear partitioning pattern where potentially toxic elements like Cd and Zn were present in more labile fractions, whereas Fe, Al, Cr, Cu, and Pb were stabilised within less mobile pools.

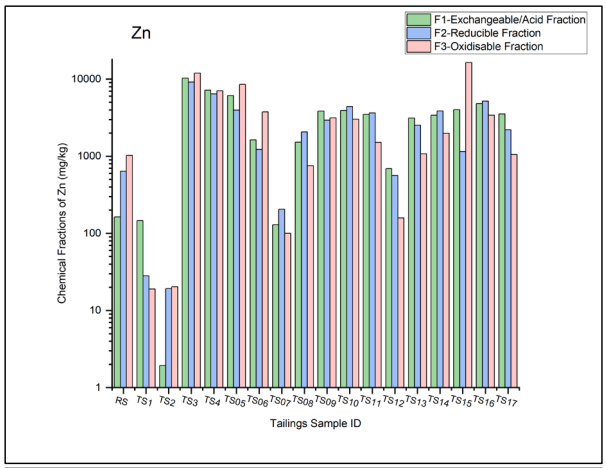
Zn
F1-Exchangeable/Acid Fraction
F2-Reducible Fraction
F3-Oxidisable Fraction
Chemical Fractions of Zn (mg/kg)
Tailings Sample ID

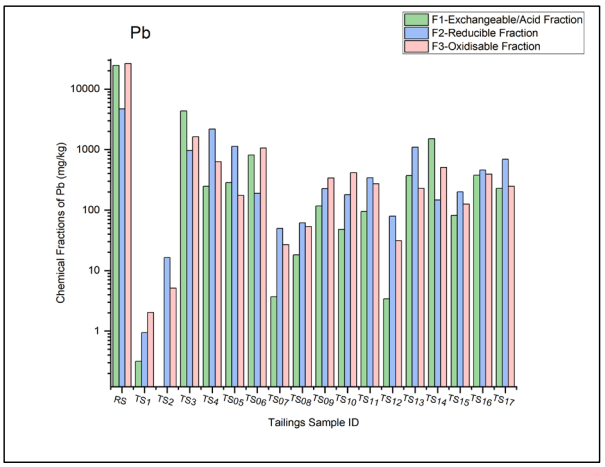
Pb
F1-Exchangeable/Acid Fraction
F2-Reducible Fraction
F3-Oxidisable Fraction
Chemical Fractions of Pb (mg/kg)
Tailings Sample ID

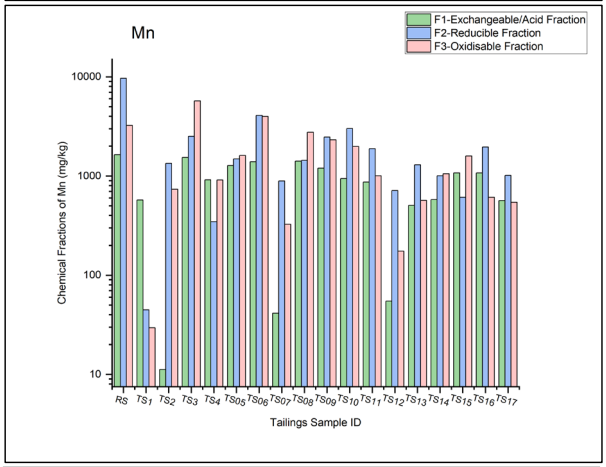
Mn
F1-Exchangeable/Acid Fraction
F2-Reducible Fraction
F3-Oxidisable Fraction
Chemical Fractions of Mn (mg/kg)
Tailings Sample ID

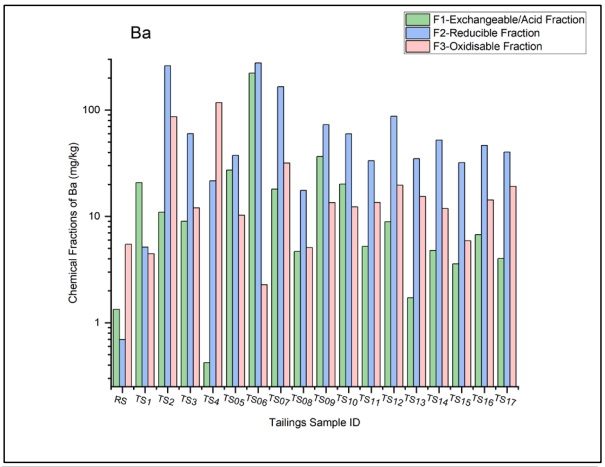
Ba
F1-Exchangeable/Acid Fraction
F2-Reducible Fraction
F3-Oxidisable Fraction
Chemical Fractions of Ba (mg/kg)
Tailings Sample ID

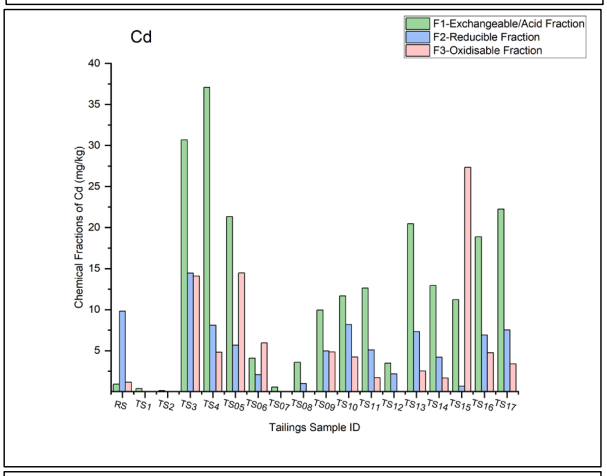
Cd
F1-Exchangeable/Acid Fraction
F2-Reducible Fraction
F3-Oxidisable Fraction
Chemical Fractions of Cd (mg/kg)
Tailings Sample ID

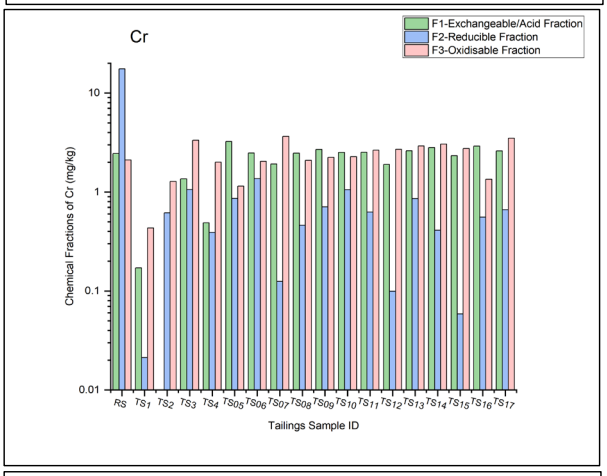
Cr
F1-Exchangeable/Acid Fraction
F2-Reducible Fraction
F3-Oxidisable Fraction
Chemical Fractions of Cr (mg/kg)
Tailings Sample ID

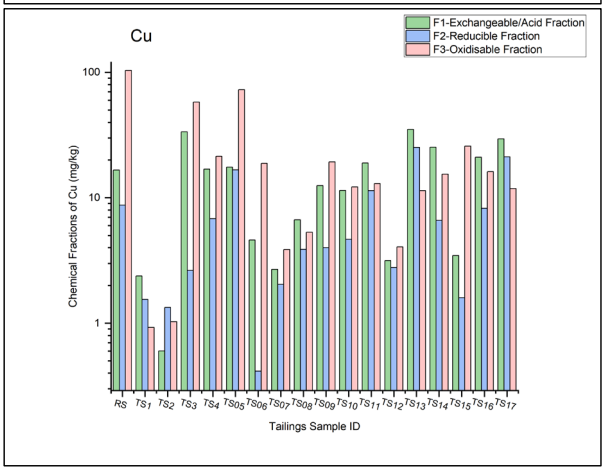
Cu
F1-Exchangeable/Acid Fraction
F2-Reducible Fraction
F3-Oxidisable Fraction
Chemical Fractions of Cu (mg/kg)
Tailings Sample ID

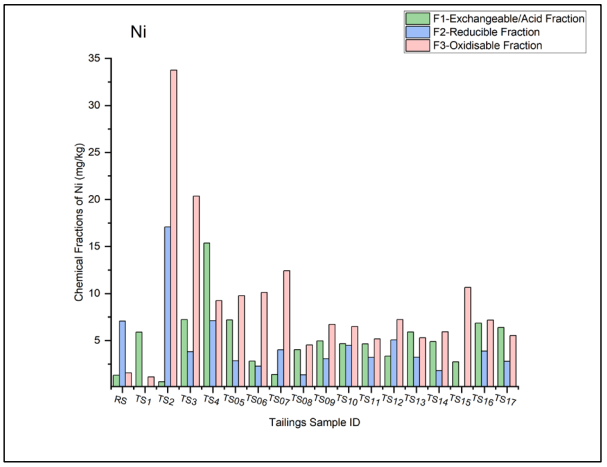
Ni
F1-Exchangeable/Acid Fraction
F2-Reducible Fraction
F3-Oxidisable Fraction
Chemical Fractions of Ni (mg/kg)
Tailings Sample ID

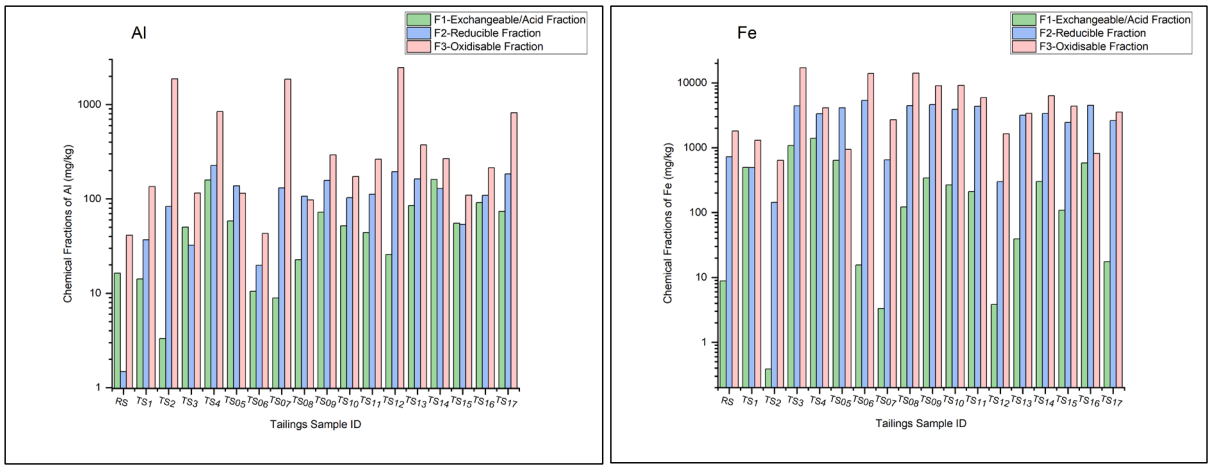

Figure 5.23: Chemical Fractions (F1, F2 and F3) for Mn, Zn, Pb, Cd, Ni, Cu, Cr, Fe, Ba, and Al in the Tailings samples collected at the Gimbi Pb/Zn AML.

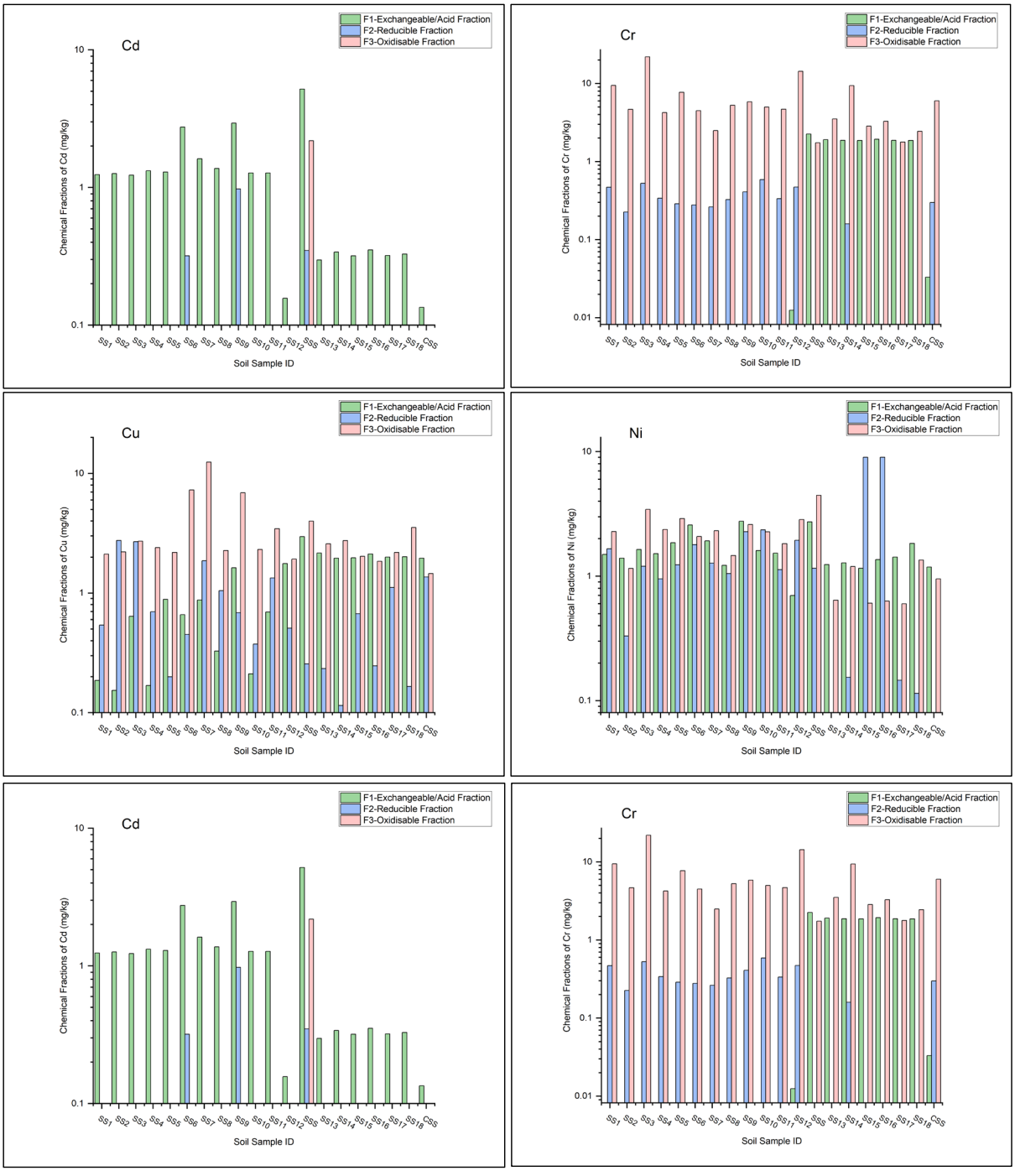

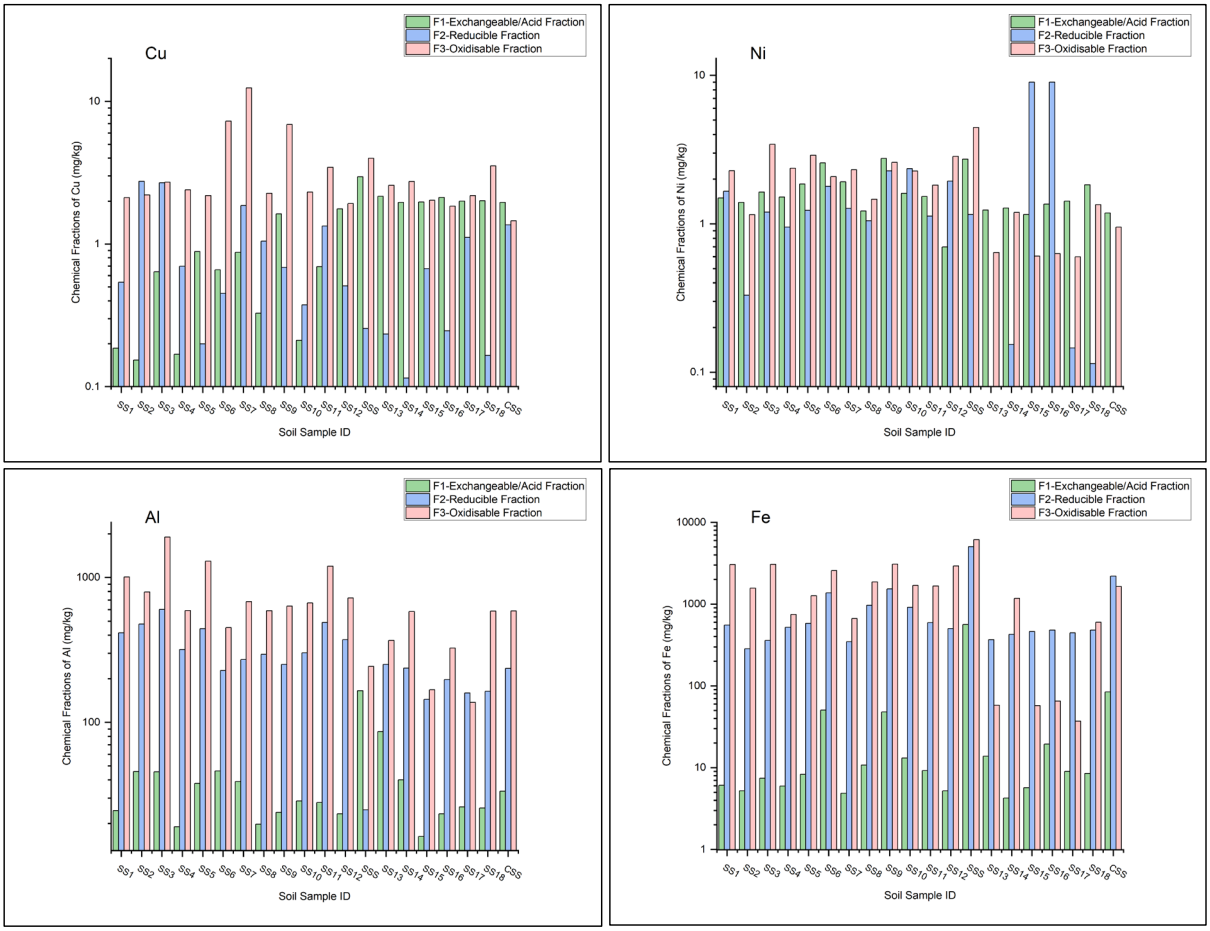

Figure 5.24: Chemical Fractions (F1, F2 and F3 for Mn, Zn, Pb, Cd, Ni, Cu, Cr, Fe, Ba, and Al) in the Soil samples collected at the Gimbi Pb/Zn AML.

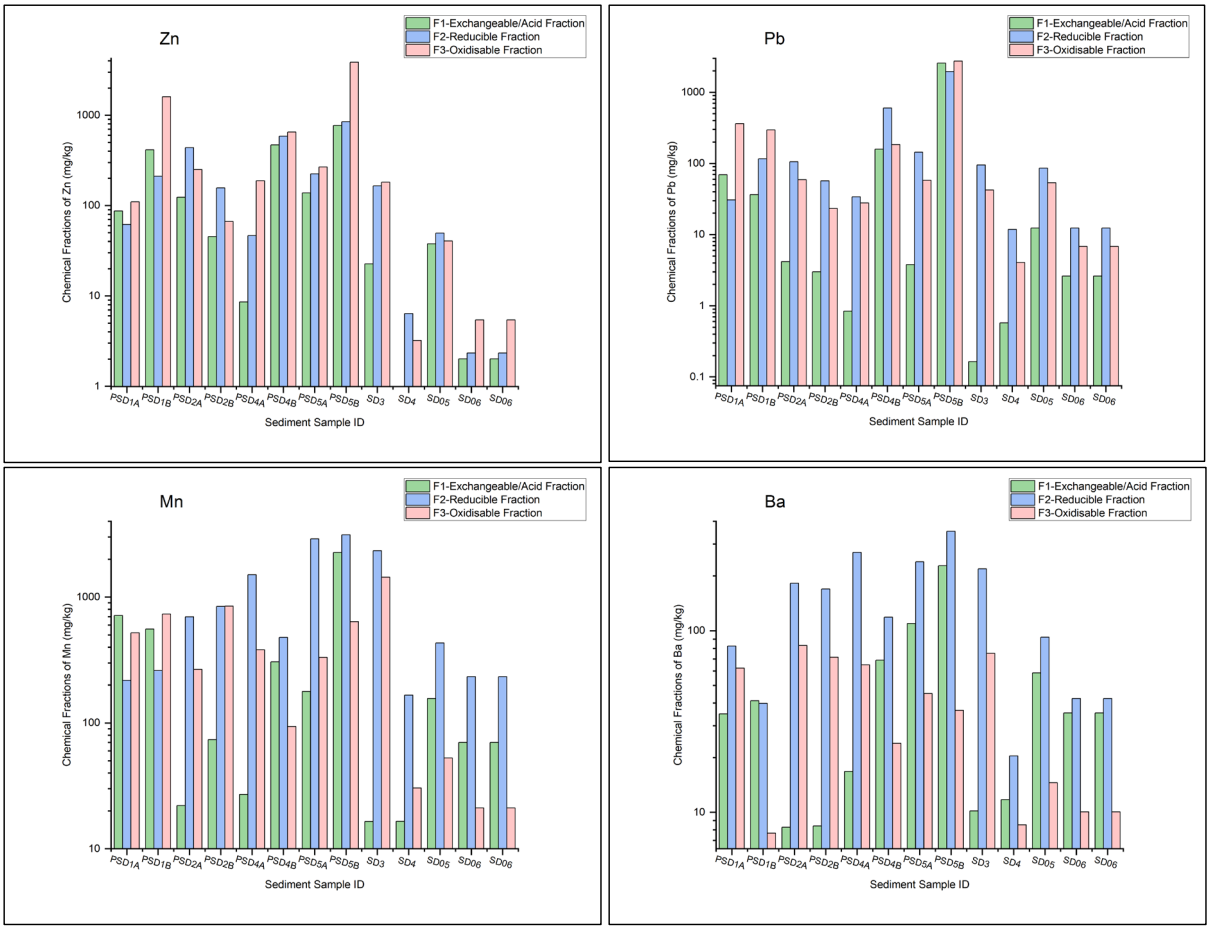

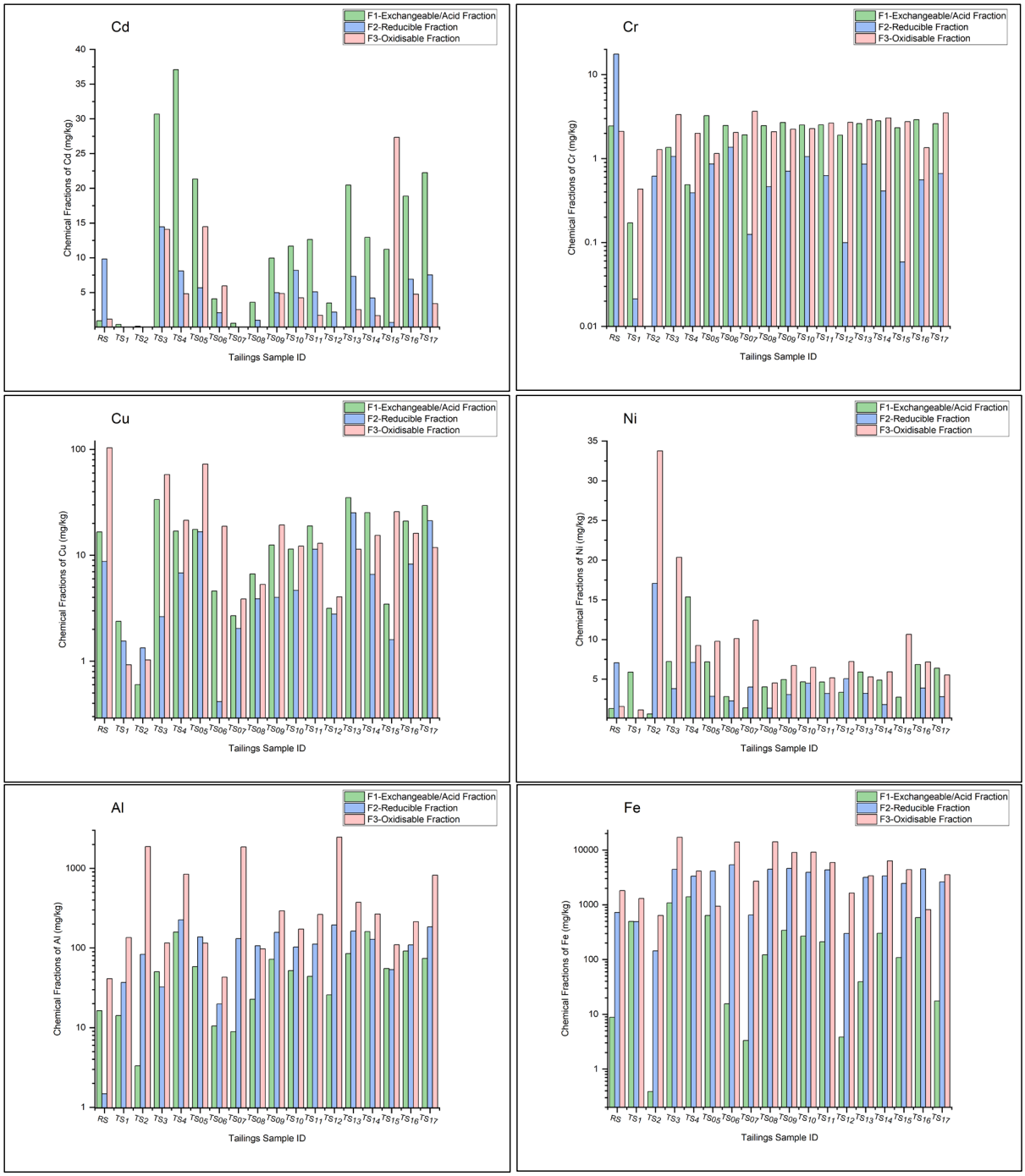

Figure 5.25: Chemical fractions F1, F2 and F3 for Mn, Zn, Pb, Cd, Ni, Cu, Cr, Fe, Ba, and Al in the Sediment samples collected at the Gimbi Pb/Zn AML.

In the sediment samples (Figure 5.25), the metal partitioning showed intermediate patterns between tailings and soils. Zinc was widely distributed across F1 to F3, with F2 and F3 generally dominant but substantial amounts still present in F1, suggesting both mobility and partial stabilisation. Compared to soils, Pb occurred mainly in F2 and F3, with smaller but consistent proportions in F1, indicating stronger reducible and oxidisable associations. In F2, Mn was strongly dominated, consistent with its association with Fe/Mn oxides, but with higher F1 contributions than in soils. Barium was also predominantly reducible, though substantial shares in F1 and F3 indicated intermediate stability. Concentration of Cd occurred mainly in F1, with enrichment in a few samples, confirming its strong lability in sediments, as in tailings and soils. Meanwhile, Cr occurred overwhelmingly in F3, pointing to its stabilisation in

mineral-bound or organic/sulfidic phases, whereas Cu was partitioned across all three fractions, with F3 consistently dominant, indicating strong mineral or organic associations with moderate mobility. A balanced distribution of Ni was observed across fractions, with a recurring tendency toward F3, similar to that in soils. As expected, Al and Fe were overwhelmingly concentrated in F3, reflecting their incorporation in aluminosilicate and Fe-oxide mineral phases, with minor contributions in F1 and F2.

Sediment samples generally displayed a higher reducible fraction for Pb, Mn, and Ba than soils, but less evenly distributed patterns than tailings. This suggests sediments serve as both a sink and a potential secondary source of metals, particularly under changing redox conditions.

Gimbi Rikaya AML Site

The speciation analysis for Gimbi Rikaya revealed a distinct pattern of metal partitioning across the soils, sediments, and tailings samples (Figure 5.26). A broad distribution of Zn was seen among the three fractions; however, sediment exhibited markedly higher concentrations with a pronounced dominance in the F2 phase, suggesting a strong association with Fe/Mn oxides, although the SD2P sediment sample was F1 up to (8261 mg/kg), this sample was collected from a dry mine pond, indicative of it bioavailability potential in the event of precipitation. In soil samples, Zn was more evenly distributed between the F1 and F2 fractions, indicating greater relative mobility in this medium. In F2 and F3 fractions across all sample types, Pb consistently dominated, with the highest concentrations occurring in tailings (TS2, 735 mg/kg) and sediment (SD2P, 759 mg/kg). Most of the soil samples contained lower levels of exchangeable Pb, pointing to limited immediate mobility but persistent binding to Fe/Mn oxide phases.

Manganese was dominantly associated with the F2, with sediments showing the highest concentrations (4373 mg/kg). This distribution reflects strong binding to Fe/Mn oxides, suggesting a susceptibility to release under reducing conditions rather than immediate mobility from F1 pools. Similarly, Ba was largely associated with the F2, with soil samples showing the highest concentrations (up to 277 mg/kg), with a relatively even distribution of F1. The sediments were more of F1 and F2, indicating potential mobility under favourable conditions. By contrast, Cd was overwhelmingly concentrated in the F1, with very low levels in soils and tailings, but with striking enrichment in one of the sediment samples, where concentrations exceeded 10 mg/kg, while the others were 0 mg/kg. This highlights its strong mobility and potential bioavailability. Chromium partitioned predominantly into the F3, especially in the soil samples, although all occurred at very low levels, indicating an affinity for organic matter and sulphide phases. Sediments also exhibited this trend, albeit at higher concentrations.

Copper and Ni were both dominant in the F3, particularly in soil samples, though at very low concentrations. Sediment samples contained higher concentrations up to 17 mg/kg for Cu and 6 mg/kg for Ni, but displayed comparable fractionation patterns, especially for Cu. On the other hand, Ni was

comparable with the F2, indicating potential mobility given favourable conditions. Aluminium and Fe were overwhelmingly concentrated in the F2 and F3 fractions across all media, with smaller contributions from the F1 fraction. Their distribution was broadly consistent across all media at elevated concentrations, although concentrations were notably higher in sediments, up to 3018 mg/kg, and in the F3 fraction, up to 5835 mg/kg.

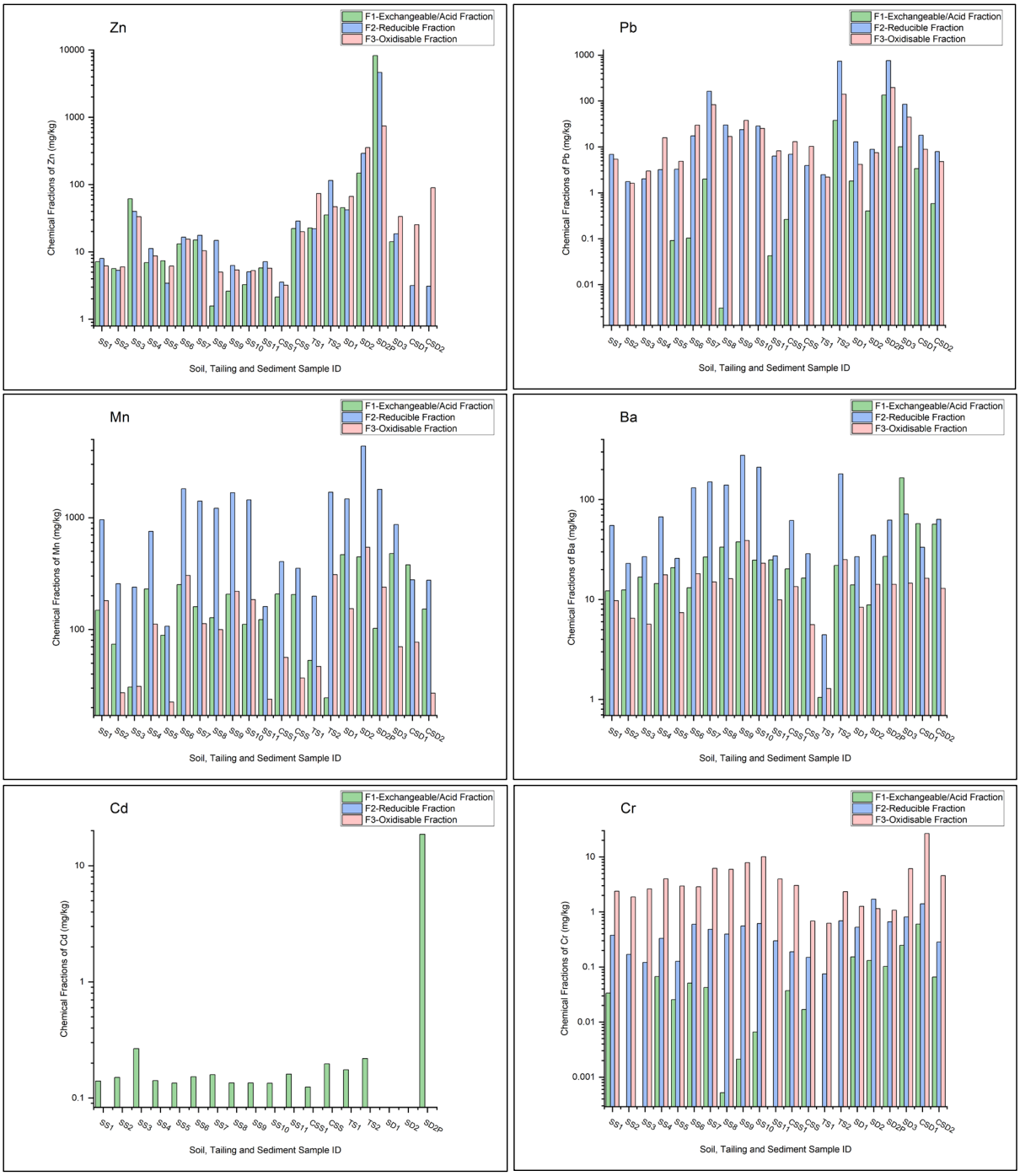

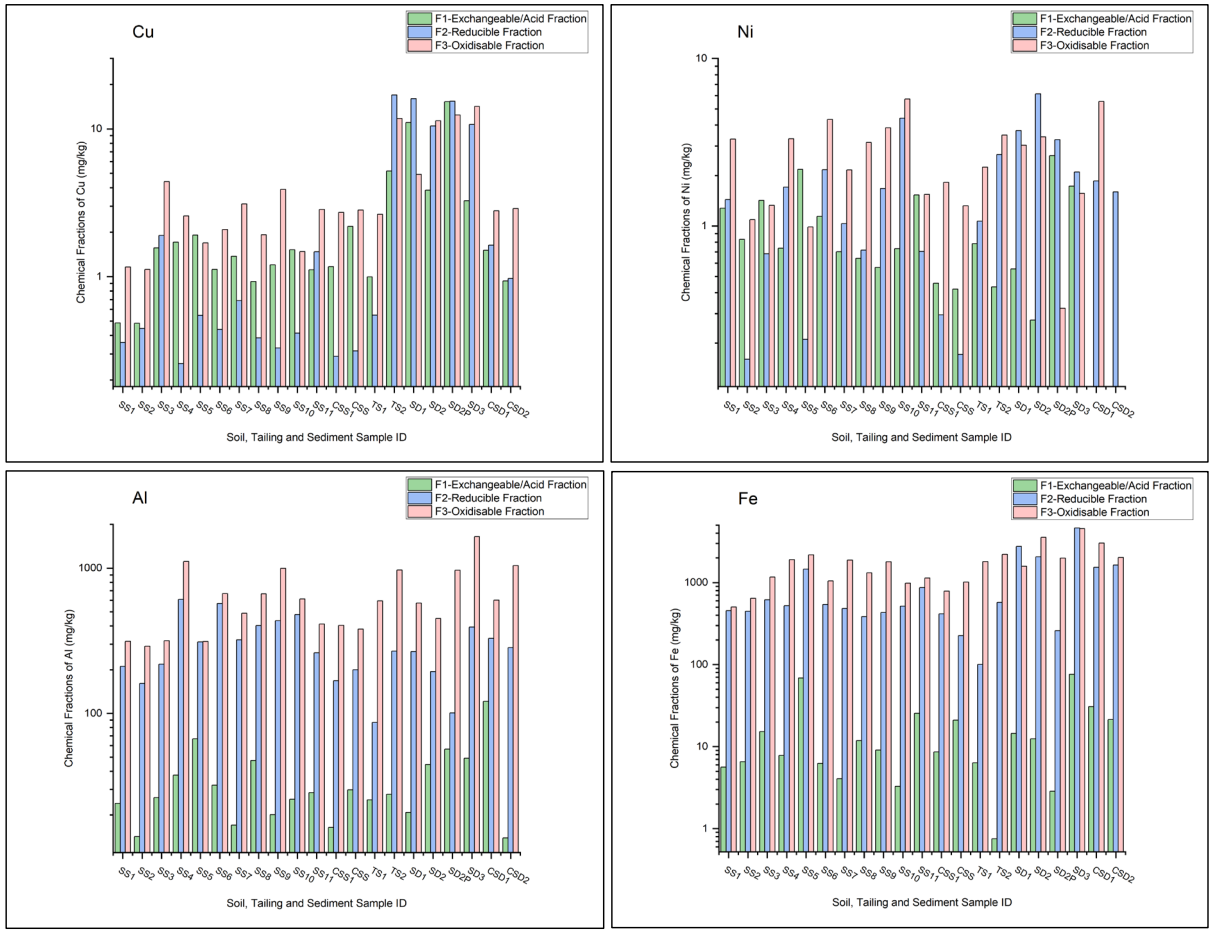

Figure 5.26: Chemical Fractions (F1, F2 and F3) for Mn, Zn, Pb, Cd, Ni, Cu, Cr, Fe, Ba, and Al in the Soil, Tailings and Sediment samples collected at the Gimbi/Rikaya Pb/Zn AML.

5.3.8 Heavy Metal Contamination and Risk Assessment

Enrichment factor

Enrichment patterns varied across the sampled media in Abakaliki, Gimbi, and Gimbi-Rikaya sites (Table 5.17). Control soils generally recorded values close to or below one, consistent with natural background levels, whereas mining-related media showed moderate to extreme enrichment for most metals.

In soil samples, Pb displayed very high to extremely high enrichment, with values of 22.2 in soil, 30.3 in sediment, and 39.8 in tailings at Abakaliki. Cadmium reached extreme levels in tailings (117.9) and remained significant in both soil (5.8) and sediment (6.3). Strong enrichment was recorded for Zn, particularly in tailings (53.7) and sediment (16.9), while soil values were lower but still significant (4.3). Barium showed very high enrichment in sediment (25.8). By contrast, Mn, Cr, Cu, Ni, and Sr generally reflected only minimal to moderate enrichment.

For the Gimbi site, the strongest enrichment was recorded in tailings, especially for Zn (96.9), Cd (111.6), and Pb (38.8), corresponding to very high to extreme levels. In soils, enrichment was significant for Zn (8.0) and Cd (4.0), while Pb was only moderate (3.1). Sediments were enriched in Zn (10.7) and

Pb (6.8), both within the significant range, whereas Ba was exceptionally enriched (164.4). Other metals, including Mn, Cu, Ni, and Cr, remained within minimal to moderate levels. Control soils consistently showed values below one, confirming background conditions.

Minimal enrichments were observed in Gimbi-Rikaya, with only Mn (2.5) and Zn (1.9) in soils showing enrichment. Sediments, however, showed very high enrichment in Pb (24.0), significant levels of Cd (7.0), and extreme enrichment in Zr (64.7). Tailings were strongly enriched in Zn (15.5) and moderately enriched in Pb (8.1) and Mn (2.7), while Cd was absent (≈0).

Across all three sites, Pb, Zn, and Cd consistently displayed the greatest enrichment, particularly in tailings and sediments, (Cd>Zn>Pb) were highest in tailings at Abakaliki and Gimbi, followed by sediment (Pb>Ba>Zn>Cd) in Abakaliki and (Ba>Zn> Pb>Al>Mn>Cr>Ni>Cd) at Gimbi, highlighting their strong association with mining activities. In contrast, Ti, Sr, Ce, and Al generally reflected negligible or background levels, except for anomalously high Zr in Gimbi-Rikaya control soils, which likely reflects lithological variations rather than mining influence.

Table 5.17: Mean Enrichment factor across soil, sediment tailings, and control soil samples at Abakaliki, Gimbi, and Gimbi Rikaya AMLs

Media/Pollutant	*Mn*	*Pb*	*Zn*	*Cr*	*Cu*	*Ba*	*Ce*	*Ti*	*Sr*	*Ni*	*Zr*	*Cd*	*Al*
Abakaliki - EF													
Tailing (n =18)	0.5	39.8	53.7	0.7	1.8	0	0.1	0	0.1	1.3	0	117.9	0.2
Soil (n =12)	1.3	22.2	4.3	1.6	0.7	0	0.3	0	0.1	0.5	0	5.8	0.2
Sediment (n =3)	0.39	30.3	16.87	1.54	0.8	25.84	0.08	0	0.16	1.59	0	6.3	1.51
Control Soil (2)	0.9	1.7	0.9	0.9	0.7	0.1	0.3	0	0.1	0.7	0	0	0.2
Gimbi - EF													
Tailing (n =17)	7	38.8	96.9	0.2	2.8	0.1	0.1	0	0.2	1.1	0	111.6	0.1
Soil (n =19)	1.5	3.1	8	1.1	0.5	0.1	0	0	0.1	0.4	0	4	0.1
Sediment (n =12)	2.26	6.77	10.72	1.49	0.93	164.38	0.44	0.03	0.78	1.32	0.01	0.66	3.28
Control Soil (2)	0.4	0.3	0.1	0.6	0.3	0.1	0.3	0	0	0	0	0	0.1
Gimbi-Rikaya - EF													
Tailing (n =2)	2.7	8.1	15.5	0.9	0.3	3.2	0	0	0.5	0.1	0.1	0	0.2
Soil (n =11)	2.5	0.9	1.9	0.5	0.6	0.5	0	0	0.7	0.1	0.2	0.1	0.1
Sediment (n =4)	2.3	24	6.4	0.8	0.4	0.9	0	0	0	0.3	64.7	7	0.1
Control Soil (2)	1.9	1.1	1.9	0.4	0.6	0	0.1	0.4	0.1	0.3	0	0	0.1

Geo-accumulation Index (Igeo)

Geoaccumulation values (Table 5:18) varied across all sample media at the studied sites, with background soils generally reflecting unpolluted conditions, whereas mine tailings showed enrichment ranging from moderate to extreme. Negative Igeo values indicate uncontaminated conditions and occur when measured concentrations are lower than 1.5 times the geochemical background concentration.

The highest contamination was observed for Pb at the Abakaliki site, reaching the extremely polluted class in soils (5.1), sediments (5.3), and tailings (5.5). A similar trend was observed in Zn, ranging from moderately polluted in soil (2.7) to extremely polluted in tailings (6.0). Whereas Cd was particularly

elevated, attaining strongly to very strongly polluted levels in soil (3.8) and sediment (3.1), and rising to extreme pollution in tailings (7.1). Unpolluted to moderately polluted (1.0–1.3) were generally seen in Cr and Mn, while Cu, Sr, Ce, Ti, and Al remained in the unpolluted range. A contrasting pattern was observed in Ba, with sediments strongly polluted (5.1) but unpolluted in tailings and soil samples.

Tailings were most impacted in Gimbi, with Zn (6.7), Pb (5.4), and Cd (6.9) classified as extremely polluted. Mn in tailings (3.0) was strongly polluted, while Cu (1.6) indicated moderate enrichment. Soils showed more moderate impacts, with Zn (2.8) at moderately to strongly polluted levels and Cd (1.8) at moderately polluted levels. Sediments showed diverse contamination, with Zn (3.3) and Pb (2.6) in the moderately to strongly polluted category, and Ba exceptionally elevated (7.2), placing it in the extremely polluted range. Most other elements, including Cr, Ni, Sr, and Al, remained unpolluted to moderately polluted.

Across Gimbi-Rikaya, soils largely indicated background or minimal enrichment, with Mn (0.9) and Zn (0.5) classified as unpolluted to moderately polluted. Sediments revealed more severe impacts: Pb (4.7) and Zr (6.2) were within the strongly to extremely polluted range, while Mn (1.4) and Zn (2.8) indicated moderate to strong pollution. Tailings also showed moderate impacts, with Pb (2.6) and Zn (3.5) in the moderately to strongly polluted category. Other metals, such as Cu, Ni, Cr, Ce, and Ti, consistently remained in the unpolluted range across this site.

Overall, tailings and sediments exhibit the most severe accumulation across the three mining districts, with Pb, Zn, and Cd emerging as the dominant contaminants. Ba was notable at the Gimbi sediments, while Zr stood out in the Gimbi-Rikaya sediments. In contrast, elements such as Ti, Sr, Ce, and Al generally indicated background conditions, reinforcing the selective influence of mining activity on specific metals.

Table 5.18: Mean Geo-accumulation Index across soil, sediment tailings, and control soil samples at Abakaliki, Gimbi, and Gimbi Rikaya AMLs

Media/Pollutant	*Mn*	*Pb*	*Zn*	*Cr*	*Cu*	*Ba*	*Ce*	*Ti*	*Sr*	*Ni*	*Zr*	*Cd*	*Al*	*Fe*
						Abakaliki - Igeo								
Tailing (n =18)	-0.8	5.5	6	-0.4	1.1	-4.3	-3.4	-9	-3.8	0.6	-6.7	7.1	-2	0.2
Soil (n =12)	1	5.1	2.7	1.3	0.1	-4.4	-1.4	-6.9	-3.7	-0.6	-5.9	3.8	-2.1	0.9
Sediment (n =3)	-1	5.3	4.5	1	0.1	5.1	-3.3	-8.9	-2.2	1.1	0	3.1	1	0.4
Control Soil (2)	0	1	0.1	0.1	-0.4	-3.5	-1.6	-7.8	-2.6	-0.2	-4.9	0	-2	0.4
						Gimbi - Igeo								
Tailing (n =17)	3	5.4	6.7	-2	1.6	-2.8	-2.7	-10.7	-1.9	0.3	-6.1	6.9	-3.9	0.1
Soil (n =19)	0.3	1.4	2.8	-0.1	-1.2	-3	-1.7	-6.2	-3.3	-1.6	-5.6	1.8	-3.4	-0.3
Sediment (n =12)	1	2.6	3.3	0.4	-0.2	7.2	-1.3	-8.3	-0.5	0.3	-6.3	-0.7	1.6	-0.1
Control Soil (1)	-1.3	-1.5	-3.3	-0.7	-1.8	-3.7	-1.5	-7	-4.5	0	-5.7	0	-3.6	-1.1
						Gimbi-Rikaya - Igeo								
Tailing (n =2)	1	2.6	3.5	-0.5	-2	1.3	-8.3	-6.7	-1.4	-3.2	-3.3	-3.1	-0.4	0
Soil (n =11)	0.9	-0.6	0.5	-1.5	-1.1	-1.3	-6.6	-6.4	-1	-3.7	-2.8	-3.8	-0.4	0

Sediment (n =4)	1.4	4.7	2.8	-0.1	-1.2	0.1	-8.5	-7.6	-2	-1.6	6.2	0.4	0.1	3
Control Soil (2)	0.5	-0.3	0.5	-1.7	-1.1	-9.9	-2.5	-2.5	-4	-2	-5.3	0	-2.4	0

Contamination Factor and Degree of Contamination

The evaluation of contamination factors (Table 5:19) showed minimal influence in controls but considerable to extreme contamination in mine-impacted soils, sediments, and tailings.

At Abakaliki, Pb was the dominant contaminant, with very high contamination across all media (49.9 in soils, 60.2 in sediments, and 68.9 in tailings). This was followed closely by Cd, reaching 20.4 in soils, 12.5 in sediments, and 206.6 in tailings, all within the very high category. Also, Zn exhibited elevated values, ranging from 9.7 in soils to 93.0 in tailings. By comparison, Mn and Cr were generally in the moderate to considerable range, while Cu, Ni, and Fe remained moderate. The overall degree of contamination was considerable in soils (93.2) and sediments (171.5), and very high in tailings (378.5), in sharp contrast to the control soils (13.9).

A moderate degree of contamination (25.8) was noted for soils in Gimbi, mainly influenced by Zn (10.1) and Cd (5.1), and categorised as considerable. Sediments displayed far higher values, with Ba (225.9) very high and the leading contributor, alongside Pb (9.3), Zn (14.7), and Mn (3.1) in the considerable to very high range. The cumulative index for sediments reached 266.7, confirming a very high degree of contamination. Tailings exhibited the most extreme impacts, with Zn (160.8), Pb (64.4), and Cd (185.3) all in the very high class, resulting in an overall contamination degree of 431.6. Control soils, in contrast, showed negligible contamination (4.2).

Results from Gimbi-Rikaya indicated lower impacts in soils, where most metals were within the low to moderate class, and the overall index reached only 10.0. Sediments, however, revealed very high contamination, driven by Pb (10.7), Zn (39.9), Ba (107.5), and Cd (11.7), resulting in a cumulative value of 181.8. Tailings showed mixed results: Pb (17.4) was very high, Zn (9.1) considerable, and Mn (3.1) considerable, elevating the index to 36.9, which is also within the very high category.

In general, Pb, Zn, and Cd consistently emerged as the most problematic contaminants, particularly in tailings and sediments where values reached extreme levels. Ba was particularly significant in the Gimbi and Gimbi-Rikaya sediments, whereas elements such as Ti, Sr, and Ce remained negligible across all sites.

Table 5.19: Mean Contamination Factor and Degree of Contamination across soil, sediment, tailings, and control soil samples at Abakaliki, Gimbi, and Gimbi Rikaya AMLs

Media/Pollutant	*Mn*	*Pb*	*Zn*	*Cr*	*Cu*	*Ba*	*Ce*	*Ti*	*Sr*	*Ni*	*Zr*	*Cd*	*Al*	*Fe*	Cd=∑CFi
Abakaliki CF and Cd															
Tailing (n =18)	0.9	68.9	93	1.1	3.2	0.1	0.1	0	0.1	2.3	0	206.6	0.4	1.7	378.5

Media/Pollutant	*Mn*	*Pb*	*Zn*	*Cr*	*Cu*	*Ba*	*Ce*	*Ti*	*Sr*	*Ni*	*Zr*	*Cd*	*Al*	*Fe*	Cd=∑CFi
Soil (n =12)	2.9	49.9	9.7	3.7	1.6	0.1	0.6	0	0.1	1	0	20.4	0.4	2.7	93.2
Sediment (n =3)	0.8	60.2	33.5	3.1	1.6	51.3	0.1	0	0.3	3.2	0	12.5	3	2	171.5
Control Soil (n=2)	1.5	3	1.6	1.6	1.1	0.1	0.5	0	0.2	1.3	0.1	0	0.4	2.5	13.9
Gimbi CF and Cd															
Tailing (n =17)	11.6	64.4	160.8	0.4	4.6	0.2	0.2	0	0.4	1.8	0	185.3	0.1	1.7	431.6
Soil (n =19)	1.9	3.9	10.1	1.4	0.7	0.2	0.5	0	0.2	0.5	0	5.1	0.1	1.3	25.8
Sediment (n =12)	3.1	9.3	14.7	2	1.3	225.9	0.6	0	1.1	1.8	0	0.9	4.5	1.4	266.7
Control Soil (n=1)	0.6	0.5	0.2	0.9	0.4	0.1	0.5	0	0.1	0	0	0	0.1	0.7	4.2
Gimbi-Rikaya CF and Cd															
Tailing (n =2)	3.1	17.4	9.1	0.4	3.6	0.2	0.6	0	0.2	1.1	0	0	0.2	1.1	36.9
Soil (n =11)	2.7	2.1	1	0.7	0.6	0.2	0.7	0	0.1	0.5	0	0	0.1	1.1	10
Sediment (n =4)	3.8	10.7	39.9	0.7	1.6	107.5	0.4	0	0.5	1.4	0	11.7	2	1.7	181.8
Control Soil (n=2)	2.1	1.2	2.2	0.5	0.7	0.2	0.5	0	0.3	0.4	0	0	0.1	1	9.2
Control Sediment (n=2)	1.1	1	0.3	4.6	0.4	100.9	0.7	0	0.2	0.8	0	0	3.7	1.4	115.1

Potential Ecological Risk (RI) Assessment

The potential ecological risk (Table 5.20) values varied widely across the study areas, with control samples consistently indicating low risk, whereas mine-affected soils, sediments, and tailings reflected moderate to very high risk.

The dominant contributor was Cd in Abakaliki, with risk values reaching 611.0 in soils, 375.3 in sediments, and an extreme 6198.5 in tailings. Considerable to high risk was observed in Pb, ranging from 249.7 in soils to 344.7 in tailings. Zn showed low to moderate levels in soils (9.7) but rose to 93.0 in tailings, while other metals, such as Mn, Cr, Cu, and Ni, remained within the low category. The overall ecological risk was very high in soils (RI = 894.0), sediments (RI = 791.6), and especially tailings (RI = 6667.0), in contrast to the low value observed in control soils (RI = 33.3).

For Gimbi, soils showed a moderate overall risk (RI = 192.9), driven mainly by Cd (152.5), with other metals contributing at low levels. Sediments reached a considerable risk level (RI = 337.0), with Pb (46.5, moderate), Zn (14.7, low), and Ba (225.9, very high) as the main contributors. Tailings presented extreme contamination, with Cd (5559.5) and Pb (322.0) far exceeding the very high risk threshold, resulting in a composite risk of 6087.2. Control soils (RI = 7.5) confirmed a negligible influence compared to mine-affected matrices.

Within Gimbi-Rikaya, soils showed only low ecological risk (RI = 15.0). Sediments, however, indicated severe impacts, with Cd (1071.4) and Pb (53.5) contributing to a very high composite risk (RI = 1292.3). Tailings showed mixed results, with Pb (87.1, considerable) and Cu (18.2, low to moderate) driving the

risk level, but the total index (RI = 123.6) remained within the moderate class. Control soils (16.8) and control sediments (122.4) indicated low to moderate background levels.

Across all three sites, Cd consistently represented the single largest risk factor, especially in tailings, where values exceeded 5000, placing them in the very high-risk category. Pb was the second most critical element, contributing moderate to considerable risk in all sites. Zn and Ba also presented significant localised impacts, particularly in Gimbi sediments. Other metals, including Mn, Cr, Cu, and Ni, generally remained within the low-risk range, highlighting the selective ecological threat posed by Cd, Pb, and Zn.

Table 5.20: Mean Potential risk index across soil, sediment tailings, and control soil samples at Abakaliki, Gimbi, and Gimbi Rikaya AMLs

Media/Pollutant	*Mn*	*Pb*	*Zn*	*Cr*	*Cu*	*Ba*	*Ni*	*Cd*	RI = ∑ Er_i
				Abakaliki - Er_i					
Tailing (n =18)	0.9	344.7	93	2.3	16	0.1	11.7	6198.5	6667
Soil (n =12)	2.9	249.7	9.7	7.4	8.1	0.1	5.1	611	894
Sediment (n =3)	0.8	300.9	33.5	6.1	8	51.3	15.8	375.3	791.6
Control Soil (n=2)	1.5	14.8	1.6	3.1	5.7	0.1	6.3	0	33.3
				Gimbi - Er_i					
Tailing (n =17)	11.6	322	160.8	0.7	23.2	0.2	9.1	5559.5	6087.2
Soil (n =19)	1.9	19.7	10.1	2.8	3.3	0.2	2.4	152.5	192.9
Sediment (n =12)	3.1	46.5	14.7	4.1	6.4	225.9	9.1	27.2	337
Control Soil (n=1)	0.6	2.6	0.2	1.9	2.2	0.1	0	0	7.5
				Gimbi-Rikaya - Er_i					
Tailing (n =2)	3.1	87.1	9.1	0.8	18.2	0.2	5.3	0	123.6
Soil (n =11)	2.7	2.1	5.1	3.4	0.6	0	1.1	0	15
Sediment (n =2)	3.8	53.5	39.9	1.3	7.9	107.5	7	1071.4	1292.3
Control Soil (n=2)	2.1	6.1	2.2	0.9	3.5	0.2	1.9	0	16.8
Control Sediment (n=2)	1.1	5	0.3	9.1	2	100.9	4.1	0	122.4

Risk Assessment Code (RAC)

The RAC, calculated as the ratio of F1 (exchangeable/carbonate fraction) to the total metal concentration, multiplied by 100, was used to evaluate the potential mobility and ecological risk of trace elements in soils, sediments, and tailings across the three study areas. This approach classifies risk as no, low, medium, high, or very high, depending on the percentage of metals present in the most labile fraction. The detailed distribution of %F1 values for individual elements and media for each site is presented in Tables 5.21-23.

At the Abakaliki site, based on the proportion of metals in the F1, RAC indicates varying degrees of potential mobility across the media. In tailings, most metals fall within the low-to-medium risk range, including Mn (11.9%), Zn (25.2%), Pb (8.1%), Ni (9.1%), and Cu (11.9%). However, Cd (40.2%) and Zr (148.4%) exhibit elevated mobility, placing them in the high-risk to very high-risk categories. Soils

show the highest overall risk profile, with exceptionally high RAC values for Cd (298.5%) and Zr (238.1%), indicating extreme mobility. Pb (37.2%) and Sr (41.9%) also fall within the high-risk range, suggesting substantial environmental availability, while other metals such as Ni (12.7%) and Cu (4.1%) remain in lower-risk classes. Sediments also display significant mobility, particularly for Ti (64.7%), Cd (135.3%), and Zn (48.8%), which fall within the high to very high-risk categories. Other elements, including Mn (23.4%), Ce (20.3%), and Sr (36.4%), indicate moderate mobility, whereas Pb (4.5%) and Cu (6.5%) are less mobile. Reference soils, as expected, show predominantly low-to-moderate risk, with Sr as the only metal reaching the high-risk threshold. Across all media, Cd, Zr, Ti, Zn, and Sr consistently present the greatest mobility concerns, whereas Cr, As, Fe, and Al remain largely immobile.

Gimbi site indicates varying degrees of potential mobility across the media. In tailings, most metals fall within the low-to-medium risk range, including Mn (22.1%), Zn (40.4%), Pb (36.5%), Ni (24.0%), Cu (17.4%), and Ba (27.1%). However, Cd (58.0%) and Ti (67.3%) exhibit elevated mobility, placing them in the high- to very-high-risk categories, while Sr (38.8%) and Zr (30.8%) approach the upper-medium- to high-risk range. Soils show the highest overall risk profile, with exceptionally high RAC values for Cd (107.9%), indicating extreme mobility. Sr (91.3%) also falls within the very high-risk category, while Zn (37.4%), Ni (29.5%), Zr (33.2%), and Ba (35.1%) indicate moderate to high mobility. In contrast, Pb (9.6%) and Cr (5.3%) remain within the low-risk range. Sediments also exhibit significant mobility, particularly for Cd (217.2%), Sr (55.1%), and Ba (40.7%), which fall within the high- to very-high-risk classes. Ti (31.0%) and Zr (25.3%) indicate moderate mobility, while Mn (27.8%) and Zn (27.0%) remain within the medium risk range. Lower mobility is observed for Pb (38.0%)—though relatively elevated compared to other media—and Ni (11.1%) and Cu (18.3%). Reference soils mainly show low to moderate risk, with Sr as the only metal clearly within the very high-risk category. Consistently, in all media, Cd, Zr, Ti, Zn, and Sr present the greatest mobility concerns, whereas Cr, As, Fe, and Al remain largely immobile.

Across the Gimbi/Rikaya site, Sr, Ba, Zn, Cd, Ti, and Zr consistently show elevated RAC values, indicating high potential mobility and environmental risk, particularly in soils and sediments. Strontium (55.1–92.0%), barium (40.7–61.9%), zinc (27.0–40.4%), cadmium (58.0–217.2%), titanium (31.0–67.3%), and zirconium (25.3–33.2%) show persistently high to very high mobility across the different media. Tailings generally reflect moderate mobility, with Mn (22.1%), Ni (24.0%), Cu (17.4%), and Ba (27.1%) falling within the low-to-medium risk range; however, Cd (58.0%) and Ti (67.3%) reach high-risk levels, indicating localised enrichment. Both control soils and control sediments display unexpectedly elevated mobility for Sr (50.7–92.0%), Ba (21.0–61.9%), Mn (12.6–45.7%), and Zr (30.8%), suggesting that the background environment may not be entirely pristine. In contrast, Cr (0.0–5.3%), As (0.0%), Fe (0.0–1.6%), Al (0.2–2.0%), and Pb (2.1–9.6%) remain largely immobile across most media, indicating low environmental availability.

Summarily, Cd consistently emerged as the dominant ecological risk factor across all three sites, particularly in soils, sediments, and tailings, where the proportion in the mobile fraction often exceeded 40%. Also, Zr and Sr showed very high, widespread mobility, while Zn, Pb, and Cu posed medium-to-high risk depending on the medium and site. By contrast, Fe, Al, and Cr generally remained in the no-risk to low-risk categories, indicating limited ecological concern compared with trace metals more directly associated with mining activities.

Table 5.21: Mean Risk Assessment Code (RAC) across soil, sediment tailings, and control soil samples at Abakaliki AMLs

Abakaliki site	Tailing (n=19)	Soil (n=12)	Sediment (n=3)	Reference soil (n=2)
Mn	11.9	9.8	23.4	12.6
Zn	25.2	25.0	48.8	12.7
Pb	8.1	37.2	4.5	2.1
Ni	9.1	12.7	9.8	0.0
Cr	0.0	0.0	0.0	0.0
Cu	11.9	4.1	6.5	7.2
Ti	17.0	9.2	64.7	1.9
Zr	148.4	238.1	0.0	5.7
Ce	6.1	5.0	20.3	1.9
Sr	31.4	41.9	36.4	50.7
Ba	21.2	29.1	14.0	21.0
Cd	40.2	298.5	135.3	0.0
Al	0.3	0.8	0.2	0.3
Fe	0.1	0.1	0.3	0.0
As	0.0	0.0	0.0	0.0

Table 5.22: Mean Risk Assessment Code (RAC) across soil, sediment tailings and control soil samples at Gimbi AMLs

Gimbi site	Tailing (n=18)	Soil (n=20)	Sediment (n=12)	Control/Reference soil (n=1)
Mn	22.1	24.5	27.8	45.7
Zn	40.4	37.4	27.0	30.8
Pb	36.5	9.6	38.0	7.4
Ni	24.0	29.5	11.1	45.3
Cr	18.5	5.3	3.2	0.1
Cu	17.4	15.8	18.3	26.6
Ti	67.3	14.3	31.0	13.4
Zr	30.8	33.2	25.3	13.0
Ce	15.8	10.1	9.3	5.9
Sr	38.8	91.3	55.1	92.0
Ba	27.1	35.1	40.7	61.9
Cd	58.0	107.9	217.2	0.0
Al	2.0	1.0	0.3	0.6
Fe	1.6	0.3	1.3	1.1
As	0.0	0.0	0.0	0.0

Table 5.23: Mean Risk Assessment Code (RAC) across soil, sediment tailings and control soil samples at Gimbi-Rikaya AMLs

Gimbi/Rikaya site	Tailing (n=2)	Soil (n=12)	Sediment (n=4)	Control soil (n=2)	Control Sediment (n=2)
Mn	4.3	23.0	27.1	29.6	60.6
Zn	6.6	23.3	59.3	12.0	0.0
Pb	3.5	0.4	14.4	0.9	10.1
Ni	4.3	26.9	13.5	9.0	0.0
Cr	0.1	0.2	4.1	0.2	0.5
Cu	6.0	14.9	20.6	14.1	13.1
Ti	54.8	14.3	16.7	8.7	0.0
Zr	38.8	31.8	0.0	48.3	0.0
Ce	4.5	2.6	0.7	3.9	4.5
Sr	45.7	91.8	54.2	74.9	48.6
Ba	12.0	30.1	53.5	25.3	82.5
Cd	0.0	0.0	55.2	0.0	0.0
Al	0.3	0.8	1.0	0.5	0.9
Fe	0.0	0.2	0.2	0.1	0.2
As	0.0	0.0	0.0	0.0	0.0

5.4 Discussion

This study set out to evaluate the chemical contamination, fate, and transport of heavy metals in and around Abakaliki and Gimbi Pb/Zn AMLs, with particular emphasis on Pb, Zn, and other trace metals. The assessment began with in-field XRF screening to rapidly identify metals associated with the legacy of lead–zinc mining, which provided an initial indication of contaminant hotspots. Subsequent laboratory analyses of tailings, soils, sediment, and water samples enabled more precise quantification of elemental concentrations and their comparison with regulatory standards, providing insight into the extent of contamination relative to environmental safety thresholds.

The analysis of metal partitioning and speciation further highlighted the fractions most bioavailable to ecological receptors (to avoid overestimating risk based solely on metal content), a critical step for understanding potential risks to both terrestrial and aquatic systems. Together, these form the basis for interpreting the environmental implications of contamination at the sites and for prioritising remediation strategies.

5.4.1 In-situ XRF and Laboratory ICP-OES Metal Concentrations

An initial screening using pXRF was conducted to guide sampling design and identify major elements and heavy metals, particularly given that the site is an abandoned lead-zinc mine where Pb and Zn are expected to be the primary contaminants. However, other contaminants are often associated with AMLs,

making this screening essential for detecting additional contaminants of concern and mapping metal distribution across the site, including hotspots in soil, mine tailings, and waste rock. The pXRF technology is increasingly favoured for in situ screening and rapid identification of contaminant hotspots, allowing for real-time data collection and subsequent confirmation through traditional laboratory analysis (Sikora et al., 2021).

Figure 5.27 shows the box plots comparing heavy metal concentrations in soil and tailings samples from the Abakaliki AML, based on field XRF and laboratory ICP-OES measurements. In the field XRF data, Ti, Pb, and Zn showed the highest concentrations, with Ti exceeding 6,000 mg/kg and several extreme outliers. Other metals such as Mn, Ba, Zr, and Ce were also detected at moderate levels, while elements like Cd, Cu, Ni, and As were present at low concentrations.

In contrast, the ICP-OES results showed extremely high Zn concentrations (up to 14,000 mg/kg), followed by Pb and Mn. Most other metals, including Ce, Ti, and Ba, were present at much lower concentrations. The variation in detection ranges between the two methods highlights differences in sensitivity and precision, with laboratory analysis providing more accurate quantification, particularly at higher concentration ranges (see Tables 5.4 and 5.6).

The pXRF results indicated elevated levels of Ti>Pb>Zn>Mn>Ba>Zr> Ce (see Table 5.4 and Figure 5.8). Elevated Pb and Zn were expected, as the site is an abandoned lead-zinc mine, explaining the high levels of Pb and Zn. However, the ICP-OES analysis showed elevated Zn > Pb > Mn levels in increasing order. The level of Zn was higher than Pb, both exceeding local reference values RSS1 and RSS2 (Table 5.6), while Cr, Cd, Ni, Cu, and Ce remained at background levels, in contrast to the pXRF measurement.

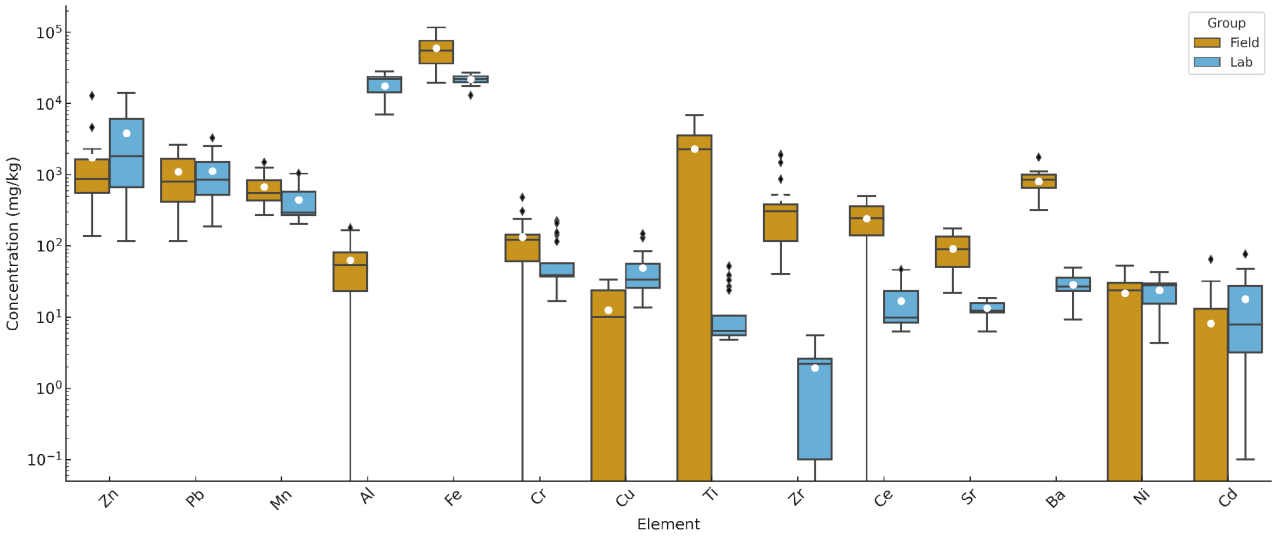

Figure 5.27: Comparison of field and laboratory Heavy Metal concentrations at the Abakaliki site

Linear Regression Analysis

Field XRF and laboratory ICP-OES measurements for Zn, Pb, Mn, Fe, Ti and Ce were compared using linear regression analysis to assess the level of agreement between the two methods (Figure 5.28). The analysis revealed a strong, statistically significant correlation for Mn, with an R^2 of 0.73 and $p < 0.005$, indicating good agreement. Lead also showed a statistically significant relationship ($R^2 = 0.35$, $p < 0.0045$), though the data exhibited considerable scatter, suggesting moderate agreement. In contrast, zinc (Zn) and iron (Fe) did not show significant correlations ($R^2 = 0.3179$, $p<0.8049$) and ($R^2 = 0.2199$, $p<0.9202$), respectively. The Zn plot showed a consistent underestimation of field XRF relative to laboratory values, with most data points falling below the 1:1 reference line. This observation aligns with findings by (Sikora et al., 2021), who also reported that field XRF tends to underreport Zn. Conversely, Mn and Fe were generally overestimated by the field XRF, particularly at lower concentrations.

Similarly, the regression for Ti showed a statistically significant correlation ($R^2 = 0.3254$, $p < 0.0388$), though the relationship was relatively weak. Most laboratory Ti values clustered at low concentrations (<100 mg/kg), whereas field XRF measurements showed a much broader range, from approximately 1,000 to over 7,000 mg/kg. The slope of the regression line (85.005) and the positive intercept (1161.3) suggest a systematic overestimation of Ti by the field XRF method. This overestimation is further highlighted by the consistent deviation of field measurements above the 1:1 reference line. While the statistical significance indicates some level of agreement, the discrepancy in scale and variance between the two methods points to potential challenges in using field XRF for accurate quantification of titanium in this context, although in a related study around an active mine in Abakaliki, where laboratory XRF was used to measure the concentration of Ti in top soil yielded over 5000 mg/kg of Ti (Umeh et al., 2023). Cerium showed a statistically significant ($p<0.007$) and low coefficient of determination ($R^2 = 0.3254$), indicating a weak and unreliable correlation between the two methods. The data spread and the fitted regression line suggest considerable variability and systematic overestimation in the field data. Several environmental and sample-related factors have been reported, including surface irregularities, moisture content, and grain size, etc., to influence field measurements (Jang, 2010; Sahraoui & Hachicha, 2017), especially when compared with laboratory-based analyses.

In this study, the pXRF detection limits for toxic trace elements are known to fall below regulatory concentrations (Gałuszka et al., 2015). The instrument used had a low detection limit of 3 mg/kg, making the pXRF screening results reliable in identifying potential contaminants at the site. Secondly, pXRF in-situ measurements often report lower values compared to laboratory-based methods because studies show that soil samples with moisture contents greater than 20% cause errors in the readings, which leads to underreporting of actual values as X-rays interact with water (Jang, 2010; Sahraoui & Hachicha, 2017; Sikora et al., 2021). This factor could have interfered with the outcome for heavy metals that were under- or over-reported. Lastly, particle size and sample preparation influence the results of XRF readings. The heterogeneity of soil particle sizes in situ contributes to variability in XRF

readings, as finer particles tend to exhibit higher metal concentrations due to their larger surface area and greater sorptive capacity. Therefore, for environmental assessments, soil and sediment samples are typically homogenised, air-dried, and sieved to improve accuracy and consistency in laboratory results (Sikora et al., 2021). The results highlight the limitations of field XRF for certain metals and emphasise the need for calibration or laboratory confirmation when precise quantification is required. While field XRF data are valuable for rapid screening and provide qualitative to semi-quantitative insights, laboratory analyses remain the most reliable means of accurately determining the extent and impact of contamination in the environment.

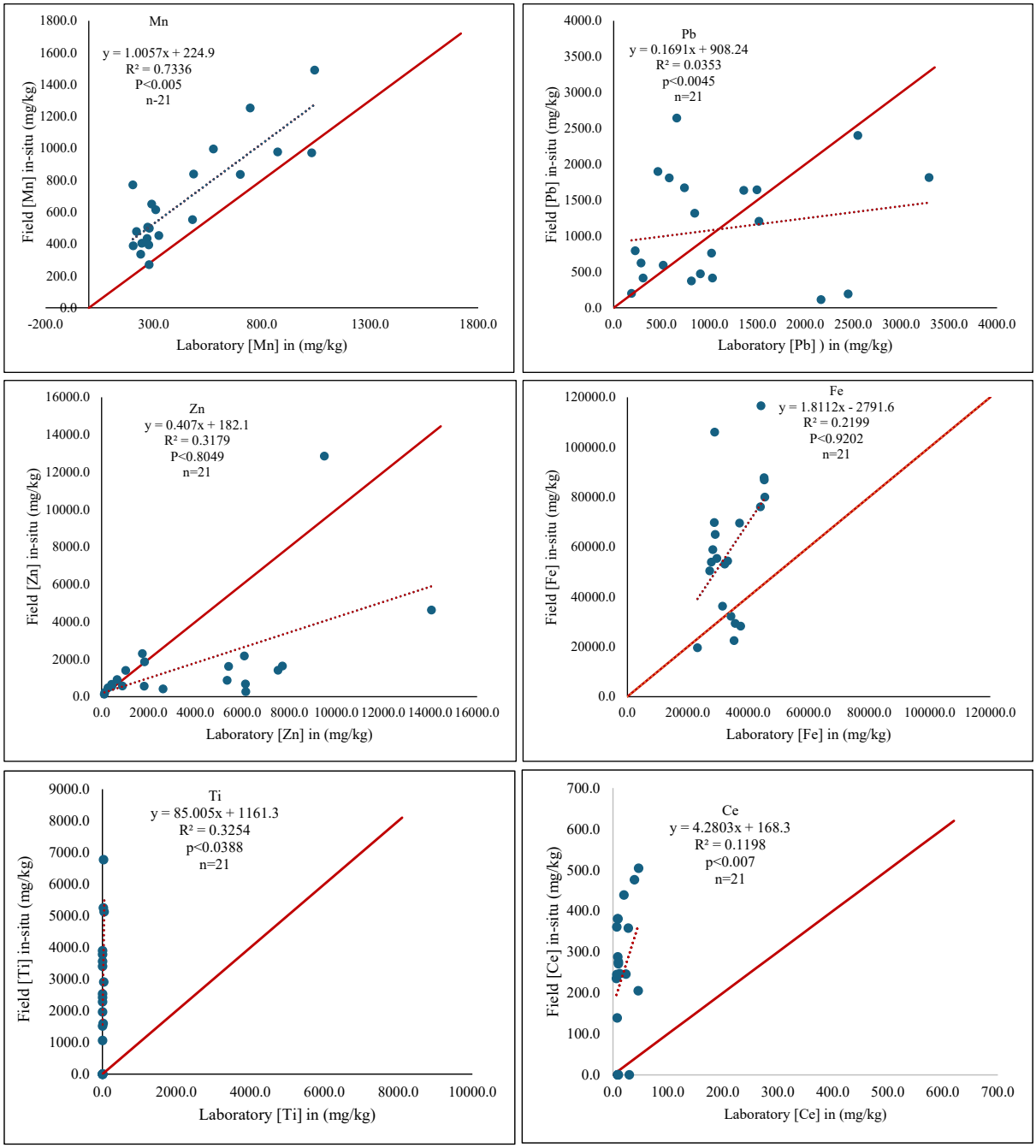

Figure 5.28: Regression of field XRF measurements against laboratory ICP-OES measurements for Zn, Pb, Mn, Fe, Ti and Ce. The estimated relationship (dashed line) and 100% recovery (solid red) are provided.

5.4.2 Evaluation of Metal Concentrations

The elemental concentrations in the water, soil, sediment, and tailings samples are a prerequisite for evaluating the extent of chemical contamination in the selected case studies. The analysis was carried out using ICP-OES, as it is widely used for heavy metal quantification, which provides a better understanding of potential ecological risk (Necula et al., 2021; Oyourou et al., 2019) compared to pXRF.

Analysis of soil, tailings, and sediment samples revealed significant variation in concentrations of potentially toxic elements (PTEs), indicating differential contamination across all media. At the Abakaliki site, soil, tailings, and sediment samples reveal a distinct spatial distribution of heavy metal concentrations: tailings > sediment > soil, with Zn, Pb, and Cd posing the most significant environmental concern. Similar trends were reported by Han around an abandoned Pb–Zn mine (W. Han et al., 2023), where Zn, Pb, and Cd exhibited the highest metal concentrations. While at the Gimbi/Rikaya site, metal concentrations followed a similar gradient across the three media: Tailings > Sediment > Soil, indicating mine-derived contamination. The primary contaminants, in decreasing order, are Zn > Mn > Fe > Pb > Cu > Cr > Ni > Cd. These patterns suggest an ongoing dispersion of metals from tailings (source) through erosion, runoff, sediment transport, and leaching processes into surrounding environments, with sediments acting as secondary sinks for contaminant accumulation (Stanley et al., 2021). The elevated metal concentrations observed in sediments and nearby soils indicate that contaminants are dispersed beyond the immediate mine waste areas and demonstrate the broader environmental footprint of the abandoned mine lands.

Interestingly, we found that soils exhibited the highest concentrations of Al and Fe, which primarily serve as a reflection of their derivation from weathered parent material rich in aluminosilicate and iron-bearing minerals (Nwajide, 2013). On the other hand, sediment samples had notably higher levels of Mg and K, which may reflect selective accumulation from mineral weathering or redistribution via water movement. Calcium and sodium were more variable but reached the highest levels in tailings, more pronounced in Gimbi, possibly due to the original ore mineralogy (Nwajide, 2013).

Broadly, aluminium concentrations were high at the Abakaliki site but low at Gimbi. In contrast, Mg, Ca, Na, and K were more abundant at Gimbi and comparatively depleted at Abakaliki. This geochemical partitioning reflects the contrasting host lithologies of the two mining environments: although both Pb–Zn districts lie within the Benue Trough (Nwajide, 2013), they occur in different segments and stratigraphic units, Wase–Gimbi in the Middle Benue and Abakaliki in the Lower Benue. Abakaliki mineralisation is hosted by the Asu River Group (shales and siltstones), whereas Gimbi is hosted by carbonates with interbedded sandstones and shales (Oha et al., 2017; Yusuf et al., 2022). The geology is illustrated schematically in Figure 5.29. Accordingly, the Abakaliki assemblage is richer in aluminosilicate phases (consistent with elevated Al), while the Gimbi assemblage is dominated by carbonate minerals (consistent with higher Mg, Ca, Na, and K). At Abakaliki, strong weathering of

shales/mudstone outcrop is consistent with the observed geochemical signature; however, collection of fresh Pb/Zn ore samples was not possible because the mine pit was flooded.

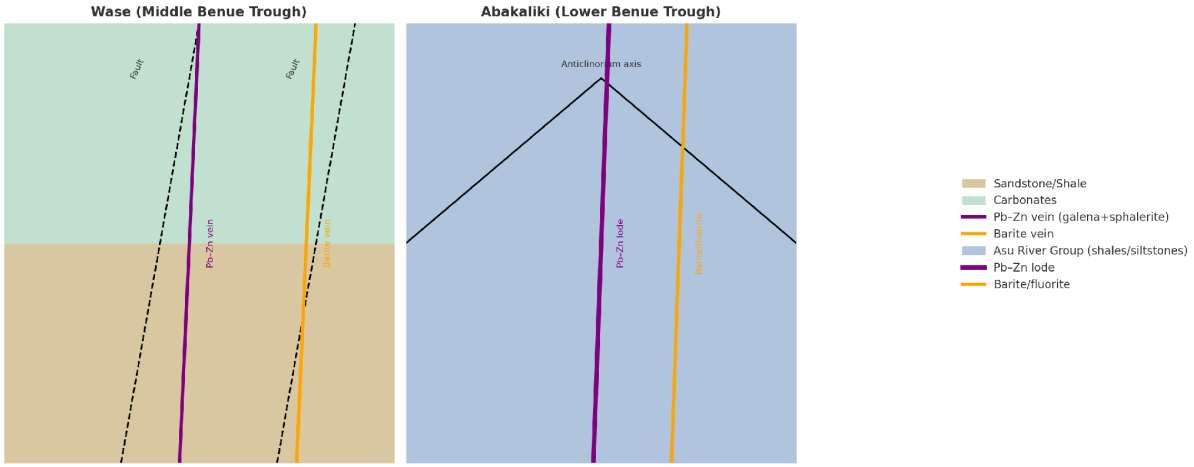

Figure 5.29: Schematic representation of the host rocks of Gimbi and Abakaliki lead-zinc mineralisation

Analysed surface water samples from both sites also showed significant concentrations of heavy metals and major elements. Abakaliki was dominated by Zn, Cd, Pb, and Mn, which indicates substantial anthropogenic contamination linked to the abandoned mine. Wase-Gimbi has lower trace metal concentrations but still shows elevated levels of Zn, Mn, Fe, and major elements. Both sites showed elevated levels of major elements, but the levels were more pronounced at the Gimbi site. This points to intense water–rock interaction, with carbonate and silicate weathering being the likely source.

5.4.3 Comparison with Regulatory Standards and Literature

The concentrations of Pb, Zn, and other metals observed across the study sites exceeded regulatory thresholds, underscoring their potential for adverse ecological impacts. Compared with values reported for other abandoned mine sites, contamination levels at Abakaliki and Gimbi AMLs are consistent with those reported in the literature, reflecting both the influence of local geology and the legacy of mining activities.

Related studies by (Chukwu & Obiora, 2023; Obiora et al., 2019) in active and abandoned Pb–Zn mine sites in southwestern Nigeria reported heavy metal concentrations in agricultural soils with mean values of Pb (1490.71–3515.46 mg/kg), Zn (181.38–1036.11 mg/kg), Mn (1034.69–2747.58 mg/kg), and Cd (4.07 mg/kg). These results show similarities with those obtained in soils around Abakaliki. Likewise, in a study of two derelict Pb mines in Wales (Sartorius, 2023), mean concentrations in sediments were reported as Pb (4080 ± 1160 mg/kg), Cd (4.03 ± 5.17 mg/kg), Zn (2030 ± 2850 mg/kg), and Cu (46.0 ± 11.3 mg/kg). These values are comparable to those obtained in Gimbi-Rikaya sediments, particularly for Zn, and across both sites for Cd and Cu, although Pb was lower than those reported. For water samples, Sartorius reported mean concentrations of Pb (369 ± 186 µg/L), Cd (4.13 ± 4.69 µg/L), Zn (1370 ± 1690 µg/L), and Cu (3.32 ± 2.17 µg/L) (Sartorius, 2023), which were lower than those from

Abakaliki but comparable to values at Gimbi-Rikaya. Similarly, Domingos reported comparable results for mining-impacted sediments in the Philippines (Domingo et al., 2023). Parallel findings have also been documented in other abandoned mine sites, including Zeida, Morocco (Nassiri et al., 2022); Sonoran Desert, Mexico(Del Rio-Salas et al., 2019); Agios Philippos mine in the Kirki region, Greece (Nikolaidis et al., 2010); Indae, South Korea (Chang et al., 2019); and São Pedro da Cova, Portugal (P. Santos et al., 2023), among others.

Threshold comparisons further revealed that the Abakaliki and Gimbi-Rikaya sites most frequently exceeded PEL values for sediments as well as soil and tailings in agricultural and residential parklands, particularly for Zn, Pb, and Cd, indicating a higher ecological risk.

5.4.4 Chemical Contamination Assessment

Given the levels of metal concentrations and exceedances when compared with regulatory standards and literature, we looked at the nature of the rocks that hosted the abandoned lead-zinc mines in the study sites to assess chemical contamination, as geology and geologic structures play a role in the enrichment of metals in the environment (Ciszewski & Aleksander-Kwaterczak, 2020; Kodirov et al., 2018).

The geology of the Abakaliki and Gimbi sites (part of the Wase mining district) in the literature was described in section 5.1.1, highlighting their mineralisation and lithological formations. In the field, we found exposed outcrops which were observed and studied (Figure 5.30D-F). The local geology from the exposed outcrops at Gimbi revealed sedimentary rocks hosting lead-zinc minerals that generally dip southwest. Within the sedimentary sequences, the shales were dark coloured and contained lots of Bivalves associated with carbonates, fitting the description of (Yusuf et al., 2022). The rocks were highly tectonised, with evidence of faults and fractures. Two fracture patterns were observed: vertically, running northwest to southeast, and horizontally, northeast to southwest, crosscutting each other (Figure 5.30D-F), aligning with Yusuf's report on their structural fabric and rock types (Yusuf et al., 2022).

The exposed section at Abakaliki (Figure 5.30A–C) is a very fine-grained, strongly weathered, ferruginous shale/mudrock. It is fissile to locally blocky where weathering has disrupted bedding, with yellow–orange to reddish-brown weathered surfaces, pale-grey fresh breaks, and pervasive iron-oxide staining along fractures and partings. The orange staining indicates iron oxyhydroxides from oxidation of Fe-bearing minerals (and minor pyrite), typical of mine-affected settings, consistent with (Oha et al., 2017).

Bedrock geology provides information about the mineralogy and background values that inform contamination and ongoing enrichment around mining sites (Armiento et al., 2022; John & Leventhal, 2004). Developed regions and countries have established Regional or National Background Levels (NBL) of metals to help monitor contamination. However, there are no NBLs currently established in

Nigeria (Adeyi & Babalola, 2017; Umeh et al., 2023). Hence, we used established values sourced from the literature.

Various approaches have been employed to assess heavy metal contamination factor and degree of contamination using background values, average shale values (Armiento et al., 2022), mean upper continental crust values (Yahyaoui & Ben Amor, 2024), regional background values (Peña-Ortega et al., 2019), urban values and site-specific values, in this study, we used the mean (Buchman, 2008) and upper continental crust values (S. R. Taylor & McLennan, 1985) to evaluate the enrichment factor (using Fe as the reference element), Geo-accumulation index, contamination factor, and degree of contamination.

Figure 5.30: A-F: Exposed outcrops at Abakaliki and Gimbi AMLs showing lithologic units, weathered and tectonically disturbed sedimentary sequences.

Table 5.17 shows the enrichment factors in each sample, with tailings and sediment showing the highest enrichment at Gimbi and Abakaliki. Figure 5.31A shows the enrichment factor across the three sites, with Cd displaying extremely high enrichment followed by very high enrichment of Zn and Pb among the potentially toxic elements, more pronounced in Abakaliki and Gimbi. The geo-accumulation index (Igeo) (Figure 3.31B) also followed a similar trend, with Cd, Pb, Zn, and Mn emerging as the most dominant contaminants across the three sites. The contamination factor and degree of contamination

(Figure 3.31C&D) also showed Cd, Pb and Zn as very high contamination in the Abakaliki and Gimbi sites.

The extremely high enrichment, extreme contamination and high degree of contamination of the potentially toxic elements (Cd, Pb and Zn) in Abakaliki and Gimbi Rikaya sediment is evidence of ongoing transport and deposition of contaminants from the surrounding tailings heaps and particularly an ongoing acid mine drainage, pointing to the strongly acidic pH range of 3.56–3.72 of the water. Although the pond has no visible outlet, the resulting contamination is likely infiltrating the groundwater system.

Tailings are a source of contamination in both Abakaliki and Gimbi, as the AMLs have no outlet for the mine water. While this may be considered an advantage because there is no immediate threat to surface water, it is harmful to groundwater resources. This is particularly so because of the nature of the geology, which contains permeable formations and structures (Fatoye et al., 2014) that favour the movement of contaminants within the study areas. Specifically, the most effective contaminant highways are the fracture/fault–vein corridors and the permeable, carbonate-rich or sandy units; but with clay-rich shales, usually movement is retarded unless they're heavily fractured or weathered, which was the case as the host rock exposures revealed highly fractured and weathered materials.

The lithological and structural characteristics of the sites directly influence contaminant behaviour: fracture and cleavage networks provide preferential flow paths, whereas the clay-rich shale matrix and iron oxyhydroxide coatings act as geochemical sinks that sorb Pb (and to a lesser extent Zn); conversely, carbonate interbeds, and veining can buffer acidity and promote Pb precipitation, while Zn remains relatively mobile under circumneutral conditions (Dzombak & Morel, 1990; Shi et al., 2021). This combination of transmissive structures and reactive media explains spatial variability in contamination at both sites.

The high degree of similarity between dissolved and total concentrations in water samples at the two sites suggests that most metals are present in dissolved ionic or complexed forms rather than adsorbed onto particulates or colloids. The water chemistry in Abakaliki shows low pH and low DOC, which favours metal solubility. Also, there is limited sediment load or particulate matter, which reduces opportunities for metal adsorption or co-precipitation, because water samples collected from stagnant, low-flow, non-draining impoundments allow sustained dissolution of metals without significant sedimentation.

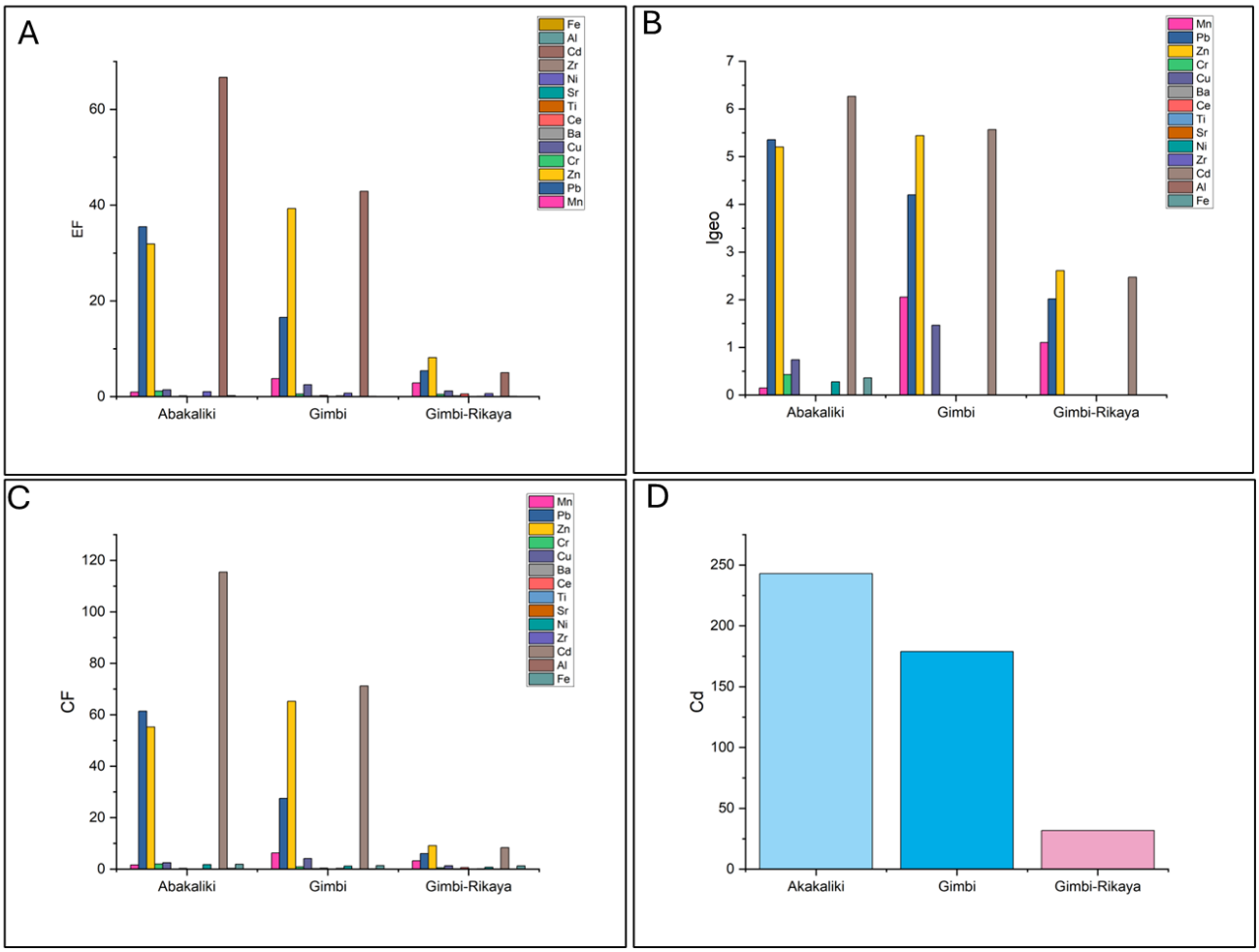

Figure 5.31: Mean enrichment factor (EF), geo-accumulation index (Igeo), contamination factor (Cf), and degree of contamination (Cd) values for soil, sediment, and tailings samples from the Abakaliki, Gimbi, and Gimbi-Rikaya AML sites.

5.4.4.1 Spatial Trends in Contaminant Distribution

Abakaliki exhibited the highest overall contamination levels, followed by Gimbi and Rikaya. Across all three sites, contaminant concentrations generally decreased with increasing distance from mine-related sources, including tailings, mine waste, and mine water discharges. Tailings consistently showed the highest contaminant accumulation, confirming their role as the primary source of contamination within the mine environments.

In Abakaliki, contamination was more strongly associated with soils than with sediments, whereas at Gimbi, sediments generally exhibited greater contaminant accumulation than soils. Sediments collected from mining-impacted ponds at mine sites also showed higher contaminant concentrations than from non-impacted ponds, highlighting the role of hydrological transport and sedimentation in redistributing contaminants. Similarly, borehole water samples used as control water sources consistently exhibited lower contaminant concentrations than mine-impacted water samples.

Although most control samples reflected background conditions, one control sediment sample (SD2) exhibited unexpectedly elevated metal concentrations relative to the mean sediment values. This may indicate localised anthropogenic influence, natural geological enrichment, or wider contaminant dispersion beyond the immediate mine footprint. Furthermore, while some metals displayed widespread spatial distribution across the study areas, others remained more localised, likely reflecting differences in contaminant mobility, geochemical behaviour, and source-specific mineralisation.

5.4.5 Metal Speciation and Bioavailability

Metal Speciation

Metal speciation was conducted to accurately estimate environmental risk. As revealed in the contamination assessment (Table 5.19), the order of contamination is Abakaliki > Gimbi > Gimbi-Rikaya, all of which exhibit a very high degree of contamination, and according to the Hakanson classification, this risk category indicates a serious anthropogenic pollution (Hakanson, 1980). Hence, metal speciation was performed to isolate bioavailable fractions of potentially toxic elements. John and Leventhal noted that, in order to estimate the effects and potential risks associated with contamination from mining or other related industrial activities, it is necessary to identify the fractions of total elemental concentrations in water, soil and sediments (John & Leventhal, 2004).

Metal speciation refers to the distribution of a metal among distinct chemical forms that control its reactivity, mobility, and environmental behaviour. In soils, sediments, and wastes, metals are not uniformly distributed but occur as free ions, inorganic or organic complexes, precipitates, or mineral-bound species, each responding differently to changes in pH, redox potential, and organic matter content (Bao et al., 2016; Chowdhury & Singer, 2023; H. Li & Ji, 2017).

Chemical sequential extraction is used to partition metals into fractions of differing stability. Among the most widely applied protocols are the Tessier sequential extraction scheme (Tessier et al., 1979), which partitions metals into operationally defined fractions (exchangeable, carbonate-bound, Fe–Mn oxide-bound, organic/sulphide-bound, and residual), and the BCR method, developed to harmonise sequential extraction procedures across laboratories in Europe (Quevauviller et al., 1993; Rauret et al., 1999), targeting the acid-soluble fraction (F1), representing metals bound to carbonates and readily mobilised under acidic conditions; the reducible fraction (F2), where metals are associated with Fe and Mn oxides and released when these phases dissolve under reducing conditions; and the oxidisable fraction (F3), encompassing metals bound to organic matter and sulphides, which may be liberated under oxidising environments (Y. Han et al., 2023). Both methods aim to distinguish between the mobile and immobile pools of metals in soils and sediments, thereby providing insight into their potential mobility and bioavailability.

In this study, a modified sequential extraction method was employed, combining elements of the Tessier and BCR procedures and the approach of Bean (see Section 5.3.6). The results presented in Section

5.3.6 highlight the distribution of the F1, F2, and F3 fractions across tailings, soils, and sediments, reflecting the heterogeneous conditions of these environments. Figure 5.32 shows the percentage metal speciation across the three sites. At Abakaliki, F1 contributions were Pb (11–35%), Cd (40–92%), Zn (38–47%), Cu (19–27%), Ni (23–43%) and Mn (8–38%), while F2 fractions of Pb (47–59%), Cd (8%), Zn (13-25%), Cu (21–27%), Ni (23–42%) and Mn (42–81%). At Gimbi, F1 comprised Pb (6–42%), Cd (35–87%), Zn (17-34%), Cu (22–32%), Mn (17–19%) and Ni (14-30%), with F2 again showing Pb (16–53%), Cd (15–37%), Zn (23-39%), Cu (15–37%), Mn (44–70%) and Ni (22-35%), At Gimbi-Rikaya, F1 levels were Pb (4–12%), Cd (100%), Zn (18-58%), Cu (16–29%), Mn (3–12%) and Ni (11-20%), while F2 for Pb (55–80%), Cd (41-100%), Zn (34-44%), Cu (15–46%), Mn (77–81%) and Ni (28–33%).

Across all sites, the most concerning toxic metals in the F1 + F2 fractions were Pb, Cd, Zn, Ni, Cu, and Mn because they exhibited significant percentage partitioning within the exchangeable and reducible fractions, indicating greater potential mobility and bioavailability. Notably, Pb and Cd are of particular concern, as they consistently occur in the F1 fraction, representing the most mobile and bioavailable form as well as ecotoxicologically relevant metals, posing immediate risks to ecological receptors. Furthermore, the dominance of Pb and Cd in the exchangeable fraction suggests high potential for leaching and uptake. In contrast, Cr and Al were largely associated with the oxidisable fraction, indicating lower short-term mobility but possible release under changing redox conditions, thus representing a longer-term risk. This distinction is critical because it shows that not all elevated concentrations translate into ecological risk; instead, risk is determined by the mobility and chemical form of the metal (Gutiérrez et al., 2016).

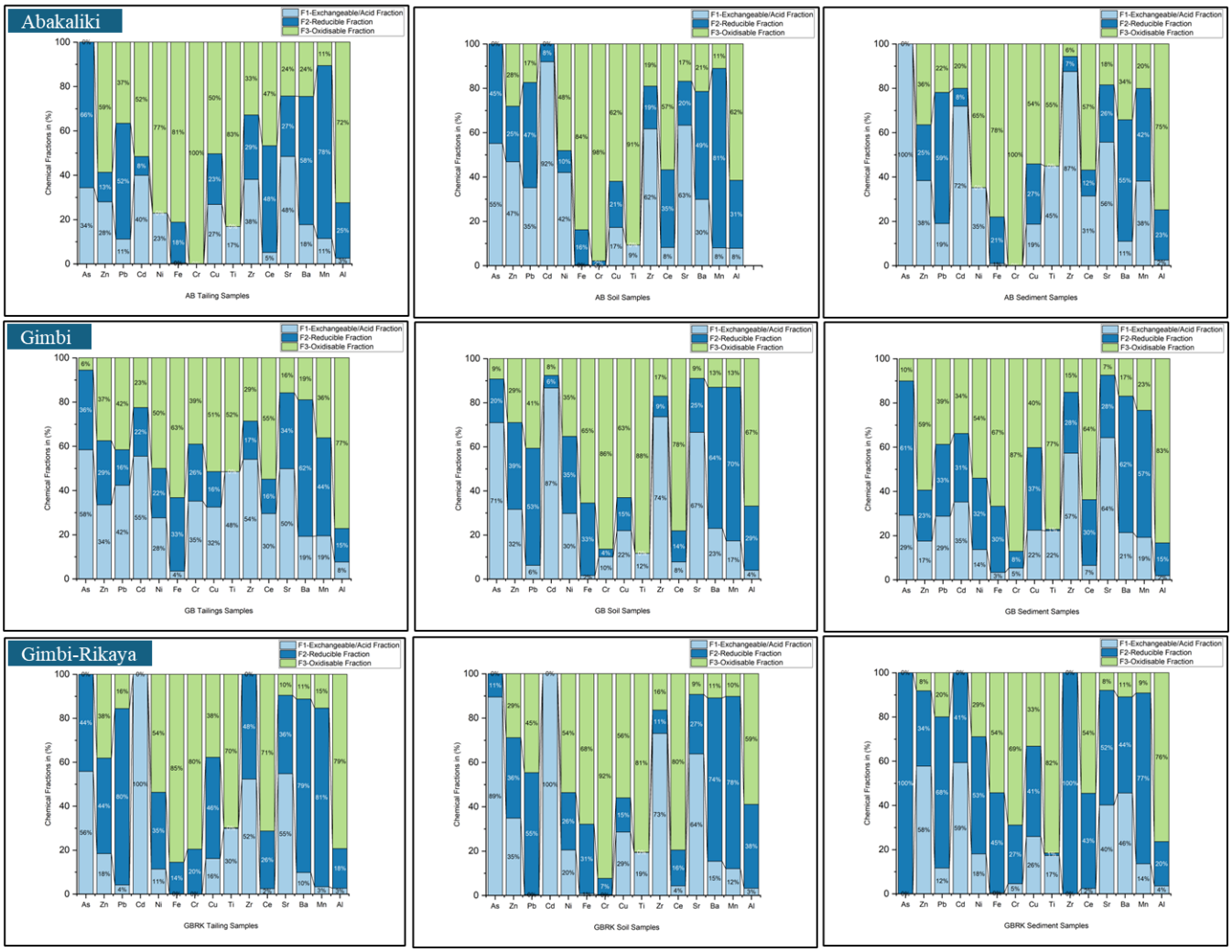

Figure 5.32: Percentage chemical fractions of Pb, As, Zn, Cr, Cu, Cd, Ni, Ba, Mn, Fe, Al, Zr, Sr, Ce, and Ti, Abakaliki, Gimbi and Gimbi-Rikaya AMLs

Bioavailability

Bioavailability represents the fraction of a contaminant that is available for uptake by ecological receptors; in other words, the proportion that is available for incorporation into biota, which is bioaccumulation (Kirk et al., 2004). So, total metal concentration is not equivalent to metal bioavailability; concentration may be high, but it is not readily available for absorption into biota, and effects may be low (John & Leventhal, 2004).

The concept of bioavailability gained prominence as researchers realised that total metal concentrations often overestimate ecological and human health risks (M. Sun et al., 2024). Early contamination assessments assumed that all measured metal content was equally available for uptake; however, evidence soon showed that metals bound within stable mineral matrices (e.g., crystalline sulphides, silicates) are effectively unavailable to organisms (Gutiérrez et al., 2016). Bioavailability-based approaches were developed to address this gap by quantifying the fraction of metals that can dissolve, desorb, or otherwise transfer into biologically accessible forms (Wilson et al., 2023).

Sequential extraction procedures fractionate metals into operationally defined forms or phases (Section 5.4.5) to isolate their geochemical associations, potential mobility, and environmental bioavailability (Filgueiras et al., 2002; Tessier et al., 1979). Although weakly bound fractions may indicate increased potential for remobilisation under changing environmental conditions, they do not necessarily translate directly into true biological bioavailability, because bioavailability is not absolute; only certain chemical forms of metals can be absorbed and assimilated by organisms. In aquatic systems, frameworks such as the Free Ion Activity Model (FIAM) and the Biotic Ligand Model (BLM), among others, are used to predict how dissolved species interact with biotic surfaces (Kirk et al., 2004). The Biotic Ligand Model (BLM) integrates chemical speciation with biological uptake by simulating how dissolved metal species compete with major ions to bind at biological receptor sites. It provides a predictive framework for assessing metal bioavailability and toxicity in aquatic systems under varying water chemistry conditions (Kirk et al., 2004; Rawlins et al., 1998).

Several recent studies of abandoned mine sites illustrate this method in assessing risk. For example, Son (Son et al., 2019) found that $CaCl_2$-extractable fractions of Cu, Mn, and Ni in soils from abandoned Korean metal mines better predicted ecological toxicity in soil invertebrates than total concentrations, underscoring that extractable (bioavailable) pools are the relevant drivers of biological effects. Other case studies highlight how environmental conditions influence bioavailability. In Russian riverine sediments, Ushakova reported (Ushakova et al., 2022) that bioavailability of trace elements was enhanced in finer sediment fractions and under lower pH conditions, which increased solubility and toxicity to aquatic organisms (*Daphnia magna* and algae). Likewise, Zineb showed that the acid-generating potential of sulphide tailings in Algeria directly controlled the mobility and release of potentially toxic metals (PTMs), with seasonal oxidation processes increasing the availability of Zn, Pb, and Cu to the surrounding environments (Zineb et al., 2024).

Our study revealed that at Abakaliki, the F1 fraction in soil contained the highest proportions of Pb (35%), Zn (47%), and Cd (92%), indicating their bioavailability after fractionation (Table 21), although these metals were also readily available in tailings and sediment, but in the reducible form (Figure 5.32). These high proportions in the F1 fractions indicate substantial potential mobility and bioavailability. The proportion of mobile fractions exceeded 35% for Pb, suggesting that the site's geochemical conditions favour the release of metals from solid phases into the surrounding environment.

At Gimbi, however, Pb displayed low mobility in soils, with only about 6% of the total Pb found in F1, whereas Zn (32%) and Cd (87%) were mobile. This suggests that Pb was predominantly associated with Fe–Mn mineral phases, indicating relatively limited mobility under oxidising conditions. However, the redox-sensitive nature of Fe–Mn oxides means that changes in environmental conditions may enhance Pb remobilisation and mobility. The carbonate-rich geology of the Gimbi area likely promotes metal precipitation and adsorption, reducing Pb solubility and mobility. Consequently, while Pb concentrations in tailings are measurable and available, their migration into soils and sediments is minimal.

In the surface water samples studied, most dissolved metal concentrations exceeded the EQS bioavailable guideline values (Table 5.14). However, after applying the Biotic Ligand Model (BLM), with DOC, pH, and hardness as input parameters, the risk evaluation was refined by estimating the bioavailable fraction of these metals to aquatic organisms (Figures 5.33 and 5.34). Strikingly, while BLM-derived bioavailability for Cu, Zn, Pb, Ni, and Mn at Abakaliki confirmed their bioavailability, their concentrations were notably lower than the direct EQS values (Figure 5.14).

In contrast, metals at the Gimbi and Rikaya sites were far less bioavailable, underscoring the importance of site-specific geochemical conditions (such as higher pH, DOC, and increased calcium concentrations indicative of hardness, complexation, etc.) in determining actual exposure risks to aquatic ecosystems. The elevated pH and DOC concentrations (Table 5.4) observed at these sites likely reduced the activity of free dissolved metal ions through complexation and competitive binding processes. These conditions decrease metal bioavailability and consequently reduce potential toxicity to aquatic organisms, consistent with BLM predictions. This suggests that the Gimbi environment may be inherently protective, which is similar to certain UK freshwater systems where elevated total metal concentrations do not necessarily translate to ecological risk due to low bioavailable fractions that remain below EQS thresholds (WFD-UKTAG, 2014).

According to (Peters et al., 2019; Wilson et al., 2023), Tier 1 assessments, based on measured dissolved concentrations and comparisons with thresholds, do not account for bioavailability and may overestimate risk. Tier 2 assessments incorporate bioavailability to evaluate actual risk, while Tier 3 involves a full BLM application to quantify the level of risk for each contaminant. At the Abakaliki site, a Tier 3 assessment would be required due to the elevated bioavailable concentrations; however, this lies beyond the scope of the present study.

Overall, although elevated total metal concentrations indicate contamination, speciation and bioavailability assessments provide a more accurate understanding of ecological risk. The interplay of environmental conditions and metal fractions ultimately governs whether contaminants remain sequestered or become available to biota, and therefore, these factors should be central to risk assessment and management of abandoned mine lands.

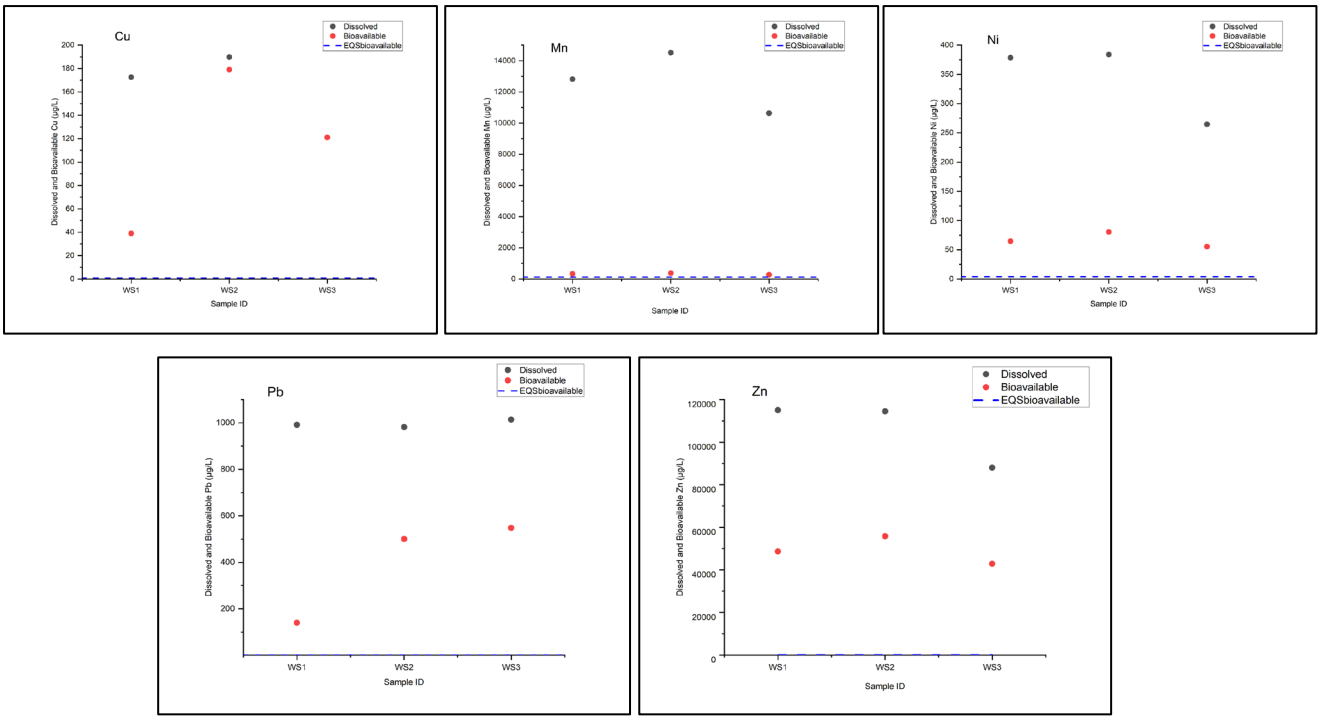

Figure 5.33: Measured dissolved Cu, Pb, Mn, Ni and Zn concentrations (grey) and model-derived bioavailable Cu, Pb, Mn, Ni and Zn concentrations (Red) at Abakaliki Pb/Zn AML Pond. The horizontal dashed blue line indicates the $EQS_{bioavailable}$ for Cu, Pb, Mn, Ni and Zn of 1, 1.2, 123, 4 and 10.9 µg/L, respectively. EQS is Environmental Quality Standard

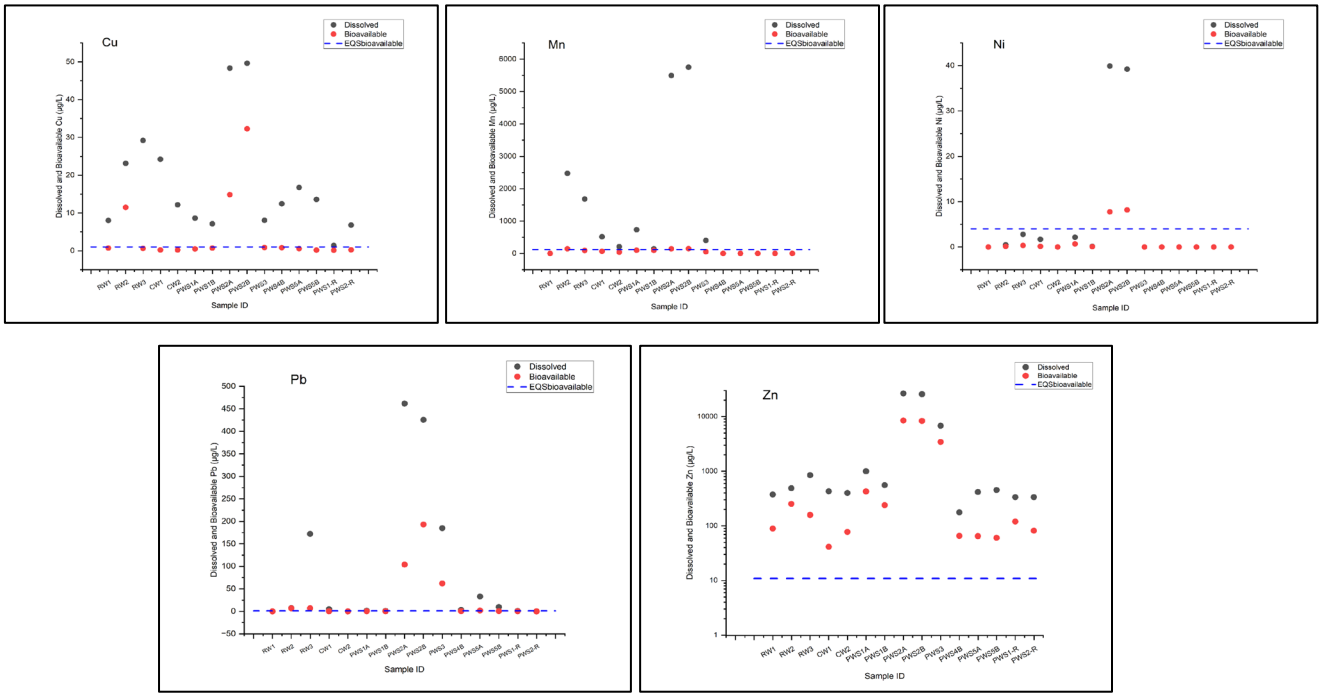

Figure 5.34: Measured dissolved Cu, Pb, Mn, Ni and Zn concentrations (grey) and model-derived bioavailable Cu, Pb, Mn, Ni and Zn concentrations (Red) at Wase-Gimbi Pb/Zn AML. The horizontal dashed blue line indicates the $EQS_{bioavailable}$ for Cu, Pb, Mn, Ni and Zn of 1, 1.2, 123, 4 and 10.9 µg/L, respectively. EQS is Environmental Quality Standard

Bioavailable concentrations (that is, model-derived bioavailable concentrations) were estimated using the BLM/Bio-met model by adjusting dissolved metal concentrations for site-specific water chemistry parameters, including pH, calcium/hardness, and dissolved organic carbon; therefore, these are not directly measured concentrations.

5.4.6 Ecological Risk Assessment

Ecological risk assessment (ERA) is a systematic process for evaluating the potential adverse effects of site-specific contaminants on ecological receptors and ecosystems. It combines site data on source, fate, exposure pathways, and receptor sensitivity to quantify risks and support decision-making (Rattner et al., 2024).

The results of the ecological risk assessment of the pollutants detected in the sampled media across the 3 sites are presented in Table 5.18. Threshold comparison shows that most contaminants exceed the TEL (the concentration below which adverse effects are expected to occur only rarely), while PEL (the concentration above which adverse effects are expected to occur frequently) is exceeded in sediments across the three sites, with Mn, Pb, Zn, and Cd as the most concerning.

The potential ecological risk and risk index for each site (Figure 5.35a and b), following the interpretation of Håkanson's scheme, indicate that the order of risk is Abakaliki > Gimbi > Gimbi–Rikaya, showing very high to considerable ecological risk (Hakanson, 1980). The risk index (RI) ranged from approximately 3,750 at Abakaliki to 2,300 at Gimbi (Figure 5.35b).

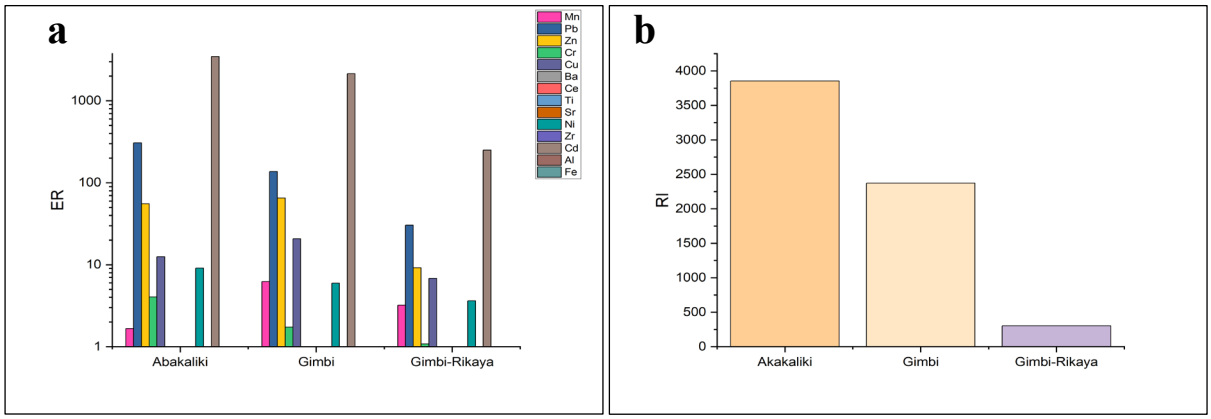

Figure 5.35a and b: ER and RI for Abakaliki, Gimbi and Gimbi-Rikaya sites

In addition to ER and RI, a cumulative pollution risk score (CRS) was applied to provide a more integrative measure of contamination pressure across metals. The CRS results (Figure 5.36) reinforced the patterns observed in ER/RI: Abakaliki and Gimbi recorded the highest scores, reflecting multiple metals contributing to elevated ecological risk, while Gimbi–Rikaya exhibited substantially lower cumulative pressure. The CRS therefore supports the view that risk at Abakaliki and Gimbi is not driven by a single contaminant but by the combined effect of several metals acting through multiple pathways.

These patterns are consistent with findings from mining-impacted environments globally, where Cd, Pb, Zn, and Cu frequently dominate ecological risk; many studies report very high RI values in metal-mining areas, often driven disproportionately by Cd (Custodio et al., 2025; Mensah & Addai, 2024; Ngole-Jeme & Fantke, 2017; W. Xu et al., 2025). The use of integrative indices such as CRS has also been emphasised in recent ecological risk studies for capturing the cumulative burden of multi-metal contamination, as single-index approaches may underrepresent combined pressures (L. Jiang et al., 2021; Yu et al., 2025).

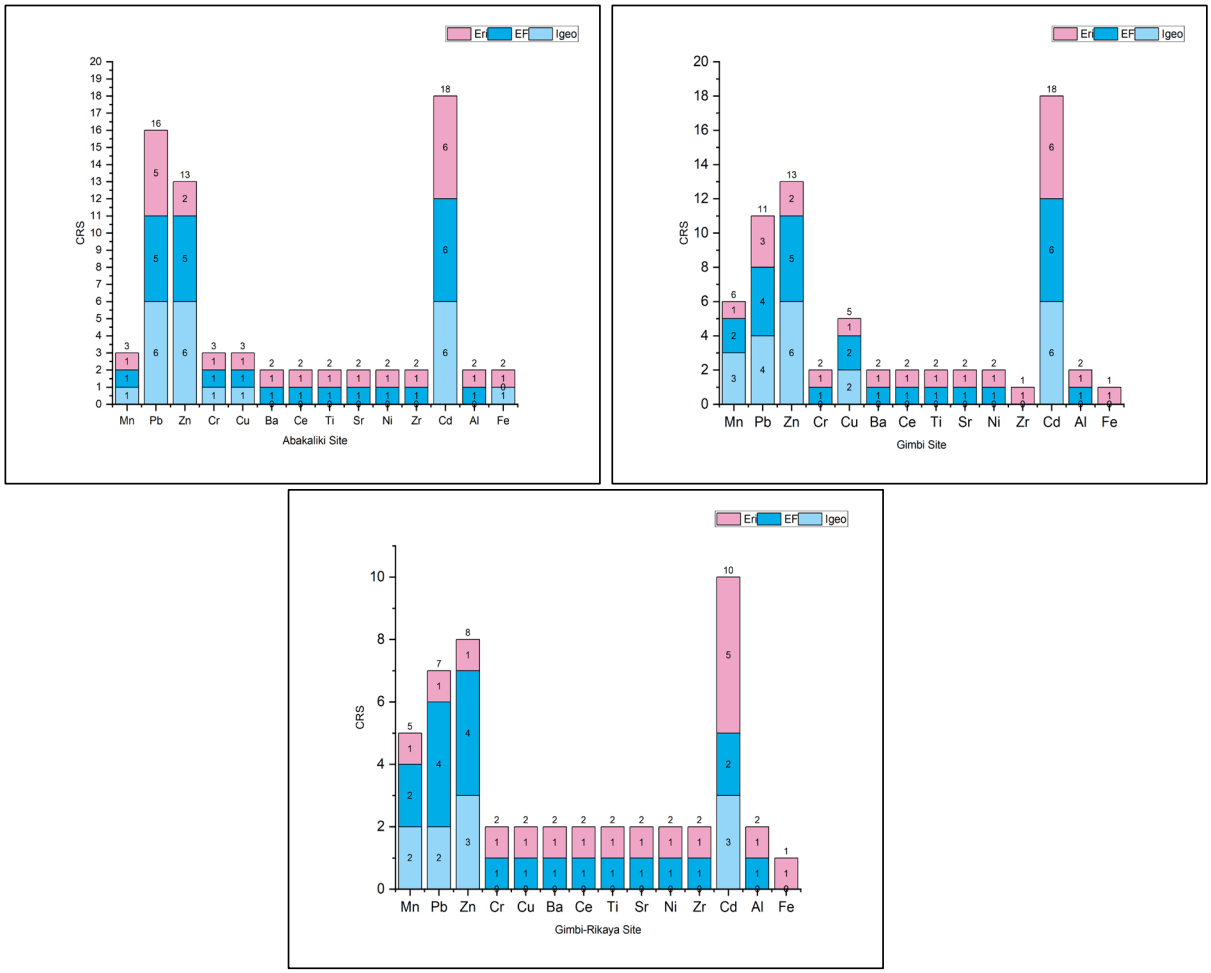

Figure 5.36: Cumulative Risk Score for Abakaliki, Gimbi and Gimbi-Rikaya sites

The conceptual site model (Figure 5.37) illustrates the concurrent operation of soil, sediment, water, and plant pathways, highlighting the complex interactions that govern contaminant transport and exposure at mine-impacted sites. These simultaneous pathways demonstrate how contaminants originating from tailings, waste rock, and mine water can migrate through multiple environmental media via leaching, erosion, runoff, hydrological transport, and root uptake. Such multi-media connectivity strengthens the coupling between sources and receptors, resulting in overlapping exposure routes (ingestion, dermal contact, inhalation, and plant uptake) across terrestrial and domestic animals and aquatic organisms. Consequently, sites exhibiting stronger source–pathway coupling tend to show elevated ecological risk indices (ER/RI) and contamination risk scores (CRS), reflecting the

compounded influence of concurrent transport and exposure mechanisms within the system.

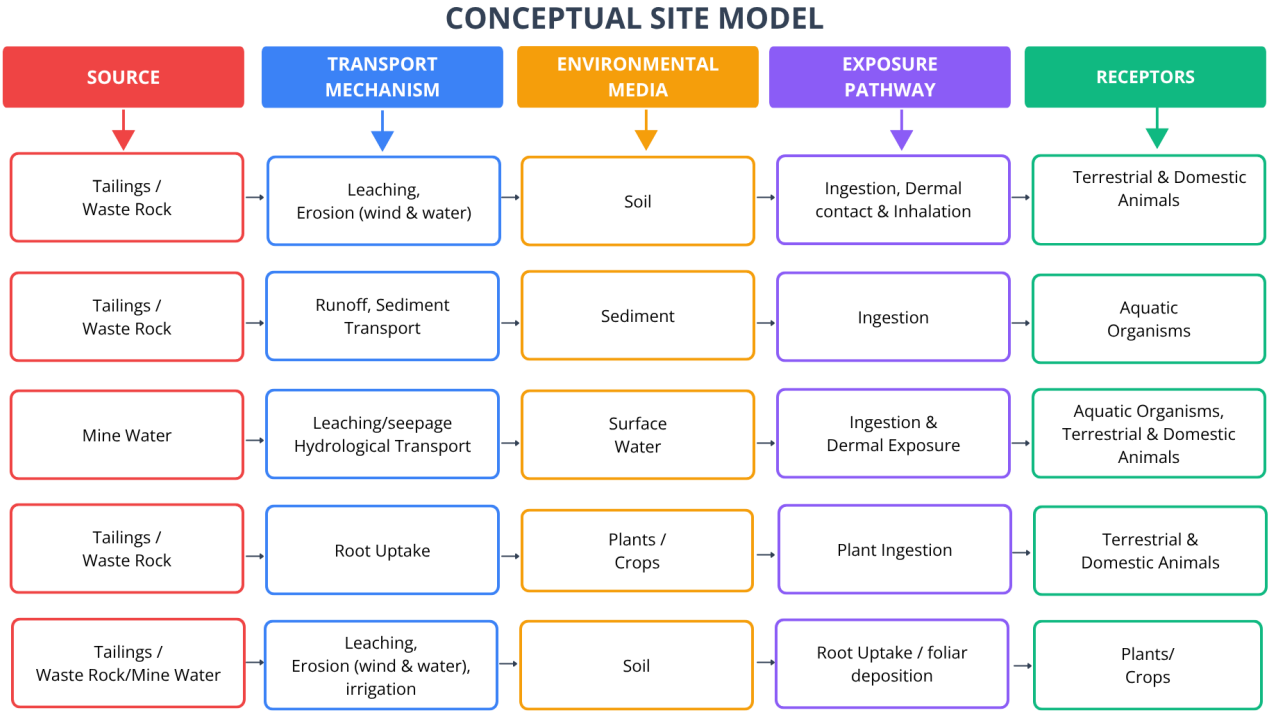

Figure 5.37: Schematic conceptual site model (CSM) of source-pathway-receptor for Abakaliki, Gimbi and Gimbi-Rikaya sites

Comparable studies also document substantial mine-related risk footprints, with high ER/RI and cumulative indices linked to Pb–Zn AMLs and mixed sulphide tailings, aligning with our Abakaliki and Gimbi profiles (L. Jiang et al., 2021; H. Liu et al., 2022), reinforcing that the very high RI and CRS at Abakaliki and Gimbi reflect not only elevated concentrations, but also efficient exposure pathways identified in the CSM, implying heightened potential for bioaccumulation, trophic transfer, and habitat-level effects on both aquatic domestic and terrestrial receptors. This is demonstrated in the RAC outcomes in Table 5.21-23, which highlight Cd, Zn, and Pb as the dominant high-risk metals.

Abakaliki shows higher levels of contamination and metal mobility than Gimbi. The consistent presence of Zn, Pb, and Cd across tailings, soils, and sediments at Abakaliki confirms extensive dispersion and a greater ecological risk potential, although Pb showed low risk and was less mobile in tailings and sediments. At Gimbi, on the other hand, although Zn concentrations are high and mobile across all media, Pb remains mainly less mobile in soils. This difference underscores the role of local geology and mineralogy in influencing metal mobility and availability, because at Abakaliki, the sulphide-rich Pb–Zn lode mineralisation hosted within the Asu River Group shales and siltstones likely promotes enhanced sulphide weathering and metal mobilisation. In contrast, the vein-style mineralisation and associated lithological conditions at Gimbi/Wase may favour stronger Pb retention within relatively stable mineral phases, including Fe–Mn oxides and carbonate-associated phases, thereby limiting Pb mobility under prevailing geochemical conditions.

The findings also highlight that elevated total metal concentrations, particularly Pb, do not necessarily correspond to higher ecological or health risks. Where metals are geochemically immobilised, their actual bioavailability is limited, reducing their capacity to cause harm to receptors.

5.5 Conclusion

This study evaluated the chemical contamination, fate, and transport of heavy metals in and around the Abakaliki and Gimbi Pb/Zn AMLs, combining field pXRF screening, laboratory ICP-OES analysis, geochemical assessments, metal speciation, and ecological risk evaluation. Although field XRF provided rapid, valuable screening of hotspots and distributions, laboratory ICP-OES offered more reliable quantification, particularly for Zn and Ti, which were systematically under- or overestimated by the in situ method.

The results demonstrated that both sites are heavily impacted by Pb, Zn, and Cd, with concentrations far exceeding regulatory thresholds and greater impacts at the Abakaliki site. Tailings emerged as the principal source of contamination, while sediments and soil serve as sinks. Geochemical analysis further revealed that site geology and structural features play a crucial role in contaminant behaviour: at Abakaliki, weathered shales and pervasive fractures facilitated contaminant movement, whereas at Gimbi, carbonate-rich formations buffered acidity but promoted Zn mobility.

Sequential extraction and bioavailability assessments confirmed that Pb, Cd, and Zn occur predominantly in the exchangeable and reducible fractions, making them highly mobile and ecotoxicologically relevant. This distinction emphasised that total concentrations alone may overestimate or underestimate ecological risk, and that bioavailable fractions provide a more accurate indication of actual risk.

At the Abakaliki AML site, dissolved metals (Pb, Zn, Ni, Cu, and Mn) in surface water exceed both the EQS and bioavailability values. The BLM results confirm high bioavailability and potential risk to aquatic organisms. At the Gimbi site, dissolved levels of Zn, Cu, Ni, and Mn exceeded the EQS, except for Pb. Bioavailability results fall below the EQS, except for Zn, which is above the EQS, indicating its high mobility. The BLM results for the Gimbi site showed that the environment is protective. The behaviour of Pb at the Gimbi site showed it has low mobility based on its low concentration in soils and bioavailability in water samples compared to tailings.

Ecological risk indices (ER, RI) and the cumulative risk score (CRS) consistently indicated that Abakaliki and Gimbi pose very high ecological risk, while Gimbi–Rikaya represents a considerable risk. The risk assessment code outcomes further demonstrated that Cd and Pb are the dominant high-risk metals, underscoring their disproportionate role in driving site-wide ecological hazards.

The CSM reveals multiple, concurrent pathways for soil, sediment, water, and vegetation, linking sources to both terrestrial, domestic and aquatic receptors, thereby increasing the potential for cumulative effects, bioaccumulation, and food-web transfer.

Taken together, these findings confirm that abandoned Pb/Zn mine lands in southeastern Nigeria represent significant ecological risk zones, where Cd and Pb should be considered priority pollutants. The results point to the need for targeted management measures, including the containment of tailings, remediation of contaminated sediments, and monitoring of groundwater pathways, to mitigate long-term ecological risks. At the Abakaliki site, bioaccumulation studies should be undertaken for aquatic organisms and invertebrates to determine internal metal burdens. Biological monitoring should be conducted for domestic and livestock in the area. For Gimbi, additional investigation should focus on understanding the geochemical processes controlling Pb mobility and retention.

6.1 Introduction

Environmental sustainability refers to the capacity to maintain the valued qualities and functions of the physical environment for present and future generations (Sutton, 2004). Its increasing global significance stems from the ongoing degradation of ecosystems and the unsustainable exploitation of natural resources (Maina et al., 2016).

Among the major contributors to environmental degradation are coal mining activities, which generate extensive waste and long-term contamination of surrounding ecosystems (J. Li et al., 2024; US EIA, 2024). Mining activities, including surface, underground and mountaintop, disturb the land, producing overburden and waste materials that lead to soil erosion, water pollution, and a decline in air quality (Badakhshan et al., 2023; Luís et al., 2011; Palmer et al., 2010). Failure to properly close mines or the complete abandonment of sites often leaves behind contaminated soils, sediments, and water bodies (Tozsin et al., 2022; Z. Zhang et al., 2011). Studies have shown that high levels of heavy metals and persistent organic pollutants are common in historic mining areas (Anawar, 2013; Hufty, 2019; S. Kim et al., 2008; Klawans, 2024; Tozsin et al., 2022). These pollutants can persist in key environmental media for extended periods and may pose risks to humans through ingestion, inhalation, and skin contact. Some chemicals have known links to cancer, neurological issues or may cause multi-organ damage (IARC, 2010; K. H. Kim et al., 2013; US EPA, 2011a, 2011c, 2011b).

Coal mining in Nigeria exemplifies the environmental and health issues linked to extractive industries. The sector has played a significant role in the country's industrial growth, especially in Enugu and the southeastern regions (BPE, 2006; Nwaobi, 2005). However, decades of abandonment, along with the lack of comprehensive monitoring and cleanup efforts, have led to ongoing contamination of local ecosystems, increased dangers for local communities, and hindered effective risk reduction (Asogwa, 1988; Ezeigbo & Ezeanyim, 1993; Ogbonna et al., 2015; Sikakwe et al., 2015). Therefore, a thorough evaluation of environmental contamination and health threats posed by abandoned coal mines is essential not only for local safety but also for developing policies aimed at protecting public health and promoting long-term environmental sustainability in Nigeria.

6.1.1 Geology and Characteristics of Coal Mining in Nigeria

Enugu State, in southeastern Nigeria, hosts a diverse geological landscape, featuring sedimentary rocks, significant coal deposits, and igneous intrusions. Historically, the development of the state has been influenced by extensive coal seams in the Afuze Formation of the Anambra Basin, dating back to the Early Cretaceous period (Nwajide, 2013). In terms of geology, the Enugu Coal Mines are underlain by three unconformable formations of Cretaceous age, namely the Enugu Shale Formation, Mamu

Formation, and Ajali Sandstone (Nwajide, 2013), from oldest to youngest, respectively, all within the lower or Southern Benue Trough (Figure 6.1). The Onyeama mine coal seam is of the Mamu Formation, which is associated with Pyrite and Siderite (Nwajide, 2013). The topography varies from lowlands in river valleys to uplands and plateaus. The uplands are underlain by the Ajali and Mamu Sandstone, while the lowlands are underlain by the Enugu Shale. The Enugu Escarpment stands out as a notable feature, separating the lower plains from the higher elevations. Erosion has shaped the landscape, with rivers and streams carving through the terrain (Akpan et al., 2021).

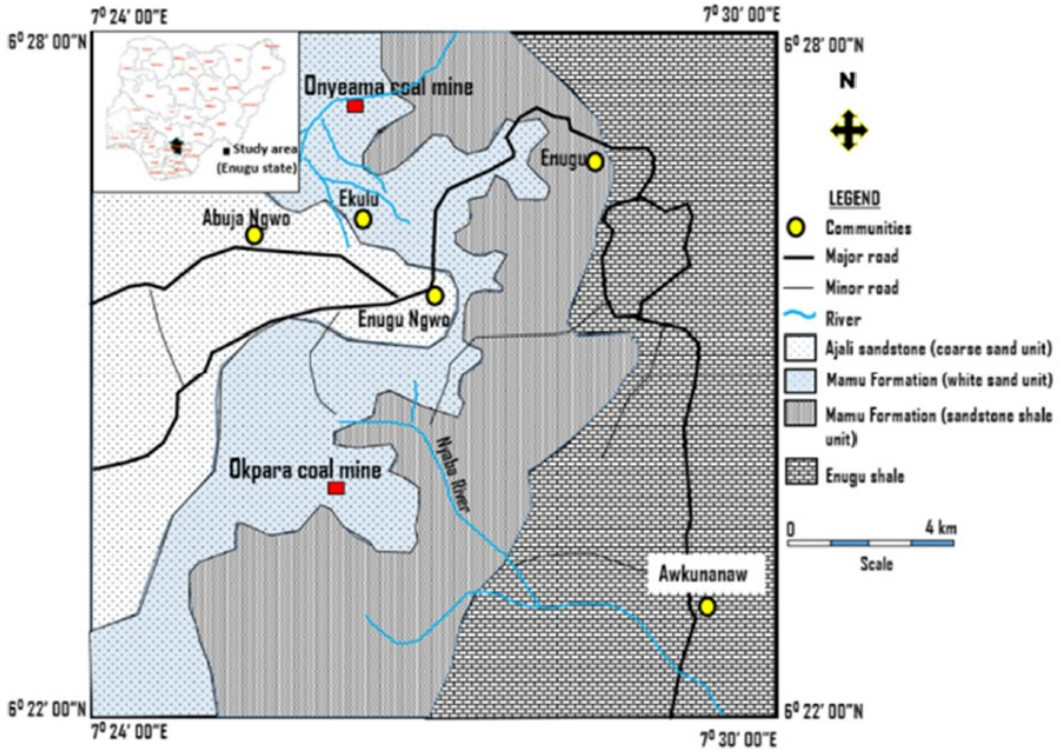

Figure 6.1 Geological map with the location of abandoned coal mines (Akpan et al., 2021)

6.1.2 Background to Coal Mining in Nigeria

Coal has historically fuelled energy generation and industrial growth, particularly during Nigeria's colonial era. Coal was initially discovered by Albert Kitson, a British engineer, in 1909 at Udi Ridge, Enugu, and mining started at Ogbete in 1915 (Nwaobi, 2005). The Ogbete mine achieved full operational status by 1916, yielding a total of 24.11 million metric tons (MT) of coal (Baiyewu-Teru, 2015). Over time, additional mines emerged in the region, collectively known as the Onyeama complexes, laying the foundation for the modern Enugu State. During its peak, production of coal soared to as high as 790,030 MT as of 2015; the estimated coal deposit stands at about 2.8 billion MT (Asogwa, 1988; Baiyewu-Teru, 2015).

The heyday of coal production was followed by a decline, primarily attributed to the Nigerian Railway Corporation and the Electric Power Company of Nigeria shifting from coal as a source of power to diesel, which were the major clients at the time (Nwaobi, 2005). This shift was predominantly influenced by the discovery of crude oil in the late 1950s. The Nigerian civil war between 1966 and

1970 also played a role in the decline, alongside failed attempts to mechanise the mines in the late 70s and 80s, as well as poor management of the Nigerian Coal Corporation and the mines in the 90s. All these factors played a significant role in the abandonment of most of the mines (Ogunsola, 1990). The Privatisation of the Nigeria Coal Corporation in 1999 and access granted to large private marketers into the nation's solid minerals gave a final blow to the sector, which led to its closure in 2002. Some of the assets of the corporation were sold in 2013 by the federal government (Nwaobi, 2005; Ogunsola, 1990).

Coal mining brought wealth and employment opportunities to the area, but it also led to extensive land degradation. Subsidence, mine waste dumps, changes in topography, erosion, acid mine water from the mines, and flooding characterise the mined lands, which are still affecting those living around the area (Akpan et al., 2021; Aroh, 2021; Omotehinse & Ako, 2019).

6.1.3 Environmental Contamination of Abandoned Coal Mine

Abandoned coal mines pose significant environmental and public health risks, including the generation of AMD, which contaminates water bodies with heavy metals and increases acidity. Additionally, accumulated methane emissions in these mines contribute to climate change, while soil contamination with coal residues and leachates can harm vegetation and potentially affect human health. Runoff from abandoned mines contaminates surface water, endangering aquatic ecosystems, and dust emissions from mine sites further degrade air quality, impacting both human and ecological health (Fields, 2003; Hasheela et al., 2015; UK EA, 2008).

Coal waste tips and spoil heaps associated with abandoned coal mines may also act as significant long-term sources of contamination (Kirby et al., 2010). These waste materials commonly contain sulphide-bearing minerals and residual hydrocarbons that undergo weathering upon prolonged exposure to oxygen and infiltrating water. As a result, coal waste tips can contribute to acid mine drainage generation, sulphate release, metal leaching, sediment mobilisation, and the release of particulate matter and PAHs into surrounding environments. In some cases, spontaneous combustion of coal waste piles may further increase atmospheric emissions and environmental degradation, reinforcing their role as persistent diffuse pollution sources long after mine abandonment (Kirby et al., 2010; Rouhani et al., 2023).

Environmental pollutants are notably prevalent in urban, agricultural, and industrial areas, including active and abandoned mine sites, where they affect soil, water, and air quality (Coelho et al., 2011). Among these pollutants, metals and PAHs are particularly concerning due to their persistence and toxicity, originating from industrial processes, mining operations, hydraulic fracturing, and accidental releases (Fayemiwo, 2018). Their ability to dissolve in water raises concerns about their impact on human health, necessitating continued attention to monitoring and mitigating their presence in various environmental contexts (Coelho et al., 2011; Ogodo, 2018).

PAHs are a group of organic contaminants composed of two or more fused aromatic rings (Public Health England, 2017). They are generated predominantly through the incomplete combustion of organic matter, including coal, petroleum products, biomass, and waste materials (Halfadji et al., 2021). Anthropogenic activities such as fossil fuel combustion, mining, smelting, and industrial processing significantly contribute to their release into the environment (Achten & Hofmann, 2009; Public Health England, 2017). PAHs are also present in unburnt materials such as native coal, which can contain concentrations up to several thousand mg/kg and act as an unrecognised but persistent source of contamination in soils and sediments (Achten & Hofmann, 2009). Because of their lipophilic and hydrophobic nature, PAHs have a strong affinity for organic matter and tend to accumulate in sediments and soils, where they persist for extended periods due to their resistance to biodegradation and photolysis (Ugochukwu et al., 2021).

Recent studies have reinforced the complexity of assessing PAH-related health risks in diverse environmental settings. For instance, Halfadji found that PAHs in Algerian soils posed carcinogenic risks primarily through dermal and ingestion pathways (Halfadji et al., 2021), with benzo[a]pyrene and dibenzo[a,h]anthracene contributing over 70% of total toxicity equivalents. Similarly, (C. Sun et al., 2015) and (Grmasha et al., 2023) reported potential carcinogenic risks associated with PAHs in surface water and sediment, with incremental lifetime cancer risk (ILCR) values ranging between 10^{-5} and 10^{-3}, particularly in areas affected by industrial and petroleum activities. In Nigeria, (Ugochukwu et al., 2021) and (Ugwu & Ukoha, 2016) linked PAH contamination in sediments and soils to petrogenic and pyrogenic sources from coal mining activities and vehicle emissions, observing that although ecological risks were elevated, most human health hazard indices remained within acceptable limits. Collectively, these findings indicate that exposure to PAHs, especially high-molecular-weight, carcinogenic compounds, remains a significant public health concern, requiring ongoing monitoring, site-specific risk characterisation, and the adoption of risk management and remediation strategies to minimise human exposure.

6.1.4 Case study of Onyeama Abandoned Coal Mine

Onyeama coal mine was an underground mine, lying within Latitude 060 22’ 00’’ N and 060 28’ 00’’ N and Longitude 070 24’ 00’’E to 070 30’ 00’’ E, which is part of the mine fields of Enugu state (Figure 6.2) Onyeama mine is within Ngwo community, which is the only town in Nigeria that is in three local government areas: Udi, Enugu North and Enugu South (Figure 6.2). It was opened in 1958 and operated by the Nigeria Coal Corporation, of the federal government of Nigeria. It was abandoned over 4 decades ago due to the challenges highlighted in section 6.1.2.

The operational phase of the mine is shown in Figures 6.3a and 6.3b, while its current state of abandonment is illustrated in Figure 6.4. The mine has two tunnels and, since its abandonment, the mine’s two tunnels have continuously discharged orange-coloured mine water, an acidic effluent

produced by oxidation of sulphide minerals (particularly pyrite) in the coal-bearing Mamu Formation. The iron-rich water flows into the Ekulu River, which could significantly deteriorate the water quality.

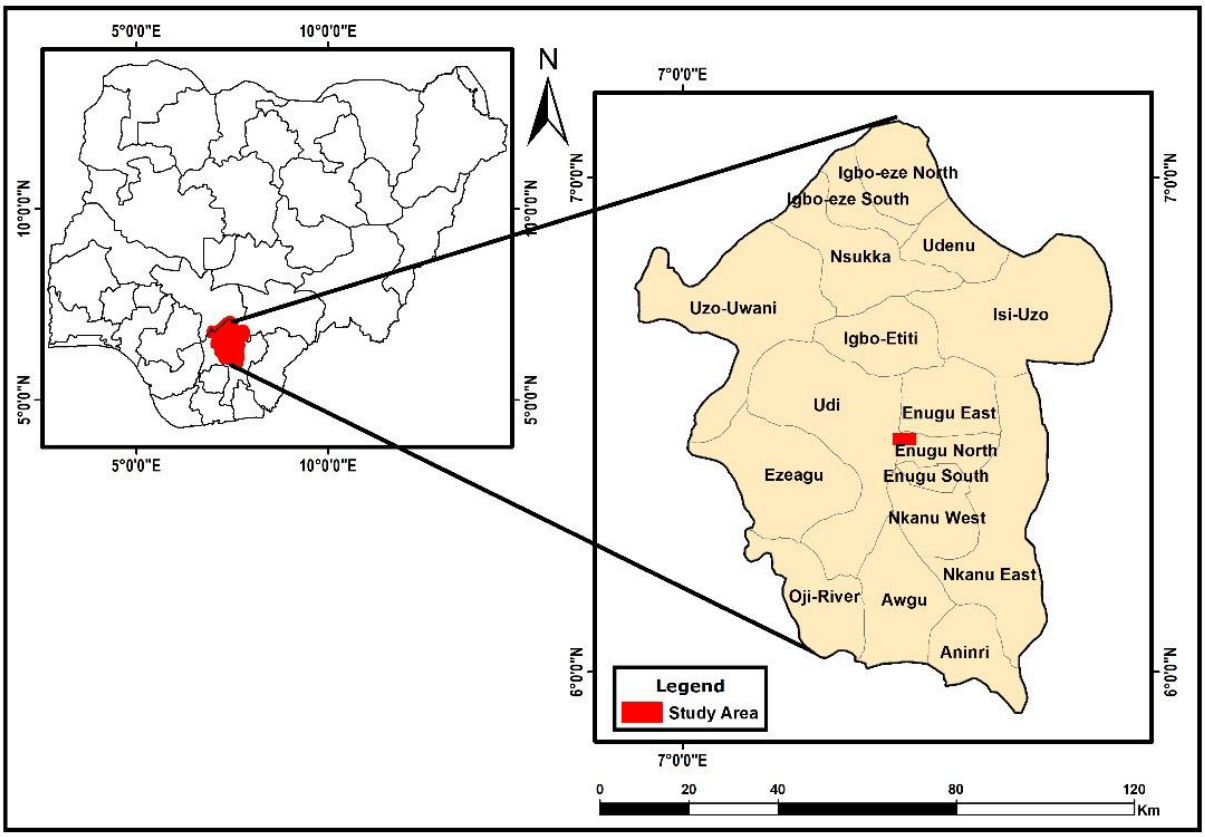

Figure 6.2: Location map of the study area. Enugu State is shown in red on the main map, with the primary study site situated within Enugu North and Enugu South Local Government Areas, indicated by the red rectangle.

.

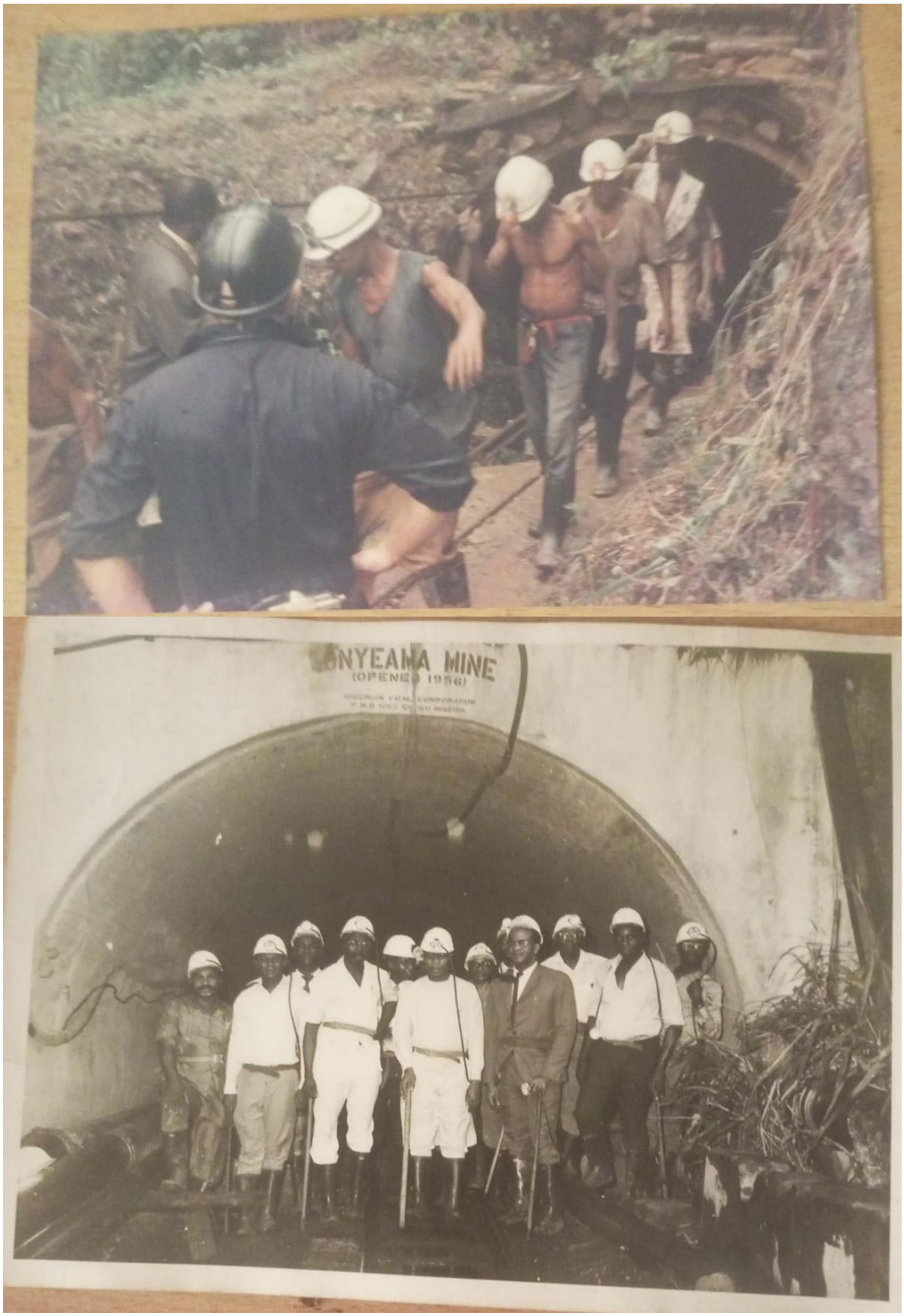

Figure 6.3: Onyeama Mine before abandonment. (a) Mine workers during operations prior to full construction; (b) Mine workers and officials after full construction (Source: NCC archive).

Figure 6.4: Onyeama Abandoned Underground Coal Mine. (a) Mine Adit on the left wing with acid mine drainage flowing into a stream; (b) second mine Adit on the right discharging into a stream; (c) receiving stream from both mine Adits; (d) mine area currently used for agriculture, with vegetables planted within the ridges.

6.1.5 Chapter Aim and Objectives

This chapter aims to identify and quantify organic and inorganic contaminants, evaluate human health risks associated with an abandoned coal mine in Nigeria, and inform risk management and remediation strategies to protect exposed populations. Specific objectives are to:

- Determine the concentrations of heavy metals and PAHs around the abandoned coal mine.

- Compare the measured contaminant levels with national and international guideline values for human health protection.
- Determine potential PAH toxicity from the hydrocarbon contamination.
- Estimate human exposure levels to identified contaminants through relevant pathways (ingestion, dermal contact, and inhalation).
- Assess the potential non-carcinogenic and carcinogenic health risks associated with exposure to contaminants from the abandoned mine.
- Provide recommendations for mitigating contamination impacts and managing human health risks in and around the abandoned mine site.

6.2 Materials and Methods

The methods employed in this study encompass sample collection, sample processing, chemical analysis, and data analysis techniques developed to achieve the objectives of this chapter. Prior to sampling, a Field Sampling Plan (FSP) for the environmental assessment was developed to provide structure and guidance for all field activities. The FSP defined the sampling design, procedures, and quality assurance measures necessary to ensure that representative and reliable data were obtained. In addition, a protocol for Sample collection was prepared to outline site-specific procedures, ensuring that all sampling activities were consistent with the study objectives and adapted to local conditions. Standard Operating Procedures (SOPs) for sediment, soil, and water sampling were also established to promote uniformity, minimise sampling errors, and maintain the integrity and comparability of collected samples.

Furthermore, protocols for chemical analysis were developed to guide laboratory procedures for the determination of contaminants in the collected samples. These protocols ensured the use of standardised analytical methods, proper instrument calibration, and adherence to quality control and assurance measures. Collectively, these documents provided a robust framework for methodological rigour, reproducibility, and data quality throughout the study.

The following sections describe the study area and the procedures adopted for sample collection, processing, and chemical analysis. Emphasis is placed on ensuring the representativeness of samples, adherence to established protocols, and maintaining data quality throughout the investigation.

6.2.1 Study Area

The study was conducted at the site described in section 6.1.4. The areas covered were the mine drainage area, surrounding rivers, agricultural land, and waste and tailings dumps within the abandoned mine site. The location map of the sample points is shown in Figure 6.5.

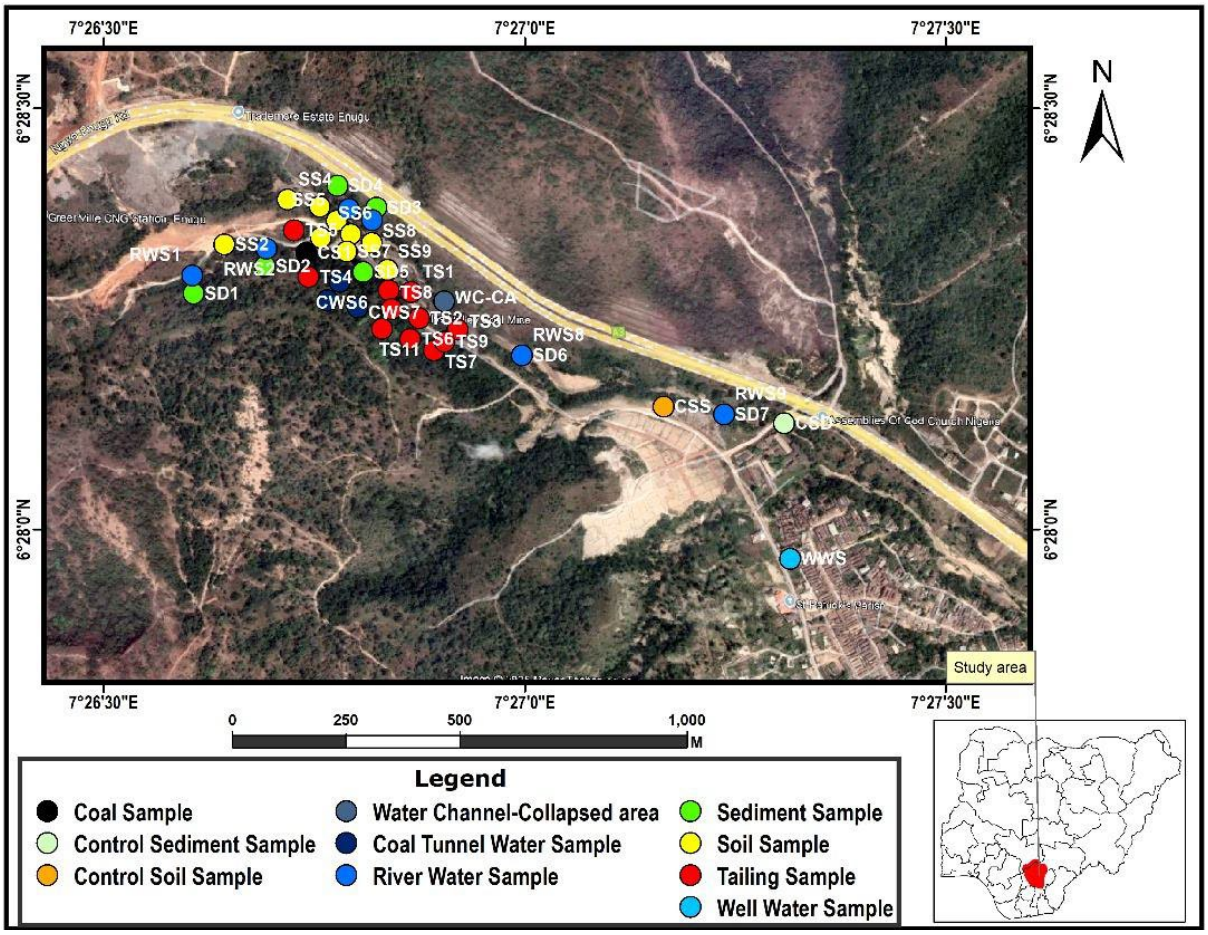

Figure 6.5: Map of the study area showing water, soil, and sediment sample locations, colour-coded and labelled within the map. The sampling points are concentrated around the abandoned mine adits and the surrounding arable land.

6.2.2 Field Measurements

Temperature, pH, total dissolved solids (TDS), electrical conductivity (EC), and dissolved oxygen (DO) were measured in situ at each water sampling point. A portable X-ray fluorescence (pXRF) analyser (S1 Titan, Bruker Nano Analytics, Germany) was used for in situ, simultaneous, multi-element analysis of soils and tailings dumps at the abandoned underground coal mine site. A detailed description of the measurement procedure is provided in Section 5.2.2. Sampling details, including elevation and GPS coordinates, are presented in Appendix 6.1.

6.2.3 Sample Collection

Samples were collected at the abandoned mine site over an area of 0.30 km^2, covering mine waste dumps, mine adits, rivers and soils within the mine. Soil, sediment and tailings samples were collected in 250 mL glass jars and kept in a cooler. At each sampling point, additional samples were collected in 50 mL plastic tubes for metal analysis.

Water samples were collected for PAH analysis in 500 mL glass jars from river channels draining the site and at the entrance of the two tunnels leading to the underground mines (Figure 6.4). For metals analysis, 50 mL water samples each were collected and transferred unfiltered to a 50 mL plastic tube (for analysis of total metals) and adjusted to pH <2 using ICP-MS grade nitric acid. For stream and river water samples, a second sub-sample was filtered with a 0.2 micrometre syringe filter and transferred to a 50 mL plastic tube (for analysis of dissolved metals) and adjusted to pH <2 using ICP-MS grade nitric acid. Sediment samples were collected in 250 mL glass jars at the same point where water samples were collected, except at the mine tunnel, where this was difficult. A total of 10 water, 7 sediment, 10 soil, and 10 tailings samples were collected for each analysis of interest.

The samples were packed in a polystyrene box, with ice packs and shipped through FedEx courier to the laboratory. Upon arrival, the samples were logged and stored in the refrigerator at (4°C) before preparation and analysis. Sample details are provided in Appendix 6.2.

6.2.4 Reagents and Chemicals

The reagents and chemicals established for metal analysis using ICP-OES are as described in Section 5.2.4. While for PAHs analysis using GC-MS, all solvents, including methanol, hexane, acetone and ethyl acetate (EtAc), are of HPLC grade. PAH Mix (2000 µg/mL in benzene: dichloromethane (50:50)) standard including naphthalene (Nap), acenaphthene (Ace), acenaphthylene (Acy), fluorene (Flo), phenanthrene (Phe), anthracene (Ant), fluoranthene (Fla), pyrene (Pyr), benz(a)anthracene (BaA), chrysene (Chr), benzo(b)fluoranthene (BbF), benzo(k)fluoranthene (BkF), benzo(a)pyrene (BaP), dibenz(a,h)anthracene (DahA), indeno(1,2,3-cd)pyrene (IcdP) and benzo(g,h,i)perylene (BghiP) were obtained from Supelco, while PAHs internal standard (IS); including Phenanthrene-d10, Nephthalene-d8, Fluorene-d10, Anthracene-d10, and Fluoranthene-d10 were obtained from Sigma-Aldrich.

In all sample preparation and analysis, deionised water from a Milli-Q system with a resistivity of 18.2 MΩ•cm was used.

Equipment and consumables

Pipettes/tips, plasticware; syringes, syringe adaptors, filters, plastic bottles, glassware; beakers, 200 ml conical flask, centrifuge tubes, Tubovap tube, HPLC vials, manifold and accessories: weights, straws, stoppers, reservoirs, taps, SPE cartridges (C18 solid phase cartridges (500mg/3ml), Tubovap

evaporator, nitrogen blow-down apparatus, PTFE syringe filters (0.2 and 0.45 µm), filter paper (0.45 µm glass fibre filter (Whatman)) and Buchner flask and funnels, vacuum pump and tubing, trap to protect vacuum pump and ultra-sonic instrument.

6.2.4 General Parameter Analysis

Dissolved organic carbon (DOC) and pH measurement using the TOC-V CPN analyser (Shimadzu, Japan) and pH meter, respectively, were carried out for the water samples. A description of the procedures and analysis is provided in Section 5.2.5.

6.2.5 Sample Preparation for Metal and Organic Analysis

The concentrations of the 16 PAHs recommended as priority pollutants by the United States Environmental Protection Agency (US EPA) were considered for organic contaminants. At the same time, Zinc, Lead, Copper, Arsenic, Nickel, Titanium, Cadmium, Chromium, Cerium, Strontium, Zirconium, Manganese, Mercury, Iron, Barium, Aluminium, Magnesium, Calcium, Potassium and Sodium were the heavy metals and macro elements considered.

6.2.5.1 Heavy Metals (HMs)

Total and dissolved metals in water samples, total metal concentrations, as well as a three-step sequential chemical extraction (SCE) in soil and sediment samples, were prepared and analysed according to the procedures described in Sections 5.2.6 and 5.2.7.

6.2.5.2 PAHs

All sample preparations were conducted within a Class I microbiological safety cabinet to minimise contamination.

Solid Phase Extraction (SPE)

PAHs were extracted from water samples following a protocol developed by the Division of Environmental Science lab protocols, which are in line with standard protocols of the US EPA, using C18 solid phase extraction (SPE) cartridges (500 mg/3 mL). Samples were brought to room temperature and filtered through 0.45 µm glass fibre filters (Whatman) using a vacuum filtration apparatus. Filtered samples (200 mL each) were transferred to pre-cleaned 200 mL glass bottles (rinsed with methanol) and spiked with 500 µL of PAH-internal standard mix (0.2 ug/mL) solution. The SPE procedure was carried out using a Visiprep vacuum manifold under a fume hood.

Cartridges were conditioned sequentially with 5 mL of methanol followed by double-distilled water, ensuring they did not run dry between steps. Filtered water samples were loaded onto the cartridges at

a flow rate of approximately 5 mL/min under a vacuum pressure of 5–10 inHg. After loading, the cartridges were dried under vacuum for 30 minutes and subsequently eluted under reduced pressure (2.5–5 inHg) with 5 mL of EtAc, which was allowed to stand for 2 minutes before complete drainage. This step was followed by a second elution with 5 mL of an ethyl acetate/acetone mixture (50:50 v/v) following the same procedure. The eluates were collected in pre-washed 10 mL glass conical tubes (rinsed with methanol) and stored at −16 to −20 °C overnight.

The extracts were then concentrated using a Turbovap evaporator at 25 °C for approximately 90 minutes until the volume was reduced to about 1 mL. Each sample was transferred into a 2 mL HPLC vial using a glass pipette and further concentrated to approximately 0.2 mL under a gentle stream of nitrogen using the Turbovap nitrogen blowdown apparatus. The final concentrates were transferred into low-volume (250 µL) inset vials and prepared for GC–MS analysis. To prevent compound loss, each sample was vortexed before nitrogen blowdown and again after drying to mobilise any analytes that may have adhered to the glass walls back into solution.

Soil and sediment extraction

The ultrasonic-assisted solvent extraction method modified from (Silalahi et al., 2021) was used for the extraction of PAHs from soil and sediment samples under a fume hood. Approximately 5 g of homogenised soil or sediment was weighed into a 20 mL glass tube, followed by the addition of 7 mL of acetone and 525 µL of PAH-Internal Standard mix solution (20 µg/mL). The samples were extracted using ultrasonication and were sonicated in an ultrasonic water bath for 20 minutes. The resulting extract was transferred using a 7 mL pipette into a clean 25 mL glass tube (methanol rinsed). The extraction process was repeated twice more, each time with an additional 7 mL of acetone and a 20-minute sonication period, and the extracts were combined in the same collection tube.

Combined extracts were stored under refrigeration at -16 to -20 °C prior to analysis. Before instrumental analysis, a 1 mL aliquot of the extract was removed and filtered through a 0.2 µm PTFE syringe filter into a 2 mL HPLC vial for PAH analysis using Gas Chromatography–Mass Spectrometry (GC–MS).

6.2.6 GC-MS Analysis

Sample extracts were analysed using an Agilent 8890 gas chromatograph coupled with an Agilent 5977B mass spectrometer. Sample injections (1 µL) were performed using a PAL RSI 85 autosampler in pulsed splitless mode with an injection pulse pressure of 50 psi maintained for 0.7 min, followed by a purge flow to the split vent of 50 mL/min at 0.75 min. The inlet temperature was set to 320 °C, and the septum purge flow was maintained at 3 mL/min. Separation was achieved on an Agilent HP-5MS UI capillary column (30 m × 0.25 mm i.d., 0.25 µm film thickness) with helium carrier gas at a constant flow rate of 1.0 mL/min. The GC oven temperature program was as follows: initial temperature 80 °C (held for 1 min), ramped at 25 °C/min to 200 °C (no hold), then at 8 °C/min to 289 °C and held for 6.3

min, giving a total run time of approximately 23.3 min. The transfer line temperature was maintained at 300 °C. The mass spectrometer operated in selected ion monitoring (SIM) mode under electron ionisation (EI) conditions, with a solvent delay of 4 min. The electron multiplier gain was set to 1.0, and the instrument was tuned using PFTBA. Data acquisition and processing were carried out using Agilent MassHunter software.

Prior to analysis, the GC–MS was calibrated for the 16 USEPA priority PAHs using a series of standard solutions. The calibration range included blank (0), 1, 2, 10, 20, 100, 200, and 1000 ng/mL, with PAH-Internal Standard mix solution (500 ng/mL) added to each calibration level. The resulting curves exhibited excellent linearity, with correlation coefficients (R^2) greater than 0.99 for all analytes across the calibration range, confirming the instrument's reliability and accuracy. PAH were quantified using internal standard quantitation. Quality assurance and control (QA/QC) procedures were incorporated into each analytical batch. These included method blanks, control samples, and continuing calibration verification standards.

6.2.7 Data and Statistical Analysis

Quantitative data were processed using Agilent MassHunter software, and analyte concentrations were determined from the respective calibration curves using internal standard normalisation calibration.

Method validation was performed for both water and soil matrices to assess the analytical procedure's accuracy and precision. Validation included the analysis of three low-spike samples, three high-spike samples, and three blanks for each matrix. The recovery, precision, and method detection limits (LODs) obtained from these validation experiments were used to assess the method's performance. Detailed results for the validation parameters and LOD values are provided in Appendices 6.3-6.4.

6.2.7.1 Data Analysis for Metals and Organic Contaminants

6.2.7.1.1 Heavy Metal Evaluation

The data processing procedures for heavy metals, including the evaluation of total metal concentrations, sequential extraction procedure, calculation of enrichment factors (EF), contamination factors (C_f), degree of contamination (C_d) and the geoaccumulation index (Igeo), have been described previously in Section 5.2.8 and are therefore not repeated here. The results are in Appendices 6.8-13.

6.2.7.1.2 PAH Toxicity

The toxicity of PAHs in soil and water was evaluated using the toxic equivalency factor (TEF) approach, recommended by (CCME, 2010; US EPA, 1993; WHO, 2003) which normalises the toxicity of individual PAHs to that of BaP, a reference compound with a TEF of 1 based on its known potency (Bukowska et al., 2022; Nisbet & Lagoy, 1992). The concentration of each PAH (C_i) was multiplied by

its corresponding TEF (TEF_i) to obtain its benzo(a)pyrene equivalent concentration (BaPeq), as shown in equation (1):

$$BaPeq_i = (C_i \times TEF_i) \quad \text{Eq. 1}$$

$$TEQ = \sum BaPeq \quad \text{Eq. 2}$$

The sum of all 16 PAH BaPeq values in equation 2 represents the total toxic equivalent (TEQ), which reflects the cumulative carcinogenic potency of the PAH mixture relative to BaP. TEFs were adopted from the work of Nisbet and Lagoy (Nisbet & Lagoy, 1992). The total BaPeq concentration in the environmental media (soil) was then used to estimate potential human health risks.

6.2.7.2 Human Exposure Assessment

In this study, chronic daily intakes (CDIs) were estimated in accordance with the USEPA human health risk assessment guidelines (US EPA, 1989a, 1991, 2001, 2004). The assessment considered exposure to PAHs in soil via ingestion, dermal contact, and inhalation pathways, and in water via ingestion and dermal contact only. The inhalation pathway was not considered for water because PAHs have low volatility, and their transfer from water to air is negligible compared to ingestion and dermal exposure routes (ATSDR, 1995; CCME, 2010; Grmasha et al., 2023; US EPA, 2004). This approach is consistent with previous studies (Singovszka et al., 2020; C. Sun et al., 2015; Zoveidadianpour et al., 2023) which typically focus on ingestion and dermal exposure as the dominant pathways for assessing PAH risk in water. The CDIs for each exposure pathway were calculated using the following equations:

Soil (Residential/Industrial Exposure)

Ingestion of soil -

$$CDI_{ingestion} = \frac{Cs \times IRs \times EF \times ED \times CF}{BW \times AT} \quad \text{Eq. 3}$$

The definitions of each variable in this equation and subsequent equations, as well as the exposure pathways and parameter values, are presented in Table 6.1.

Inhalation of soil particulates (dust) -

$$CDI_{inhalation} = \frac{C_{air} \times InhR \times EF \times ED}{BW \times AT}$$

Where: $C_{air} = \frac{C_{soil}}{PEF}$

(C_{air} is air concentration, C_{soil} is soil concentration, and PEF is the particulate emission factor)

Therefore,

$$CDI_{inhalation} = \frac{Cs \times InhR \times EF \times ED}{BW \times AT \times PEF} \quad \text{Eq. 4}$$

Dermal contact with soil -

$$CDI_{dermal} = \frac{Cs \times CF \times SA \times AF \times ABS \times ED \times EF}{BW \times AT} \quad \text{Eq. 5}$$

It should be acknowledged that the inhalation exposure assessment was based on the US EPA's particulate emission factor (PEF) methodology as defined in the Soil Screening Guidance Technical Background Document (US EPA, 1996). This estimates airborne contaminant concentrations from total soil contaminant levels rather than from directly measured inhalable or respirable particulate fractions (e.g., PM_{10} or $PM_{2.5}$). As a result, the calculated CDI inhalation values represent screening-level estimates and may not fully capture the proportion of particulates capable of entering the respiratory tract under actual environmental conditions.

Furthermore, the exposure assessment relied on total contaminant concentrations and did not incorporate site-specific bioaccessibility or bioavailability within lung fluids or the gastrointestinal environment. Consequently, the resulting inhalation and ingestion risk estimates are likely to be conservative and may overstate potential exposures.

Table 6.1: Exposure parameters and default values used to estimate CDI for soil exposure pathways (ingestion, dermal contact, and inhalation) for adult and child receptors. Parameter values were adopted primarily from the U.S. EPA Risk Assessment Guidance for Superfund (US EPA, 1989b, 1991, 2004) and the Exposure Factors Handbook (US EPA, 2011b).

Exposure Pathway / Parameter	Symbol	Adult	Child	Units
Soil ingestion				
Chemical Concentration in Soil	Cs	Measured	Measured	mg/kg
Soil ingestion rate	IRs	100	200	mg/day
Fraction Ingested	FI	1	1	
Exposure frequency	EF	350	350	days/yr
Exposure duration	ED	24	6	yr
Body weight	BW	70	15	kg
Conversion Factor	CF	$1x10^{-06}$	$1x10^{-06}$	Kg/mg
Lifetime	ED (lifetime)	70	70	years
Averaging time (non-cancer)	AT	8,760	2,190	days
Averaging time (cancer)	AT	25,550	25,550	days
Dermal contact with soil				
Exposed skin surface area	SA	5,700	2,800	cm^2
Soil adherence factor	AF	0.07	0.2	mg/cm^2
Dermal absorption fraction	ABS	0.13	0.13	—
Event Frequency	EV	1	1	Events/day
Inhalation of particulates				
Particulate emission factor	PEF	1.36×10^9	1.36×10^9	m^3/kg
Inhalation rate	IHR	16	10	m^3/day

Water (Drinking, Bathing/Showering and Swimming Exposure)

Ingestion of water -

$$CDI_{ingestion} = \frac{Cw \times IRw \times EF \times ED}{BW \times AT} \quad \text{Eq. 6}$$

Dermal absorption -

$$CDI_{dermal} = \frac{Cw \times SA \times Kp \times ET \times EF \times ED \times CF}{BW \times AT} \quad \text{Eq. 7}$$

The definitions of each variable in the equations and the values for the exposure parameters are presented in Table 6.2. Where CDI is in mg/kg BW/day, and Cs and Cw are the concentrations of HMs and PAHs in soil and water samples (mg/kg).

Table 6.2: Exposure parameters and values adopted from (US EPA, 2004, 2011c) used to estimate CDI for human health risk assessment of adults and children through water ingestion and dermal exposure pathways.

Exposure Pathways/Parameters	Symbol	Adult	Child	Unit
Ingestion of Water				
Chemical Concentration in Water	Cw	Measured	Measured	mg/L
Ingestion Rate of Water	IRw	2	1	l/day
Exposure frequency	EF	350	350	days/year
Exposure Duration	ED	24	6	years
Lifetime for carcinogenic risk	LT	70	70	years
Body Weight	BW	70	15	kg
Averaging Time- Cancer	AT	25,550	25,550	days
Averaging Time - Non-Cancer	AT	8,760	2,190	days
Dermal contact with water				
Permeability Constant	K_p	Chemical specific	Chemical specific	cm/hr
Skin Surface Area	SA	18000	6,600	cm^2
Exposure Frequency	EF	350	350	day/year
Volumetric Conversion Factor for Water	CF	0.001	0.001	l/cm^3
Gastrointestinal absorption factor (PAHs)	ABS_{GI}	Chemical specific	Chemical specific	unitless
Body Weight	BW	70	15	kg
Event Duration or Event Time or Exposure Time	ET	0.58	1	hours/event

The dermal permeability constant (Kp) is a chemical-specific dermal permeability coefficient used to estimate what fraction of a contaminant in water can pass through the skin and be absorbed. The values used to estimate dermal contact exposure to water are presented in Table 6.3. The gastrointestinal absorption factor (ABS_{GI}) used to estimate risk via this route is also included in the table.

Table 6.3: The values of (K_p) and (ABS_{GI}) used for dermal exposure and risk calculations. These were obtained from the US EPA guidance for dermal risk assessment (US EPA, 2004).

PAHs	Kp (cm/h) predicted	ABS_{GI}

Nap	0.0466	0.58
Acy	0.0860	,,
Ace*	0.0325	,,
Fl	0.11	,,
Phe	0.14	,,
Ant	0.142	,,
Flu	0.22	,,
Pyr	0.201	,,
BghiP**	0.0001	,,
BaA	0.47	,,
Chr	0.47	,,
BbF	0.417	,,
BkF	0.6910	,,
BaP	0.7	,,
IND	1	,,
DBA	0.9530	,,
HMs		
As	0.001	0.95
Ba	0.001	0.07
Cu	0.001	0.1
Mn	0.001	0.04
Cd	0.001	0.025
Cr	0.002	0.025
Ni	0.0002	0.04
Pb	0.00013	0.1
Zn	0.0006	0.1
Hg	0.001	0.1
Fe, Ti, Zr, Ce, Sr, and Al.	0.0001	0.1

6.2.7.3 Human Health Risk Assessment (HHRA)

The risk assessment was conducted to evaluate the potential non-carcinogenic and carcinogenic risks associated with human exposure to contaminant concentrations in soil and water. HHRA generally considers multiple exposure pathways while accounting for the variability in PAH composition, persistence, and toxicity. Hence, the assessments were based on the CDIs derived for each relevant pathway, including ingestion, dermal contact, and inhalation. These exposure estimates were compared with established toxicological reference values to quantify potential health risks. Toxicity values are not available for all carcinogenic PAHs as well as the noncarcinogenic ones, several regulatory and health agencies, including the World Health Organization (WHO, 2003), the Canadian Council of Ministers of the Environment (CCME, 2010), Public Health England (Public Health England, 2017) and US EPA (ASTDR, 2022) recommends a surrogate marker approach typically using BaP to assess genotoxic PAH mixtures in contaminated soils and water. This method assumes that the carcinogenic

risk of a PAH mixture is proportional to the BaP concentration, allowing comparison against benchmark values.

Non-carcinogenic Risk

Potential non-carcinogenic risk was assessed by comparing the estimated exposure doses (CDIs) with the corresponding reference doses (RfDs) to obtain the hazard quotient (HQ) for each organic and inorganic contaminant. The following expressions were used for the calculations:

Ingestion (soil/water) -

$$HQ_{ing} = \frac{CDI_{ing}}{RfD_{ing}} \quad \text{Eq.8}$$

where RfDing (mg/kg/day) is the oral reference dose, and HQing is the hazard quotient via ingestion.

Dermal contact (soil/water) -

The dermal reference doses (RfD_{dermal}) were derived from oral RfDs as:

$$RfD_{dermal} = RfD_{ing} \times ABS_{GI} \quad \text{Eq. 9}$$

where ABS_{GI} refers to the gastrointestinal absorption fraction (Table 6.3). Dermal hazards (HQ_{dermal}) were then calculated using:

$$HQ_{dermal} = \frac{CDI_{dermal}}{RfD_{dermal}} \quad \text{Eq. 10}$$

Inhalation (soil particulates) -

The inhalation non-cancer risk (HQ_{inh}) was evaluated using exposure concentration in air (EC) (expressed as CDI_{inh}) and the inhalation reference concentration (RfC_{inh}):

$$HQ_{inh} = \frac{CDI_{inh}}{RfC_{inh}} \quad \text{Eq. 11}$$

Note that EC was obtained from soil concentration via the particulate emission factor (PEF) (Equation 5).

The toxicity parameters used for PAHs are listed in Table 6.4 and for HMs in Table 6.5. As shown in Table 6.4, RfC values are not available for most non-carcinogenic PAHs (except naphthalene). Therefore, the benzo[a]pyrene BaP RfC was cautiously applied as a surrogate for screening-level assessment.

Table 6.4: The Reference doses (RfD) and reference concentrations (RfC) for noncarcinogenic PAHs, obtained from the IRIS assessment database (IRIS, 2025) and BaP cancer slope factor (CSF) and inhalation unit risk (IUR) retrieved from the US EPA (IRIS, 2017).

PAHs	RfD (mg/kg-day)	RfC (mg/m^3)	CSF (mg/kg-day)	IUR (µg/m^3)
Acenaphthene	0.06			
Fluoranthene	0.04			
Fluorene	0.04			
Naphthalene	0.02	0.003		
Pyrene	0.03			
Anthracene	0.3			
Benzo(a)pyrene	0.0003	0.000006	2	0.001

*Table 6.5: The Reference doses (RfD) and reference concentrations (RfC) for noncarcinogenic HMs were sourced from the IRIS assessment database (IRIS, 2025). RfD for Pb and Cu were from *(EFSA, 2010) and **(A. A. Taylor et al., 2023). RfCs for As, Pb, and Ba were from (Barraza et al., 2018), as well as CSF for Cd, while Zn, Cd, Cu and Ni were obtained from (Z. Sun et al., 2020). Cancer slope factor (CFS) and Inhalation unit risk (IUR) for HMs in bold were sourced from (OEHHA, 2025), while the rest are from (IRIS, 2025).*

HMs	RfD mg/kg-day	RfC mg/m3	CSF (mg/kg-day)	IUR (µg/m^3)
As	0.00006	0.00003	0.32	0.0043
Zn	0.3	0.3		
Pb*	0.00034	0.00352	0.042	0.000012
Cd	0.0005	0.00001	0.38	0.0042
Ni	0.02	0.0206	0.91	0.00026
Cr	0.0009	0.00005	0.27	0.018
Cu**	0.04	0.04		
Sr	0.6			
Ba	0.2	0.000143		
Mn	0.14	0.00005		

Hazard Index (HI)

The overall potential for combined or cumulative non-carcinogenic effects resulting from simultaneous exposure to multiple contaminants or pathways was assessed using the hazard index (HI). The HI was calculated as the sum of the individual hazard quotients (HQs) associated with each contaminant and exposure route for a given receptor (adult or child), as expressed below:

$$HI = \sum HQ_i \quad \text{Eq. 12}$$

An HI value less than 1 indicates that non-carcinogenic adverse health effects are unlikely to occur, whereas an HI greater than 1 suggests a potential for adverse effects, depending on the magnitude and exposure context (US EPA, 1989b, 2004).

Carcinogenic Risk

The incremental lifetime cancer risk (ILCR) was used to assess the risk to site users exposed to the US EPA recognised carcinogenic PAHs: BaA, BkF, BbF, Chy, BaP, DahA and IcdP in water and soil. Carcinogenic risk was quantified using BaP-specific oral Cancer Slope Factors (CSFo) for ingestion and Inhalation Unit Risk (IUR) values (2.0 mg/kg/day and 0.001 µg/m3, respectively) obtained from US EPA (IRIS, 2017). Oral CSFs and IURs for other PAHs were derived using Potency Equivalence Factors (PEFs) relative to BaP using equations 13 and 14; the values were retrieved from (ASTDR, 2022; US EPA, 1993).

$$CSF_{PAHi} = CSF_{OBaP} \times PEF_i \quad \text{Eq. 13}$$

$$IUR_{PAHi} = IUR_{BaP} \times PEF_i \quad \text{Eq. 14}$$

The ILCR for ingestion and inhalation were calculated as follows:

$$ILCR_{ing} = CDI_{ing} \times CSF_i \quad \text{Eq. 15}$$

$$ILCR_{inh} = CDI_{inh} \times IUH_i \quad \text{Eq. 16}$$

A similar approach using PEF has been applied by different researchers for site-specific HHRA studies (Ugochukwu et al., 2018, 2021). Others studies (S. C. Chen & Liao, 2006; Halfadji et al., 2021; Peng et al., 2011; Zoveidadianpour et al., 2023) used BaP cancer slope factor values of 7.3 mg/kg/day for ingestion (IRIS, 1994), 25 mg/kg/day for dermal (Knafla et al., 2006) and 3.85 (3.9) mg/kg/day for inhalation (OEHHA, 2010) for the assessments, although these are legacy Health Effect Assessment Summary Table (HEAST) values. The PEF values and corresponding CSFs and IUHs for the carcinogenic PAHs are shown in Table 6.6.

The US EPA doesn't provide a separate dermal cancer slope factor (CSF_{dermal}) for risk assessment. Instead, carcinogenic risk from dermal exposure is evaluated using the oral CSF on an absorbed-dose basis (US EPA, 2004). The dermal absorbed dose (DAD) was not calculated separately, as the CDI for dermal exposure (CDI_{dermal}) already accounts for absorption through inclusion of the permeability coefficient (K_p), exposure time, and exposed skin surface area. This approach avoids double-counting absorption and aligns with the current US EPA methodology for estimating systemic dermal exposure to PAHs (US EPA, 2004, 2011c). Therefore, dermal carcinogenic risk was computed as:

$$ILCR_{dermal} = CDI_{dermal} \times CSF_{dermal} \quad \text{Eq. 17}$$

Where:

$$CSF_{dermal} = \frac{CSF_{oral}}{ABS_{GI}} \quad \text{Eq. 18}$$

Where ABS_{GI} is the gastrointestinal absorption fraction, representing the proportion of an ingested chemical absorbed through the GI tract. For many organic compounds, including PAHs, the guidance assumes full absorption via ingestion (ABSGI = 1 or 100%). In this study, because chemical-specific

data were unavailable for most PAHs, an absorption factor of 58% was adopted, corresponding to the starch-based absorption rate recommended for PAHs (the alternative dietary value being 89%). For metals, an ABS_{GI} of 10% was applied to elements not specifically listed in the (US EPA, 2004) guidance document; these details are in Table 6.3.

Table 6.6: The PEF values, oral cancer slope factors (CSF_ing), and inhalation unit risks (IUR_inh) for Carcinogenic PAHs obtained from the US EPA (ASTDR, 2022; IRIS, 2017).

PAHs	PEF (unitless)	CSF_ing (mg/kg-day)	IUR_inh (µg/m3)
Benzo(a)pyrene	1	2	0.001
Benzo[a]anthracene	0.1	0.2	0.0001
Chrysene	0.01	0.02	0.00001
Benzo[b]fluoranthene	0.1	0.2	0.0001
Benzo[k]fluoranthrene	0.1	0.2	0.0001
Indeno(1,2,3-cd)pyrene	0.1	0.2	0.0001
Dibenz[a,h]anthracene	2.4	4.8	0.0024

Cumulative Cancer Risk (CCR)

The CCR represents the combined probability of developing cancer over a lifetime from exposure to carcinogenic contaminants through all relevant pathways. This was calculated as the sum of the ILCRs for each exposure route, as shown below:

$$CCR = \sum ILCR_i \quad \text{Eq.19}$$

where $ILCR_i$ is the incremental lifetime cancer risk associated with the i^{th} exposure pathway (ingestion, dermal contact, or inhalation).

The CCR represents the overall lifetime probability of developing cancer due to exposure to carcinogenic contaminants across all pathways. The US EPA (US EPA, 1989b, 2004). and related international guidelines (CCME, 2016; WHO, 2003), consider a CCR value of $\leq 1 \times 10^{-6}$ negligible or within the acceptable risk range for regulatory purposes. Values between 1×10^{-6} and 1×10^{-4} fall within the tolerable or acceptable range, while those exceeding 1×10^{-4} indicate a potentially unacceptable risk that may require remedial or management actions. These benchmark ranges were used to interpret the cancer risk levels estimated for PAHs and heavy metals in the study area.

6.3 Results

The results from the evaluation include the physicochemical properties of surface water samples, concentrations and spatial distributions of HMs and PAHs in environmental media, alongside comparisons with national and international guideline values to evaluate potential exceedances of

health-based thresholds. Furthermore, the section outlines the toxicity of PAHs to estimate the potential carcinogenic potency of hydrocarbon contamination. Finally, estimated exposure levels and corresponding human health risk indices, both non-carcinogenic and carcinogenic, are presented to characterise the potential health implications for populations living, farming or working in proximity to the site. All raw datasets (PAHs, pXRF, ICP–OES, and sequential extraction analyses) are provided in Appendices 6.5-6.10, while the pollution indices results are in Appendices 6.11-6.13.

6.3.1 Physicochemical Properties of Surface Water

The physicochemical characteristics of surface water samples collected from the abandoned Onyeama coal mine are presented in Table 6.7. The pH of the samples ranged from 5.98 to 7.79, indicating slightly acidic to neutral conditions. The lowest pH values were recorded in samples from the mine tunnels (CWS5–CWS7), suggesting possible acid mine drainage (AMD) influence, as evidenced by the orange colouration of water emerging from the tunnel adits (Figure 6.6).

Electrical conductivity (EC) values ranged from 60 to 556 µS/cm, reflecting differences in the ionic content of the water. The highest EC was recorded at CWS1, which may indicate elevated dissolved ions resulting from the leaching of minerals from coal-bearing strata or from tailings. Total dissolved solids (TDS) showed a similar pattern, ranging from 30 to 129 ppm, and were generally within the acceptable range for freshwater quality.

Dissolved oxygen (DO) values spanned 40.4% to 74.9%, with markedly lower concentrations in tunnel waters. This reduction is indicative of limited aeration and potential microbial oxygen consumption within stagnant mine drainage systems. The lowest DO levels were recorded in the mine adit. Temperature ranged from 28.6°C to 32.4°C, aligning with the warm tropical setting of the study area and showing minimal spatial variation.

These measurements reveal that while surface waters around the mine are mostly neutral and moderately mineralised, the moderately acidic, iron-stained tunnel effluents point to active geochemical alteration processes associated with AMD generation and discharge.

Table 6.7: Physicochemical Properties of surface water samples collected at the abandoned coal mine site. The DOC for the samples were measured in the laboratory.

Sample Id	pH	EC (uS/cm)	TDS (ppm)	DO (%)	Temp. (°C)	DOC (mg/L)
CWS1	6.83	556	129	65.20	32.4	3.578
CWS2	7.22	60	31	66.20	31.7	2.29
CWS3	7.66	62	30	72.30	32.1	2.964
CWS4	7.79	196	88	67.40	31.3	2.434
CWS5 (Tunnel 1) T1	5.98	186	92	40.40	30.7	3.388
CWS6 (Tunnel 2) T2	6.05	184	93	51.50	30.8	6.884
CWS7 (BTW T1&T2)	6	180	90	54.40	30.2	2.883
CWS8	6.78	162	80	68.10	30.8	1.899

CWS9	7.64	130	65	74.90	30.5	3.021
CWS10 Well water	7.03	NR	NR	NR	28.6	8.011

NR - Not Recorded

Figure 6.6: Mine water discharge points at the abandoned Onyeama coal mine. (1) Tunnel 1 (Adit 1), (2) Tunnel 2 (Adit 2), and (3) surface flow between the two tunnels. The orange colouration indicates the influence of acid mine drainage and iron oxide precipitation.

The DOC varies across the sampled locations, with relatively low DOC levels observed in the surface stream samples (CWS2–CWS5), where values generally remained below 3.1 mg/L. These modest concentrations suggest limited input of organic matter from surface runoff or biological activity in those locations.

In contrast, elevated DOC values were recorded in samples associated with the mine tunnels and the groundwater, which is the well water sample. Tunnel 2 (CWS7) exhibited a markedly high DOC concentration of 6.884 mg/L, while the well water sample (CWS10) showed the highest level at 8.011 mg/L. The enrichment in DOC at these points may reflect the dissolution of organic-rich materials within subsurface strata, microbial degradation of coal residues, or prolonged contact between water and organic-bearing sediments.

Moderate DOC levels in Tunnel 1 (CWS6; 3.388 mg/L) and the drainage between the two tunnels (CWS8; 2.883 mg/L) indicate partial organic contribution from mine effluents to adjacent watercourses. The observed pattern underscores the influence of subsurface and mine-related processes on organic carbon mobilisation in the study area, distinguishing these sources from the more dilute, oxidised surface waters.

6.3.2 Field pXRF Measured Metal Concentrations

The field XRF analysis of major and trace metals measured at the AML revealed clear concentration contrasts among soils, tailings, and the control sample, as illustrated in Figure 6.7 and summarised in Table 6.8. Iron and Ti were the dominant elements across all samples, confirming their potential

abundance in the geology of the study area. Fe showed the widest range (5,443–32,224 mg/kg in soils; 178–33,300 mg/kg in tailings) and several outliers. The tailings generally contained higher and more variable metal concentrations than the soils, reflecting their origin from concentrated mine waste. In contrast, the control soil Fe (18,071 mg/kg) and Ti (8,597 mg/kg) are the principal constituents, and lower values for most HMs, Pb (18 mg/kg) and Zn (54 mg/kg), providing a clear compositional distinction from the mine-impacted materials.

Lead displayed particularly striking variability, with mean concentrations increasing from 19.6 mg/kg in soils to 421 mg/kg in tailings, and a maximum tailings value of 1,624 mg/kg, indicating localised enrichment likely linked to ore residues. Chromium and Cu were moderately elevated in both matrices, while As and Cd occurred at low to near-detection levels.

Notably, the boxplot highlights the dominance of Fe, Ti, Zr, and Ba in both soils and tailings, while Cd, As, and Ni occurred at near-detection levels. Metals such as Pb, Cr, and Cu displayed skewed distributions with distinct outliers, reflecting localised accumulation within specific sampling points. The data collectively indicate marked compositional diversity across sample types and suggest different degrees of metal association with the mine-derived materials.

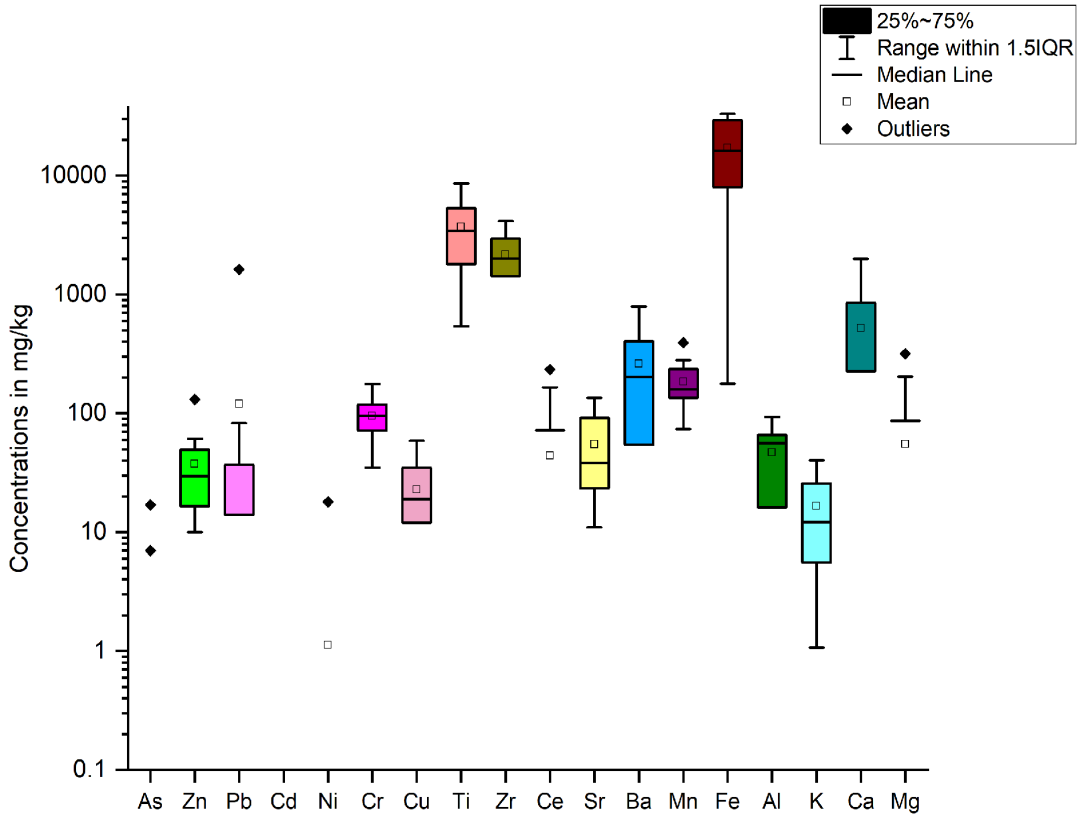

Figure 6.7: HMs and major elements concentrations at Onyeama abandoned coal mine field measurement using pXRF

Table 6.8: Descriptive statistics of heavy metals and major element concentrations measured using pXRF (mg/Kg)

Statistical Parameters	*As*	*Zn*	*Pb*	*Ni*	*Cr*	*Cu*	*Ti*	*Zr*	*Ce*	*Sr*	*Ba*	*Mn*	*Fe*	*Al*	*K*	*Ca*	*Mg*
								Tailings(n=4)									
Minimum	0	10	0	0	55	7	540	0	0	11	0	127	178	0	6.1	0	0
Maximum	7	61	1624	18	177	39	6639	3642	165	104	607	393	33300	93.1	38.4	1133	317.6
Mean	1.8	36	421.3	4.5	106.3	21	4455.5	2383.5	81.5	71.5	354	235.8	19181.8	55	23.9	283.3	130.5
Standard Deviation	3.5	23.2	802.3	9	51.5	13.3	2685	1624.8	94.1	43.4	254.8	125.3	15635.2	39.5	13.7	566.5	157.6
Standard Error	1.8	11.6	401.2	4.5	25.8	6.6	1342.5	812.4	47.1	21.7	127.4	62.7	7817.6	19.8	6.8	283.3	78.8
Median	0	36.5	30.5	0	96.5	19	5321.5	2946	80.5	85.5	404.5	211.5	21624.5	63.4	25.5	0	102.1
Sample Variance	12	538	643764	81	2656	177	7209095	2639919	8859	1884	64930	15705	244459059	1561	187	320922	24836
Kurtosis	4	-3.2	4	4	1.7	1.8	3.1	3.3	-6	0.9	2.2	-2.3	-3	1.9	0.4	4	-3.6
Skewness	2	-0.1	2	2	1	0.9	-1.7	-1.7	0	-1.3	-1.1	0.6	-0.5	-1.2	-0.6	2	0.4
Range	7	51	1624	18	122	32	6099	3642	165	93	607	266	33122	93.1	32.3	1133	317.6
Control soil sample (n=1)	0	54	18	0	143	20	8597	4159	234	135	510	276	18071	90.5	38.2	1996	0
								Soil (n=11)									
Minimum	0	10	0	0	35	0	681	884	0	20	0	74	5443	0	1.1	0	0
Maximum	17	131	83	0	130	59	5788	3409	145	106	794	266	32224	91.1	40.5	1999	191.1
Mean	1.5	36.8	19.6	0	86.7	23.9	2995.6	1900.3	13.2	41.5	205.2	157.8	16275.5	40.5	12	474.3	33.1
Standard Deviation	5.1	33.9	26.2	0	32.1	18.7	1732.8	719.2	43.7	27.4	231.6	54.6	10120.6	27.7	11.9	633	73.8
Standard Error	1.5	10.2	7.9	0	9.7	5.6	522.5	216.9	13.2	8.3	69.8	16.5	3051.5	8.4	3.6	190.8	22.3
Median	0	26	10	0	81	19	2616	1675	0	34	140	152	15697	37.3	8.7	300	0
Sample Variance	26	1151	685	0	1028	348	3002612	517281	1911	751	53622	2978	102425881	769	142	400635	5449
Kurtosis	11	6.9	2.6	0	-0.8	-0.5	-1.2	0.6	11	2.4	3.9	0.3	-1.2	-0.7	2.3	2.8	2.1
Skewness	3.3	2.5	1.6	0	-0.3	0.7	0.4	0.9	3.3	1.8	1.8	0.4	0.6	0.2	1.5	1.8	1.9
Range	17	121	83	0	95	59	5107	2525	145	86	794	192	26781	91.1	39.4	1999	191.1

6.3.3 Heavy Metal Concentrations – Soil and Sediment Samples

Figure 6.8 summarises the concentrations of HMs determined from laboratory analysis of soil, tailings and sediment samples collected in the arable lands around the AML. The results showed distinct variability across the analysed samples, with elements such as Fe, Al, Ca, and K prevalent at relatively higher concentrations, while trace elements, including As, Cd, and Ni, were present at much lower levels. The spread and distribution patterns highlight differences in metal abundance and potential geochemical associations within the environmental samples.

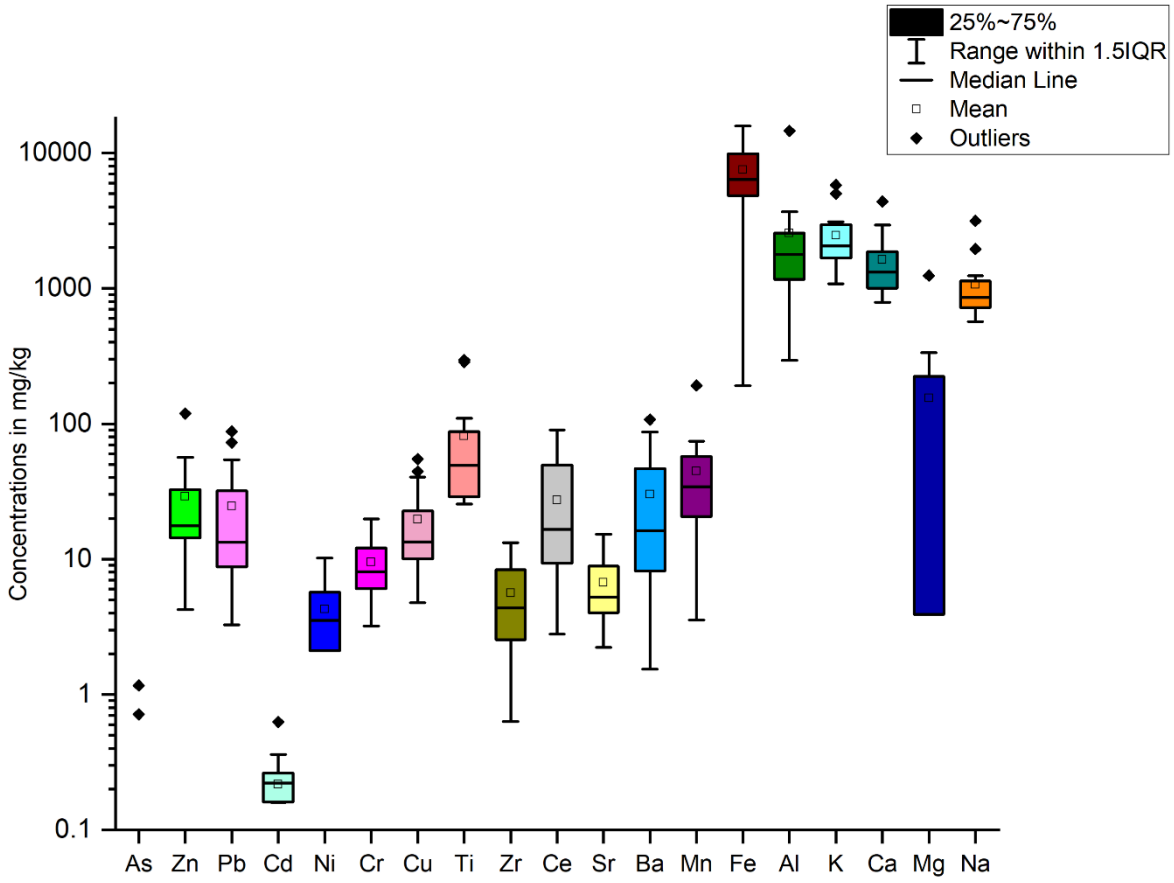

Figure 6.8: HMs and major elements concentrations (for soil, sediment and tailings) at Onyeama abandoned coal mine land determined in the laboratory using ICP-OES

Figure 6.8: HMs and major elements concentrations (for soil, sediment and tailings) at Onyeama abandoned coal mine land determined in the laboratory using ICP-OES. The descriptive statistics of the different environmental samples are outlined in Table 6.9. Major elements such as Fe, Al, Ca, and K consistently dominated all matrices, reflecting their geochemical prevalence in the AML environment.

Soils exhibited wide concentration ranges, with Fe (4,102.5–15,821 mg/kg) and Al (1,006–14,545 mg/kg) showing high variability. Mean values for Mn, Zn, Pb, and Cu (40.6, 35.1, 36.7, and 25.6 mg/kg, respectively) indicate moderate enrichment, while As and Cd remained very low (≤0.3 mg/kg). As illustrated in Figure 6.9, Fe and Al were dominant across all soil samples, with notably higher

concentrations in CSS02, CSS03, and CSS09. Mn and Ba were relatively elevated in CSS04 and CSS08, while Zn and Pb showed variable but appreciable levels, particularly in CSS01 and CSS05. Trace elements such as Cu, Cr, and Ni were present in moderate amounts throughout, whereas Cd and As were near the detection limits. The control sample (CSS) exhibited a similar elemental profile but with generally lower concentrations, suggesting localised enrichment of mine-affected soils around the Onyeama site.

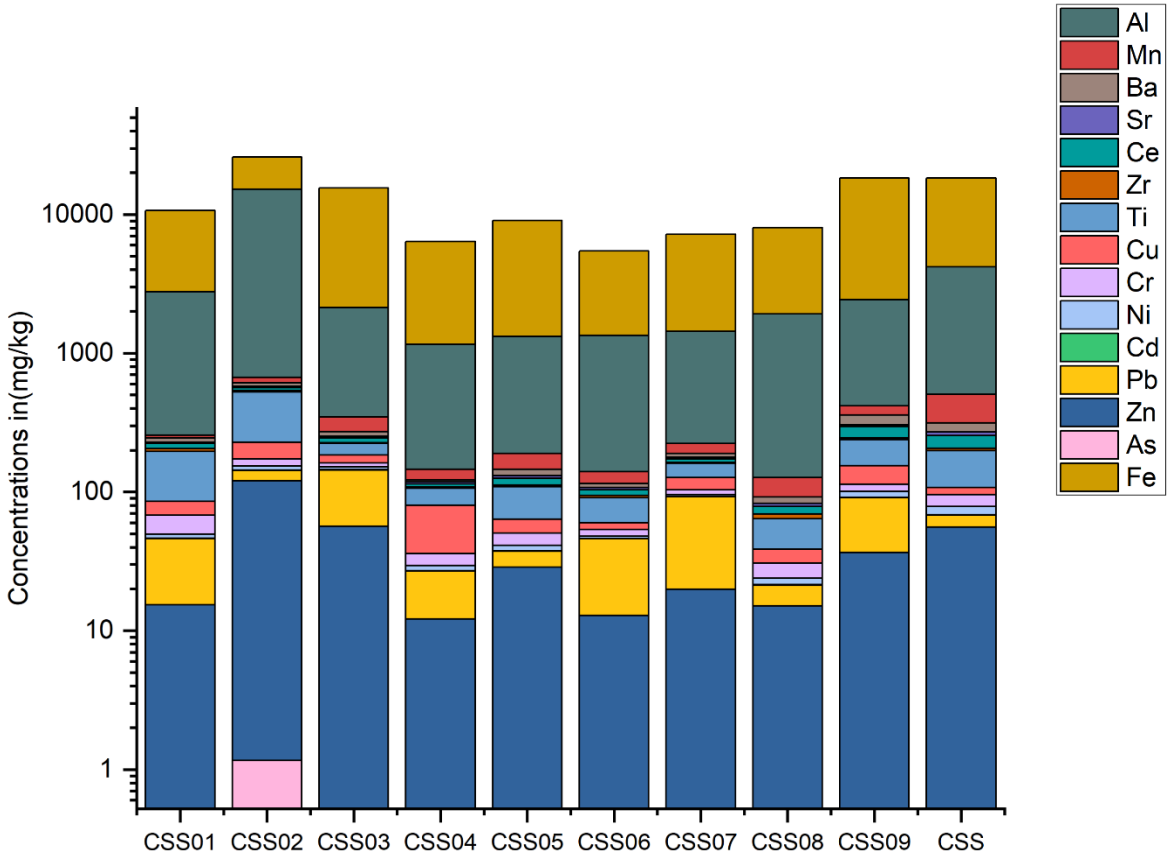

Figure 6.9: Distribution of HMs in soil samples from the Onyeama coal mine area, showing variations in elemental composition across sampling locations (CSS01–CSS09) and the control soil (CSS).

In the tailings samples, Fe and Al remained the dominant constituents, with mean concentrations of 6,836 mg/kg and 2,272 mg/kg, respectively (Table 6.9). Mn and Zn showed moderate enrichment, averaging 46.1 mg/kg and 21.0 mg/kg, while Pb, Cu, and Cr were generally lower but spatially variable. Fe and Al concentrations were consistently high across all tailings samples (Figure 6.10), reflecting the mineralogical composition of the mining wastes. CTS02 exhibited slightly higher levels of Fe and Al, followed by CTS07 and CTS08, compared to other locations, whereas Zn, Pb, and Cu were most prominent in CTS03, CTS04, CTS06, CTS07, and CTS08. Minor elements such as Ni, Cd, and As occurred at near-detection limits across all samples. The coal sample (CS EG) showed comparatively

higher Ti proportions than at other locations but lower Fe and Al, suggesting compositional differences between the waste materials and the raw coal source.

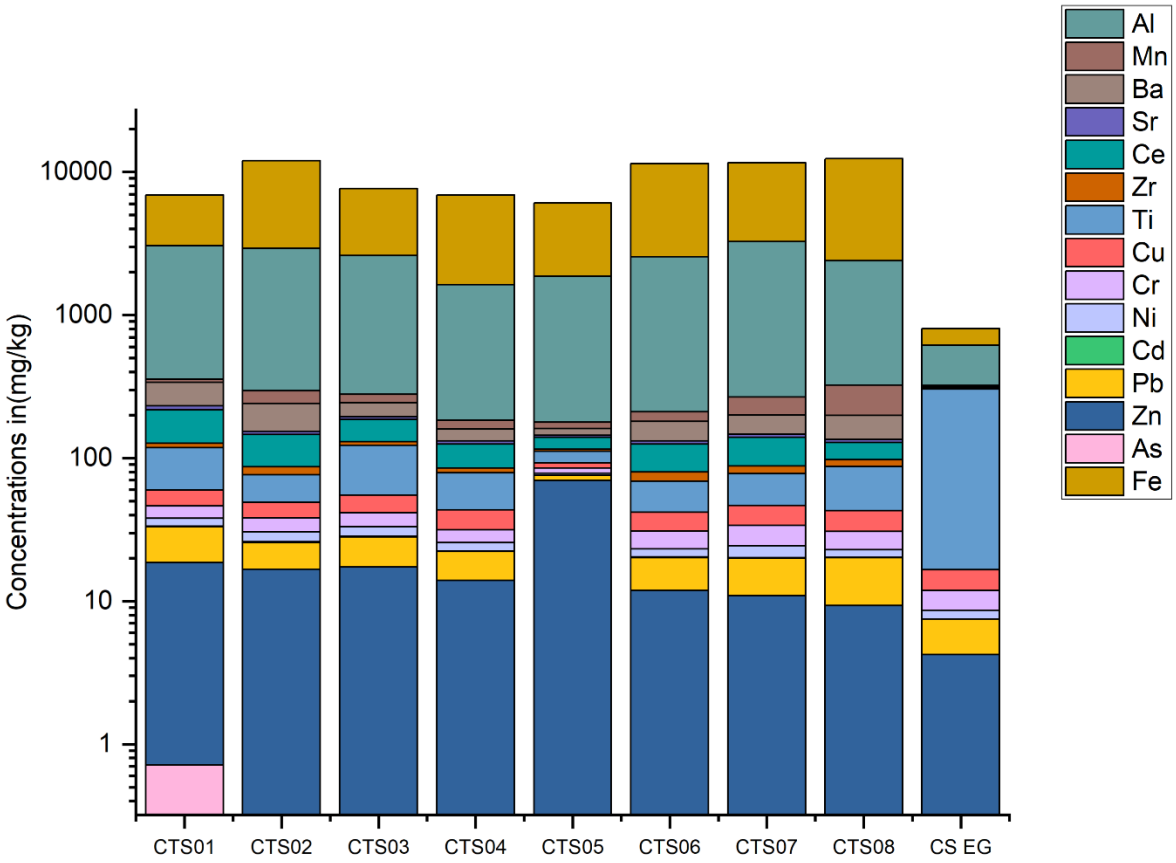

Figure 6.10: HMs concentration in tailings samples (CTS01–CTS08) from the AML, illustrating variability in Fe, Al, Zn, Pb, and other elements relative to the coal sample (CS EG).

In sediments, Fe and Al were again the most abundant elements, with mean concentrations of 4,861 mg/kg and 732 mg/kg, respectively. As shown in Figure 6.11, Fe exhibited distinct elevation in CSD02, CSD06 and CSD08, while Al was comparatively higher in CSD02, CSD04, CSD06, CSD07 and CSD08. Manganese and Zn were present at low levels across most sites, with slightly higher levels in CSD06. Other metals, including Cu, Cr, Ni, and Pb, occurred in trace or minor quantities, displaying little variation among samples. Cd and As remained below or near detection limits throughout. The compositional pattern indicates broadly similar metal distribution across the sediment samples, with localised enrichment in Fe and Al, likely reflecting depositional input from mine drainage channels.

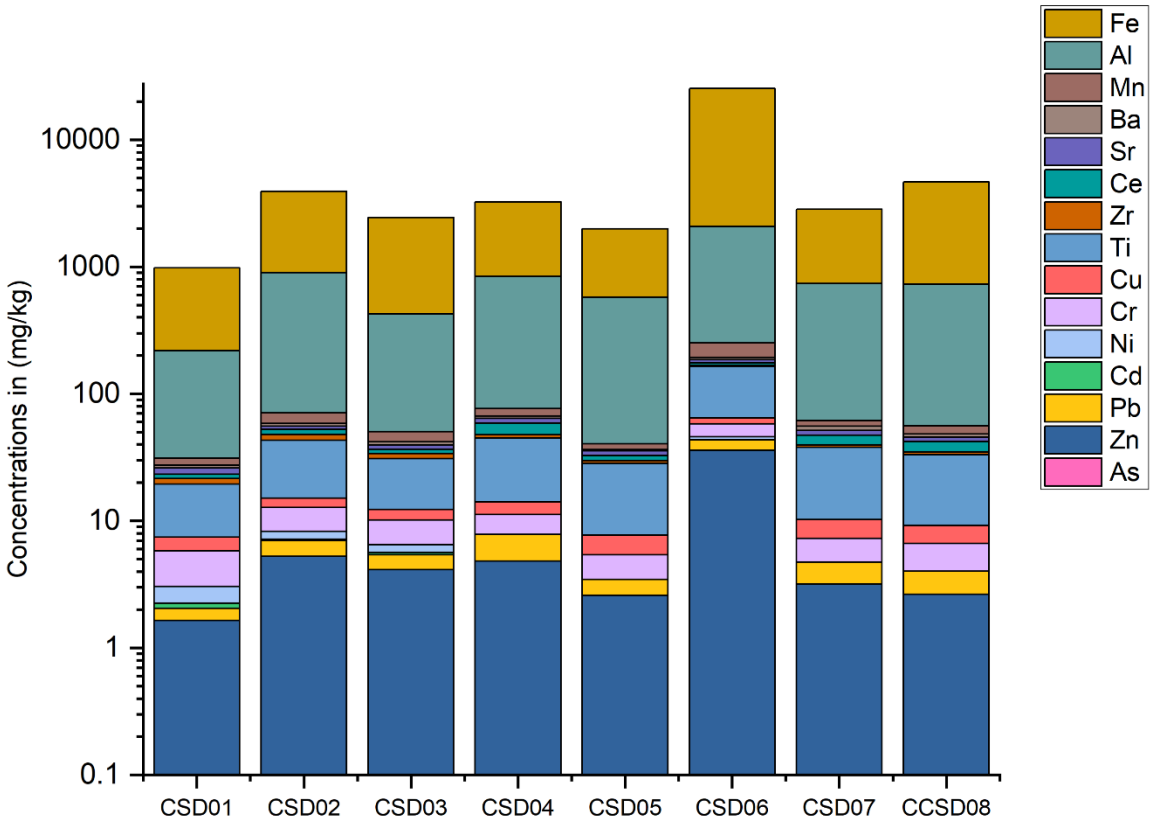

Figure 6.11 Distribution of HMs in sediment samples (CSD01–CSD08) collected upstream and downstream of the AML, highlighting localised enrichment in Fe and Al relative to other metals.

Across all matrices, Fe and Al dominated the elemental composition, while Mn, Zn, Pb, and Cu showed moderate enrichment, particularly in soils and tailings. Sediments contained comparatively lower HM levels than tailings and soil but reflected similar compositional patterns, suggesting a common geochemical source influenced by mine drainage and weathering processes.

Table 6.9: Summary of metal concentrations (mg/kg) in soils, tailings, and sediments from the Onyeama coal mine area, including descriptive statistics, background values, and soil quality guideline (SQG) limits.

Statistical Parameter	*Mn*	*Zn*	*Pb*	*Ni*	*Cr*	*Cu*	*Ti*	*Zr*	*Ce*	*Sr*	*Ba*	*Cd*	*As*	*Al*	*Fe*	*Mg*	*Ca*	*Na*	*K*
										Tailings (n=8)									
Minimum	16.6	9.3	5.7	2.6	5.9	7.9	18.6	3.8	24.6	4.5	16.9	0.1	0	1444.2	3838.8	0	588.1	624.4	1853.4
Maximum	125	69.9	14.5	4.7	9.3	13.5	67.7	10.9	89.7	14.2	107.1	0.2	0.7	2978.9	9958	634	1078.3	1094.5	3095.1
Mean	46.1	21	9.5	3.7	7.7	11.6	38.8	8.4	49.8	7.8	56.5	0.2	0.1	2271.5	6835.9	221.9	897	787.8	2267.7
Median	32	15.3	9	3.8	7.9	11.9	33.3	9.3	48.3	7.1	51	0.2	0	2333.6	6807	173.6	891.2	735.4	2018.1
Standard Error	12.9	7.1	0.9	0.3	0.4	0.7	6	0.9	7.1	1	10.3	0	0.1	183.4	875	68.9	52.9	57.4	186.8
Standard Deviation	36.5	20	2.6	0.9	1.1	1.8	16.9	2.4	20	2.9	29.2	0	0.3	518.6	2474.8	194.8	149.5	162.4	528.4
Sample Variance	1335	401	7	1	1	3	287	6	401	8	855	0	0	268985	6124878	37937	22348	26387	279164
Kurtosis	2.9	7.4	1.7	-2.4	0.1	1.7	-0.5	0.3	1.6	3.9	0	-1.2	8	-0.7	-2.3	2.7	2.3	0.4	-0.5
Skewness	1.7	2.7	0.7	-0.1	-0.7	-1.2	0.8	-1	1	1.7	0.6	-0.4	2.8	-0.4	0	1.5	-1.2	1	1.1
Range	108.5	60.7	8.8	2.1	3.4	5.6	49.1	7.2	65	9.7	90.2	0.1	0.7	1534.8	6119.1	634	490.1	470.2	1241.8
										Soil (n=9)									
Minimum	10.9	12.2	6.1	1.9	5.8	6.3	25.5	2	5.7	3.6	4.3	0.2	0	1006	4102.5	0	790.6	569.3	1084.1
Maximum	74.1	119	87.7	10.2	19.7	54.8	296.1	13.2	50.7	9	53.1	0.6	1.2	14544.7	15821	290.9	2945.7	956.5	2824.6
Mean	40.6	35.1	36.7	4.8	10.9	25.6	76.8	5.6	17.9	5.7	19.7	0.3	0.1	3021.5	8521.2	50.4	1543	787.6	1766.5
Median	35.1	19.9	30.7	3.3	9.2	22	39.1	3.6	13.2	5.1	14.6	0.2	0	1783.5	7726.1	2.2	1444.9	792.9	1739.6
Standard Error	6.8	11.5	9.6	1	1.7	5.7	29.1	1.3	4.7	0.7	5.3	0	0.1	1449.8	1325.8	33.9	214.7	45.1	185.4
Standard Deviation	20.4	34.6	28.9	3.1	5.2	17.1	87.2	3.8	14	2	15.9	0.1	0.4	4349.4	3977.3	101.6	644.2	135.3	556.2
Sample Variance	416	1197	834	10	28	293	7602	15	196	4	253	0	0	18916969	15819284	10329	415024	18294	309405
Kurtosis	-0.8	4.9	-0.6	-0.6	-0.6	-0.9	6.3	0.5	3.8	-0.3	1.5	4.4	9	8.7	-0.3	4.1	2.3	-0.8	0.3
Skewness	0.3	2.2	0.8	1	0.9	0.6	2.4	1.2	1.9	1	1.4	1.9	3	2.9	0.9	2.1	1.3	-0.4	0.9
Range	63.2	106.8	81.6	8.3	14	48.5	270.6	11.2	45	5.4	48.8	0.5	1.2	13538.6	11718.5	290.9	2155.1	387.2	1740.5
CSS (n=1)	191.4	56	12.1	10.2	17.3	11.6	91.5	8	48.3	15.3	44.2	0	0	3692.1	14101	1241.7	4373.7	1952.3	5000.9

CS (n=1)	3.6	4.2	3.3	0	3.2	4.8	285.7	2.8	0	4	4.7	0	0	293.8	190.7	0	2522.1	3150.7	5801.4
*SBVs	330	48	16	13	<37	17	2200	190	64	120	440	0.098	1.5	47,000	18,000	13,300	30,000	28,900	28,000
**SQGs	–	250	61	45	64	63	–	–	–	–	759	1.4	12	–	–	–	–	–	–
Sediment (n=8)																			
Minimum	3.7	1.6	0.4	0	2	1.6	12	1.4	1.6	2.8	0.6	0	0	187.3	758.3	0	311.1	414.3	702.4
Maximum	57.5	35.8	7.5	2.4	12.4	6.4	100	4.8	11.5	9.2	8.9	0.2	0	1821.3	23251.5	296.4	1748.8	925.3	1597.7
Mean	13.7	7.5	2.2	0.6	4.2	2.9	32.7	2.6	5.7	4.2	3.3	0.1	0	732.3	4861.4	37	841.7	609.9	1052.6
Standard Error	8.1	3.6	1.5	0.4	3.1	2.5	25.9	2.4	6.1	3.3	2.7	0	0	674.2	2244	0	674.4	594.3	965.6
Median	6.3	4.1	0.8	0.3	1.2	0.5	9.8	0.4	1.2	0.8	0.9	0	0	172.5	2649.1	37	163.4	60.1	113.5
Standard Deviation	17.9	11.5	2.3	0.8	3.4	1.5	27.8	1.2	3.3	2.2	2.5	0.1	0	488	7492.8	104.8	462.3	170	321.2
Sample Variance	322	132	5	1	11	2	774	1	11	5	6	0	0	238152	56142771	10981	213722	28894	103149
Kurtosis	7.4	7.7	5.6	2	6.8	6.2	6.9	0	-0.5	5.4	3.9	-2	0	4.2	7.6	8	1	0.4	-0.3
Skewness	2.7	2.8	2.3	1.4	2.5	2.4	2.6	0.9	0.5	2.3	1.8	0.7	0	1.8	2.7	2.8	1.1	0.9	0.8
Range	53.8	34.2	7.1	2.4	10.4	4.7	87.9	3.4	9.9	6.4	8.2	0.2	0	1633.9	22493.2	296.4	1437.8	511	895.4
*SBVs	400	7 – 38	4 – 17	9.9	7 – 13	10 – 25	–	–	–	49	0.7	0.1 – 0.3	1.1	2,600	9,900 – 18,000	–	–	–	–

*Soil Background Values – source: (Buchman, 2008) and (S. R. Taylor & McLennan, 1985) (for the values in bold)

**Soil Quality Guidelines – source: CCME: Canadian Council of Ministers of the Environment soil quality guidelines, (CCME, 1999)

***Sediment Background Values - (Buchman, 2008)

+Control Soil Sample

++Coal sample

6.3.4 Comparison with Guideline and Background Values

Measured HMs in the soil and tailings samples were compared with background and SQG values (Table 6.9). Sediment samples were compared with background values. The Canadian soil quality guidelines for the protection of the environment and Human Health (CCME, 1999, 2010) were adopted, as Nigeria does not have established national guidelines. The potential for environmental and human health risks was evaluated by determining whether contaminant levels exceed established safety or quality limits. The limits set for agricultural and residential/ parkland were used for comparison. Several metals exceeded natural background levels but remained below SQG thresholds.

In soils, Fe and Al showed very high mean concentrations (8,521 and 3,022 mg/kg, respectively), though both were below the upper crustal background levels reported for typical soils. In contrast, Mn, Zn, Pb, and Cu displayed enrichment relative to their background values (330, 48, 16, and 17 mg/kg, respectively). The mean Pb concentration (36.7 mg/kg) exceeded the soil background (16 mg/kg) but remained below the SQG value (61 mg/kg). Copper also surpassed its background level, indicating moderate accumulation likely influenced by mine-derived particulates. Chromium (10.9 mg/kg) and Ni (4.8 mg/kg) were below their respective SQG thresholds (64 and 45 mg/kg), while Cd and As remained very low across all matrices, far below both background and guideline limits.

Tailings samples exhibited consistently higher Fe (6,836 mg/kg) and Al (2,272 mg/kg) compared to sediments, but these elements generally reflected mineralogical dominance rather than contamination. Notably, Mn and Zn in tailings (means = 46.1 and 21.0 mg/kg) were below soil background levels, while Pb, Cu, and Cr were within acceptable limits.

Sediment samples contained lower overall metal concentrations, although the mean of Fe (4,861 mg/kg) and Al (732 mg/kg) remained elevated relative to background values for unimpacted sediments. Trace metals such as Pb (2.2 mg/kg), Cd (0.1 mg/kg), and As (<0.1 mg/kg) were below both background and SQG levels, indicating limited accumulation.

In general, the soils around the mine exhibited moderate enrichment in Mn, Zn, Pb, and Cu, whereas tailings and sediments displayed lower but detectable levels of the same metals. These findings suggest localised contamination within the mine environment, with concentrations largely remaining below guideline thresholds for environmental and human health concerns.

6.3.5 Heavy Metal Concentrations - Water Samples

Concentrations of dissolved and total metals in surface and groundwater samples from the Onyeama coal mine area are presented in Table 6.10 and illustrated in Figure 6.12. The results show considerable variability across sampling locations, with Fe, Ca, Na, and K being the dominant elements in both dissolved and total fractions.

Dissolved metal concentrations ranged widely, with Fe (62.1–8,056.1 µg/L) showing the greatest variability and highest mean (2,731.6 µg/L). This mean concentration exceeds both the WHO (1,000 µg/L) and NSDWQ (300 µg/L) limits for drinking water guideline values, indicating significant Fe enrichment in mine-impacted waters. Similarly, the mean of Mn (256.4 µg/L) exceeded the NSDWQ guideline value of 200 µg/L in several samples, Ba (780.6 µg/L) exceeded the NSDWQ limit (700 µg/L) but remains below the WHO guideline (1300 µg/L), while Al (191.4 µg/L) approached the WHO guideline value of 200 µg/L. Calcium and Na occurred at particularly high concentrations (mean: 13,711.8 and 30,295.7 µg/L, respectively), reflecting mineral dissolution and water–rock interactions within the coal-bearing strata. Trace metals such as Zn, Cu, and Sr remained below their respective drinking water guideline values despite occurring at relatively elevated concentrations. Cadmium, Ni, and Pb were present at very low concentrations, with mean values of 0.3, 0.0, and 0.6 µg/L, respectively, all well below their respective guideline thresholds. Although Hg concentrations were generally low, the maximum dissolved concentration (140.2 µg/L) substantially exceeded the WHO guideline of 6 µg/L, indicating a localised enrichment event requiring further investigation.

The control water sample (WWS) generally exhibited lower concentrations of most dissolved metals compared with the mine-impacted waters. For example, dissolved Fe in the control water was 40.4 µg/L compared with a mean of 2,731.6 µg/L in mine-impacted samples, while dissolved Al was 177.5 µg/L compared with a mean of 191.4 µg/L. However, Ba (871.5 µg/L) and some major ions, including Ca, Na, and K, were substantially elevated in the control sample, suggesting that regional geological controls and natural groundwater chemistry also contribute to water composition.

Total metal concentrations followed a similar pattern but were generally higher than dissolved concentrations, reflecting the contribution of particulate-bound metals within the water column. Iron again dominated the metal profile with concentrations ranging from 1,286.5 to 13,077.0 µg/L and a mean concentration of 4,849.7 µg/L, substantially exceeding both WHO and NSDWQ drinking water limits. Manganese and Al (mean values of 284.6 µg/L and 400.2 µg/L, respectively) also exceeded their respective guideline values, highlighting the importance of particulate-associated transport. However, Ba (672.7 µg/L) is below both the NSDWQ and WHO guideline values. Other metals, including Zn, Cu, Ni, Pb and Cd, remained below their respective drinking water standards, although Zn exhibited relatively high concentrations (mean: 464.9 µg/L), reflecting its association with mine-derived materials.

Comparison with the control sample further demonstrated enrichment of Fe, Mn, Al, and Zn in mine-impacted waters, supporting the interpretation that mine drainage and weathering of coal-associated waste materials are important contributors to water contamination in the site. The elevated concentrations of Ba (1040.1 µg/L) and major ions, Ca (123,719.6 µg/L), Na (36,073.1 µg/L), K (151,465.8 µg/L), and Mg (28,905.2 µg/L) suggest that regional hydrogeological and lithological controls contribute significantly to groundwater chemistry.

As illustrated in Figure 6.12, Fe, Al, and Ba dominated the metal composition across the sampled waters, with particularly high Fe concentrations observed in CWS5 and CWS6, which were samples from the two mine adits (Tunnels 1 and 2). CWS7 was from the stream receiving drainage from both tunnels and also recorded elevated Fe and Al levels, indicating a strong geochemical influence from the mine effluent. Mn and Sr were moderately elevated in CWS4 and CWS8, while Pb, Cd, and Ni occurred in trace amounts across all sites. The well water sample (WWS) exhibited comparatively lower Fe but higher Ba and Al, suggesting minor compositional differences between groundwater and surface mine drainage sources.

Summarily, the water chemistry indicates elevated Fe, Mn, and Al levels consistent with mine drainage influence, while most trace metals remained within international and national guideline thresholds. The relative difference between dissolved and total metal fractions implies active interactions between suspended particulates and the aqueous phase within the mine drainage system.

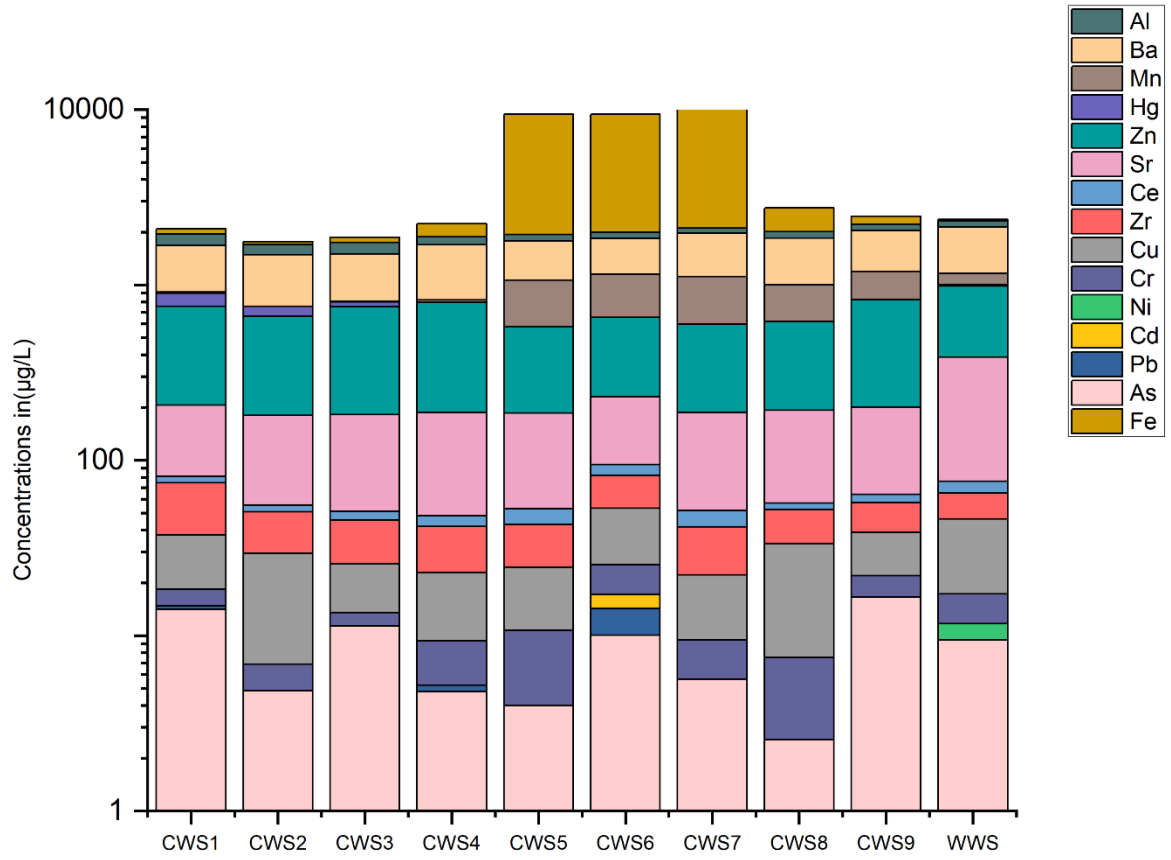

Figure 6.12: Distribution of heavy metals (HMs) in surface water from the Onyeama coal mine area. Samples CWS1–CWS4 and CWS8–CWS9 were collected from the Ekuku River, while CWS5 and CWS6 were obtained from the mine adits, which exhibited elevated Fe and Al concentrations in the discharges. Sample CWS7 was collected from the receiving stream located between the two adits, which drains into the Ekulu River.

Table 6.10: Summary statistics of dissolved and total metal concentrations (µg/L) in surface water samples from the Onyeama abandoned coal, compared with World Health Organisation (WHO) and Nigerian Standard for Drinking Water Quality (NSDWQ) guideline limits.

	As	*Zn*	*Pb*	*Cd*	*Ni*	*Fe*	*Cr*	*Cu*	*Ti*	*Zr*	*Ce*	*Sr*	*Ba*	*Hg*	*Mn*	*Al*	*Mg*	*Ca*	*Na*	*K*
Dissolved Metals (n=9)																				
Min	2.6	394.0	0.0	0.0	0.0	62.1	2.0	12.2	0.0	18.5	4.6	124.8	689.8	0.0	0.0	142.5	0.0	7162.4	23507.7	17169.1
Max	16.6	626.2	4.2	2.9	0.0	8056.1	8.2	28.0	0.0	36.6	12.5	138.6	871.5	140.2	518.3	270.8	0.0	27742.7	42741.2	42186.8
Mean	8.2	499.1	0.6	0.3	0.0	2731.6	4.6	18.3	0.0	22.3	7.4	133.1	780.6	31.4	256.4	191.4	0.0	13711.8	30295.7	26858.3
SD	5.0	90.8	1.4	1.0	0.0	3695.6	2.0	5.9	0.0	6.2	2.8	5.0	74.4	52.0	237.3	44.0	0.0	7366.3	6863.6	7765.4
WWS (Control)	9.5	596.2	0.0	0.0	2.3	40.4	5.6	29.0	0.0	18.5	11.2	311.4	980.8	24.3	153.7	177.5	29114.1	120946.1	396140.8	164369.0
Total Metals (n=9)																				
Min	3.9	405.5	0.0	0.0	0.0	632.0	2.4	11.3	0.0	18.1	6.8	122.6	616.1	0.0	22.5	166.4	0.0	5935.4	17219.1	12873.6
Max	18.5	627.9	6.3	4.3	9.4	13077.0	10.6	28.1	0.0	31.4	13.8	151.5	739.5	79.4	595.1	691.8	0.0	45377.6	54860.0	71114.4
Mean	8.9	464.9	0.8	0.9	3.3	4849.7	6.2	19.1	0.0	21.5	9.6	134.4	672.7	14.8	284.6	400.2	0.0	16865.4	28074.1	27017.7
SD	4.6	71.1	2.1	1.7	3.7	4490.5	3.3	5.9	0.0	5.4	2.6	8.4	41.7	28.3	239.4	177.0	0.0	12511.5	11401.5	17746.4
WWS (Control)	2.2	846.7	2.1	0.6	28.5	1286.5	8.8	33.3	0.0	19.0	32.5	319.4	1040.1	0.0	326.6	995.3	28905.2	127319.6	360731.5	151465.8
Water Quality Standards																				
WHO	10	3000	10	3	70	1000	50	2000	NA	NA	NA	*NA	1300	6	400	200	NA	NA	NA	NA
NSDWQ	10	3000	10	3	20	300	50	1000	NA	NA	NA	*NA	700	1	200	200	20,000	NA	200000	NA

WWS - Well water sample
WHO - World Health Organisation Guidelines for Drinking Water Quality (WHO, 2011)
NSDWQ – Nigerian Standard for Drinking Water Quality (SON, 2015)
*Neither the WHO nor the NSDWQ has established a drinking water guideline for strontium. However, Health Canada (HC, 2019) has set a guideline value of 7 mg/L (7000 µg/L) and references the U.S. EPA's non-cancer, drinking-water-based health reference level (HRL) of 1.5 mg/L (1500 µg/L) and a lifetime health advisory level of 4 mg/L for strontium in drinking water or water used to prepare food, beverages, or infant formula. Direct dermal exposure to water containing strontium is not considered a health risk.

6.3.6 PAH Concentrations – Soils Samples

PAHs were detected in all sampled matrices, with concentrations varying among compounds and the sampled media; the summary statistics are outlined in Table 6.11. The main data sets are in Appendix 6.5. The sixteen priority PAHs were identified, and their concentration profiles are presented in Figure 6.13. The data reveal marked variability in individual compound abundances, reflecting differing contamination intensities and environmental behaviours across the mine area. Nap, Flu, and Pyr exhibited the highest concentrations, while Ace, Fl, and Ant occurred at lower levels. Heavy Molecular Weight (HMW) PAHs such as BaA, Chr, BbF, and BaP were moderately abundant, indicating association with coal residues present at the site rather than combustion processes. Soils contained the highest total PAH levels, followed by tailings, while sediments recorded considerably lower concentrations.

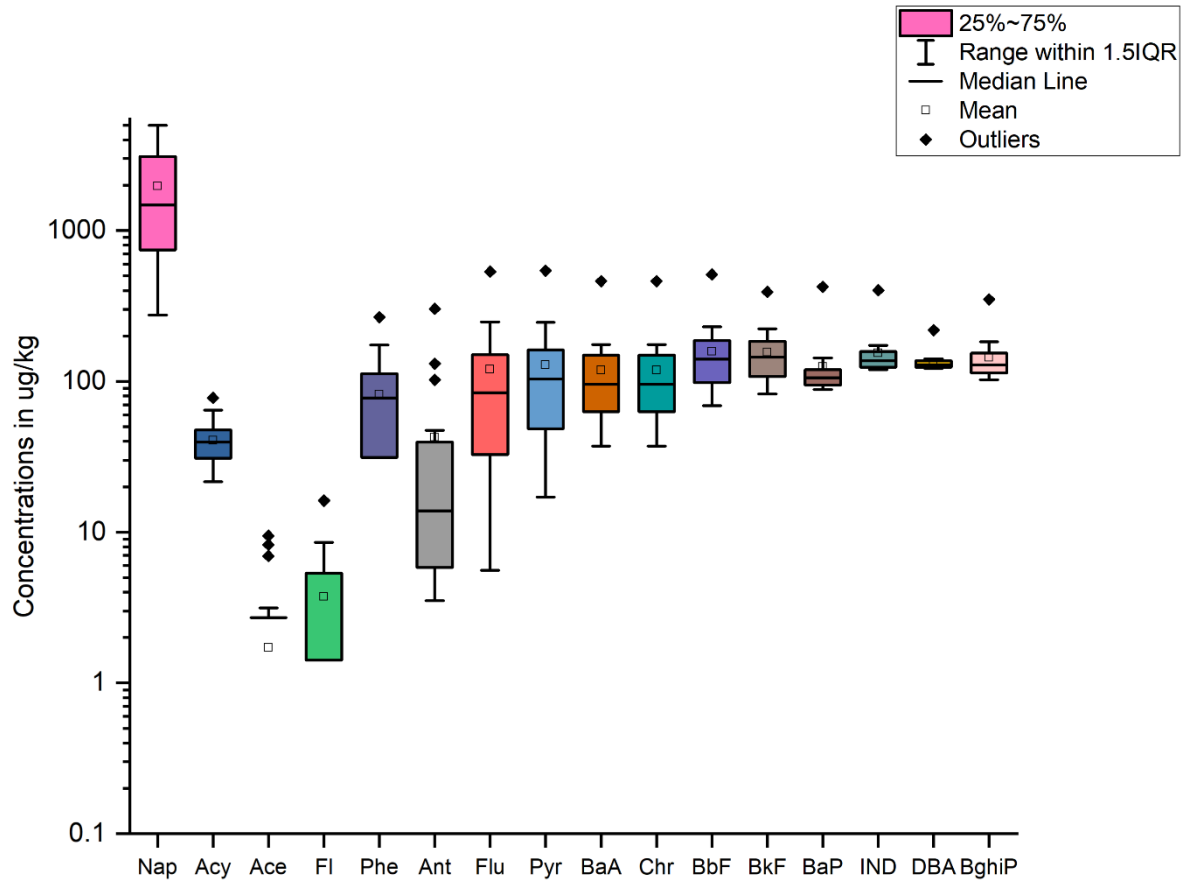

Figure 6.13: Distribution of individual PAH concentrations in the AML. Nap, Flu, and Pyr exhibited the highest concentrations, while Ace, Fl, and Ant occurred at lower levels. HMW PAHs such as BaA, Chr, BbF, and BaP were moderately abundant. indicating inputs from past coal mining processes associated with coal residues.

In soils, total PAHs ranged from 564.8 to 7,351.8 µg/kg with a mean of 2,421.6 µg/kg, dominated by Nap, Flu, and Pyr, which together accounted for a large share of the total burden. HMW compounds such as BaA, Chr, and BbF were present at notable levels, whereas Ace and Fl were relatively minor

constituents. In Figure 6.14, soils generally exhibited higher total PAH concentrations than tailings, particularly at CSS01, CSS03, CSS05, and CSS09, where Nap, Flu, and Pyr dominated.

Tailings showed mean total PAH concentrations of 1,678.5 µg/kg, characterised by the predominance of Nap, Phe, and Ant. HMW species including BbF, BaP, and BghiP were consistently detected but in lower amounts than in soils, suggesting persistent residues from past coal handling activities.

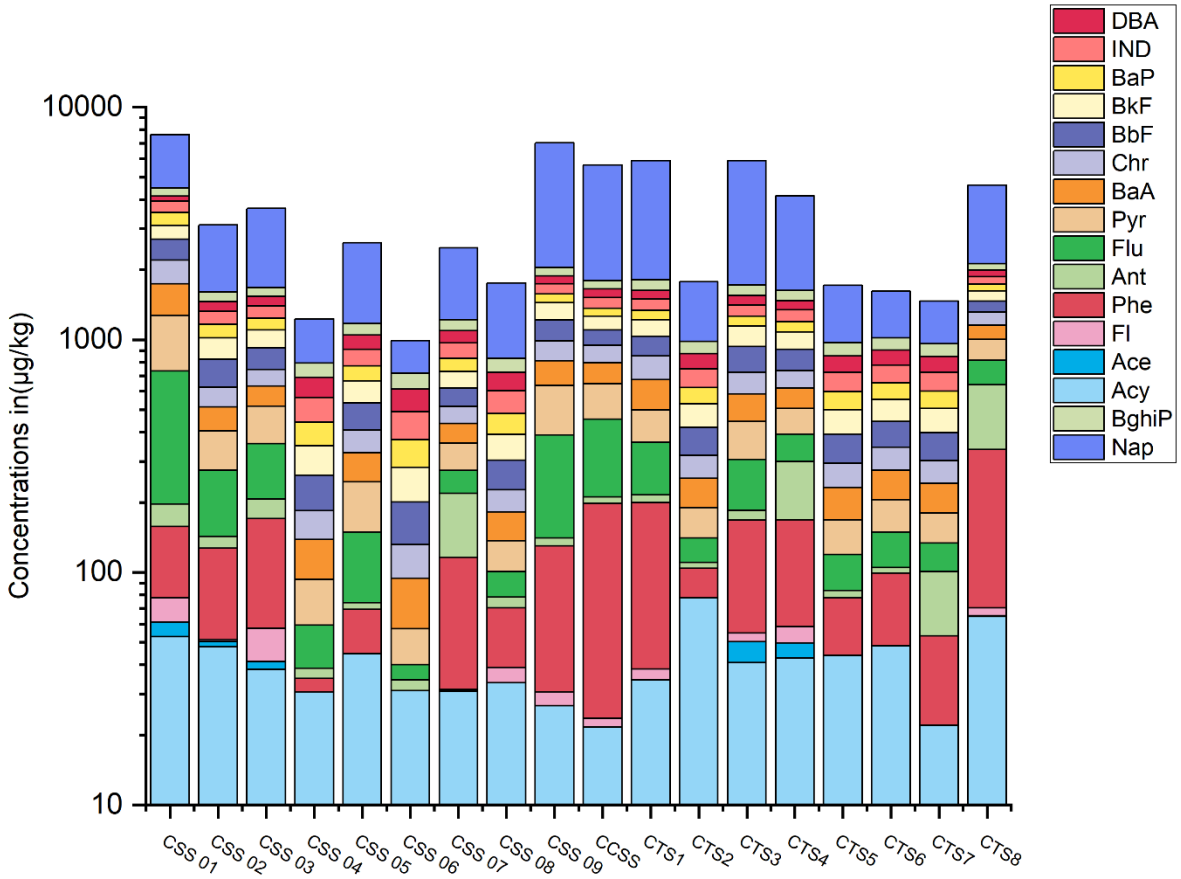

Figure 6.14: Distribution of PAH compounds in soil and tailings samples from the AML. The profiles highlight the predominance of Nap, Flu, and Pyr across all sites, while HMW compounds such as BaA, BbF, and BaP are more pronounced in tailings, indicating potential petrogenic influence from coal residues.

Tailings CTS1, CTS3, CTS4, and CTS8 displayed relatively higher concentrations than at other locations, with enrichment in Nap, Phe, Flu, BaP, and BghiP. Relatively uniform profiles were observed in other locations, though moderate enrichment in BbF, BaP, and IND was observed in CTS5, CTS6 and CTS7.

Table 6.11: Statistical summary of PAH concentrations (ug/kg) in soil, tailings, and sediment samples from the abandoned mine.

Statistical Parameter	*Nap*	*Acy*	*Ace*	*Fl*	*Phe*	*Ant*	*Flu*	*Pyr*	*BaA*	*Chr*	*BbF*	*BkF*	*BaP*	*IND*	*DBA*	*BghiP*
								Tailings n=8								
Minimum	499.8	21.9	0.0	0.0	26.2	5.7	29.9	46.4	61.4	61.4	96.8	106.7	93.4	122.8	123.7	112.4
Maximum	4168.6	77.7	9.5	8.6	266.4	302.8	174.1	187.0	175.2	175.2	212.2	207.5	119.7	157.5	137.4	182.9
Mean	1985.7	46.8	2.1	2.8	99.0	66.5	84.6	97.0	105.5	105.5	140.1	144.5	104.9	136.0	128.4	137.4
Standard Deviation	1547.2	17.3	3.8	3.3	83.4	104.4	57.3	54.1	46.8	46.8	46.8	40.8	10.7	13.1	5.2	27.3
								Soil n=9								
Minimum	276.2	26.7	0.0	0.0	0.0	3.5	5.6	17.1	37.1	37.1	68.8	82.4	88.6	119.6	122.2	102.8
Maximum	4980.8	52.9	8.3	16.2	112.4	102.4	534.9	542.2	461.7	461.7	511.2	392.6	423.8	401.8	219.0	350.1
Mean	1770.0	37.4	1.6	4.8	56.9	25.0	138.3	149.7	127.5	127.5	174.5	166.1	145.3	170.2	140.9	150.1
Standard Deviation	1470.8	9.1	2.8	6.7	42.2	32.1	167.9	163.9	132.6	132.6	139.2	99.1	106.6	88.9	30.2	77.3
Control soil	3841.7	21.6	0.0	1.9	174.8	12.2	244.7	190.8	149.0	149.0	157.2	159.5	105.2	151.4	132.3	141.2
								Sediment n=8								
Minimum	0.0	21.8	0.0	0.0	0.0	2.0	0.0	7.2	30.4	30.4	59.2	73.9	85.7	116.8	121.5	99.1
Maximum	153.7	64.4	123.1	0.0	0.3	9.7	5.5	18.3	35.7	35.7	65.7	79.6	88.7	119.2	128.5	103.5
Mean	19.2	37.4	15.4	0.0	0.0	5.3	0.9	11.1	32.0	32.0	61.0	75.5	87.3	117.6	123.4	100.3
Standard Deviation	54.4	16.2	43.5	0.0	0.1	3.2	2.0	3.5	1.9	1.9	2.6	2.2	1.1	0.9	2.3	1.6

Table 6.12: Statistical summary of PAH concentrations (µg/L) in surface and groundwater samples from the abandoned mine.

Statistical Parameter	*Nap*	*Acy*	*Ace*	*Fl*	*Phe*	*Ant*	*Flu*	*Pyr*	*BaA*	*Chr*	*BbF*	*BkF*	*BaP*	*IND*	*DBA*	*BghiP*
								Water (n=9)								
Mean	675.56	43.31	84.76	87.16	77.72	19.05	19.00	20.15	217.48	218.16	141.59	141.59	28.61	23.54	25.74	42.95
Standard Deviation	119.53	61.53	74.19	120.08	56.44	14.15	16.18	16.08	599.78	599.43	248.84	248.84	26.18	7.32	14.25	79.11
Minimum	546.30	8.72	28.41	0.85	38.87	9.81	6.92	8.82	8.62	10.97	10.46	10.46	10.96	16.11	15.54	13.23
Maximum	887.85	201.94	265.56	327.50	226.71	44.51	47.56	50.58	1816.80	1816.54	656.43	656.43	80.66	41.04	58.57	253.83
WWS10	472.5	29.5	34.8	82.3	55.4	19.3	1.6	18.1	39.0	39.1	50.9	50.9	37.2	32.7	18.2	14.8

6.3.7 PAH Concentrations - Water Samples

Table 6.12 presents summary statistics for the PAHs detected in surface and groundwater samples from the AML site. All 16 priority PAHs were detected at varying levels, with total concentrations ranging from low to moderate, comparable to those in soil and tailings. The primary dataset is in Appendix 6.6.

Among the detected compounds, Nap was the most abundant (mean = 675.6 µg/L), followed by Chr (218.2 µg/L) and BaA (217.5 µg/L). The HMW compounds, including BbF, BkF, and BaP, were detected at moderate levels with a mean of 141.6 µg/L. Lower-molecular-weight (LMW) compounds such as Flu, Pyr, and Ant occurred at comparatively lower concentrations, averaging below 90 µg/L.

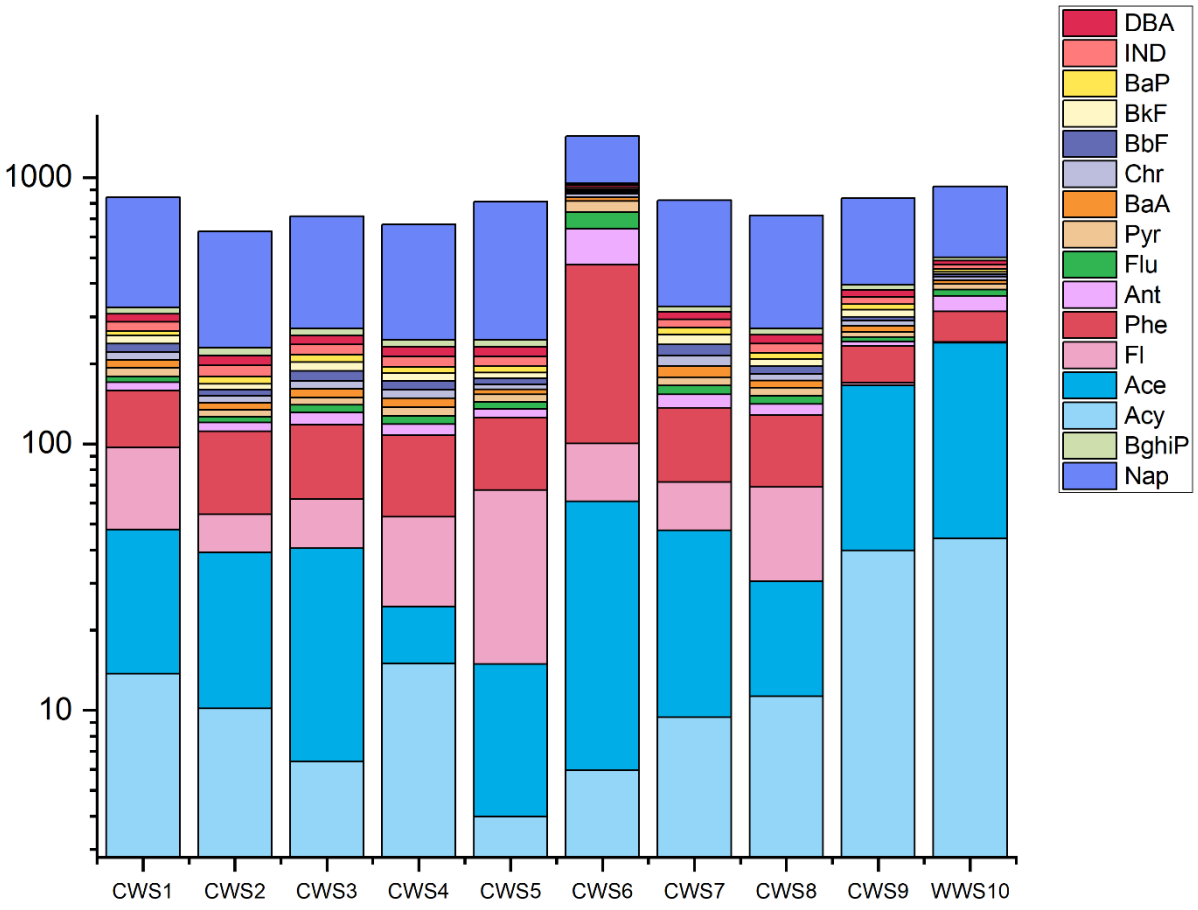

Figure 6.15: Distribution of PAH compounds in surface and groundwater samples from the mine area. LMW PAHs (Nap, Acy, Ace, Fl, and Phe) dominated across all samples, particularly in CWS5–CWS7, whereas heavier PAHs such as BaA, Chr, and BaP appeared in smaller proportions. The well water (WWS10) showed the lowest overall PAH concentrations, indicating reduced surface influence.

Marked variability was observed across sampling locations (Figure 6.15). The highest concentrations were observed at CWS6, located at one of the mine adits, followed by the second adit (CWS5) and in the receiving stream (CWS7). Elevated concentrations were also detected at CWS9, located downstream of the River Ekulu, while well water (WWS10) showed moderate levels of Acy, Ace, and Phe.

PAH concentrations in the water samples indicate the predominance of dissolved LMW compounds, mainly Nap, Acy, Ace, Fl, and Phe, reflecting inputs from coal residues and leaching processes. The relatively low levels of HMW PAHs and the attenuation observed in the cleaner water suggest limited contamination and gradual dilution away from the mine adits.

6.3.8 PAH Toxic Equivalent Concentration (TEQ) and Threshold Comparison

The concentration data provide a basis for evaluating the potential toxicity of PAHs in the study area. To quantify the relative toxic potency of the detected compounds and assess potential human health risks, TEFs were applied to estimate TEQ for soil samples. The calculated TEQs were then compared with the Canadian guideline values for human health protection based on TEF assessment.

The estimated BaPeq for individual compounds and total TEQs are shown in Table 6.13. Among the detected PAHs, DBA exhibited the highest mean BaPeq value (6.75×10^{-1} mg TEQ/kg), accounting for the largest share of the overall toxicity. BaP, assigned a TEF of 1, also showed a substantial contribution (1.26×10^{-1} mg TEQ/kg). Other compounds, such as BbF, BkF, and IND, contributed moderately, with mean BaPeq values of approximately 1.5×10^{-2} mg TEQ/kg. In contrast, low-molecular-weight PAHs, including Nap, Acy, Ace, and Fl, contributed minimally ($\leq 10^{-4}$ mg TEQ/kg) due to their low TEFs and limited persistence.

The total TEQ for the soil samples ranged from 6.67×10^{-1} to 1.71 mg TEQ/kg, with a mean value of 8.65×10^{-1} mg TEQ/kg. Compared with the Canadian Soil Quality Guideline for human health protection (0.6 mg BaP TEQ/kg), the mean TEQ slightly exceeded the threshold, suggesting potential concern for chronic exposure through soil contact or ingestion near contaminated areas.

It is noteworthy that, as shown in the table, a TEF of 5 was applied for DBA, following Nisbet and Lagoy's recommendation (Nisbet & Lagoy', 1992), to account for its comparatively higher carcinogenic potency relative to BaP.

The results suggest that the overall PAH toxicity in the abandoned coal mine soils is dominated by high-molecular-weight carcinogenic compounds, particularly DBA and BaP, reflecting petrogenic origins associated with coal residues from past mining activities. Although the observed potential risk is not alarmingly high, the carcinogenic potency of key compounds warrants attention.

Table 6.13: Toxic equivalent concentrations (TEQs) of PAHs in soil (n=17) samples from Onyeama abandoned coal mine site, calculated using toxicity equivalency factors (TEFs) relative to BaP. A TEF of 5 was applied for DBA following the recommendation of (Nisbet & Lagoy, 1992). The total TEQ values were compared with the Canadian soil quality guideline of 0.6 mg BaP TEQ/kg for human health protection.

				BaPeq(mg Teq/kg)		
Contaminant	Symbol	Aromatic Ring	*TEF	Mean	Min	Max
Napthalene	Nap	2	0.001	1.8715E-03	2.7621E-04	0.0050
Acenaphthylene	Acy	3	0.001	4.1803E-05	2.1933E-05	0.0001
Acenaphthene	Ace	3	0.001	1.8184E-06	0.0000E+00	0.0000
Fluorene	Fl	3	0.001	3.8513E-06	0.0000E+00	0.0000
Phenanthrene	Phe	3	0.001	7.6734E-05	0.0000E+00	0.0003
Anthracene	Ant	3	0.01	4.4513E-04	3.5154E-05	0.0030
Fluoranthene	Flu	4	0.001	1.1304E-04	5.5881E-06	0.0005
Pyrene	Pyr	4	0.001	1.2490E-04	1.7066E-05	0.0005
Benzo(ghi)perylene	BghiP	6	0.01	1.4415E-03	3.7142E-04	0.0035
Benzo(a)anthracene	BaA	4	0.1	1.1711E-02	3.7142E-03	0.0462
Chrysene	Chr	4	0.01	1.1711E-03	6.8812E-04	0.0046
Benzo(b)fluoranthene	BbF	5	0.1	1.5828E-02	8.2353E-03	0.0511
Benzo(k)fluoranthene	BkF	5	0.1	1.5596E-02	8.8572E-03	0.0393
Benzo(a)pyrene	BaP	5	1	1.2629E-01	1.1961E-01	0.4238
Indeno(1,2,3,-cd)pyrene	IND	6	0.1	1.5410E-02	1.2219E-02	0.0402
Dibenz(a,h)anthracene	DBA	5	5	6.7498E-01	5.1396E-01	1.0948
TEQ		∑PHA7Bapq		0.86098	0.66728	1.6999
		∑PAHBapeq		0.86510	0.66801	1.7129
**SQGs				0.6 mg/kg BaP TPE		

*Source: (Nisbet & Lagoy, 1992) **source (CCME, 2010) ∑PHA7Bapeq of the seven carcinogenic PAHs. SQGs - Soil quality guideline values.

6.3.9 Human Exposure Assessment

The assessment considered three exposure pathways, ingestion, dermal contact, and inhalation for both adults and children, representing key receptors in the affected communities. This was achieved through the estimation of CDI of PAHs and HMs in soil and water to characterise potential exposure through direct and indirect contact.

6.3.9.1 PAH Exposure (soil and water)

The CDI outcomes for PAHs in soil and water are presented in Tables 6.14 and 6.15, respectively. Among the three exposure pathways, ingestion contributed the most significantly to total PAH intake, followed by dermal contact, while inhalation accounted for the least exposure. This trend was consistent across both adults and children.

For soil, total mean CDI values across all pathways were 3.77×10^{-6}, 4.44×10^{-6}, and 1.96×10^{-6} mg/kg BW/day for adult ingestion, inhalation, and dermal routes, respectively, while corresponding values for children were 3.20×10^{-5}, 1.18×10^{-9}, and 1.17×10^{-5} mg/kg BW/day. The higher CDI values observed for children reflect their lower body weight and higher soil ingestion rates relative to adults, resulting in greater exposure per unit body mass.

In water, mean total CDI values followed a similar pathway hierarchy, with ingestion as the dominant route. Adult exposure ranged from 3.27×10^{-2} mg/kg BW/day (ingestion) to 2.28×10^{-2} mg/kg BW/day (dermal contact), while child exposure was notably higher, reaching 6.85×10^{-2} mg/kg BW/day via ingestion and 3.89×10^{-2} mg/kg BW/day through dermal absorption. Elevated exposure levels via water ingestion suggest that leaching and surface runoff from the coal mine significantly contribute to hydrocarbon contamination in the aquatic environment.

The CDI estimates indicate that children are more susceptible to PAH exposure than adults, with ingestion being the most important exposure pathway in both environmental media.

This assessment provides the foundation for subsequent evaluations of non-carcinogenic and carcinogenic risk by linking contaminant concentrations to receptor-specific exposure rates and physiological parameters.

Table 6.14: Exposure estimates (mg/kg BW/day) of PAHs in soil samples through ingestion, inhalation, and dermal contact pathways for adults and children. CDI values were calculated to quantify potential exposure from contaminated soils.

	Mean PAHs in Soil (n=17)					
	$CDI_{ingestion}$		$CDI_{inhalation}$		CDI_{dermal}	
Individual PAH	Adult	Child	Adult	Child	Adult	Child
Napthalene	2.56E-06	2.39E-05	3.02E-10	8.80E-10	1.33E-06	8.71E-06
Acenaphthylene	5.73E-08	5.34E-07	6.74E-12	1.96E-11	2.97E-08	1.95E-07
Acenaphthene	2.49E-09	2.32E-08	2.93E-13	8.55E-13	1.29E-09	8.46E-09
Fluorene	5.28E-09	4.92E-08	6.21E-13	1.81E-12	2.74E-09	1.79E-08
Phenanthrene	1.05E-07	9.81E-07	1.24E-11	3.61E-11	5.45E-08	3.57E-07
Anthracene	6.10E-08	5.69E-07	7.17E-12	2.09E-11	3.16E-08	2.07E-07
Fluoranthene	1.55E-07	1.45E-06	1.82E-11	5.31E-11	8.03E-08	5.26E-07
Pyrene	1.71E-07	1.60E-06	2.01E-11	5.87E-11	8.87E-08	5.81E-07
Benzo(ghi)perylene	1.97E-07	1.84E-06	2.32E-11	6.78E-11	1.02E-07	6.71E-07
Benzo(a)anthracene	5.50E-08	1.28E-07	6.47E-12	4.72E-12	2.85E-08	4.67E-08
Chrysene	5.50E-08	1.28E-07	6.47E-12	4.72E-12	2.85E-08	4.67E-08
Benzo(b)fluoranthene	7.43E-08	1.73E-07	8.75E-12	6.38E-12	3.86E-08	6.31E-08
Benzo(k)fluoranthene	7.32E-08	1.71E-07	8.62E-12	6.28E-12	3.80E-08	6.22E-08
Benzo(a)pyrene	5.93E-08	1.38E-07	6.98E-12	5.09E-12	3.08E-08	5.04E-08
Indeno(1,2,3,-cd)pyrene	7.24E-08	1.69E-07	8.52E-12	6.21E-12	3.75E-08	6.15E-08
Dibenz(a,h)anthracene	6.34E-08	1.48E-07	7.46E-12	5.44E-12	3.29E-08	5.39E-08
∑CDI	3.77E-06	3.20E-05	4.44E-10	1.18E-09	1.96E-06	1.17E-05

Table 6.15: Estimated CDI of PAHs in water through ingestion and dermal contact pathways for adults and children (mg/kg BW/day). The results reflect potential exposure associated with the use of contaminated surface and groundwater near the abandoned mine.

	Mean PAH in Water (n=18)			
	$CDI_{ingestion}$		CDI_{dermal}	
Individual PAH	Adult	Child	Adult	Child
Napthalene	1.86E-02	4.33E-02	4.52E-03	1.33E-02
Acenaphthylene	7.43E-04	1.73E-03	3.33E-04	9.84E-04
Acenaphthene	1.75E-03	4.09E-03	2.98E-04	8.78E-04
Fluorene	1.78E-03	4.16E-03	1.02E-03	3.02E-03
Phenanthrene	2.71E-03	6.33E-03	1.98E-03	5.85E-03
Anthracene	7.23E-04	1.69E-03	5.36E-04	1.58E-03
Fluoranthene	5.80E-04	1.35E-03	6.66E-04	1.96E-03
Pyrene	5.68E-04	1.33E-03	5.96E-04	1.76E-03
Benzo(ghi)perylene	8.40E-04	1.96E-03	6.56E-07	1.94E-06
Benzo(a)anthracene	1.11E-03	6.47E-04	2.72E-03	2.01E-03
Chrysene	1.11E-03	6.48E-04	2.73E-03	2.01E-03
Benzo(b)fluoranthene	7.54E-04	4.40E-04	1.64E-03	1.21E-03
Benzo(k)fluoranthene	7.60E-04	4.43E-04	2.74E-03	2.02E-03
Benzo(a)pyrene	2.09E-04	1.22E-04	7.63E-04	5.63E-04
Indeno(1,2,3,-cd)pyrene	2.20E-04	1.28E-04	1.15E-03	8.47E-04
Dibenz(a,h)anthracene	2.27E-04	1.33E-04	1.13E-03	8.34E-04
∑CDI	0.0327	0.0685	0.0228	0.0389

6.3.9.2 HMs Exposure (soil and water)

Human exposure to HMs was evaluated to estimate the potential intake of toxic metals from soil and water around the abandoned coal mine. Exposure assessment was conducted for adults and children through ingestion, dermal contact, and inhalation pathways, using measured concentrations of HMs in environmental media. The estimated CDI values provide insight into the magnitude of human exposure and the relative contribution of each exposure route, serving as the foundation for subsequent non-carcinogenic risk evaluations.

The computed CDI values for HMs in soil and water are shown in Tables 6.16 and 6.17, respectively. In soils (Table 6.17), ingestion represented the dominant exposure pathway, followed by dermal absorption, while inhalation contributed minimally. Fe and Al exhibited the highest CDI values among all metals, with mean ingestion CDIs of 1.06×10^{-2} and 3.66×10^{-3} mg/kg BW/day for adults, respectively. Moderate exposures were observed for Zn, Pb, Cu, and Mn, whereas As, Cd, and Ni showed comparatively lower CDI values. Children recorded higher exposure estimates across all pathways due to their lower body weight and higher soil intake rates.

In water (Table 6.17), the ingestion pathway also accounted for the greatest contribution to total exposure, with Fe (2.21×10^{-1} mg/kg BW/day), Ba (2.69×10^{-2} mg/kg BW/day), and Zn (1.72×10^{-2} mg/kg BW/day) showing the highest mean CDIs. Dermal contact contributed less significantly but remained non-negligible, particularly for Fe and Ba. Similar to estimates in soil, children's CDIs were higher than those of adults, emphasising increased susceptibility in younger receptors.

Table 6.16: The CDI of heavy metals in soil from the Onyeama coal mine area for adults and children through ingestion, inhalation, and dermal contact pathways (mg/kg BW/day).

	Mean HMs in Soil (n=17)					
	$CDI_{ingestion}$		$CDI_{inhalation}$		CDI_{dermal}	
Analyte	Adult	Child	Adult	Child	Adult	Child
As	1.51E-07	1.41E-06	1.78E-11	5.19E-11	7.84E-08	5.14E-07
Zn	3.90E-05	3.64E-04	4.59E-09	1.34E-08	2.02E-05	1.33E-04
Pb	3.28E-05	3.06E-04	3.86E-09	1.12E-08	1.70E-05	1.11E-04
Cd	3.29E-07	3.07E-06	3.87E-11	1.13E-10	1.70E-07	1.12E-06
Ni	5.83E-06	5.44E-05	6.86E-10	2.00E-09	3.03E-06	1.98E-05
Cr	1.29E-05	1.20E-04	1.51E-09	4.41E-09	6.67E-06	4.37E-05
Cu	2.61E-05	2.43E-04	3.07E-09	8.94E-09	1.35E-05	8.85E-05
Ti	8.07E-05	7.53E-04	9.49E-09	2.77E-08	4.18E-05	2.74E-04
Zr	9.43E-06	8.80E-05	1.11E-09	3.24E-09	4.89E-06	3.20E-05
Ce	4.51E-05	4.21E-04	5.30E-09	1.55E-08	2.34E-05	1.53E-04
Sr	9.18E-06	8.57E-05	1.08E-09	3.15E-09	4.76E-06	3.12E-05
Ba	5.07E-05	4.73E-04	5.96E-09	1.74E-08	2.63E-05	1.72E-04
Mn	5.92E-05	5.52E-04	6.96E-09	2.03E-08	3.07E-05	2.01E-04
Al	3.66E-03	3.41E-02	4.30E-07	1.25E-06	1.90E-03	1.24E-02
Fe	1.06E-02	9.88E-02	1.25E-06	3.63E-06	5.49E-03	3.60E-02
∑CDI	1.46E-02	1.36E-01	1.72E-06	5.01E-06	7.58E-03	4.96E-02

Table 6.17: The CDI of heavy metals in soil from the Onyeama coal mine area for adults and children through ingestion, inhalation, and dermal contact pathways (mg/kg BW/day).

	Mean HMs in Water (n=18)			
	$CDI_{ingestion}$		CDI_{dermal}	
Analyte	Adult	Child	Adult	Child
As	4.55E-04	2.27E-04	2.37E-06	7.00E-06
Zn	1.72E-02	8.58E-03	5.37E-05	1.59E-04
Pb	1.16E-04	5.80E-05	7.88E-08	2.32E-07
Cd	8.04E-05	4.02E-05	4.20E-08	1.24E-07
Ni	6.22E-05	3.11E-05	6.49E-08	1.91E-07
Fe	2.21E-01	1.10E-01	1.15E-04	3.40E-04
Cr	2.26E-04	1.13E-04	2.35E-06	6.95E-06
Cu	7.96E-04	3.98E-04	4.15E-06	1.23E-05
Ti	0.00E+00	0.00E+00	0.00E+00	0.00E+00
Zr	1.00E-03	5.01E-04	5.24E-07	1.54E-06
Ce	3.44E-04	1.72E-04	1.79E-07	5.29E-07

Sr	8.53E-03	4.27E-03	4.45E-06	1.31E-05
Ba	2.69E-02	1.34E-02	1.40E-04	4.14E-04
Hg	3.84E-03	1.92E-03	2.01E-05	5.92E-05
Mn	1.42E-02	7.10E-03	7.41E-05	2.19E-04
Al	7.42E-03	3.71E-03	3.87E-06	1.14E-05
∑CDI	3.02E-01	1.51E-01	4.21E-04	1.24E-03

6.3.10 Human Health Risk Assessment

6.3.10.1 Non-carcinogenic Risk Assessment (HQ and HI)

Non-carcinogenic risks associated with exposure to contaminants in soil and water were evaluated using the HQ and HI. This assessment was conducted for both PAHs and HMs, considering ingestion, dermal contact, and inhalation pathways for adult and child receptors.

PAHs (Soil and Water)

The evaluated HQ for the non-carcinogenic PAHs and the HI for cumulative exposure across the three pathways of exposure for soil and water are outlined in Tables 6.18 and 6.19. These metrics help determine whether chronic exposure to PAHs may pose potential health concerns, with values exceeding one (HQ or HI > 1) indicating possible non-carcinogenic risk.

Across all soil pathways (Table 6.19), HQs were generally below the threshold of 1, indicating no significant non-carcinogenic risk for either adults or children. Ingestion was the dominant exposure route, contributing the highest HQ values, followed by dermal contact, while inhalation showed minimal influence. Among the individual compounds, Nap, Pyr, and Flu exhibited comparatively higher HQs, although still within safe limits. The total HQs (HI), that is, HI for soil, were 1.39×10^{-4} (adult ingestion) and 1.30×10^{-3} (child ingestion), confirming that non-carcinogenic effects from PAHs in soil are unlikely for both receptor groups.

Estimated HQs for surface and groundwater are presented in Table 6.20. Like soil, ingestion represented the primary exposure pathway, contributing more significantly to total non-carcinogenic risk than dermal contact. HQs varied among compounds and pathways, with values for several PAHs approaching or exceeding the threshold of 1, particularly in the child receptor group. Nap showed the highest HQs for both ingestion (2.17) and dermal contact (1.15) in children, indicating potential non-carcinogenic concern through water exposure. Moderate HQs were observed for Flu, Pyr, and Acy, while other PAHs remained below critical limits. The total HQs (HI) values reached 1.02 (adult ingestion) and 2.38 (child ingestion), suggesting that chronic exposure to PAHs in contaminated water may pose a potential non-carcinogenic risk, especially for children who exhibit higher exposure sensitivity.

The HQ results for PAHs in soil were well below unity, indicating negligible non-carcinogenic risk, while water samples showed higher HQs, particularly for Nap, suggesting potential health concern through ingestion and dermal exposure, especially among children.

Table 6.18: Mean HQ and HI for non-carcinogenic risk from PAHs in soil from the Onyeama AML for adults and children via ingestion, inhalation, and dermal contact pathways.

	Mean PAH in Soil (n=17)					
	$HQ_{ingestion}$		$HQ_{inhalation}$		HQ_{dermal}	
Non-carcinogenic PAHs	Adult	Child	Adult	Child	Adult	Child
Napthalene	1.28E-04	1.20E-03	1.01E-07	2.93E-07	1.15E-04	1.68E-05
Acenaphthylene	9.54E-07	8.91E-06	1.12E-06	3.27E-06	8.54E-07	2.43E-07
Acenaphthene	0	0	4.88E-08	1.42E-07	0	0
Fluorene	1.32E-07	1.23E-06	1.03E-07	3.02E-07	1.18E-07	1.54E-05
Phenanthrene	0	0	2.06E-06	6.01E-06	0	0
Anthracene	2.03E-07	1.90E-06	1.20E-06	3.49E-06	1.82E-07	3.02E-06
Fluoranthene	3.87E-06	3.61E-05	3.04E-06	8.86E-06	3.46E-06	2.51E-05
Pyrene	5.70E-06	5.32E-05	3.35E-06	9.78E-06	5.10E-06	3.86E-05
Benzo(ghi)perylene	0	0	3.87E-06	1.13E-05	0	0
∑HQ=H1	1.39E-04	1.30E-03	1.49E-05	4.34E-05	1.24E-04	9.90E-05

Table 6.19: Mean HQ and HI for non-carcinogenic risk from PAHs in surface and groundwater from the Onyeama abandoned coal mine for adults and children via ingestion and dermal contact pathways.

	Mean PAH in Water (n=18)			
	$HQ_{ingestion}$		HQ_{dermal}	
Non-carcinogenic PAHs	Adult	Child	Adult	Child
Napthalene	9.29E-01	2.17E+00	3.89E-01	1.15E+00
Acenaphthylene	1.24E-02	2.89E-02	9.58E-03	2.83E-02
Acenaphthene	0	0	0	0
Fluorene	4.45E-02	1.04E-01	4.41E-02	1.30E-01
Phenanthrene	0	0	0	0
Anthracene	2.41E-03	5.62E-03	3.08E-03	9.08E-03
Fluoranthene	1.45E-02	3.38E-02	2.87E-02	8.47E-02
Pyrene	1.89E-02	4.42E-02	3.43E-02	1.01E-01
Benzo(ghi)perylene	0	0	0	0
∑HQ=H1	1.02E+00	2.38E+00	5.09E-01	1.50E+00

Heavy Metals (soil and water)

The estimated HQ and HI values for heavy metals in soil and water are summarised in Tables 6.20 and 6.21. Among the assessed pathways for soil (Table 6.21), dermal contact and ingestion contributed most to total non-carcinogenic risk, while inhalation was negligible. The HQs for individual metals were generally below unity for adults but exceeded 1 in children for certain metals, notably Pb (HQ = 3.28)

and Cr (HQ = 1.94) via dermal contact, indicating potential non-carcinogenic concern for younger receptors. Moderate HQs were also observed for As and Cr, whereas Zn, Cu, and Mn showed relatively low values for the child receptors via the ingestion pathway. The hazard index (∑HQ) for children (5.42) exceeded the acceptable limit, suggesting possible health effects from combined metal exposure through dermal contact with soil, particularly for lead and chromium.

The HQ values (Table 6.21) for HMs in water reveal that ingestion was the predominant exposure route, accounting for most of the total non-carcinogenic risk, while dermal contact contributed moderately. HQs for As and Cr notably exceeded the threshold value of 1 for both adults and children, indicating potential health concern through water consumption and skin contact. The highest HQs were recorded for As (3.81 in adults; 1.91 in children) and Cr (1.28 in adults; 0.64 in children via ingestion), suggesting that these elements are the primary contributors to cumulative non-carcinogenic risk. Other metals such as Zn, Pb, Cu, and Mn showed HQs well below unity, implying minimal health concern from these metals. The HI values of 5.38 (adults) and 2.69 (children) suggest that combined exposure to metals in water may pose potential non-carcinogenic health risks, primarily due to arsenic and chromium contamination.

The HQ values for HMs in soil and water indicated potential non-carcinogenic risk, particularly for children, with Pb, Cr, and As emerging as key contributors. The total HQ (HI) values exceeding unity suggest that chronic exposure, especially through ingestion and dermal contact, may pose health concerns around Onyema AML.

Table 6.20: Estimated HQ values for HMs in soil from the Onyeama abandoned coal mine area for adults and children via ingestion, inhalation, and dermal contact pathways.

Mean HMs in Soil (n=17)						
Analyte	$HQ_{ingestion}$		$HQ_{inhalation}$		HQ_{dermal}	
Heavy Metals	Adult	Child	Adult	Child	Adult	Child
As	2.52E-03	2.35E-02	5.93E-07	1.73E-06	1.38E-03	9.01E-03
Zn	1.30E-04	1.21E-03	1.53E-08	4.46E-08	6.75E-04	4.42E-03
Pb	9.64E-02	9.00E-01	1.10E-06	3.20E-06	5.00E-01	3.28E+00
Cd	6.57E-04	6.14E-03	3.87E-06	1.13E-05	1.36E-02	8.93E-02
Ni	2.92E-04	2.72E-03	3.33E-08	9.72E-08	3.78E-03	2.48E-02
Cr	1.43E-02	1.33E-01	3.03E-05	8.83E-05	2.97E-01	1.94E+00
Cu	6.51E-04	6.08E-03	7.66E-08	2.24E-07	3.38E-03	2.21E-02
Sr	1.53E-05	1.43E-04	0.00E+00	0.00E+00	7.93E-05	5.20E-04
Ba	2.53E-04	2.37E-03	4.17E-05	1.22E-04	1.88E-03	1.23E-02
Mn	4.23E-04	3.95E-03	1.39E-04	4.06E-04	5.48E-03	3.59E-02
∑HQ=H1	0.116	1 08	2.17E-04	6.33E-04	0.827	5.42

Table 6.21: Estimated HQ values for HMs in water from Onyeama abandoned coal mine area for adults and children through ingestion and dermal contact pathways.

	Mean HMs in Water (n=10)	
	$HQ_{ingestion}$	HQ_{dermal}

Heavy Metals	Adult	Child	Adult	Child
As	3.81E+00	1.91E+00	1.90E-01	5.59E-01
Zn	4.65E-02	2.32E-02	1.46E-03	4.29E-03
Pb	4.23E-02	2.12E-02	2.87E-04	8.48E-04
Cd	1.61E-02	8.04E-03	3.36E-04	9.91E-04
Ni	3.11E-04	1.55E-04	8.11E-06	2.39E-05
Cr	1.28E+00	6.40E-01	5.35E-01	1.58E+00
Cu	1.33E-02	6.64E-03	6.93E-04	2.04E-03
Sr	6.89E-03	3.45E-03	3.60E-05	1.06E-04
Ba	1.10E-01	5.48E-02	8.18E-03	2.41E-02
Mn	4.82E-02	2.41E-02	6.29E-03	1.85E-02
∑HQ=H1	5.38	2.69	0.741	2.19

6.3.10.2 Carcinogenic Risk Assessment (ILCR)

Carcinogenic risk was estimated using the ILCR model, which quantifies the probability of developing cancer over a lifetime of exposure to carcinogenic contaminants. Risks were calculated for only PAHs and HMs in soil and water through ingestion, dermal, and inhalation pathways for adults and children. Acceptable ILCR values typically range between 1×10^{-6} and 1×10^{-4}, corresponding to low to moderate cancer risk levels. This analysis identifies the key compounds and exposure routes contributing most to potential carcinogenic effects within the Onyeama Abandoned coal mine land.

PAH (Soil and Water)

The estimated ILCR values for PAHs in soil are presented in Table 6.22. ILCRs across all pathways ranged from 6.47×10^{-17} to 4.00×10^{-8}, with ingestion being the dominant contributor to potential cancer risk for children, followed by dermal contact, while inhalation pathways were negligible. Among the individual compounds, DBA and BaP exhibited the highest ILCRs, with mean ingestion values of 3.04×10^{-7} and 1.19×10^{-7} for adults, respectively, reflecting their strong carcinogenic potency. The cumulative CR (∑ILCR) for children (1.12×10^{-6}) slightly exceeded the upper acceptable risk limit of 1×10^{-6}, indicating potential long-term carcinogenic concern, whereas adult risk values remained within the tolerable range. These findings suggest that carcinogenic risk from soil exposure is primarily associated with high-molecular-weight PAHs such as DBA and BaP.

The ILCR values for carcinogenic PAHs in water are summarised in Table 6.23. The estimated risks ranged from 2.22×10^{-5} to 1.37×10^{-3}, with ingestion contributing more substantially than dermal contact, although both pathways indicated potential concern. DBA and BaP were the most significant contributors to the total carcinogenic risk, with ingestion ILCRs of 1.09×10^{-3} and 4.18×10^{-4} for adults, respectively. The cumulative CRs exceeded the upper acceptable limit of 1×10^{-4} for both adults (2.10×10^{-3}) and children (1.22×10^{-3}) via ingestion, suggesting elevated carcinogenic risk associated with long-term exposure to PAHs in contaminated water. The results indicate that waterborne PAHs,

especially DBA and BaP, pose a more substantial cancer risk than those in soil, emphasising the importance of monitoring and mitigating hydrocarbon contamination in the mine-affected area.

The ILCR values for PAHs in soil were mostly within or slightly above the acceptable risk range, while water samples showed markedly higher carcinogenic potentials. The elevated risks, primarily driven by DBA and BaP, highlight water ingestion as the dominant exposure pathway and suggest greater long-term cancer concern for populations near the Onyeama abandoned coal mine.

Table 6.22: Estimated ILCR values for carcinogenic PAHs in soil from the Onyeama abandoned coal mine for adults and children via ingestion, inhalation, and dermal contact pathways.

	PAH in Soil Mean (n=17)					
	$ILCR_{ingestion}$		$ILCR_{inhalation}$		$ILCR_{dermal}$	
Carcinogenic PAHs	Adult	Child	Adult	Child	Adult	Child
Benzo(a)anthracene	1.10E-08	2.57E-08	6.47E-15	4.72E-15	9.84E-09	1.61E-08
Chrysene	1.10E-09	2.57E-09	6.47E-16	4.72E-16	9.84E-10	1.61E-09
Benzo(b)fluoranthene	1.49E-08	3.47E-08	8.75E-17	6.38E-17	1.33E-08	2.18E-08
Benzo(k)fluoranthene	1.46E-08	3.42E-08	8.62E-16	6.28E-16	1.31E-08	2.15E-08
Benzo(a)pyrene	1.19E-07	2.77E-07	6.98E-16	5.09E-16	1.06E-07	1.74E-07
Indeno(1,2,3,-cd)pyrene	1.45E-08	3.38E-08	8.52E-16	6.21E-16	1.29E-08	2.12E-08
Dibenz(a,h)anthracene	3.04E-07	7.10E-07	1.79E-14	1.31E-14	2.72E-07	4.46E-07
∑ILCR=CCR	4.79E-07	1.12E-06	2.75E-14	2.01E-14	4.28E-07	7.02E-07

Table 6.23: Estimated ILCR values for carcinogenic PAHs in water for adults and children through ingestion and dermal contact pathways at the Onyeama AML site.

	Mean PAHs in Water (n=18)			
	$ILCR_{ingestion}$		$ILCR_{dermal}$	
Carcinogenic PAHs	Adult	Child	Adult	Child
Benzo(a)anthracene	2.22E-04	1.29E-04	6.49E-05	4.78E-05
Chrysene	2.22E-05	1.30E-05	2.20E-05	1.62E-05
Benzo(b)fluoranthene	1.51E-04	8.79E-05	1.93E-04	1.42E-04
Benzo(k)fluoranthene	1.52E-04	8.86E-05	2.75E-04	2.03E-04
Benzo(a)pyrene	4.18E-04	2.44E-04	8.27E-04	6.10E-04
Indeno(1,2,3,-cd)pyrene	4.40E-05	2.57E-05	5.93E-08	4.37E-08
Dibenz(a,h)anthracene	1.09E-03	6.36E-04	1.37E-03	1.01E-03
∑ILCR=CCR	2.10E-03	1.22E-03	2.76E-03	2.03E-03

HMs (Soil and Water)

Table 6.24 outlines the estimated ILCR levels for carcinogenic heavy metals (HMs) in soil. Ingestion contributes the greatest potential cancer risk, followed by dermal contact, while inhalation remains negligible from the calculated ILCRs. Lead and Ni exhibited the highest ILCR values, particularly for children, with ingestion risks of 1.28×10^{-5} and 4.95×10^{-5}, respectively, among the assessed metals.

Moderate carcinogenic potential was observed in Cr and Cd, while As presented relatively low ILCRs. Adults ranged from 4.84 x 10^{-8} (As) to 5.31 x 10^{-6} (Cr). The cumulative CR for children (9.64×10^{-5}) approached the upper bound of the acceptable risk range (1×10^{-4}), indicating possible long-term cancer concern for highly exposed populations. Conversely, adult cumulative risk (1.03×10^{-5}) remained within the tolerable range. These findings suggest that children face a greater carcinogenic risk from soil exposure, primarily due to lead and nickel contamination.

The ILCR values for water are summarised in Table 6.25. The dominant route of potential cancer risk identified from the estimated risks across the three exposure pathways was ingestion. The highest ILCRs were recorded for As and Cr, with ingestion values of 7.32×10^{-5} and 3.46×10^{-5} for adults, respectively, and slightly lower but comparable values for children. Other metals, including Pb, Cd, and Ni, exhibited relatively low carcinogenic potentials. For adults, cumulative CR through ingestion reached 1.17×10^{4}, slightly exceeding the upper acceptable risk limit (1×10^{-4}), suggesting a potential carcinogenic concern from long-term water exposure near the AML site. Meanwhile, dermal exposure contributed minimally to total cancer risk, indicating that As and Cr are the principal drivers of carcinogenic risk in water via ingestion.

The assessments highlight that children are more vulnerable to carcinogenic risk than adults, with As, Cr, Pb, and Ni as the main contributors. While soil risks largely fall within the acceptable range, waterborne exposures slightly exceed the safety threshold, pointing to potential long-term cancer risks for residents around and users of the AML.

Table 6.24: Estimated ILCR values in soil from the Onyeama AML for adults and children through ingestion, inhalation, and dermal contact pathways with carcinogenic HMs.

	Mean HMs in Soil (n=17)					
	$ILCR_{ingestion}$		$ILCR_{inhalation}$		$ILCR_{dermal}$	
Carcinogenic HMs	Adult	Child	Adult	Child	Adult	Child
As	4.84E-08	4.52E-07	7.65E-14	2.23E-13	4.33E-08	2.83E-07
Pb	1.38E-06	1.28E-05	4.63E-14	1.35E-13	1.23E-06	8.06E-06
Cd	1.25E-07	1.17E-06	1.62E-13	4.74E-13	1.12E-07	7.32E-07
Ni	5.31E-06	4.95E-05	1.78E-13	5.20E-13	4.75E-06	3.11E-05
Cr	3.47E-06	3.24E-05	2.72E-11	7.95E-11	3.11E-06	2.03E-05
∑ILCR=CCR	1.03E-05	9.64E-05	2.77E-11	8.08E-11	9.24E-06	6.05E-05

Table 6.25: Results of estimated ILCR in water from Onyeama AML for adults and children through ingestion and dermal contact with carcinogenic HMs.

	Mean HMs in Water (n=10)			
	$ILCR_{ingestion}$		$ILCR_{dermal}$	
Carcinogenic HMs	Adult	Child	Adult	Child
As	7.32E-05	3.66E-05	6.59E-07	1.94E-06
Pb	6.05E-07	3.02E-07	7.07E-10	2.09E-09
Cd	3.06E-06	1.53E-06	2.75E-09	8.11E-09

Ni	5.66E-06	2.83E-06	1.02E-08	3.00E-08
Cr	3.46E-05	1.73E-05	6.22E-07	1.84E-06
∑ILCR=CCR	1.17E-04	5.85E-05	1.29E-06	3.82E-06

6.3.10.3 Cumulative HI and ILCR

PAHs (Soil and Water)

The cumulative HI and cancer risk (CCR) values for PAHs in soil and water are summarised in Table 6.26. For soil, all cumulative HI values were well below 1, confirming non-carcinogenic risk for both adults (2.78×10^{-4}) and children (1.44×10^{-3}). Corresponding CCR values remained within or slightly above the acceptable risk range (1×10^{-6} to 1×10^{-4}), with children exhibiting higher values (1.82×10^{-6}) than adults (9.07×10^{-7}). Meanwhile, cumulative HI values for water exceeded unity (3.88) for children and (1.53) for adults through ingestion and dermal exposure, indicating potential non-carcinogenic concern, particularly among children. The cumulative CCRs for water (4.86×10^{-3}–3.25×10^{-3}) for adults and children were above the acceptable threshold, suggesting that prolonged exposure to waterborne PAHs poses a notable carcinogenic risk relative to soil.

Table 6.26: Mean cumulative HI and Cancer Risk (CR) results for PAHs in soil and water across different exposure pathways and receptors (adults and children).

Mean Cumulative HI and CCR of PAHs in soil (n = 17)					
Exposure Pathway	Adult	Child	Exposure Pathway	Adult	Child
$HI_{ingestion}$	1.39E-04	1.30E-03	$CCR_{ingestion}$	4.79E-07	1.12E-06
$HI_{inhalation}$	1.49E-05	4.34E-05	$CCR_{inhalation}$	2.75E-14	2.01E-14
HI_{dermal}	1.24E-04	9.90E-05	CCR_{dermal}	4.28E-07	7.02E-07
∑HI	2.78E-04	1.44E-03	∑CCR	9.07E-07	1.82E-06

Mean Cumulative HI and CCR of PAHs in Water (n = 18)					
Exposure Pathway	Adult	Child	Exposure Pathway	Adult	Child
$HI_{ingestion}$	1.02	2.38	$CCR_{ingestion}$	2.10E-03	1.22E-03
HI_{dermal}	0.509	1.50	CCR_{dermal}	2.76E-03	2.03E-03
∑HI	1.53	3.88	∑CCR	4.86E-03	3.25E-03

HMs (Soil and Water)

Heavy metals combined HI and CCR risk estimates in soil and water are summarised in Table 6.27. For soil, the total HI values indicate low to moderate non-carcinogenic risk for adults (0.94) but a significantly higher risk for children (6.50), largely attributable to dermal and ingestion exposure. Corresponding CCR values for soil were 1.96×10^{-5} for adults and 1.57×10^{-4} for children, the latter slightly exceeding the upper acceptable limit (1×10^{-4}), suggesting potential long-term carcinogenic concern.

Conversely, water samples exhibited elevated cumulative HI values for both adults (6.12) and children (4.87), exceeding the safety threshold (HI = 1), thereby signalling a clear non-carcinogenic risk from metal exposure. The cumulative cancer risks in water were 1.18×10^{-4} for adults and 6.24×10^{-5} for children, slightly above and within the upper acceptable range, respectively. Ingestion was the dominant exposure route for both risk types, while dermal pathways made secondary contributions. Collectively, these results emphasise that metal contamination in water poses greater overall health risks than in soil.

Table 6.27: Mean cumulative HI and Cancer Risk (CR) results for HMs in soil and water across different exposure pathways and receptors (adults and children).

Mean Cumulative HI of HMs in soil (n = 17)			Mean Cumulative CR of HMs in soil (n = 17)		
Exposure Pathway	Adult	Child	Exposure Pathway	Adult	Child
$HI_{ingestion}$	1.16E-01	1.08	$CCR_{ingestion}$	1.03E-05	9.64E-05
$HI_{inhalation}$	2.17E-04	6.33E-04	$CCR_{inhalation}$	2.77E-11	8.08E-11
HI_{dermal}	8.27E-01	5.42	CCR_{dermal}	9.24E-06	6.05E-05
∑HI	9.43E-01	6.50	∑CCR	1.96E-05	1.57E-04

Mean Cumulative HI in HMs in Water (n = 10)			Mean Cumulative CR in HMs in Water (n = 10)		
Exposure Pathway	Adult	Child	Exposure pathway	Adult	Child
$HI_{ingestion}$	5.38	2.69	$CCR_{ingestion}$	1.17E-04	5.85E-05
HI_{dermal}	70..41	2.19	CCR_{dermal}	1.29E-06	3.82E-06
∑HI	6.12	4.87	∑ILCR	1.18E-04	6.24E-05

The integrated risk assessment of HMs and PAHs across the environmental media reveals that soil exposure presents relatively low non-carcinogenic and carcinogenic risks, whereas water exhibited higher risks, particularly through ingestion. Among HMs, As, Cr, Pb, and Ni were the dominant contributors to both non-cancer and cancer risks, whereas BaP and DBA were the key PAH drivers of carcinogenicity. Children consistently showed higher exposure and risk levels than adults across all pathways, emphasising their greater vulnerability. These findings underscore varying degrees of human health concern around the abandoned Onyeama coal mine and emphasise the need for targeted risk management, continuous monitoring, and remediation strategies to mitigate the potential human health impacts associated with prolonged exposure to contaminated water and soils.

6.4 Discussion

The levels of organic (PAHs) and inorganic (HMs) contaminants in environmental media around the Onyeama abandoned coal mine in Nigeria, with emphasis on assessing human health risks and informing management strategies, were assessed. Field measurements provided semi-quantitative concentrations of trace and major elements, followed by laboratory analyses for accurate quantification. Organic contaminants were assessed solely through laboratory analysis of environmental samples. The

measured concentrations of HMs and PAHs were compared with national and international guideline values to identify potential exceedances.

Results showed that both contaminant classes were present in soil and water at varying levels, with corresponding HI and cancer risk estimates (CR/CCR) differing across exposure pathways and receptor groups. PAH concentrations contributed significantly to carcinogenic risk, particularly through ingestion and dermal contact. Children exhibited higher incremental lifetime cancer risks (ILCRs) than adults across all exposure routes, underscoring their greater vulnerability. These findings align with global concerns regarding legacy mining sites and highlight the urgent need for targeted risk management and remediation interventions in the affected communities.

6.4.1 Distribution and Concentration of Metals

The pXRF field results (Table 6.8) provided an initial overview of the spatial distribution of both trace and major elements around the abandoned coal mine site. Among the significant elements, Fe and Ti were dominant across all sampled media, with soil concentrations averaging 16,275.5 mg/kg and 2,995.6 mg/kg, respectively. Ca and Mn followed these, while lighter elements such as Mg, K, and Sr occurred at relatively lower levels, exhibiting a distribution pattern (Fe > Ti > Ca > Ba > Mn > Sr > Mg > K). The trace metals showed concentration gradients of Mn > Ce > Zn > Cu > Pb > Zr > Cr > Ni > Cd > As in tailings, and Cr > Zn > Cu > Pb > Ce > As > Ni in soils. Cr displayed the highest mean concentration (86.7 mg/kg), followed by zinc (36.8 mg/kg), copper (23.9 mg/kg), and lead (19.6 mg/kg), while arsenic (1.5 mg/kg) occurred at background levels, and nickel was non-detectable. The overall distribution pattern observed in the field data was Fe > Ti > Cr > Zn > Cu > Pb > Ba > Mn > Ca > Sr > K > Mg > As > Ni.

The laboratory results (Table 6.9) confirmed these concentration patterns, providing more precise quantification of both trace and major elements in soils, tailings, and sediments. Consistent with the field data, Fe remained the most abundant major element across all media, followed by Al, K, Mg, and Na. In tailings, the concentration gradient (Fe > K > Al > Mg > Na > Ca > Ti > Ba > Sr) reflected the dominance of Fe- and Al-bearing minerals and the accumulation of K-bearing aluminosilicates (Ushakova et al., 2022). In soils, the pattern (Fe > Al > K > Mg > Na > Ti > Ca > Ba > Sr) was similar. However, Fe and Al were comparatively higher, reflecting both the natural geochemical background and secondary enrichment from weathering of tailings. Sediments exhibited lower overall metal concentrations, following a general trend of Fe > K > Mg > Na > Al > Ti > Ca > Sr > Ba, indicating dilution by fine detrital materials and hydrodynamic sorting.

For trace elements, laboratory results showed a trend similar to the pXRF data, but with magnitude variations across different media. Manganese, Zn, and Pb were the most enriched trace elements in both tailings and soils, while As and Cd remained relatively low. The overall gradient across all matrices was Mn > Zn > Pb > Cu > Cr > Ce > Ni > Zr > Cd > As, indicating potential contamination from mining

residues and weathering of metalliferous minerals. These concentration patterns are similar to those reported in other abandoned coal mines (Table 6.30). The high Mn and Zn concentrations, especially in tailings and soils, suggest both geogenic and anthropogenic sources. Conversely, sediments exhibited lower overall trace metal concentrations, consistent with attenuation during transport and deposition.

The observed concentration gradient of total metals in mine and surface water shows that Na > K > Ca > Fe > Mg > Ba > Sr > Al, and Zn > Mn > Cu > Cr ≈ As > Ce > Zr > Ni > Pb > Cd > Hg. This pattern demonstrates the dominance of alkali and alkaline earth metals in the aqueous phase, indicating mineral dissolution processes, particularly from silicate and calcareous-bearing strata that characterise the geology of groundwater-bearing formations in the abandoned underground coal mines. Such geogenic inputs are further intensified by saline intrusion and hydrogeochemical evolution as groundwater interacts with host rock minerals and residual mine materials. Elevated levels of Fe, Zn, and Mn suggest trace-metal enrichment resulting from mine drainage and geochemical weathering of exposed tailings and soil materials (Jiao, Liu, et al., 2023).

Field and laboratory data confirm that Fe, Mn, Zn, and Pb are the dominant metals of concern in the study area. Their spatial variability reflects a combination of natural geochemical background, inputs from historical mine waste, and post-mining weathering processes. The observed strong correlation between Fe and trace metals suggests that secondary iron oxides may act as sinks or carriers for trace metal accumulation through adsorption and co-precipitation mechanisms (Chowdhury & Singer, 2023; T. Yang et al., 2021). While specific mineral phases were not identified in this study, similar environments often report associations with poorly crystalline and amorphous iron oxides and oxyhydroxides, such as ferrihydrite, goethite, and schwertmannite, which are recognised as important scavengers of trace metals due to their high surface area and strong adsorption capacity (Acero et al., 2006; Dzombak & Morel, 1990; Nordstrom et al., 2015). Spatially, elevated levels of Fe, As, Cr, and Cu were detected at and near the mine adits (CWS5–CWS7), where seepage water interacts directly with coal and overburden materials. Soils adjacent to these discharge points exhibited accumulation of less mobile metals such as Pb, Cr, and Ba. Although mineralogical analyses were not undertaken in this study, the observed enrichment is consistent with the retention of these metals through adsorption onto iron and aluminium oxide phases and their association with fine-grained clay fractions, processes that have been widely reported in mining-impacted soils and sediments (Acero et al., 2006; Dzombak & Morel, 1990; W. Wang et al., 2024). In contrast, more soluble elements (Zn and Mn) showed greater dispersion, indicating secondary migration via runoff and infiltration.

6.4.2 Metal Contamination and Geochemical Behaviour

The distribution of HMs in the Onyeama mine environment reflects the combined influence of coal mineralogy, weathering of waste materials, and hydrogeochemical processes driven by mine drainage. Elevated concentrations of Fe and Al in both soil and water indicate active oxidation of pyrite-bearing strata and subsequent hydrolysis, producing ferric hydroxides that impart the characteristic orange

colouration observed in mine adits and drainage tunnels (Simate & Ndlovu, 2014). This is consistent with the geology of the abandoned underground mine, which is hosted in layers of sandstones, siltstones, and shale (Nwajide, 2013; Salufu et al., 2014). These host rocks contain iron-bearing pyrite and siderite (Ozoko, 2015), which are released during weathering processes and transported through leaching, thereby increasing iron concentration (Kefeni et al., 2017). The mean concentrations of iron in soil and water are 8521 mg/kg and 4.5 mg/L, respectively. Previous studies at the site reported 9.21 mg/L for water (Akpan et al., 2021), and other related studies reported similar or lower concentrations of Fe and other HMs (Table 6.30).

In this study, the pH of the underground mine water ranged from 5.98 to 6.05, indicating near-neutral conditions. This contrasts with earlier reports of more acidic mine drainage at the same site, including pH values of 3.39–5.84 (Akpan et al., 2021), 3.1 (Salufu et al., 2014), and 2.80 (Ezeigbo & Ezeanyim, 1993). The observed shift toward neutrality suggests natural attenuation processes are occurring within the mine, primarily due to acid buffering and geochemical interactions over time. The Onyeama coal mine lies beneath the Ajali Formation, composed of coarse sandstone that serves as the regional aquifer, while the mine itself is hosted within the Mamu Formation, consisting of alternating sandstone and shale layers (Ezeigbo & Ezeanyim, 1993; Nwajide, 2013) (Figure 6.1). The area is further characterised by two subsurface faults that influence groundwater flow and promote periodic flooding within the mine (Ozoko, 2015).

The gradual flooding of the mine likely facilitated sustained interaction between acidic drainage and calcareous shale strata, allowing carbonate-rich minerals to dissolve and neutralise acidity generated by the oxidation of pyrite and siderite within the sandstone units. Over time, this buffering effect would have progressively raised the pH, explaining the current near-neutral conditions. Such natural pH recovery in flooded or partially saturated mine systems has been widely reported elsewhere (Akcil & Koldas, 2006; Banks et al., 1997; Blowes et al., 2003; Nordstrom et al., 2015; Younger, 1997), where carbonate dissolution, dilution, and reduced sulphide oxidation collectively drive the attenuation of acidity. Thus, the improvement in mine water quality at Onyeama likely reflects a naturally evolving hydrogeochemical equilibrium, dominated by carbonate buffering and secondary mineral formation that limit further acid generation.

The near-neutral pH conditions observed in the mine water also provide a plausible explanation for the relatively low concentrations of dissolved heavy metals recorded in this study compared with previous reports. As acidity decreases, most metals become less soluble due to hydrolysis, precipitation, and sorption processes (Banks et al., 1997; Younger, 1997). At pH values approaching neutrality, metals such as Fe, Al, and Mn tend to form hydroxides and oxyhydroxides, which subsequently adsorb trace metals including Pb, Zn, and Cu, thereby reducing their mobility and bioavailability (Cravotta III, 2008). Additionally, carbonate buffering from the calcareous shale layers enhances metal precipitation and coprecipitation with secondary minerals, while mine flooding limits oxygen availability and suppresses further sulphide oxidation. These geochemical conditions collectively indicate that natural

attenuation and buffering mechanisms are actively mitigating metal release within the abandoned Onyeama mine environment. Similar conditions have been reported in other flooded coal mines, where carbonate-rich lithologies and reduced oxygen levels contribute to trace metal attenuation and geochemical stability (D. Chen et al., 2021; X. Li et al., 2021; Pan et al., 2021). These patterns are typical of weathered mine sites where alternating oxidation and reduction conditions promote metal partitioning between aqueous and solid phases (Ciszewski & Aleksander-Kwaterczak, 2020; Gomo & Vermeulen, 2014).

Also, the measurable DOC and DO indicate an environment transitioning from active acid mine drainage to a more buffered state. DOC likely enhances the complexation and mobility of metals such as Cu, Ni, and Zn, while simultaneously contributing to partial neutralisation of acidity through humic buffering. Nevertheless, the persistence of high Fe and Cr levels demonstrates ongoing geochemical release from the coal-bearing strata and tailings materials. Overall, the geochemical evidence points to a system in which hydrolysis of sulphide minerals, adsorption–desorption dynamics, and organic complexation collectively govern the observed metal distribution and potential bioavailability (X. Li et al., 2021; Ushakova et al., 2022).

Comparison with national (NSDWQ) and international (WHO) guideline limits showed that mean levels of Fe, Mn, Ba, and Al in surface water exceeded permissible values for human consumption, while Pb, Cu, Cr, Cd, and Ni were within safe limits. However, some maximum values surpassed these limits.

In summary, although contaminant concentrations in mine-affected soils and waters are sometimes low, the risk to human health persists due to the persistence, bioavailability, and cumulative nature of toxic elements. Metals such as Cd, As, Pb, and Cr can bioaccumulate, become remobilised under changing redox or pH conditions, and enter the food chain or groundwater used for drinking and surface water for communities with no access to groundwater, as observed at the site. The speciation data, depicting the bioavailability of the studied metals, are presented in Appendix 6.10. Therefore, even near-background levels can sustain chronic exposure pathways and exceed acceptable risk thresholds, especially for sensitive populations.

Table 6.28: Concentrations of heavy metals in previous and related studies in abandoned coal mines

Location / Medium	pH (avg / range)	As	Cd	Cr	Cu	Pb	Ni	Zn	Fe	Mn	Al	Hg	Reference
Soil (mg/kg)													
Guizhou, China — Soil (AMD-impacted vs reference)	Ref: 7.04–8.22; AMD: 2.53–6.79	28.84	0.65	75.84	13.52	30.55		56.44	321800	131.45			(D. Chen et al., 2021)
Southwestern China — Soil (abandoned coal mine)	Mean 5.28	8.74	1.12	86.06	62.68	18.4	25.95	72.52	35575.95	593.6		0.01	(Pan et al., 2021)
São Pedro da Cova, Portugal — Soil		22.55	0.11	74.1	50.18	50.22	24.29	96.97					(Sartorius, 2023)
Perm Krai, Russia — Sediment (AMD-impacted)	AMD pH 2–3; sediment ~5	2.91	0.93	77.26	33.05	36.54	41.92	61.46					(Ushakova et al., 2022)
Huaibei coalfield, China — Soil (wasteland & farmland)		15	0.08	58.52	21.23	16.26	27.2	95.7		450			(Fang et al., 2021)
Enugu, Nigeria, Oyeama abandoned mine - soil		0.1	0.3	10.9	25.6	36.7	4.8	35.1	8521	46.1			This study
Water (mg/L)													
Yudong River, Guizhou — AMD water & river water	Mine: 2.8–6.6; River: ~6.0–7.5		0.03–0.09		0.3–0.9			up to ~7	up to ~80	~5			(X. Li et al., 2021)
Hongshan, China — Groundwater (Ordovician aquifer)									0.1–2.5	0.05–0.2			(Feng et al., 2020)
Zhangqiu, China — Groundwater (karst)		0.012	0.002	0.017	0.024	0.014	0.035	0.32				0.001	(Y. Han et al., 2023)
Enugu, Nigeria-Opkara abandoned coal mine	Surface water: 4.22		0.0003	0.001	0.008	0.006	0.051	0.254	5.14	3.35	4.3		(Sikakwe et al., 2015)
Enugu, Nigeria, Onyeama abandoned coal mine	Surface water 4.05	1.07		0.08	14.45	16.96	0.02	15.42	9.21	0.06			(Akpan et al., 2021)
Enugu Oyeama abandoned mine	Surface water: 5.98 to 6.05	0.0082	0.0008	0.0065	0.0205	0.0009	0.0058	0.5	4.5	0.29	0.46	0.0134	This study

6.4.3 PAHs Distribution and Source Characterisation

The distribution and compositional patterns of PAHs across the Onyeama coal mine environment reveal important insights into their origin, transport, and potential ecological persistence. Sixteen priority PAHs were detected in all sampled media, with total concentrations varying substantially between soils, tailings, and surface waters. Soils recorded the highest total PAH levels (mean = 2,421.6 µg/kg), followed by tailings (mean = 1,678.5 µg/kg), while sediments exhibited comparatively lower values (mean = 79.7 µg/kg). This gradient reflects differences in contaminant retention capacity, with soils and tailings acting as major sinks due to their high organic matter content and surface area. In contrast, hydrological dilution and microbial degradation likely reduced concentrations in sediments and water.

The analysis of PAH composition helps in the understanding of their source, transport and transformation in the environment (Deng et al., 2023). The compositional profiles of the 16 PAHs were dominated by Nap, Flu, and Pyr among LMW PAHs, and by BaA, Chr, BbF, and BaP among HMW species. The predominance of HMW compounds, coupled with elevated BaPeq concentrations, suggests that spontaneous oxidation and leaching of coal residues in the environmental media and exposed seams are the principal sources of contamination. Compositional interpretation is supported by (Achten & Hofmann, 2009; Bowers & Smith, 2014; Kapley et al., 2020).

Tailings and topsoil near the adits showed pronounced enrichment in BaP, DBA, and BghiP, indicating the presence of coal-processing residues. In contrast, lower levels in sediments reflect both dilution during transport and biodegradation of less stable LMW species (C. Li et al., 2019; Mukhopadhyay et al., 2017).

The TEQ assessment outcome, based on toxicity TEFs, confirmed that DBA and BaP were the most toxic constituents, together accounting for the majority of the total PAH toxic potential. The average ∑BaPeq value (0.86 mg TEQ/kg) slightly exceeded the Canadian Soil Quality Guideline (0.6 mg TEQ/kg) for human health protection, indicating a moderate carcinogenic risk associated with exposure to soil and tailings.

The persistence of these HMW compounds, despite potential weathering and oxidation, reflects their low volatility, hydrophobicity, strong binding to soil organic matter and mineral surfaces (K. Chen et al., 2024; Deng et al., 2023; Mukhopadhyay et al., 2017). This reinforces the need for long-term monitoring and site-specific remediation strategies around abandoned coal mines.

6.4.4 Human Exposure and Risk Implications

The HHRA revealed distinct exposure trends associated with both inorganic and organic contaminants at the Onyeama coal mine environment.

The estimated CDI values for HMs and PAHs varied across pathways and receptors, indicating differences in environmental concentrations and exposure behaviours among the evaluated receptors. In all pathways, ingestion was the dominant exposure route, followed by dermal contact, while inhalation contributed minimally. Children consistently exhibited higher CDI values than adults, mainly due to their lower body weight and greater frequency of soil and water contact. Halfadji compared children, adolescents, and adults in their study, explaining why children often show higher CDI or cancer risk values as a function of their frequent hand-to-mouth or object-to-mouth activities, which facilitate ingestion of contaminated soils (Halfadji et al., 2021). Therefore, they are considered the most sensitive age group likely to be exposed to environmental pollutants. For adults, a longer exposure time to the indoor/outdoor environment, greater body weight and greater skin surface area can also lead to a higher potential cancer risk (Halfadji et al., 2021; Zoveidadianpour et al., 2023).

For heavy metals, ingestion of contaminated water and soil accounted for the highest exposure burden. Metals such as As, Cr, and Pb were the principal contributors to both non-carcinogenic and carcinogenic risk, with elevated HQ and ILCR values indicating potential long-term health concerns. The cumulative hazard index (HI) for HMs in soil (6.50 for children; 0.94 for adults) and water (4.87 for children; 6.12 for adults) exceeded unity, indicating a likelihood of non-carcinogenic effects, particularly among children. Similar outcomes were reported for adults and children (Ayari et al., 2021; Mehta et al., 2020; Singovszka et al., 2020). The corresponding cumulative cancer risks (∑CCR) for soil (1.57×10^{-4}) and water (1.18×10^{-4}) also exceeded the upper acceptable limit (1×10^{-4}), signifying possible carcinogenic concern through chronic exposure. Barraza reported a range of 2-13 x 10^{-4} for adults and children through ingestion and inhalation (Barraza et al., 2018). HI values over 10 were reported (Singovszka et al., 2020) for adults and children via ingestion of contaminated water and dermal contact.

In the same vein, non-carcinogenic risk estimates for PAHs showed moderate hazard levels from soil ingestion and risk for water ingestion, dominated by Nap, Flu, and Pyr. Cumulative HI for soil (2.78×10^{-4} to 1.44×10^{-3}) and for water (1.53 to 3.88), while carcinogenic PAHs such as BaP and DBA yielded the highest ILCR values. The cumulative CRs for PAHs in soil (9.07×10^{-7} to 1.82×10^{-6}) were within the tolerable risk range (10^{-6}–10^{-4}), whereas those for water (4.86×10^{-3} to 3.25×10^{-3}) exceeded acceptable thresholds, suggesting significant concern for chronic exposure via drinking water and dermal contact. Other studies reported similar findings where BaP, BbF, or DahA were dominant contributors (Aralu et al., 2023; Halfadji et al., 2021; Yusuf et al., 2022; Zoveidadianpour et al., 2023).

Comparatively, although the overall contribution of organic contaminants (PAHs) to total cancer risk was less than that of heavy metals, their persistence, bioaccumulative nature, and additive toxic effects, particularly for BaP and DBA, cannot be overlooked. The observed pattern demonstrates that

waterborne exposure poses the most significant health threat, consistent with previous studies in coal-mining regions, where acidic drainage, poor waste containment, and tailings leaching sustain long-term contamination (Deng et al., 2023; C. Li et al., 2019; Mukhopadhyay et al., 2017).

The elevated HI and CCR values, especially among children, underscore the vulnerability of local populations living near the Onyeama mine and of farmers using the arable land surrounding it (Figure 6.15) to cultivate vegetables and other crops. Without adequate containment and remediation, continued exposure through drinking, bathing, swimming and food chain transfer could amplify both non-carcinogenic and carcinogenic risks over time. In mining-impacted environments, metals and PAHs may accumulate in edible crops through root uptake, irrigation with contaminated water, atmospheric deposition, and adherence of contaminated soil particles to plant surfaces. Consequently, consumption of locally cultivated food crops may represent an additional chronic exposure pathway for nearby communities, particularly where agricultural activities occur within or around contaminated mine lands. Although direct food-chain exposure assessment was beyond the scope of the present study, this pathway warrants further investigation in future site-specific human health risk assessments. This is so important because the immediate stream where the mine adits are draining into is being used for swimming, bathing, washing, and drinking, as a result, calling for urgent risk management interventions, including treatment of mine water effluents, restriction of human access to contaminated zones, and regular monitoring of soil and water quality to safeguard community health.

Figure 6.16: Potential vulnerability of local populations to contaminant exposure. A red arrow indicates a mine adit discharging mine water to the stream where children bathe, swim and wash. B. Children and parents are washing a tricycle, bathing and swimming (blue arrows indicating the stream). C. Vegetable ridges, researcher collecting soil sample from one of the ridges. D. Vegetable farm.

6.4.5 Implications for Risk Management and Environmental Remediation

The findings from this study underscore the urgent need for targeted environmental management and remediation strategies in and around the Onyeama coal mine area. Other abandoned coal mines (Okpara mine, Iva Valley, and Obwetti Fireclay, associated with the Onyeama mines) (Ezeigbo & Ezeanyim, 1993) need to be addressed to safeguard the environment and human health.

Elevated concentrations of heavy metals and PAHs in soil and water, together with HI and cumulative cancer risk CCR values exceeding acceptable limits, demonstrate that contamination from abandoned coal mine workings constitutes a continuing risk to human health and surrounding ecosystems. The predominance of waterborne pathways, mainly through ingestion and dermal contact, emphasises the need to prioritise mine water treatment and containment of contaminated discharges to prevent further downstream migration of pollutants. This is because mine-water discharges from abandoned coal workings have been shown to act as persistent sources of downstream contamination, emphasising the need for targeted treatment and containment strategies (UK EA, 2008; Z. Wang et al., 2021).

Effective risk reduction in coal mine-impacted environments should begin with mine drainage control, particularly through passive treatment systems such as limestone drains, constructed wetlands, and anoxic limestone drains (ALDs). These systems have proven effective in neutralising acidity and promoting metal precipitation without the need for continuous chemical inputs (J. Li et al., 2024; Pat-Espadas et al., 2018; Younger, 2000). To ensure long-term effectiveness, regular monitoring of water quality parameters, including pH, DO, TDS, temperature, and key contaminants such as As, Cr, Pb, Fe, and BaP, should be institutionalised. Such monitoring is critical for tracking contaminant behaviour and guiding adaptive management strategies.

In parallel, stabilisation or phytoremediation of mine tailings and contaminated soils using tolerant plant species offers a sustainable remediation pathway. This approach can immobilise heavy metals, reduce dust dispersion, and gradually restore ecological function, particularly in areas with limited access to engineered solutions. Species selection should prioritise native flora with demonstrated metal uptake or stabilisation capacity (Deepika et al., 2025).

Given the elevated child-specific exposure and risk values observed in this study, public health protection measures are essential. These include restricting access to mine drainage channels, providing safe alternative water sources, and implementing public awareness campaigns to reduce inadvertent exposure. Establishing community-based monitoring initiatives in collaboration with local environmental agencies can further enhance sustainability and accountability by fostering local stewardship and trust, a standard practice in developed nations.

At a broader scale, the findings underscore the need to integrate health risk assessment into mine closure and post-mining land management policies. Frameworks such as those outlined by the ICMM (ICMM, 2025) and national closure guidelines advocate for early incorporation of environmental and health considerations into closure planning. Site-specific assessments, such as the one conducted at the Onyeama coal mine, can inform prioritisation of remediation zones, support regulatory decision-making, and guide adaptive management to minimise exposure pathways.

In conclusion, mitigating the risks identified at Onyeama will require a coordinated approach that combines scientific assessment, community engagement, and regulatory enforcement. Such integration

is essential to achieve long-term environmental recovery and protect vulnerable populations from ongoing exposure.

6.5 Conclusion

This study investigated the chemical contamination and human health risks associated with the abandoned Onyeama coal mine in southeastern Nigeria, with emphasis on identifying and quantifying inorganic and organic contaminants, evaluating their spatial distribution, and assessing potential health implications for exposed populations. The integrated chemical analysis, field observations, and risk assessment revealed that the legacy of coal mining continues to influence the environmental quality of soil and water in the area.

Elevated concentrations of Fe, Al, Cr, Mn, Pb, and Zn, along with detectable levels of priority PAHs, indicate persistent contamination from both geogenic weathering and anthropogenic sources, such as historical coal mining activities and waste discharge.

The risk assessment results demonstrated that ingestion and dermal contact are the dominant exposure pathways for both heavy metals and PAHs. Waterborne exposure contributed the highest non-carcinogenic and carcinogenic risk, with cumulative HI and CR values exceeding acceptable thresholds, particularly for children. The presence of Pb, Cr, BaP, and DBA as major risk drivers highlights the potential for chronic health effects if exposure persists. Conversely, soil contamination presented relatively lower risks but still indicated localised enrichment near the mine adits and waste dumps.

The findings underscore the significant environmental and public health implications of poorly managed abandoned coal mines in Nigeria. The persistence of contaminants, combined with the vulnerability of surrounding communities that rely on untreated surface and groundwater sources and on contaminated land for regular vegetable cultivation, emphasises the need for immediate intervention, monitoring, and long-term remediation strategies.

Although the environmental impacts of heavy metals and acid mine drainage from abandoned coal mines have been widely documented, the potential human health risks associated with organic contaminants, particularly PAHs, have received limited attention. Abandoned coal mines act as long-term sources of both inorganic and organic pollutants, creating pathways for human exposure through contaminated soil and water. Findings from this study confirm that such contamination poses measurable non-carcinogenic and carcinogenic risks to local populations, thereby emphasising the need for continuous monitoring and remediation. This research contributes to bridging the knowledge gap by characterising PAH concentrations and quantifying associated health risks in soil, tailings, and water from the Onyeama abandoned coal mine area.

Chapter 7: General Conclusion

7.1 Background

The primary aim of this research was to conduct an environmental assessment of chemical contamination from abandoned coal and lead-zinc mines. AMLs are legacy sites of historical mining operations that were closed without adequate reclamation, leaving waste dumps and tailings that continue to release toxic metals, metalloids, and organics into the surrounding environment (J. Yang et al., 2015). These mine wastes undergo weathering, oxidation, and leaching, generating AMD and mobilising contaminants such as Cd, Pb, As, and Zn into soils, sediments, surface waters and groundwater systems (El Azhari et al., 2016; Pan et al., 2021). Persistent contamination from these abandoned mine sites disrupts terrestrial and aquatic ecosystems, threatens agricultural productivity, and poses long-term health risks to nearby populations through ingestion, inhalation, and dermal exposure pathways (Son et al., 2019; Q. Xu et al., 2024). Despite the cessation of mining activities, the geochemical and hydrological legacies of AMLs can persist for decades or longer, leading to cumulative and transboundary contamination (J. Y. Kim et al., 2005).

While many countries, such as the US, Canada, Australia, and the UK, operate under strong environmental oversight (e.g., in the US, the Abandoned Mine Land Reclamation Program, which funds remediation of legacy coal sites through fees collected from active mines and in the UK, the Coal Authority, Environment Agency, and Scottish Environment Protection Agency (SEPA) are the primary regulators for abandoned mines, with a particular focus on coal mine pollution. The Mining Remediation Authority also manages some disused colliery tips, and the Local Authorities have a role in managing the safety of tips under the Mines and Quarries (Tips). Diffuse, legacy discharges from AMLs remain challenging to manage. In Nigeria, the regulatory structure is still evolving. Mining governance is coordinated by the Ministry of Solid Mineral Development (MSMD), with agencies and departments responsible for geological surveys, minerals licensing, and environmental protection. Also, the National Environmental Standards and Regulations Enforcement Agency (NESREA), under the Federal Ministry of Environment, enforces environmental laws, including those governing the mining and processing of coal, ores and industrial minerals. However, coordinated legal and operational frameworks for addressing chemical contamination from abandoned mine sites remain limited. This gap underscores the need for research-driven approaches, such as the present study, to inform evidence-based policy and integrated environmental management of AMLs in Nigeria. This thesis aimed to conduct an environmental assessment of chemical contamination from abandoned coal and minerals mines in Nigeria to determine the risks these contaminants pose to ecological and human receptors. To address this, (1) a SEM protocol was developed, and a narrative evidence review was undertaken to evaluate the current methods for assessing chemical contamination risk from abandoned coal and Pb-Zn mines, (2) chemical contamination of abandoned coal and Pb-Zn mines was evaluated, and (3) ecological and human health risk assessments were conducted at these AML sites.

7.2 Systematic Evidence Map of Current Methods

To address the first objective, a SEM protocol was developed (Chapter 3) using a structured approach to identify, extract, and synthesise literature on chemical contamination risk from abandoned coal and Pb-Zn mines. This approach provided a comprehensive overview of existing methodologies and current practices. To our knowledge, no previous synthesis of this kind has been reported. The SEM protocol (Chapter 3) clearly defined eligibility criteria to include studies addressing abandoned coal and Pb/Zn mines that conducted chemical risk assessments. The protocol development, refined through iterative piloting and peer review, established a robust and transparent methodological foundation consistent with open science principles. By systematising the mapping of methodological practices rather than research outcomes, the SEM protocol enhances the organisation, interpretation, and application of evidence on CRA in AMLs. The process also underscored the importance of reflective, collaborative practices for improving research quality and reproducibility.

Using the published protocol, a narrative evidence review (Chapter 4) from 41 studies (published between 2000 and 2024) was completed during the thesis submission period, rather than the planned evidence map, due to the extended peer-review process for protocol publication and time constraints.

Key findings indicate that most studies did not report mining methods or the year of site abandonment—details critical to understanding contamination pathways and persistence. Soils, sediments, tailings, and water were the most frequently assessed environmental media, while air and rock matrices were rarely investigated. Contaminants were dominated by metals and metalloids (Pb, Zn, Cd, As, Fe, Mn), with coal sites predominantly framed through acid mine drainage (AMD). Organic contaminants, particularly PAHs, were underreported; only one study addressed total petroleum hydrocarbons (TPH).

Risk assessment methods frequently applied were found to rely primarily on traditional indices such as Igeo, HQ, Er, Cf, SQGs, CR, Ef, and BVs, with mixture risk assessments using approaches such as RI, HI, HPI, Pn, and TCR. Evolving data-driven and probabilistic RA methods included logistic and linear regression models, while Bayesian Kernel Machine Regression (BKMR), cumulative probability distribution analyses for HI, and Incremental Lifetime Cancer Risk (ILCR) for MRA. The diversity of risk assessment methods identified reflects the increasing recognition that contamination risks in abandoned mine environments are complex, site-specific, and influenced by multiple interacting contaminants and exposure pathways. Traditional index-based approaches provide useful screening-level assessments but may oversimplify contaminant behaviour by relying on total concentrations and generic thresholds. In contrast, probabilistic and data-driven approaches offer improved capacity to address uncertainty, contaminant interactions, and site-specific exposure dynamics, thereby supporting more realistic risk characterisation and informed remediation decision-making.

The study further revealed that biomonitoring investigations focusing on biological effects reported significant adverse outcomes in approximately three-quarters of the tests reviewed. This validates the ecological relevance of observed contamination and highlights the value of bioindicator-based assessments in complementing chemical data to strengthen the evidence base for risk characterisation.

7.3 Evaluation of Ecological Risk Assessment

To evaluate chemical contamination and ecological risk associated with abandoned Pb-Zn mines, two case studies were presented in Chapter 5: the Gimbi/Rikaya site in Plateau State and the Abakaliki site in Ebonyi State, Nigeria. Combining field pXRF screening, laboratory ICP-OES analysis, geochemical assessments, metal speciation, bioavailability and ecological risk evaluation. Tailings, soil, sediment, and water samples from the two sites were collected and analysed.

The findings revealed that field pXRF provided rapid, valuable screening of hotspots for trace and major elements, while laboratory ICP-OES offered more reliable quantification. Among the metals evaluated, only Mn showed a strong, statistically significant correlation ($R^2 = 0.73$, $p < 0.005$) between field and lab results; Pb also showed a statistically significant relationship ($R^2 = 0.35$, $p < 0.0045$). Zn was underestimated, whereas Mn, Fe, and Ti were overestimated by the in situ method.

Chemical analysis results showed that both sites were heavily impacted by Pb, Zn, and Cd, with concentrations well above regulatory thresholds and greater impacts at the Abakaliki site. At the Abakaliki site, soil, tailings, and sediment samples reveal a distinct spatial distribution of heavy metal concentrations, with tailings > sediment > soil, with Zn, Pb, and Cd posing the most significant environmental concern. At the Gimbi/Rikaya site, metal concentrations followed a similar gradient across the three media: Tailings > Sediment > Soil, indicating mine-derived contamination. The primary contaminants, in decreasing order, are Zn > Mn > Fe > Pb > Cu > Cr > Ni > Cd. Tailings emerged as the principal source of contamination, while sediments and soil serve as sinks.

Analysed surface water samples from both sites also showed significant concentrations of heavy metals and major elements. Abakaliki was dominated by Zn, Cd, Pb, and Mn, which indicates substantial anthropogenic contamination linked to the abandoned mine. Lower trace metal concentrations were found at the Gimbi/Rikaya sites, but elevated levels of Zn, Mn, Fe, and major elements were observed.

Sequential extraction and bioavailability assessments revealed that at the Abakaliki site, the proportion of mobile Pb fractions exceeded 34% in soils, indicating that the site's geochemical conditions promote the release of Pb into the surrounding environment. At Gimbi, however, it is slightly different. Pb displayed high mobility in tailings 42% but low mobility in soils, with only about 6% of F1 in soils. This suggests that Pb remains largely immobile and bound to mineral components, particularly Fe and Mn in soil. The carbonate-rich geology of the Gimbi area likely promotes metal precipitation and

adsorption, thereby reducing Pb solubility and mobility. Consequently, while Pb concentrations in tailings are measurable, its migration into soils and sediments is minimal.

Also, at the Abakaliki AML site, the BLM results confirm high bioavailability and potential risk to aquatic organisms. This was observed from the dissolved metals of Pb, Zn, Ni, Cu, and Mn in surface water, which exceeded both the EQS and bioavailability values. At the Gimbi site, dissolved levels of Zn, Cu, Ni, and Mn exceeded the EQS, except for Pb. However, the BLM bioavailability results fell below the EQS values, except for Zn, which exceeded the EQS, indicating its high solubility and mobility.

Ecological risk indices (ER and RI) and the cumulative risk score (CRS) consistently indicated that both Abakaliki and Gimbi pose very high ecological risks. However, the actual toxicity of these metals depends on their bioavailability, as demonstrated by the speciation analysis. Cr was predominantly associated with the F3 fraction, indicating low mobility, whereas Ba and Mn were primarily associated with the F1 and F2 fractions, suggesting higher potential mobility. Across the sites, changes in environmental conditions could exacerbate risk by promoting the release of these metals.

The CSM revealed multiple exposure pathways for soil, sediment, water, and vegetation, linking sources to both terrestrial and aquatic receptors, increasing the potential for cumulative effects, bioaccumulation, and food-web transfer.

7.4 Assessment of Human Health Risk Assessment

The chemical contamination and human health risks associated with the abandoned Onyeama coal mine at Enugu, southeastern Nigeria, were assessed in Chapter 6. The study revealed notable spatial variability and enrichment of major and trace metals, as well as PAHs, across environmental media surrounding the abandoned coal mine.

Fe was the dominant element in all matrices, followed by Ti, Al, and other lithogenic constituents, reflecting both geogenic background and secondary enrichment from weathered tailings. Among trace metals, Mn, Zn, Pb, and Cr were most elevated, indicating contamination from historical mining residues. In water, elevated levels of Na, K, Ca, Fe, Zn, and Mn suggested mineral dissolution, the influence of mine drainage, and geochemical weathering of exposed materials. Strong correlations between Fe and trace metals implied that secondary Fe oxides act as sinks or carriers through adsorption and co-precipitation mechanisms (Chowdhury & Singer, 2023; X. Liu et al., 2021). Spatially, elevated concentrations of Fe, Cr, and Cu were recorded near mine adits. At the same time, more soluble elements, such as Zn and Mn, showed greater dispersion through runoff and infiltration. These findings indicate mixed lithogenic and anthropogenic sources in the post-mining environment (Jiao, Liu, et al., 2023; Ushakova et al., 2022). Elevated Fe and Al indicate pyrite oxidation and ferric hydroxide formation(Simate & Ndlovu, 2014), while mean Fe levels in soil (8,521 mg/kg) and water (4.5 mg/L)

align with previous studies (Akpan et al., 2021). A near-neutral pH (5.98–6.05) suggests natural attenuation through carbonate buffering and reduced sulphide oxidation (Akcil & Koldas, 2006; Banks et al., 1997; Nordstrom, 2011). Although these conditions limit metal solubility, exceedances of NSDWQ and WHO limits for Fe, Mn, Ba, and Al, along with the persistence of Fe, Cr, Cd, As, Pb, and Zn, indicate potential long-term exposure risks.

Sixteen priority PAHs were detected across all media, with concentrations highest in soils (mean = 2,421.6 µg/kg), followed by tailings (1,678.5 µg/kg) and sediments (79.7 µg/kg). This gradient reflects the higher retention capacity of soils and tailings and attenuation through dilution and biodegradation in sediments. The distribution of PAH compounds in surface and groundwater samples from the mine area showed that LMW PAHs (Nap, Acy, Ace, Flu, and Phe) were dominant across all samples, particularly in the mine adits. In contrast, heavier PAHs, such as BaA, Chr, and BaP, were present at lower proportions. Compositional patterns in soil/tailing samples were dominated by Nap, Flu, Pyr (LMW) and BaA, Chr, BbF, and BaP (HMW) species. The predominance of HMW compounds, coupled with elevated BaP, DBA, and BghiP near adits, indicates contamination primarily from coal-processing residues and weathering of exposed seams (Achten & Hofmann, 2009; Kapley et al., 2020; C. Li et al., 2019). The ∑BaPeq value (0.86 mg TEQ/kg) exceeded the Canadian Soil Quality Guideline (0.6 mg TEQ/kg), indicating that DBA and BaP are the dominant toxic contributors. The persistence of HMW PAHs, driven by their hydrophobicity and strong binding to soil organic matter (K. Chen et al., 2024; Deng et al., 2023), underscores long-term ecological and carcinogenic risks.

These findings underscore the need for HHRA to evaluate the cumulative and chronic health implications of metal bioavailability and remobilisation in local communities dependent on contaminated soil and water resources.

The HHRA revealed distinct exposure patterns for both HMs and PAHs at the Onyeama AML. Ingestion was the dominant pathway, followed by dermal contact, while inhalation contributed minimally. Children consistently showed higher CDI, HI, and ILCR values than adults, reflecting greater exposure frequency and lower body weight (Halfadji et al., 2021; Zoveidadianpour et al., 2023). For HMs, As, Cr, and Pb were the main contributors to both non-carcinogenic and carcinogenic risks. The cumulative HI for soil (6.50 – children; 0.94 – adults) and water (4.87 – children; 6.12 – adults) exceeded 1, indicating potential adverse effects, while ∑CCR values for soil (1.57×10^{-4}) and water (1.18×10^{-4}) surpassed the acceptable limit (1×10^{-4}), suggesting possible carcinogenic concern.

For PAHs, moderate non-carcinogenic risk was associated with Nap, Flu, and Pyr via soil and water ingestion, while BaP and DBA contributed most to carcinogenic risk (Aralu et al., 2023; Yusuf et al., 2022). Although PAH-related cancer risks in soil ($9.07 \times 10^{-7} – 1.82 \times 10^{-6}$) were within tolerable limits, waterborne risks ($4.86 \times 10^{-3} – 3.25 \times 10^{-3}$) exceeded acceptable thresholds, identifying contaminated water as the primary exposure route. The elevated HI and CCR values, particularly among children and

farmers who use the site for vegetable cultivation, highlight significant vulnerability and justify urgent risk management actions.

While the environmental and human health impacts of heavy metals and acid mine drainage from abandoned coal mines have been widely documented, the potential human health risks associated with organic contaminants, particularly PAHs, have received limited attention. Abandoned coal mines act as long-term sources of both inorganic and organic pollutants, creating pathways for human exposure through contaminated soil and water. Findings from this study confirm that such contamination poses measurable non-carcinogenic and carcinogenic risks to local populations, thereby emphasising the need for continuous monitoring and remediation. This research helps bridge the knowledge gap by characterising PAH concentrations and quantifying associated human health risks in soil, tailings, and water from the Onyeama abandoned coal mine area.

7.5 Policy Recommendations for Managing Abandoned Mine Lands in Nigeria

AMLs in Nigeria continue to pose serious environmental and public health risks due to persistent contamination from HMs and PAHs. Findings from this study, based on investigations at two abandoned lead–zinc mines at Gimbi in the Wase mining district in Plateau State and at Abakaliki in Ebonyi State and an abandoned coal mine in Enugu State, revealed elevated concentrations of Pb, Zn, Cd, and PAHs in soils, sediments, and water bodies that exceed international guideline values. Ecological risk assessment indicated a high potential for toxicity to soil, aquatic, and terrestrial receptors. In contrast, human health risk assessment identified potential non-carcinogenic and carcinogenic risks, particularly through ingestion and dermal contact. These results underscore the cumulative pollution burden and the lack of coordinated monitoring, remediation, and risk communication within Nigeria's post-mining landscape.

Despite ongoing mining activities and a longstanding history of abandoned operations, Nigeria lacks a robust, dedicated policy framework for managing chemically contaminated land. Existing regulations mainly focus on physical reclamation and mine safety, with limited attention to long-term chemical exposure or ecological and human health risks. Drawing from international best practices such as the United Kingdom's Part 2A Contaminated Land Regime (UK EA, 2020), the Netherlands' risk-based soil management framework (Swartjes et al., 2012), and the community health prioritisation model used in Appalachia (Surber, 2021). Nigeria should establish a National Contaminated Land Management Framework under the Federal Ministry of Environment, in collaboration with the Ministry of Solid Minerals Development. This framework should legally define contaminated land, utilise risk-based assessment tools to prioritise remediation, and develop a national inventory and database of contaminated mine sites supported by environmental monitoring and transparent reporting, which are currently not in place.

Nigeria's existing institutional structure already provides a foundation for such a framework. The National Environmental Standards and Regulations Enforcement Agency (NESREA) under the Ministry of Environment and the Mines Environmental Compliance Department (MEC) under the Ministry of Solid Minerals Development both have relevant but separate mandates. NESREA enforces environmental standards and pollution control, while MEC focuses on environmental compliance during active mining and mine closure. However, this division leaves post-closure and legacy contamination, especially from abandoned or orphaned mines, inadequately addressed. Rather than establishing a new agency, Nigeria should promote an integrated contaminated land management arrangement that formalises collaboration between NESREA and MEC. NESREA would serve as the lead regulatory body for enforcement, monitoring, and community reporting, while MEC would provide technical expertise in mining-related contamination, risk assessment, and remediation. Such coordination would enable a comprehensive, risk-based, and health-centred approach to addressing contamination from abandoned mine lands.

Remediation targets should follow a "fitness-for-use" principle, allowing for safe land reuse while safeguarding human and ecological receptors. A dedicated remediation fund, financed through mining royalties and public-private partnerships, should support the cleanup of high-risk AMLs. Integrating community health data, local participation, and innovative low-cost remediation technologies such as phytoremediation and tailings reprocessing will enhance cost-effectiveness and trust. Grounding these policy measures in scientific evidence from Nigerian case studies, such as the contamination patterns and risk assessments presented in this research, ensures that AML management becomes science-based, locally relevant, and aligned with global best practices for sustainable post-mining land governance.

7.6 Limitations to the Study

The main limitation of these studies lies in the limited number of case studies and the absence of comprehensive temporal and spatial assessments to elucidate contaminant behaviour across seasons. The small number of investigated sites, relative to the number of AMLs in Nigeria, restricts comparative evaluation and generalisation of findings. Notably, only one coal mine was surveyed; expanding the scope to include other abandoned coal mines within the Enugu coalfield would have provided broader insights into spatial variability and contaminant dynamics across similar geological and operational settings. The US EPA recommends incorporating both temporal and spatial assessments to better characterise contaminant distribution, seasonal variations, and potential exposure pathways.

Additionally, the samples were handled under an APHA License, which was not possible without greater effort in writing SOP and lab modifications; this imposed restrictions on the analysis of potentially contaminated materials to prevent the release of pollutants into the environment. As a result, laboratory determinations of key soil parameters influencing contaminant bioavailability, such as pH, organic matter content, cation exchange capacity (CEC), texture and clay fraction, redox potential (Eh),

and soil moisture content, were not possible. The absence of these supporting data limited the interpretation of the geochemical and physicochemical controls on contaminant mobility and bioavailability at the study sites, thereby constraining the formulation of site-specific management recommendations.

Furthermore, X-ray diffraction (XRD) and scanning electron microscopy (SEM) analyses were not conducted to characterise the mineralogical composition and microstructural features of the environmental samples. These techniques would have provided valuable insights into the mineral phases, surface morphology, and particle associations influencing contaminant retention and release. The absence of this information limits the interpretation of the mineral–contaminant interactions and geochemical mechanisms governing contaminant mobility and potential release from tailings and soils.

Lastly, the initial study design included the use of Microtox bioassays to evaluate the toxicity of contaminated environmental samples. However, these analyses could not be conducted due to time constraints associated with thesis submission. The absence of bioassay data limited the ability to validate chemically predicted risks with empirical ecotoxicological evidence, thereby further strengthening the overall risk characterisation and providing a more comprehensive assessment of contaminant effects.

7.7 Future Perspectives

Future research should prioritise comprehensive spatial and temporal assessments of contaminant dynamics across the Wase, Abakaliki abandoned Pb-Zn, and the Enugu abandoned coalfield in Nigeria. Expanding sampling to multiple sites and monitoring across wet and dry seasons would enhance understanding of the seasonal variability of contaminant mobility, transformation, and exposure potential.

The evidence narrative indicates a paucity of studies addressing airborne exposure pathways around abandoned Pb/Zn mines, and coal mine environments remain underexplored; future research should consider this. Additionally, limited studies have investigated organic contamination and risk assessment in abandoned coal mines. Future research should therefore focus on the Enugu coalfield, assessing organic contaminant profiles and conducting associated ecological and human health risk evaluations, such as the Alkylated PAHs, e.g. 7,12-dimethylbenzene(a)anthracene.

Integrating mineralogical and microstructural analyses (XRD and SEM) with chemical and biological data would help clarify contaminant–mineral interactions and support predictive modelling of contaminant release and retention. This should be considered in assessing abandoned Pb-zinc and coal mines. In addition, Risk assessment frameworks should also incorporate effect-based tools and biomarkers to align predicted chemical risks with observed ecological and biological outcomes.

Moreover, combining bioassay-based toxicity testing (e.g., Microtox, earthworm, or algal assays) with chemical analyses is essential for validating modelled risks and strengthening risk characterisation.

At the Abakaliki site, biological monitoring should be conducted on domestic animals and livestock to evaluate contaminant uptake. At the same time, bioaccumulation studies on aquatic organisms and benthic invertebrates are recommended to determine internal metal burdens. Additionally, toxicological assessments should be undertaken to evaluate potential carcinogenic and non-carcinogenic effects, particularly for Pb and Cd exposure for adults and children living next to the AML site. For the Gimbi site, further investigation should focus on elucidating the geochemical processes controlling Pb immobility, thereby improving understanding of metal transport and stability under varying redox and pH conditions.

Given the high acidity of mine water and lack of tailings containment observed at the Abakaliki Pb/Zn mine, future work should focus on developing and evaluating cost-effective remediation and containment strategies suitable for tropical, resource-limited contexts. Potential approaches include passive treatment systems such as anoxic limestone drains, open limestone channels, and constructed wetlands to promote pH neutralisation and metal precipitation. Active remediation techniques, including alkaline amendment of tailings, selective backfilling, and engineered cover systems, should also be explored to limit oxygen ingress and prevent further acid generation. In addition, phytoremediation and microbial-assisted bioremediation could offer sustainable, low-maintenance solutions for stabilising contaminated soils and tailings. Future studies should integrate these remedial options into site-specific hydrogeochemical models to assess their long-term effectiveness in reducing contaminant fluxes, improving water quality, and mitigating ecological and human health risks associated with abandoned Pb/Zn mines.

At the Gimbi site, the existing tailings dam, which lacks an engineered outlet, presents a potential risk to groundwater through seepage and subsurface contaminant migration. Continuous monitoring of groundwater pathways is therefore essential for evaluating potential leaching of metals and other contaminants into underlying aquifers. Future investigations should include hydrogeochemical profiling and isotopic tracing to characterise contaminant transport mechanisms and identify early warning indicators of groundwater pollution. Developing a comprehensive groundwater monitoring network will be crucial for assessing cumulative contamination risks and informing sustainable water resource management in communities surrounding the site.

References

911Metallurgist. (2020, December 23). *Water in Mining*. Https://Www.911metallurgist.Com/. https://www.911metallurgist.com/blog/water-mining/

Abdelnour, S. A., Abd El-Hack, M. E., Khafaga, A. F., Noreldin, A. E., Arif, M., Chaudhry, M. T., Losacco, C., Abdeen, A., & Abdel-Daim, M. M. (2019). Impacts of rare earth elements on animal health and production: Highlights of cerium and lanthanum. *Science of the Total Environment*, *672*, 1021–1032. https://doi.org/10.1016/J.SCITOTENV.2019.02.270

Abiye, T. A. (2014). Mine water footprint in the Johannesburg area, South Africa: Analysis based on existing and measured data. *South African Journal of Geology*, *117*(1), 87–96. https://doi.org/10.2113/GSSAJG.117.1.87

Acero, P., Ayora, C., Torrentó, C., & Nieto, J. M. (2006). The behavior of trace elements during schwertmannite precipitation and subsequent transformation into goethite and jarosite. *Geochimica et Cosmochimica Acta*, *70*(16), 4130–4139. https://doi.org/10.1016/J.GCA.2006.06.1367

Achten, C., & Hofmann, T. (2009). Native polycyclic aromatic hydrocarbons (PAH) in coals - A hardly recognized source of environmental contamination. In *Science of the Total Environment* (Vol. 407, Number 8, pp. 2461–2473). https://doi.org/10.1016/j.scitotenv.2008.12.008

Adebayo, A. (2015, August 15). *Developing artisanal small-scale mining in Nigeria – Daily Trust*. Daily Trust. https://dailytrust.com/developing-artisanal-small-scale-mining-in-nigeria/

Adeyi, A. A., & Babalola, B. A. (2017). Lead and Cadmium Levels in Residential Soils of Lagos and Ibadan, Nigeria. *Journal of Health & Pollution*, *7*(13), 42–55. https://doi.org/10.5696/2156-9614-7-13.42

Ahmed, Y. M., & Oruonye, E. D. (2018). Inventorization of Abandoned Mines and quarry Pits in Taraba State, Nigeria. *International Journal of Environment, Agriculture and Biotechnology*, *3*(5), 1804–1815. https://doi.org/10.22161/IJEAB/3.5.32

Aigbedion, I., & Iyayi, S. E. (2007). Environmental effect of mineral exploitation in Nigeria. *International Journal of Physical Sciences*, *2*(2), 33–38. https://doi.org/10.5897/IJPS.9000228

Akande, S. O., & Mücke, A. (1993). Coexisting copper sulphides and sulphosalts in the Abakaliki Pb-Zn deposit, lower Benue Trough (Nigeria) and their genetic significance. *Mineralogy and Petrology*, *47*(2–4), 183–192. https://doi.org/10.1007/BF01161566/METRICS

Akbar, K. A., & Kallawicha, K. (2024). Black Lung Disease among Coal Miners: First Ever Evidence from Indonesia's National Coal Production Report. *Aerosol and Air Quality Research*, *24*(12), 240161. https://doi.org/10.4209/AAQR.240161

Akcil, A., & Koldas, S. (2006). Acid Mine Drainage (AMD): causes, treatment and case studies. *Journal of Cleaner Production*, *14*(12-13 SPEC. ISS.), 1139–1145. https://doi.org/10.1016/J.JCLEPRO.2004.09.006

Akpan, L., Tse, A. C., Giadom, F. D., & Adamu, C. I. (2021). Chemical Characteristics of Discharges from Two Derelict Coal Mine Sites in Enugu Nigeria : Implication for Pollution and Acid Mine Drainage. *Journal of Mining and Environment (JME) Chemical*, (August). https://doi.org/10.22044/jme.2020.10181.1956

Alao, O., & Ibrahim, H. (2014). Plateau bears scars of tin mining - Daily Trust. In *Daily Trust*. https://dailytrust.com/plateau-bears-scars-of-tin-mining/

Alonzo, D., Tabelin, C. B., Dalona, I. M., Abril, J. M. V., Beltran, A., Orbecido, A., Villacorte-Tabelin, M., Resabal, V. J., Promentilla, M. A., Suelto, M., Brito-Parada, P. R., Plancherel, Y., Jungblut, A. D., Armstrong, R., Santos, A., Schofield, P. F., & Herrington, R. (2024). Working with the community for the rehabilitation of legacy mines: Approaches and lessons learned from the literature. *Resources Policy*, *98*, 105351. https://doi.org/10.1016/J.RESOURPOL.2024.105351

Alpers, C. N., Hunerlach, M. P., May, J. T., & Hothem, R. L. (2005). *Mercury Contamination from Historical Gold Mining in California*. https://pubs.usgs.gov/fs/2005/3014/

Alvarenga, P., Laneiro, C., Palma, P., de Varennes, A., & Cunha-Queda, C. (2013). A study on As, Cu, Pb and Zn (bio)availability in an abandoned mine area (São Domingos, Portugal) using chemical and ecotoxicological tools. *Environmental Science and Pollution Research*, *20*(9), 6539–6550. https://doi.org/10.1007/s11356-013-1649-2

Anawar, H. M. (2013). Impact of climate change on acid mine drainage generation and contaminant transport in water ecosystems of semi-arid and arid mining areas. *Physics and Chemistry of the Earth, Parts A/B/C*, *58–60*, 13–21. https://doi.org/10.1016/J.PCE.2013.04.002

Anawar, H. M. (2015). Sustainable rehabilitation of mining waste and acid mine drainage using geochemistry, mine type, mineralogy, texture, ore extraction and climate knowledge. *Journal of Environmental Management*, *158*, 111–121. https://doi.org/10.1016/J.JENVMAN.2015.04.045

Anzecc, & Armcanz. (2000). *Australian and New Zealand Guidelines for Fresh and Marine Water Quality The Guidelines Australian and New Zealand Environment and Conservation Council Agriculture and Resource Management Council of Australia and New Zealand*.

Aralu, C. C., Okoye, P. A. C., Abugu, H. O., Eboagu, N. C., & Eze, V. C. (2023). Characterization, sources, and risk assessment of PAHs in borehole water from the vicinity of an unlined dumpsite in Awka, Nigeria. *Scientific Reports*, *13*(1). https://doi.org/10.1038/s41598-023-36691-3

Arinze, I. J., Emedo, C. O., & Ugbor, C. C. (2019). A scalar-geometric approach for the probable estimation of the reserve of some Pb-Zn deposits in Ameri, southeastern Nigeria. *Journal of Sustainable Mining*, *18*(4), 208–225. https://doi.org/10.1016/J.JSM.2019.07.004

Ariyarathna, T., Vlahos, P., Tobias, C., & Smith, R. (2016). Sorption kinetics of TNT and RDX in anaerobic freshwater and marine sediments: Batch studies. *Environmental Toxicology and Chemistry*, *35*(1), 47–55. https://doi.org/10.1002/ETC.3149

Armiento, G., Barsanti, M., Caprioli, R., Chiavarini, S., Conte, F., Crovato, C., De Cassan, M., Delbono, I., Montereali, M. R., Nardi, E., Parrella, L., Pezza, M., Proposito, M., Rimauro, J., Schirone, A., & Spaziani, F. (2022). Heavy metal background levels and pollution temporal trend assessment within the marine sediments facing a brownfield area (Gulf of Pozzuoli, Southern Italy). *Environmental Monitoring and Assessment*, *194*(11), 1–21. https://doi.org/10.1007/S10661-022-10480-3/FIGURES/9

Aroh, B. (2021, September 3). *Living On The Edge: Abandoned Coal Mines In Enugu Are Eclipsing Communities*. Saharareporters.Com. http://saharareporters.com/2021/09/03/living-edge-abandoned-coal-mines-enugu-are-eclipsing-communities

Ashby, A., & van-Etten, E. (2021). Exploring abandoned mines through a public lens. *Proceedings of the 14th International Conference on Mine Closure*, 1–14. https://papers.acg.uwa.edu.au/p/2152_46_Ashby/

Ashim Sikdar, Md. Shakhawat Hossain, & Shulin Feng. (2020). Heavy Metal Pollution of Environment by Mine Tailings and the Potential Reclamation Techniques: A Review. *Journal of Biology, Agriculture and Healthcare*. https://doi.org/10.7176/jbah/10-16-05

Ashley, P. M., Lottermoser, B. G., & Chubb, A. J. (2003). Environmental geochemistry of the Mt Perry copper mines area,SE Queensland, Australia. *Geochemistry: Exploration, Environment, Analysis*, *3*(4), 345–357. https://doi.org/10.1144/1467-7873/03-014

Asogwa, S. E. (1988). The health benefits of mechanization at the Nigerian Coal Corporation. *Accident; Analysis and Prevention*, *20*(2), 103–108. https://doi.org/10.1016/0001-4575(88)90025-5

ASTDR. (2022). *Guidance for Calculating Benzo(a)pyrene Equivalents for Cancer Evaluations of Polycyclic Aromatic Hydrocarbons*.

Atik, M. D., Taylan, A., & Uçan, E. S. (2022). Radiological Findings in the Case Exposed to Zirconium. *Turkish Thoracic Journal*, *23*(6), 426–429. https://doi.org/10.5152/TURKTHORACJ.2022.22109,

ATSDR. (1995). *Toxicological Profile for Polycyclic Aromatic Hydrocarbons*.

ATSDR. (1999). Toxicological profile for total petroleum hydrocarbons (TPH). In *Atlanta, GA: U.S. Department of Health and Human Services, Public Health Service.* www.atsdr.cdc.gov/

ATSDR. (2000). *Toxicological Profile For Polychlorinated Biphenyls (Pcbs)*.

ATSDR. (2024). Toxicological Profile for Benzene. In *Atlanta, GA: U.S. Department of Health and Human Services, Public Health Service.* www.regulations.gov.

Ayari, J., Barbieri, M., Agnan, Y., Sellami, A., Braham, A., Dhaha, F., & Charef, A. (2021). Trace element contamination in the mine-affected stream sediments of Oued Rarai in north-western Tunisia: a river basin scale assessment. *ENVIRONMENTAL GEOCHEMISTRY AND HEALTH*, *43*(10), 4027–4042. https://doi.org/10.1007/s10653-021-00887-1

Ayari, J., Barbieri, M., Barhoumi, A., Boschetti, T., Braham, A., Dhaha, F., & Charef, A. (2023). Trace metal element pollution in media from the abandoned Pb and Zn mine of Lakhouat, Northern Tunisia. *Journal of Geochemical Exploration*, *247*. https://doi.org/10.1016/j.gexplo.2023.107180

Azubuike, S. I., Nakanwagi, S., Pinto, J., I, A. S., Susan, N., & Jaqueline, P. (2022). Mining Resource Corridor development in Nigeria: critical considerations and actions for a diversified and sustainable economic future. *Mineral Economics*, *1*, 1–17. https://doi.org/10.1007/s13563-022-00307-5

Badakhshan, N., Shahriar, K., Afraei, S., & Bakhtavar, E. (2023). Evaluating the impacts of the transition from open-pit to underground mining on sustainable development indexes. *Journal of Sustainable Mining*, *22*(2), 155–168. https://doi.org/10.46873/2300-3960.1382

Baiyewu-Teru, A. (2015). The History of Coal in Nigeria. In *Heinrich Böll Stiftung _ Abuja office - Nigeria*.

Balasubramanian, A. (2017). An overview of mining Methods. *DOI: 10.13140/RG.2.2.15761.63845. Https://Www.Researchgate.Net/Publication/ 314502989*, (February), 1–8. https://doi.org/10.13140/RG.2.2.15761.63845

BAM. (2004, October 1). *Introducing tailsafe*. Tailsafe.Com. https://www.tailsafe.com/introducing_tailsafe.html

Banks, D., Younger, P. L., Road, H., Younger, P. L., Arnesen, R.-T., Iversen, E. R., & Banks, S. B. (1997). Mine-water chemistry: the good, the bad and the ugly. In *Environmental Geology* (Vol. 32, Number 3). Springer-Verlag.

Bao, J., Wang, L., & Xiao, M. (2016). Changes in speciation and leaching behaviors of heavy metals in dredged sediment solidified/stabilized with various materials. *Environmental Science and Pollution Research*, *23*(9), 8294–8301. https://doi.org/10.1007/S11356-016-6184-5/FIGURES/3

Barraza, F., Maurice, L., Uzu, G., Becerra, S., López, F., Ochoa-Herrera, V., Ruales, J., & Schreck, E. (2018). Distribution, contents and health risk assessment of metal(loid)s in small-scale farms in the Ecuadorian Amazon: An insight into impacts of oil activities. *Science of The Total Environment*, *622–623*, 106–120. https://doi.org/10.1016/J.SCITOTENV.2017.11.246

Basu, N., Clarke, E., Green, A., Calys-Tagoe, B., Chan, L., Dzodzomenyo, M., Fobil, J., Long, R. N., Neitzel, R. L., Obiri, S., Odei, E., Ovadje, L., Quansah, R., Rajaee, M., & Wilson, M. L. (2015). Integrated Assessment of Artisanal and Small-Scale Gold Mining in Ghana—Part 1: Human Health Review. *International Journal of Environmental Research and Public Health*, *12*(5), 5143–5176. https://doi.org/10.3390/IJERPH120505143

Beane, S. J., Comber, S. D. W., Rieuwerts, J., & Long, P. (2016). Abandoned metal mines and their impact on receiving waters: A case study from Southwest England. *Chemosphere*, *153*, 294–306. https://doi.org/10.1016/j.chemosphere.2016.03.022

Bebbington, A., & Williams, M. (2008). Water and Mining Conflicts in Peru. *Https://Doi.Org/10.1659/Mrd.1039*, *28*(3), 190–195. https://doi.org/10.1659/MRD.1039

Bennett, K. (2016). Abandoned mines — environmental, social and economic challenges. *Proceedings of the 11th International Conference on Mine Closure*, 241–252. https://doi.org/10.36487/acg_rep/1608_16_bennett

Benson, R., Kaufmann, R., Yuhr, L., & Hopkins, R. (2003). Locating and Characterizing Abandoned Mines Using Microgravity. *Technos, Inc*. https://www.fhwa.dot.gov/engineering/geotech/hazards/mine/workshops/ktwkshp/ky0316.pdf

Bes, C. M., Pardo, T., Bernal, M. P., & Clemente, R. (2014). Assessment of the environmental risks associated with two mine tailing soils from the La Unión-Cartagena (Spain) mining district. *Journal of Geochemical Exploration*, *147*(PB), 98–106. https://doi.org/10.1016/J.GEXPLO.2014.05.020

Beyer, A., & Biziuk, M. (2009). Environmental Fate and Global Distribution of Polychlorinated Biphenyls. *Reviews of Environmental Contamination and Toxicology*, *201*, 137–158. https://doi.org/10.1007/978-1-4419-0032-6_5

Bigham, J. M., & Cravotta, C. A. (2016). Acid Mine Drainage. In *USGS Publications Warehouse* (pp. 6–10). CRC Press Taylor and Francis Group. https://doi.org/10.1081/E-ESS3-120053867

Bio-Met. (2022). *Bioavailability Tool - Bio-met* (5.1). www.bio-met.net. https://bio-met.net/bioavailability-tool/

Blowes, D. W., Ptacek, C. J., Jambo, J. L., Weisener C G, Paktunc D, Gould W D, & Johnson D B. (2014). The Geochemistry of Acid Mine Drainage. *Elsevier*. https://doi.org/10.1016/B978-0-08-095975-7.00905-0

Blowes, D. W., Ptacek, C. J., Jambor, J. L., & Weisener, C. G. (2003). The Geochemistry of Acid Mine Drainage. *Treatise on Geochemistry*, *9–9*, 149–204. https://doi.org/10.1016/B0-08-043751-6/09137-4

BML. (2017). Abandoned Mine Lands. In *US Department of The Interior - Bureau of Land Management*. https://www.blm.gov/programs/aml-environmental-cleanup/aml

Bonnail, E., Sarmiento, A. M., DelValls, T. A., Nieto, J. M., & Riba, I. (2016). Assessment of metal contamination, bioavailability, toxicity and bioaccumulation in extreme metallic environments

(Iberian Pyrite Belt) using Corbicula fluminea. *SCIENCE OF THE TOTAL ENVIRONMENT*, *544*, 1031–1044. https://doi.org/10.1016/j.scitotenv.2015.11.131

Bouzekri, S., El Fadili, H., El Hachimi, M. L., El Mahi, M., & Lotfi, E. M. (2020). Assessment of trace metals contamination in sediment and surface water of quarry lakes from the abandoned Pb mine Zaida, High Moulouya-Morocco. *Environment, Development and Sustainability*, *22*(7), 7013–7031. https://doi.org/10.1007/s10668-019-00525-y

Bowers, R. L., & Smith, J. W. N. (2014). Constituents of potential concern for human health risk assessment of petroleum fuel releases. *Quarterly Journal of Engineering Geology and Hydrogeology*, *47*(4), 363–372. https://doi.org/10.1144/qjegh2014-005

BPE. (2006). Nigerian Coal Corporation. In *Bureau of Public Enterprises*. https://www.bpe.gov.ng/nigerian-coal-corporation/

Breivik, K., Sweetman, A., Pacyna, J. M., & Jones, K. C. (2002). Towards a global historical emission inventory for selected PCB congeners - A mass balance approach: 2. Emissions. *Science of the Total Environment*, *290*(1–3), 199–224. https://doi.org/10.1016/S0048-9697(01)01076-2

Bridge, G., & Fredriksen, T. (2012). "Order out of chaos": Resources, hazards and the production of a tin-mining economy in northern Nigeria in the early twentieth century. *Environment and History*, *18*(3), 367–394. https://doi.org/10.3197/096734012X13400389809337;REQUESTEDJOURNAL:JOURNAL:WHPEH;PAGE:STRING:ARTICLE/CHAPTER

Buat-Menard, P., & Chesselet, R. (1979). Variable influence of the atmospheric flux on the trace metal chemistry of oceanic suspended matter. *Earth and Planetary Science Letters*, *42*(3), 399–411. https://doi.org/10.1016/0012-821X(79)90049-9

Buchman, M. F. (2008). *NOAA Screening Quick Reference Tables*. https://repository.library.noaa.gov/view/noaa/9327.

Buckley, L., Rudolph, L., & Maizlish, N. (2017). Public Health Research Roadmap on Emerging Electricity Systems. In *California Energy Commission*. http://climatehealthconnect.org/

Bukowska, B., Mokra, K., & Michałowicz, J. (2022). Benzo[a]pyrene—Environmental Occurrence, Human Exposure, and Mechanisms of Toxicity. *International Journal of Molecular Sciences*, *23*(11). https://doi.org/10.3390/IJMS23116348,

Bulovic, N., McIntyre, N., & Trancoso, R. (2024). Climate change risks to mine closure. *Journal of Cleaner Production*, *465*, 142697. https://doi.org/10.1016/J.JCLEPRO.2024.142697

Burger, A. M., & Taylor, I. (2021). *Independent Technical Report Mineral Resource and Ore Reserve Estimate, Segilola Gold Deposit, Osun Province Nigeria*. www.miningassociates.com.au

Burton, A. (2012). Massive childhood lead poisoning: the price of Nigerian gold. *Environmental Health Perspectives*, *120*(4). https://doi.org/10.1289/EHP.120-A165A

Bute, S. I., Zhou, J. X., Luo, K., Girei, M. B., & Peter, R. T. (2024). Pb-Zn-Ba deposits in the Nigerian Benue Trough: A synthesis on deposits classification and genetic model. *Ore Geology Reviews*, *166*, 105947. https://doi.org/10.1016/J.OREGEOREV.2024.105947

Bwede, D. D., Wuana, R. A., Egah, G. O., Itodo, A. U., Ogah, E., Yerima, E. A., & Ibrahim, A. I. (2021). Characterization and Evaluation of Human Health Risk of Heavy Metals in Tin Mine Tailings in Selected Area of Plateau State, Nigeria. *Journal of the Nigerian Society of Physical Sciences*, *3*(4), 406–413. https://doi.org/10.46481/JNSPS.2021.262

Byrne, P., Yendell, A., Frau, I., & Todd, A. M. L. (2021). Identification and Prioritisation of Mine Pollution Sources in a Temperate Watershed Using Tracer Injection and Synoptic Sampling. *Mine Water and the Environment 2021 40:4*, *40*(4), 980–993. https://doi.org/10.1007/S10230-021-00792-0

Cacciuttolo, C., & Cano, D. (2022). Environmental Impact Assessment of Mine Tailings Spill Considering Metallurgical Processes of Gold and Copper Mining: Case Studies in the Andean Countries of Chile and Peru. *Water 2022, Vol. 14, Page 3057*, *14*(19), 3057. https://doi.org/10.3390/W14193057

Calabro, M. R., Roqueiro, G., Tapia, R., Crespo, D. C., Bargiela, M. F., & Young, B. J. (2022). Chronic toxicity, bioavailability and bioaccumulation of Zn, Cu and Pb in Lactuca sativa exposed to waste from an abandoned gold mine. *CHEMOSPHERE*, *307*. https://doi.org/10.1016/j.chemosphere.2022.135855

Calvert, A. F. (1977). *Nigeria and Its Tin Fields*. Arno Press. http://books.google.co.uk/books?id=TtpFeNysW2cC23/03/08

Candeias, C., Avila, P. F., da Silva, E. F., & Teixeira, J. P. (2015). Integrated approach to assess the environmental impact of mining activities: estimation of the spatial distribution of soil contamination (Panasqueira mining area, Central Portugal). *ENVIRONMENTAL MONITORING AND ASSESSMENT*, *187*(3). https://doi.org/10.1007/s10661-015-4343-7

Carvalho, F. P. (2017). Mining industry and sustainable development: Time for change. *Food and Energy Security*, *6*(2), 61–77. https://doi.org/10.1002/FES3.109

Casey, J. (2018, September 19). *Top Mined Minerals in the World: Coal, Iron, Bauxite, and More*. Mining Technology. https://www.mining-technology.com/features/coal-iron-bauxite-top-list-mined-minerals-world/?utm_source=chatgpt.com&cf-view

CCME. (1999). *Canadian Environmental Quality Guidelines Canadian Council of Ministers of the Environment Canadian Soil Quality Guidelines for the Protection of Environmental and Human Health SUMMARY TABLES*. http://www.ccme.ca/publications/ceqg_rcqe.html?category_id=125]

CCME. (2002). *Canadian Sediment Quality Guidelines for the Protection of Aquatic Life*.

CCME. (2006). A Protocol for the Derivation of Environmental and Human Health Soil Quality Guidelines. *Canadian Council of Ministers of the Environment*.

CCME. (2010). *Canadian Soil Quality Guidelines for the Protection of Environmental and Human Health*.

CCME. (2016). Guidance manual for environmental site characterization in support of environmental and human health risk assessment. In *Canadian Council of Ministers of the Environment*. Canadian Council of Ministers of the Environment.

Chang, J. Y., Ahn, S. C., Lee, J. S., Kim, J. Y., Jung, A. R., Park, J., Choi, J. W., & Do Yu, S. (2019). Exposure assessment for the abandoned metal mine area contaminated by arsenic. *Environmental Geochemistry and Health*, *41*(6), 2443–2458. https://doi.org/10.1007/s10653-019-00296-5

Chanpiwat, P., & Numprasanthai, A. (2024). Factors affecting cadmium toxicity to rice germinated in soils collected from downstream areas of abandoned zinc mines. *Global Journal of Environmental Science and Management*, *10*(1), 133–154. https://doi.org/10.22034/gjesm.2024.01.10

Chen, D., Feng, Q., & Liang, H. (2021). Effects of long-term discharge of acid mine drainage from abandoned coal mines on soil microorganisms: microbial community structure, interaction

patterns, and metabolic functions. *Environmental Science and Pollution Research*. https://doi.org/10.1007/s11356-021-14566-2/Published

Chen, K., Shen, H., Zang, S., & Sun, L. (2024). Spatial heterogeneity of polycyclic aromatic hydrocarbons pollution in surface soil of China and its response to regional energy consumption. *Frontiers in Environmental Science*, *12*. https://doi.org/10.3389/fenvs.2024.1496826

Chen, S. C., & Liao, C. M. (2006). Health risk assessment on human exposed to environmental polycyclic aromatic hydrocarbons pollution sources. *Science of The Total Environment*, *366*(1), 112–123. https://doi.org/10.1016/J.SCITOTENV.2005.08.047

Chowdhury, M. A. R., & Singer, D. M. (2023). Complex Speciation and Distribution of Iron, Sulfur, and Trace Metals in Coal Mine Soils Reflect Grain- and Sub-Grain-Scale Heterogeneity during Pyrite Oxidative Dissolution. *Soil Systems 2024, Vol. 8, Page 2*, *8*(1), 2. https://doi.org/10.3390/SOILSYSTEMS8010002

Chukwu, A., & Obiora, S. C. (2023). Effect of Lead–Zinc Mining on Socio-Economic and Health Conditions of Enyigba and Ishiagu Lead–zinc Mining Districts of Southeastern Nigeria. In *Mining, Metallurgy and Exploration* (Vol. 40, Number 2, pp. 691–701). Springer Science and Business Media Deutschland GmbH. https://doi.org/10.1007/s42461-023-00745-x

Ciszewski, D., & Aleksander-Kwaterczak, U. (2020). Metal mobility in a mine-affected floodplain. *Minerals*, *10*(9), 1–20. https://doi.org/10.3390/min10090814

Climate Analytics. (2022). National 1.5°C Compatible Emissions Pathways and Consistent Power Sector Benchmarks in Africa. In *www.climateanalytics.org*. www.climateanalytics.org/publications

Coelho, P., Silva, S., Roma-Torres, J., Costa, C., Henriques, A., Teixeira, J., Gomes, M., & Mayan, O. (2007). Health impact of living near an abandoned mine - Case study: Jales mines. *International Journal of Hygiene and Environmental Health*, *210*(3–4), 399–402. https://doi.org/10.1016/j.ijheh.2007.01.004

Coelho, P., Teixeira, J. P., & Gonçalves, O. N. B. S. M. (2011). Mining Activities: Health Impacts. *Encyclopedia of Environmental Health*, 788–802. https://doi.org/10.1016/B978-0-444-52272-6.00488-8

Cortes-Ramirez, J., Mengersen, K., Morawska, L., Sly, P., Jagals, P., & Wraith, D. (2024). The hospitalisation risk of chronic circulatory and respiratory diseases associated with coal mining in the general population in Queensland, Australia. *Science of The Total Environment*, *949*, 174989. https://doi.org/10.1016/J.SCITOTENV.2024.174989

Cravotta III, C. A. (2008). Dissolved metals and associated constituents in abandoned coal-mine discharges, Pennsylvania, USA. Part 2: Geochemical controls on constituent concentrations. *Applied Geochemistry*, *23*(2), 203–226. https://doi.org/10.1016/j.apgeochem.2007.10.003

Cravotta III, C. A., Brightbill, R. A., & Langland, M. J. (2010). Abandoned Mine Drainage in the Swatara Creek Basin, Southern Anthracite Coalfield, Pennsylvania, USA: 1. Stream Water Quality Trends Coinciding with the Return of Fish. *Mine Water and the Environment*, *29*(3), 176–199. https://doi.org/10.1007/S10230-010-0112-6/FIGURES/13

Custodio, M., Pizarro, S., Huarcaya, J., Ortega, K., & Ccopi, D. (2025). Ecological and Human Health Risk Assessment of Heavy Metals in Mining-Affected River Sediments in the Peruvian Central Highlands. *Toxics*, *13*(9), 783. https://doi.org/10.3390/TOXICS13090783

Dales, J., & Ramasamy, K. (2019). Mapping & Assessing Environmental Hazards of Abandoned Mines in Sub-Saharan African Countries. *UNESCO. Nairobi, Kenya*, 28.

Dash, S., Borah, S. S., & Kalamdhad, A. (2019). A modified indexing approach for assessment of heavy metal contamination in Deepor Beel, India. *Ecological Indicators*, *106*, 105444. https://doi.org/10.1016/J.ECOLIND.2019.105444

David, E., & Niculescu, V. C. (2021). Volatile Organic Compounds (VOCs) as Environmental Pollutants: Occurrence and Mitigation Using Nanomaterials. *International Journal of Environmental Research and Public Health*, *18*(24), 13147. https://doi.org/10.3390/IJERPH182413147

DCC_FMEN. (2021). 2050 Long-Term Vision for Nigeria (LTV-2050)-Towards the Development of Nigeria's Long-Term Low Emissions Development Strategy (LT-LEDS). In *Department of Climate Change, Federal Ministry of Environment, Nigeria*.

De Gaff, J. V. (2018). Mine Closure. *Encyclopedia of Earth Sciences Series*, 1–5. https://doi.org/10.1007/978-3-319-12127-7_199-1/COVER

Deepika, Tyagi, A., & Haritash, A. K. (2025). Environmental impacts of mine tailings and phytoremediation as a sustainable management strategy: A review. *Acta Geochimica 2025 44:5*, *44*(5), 1142–1165. https://doi.org/10.1007/S11631-025-00804-8

Del Rio-Salas, R., Ayala-Ramírez, Y., Loredo-Portales, R., Romero, F., Molina-Freaner, F., Minjarez-Osorio, C., Pi-Puig, T., Ochoa–Landín, L., & Moreno-Rodríguez, V. (2019). Mineralogy and Geochemistry of Rural Road Dust and Nearby Mine Tailings: A Case of Ignored Pollution Hazard from an Abandoned Mining Site in Semi-arid Zone. *Natural Resources Research*, *28*(4), 1485–1503. https://doi.org/10.1007/s11053-019-09472-x

Deng, X., Chen, G., Wang, H., & Sun, H. (2023). Pollution Characteristics and Risk Evaluation of PAHs in Subsidence Water Bodies in Huainan Coal Mining Area, China. *Sustainability (Switzerland)*, *15*(18). https://doi.org/10.3390/su151814003

Dennis, A. (2022). Nigeria's Mineral Production Grew by 39.19% and this is Why it's a Good Thing | Dataphyte. In *DATAPHYTE*. https://www.dataphyte.com/latest-reports/nigerias-mineral-production-grew-by-39-19-and-this-is-why-its-a-good-thing/

DEP. (2015). Abandoned Mine Land Hazards: Problems and Solutions. In *Pennsylvania Department of Environmental Protection*. https://www.pa.gov/agencies/dep/programs-and-services/mining/abandoned-mine-reclamation/aml-program-information/abandoned-mine-land-hazards-and-problem-types.html

Djebbi, C., Chaabani, F., Font, O., Queralt, I., & Querol, X. (2017). Atmospheric dust deposition on soils around an abandoned fluorite mine (Hammam Zriba, NE Tunisia). *ENVIRONMENTAL RESEARCH*, *158*, 153–166. https://doi.org/10.1016/j.envres.2017.05.032

Domingo, J. P. T., Jenkin, G. R. T., Quick, L., Williams, R. D., Hudson-Edwards, K. A., Tortajada, C., Byrne, P., Coulthard, T. J., Padrones, J. T., Crane, R., Gibaga, C. R. L., Vasilopoulos, G., Tungpalan, K., Samaniego, J. O., Biles, E., Tanciongco, A. M., Chambers, J. E., Quimado, M. O., Bautista, A. T., … Arcilla, C. A. (2024). Sustainable mining in tropical, biodiverse landscapes: Environmental challenges and opportunities in the archipelagic Philippines. In *Journal of Cleaner Production* (Vol. 468). Elsevier Ltd. https://doi.org/10.1016/j.jclepro.2024.143114

Domingo, J. P. T., Ngwenya, B. T., Attal, M., David, C. P. C., & Mudd, S. M. (2023). Geochemical fingerprinting to determine sediment source contribution and improve contamination assessment in mining-impacted floodplains in the Philippines. *Applied Geochemistry*, *159*. https://doi.org/10.1016/j.apgeochem.2023.105808

Dooyema, C. A., Neri, A., Lo, Y. C., Durant, J., Dargan, P. I., Swarthout, T., Biya, O., Gidado, S. O., Haladu, S., Sani-Gwarzo, N., Nguku, P. M., Akpan, H., Idris, S., Bashir, A. M., & Brown, M. J.

(2012). Outbreak of fatal childhood lead poisoning related to artisanal gold mining in northwestern Nigeria, 2010. *Environmental Health Perspectives*, *120*(4), 601–607. https://doi.org/10.1289/EHP.1103965

Downham, R. (2022). Understanding environmental impact through the study of sediments. In *British Geological Survey* (pp. 1–2). https://www.bgs.ac.uk/news/understanding-environmental-impact-through-the-study-of-sediments/

Dzombak, D. A., & Morel, F. M. M. (1990). SURFACE COMPLEXATION MODELING Hydrous Ferric Oxide. *A Wiley-Interscience Publication*.

Edun, E. O., & Davou, D. D. (2013). Inventory Of Abandoned Mine Ponds/Dams On The Jos-Bukuru North-Central Nigeria Using G.I.S And Remote Sensing Technique. *The International Journal Of Engineering And Science*. www.theijes.com

Edwards, D. P., Sloan, S., Weng, L., Dirks, P., Sayer, J., & Laurance, W. F. (2014). Mining and the African environment. *Conservation Letters*, *7*(3), 302–311. https://doi.org/10.1111/CONL.12076

EEA. (2004). Mining, mining waste and related environmental issues: Problems and solutions in Central and Eastern European Candidate Countries. *European Environmental Agency*, (Lsi 003), CSI 015/LSI 003. https://doi.org/10.2788/4658

EEA. (2020). Chapter 6: Ecological Risk Assessment. In *European Environmental Agency*. https://www.eea.europa.eu/publications/GH-07-97-595-EN-C2/chapter6h.html#:~:text=Ecological%20Risk%20Assessment%20(EcoRA)%20involves,which%20make%20up%20the%20environment.

EFSA. (2010). Scientific Opinion on Lead in Food. *EFSA Journal*, *8*(4), 151. https://doi.org/10.2903/J.EFSA.2010.1570

Ekundare, R. O. (1973). An economic history of Nigeria, 1860-1960. In *New York, Africana Pub. Co*. https://archive.org/details/economichistoryo1860unse/page/84/mode/2up?q=tin

El Azhari, A., Rhoujjati, A., & EL Hachimi, M. L. (2016). Assessment of heavy metals and arsenic contamination in the sediments of the Moulouya River and the Hassan II Dam downstream of the abandoned mine Zeïda (High Moulouya, Morocco). *Journal of African Earth Sciences*, *119*, 279–288. https://doi.org/10.1016/j.jafrearsci.2016.04.011

Elsevier. (2013). *Mendeley Reference Manager* (2.130.2).

Eludoyin, A. O., Ojo, A. T., Ojo, T. O., & Awotoye, O. O. (2017). Effects of artisanal gold mining activities on soil properties in a part of southwestern Nigeria. *Cogent Environmental Science*, *3*(1). https://doi.org/10.1080/23311843.2017.1305650

Ericsson, M. (1991). African mining: a light at the end of the tunnel? *Review of African Political Economy*, *18*(51), 96. https://doi.org/10.1080/03056249108703911

Ezeigbo, H. I., & Ezeanyim, B. N. (1993). Environmental pollution from coal mining activities in the Enugu area Anambka state Nigeria. *Mine Water and the Environment*, *12*(1), 53–61. https://doi.org/10.1007/BF02914799

Ezemokwe, D. E., & Madubuike, P. C. (2015). Impact of Coal Mining In Enugu Area of Nigeria on the Surrounding Water Quality deezemokwe@gmail.com. *IOSR Journal of Environmental Science*, *9*(12), 35–45. https://doi.org/10.9790/2402-091223545

Fallis, a. G. (2013). Guidebook for Evaluating Mining Project EIAs. In *Journal of Chemical Information and Modeling* (Vol. 53, Number 9).

Fang, H., Gui, H., Yu, H., Li, J., Wang, M., Jiang, Y., Wang, C., & Chen, C. (2021). Characteristics and source identification of heavy metals in abandoned coal-mining soil: a case study of Zhuxianzhuang coal mine in Huaibei coalfield (Anhui, China). *Human and Ecological Risk Assessment*, *27*(3), 708–723. https://doi.org/10.1080/10807039.2020.1750346

Farrington, J. L. (1952). A preliminary description of the Nigerian lead-zinc field. *Economic Geology*, *47*(6), 583–608. https://doi.org/10.2113/GSECONGEO.47.6.583

Fatoye, B. F., Ibitomi, A. M., & Omada, I. J. (2014). Lead-Zinc-Barytes mineralization in the Benue Trough, Nigeria: Their geology, occurrences and economic prospective. *Advances in Applied Science Research*, *5*(2), 86–92. www.pelagiaresearchlibrary.com

Fayemiwo, O. M. (2018). *Plant-based adsorbents for the removal of BTEX compounds from water* [University of Johannesburg]. https://ujcontent.uj.ac.za/esploro/outputs/doctoral/Plant-based-adsorbents-for-the-removal-of/9912579607691

Fecher, B., Friesike, S., Fecher, B., & Friesike, S. (2014). Open Science: One Term, Five Schools of Thought. *Opening Science*, 17–47. https://doi.org/10.1007/978-3-319-00026-8_2

Feng, H., Zhou, J., Chai, B., Zhou, A., Li, J., Zhu, H., Chen, H., & Su, D. (2020). Groundwater environmental risk assessment of abandoned coal mine in each phase of the mine life cycle: a case study of Hongshan coal mine, North China. *Environmental Science and Pollution Research*, *27*(33), 42001–42021. https://doi.org/10.1007/s11356-020-10056-z

Fernández-Lozano, J., Gutiérrez-Alonso, G., & Fernández-Morán, M. Á. (2015). Using airborne LiDAR sensing technology and aerial orthoimages to unravel roman water supply systems and gold works in NW Spain (Eria valley, León). *Journal of Archaeological Science*, *53*, 356–373. https://doi.org/10.1016/J.JAS.2014.11.003

Festin, E. S., Tigabu, M., Chileshe, M. N., Syampungani, S., & Odén, P. C. (2019). Progresses in restoration of post-mining landscape in Africa. *Journal of Forestry Research 2018 30:2*, *30*(2), 381–396. https://doi.org/10.1007/S11676-018-0621-X

Fields, S. (2003). The Earth's open wounds: Abandoned and orphaned mines. *Environmental Health Perspectives*, *111*(3), 154–161.

Filgueiras, V., A., Lavilla, I., Bendicho, & C. (2002). Chemical sequential extraction for metal partitioning in environmental solid samples. *Journal of Environmental Monitoring*, *4*(6), 823–857. https://doi.org/10.1039/B207574C

Freeman, M., Smith, L. K., Freeman, W. B., & Freeman, M. J. (1953). Mining World-Including the Export Edition. *American Trade Journals, Inc*, *15*(7).

Gallart, A. (2017, July 27). *The environmental impact of abandoned metal mines in the UK*. Groundsure. https://www.groundsure.com/the-environmental-impact-of-abandoned-metal-mines-in-the-uk/

Gałuszka, A., Migaszewski, Z. M., & Namieśnik, J. (2015). Moving your laboratories to the field - Advantages and limitations of the use of field portable instruments in environmental sample analysis. In *Environmental Research* (Vol. 140, pp. 593–603). Academic Press Inc. https://doi.org/10.1016/j.envres.2015.05.017

Gammons, C. H., Duaime, T. E., Parker, S. R., Poulson, S. R., & Kennelly, P. (2010). Geochemistry and stable isotope investigation of acid mine drainage associated with abandoned coal mines in central Montana, USA. *Chemical Geology*, *269*(1–2), 100–112. https://doi.org/10.1016/J.CHEMGEO.2009.05.026

Gandhi, S. M. (2014). Copper, zinc, lead ores — Their exploitation and metal extraction by the ancients in the northwestern India. *Journal of the Geological Society of India*, *84*(3), 253–266. https://doi.org/10.1007/S12594-014-0129-8

Gomo, M., & Vermeulen, D. (2014). Hydrogeochemical characteristics of a flooded underground coal mine groundwater system. *Journal of African Earth Sciences*, *92*, 68–75. https://doi.org/10.1016/j.jafrearsci.2014.01.014

Gong, Y., Nunes, L. M., Greenfield, B. K., Qin, Z., Yang, Q., Huang, L., Bu, W., & Zhong, H. (2018). Bioaccessibility-corrected risk assessment of urban dietary methylmercury exposure via fish and rice consumption in China. *Science of the Total Environment*, *630*, 222–230. https://doi.org/10.1016/j.scitotenv.2018.02.224

Gopinathan, P., Subramani, T., Barbosa, S., & Yuvaraj, D. (2023). Environmental impact and health risk assessment due to coal mining and utilization. In *Environmental Geochemistry and Health* (Vol. 45, Number 10, pp. 6915–6922). Springer Science and Business Media B.V. https://doi.org/10.1007/s10653-023-01744-z

Gospel, C., Rachael, C., Ulunma, O., Christian, C., Ogechi, C., Uzoamaka, F., & Gabriel, C. (2020). Assessment of Trace Metals Contamination on Soil From Abandoned Artisanal Tin Mining Paddock in Barkin-Ladi Area of Plateau State. | *Www.Ijaar.Org Journal International Journal of Advanced Academic Research*, *ISSN*(11), 2488–9849. https://doi.org/10.46654/ij.24889849

Grajal-Puche, A., Driver, E. M., & Propper, C. R. (2024). Review: Abandoned mines as a resource or liability for wildlife. In *Science of the Total Environment* (Vol. 921). Elsevier B.V. https://doi.org/10.1016/j.scitotenv.2024.171017

Grande, J. A., Borrego, J., Morales, J. A., & De La Torre, M. L. (2003). A description of how metal pollution occurs in the Tinto–Odiel rias (Huelva-Spain) through the application of cluster analysis. *Marine Pollution Bulletin*, *46*(4), 475–480. https://doi.org/10.1016/S0025-326X(02)00452-6

Grist, C. (2021, November 18). *Reinventing coal country: Reclaiming America's abandoned mine lands*. Grist. https://grist.org/sponsored/reinventing-coal-country-reclaiming-americas-abandoned-mine-lands/

Grmasha, R. A., Abdulameer, M. H., Stenger-Kovács, C., Al-sareji, O. J., Al-Gazali, Z., Al-Juboori, R. A., Meiczinger, M., & Hashim, K. S. (2023). Polycyclic aromatic hydrocarbons in the surface water and sediment along Euphrates River system: Occurrence, sources, ecological and health risk assessment. *Marine Pollution Bulletin*, *187*. https://doi.org/10.1016/j.marpolbul.2022.114568

Guerrero, J. L., Gutiérrez-Álvarez, I., Hierro, A., Pérez-Moreno, S. M., Olías, M., & Bolívar, J. P. (2021). Seasonal evolution of natural radionuclides in two rivers affected by acid mine drainage and phosphogypsum pollution. *CATENA*, *197*, 104978. https://doi.org/10.1016/J.CATENA.2020.104978

Gutiérrez, M., Mickus, K., & Camacho, L. M. (2016). Abandoned Pb-Zn mining wastes and their mobility as proxy to toxicity: A review. *Science of the Total Environment*, *565*, 392–400. https://doi.org/10.1016/j.scitotenv.2016.04.143

Hakanson, L. (1980). An ecological risk index for aquatic pollution control.a sedimentological approach. *Water Research*, *14*(8), 975–1001. https://doi.org/10.1016/0043-1354(80)90143-8

Halfadji, A., Naous, M., Bettiche, F., & Touabet, A. (2021). Human Health Assessment of Sixteen Priority Polycyclic Aromatic Hydrocarbons in Contaminated Soils of Northwestern Algeria. *Journal of Health & Pollution*, *11*(31).

Han, W., Zhao, R., Liu, W., Wang, Y., Zhang, S., Zhao, K., & Nie, J. (2023). Environmental contamination characteristics of heavy metals from abandoned lead–zinc mine tailings in China. *Frontiers in Earth Science*, *11*. https://doi.org/10.3389/feart.2023.1082714

Han, Y., Liu, Y., Wei, S., Wang, M., Ding, G., Song, X., Shen, D., Gao, S., Tang, C., & Ma, G. (2023). Source Apportionment and Health Risk Assessment of Heavy Metals in Karst Water from Abandoned Mines in Zhangqiu, China. *Water (Switzerland)*, *15*(19). https://doi.org/10.3390/w15193440

Hans, N. J. (2021, February 16). *Grim toll from Indonesia's abandoned mines may get even worse, report warns*. Mongabay. https://news.mongabay.com/2021/02/indonesia-abandoned-mining-pit-death-toll-report/

Hasheela, I., Schneider, G. I. C., Ellmies, R., Haidula, A., Leonard, R., Ndalulilwa, K., Shaningwa, O., & Walmsley, B. (2015). Risk Assessment of Abandoned Mines in Namibia_Poster. *ResearchGate*. https://doi.org/10.13140/RG.2.1.3252.8728

He, B., Wang, J., Lin, J., Chen, J., Zhuang, Z., Hong, Y., Yan, L., Lin, L., Shi, B., Qiu, Y., Pan, L., Zheng, X., Liu, F., & Chen, F. (2021). Association Between Rare Earth Element Cerium and the Risk of Oral Cancer: A Case-Control Study in Southeast China. *Frontiers in Public Health*, *9*, 647120. https://doi.org/10.3389/FPUBH.2021.647120

Health Council of the Netherlands. (2002). Zirconium and zirconium compounds. In *Committee on Updating of Occupational Exposure Limits. Zirconium and zirconium compounds; Health-based Reassessment of Administrative Occupational Exposure Limits. The Hague: Health Council of the Netherlands,* (Number 2000/15OSH/059).

Higueras, P., Esbrí, J. M., García-Ordiales, E., González-Corrochano, B., López-Berdonces, M. A., García-Noguero, E. M., Alonso-Azcárate, J., & Martínez-Coronado, A. (2017). Potentially harmful elements in soils and holm-oak trees (Quercus ilex L.) growing in mining sites at the Valle de Alcudia Pb-Zn district (Spain)–Some clues on plant metal uptake. *Journal of Geochemical Exploration*, *182*, 166–179. https://doi.org/10.1016/j.gexplo.2016.07.017

Hoek, B. (2008). Military Explosives and Health. *Source: Medicine, Conflict and Survival*, *20*(4), 326–333. https://doi.org/10.2307/27017607

Holmes, R., & Stewart, G. (2011). A guidance document for mine closure and management of long-term liabilities – examining a policy framework in Canada. *Proceedings of the Sixth International Conference on Mine Closure*, 21–28. https://doi.org/10.36487/acg_rep/1152_69_holmes

Horasan, B. Y. (2020). The environmental impact of the abandoned mercury mines on the settlement and agricultural lands; Ladik (Konya, Turkey). *Environmental Earth Sciences*, *79*, 237. https://doi.org/10.1007/s12665-020-08985-6

Huang, B., Guo, Z., Tu, W., Peng, C., Xiao, X., Zeng, P., Liu, Y., Wang, M., & Xiong, J. (2018). Geochemistry and ecological risk of metal(loid)s in overbank sediments near an abandoned lead/zinc mine in Central South China. *Environmental Earth Sciences*, *77*(3). https://doi.org/10.1007/s12665-018-7249-1

Huang, L. M., Deng, C. B., Huang, N., & Huang, X. J. (2013). Multivariate statistical approach to identify heavy metal sources in agricultural soil around an abandoned Pb-Zn mine in Guangxi Zhuang Autonomous Region, China. *Environmental Earth Sciences*, *68*(5), 1331–1348. https://doi.org/10.1007/s12665-012-1831-8

Huang, X., Sillanpää, M., Gjessing, E. T., Peräniemi, S., & Vogt, R. D. (2010). Environmental impact of mining activities on the surface water quality in Tibet: Gyama valley. *Science of the Total Environment*, *408*(19), 4177–4184. https://doi.org/10.1016/j.scitotenv.2010.05.015

Hufty, M. (2019, November). *Abandoned Mines: The Scars of the Past*. Global Challenges. https://globalchallenges.ch/issue/6/abandoned-mines-the-scars-of-the-past/

Hughes, L. (2024a, June 6). The unseen dangers of lead contamination in the UK. *Financial Times*. https://www.ft.com/content/5bcc846c-9858-4ae3-ae75-06fc17342d3d

Hughes, L. (2024b, October 12). UK food safety watchdog to probe lead levels near abandoned mines. *Financial Times*. https://www.ft.com/content/59b058c0-3f87-45fb-8a8c-f94e08a3bc7b

Human Rights Watch. (2011). *A Heavy Price: Lead Poisoning and Gold Mining in Nigeria's Zamara State*.

IARC. (2010). *Some Non-heterocyclic Polycyclic Aromatic Hydrocarbons and Some Related Exposures*.

Iatan, E.-L. (2021). Gold mining industry influence on the environment and possible phytoremediation applications. *Phytorestoration of Abandoned Mining and Oil Drilling Sites*, 373–408. https://doi.org/10.1016/B978-0-12-821200-4.00007-8

ICMM. (2007). Metals Environmental Risk Assessment Guidance. In *International Council on Mining and Metals*. www.icmm.com

ICMM. (2016). Metals Environmental Risk Assessment Guidance-Weight of evidence approach. *International Council on Mining and Metals*. www.icmm.com

ICMM. (2019). *Mine Closure*. International Council for Mining & Metals. https://www.icmm.com/en-gb/our-work/governance-and-transparency/mine-closure

ICMM. (2021). *Responsible Mine Closure*. International Council for Mining and Metals. https://pimcore.icmm.com/website/publications/pdfs/environmental-stewardship/2021/briefing_responsible-mine-closure.pdf

ICMM. (2025, February 19). *Integrated Mine Closure: Good Practice Guide*. Https://Www.Icmm.Com/Integrated-Mine-Closure. https://www.icmm.com/integrated-mine-closure

IEA News. (2023, July 27). *Global coal demand set to remain at record levels in 2023*. International Energy Agency. https://www.iea.org/news/global-coal-demand-set-to-remain-at-record-levels-in-2023

IGF. (2017). *Global trends in artisanal and small-scale mining (ASM): A review of key numbers and issues*.

IGF. (2025, March 20). *Mine Closure and Post-Mining Transition*. Intergovernmental Forum on Mining. https://www.igfmining.org/mine-closure-and-post-mining-transition/

IRIS. (1994). *Benzo [a] pyrene (BaP); CASRN 50-32-8*. http://www.epa.gov/iris/subst/0136.htmhttp://www.epa.gov/iris/subst/0136.htm

IRIS. (2017, January 9). *Benzo[a]pyrene (BaP) | CASRN 50-32-8 | DTXSID2020139*. U.S. Environmental Protection Agency. https://iris.epa.gov/ChemicalLanding/&substance_nmbr=136

IRIS. (2025). *IRIS Assessments*. US Environmental Protection Agency. https://iris.epa.gov/AtoZ/?list_type=alpha

ISO. (2017). *ISO 19204:2017(en), Soil quality — Procedure for site-specific ecological risk assessment of soil contamination (soil quality TRIAD approach)*. International Organization for Standardization. https://www.iso.org/obp/ui/#iso:std:iso:19204:ed-1:v1:en

ISO. (2018). *ISO 18400-104:2018(en), Soil quality — Sampling — Part 104: Strategies*. International Organization for Standardization. https://www.iso.org/obp/ui/en/#iso:std:iso:18400:-104:ed-1:v1:en

Jain, R., Cui, Z., & Domen, J. (2016). Environmental impacts of mining. In R. K. Jain, Z. "Cindy" Cui, & J. K. Domen (Eds.), *Environmental Impact of Mining and Mineral Processing* (pp. 53–157). Elsevier. https://doi.org/https://doi.org/10.1016/B978-0-12-804040-9.00004-8

James, K. L., Randall, N. P., & Haddaway, N. R. (2016). A methodology for systematic mapping in environmental sciences. *Environmental Evidence*, *5*(1), 1–13. https://doi.org/10.1186/S13750-016-0059-6/TABLES/2

Jang, M. (2010). Application of portable X-ray fluorescence (pXRF) for heavy metal analysis of soils in crop fields near abandoned mine sites. *Environmental Geochemistry and Health*, *32*(3), 207–216. https://doi.org/10.1007/s10653-009-9276-z

Jiang, L., Sun, H., Peng, T., Ding, W., Liu, B., & Liu, Q. (2021). Comprehensive evaluation of environmental availability, pollution level and leaching heavy metals behavior in non-ferrous metal tailings. *Journal of Environmental Management*, *290*. https://doi.org/10.1016/j.jenvman.2021.112639

Jiang, W., & Liang, J. (2023). Solute geochemistry and health risk of water quality for an abandoned rare earth mine in South Jiangxi Province, China. *Human and Ecological Risk Assessment*, *29*(2), 529–552. https://doi.org/10.1080/10807039.2022.2137780

Jiao, Y., Liu, Y., Wang, W., Li, Y., Chang, W., Zhou, A., & Mu, R. (2023). Heavy Metal Distribution Characteristics, Water Quality Evaluation, and Health Risk Evaluation of Surface Water in Abandoned Multi-Year Pyrite Mine Area. *Water (Switzerland)*, *15*(17), 3138. https://doi.org/10.3390/W15173138/S1

Jiao, Y., Zhang, C., Su, P., Tang, Y., Huang, Z., & Ma, T. (2023). A review of acid mine drainage: Formation mechanism, treatment technology, typical engineering cases and resource utilization. In *Process Safety and Environmental Protection* (Vol. 170, pp. 1240–1260). Institution of Chemical Engineers. https://doi.org/10.1016/j.psep.2022.12.083

John, D. A., & Leventhal, J. S. (2004). BIOAVAILABILITY OF METALS. *Environmental Science*.

Johnson, R. H., Blowes, D. W., Robertson, W. D., & Jambor, J. L. (2000). The hydrogeochemistry of the Nickel Rim mine tailings impoundment, Sudbury, Ontario. *Journal of Contaminant Hydrology*, *41*(1–2), 49–80. https://doi.org/10.1016/S0169-7722(99)00068-6

Johnston, D., & Rolley, S. (2008). Abandoned Mines and the Water Framework Directive in the United Kingdom. *Proc. Mine Water and the Environment. VSB– Technical University of Ostrava, Czech Republic*, 529–532.

Juhasz, A. L., & Naidu, R. (2007). Explosives: Fate, dynamics, and ecological impact in terrestrial and marine environments. *Reviews of Environmental Contamination and Toxicology*, *191*, 163–215. https://doi.org/10.1007/978-0-387-69163-3_6,

Julius Kuhn Institut. (2017). *CADIMA*. Quedlinburg, Germany. https://www.cadima.info/index.php/area/evidenceSynthesisDatabase

Kabata-Pendias, A. (2010). Trace elements in soils and plants: Fourth edition. *Trace Elements in Soils and Plants, Fourth Edition*, 1–520. https://doi.org/10.1201/B10158/TRACE-ELEMENTS-SOILS-PLANTS-ALINA-KABATA-PENDIAS/RIGHTS-AND-PERMISSIONS

Kapley, A., Kjellerup, B. V, Saxena, G., Teng, Y., Desai, C., Madamwar, D., Patel, A. B., Shaikh, S., & Jain, K. R. (2020). Polycyclic Aromatic Hydrocarbons: Sources, Toxicity, and Remediation

Approaches. *Frontiers in Microbiology*, *11*, 562813. https://doi.org/10.3389/FMICB.2020.562813

Kefeni, K. K., Msagati, T. A. M., & Mamba, B. B. (2017). Acid mine drainage: Prevention, treatment options, and resource recovery: A review. *Journal of Cleaner Production*, *151*, 475–493. https://doi.org/10.1016/j.jclepro.2017.03.082

Khan, M. A. I., Biswas, B., Smith, E., Naidu, R., & Megharaj, M. (2018). Toxicity assessment of fresh and weathered petroleum hydrocarbons in contaminated soil- a review. *Chemosphere*, *212*, 755–767. https://doi.org/10.1016/J.CHEMOSPHERE.2018.08.094

Kibria, G. (2011). Nuclear Power Plant Accidents and Its Effects. *Science*, (March), 1502–1503.

Kibria, G. (2012). Environmental/Ecological Risk Assessment (ERA) Model for Assessing Risks in Irrigation Areas (Rivers, Creeks, Channels, drains) of toxicants (Pesticides, Herbicides and Trace Metals) to Various Receptors. *National and International Research Collaboration (2001-2012) between the Goulburn Murray Rural Water Corporation, Tatura, Victoria, Australia (G-MW), and Federal, State and Regional Government Departments and the Universities*, 42. http://www.g-mwater.com.au/projects/researchanddevelopment/currentprojects

Kibria, G. (2014). Mining: Friend or Foe? Economic, Environmental & Social Impacts- An Overview. *Science & Technology Article 35*. https://doi.org/10.13140/RG.2.1.1685.0403

Kibria, G., Haroon, A., Nugegoda, D., & Rose, G. (2010). Climate change and chemicals: environmental and biological aspects. In *New India Publishing Agency, New Delhi, India, 460 pp. ISBN: 9789-38-0235-301.* https://www.semanticscholar.org/paper/Climate-change-and-chemicals%3A-environmental-and-Kibria-Haroon/adcc527036330d468cc3641c496ebda1fe24c59b

Kim, D., Kwak, J. Il, Hwang, W., Lee, Y. ho, Lee, Y. S., Kim, J. I., Hong, S., Hyun, S., & An, Y. J. (2022). Site-specific ecological risk assessment of metal-contaminated soils based on the TRIAD approach. *Journal of Hazardous Materials*, *434*. https://doi.org/10.1016/j.jhazmat.2022.128883

Kim, J. Y., Kim, K. W., Ahn, J. S., Ko, I., & Lee, C. H. (2005). Investigation and risk assessment modeling of As and other heavy metals contamination around five abandoned metal mines in Korea. *Environmental Geochemistry and Health*, *27*(2), 193–203. https://doi.org/10.1007/s10653-005-0127-2

Kim, K. H., Jahan, S. A., Kabir, E., & Brown, R. J. C. (2013). A review of airborne polycyclic aromatic hydrocarbons (PAHs) and their human health effects. *Environment International*, *60*, 71–80. https://doi.org/10.1016/J.ENVINT.2013.07.019

Kim, S., Kwon, H. J., Cheong, H. K., Choi, K., Jang, J. Y., Jeong, W. C., Kim, D. S., Yu, S., Kim, Y. W., Lee, K. Y., Yang, S. O., Ik, J. J., Yang, W. H., & Hong, Y. C. (2008). Investigation on Health Effects of an Abandoned Metal Mine. *Journal of Korean Medical Science*, *23*(3), 452. https://doi.org/10.3346/JKMS.2008.23.3.452

Kincey, M., Warburton, J., & Brewer, P. (2018). Contaminated sediment flux from eroding abandoned historical metal mines: Spatial and temporal variability in geomorphological drivers. *Geomorphology*, *319*, 199–215. https://doi.org/10.1016/J.GEOMORPH.2018.07.026

Kirby, B. M., Vengadajellum, C. J., Burton, S. G., & Cowan, D. A. (2010). Coal, Coal Mines and Spoil Heaps. *Handbook of Hydrocarbon and Lipid Microbiology*, 2277–2292. https://doi.org/10.1007/978-3-540-77587-4_166

Kirk, T. . S., Kieron, J. D., Kevin, C. J., Peter, B., Andrew, C., & Hauke, H. (2004). Defining BIOAVAILABILITY and Bioaccessibility of Contaminated Soil and Sediment is Complicated. *Environmental Science & Technology*, 229–231.

Klawans, J. (2024). Abandoned mines pose hidden safety and environmental risks. *The Week*. https://theweek.com/science/abandoned-mine-safety-risks

Knafla, A., Phillipps, K. A., Brecher, R. W., Petrovic, S., & Richardson, M. (2006). Development of a dermal cancer slope factor for benzo[a]pyrene. *Regulatory Toxicology and Pharmacology*, *45*(2), 159–168. https://doi.org/10.1016/j.yrtph.2006.02.008

Kodirov, O., Kersten, M., Shukurov, N., & Peinado, F. J. M. (2018). Trace metal(loid) mobility in waste deposits and soils around Chadak mining area, Uzbekistan. *SCIENCE OF THE TOTAL ENVIRONMENT*, *622*, 1658–1667. https://doi.org/10.1016/j.scitotenv.2017.10.049

Koski, R. A., & Mosier, D. L. (2012). *2. Deposit Type and Associated Commodities Volcanogenic Massive Sulfide Occurrence Model*. http://www.usgs.gov/pubprod

Kossoff, D., Dubbin, W. E., Alfredsson, M., Edwards, S. J., Macklin, M. G., & Hudson-Edwards, K. A. (2014). Mine tailings dams: Characteristics, failure, environmental impacts, and remediation. *Applied Geochemistry*, *51*, 229–245. https://doi.org/10.1016/J.APGEOCHEM.2014.09.010

KPMG, N. (2017). Nigerian Mining Sector Brief. *KPMG Nigeria*. https://home.kpmg/ng/en/home/insights/2017/03/nigerian-mining-sector-brief.html

Kumar, V., Parihar, R. D., Sharma, A., Bakshi, P., Singh Sidhu, G. P., Bali, A. S., Karaouzas, I., Bhardwaj, R., Thukral, A. K., Gyasi-Agyei, Y., & Rodrigo-Comino, J. (2019). Global evaluation of heavy metal content in surface water bodies: A meta-analysis using heavy metal pollution indices and multivariate statistical analyses. *Chemosphere*, *236*. https://doi.org/10.1016/J.CHEMOSPHERE.2019.124364

Kuter, N. (2013). Reclamation of Degraded Landscapes due to Opencast Mining. *Advances in Landscape Architecture*. https://doi.org/10.5772/55796

Lane, A. (2021, July 7). *How flooded coal mines could heat homes | BBC Future Planet*. British Broadcasting Corporation. https://www.bbc.com/future/article/20210706-how-flooded-coal-mines-could-heat-homes

Lar, U. A. (2018, January 18). Geology and Mineral Resources of Nigeria and Their Uses. *Product Development for Solid Minerals in Nigeria*. https://www.researchgate.net/publication/322963731_GEOLOGY_AND_MINERAL_RESOURCES_OF_NIGERIA_AND_THEIR_USES

Lar, U. A., Agene, J. I., & Umar, A. I. (2015). Geophagic clay materials from Nigeria: a potential source of heavy metals and human health implications in mostly women and children who practice it. *Environmental Geochemistry and Health*, *37*(2), 363–375. https://doi.org/10.1007/S10653-014-9653-0

Laurence, D. (2006). Optimisation of the mine closure process. *Journal of Cleaner Production*, *14*(3–4), 285–298. https://doi.org/10.1016/J.JCLEPRO.2004.04.011

Lee, J. S., & Chon, H. T. (2003). Exposure assessment of heavy metals on abandoned metal mine areas by ingestion of soil, crop plant and groundwater. *Journal De Physique IV*.

Lee, J. S., Lee, S. W., Chon, H. T., & Kim, K. W. (2008). Evaluation of human exposure to arsenic due to rice ingestion in the vicinity of abandoned Myungbong Au–Ag mine site, Korea. *Journal of Geochemical Exploration*, *96*(2–3), 231–235. https://doi.org/10.1016/J.GEXPLO.2007.04.009

Lei, L. Q., Song, C. A., Xie, X. L., Li, Y. H., & Wang, F. (2010). Acid mine drainage and heavy metal contamination in groundwater of metal sulfide mine at arid territory (BS mine, Western Australia). *Transactions of Nonferrous Metals Society of China*, *20*(8), 1488–1493. https://doi.org/10.1016/S1003-6326(09)60326-5

Lenntech. (2025). *Cerium (Ce) - Chemical properties, Health and Environmental effects*. https://www.lenntech.com/periodic/elements/ce.htm

Lenton, T. (2016). Earth System Science: A Very Short Introduction. *Oxford Academic*, 1–17. https://doi.org/10.1093/ACTRADE/9780198718871.003.0001

LePan, N. (2020, March 1). *All of the World's Metals and Minerals in One Infographic*. Visual Capitalist. https://www.visualcapitalist.com/all-the-worlds-metals-and-minerals-in-one-visualization/

Li, C., Zhang, X., Gao, X., Qi, S., & Wang, Y. (2019). The Potential Environmental Impact of PAHs on Soil and Water Resources in Air Deposited Coal Refuse Sites in Niangziguan Karst Catchment, Northern China. *International Journal of Environmental Research and Public Health*, *16*(8), 1368. https://doi.org/10.3390/IJERPH16081368

Li, H., & Ji, H. (2017). Chemical speciation, vertical profile and human health risk assessment of heavy metals in soils from coal-mine brownfield, Beijing, China. *Journal of Geochemical Exploration*, *183*, 22–32. https://doi.org/10.1016/j.gexplo.2017.09.012

Li, J., Chugh, Y. P., & Hu, Z. (2024). Coal Mine Closure Practices in China: An Overview. *THE 41ST MEETING OF THE AMERICAN SOCIETY OF RECLAMATION SCIENCES*.

Li, J., & McDonald-Gillespie, J. (2020). Airborne Lead (Pb) From Abandoned Mine Waste in Northeastern Oklahoma, USA. *GeoHealth*, *4*(9), e2020GH000273. https://doi.org/10.1029/2020GH000273

Li, W., Cao, X., Hu, Y., & Cheng, H. (2024). Source Apportionment and Risk Assessment of Heavy Metals in Agricultural Soils in a Typical Mining and Smelting Industrial Area. *Sustainability (Switzerland)*, *16*(4), 1673. https://doi.org/10.3390/SU16041673/S1

Li, W., Deng, Y., Wang, H., Hu, Y., & Cheng, H. (2024). Potential risk, leaching behavior and mechanism of heavy metals from mine tailings under acid rain. *Chemosphere*, *350*, 140995. https://doi.org/10.1016/J.CHEMOSPHERE.2023.140995

Li, X., Cai, J., Chen, D., & Feng, Q. (2021). Characteristics of water contamination in abandoned coal mines: a case study on Yudong River area, Kaili, Guizhou Province, China. *International Journal of Coal Science and Technology*, *8*(6), 1491–1503. https://doi.org/10.1007/s40789-021-00466-w

Li, Z., Yang, Q., Yang, Y., Xie, C., & Ma, H. (2020). Hydrogeochemical controls on arsenic contamination potential and health threat in an intensive agricultural area, northern China. *Environmental Pollution*, *256*. https://doi.org/10.1016/j.envpol.2019.113455

Lim, S. K., Shin, H. S., Yoon, K. S., Kwack, S. J., Um, Y. M., Hyeon, J. H., Kwak, H. M., Kim, J. Y., Kim, T. Y., Kim, Y. J., Roh, T. H., Lim, D. S., Shin, M. K., Choi, S. M., Kim, H. S., & Lee, B. M. (2014). Risk assessment of volatile organic compounds benzene, toluene, ethylbenzene, and xylene (BTEX) in consumer products. *Journal of Toxicology and Environmental Health - Part A: Current Issues*, *77*, 1502–1521. https://doi.org/10.1080/15287394.2014.955905

Liu, H., Yang, Y., Jiao, W., Wang, S., & Cheng, F. (2022). A New Assessment Method for the Redevelopment of Closed Coal Mine—A Case Study in Shanxi Province in China. *Sustainability (Switzerland)*, *14*(15). https://doi.org/10.3390/su14159759

Liu, W. H., Zhao, J. Z., Ouyang, Z. Y., Söderlund, L., & Liu, G. H. (2005). Impacts of sewage irrigation on heavy metal distribution and contamination in Beijing, China. *Environment International*, *31*(6), 805–812. https://doi.org/10.1016/J.ENVINT.2005.05.042

Liu, X., Chen, S., Yan, X., Liang, T., Yang, X., El-Naggar, A., Liu, J., & Chen, H. (2021). Evaluation of potential ecological risks in potential toxic elements contaminated agricultural soils: Correlations between soil contamination and polymetallic mining activity. *Journal of Environmental Management*, *300*. https://doi.org/10.1016/j.jenvman.2021.113679

Liu, Y., Ma, G., Han, Y., Wang, Y., Tang, C., Tian, N., Tang, X., Jiang, L., Zuo, H., Zhang, Y., Wang, S., Wang, A., Mao, D., & Liu, S. (2023). Assessment of the Impact of Abandoned Mine Water on Groundwater Environment. *Water 2023, Vol. 15, Page 2649*, *15*(14), 2649. https://doi.org/10.3390/W15142649

Lottermoser, B. (2010). Mine Wastes. Characterization, Treatment and Environmental Impacts. In *Springer Verlag Berlin Heidelberg. .ISBN 978- 3-642-12418-1. 4.* (Third edit).

Lottermoser, B. (2016). Environmental indicators in metal mining. In *Environmental Indicators in Metal Mining*. Springer Cham. https://doi.org/10.1007/978-3-319-42731-7/SAVE-RESEARCH

LSRCA. (2025). *Petroleum Hydrocarbons*. The Lake Simcoe Region Conservation Authority. https://lsrca.on.ca/index.php/home/petroleum-hydrocarbons-phcs/

Luís, A. T., Teixeira, P., Fernandes, S., Almeida, P., Matos, J. X., & Ferreira Da Silva, E. (2011). *Environmental impact of mining activities in the Lousal area (Portugal): Chemical and diatom characterization of metal-contaminated stream sediments and surface water of Corona stream*. https://doi.org/10.1016/j.scitotenv.2011.06.052

Lyu, Z., Chai, J., Xu, Z., Qin, Y., & Cao, J. (2019). A Comprehensive Review on Reasons for Tailings Dam Failures Based on Case History. *Advances in Civil Engineering*, *2019*(1), 4159306. https://doi.org/10.1155/2019/4159306

Ma, H., Bertsch, P. M., Glenn, T. C., Kabengi, N. J., & Williams, P. L. (2009). Toxicity of Manufactured Zinc Oxide Nanoparticles in the Nematode Caenorhabditis Elegans. *Environmental Toxicology and Chemistry*, *28*(6), 1324–1330. https://doi.org/10.1897/08-262.1

MacDonald, D. D., Ingersoll, C. G., & Berger, T. A. (2000). Development and evaluation of consensus-based sediment quality guidelines for freshwater ecosystems. *Archives of Environmental Contamination and Toxicology*, *39*(1), 20–31. https://doi.org/10.1007/s002440010075

Macklin, M. G., Thomas, C. J., Mudbhatkal, A., Brewer, P. A., Hudson-Edwards, K. A., Lewin, J., Scussolini, P., Eilander, D., Lechner, A., Owen, J., Bird, G., Kemp, D., & Mangalaa, K. R. (2023). Impacts of metal mining on river systems: a global assessment. *Science*, *381*(6664), 1345–1350. https://doi.org/10.1126/SCIENCE.ADG6704

MacMillan, K., Milner, G., Brown, T., Richard, J., & Sparling E. (2021). Assessing Climate Change Risk at the Kam Kotia Mine Site. In *Climate Risk Institute (CRI)*. https://climateriskinstitute.ca/

Mahlangeni, N., Kapwata, T., Laban, T., & Wright, C. Y. (2024). Health risks of exposure to air pollution in areas where coal-fired power plants are located: protocol for a scoping review. *BMJ Open*, *14*(3), e084074. https://doi.org/10.1136/BMJOPEN-2024-084074

Maina, B., Aliyuda, K., & Amin Dawa, C. C. (2016). Impact of Coal Mining on the Environment in Mainganga Community of Akko Local Government, Gombe State, Nigeria. *Global Journal of Human-Social Science: Geography, Geo-Sciences, Environmental Science & Disaster Management*, *16*(3).

Maramba, N. P. C., Reyes, J. P., Francisco-Rivera, A. T., Panganiban, L. C. R., Dioquino, C., Dando, N., Timbang, R., Akagi, H., Castillo, M. T., Quitoriano, C., Afuang, M., Matsuyama, A., Eguchi, T., & Fuchigami, Y. (2006). Environmental and human exposure assessment monitoring of communities near an abandoned mercury mine in the Philippines: A toxic legacy. *Journal of Environmental Management*, *81*(2), 135–145. https://doi.org/10.1016/J.JENVMAN.2006.02.013

Marc, S., John, B., & Dana, V. (2018, January 18). *What triggered the oil price plunge of 2014-2016 and why it failed to deliver an economic impetus in eight charts*. Let's Talk Development. https://icsid.worldbank.org/sites/default/files/parties_publications/C9734/I%20-%20Counter-Memorial%20on%20Damages%20-%2009.26.2025/4.%20Traducciones%20de%20cortes%C3%ADa%20-%20Memorial%20de%20Contestaci%C3%B3n%20sobre%20Da%C3%B1os/3.%20FTI%20exhibits/FTI-017-ENG.pdf

Marcotullio, P. J. (2007). Urban water-related environmental transitions in Southeast Asia. *Sustainability Science*, *2*, 27–54. https://doi.org/10.1007/s11625-006-0019-0

Marras, P. A., Zhou, L., De Giudici, G. B., Medas, D., & Dore, E. (2022). Modeling the fate and the transport of heavy metals in a mine-polluted river watershed. *Institutional Research Information System*. https://iris.unica.it/handle/11584/345357

Martín-Crespo, T., Gómez-Ortiz, D., Martín-Velázquez, S., Esbrí, J. M., de Ignacio-San José, C., Sánchez-García, M. J., Montoya-Montes, I., & Martín-González, F. (2015). Abandoned mine tailings in cultural itineraries: Don Quixote Route (Spain). *Engineering Geology*, *197*, 82–93. https://doi.org/10.1016/J.ENGGEO.2015.08.008

Martínez-López, S., Martínez-Sánchez, M. J., & Pérez-Sirvent, C. (2021). Do old mining areas represent an environmental problem and health risk? A critical discussion through a particular case. *Minerals*, *11*(6). https://doi.org/10.3390/min11060594

Masindi, V., Akinwekomi, V., Maree, J. P., & Muedi, K. L. (2017). Comparison of mine water neutralisation efficiencies of different alkaline generating agents. *Journal of Environmental Chemical Engineering*, *5*(4), 3903–3913. https://doi.org/10.1016/j.jece.2017.07.062

Mavrommatis, E., & Menegaki, M. (2017). Setting rehabilitation priorities for abandoned mines of similar characteristics according to their visual impact: The case of Milos Island, Greece. *Journal of Sustainable Mining*, *16*(3), 104–113. https://doi.org/10.1016/J.JSM.2017.10.003

Mayes, W. M., Potter, H. A. B., & Jarvis, A. P. (2013). Riverine flux of metals from historically mined orefields in england and wales. *Water, Air, and Soil Pollution*, *224*(2), 1–14. https://doi.org/10.1007/S11270-012-1425-9/TABLES/5

Mbaya, R. P. (2013). Land Degradation Due To Mining: The Gunda Scenario. *International Journal of Geography and Geology*, *2*(12), 144–158. https://doi.org/10.18488/journal.10/2013.2.12/10.12.144.158

Mclemore, V. T., & Frey, B. (2018). *Making Abandoned Mine Lands (AML) Profitable*. http://duraroot.com/

Mead, D., & Stiger, P. (2015). The 2014 plunge in import petroleum prices: What happened? *Beyond The Numbers*, *4*(0), 1–7.

MECD. (2022). Activities of Mines Environmental Compliance Department for Year 2022. In *msmd.gov.ng*.

Medunić, G., Kuharić, Ž., Krivohlavek, A., Đuroković, M., Dropučić, K., Rađenović, A., Oberiter, B. L., Krizmanić, A., & Bajramović, M. (2018). Selenium, sulphur, trace metal, and BTEX levels in soil, water, and lettuce from the croatian raša bay contaminated by superhigh-organic-sulphur coal. *Geosciences (Switzerland)*, *8*(11). https://doi.org/10.3390/geosciences8110408

Mehta, N., Cipullo, S., Cocerva, T., Coulon, F., Dino, G. A., Ajmone-Marsan, F., Padoan, E., Cox, S. F., Cave, M. R., & De Luca, D. A. (2020). Incorporating oral bioaccessibility into human health risk assessment due to potentially toxic elements in extractive waste and contaminated soils from an abandoned mine site. *Chemosphere*, *255*. https://doi.org/10.1016/j.chemosphere.2020.126927

Melymuk, L., Blumenthal, J., Sáňka, O., Shu-Yin, A., Singla, V., Šebková, K., Pullen Fedinick, K., & Diamond, M. L. (2022). Persistent Problem: Global Challenges to Managing PCBs. *Environmental Science and Technology*, *56*(12), 9029–9040. https://doi.org/10.1021/ACS.EST.2C01204/SUPPL_FILE/ES2C01204_SI_003.XLSX

Mensah, A. K., & Addai, P. (2024). Cadmium, Cu, Hg, Sb, Se and Ti contamination in abandoned and active mining sites in Ghana shows concerns for soil and human health risks. *Environmental Advances*, *15*, 100500. https://doi.org/10.1016/J.ENVADV.2024.100500

Merem, E. C., Twumasi, Y., Wesley, J., Isokpehi, P., Shenge, M., Fageir, S., Crisler, M., Romorno, C., Hines, A., Hirse, G., Ochai, S., Leggett, S., & Nwagboso, E. (2017). Assessing the Ecological Effects of Mining in West Africa: The Case of Nigeria. *International Journal of Mining Engineering and Mineral Processing*, *6*(1), 1–19. https://doi.org/10.5923/J.MINING.20170601.01

Mhlongo, S. E., & Amponsah-Dacosta, F. (2016). A review of problems and solutions of abandoned mines in South Africa. *International Journal of Mining, Reclamation and Environment*, *30*(4), 279–294. https://doi.org/10.1080/17480930.2015.1044046

Miake-Lye, I. M., Hempel, S., Shanman, R., & Shekelle, P. G. (2016). What is an evidence map? A systematic review of published evidence maps and their definitions, methods, and products. *Systematic Reviews*, *5*(1). https://doi.org/10.1186/s13643-016-0204-x

Microsoft Corporation. (2023). *Microsoft Excel* (Version 2509). https://www.microsoft.com

Milton, A., & Johnson, M. S. (2002). Food chain transfer of zinc within the ecosystems of old and modern metalliferous mine wastes. *Environmental Technology (United Kingdom)*, *23*(5), 525–536. https://doi.org/10.1080/09593332308618393

Mindat. (2025). *Definition of mine water*. Mindat.Org. https://www.mindat.org/glossary/mine_water

MMSD. (2016). *Nigeria's Mining and Metal Sector Investment Promotion Brochure*.

MMTA. (2016). *Cerium*. Minor Metals Trade Association (MMTA). https://mmta.co.uk/metals/ce/

Moher, D., Shamseer, L., Clarke, M., Ghersi, D., Liberati, A., Petticrew, M., Shekelle, P., Stewart, L. A., Estarli, M., Barrera, E. S. A., Martínez-Rodríguez, R., Baladia, E., Agüero, S. D., Camacho, S., Buhring, K., Herrero-López, A., Gil-González, D. M., Altman, D. G., Booth, A., … Whitlock, E. (2015). Preferred reporting items for systematic review and meta-analysis protocols (PRISMA-P) 2015 statement. *Revista Espanola de Nutricion Humana y Dietetica*, *20*(2), 148–160. https://doi.org/10.1186/2046-4053-4-1

Momčilović, M., Kovačević, J., Tanić, M., Crossed D Signorcrossed D Signević, M., Bačić, G., & Dragović, S. (2013). Distribution of natural radionuclides in surface soils in the vicinity of abandoned uranium mines in Serbia. *Environmental Monitoring and Assessment*, *185*(2), 1319–1329. https://doi.org/10.1007/S10661-012-2634-9,

Montes, L., Pavón, E., Cota, A., & Alba. (2021). Zirconium retention for minimizing environmental risk: Role of counterion and clay mineral. *Chemosphere*, *267*, 128914. https://doi.org/10.1016/J.CHEMOSPHERE.2020.128914

Montuori, P., De Rosa, E., Di Duca, F., De Simone, B., Scippa, S., Russo, I., Sarnacchiaro, P., & Triassi, M. (2022). Polycyclic Aromatic Hydrocarbons (PAHs) in the Dissolved Phase,

Particulate Matter, and Sediment of the Sele River, Southern Italy: A Focus on Distribution, Risk Assessment, and Sources. *Toxics*, *10*(7), 401. https://doi.org/10.3390/TOXICS10070401/S1

Morgan, T. (2024, May 8). *Lead: Metal mines pollution raises health risk concerns - BBC News*. BBC. https://www.bbc.co.uk/news/articles/cv2rzj3v2leo

Moulinec, A., Arle, J., Hollert, H., Hörchner, S., Johann, S., Kienle, C., Oetken, M., & Sundermann, A. (2025). Assessing chemical pollution with biomonitoring approaches in streams and rivers: a critical review. *Environmental Sciences Europe 2025 37:1*, *37*(1), 1–23. https://doi.org/10.1186/S12302-025-01110-Z

MRC. (2020). An in-depth look at the current state of mining in Nigeria. In *Mining Review Content*. https://www.miningreview.com/gold/an-in-depth-look-at-the-current-state-of-mining-in-nigeria/

Mugova, E., Leshego Molaba, ·, & Wolkersdorfer, · Christian. (2024). *Understanding the Mechanisms and Implications of the First Flush in Mine Pools: Insights from Field Studies in Europe's Deepest Metal Mine and Analogue Modelling*. *43*, 73–86. https://doi.org/10.1007/s10230-024-00969-3

Mugova, E., & Wolkersdorfer, C. (2025). Understanding the influence of stratification for mine water management: a comparative study. *Scientific Reports*, *15*(1), 2757. https://doi.org/10.1038/S41598-024-82293-Y

Mukhopadhyay, S., George, J., & Masto, R. E. (2017). Changes in Polycyclic Aromatic Hydrocarbons (PAHs) and Soil Biological Parameters in a Revegetated Coal Mine Spoil. *Land Degradation and Development*, *28*(3), 1047–1055. https://doi.org/10.1002/ldr.2593

Muller, G. (1969). Index of Geoaccumulation in Sediments of The Rhine River. *GeoJournal*, *2*(3), 108–118. https://sid.ir/paper/618491/en

Nakazawa, K., Nagafuchi, O., Kawakami, T., Inoue, T., Yokota, K., Serikawa, Y., Basir-Cyio, M., & Elvince, R. (2016). Human health risk assessment of mercury vapor around artisanal small-scale gold mining area, Palu city, Central Sulawesi, Indonesia. *Ecotoxicol Environ Saf*, *124*, 155–162. https://doi.org/10.1016/j.ecoenv.2015.09.042

Nassiri, O., Rhoujjati, A., & EL Hachimi, M. L. (2021). Contamination, sources and environmental risk assessment of heavy metals in water, sediment and soil around an abandoned Pb mine site in North East Morocco. *Environmental Earth Sciences*, *80*(3). https://doi.org/10.1007/s12665-021-09387-y

Nassiri, O., Rhoujjati, A., Moreno-Jimenez, E., & Hachimi, M. L. E. L. (2022). Assessment of metallic trace elements mobility from mine tailing and soils around abandoned Pb mine site in North East Morocco. *Journal of Taibah University for Science*, *16*(1), 933–943. https://doi.org/10.1080/16583655.2022.2128564

NBS. (2015). *Nigerian Mining and Quarrying Sector*. http://www.nigeriaembassyusa.org/index.php?page=culture-tourism

Ndinwa, G. C. C., & Ohwona, C. O. (2014). Environmental and Health Impact of Solid Mineral Exploration and Exploitation in South-Northern Nigeria: A Case Study of Igarra in Edo State. *Review of Environment and Earth Sciences*, *1*(1), 24–36. https://doi.org/10.18488/JOURNAL.80/2014.1.1/80.1.24.36

Necula, R., Zaharia, M., Butnariu, A., Zamfirache, M. M., Surleva, A., Ciobanu, C. I., Pintilie, O., Iacoban, C., & Drochioiu, G. (2021). Heavy metals and arsenic in an abandoned barite mining area: ecological risk assessment using biomarkers. *ENVIRONMENTAL FORENSICS*. https://doi.org/10.1080/15275922.2021.1976315

NEITI. (2011). *Scoping Study on the Nigerian Mining Sector*.

NEPM. (2014). National Environment Protection Measure (Assessment of Site Contamination). In *Australia National Environment Protection Council*. https://www.nepc.gov.au/nepms/assessment-site-contamination

News Tower Magazine. (2011). *History of Mining in Plateau State, Nigeria*. https://newstoweronline.blogspot.com/2011/10/history-of-mining-in-plateau-state.html

Ngole-Jeme, V. M., & Fantke, P. (2017). Ecological and human health risks associated with abandoned gold mine tailings contaminated soil. *PLOS ONE*, *12*(2), e0172517. https://doi.org/10.1371/JOURNAL.PONE.0172517

NGSA. (2017). Nigerian Geological Survey Agency. In *NGSA MMSD*. http://ngsa.minesandsteel.com/

Nigeria Vision 2020. (2009). *Nigeria Vision 2020 National Technical Working Group On Minerals & Metals Development*.

Nikolaidis, C., Zafiriadis, I., Mathioudakis, V., & Constantinidis, T. (2010). Heavy metal pollution associated with an abandoned lead-zinc mine in the Kirki Region, NE Greece. *Bulletin of Environmental Contamination and Toxicology*, *85*(3), 307–312. https://doi.org/10.1007/s00128-010-0079-9

Nisbet, I. C. T., & Lagoy, P. K. (1992). Toxic Equivalency Factors (TEFs) for Polycyclic Aromatic Hydrocarbons (PAHs). In *REGULATORY TOXICOLOGY AND PHARMACOLOGY* (Vol. 16).

Nobuntou, W., Parkpian, P., Oanh, N. T. K., Noomhorm, A., Delaune, R. D., & Jugsujinda, A. (2010). Lead distribution and its potential risk to the environment: Lesson learned from environmental monitoring of abandon mine. *Journal of Environmental Science and Health - Part A Toxic/Hazardous Substances and Environmental Engineering*, *45*(13), 1702–1714. https://doi.org/10.1080/10934529.2010.513232

Nordstrom, D. K. (2011). Mine waters: Acidic to circumneutral. *Elements*, *7*(6), 393–398. https://doi.org/10.2113/GSELEMENTS.7.6.393

Nordstrom, D. K., Blowes, D. W., & Ptacek, C. J. (2015). Hydrogeochemistry and microbiology of mine drainage: An update. *Applied Geochemistry*, *57*, 3–16. https://doi.org/10.1016/J.APGEOCHEM.2015.02.008

Nouairi, J., Rocha, F., & Medhioub, M. (2019). Geobiological assessment of the pollution effect of abandoned mine ores (Fej Lahdoum, Northwest Tunisia). *Arabian Journal of Geosciences*, *12*(24). https://doi.org/10.1007/s12517-019-4870-6

NPS. (2020). Understanding AML. In *US National Park Service*. https://www.nps.gov/subjects/abandonedminerallands/understanding-aml.htm

Nwajide, C. S. (2013). *Geology of Nigeria's Sedimentary Basins*. CSS Bookshop Ltd. https://www.scirp.org/reference/referencespapers?referenceid=1551678

Nwaobi, G. (2005). The Nigerian Coal Corporation: An Evaluation Of Production Performance(1960 1987). *Industrial Organization*. https://ideas.repec.org/p/wpa/wuwpio/0501002.html

Obasi, P. N., & Akudinobi, B. B. (2020). Potential health risk and levels of heavy metals in water resources of lead–zinc mining communities of Abakaliki, southeast Nigeria. *Applied Water Science*, *10*(7), 1–23. https://doi.org/10.1007/S13201-020-01233-Z/TABLES/5

Obiora, S. C., Chukwu, A., Chibuike, G., & Nwegbu, A. N. (2019). Potentially harmful elements and their health implications in cultivable soils and food crops around lead-zinc mines in Ishiagu, Southeastern Nigeria. *Journal of Geochemical Exploration*, *204*(April), 289–296. https://doi.org/10.1016/j.gexplo.2019.06.011

Obiora, S. C., Chukwu, A., & Davies, T. C. (2016). Heavy metals and health risk assessment of arable soils and food crops around Pb-Zn mining localities in Enyigba, southeastern Nigeria. *Journal of African Earth Sciences*, *116*, 182–189. https://doi.org/10.1016/j.jafrearsci.2015.12.025

Odinga, E. S., Gudda, F. O., Waigi, M. G., Wang, J., & Gao, Y. (2021). Occurrence, formation and environmental fate of polycyclic aromatic hydrocarbons in biochars. *Fundamental Research*, *1*(3), 296–305. https://doi.org/10.1016/J.FMRE.2021.03.003

OECD. (2010). Test No. 317: Bioaccumulation in Terrestrial Oligochaetes. *OECD Guidelines for the Testing of Chemicals,* (July), 30. http://www.oecd-ilibrary.org/environment/test-no-317-bioaccumulation-in-terrestrial-oligochaetes_9789264090934-en%5Cnhttp://www.oecd-ilibrary.org/environment/test-no-316-phototransformation-of-chemicals-in-water-direct-photolysis_9789264067585-en

OECD. (2017). *Good Laboratory Practice and Compliance Monitoring*. The Organisation for Economic Co-Operation and Development. https://www.oecd.org/en/topics/sub-issues/testing-of-chemicals/good-laboratory-practice-and-compliance-monitoring.html

OECD. (2018). *CONSIDERATIONS FOR ASSESSING THE RISKS OF COMBINED EXPOSURE TO MULTIPLE CHEMICALS Series on Testing and Assessment No. 296*. www.oecd.org/chemicalsafety/

OECD. (2021). Guidance on Key Considerations for the Identification and Selection of Safer Chemical Alternatives. In *Environment, Health and Safety, Environment Directorate, OECD*.

OEHHA. (2010). *Benzo[a]pyrene*. Office of Environmental Health Hazard Assessment. https://oehha.ca.gov/chemicals/benzoapyrene?utm_source=chatgpt.com

OEHHA. (2025). *Air Toxics Hot Spots*. https://oehha.ca.gov/air/air-toxics-hot-spots

Ogbonna, P. C., Nzegbule, E. C., & Okorie, P. E. (2015). Environmental impact assessment of coal mining at Enugu, Nigeria. *Impact Assessment and Project Appraisal*, *33*(1), 73–79. https://doi.org/10.1080/14615517.2014.941711

Ogodo, O. (2018). Tackle health, environmental impacts of abandoned mines - Sub-Saharan Africa. In *Science development network*. https://www.scidev.net/sub-saharan-africa/news/tackle-health-environmental-impacts-mines/

Ogundipe, I. E., & Obasi, R. A. (2017). Geology and Mineralisation in the Albian Sediments of the Benue Trough, Nigeria. *British Journal of Earth Sciences Research*, *5*(1), 1–15. www.eajournals.org

Ogunsola, O. I. (1990). History of Energy Sources and Their-Utilization in Nigeria. *Http://Dx.Doi.Org/10.1080/00908319008960198*, *12*(2), 181–198. https://doi.org/10.1080/00908319008960198

Oha, I. A., Onuoha, K. M., & Dada, S. S. (2017). Contrasting styles of lead-zinc-barium mineralization in the Lower Benue Trough, Southeastern Nigeria. *Earth Sciences Research Journal*, *21*(1), 7–16. https://doi.org/10.15446/ESRJ.V21N1.39703

Ojo, G. (2015). *Nigeria An Outlook on the Mining Industry*.

Olade, M. A. (2019). Solid mineral deposits and mining in Nigeria : - A sector in transitional change. *Achievers Journal of Scientific Research*, *2*(1), 1–16. https://www.researchgate.net/publication/333024301

Oladele, O. (2016). Exploration Report of SSML, Gimbi, Wase LGA, Plateau State. UNIQUE EL-MAO NIG. LTD. In *GISL, Abuja*.

Olalde, M. (2017). Unfinished business: Coal miners across South Africa walk away from clean up. In *Climate Home News*. https://www.climatechangenews.com/2017/03/22/unfinished-business-coal-miners-south-africa-walk-away-clean/

Omotehinse, A. O., & Ako, B. D. (2019). The environmental implications of the exploration and exploitation of solid minerals in Nigeria with a special focus on Tin in Jos and Coal in Enugu. *Journal of Sustainable Mining*, *18*(1), 18–24. https://doi.org/10.1016/j.jsm.2018.12.001

OriginLab Corporation. (2022). *OriginPro* (OriginPro 2022b). OriginLab Corporation, Northampton, MA, USA. https://www.originlab.com

Otamonga, J. P., & Poté, J. W. (2020). Abandoned mines and artisanal and small-scale mining in Democratic Republic of the Congo (DRC): Survey and agenda for future research. *Journal of Geochemical Exploration*, *208*, 106394. https://doi.org/10.1016/J.GEXPLO.2019.106394

Oyetibo, G. O., Enahoro, J. A., Ikwubuzo, C. A., & Ukwuoma, C. S. (2021). Microbiome of highly polluted coal mine drainage from Onyeama, Nigeria, and its potential for sequestrating toxic heavy metals. *Scientific Reports*, *11*(1). https://doi.org/10.1038/s41598-021-96899-z

Oyourou, J. N., McCrindle, R., Combrinck, S., & Fourie, C. J. S. (2019). Investigation of zinc and lead contamination of soil at the abandoned Edendale mine, Mamelodi (Pretoria, South Africa) using a field-portable spectrometer. *Journal of the Southern African Institute of Mining and Metallurgy*, *119*(1), 55–62. https://doi.org/10.17159/2411-9717/2019/v119n1a7

Ozobialu, B., Igwe, O., & Emeh, C. (2020). Lateral distribution of potential toxic elements from lead–zinc mine sites within Enyigba, Southeastern Nigeria. *Environmental Earth Sciences*, *79*(15), 1–17. https://doi.org/10.1007/S12665-020-09122-Z/FIGURES/11

Ozoko, D. C. (2015). *Heavy Metal Geochemistry of Acid Mine Drainage in Onyeama Coal Mine, Enugu, Southeastern Nigeria*. *5*(10). www.iiste.org

Palma, P., López-Orozco, R., Lourinha, C., Oropesa, A. L., Novais, M. H., & Alvarenga, P. (2019). Assessment of the environmental impact of an abandoned mine using an integrative approach: A case-study of the "Las Musas" mine (Extremadura, Spain). *Science of The Total Environment*, *659*, 84–94. https://doi.org/10.1016/J.SCITOTENV.2018.12.321

Palmer, M. A., Bernhardt, E. S., Schlesinger, W. H., Eshleman, K. N., Foufoula-Georgiou, E., Hendryx, M. S., Lemly, A. D., Likens, G. E., Loucks, O. L., Power, M. E., White, P. S., & Wilcock, P. R. (2010). Mountaintop Mining Consequences. *Science*, *327*(5962), 148–149. https://doi.org/10.1126/SCIENCE.1180543

Pan, L., Guan, X., Liu, B., Chen, Y., Pei, Y., Pan, J., Zhang, Y., & Hao, Z. (2021). Pollution characteristics, distribution and ecological risk of potentially toxic elements in soils from an abandoned coal mine area in Southwestern China. *Minerals*, *11*(3), 1–16. https://doi.org/10.3390/min11030330

Parbhakar-Fox, A. (2016). Geoenvironmental characterisation of heap leach materials at abandoned mines: Croydon au-mines, QLD, Australia. *Minerals*, *6*(2). https://doi.org/10.3390/min6020052

Passariello, B., Giuliano, V., Quaresima, S., Barbaro, M., Caroli, S., Forte, G., Carelli, G., & Iavicoli, I. (2002). Evaluation of the environmental contamination at an abandoned mining site. *Microchemical Journal*, *73*(1–2), 245–250. https://doi.org/10.1016/S0026-265X(02)00069-3

Patel, K. S., Pandey, P. K., Agarwal, C., Sahu, B. L., Sharma, S. K., Wysocka, I., Yurdakul, S., Varol, S., & Martín-Ramos, P. (2024). Characterization, variations, fluxes, and sources of contaminants in coal mine water of Korba basin, Chhattisgarh, India. *Environmental Quality Management*, *33*(3), 345–359. https://doi.org/10.1002/TQEM.22126;PAGE:STRING:ARTICLE/CHAPTER

Pat-Espadas, A. M., Portales, R. L., Amabilis-Sosa, L. E., Gómez, G., & Vidal, G. (2018). Review of Constructed Wetlands for Acid Mine Drainage Treatment. *Water 2018, Vol. 10, Page 1685*, *10*(11), 1685. https://doi.org/10.3390/W10111685

Paul, S. N., Frazzoli, C., Sikoki, F. D., Babatunde, B. B., & Orisakwe, O. E. (2022). Natural occurring radioactive materials (NORMs) from mining sites in Nigeria: A systematic review of geographical distribution and public health concern. *Journal of Environmental Radioactivity*, *249*, 106889. https://doi.org/10.1016/J.JENVRAD.2022.106889

PDH. (2023). Benzene, Toluene, Ethylbenzene & Xylenes-BTEX. *Pennsylvania Department of Health*.

Peña-Ortega, M., Del Rio-Salas, R., Valencia-Sauceda, J., Mendívil-Quijada, H., Minjarez-Osorio, C., Molina-Freaner, F., de la O-Villanueva, M., & Moreno-Rodríguez, V. (2019). Environmental assessment and historic erosion calculation of abandoned mine tailings from a semi-arid zone of northwestern Mexico: insights from geochemistry and unmanned aerial vehicles. *Environmental Science and Pollution Research*, *26*(25), 26203–26215. https://doi.org/10.1007/S11356-019-05849-W/FIGURES/7

Peng, C., Chen, W., Liao, X., Wang, M., Ouyang, Z., Jiao, W., & Bai, Y. (2011). Polycyclic aromatic hydrocarbons in urban soils of Beijing: Status, sources, distribution and potential risk. *Environmental Pollution*, *159*(3), 802–808. https://doi.org/10.1016/J.ENVPOL.2010.11.003

Pennington, J. C., & Brannon, J. M. (2002). Environmental fate of explosives. *Thermochimica Acta*, *384*(1–2), 163–172. https://doi.org/10.1016/S0040-6031(01)00801-2

Peplow, D., & Edmonds, R. (2005). The effects of mine waste contamination at multiple levels of biological organization. *Ecological Engineering*, *24*(1–2), 101–119. https://doi.org/10.1016/j.ecoleng.2004.12.011

Pérez-Sirvent, C., Hernández-Pérez, C., Martínez-Sánchez, M. J., García-Lorenzo, M. L., & Bech, J. (2016). Geochemical characterisation of surface waters, topsoils and efflorescences in a historic metal-mining area in Spain. *Journal of Soils and Sediments*, *16*(4), 1238–1252. https://doi.org/10.1007/s11368-015-1141-3

Perin, G., Craboledda, L., Lucchese, M., Cirillo, R., & Dotta, L. (1985). *Heavy Metal Speciation in the Sediments of Northern Adriatic Sea: A new Approach for Environmental Toxicity Determination*.

Perry, R. S., Dudeney, A. W. L., & Chan, B. K. C. (2016). Characteristics and treatment of mine water from three historical coal workings in Yorkshire, UK: interrelationships between rates in geochemical, environmental and operational processes. *Proceedings IMWA 2016, Freiberg/Germany | Drebenstedt, Carsten, Paul, Michael (Eds.) | Mining Meets Water – Conflicts and Solutions*.

Peters, A., Wilson, I., Merrington, G., Heijerick, D., & Baken, S. (2019). Assessing Compliance of European Fresh Waters for Copper: Accounting for Bioavailability. *Bulletin of Environmental Contamination and Toxicology*, *102*(2), 153–159. https://doi.org/10.1007/S00128-018-2515-1/FIGURES/1

Ping, J., Yan, S., Gu, P., Wu, Z., & Hu, C. (2017). Application of MIKE SHE to study the impact of coal mining on river runoff in Gujiao mining area, Shanxi, China. *PLOS ONE*, *12*(12), e0188949. https://doi.org/10.1371/JOURNAL.PONE.0188949

Pinto, M. M. S. C., Silva, M. M. V. G., & Neiva, A. M. R. (2004). *Pollution of Water and Stream Sediments Associated with the Vale De Abrutiga Uranium Mine, Central Portugal*. *23*, 66–75.

Pless-Mulloli, T., Howel, D., King, A., Stone, I., Merefield, J., Bessell, J., & Darnell, R. (2000). Living near opencast coal mining sites and children's respiratory health. *Occupational and Environmental Medicine*, *57*(3), 145–151. https://doi.org/10.1136/OEM.57.3.145

Polzin, G. M., Kosa-Maines, R. E., Ashley, D. L., & Watson, C. H. (2007). Analysis of volatile organic compounds in mainstream cigarette smoke. *Environmental Science and Technology*, *41*(4), 1297–1302. https://doi.org/10.1021/ES060609L,

Popham, C. (2019, March 1). *Acid Rock Drainage and Acid Mine Drainage*. Open University Geological Society (OUGS). https://ougs.org/southwest/local-geology/211/acid-rock-drainage-and-acid-mine-drainage/

Prathap, A., & Chakraborty, S. (2019). Hydro chemical characterization and suitability analysis of groundwater for domestic and irrigation uses in open cast coal mining areas of Charhi and Kuju, Jharkhand, India. *Groundwater for Sustainable Development*, *9*. https://doi.org/10.1016/j.gsd.2019.100244

Public Health England. (2017). *Contaminated land information sheet: risk assessment approaches for polycyclic aromatic hydrocarbons (PAHs)* land information sheet for PAHs incorporating the category 4 screening level approach*. www.facebook.com/PublicHealthEngland

Punch, T. (2022). Mining, quarrying sector contributed N5.37tn to GDP in 2021. In *Punch Newspapers*. https://punchng.com/mining-quarrying-sector-contributed-n5-37tn-to-gdp-in-2021/

Qian, G., Fan, R., Short, M. D., Schumann, R. C., Li, J., St, R. C., & Gerson, A. R. (2018). The Effects of Galvanic Interactions with Pyrite on the Generation of Acid and Metalliferous Drainage. *Environmental Science & Technology*, *52*(9), 5349–5357. https://doi.org/10.1021/ACS.EST.7B05558

Qin, W., Han, D., Song, X., & Liu, S. (2021). Sources and migration of heavy metals in a karst water system under the threats of an abandoned Pb–Zn mine, Southwest China. *Environmental Pollution*, *277*, 116774. https://doi.org/10.1016/J.ENVPOL.2021.116774

Quevauviller, P., Ure, A., Muntau, H., & Griepink, B. (1993). Speciation of Heavy Metals in Soils and Sediments. An account of the Improvement and Harmonization of Extraction Techniques Undertaken Under the Auspices of the BCR of the commission of the European Communities. *International Journal of Environmental Analytical Chemistry*, *51*(1–4), 135–151. https://doi.org/10.1080/03067319308027619

Randelovic, D., Mutic, J., Marjanovic, P., Dordevic, T., & Kasanin-Grubin, M. (2020). Geochemical distribution of selected elements in flotation tailings and soils/sediments from the dam spill at the abandoned antimony mine Stolice, Serbia. *ENVIRONMENTAL SCIENCE AND POLLUTION RESEARCH*, *27*(6), 6253–6268. https://doi.org/10.1007/s11356-019-07348-4

Rattner, B. A., Bean, T. G., Beasley, V. R., Berny, P., Eisenreich, K. M., Elliott, J. E., Eng, M. L., Fuchsman, P. C., King, M. D., Mateo, R., Meyer, C. B., O'Brien, J. M., & Salice, C. J. (2024). Wildlife ecological risk assessment in the 21st century: Promising technologies to assess toxicological effects. *Integrated Environmental Assessment and Management*, *20*(3), 725–748. https://doi.org/10.1002/IEAM.4806

Rauret, G., López-Sánchez, J. F., Sahuquillo, A., Rubio, R., Davidson, C., Ure, A., & Quevauviller, P. (1999). Improvement of the BCR three step sequential extraction procedure prior to the certification of new sediment and soil reference materials. *Journal of Environmental Monitoring*, *1*(1), 57–61. https://doi.org/10.1039/A807854H

Rawlins, B. G., Cordeiro, M. J. A. R., & Smith, B. (1998). *Exposure and Bioavailability of Cerium Through the Ingestion of Soil (Uganda)*.

Regan, A. J. (2017). Bougainville: Origins of the Conflict, and Debating the Future of Large-Scale Mining. *Large-Scale Mines and Local-Level Politics: Between New Caledonia and Papua New Guinea*, 353–414. https://doi.org/10.22459/LMLP.10.2017.12

Richard, J., Milner, G., Huntsman, P., & Cleaver, A. (2021, March 15). *Understanding the Impact of Climate Change on Abandoned Mine Sites in Canada*. Https://Changingclimate.Ca. https://changingclimate.ca/map/assessing-climate-change-risk-at-the-kam-kotia-mine/?utm_source=chatgpt.com

Riggs, D. W., Malovichko, M. V., Gao, H., McGraw, K. E., Taylor, B. S., Krivokhizhina, T., Rai, S. N., Keith, R. J., Bhatnagar, A., & Srivastava, S. (2021). Environmental Exposure to Volatile Organic Compounds is Associated with Endothelial Injury. *MedRxiv*, 2021.08.25.21262556. https://doi.org/10.1101/2021.08.25.21262556

Rodriguez-Ruiz, A., Etxebarria, J., Boatti, L., & Marigómez, I. (2015). Scenario-targeted toxicity assessment through multiple endpoint bioassays in a soil posing unacceptable environmental risk according to regulatory screening values. *Environmental Science and Pollution Research*, *22*(17), 13344–13361. https://doi.org/10.1007/s11356-015-4564-x

Ross-Hellauer, T. (2017). What is open peer review? A systematic review. *F1000Research 2017 6:588*, *6*, 588. https://doi.org/10.12688/f1000research.11369.2

Rouhani, A., Skousen, J., & Tack, F. M. G. (2023). An Overview of Soil Pollution and Remediation Strategies in Coal Mining Regions. *Minerals*, *13*(8). https://doi.org/10.3390/MIN13081064

Sahoo, A. K., Madgaonkar, S. R., Chivukula, N., Karthikeyan, P., Ramesh, K., Marigoudar, S. R., Sharma, K. V., & Samal, A. (2024). Network-based investigation of petroleum hydrocarbons-induced ecotoxicological effects and their risk assessment. *Environment International*, *194*, 109163. https://doi.org/10.1016/J.ENVINT.2024.109163

Sahraoui, H., & Hachicha, M. (2017). *Determination of trace elements in mine soil samples using a portable X-ray fluorescence spectrometer: A comparative study with ICP-OES*.

Salesforce Inc. (2025). *Tableau*. https://www.tableau.com/en-gb/products/new-features?utm_source=chatgpt.com

Salufu, S. O., Salufu, E., Samuel, S., & Salufu, E. O. (2014). *Integrated Study of Acid Mine Drainage and its Environmental Effects on Onyeama Mine and Environs, Enugu, Nigeria*. *1*. https://www.researchgate.net/publication/270272135

Sanliyuksel Yucel, D., Balci, N., & Baba, A. (2016). Generation of Acid Mine Lakes Associated with Abandoned Coal Mines in Northwest Turkey. *Archives of Environmental Contamination and Toxicology*, *70*(4), 757–782. https://doi.org/10.1007/s00244-016-0270-z

Santos, T. B. dos, Lana, M. S., Pereira, T. M., & Canbulat, I. (2019). Quantitative hazard assessment system (Has-Q) for open pit mine slopes. *International Journal of Mining Science and Technology*, *29*(3), 419–427. https://doi.org/10.1016/J.IJMST.2018.11.005

Santos, P., Ribeiro, J., Espinha Marques, J., & Flores, D. (2023). Environmental and Health Risk Assessment of Soil Adjacent to a Self-Burning Waste Pile from an Abandoned Coal Mine in Northern Portugal. *Environments - MDPI*, *10*(3). https://doi.org/10.3390/environments10030053

Sartorius, A. (2023). *Ecosystem-wide Transfer of Trace Metal Pollutants from Derelict Metalliferous Mines in the UK* [PhD thesis, University of Nottingham]. https://eprints.nottingham.ac.uk/73614/

Sartorius, A. (2024, May 22). *Abandoned lead mines are leaving a toxic legacy on Wales's farmland, wildlife and rivers*. The Conversation. https://theconversation.com/abandoned-lead-mines-are-leaving-a-toxic-legacy-on-waless-farmland-wildlife-and-rivers-228310

Sartorius, A., Johnson, M., Young, S., Bennett, M., Baiker, K., Edwards, P., & Yon, L. (2022). Human health implications from consuming eggs produced near a derelict metalliferous mine: a case study . *Food Additives and Contaminants - Part A*, *39*(6), 1074–1085. https://doi.org/10.1080/19440049.2022.2062059

Schoenberger, E. (2016). Environmentally sustainable mining: The case of tailings storage facilities. *Resources Policy*, *49*, 119–128. https://doi.org/10.1016/J.RESOURPOL.2016.04.009

Schwartz, F. W., Lee, S., & Darrah, T. H. (2021). A Review of the Scope of Artisanal and Small-Scale Mining Worldwide, Poverty, and the Associated Health Impacts. *GeoHealth*, *5*(1). https://doi.org/10.1029/2020GH000325

Selebalo, I. M., Scholes, M. C., & Clifford-holmes, J. K. (2021). A Systemic Analysis of the Environmental Impacts of Gold Mining within the Blyde River Catchment, a Strategic Water Area of South Africa. *Water 2021, Vol. 13, Page 301*, *13*(3), 301. https://doi.org/10.3390/W13030301

Sengupta, M. (1993). Environmental Impacts of Mining Monitoring, Restoration, and Control. In *USA: Lewis Publishers;* (Vol. 1). https://books.google.co.uk/books?hl=en&lr=&id=P20lkGOEkRwC&oi=fnd&pg=PA1&dq=environmental+impacts+of+mineral+extraction&ots=ekhkzrENH3&sig=FAa3MPBWS2Qm_WHYnlGhr_BGLpE&redir_esc=y#v=onepage&q=environmental impacts of mineral extraction&f=false

Shahid, M., Ferrand, E., Schreck, E., & Dumat, C. (2013). Behavior and impact of zirconium in the soil-plant system: Plant uptake and phytotoxicity. *Reviews of Environmental Contamination and Toxicology*, *221*, 107–127. https://doi.org/10.1007/978-1-4614-4448-0_2,

Shamseer, L., Moher, D., Clarke, M., Ghersi, D., Liberati, A., Petticrew, M., Shekelle, P., Stewart, L. A., & Group, P.-P. (2015). *Preferred reporting items for systematic review and meta-analysis protocols (PRISMA-P) 2015: elaboration and explanation*. https://doi.org/10.1136/bmj.g7647

Shi, M., Min, X., Ke, Y., Lin, Z., Yang, Z., Wang, S., Peng, N., Yan, X., Luo, S., Wu, J., & Wei, Y. (2021). Recent progress in understanding the mechanism of heavy metals retention by iron (oxyhydr)oxides. *Science of The Total Environment*, *752*, 141930. https://doi.org/10.1016/J.SCITOTENV.2020.141930

Shirani, M., Azadnasab, R., Baradaran, M., & Shariati, S. (2023). A Review of Toxicity Studies of Zirconium and Its Derivatives. In *Jundishapur Journal of Natural Pharmaceutical Products* (Vol. 18, Number 4). Brieflands. https://doi.org/10.5812/jjnpp-137464

Shirin, S., Jamal, A., Emmanouil, C., Singh, V. P., & Yadav, A. K. (2022). Assessment and characterization of waste material used as backfilling in an abandoned mine. *International Journal of Coal Preparation and Utilization*. https://doi.org/10.1080/19392699.2022.2118259

Sikakwe, G. U., Ephraim, B. E., Nganje, T. N., Ntekim, E. E. U., & Amah, E. A. (2015). *Geoenvironmental impact of Okpara coal mine , Enugu , Southeastern Nigeria*. *6*(4), 5–16.

Sikora, A. L., Maguire, L. W., Nairn, R. W., & Knox, R. C. (2021). A comparison of XRFS and ICP-OES methods for soil trace metal analyses in a mining impacted agricultural watershed. *Environmental Monitoring and Assessment*, *193*(8). https://doi.org/10.1007/s10661-021-09275-9

Silalahi, E. T. M. E., Sofia, A., & Teruna, H. Y. (2021). Comparison of Extraction Techniques for the Determination of Polycyclic Aromatic Hydrocarbons (PAHs) in Soil. *Journal of Physics: Conference Series*, *1819*(1). https://doi.org/10.1088/1742-6596/1819/1/012061

Simate, G. S., & Ndlovu, S. (2014). Acid mine drainage: Challenges and opportunities. *Journal of Environmental Chemical Engineering*, *2*(3), 1785–1803. https://doi.org/10.1016/j.jece.2014.07.021

Singovszka, E., Balintova, M., & Junakova, N. (2020). The impact of heavy metals in water from abandoned mine on human health. *SN Applied Sciences*, *2*(5), 1–8. https://doi.org/10.1007/S42452-020-2731-2/FIGURES/5

Sipter, E., Rózsa, E., Gruiz, K., Tátrai, E., & Morvai, V. (2008). Site-specific risk assessment in contaminated vegetable gardens. *Chemosphere*, *71*(7), 1301–1307. https://doi.org/10.1016/j.chemosphere.2007.11.039

Smedley, P. L., & Kinniburgh, D. G. (2002). A review of the source, behaviour and distribution of arsenic in natural waters. *Applied Geochemistry*, *17*(5), 517–568. https://doi.org/10.1016/S0883-2927(02)00018-5

Snilstveit, B., Vojtkova, M., Bhavsar, A., Stevenson, J., & Gaarder, M. (2016). Evidence & Gap Maps: A tool for promoting evidence informed policy and strategic research agendas. *Journal of Clinical Epidemiology*, *79*, 120–129. https://doi.org/10.1016/J.JCLINEPI.2016.05.015

SON. (2015). *Nigerian Standard for Drinking Water Quality*.

Son, J., Kim, J. G., Hyun, S., & Cho, K. (2019). Screening level ecological risk assessment of abandoned metal mines using chemical and ecotoxicological lines of evidence. *Environmental Pollution*, *249*, 1081–1090. https://doi.org/10.1016/j.envpol.2019.03.019

Srogi, K. (2007). Monitoring of environmental exposure to polycyclic aromatic hydrocarbons: a review. *Environmental Chemistry Letters*, *5*(4), 169. https://doi.org/10.1007/S10311-007-0095-0

Stanley, P., Wolkersdorfer, C., & Wolkersdorfer, K. (2021). *Source Apportionment of Trace Metals at the Abandoned Nantymwyn Lead-Zinc Mine, Wales*.

Starke, I. C., Pieper, R., Neumann, K., Zentek, J., & Vahjen, W. (2014). The impact of high dietary zinc oxide on the development of the intestinal microbiota in weaned piglets. *FEMS Microbiology Ecology*, *87*(2), 416–427. https://doi.org/10.1111/1574-6941.12233

Stuart, M., Lapworth, D., Crane, E., & Hart, A. (2012). Review of risk from potential emerging contaminants in UK groundwater. *Science of The Total Environment*, *416*, 1–21. https://doi.org/10.1016/J.SCITOTENV.2011.11.072

Su, H., Zhang, D., Antwi, P., Xiao, L., Deng, X., Liu, Z., Long, B., Shi, M., Manefield, M. J., & Ngo, H. H. (2021). Exploring potential impact(s) of cerium in mining wastewater on the performance of partial-nitrification process and nitrogen conversion microflora. *Ecotoxicology and Environmental Safety*, *209*, 111796. https://doi.org/10.1016/J.ECOENV.2020.111796

Sun, C., Zhang, J., Ma, Q., & Chen, Y. (2015). Human health and ecological risk assessment of 16 polycyclic aromatic hydrocarbons in drinking source water from a large mixed-use reservoir. *International Journal of Environmental Research and Public Health*, *12*(11), 13956–13969. https://doi.org/10.3390/ijerph121113956

Sun, M., Li, F., Li, Y., Chen, J., & Cheng, G. (2024). Assessing the Ecological and Health Risks Associated with Heavy Metals in PM2.5 Based on their Potential Bioavailability. *Water, Air, and Soil Pollution*, *235*(5). https://doi.org/10.1007/s11270-024-07118-0

Sun, T., Liu, G., Ou, L., Feng, X., Chen, A., Lai, R., & Shao, L. (2019). Toxicity induced by zirconia oxide nanoparticles on various organs after intravenous administration in rats. *Journal of Biomedical Nanotechnology*, *15*(4), 728–741. https://doi.org/10.1166/JBN.2019.2717,

Sun, Z., Hu, Y., & Cheng, H. (2020). Public health risk of toxic metal(loid) pollution to the population living near an abandoned small-scale polymetallic mine. *Science of the Total Environment*, *718*. https://doi.org/10.1016/j.scitotenv.2020.137434

Surber, S. J. (2021). A conceptual model for integrating community health in managing remediation of West Virginia and central Appalachia's abandoned coal mines. *Environment, Development and Sustainability*, *23*(2), 1563–1578. https://doi.org/10.1007/s10668-020-00638-9

Sutton, P. (2004). *A Perspective on environmental sustainability?* http://www.green-innovations.asn.au/

Swartjes, F. A., Rutgers, M., Lijzen, J. P. A., Janssen, P. J. C. M., Otte, P. F., Wintersen, A., Brand, E., & Posthuma, L. (2012). State of the art of contaminated site management in The Netherlands: Policy framework and risk assessment tools. *Science of the Total Environment*, *427–428*, 1–10. https://doi.org/10.1016/j.scitotenv.2012.02.078

Swiss Academic Software GmbH. (2024). *Citavi* (6.19.2.1). https://lumivero.com/products/citavi/

Taylor, A. A., Tsuji, J. S., McArdle, M. E., Adams, W. J., & Goodfellow, W. L. (2023). Recommended Reference Values for Risk Assessment of Oral Exposure to Copper. *Risk Analysis : An Official Publication of the Society for Risk Analysis*, *43*(2), 211–218. https://doi.org/10.1111/RISA.13906

Taylor, S. R., & McLennan, S. M. (1985). The Continental Crust: Its Composition and Evolution. In *Geological Magazine* (Vol. 122, Number 6). Blackwell Scientific Publications. https://doi.org/10.1017/S0016756800032167

Tennant, J. P., Dugan, J. M., Graziotin, D., Jacques, D. C., Waldner, F., Mietchen, D., Elkhatib, Y., B. Collister, L., Pikas, C. K., Crick, T., Masuzzo, P., Caravaggi, A., Berg, D. R., Niemeyer, K. E., Ross-Hellauer, T., Mannheimer, S., Rigling, L., Katz, D. S., Greshake Tzovaras, B., … Colomb, J. (2017). A multi-disciplinary perspective on emergent and future innovations in peer review. *F1000Research 2017 6:1151*, *6*, 1151. https://doi.org/10.12688/f1000research.12037.3

Tessier, A., Campbell, P. G. C., & Bisson, M. (1979). Sequential Extraction Procedure for the Speciation of Particulate Trace Metals. *Analytical Chemistry*, *51*(7), 844–851. https://doi.org/10.1021/ac50043a017

Tirima, S., Bartrem, C., von Lindern, I., von Braun, M., Lind, D., Anka, S. M., & Abdullahi, A. (2018). Food contamination as a pathway for lead exposure in children during the 2010–2013 lead poisoning epidemic in Zamfara, Nigeria. *Journal of Environmental Sciences*, *67*, 260–272. https://doi.org/10.1016/J.JES.2017.09.007

Tomiyama, S., & Igarashi, T. (2022). The potential threat of mine drainage to groundwater resources. *Current Opinion in Environmental Science & Health*, *27*, 100347. https://doi.org/10.1016/J.COESH.2022.100347

Tozsin, G., Arol, A. I., Duzgun, S., Soydan, H., & Torun, A. (2022). Effects of abandoned coal mine on the water quality. *International Journal of Coal Preparation and Utilization*. https://doi.org/10.1080/19392699.2022.2044320

Tran, T. Q., Banning, A., Wisotzky, F., & Wohnlich, S. (2020). Mine water hydrogeochemistry of abandoned coal mines in the outcropped Carboniferous formations, Ruhr Area, Germany. *Environmental Earth Sciences*, *79*(4). https://doi.org/10.1007/s12665-020-8821-z

Tychsen, J., Peter W.U. Appel, Hassan, U. A., Jørgensen, T., & Azubike, O. C. (2011). *ASM Handbook for Nigeria* (J. Tychsen, Ed.; 1st ed., Vol. 1). Geological Survey of Denmark and Greenland (GEUS). https://pub.geus.dk/en/publications/asm-handbook-for-nigeria/fingerprints/

Tyson, R. (2020, July 7). *Innovative ways to repurpose old mines*. Mining.Com. https://www.mining.com/web/innovative-ways-to-repurpose-old-mines/

Ugochukwu, U. C., Ochonogor, A., Jidere, C. M., Agu, C., Nkoloagu, F., Ewoh, J., & Okwu-Delunzu, V. U. (2018). Exposure risks to polycyclic aromatic hydrocarbons by humans and livestock (cattle) due to hydrocarbon spill from petroleum products in Niger-delta wetland. *Environment International*, *115*, 38–47. https://doi.org/10.1016/J.ENVINT.2018.03.010

Ugochukwu, U. C., Onuora, O. H., Kurumeh, L., Mbakwe, U. I., Okolo, O. J., & Onuorah, A. L. (2021). Risk assessment of polycyclic aromatic hydrocarbons in the sediments of the Ekulu River in Enugu State in Nigeria. *African Journal of Aquatic Science*, *46*(2), 153–160. https://doi.org/10.2989/16085914.2020.1865868

Ugwu, K. E., & Ukoha, P. O. (2016). Analysis and Sources of Polycyclic Aromatic Hydrocarbons in Soil and Plant Samples of a Coal Mining Area in Nigeria. *Bulletin of Environmental Contamination and Toxicology*, *96*(3), 383–387. https://doi.org/10.1007/s00128-016-1727-5

UK EA. (2008). Abandoned mines and the water environment. In *The Environment Agency, United Kingdom*. https://doi.org/www.environment-agency.gov.uk

UK EA. (2019). 2021 River Basin Management Plan Mine waters challenge. *Environment Agency, United Kingdom*. https://consult.environment-agency.gov.uk/environment-and-business/challenges-and-choices/user_uploads/pollution-from-abandoned-mines-challenge-rbmp-2021-1.pdf

UK EA. (2020). *Land contamination risk management (LCRM)*. https://www.gov.uk/government/publications/land-contamination-risk-management-lcrm

UK EA. (2021). Mine waters: challenges for the water environment. *The Environment Agency, United Kingdom*.

Ukhan, O., Osadcha, N., & Osadchyi V. (2022). Mine water and its impact on the Siverskyi Donets River Basin. *XVI International Scientific Conference "Monitoring of Geological Processes and Ecological Condition of the Environment."*

Umeh, C. T., Nduka, J. K., Omokpariola, D. O., Morah, J. E., Mmaduakor, E. C., Okoye, N. H., Lilian, E. E. I., & Kalu, I. F. (2023). Ecological pollution and health risk monitoring assessment of polycyclic aromatic hydrocarbons and heavy metals in surface water, southeastern Nigeria. *Environmental Analysis Health and Toxicology*, *38*(2). https://doi.org/10.5620/eaht.2023007

UPPC. (2025, May 12). *The Revival of Kilembe Mine*. Uganda Printing and Publishing Corporation (UPPC). https://govinfohub.go.ug/index.php/2025/05/12/the-revival-of-kilembe-mine/

US EIA. (2024, April 17). *Coal and the environment*. U.S. Energy Information Administration. https://www.eia.gov/energyexplained/coal/coal-and-the-environment.php

US EPA. (1989a). Ecological risk assessment of hazardous waste site. *United States Environmental Protection Agency*.

US EPA. (1989b). *Risk Assessment: Guidance for Superfund Volume 1 Human Health Evaluation Manual (Part A)*. http://www.epa.gov/swerrims/riskassessment/risk_superfund.html

US EPA. (1991). *Risk Assessment Guidance for Superfund: Volume I - Human Health Evaluation Manual (Part B, Development of Risk-based Preliminary Remediation Goals)*.

US EPA. (1993). Provisional Guidance for Quantitative Risk Assessment of Polycyclic Aromatic Hydrocarbons. In *U.S. Environmental Protection Agency.*

US EPA. (1998). *Guidelines for Ecological Risk Assessment*. United State Environmental Protection Agency.

US EPA. (2000a). *Abandoned Mine Site Characterization and Cleanup Handbook*. United State Environmental Protection Agency.

US EPA. (2000b). Supplementary Guidance for Conducting Health Risk Assessment of Chemical Mixtures. *United States Environmental Protection Agency*.

US EPA. (2001). *Risk Assessment Guidance For Superfund: Volume I Human Health Evaluation Manual (Part D, Standardized Planning, Reporting, And Review Of Superfund Risk Assessments)*.

US EPA. (2004). *Risk Assessment: Guidance for Superfund Volume I: Human Health Evaluation Manual (Part E, Supplemental Guidance for Dermal Risk Assessment)*. http://www.epa.gov/oswer/riskassessment/

US EPA. (2007). Integrated Risk Information System. *Philadelphia, PA; Washington, DC;* https://www.epa.gov/iris

US EPA. (2011a). *Exposure Factors Handbook- Chapter 5-Soil and Dust Ingestion*.

US EPA. (2011b). *Exposure Factors Handbook- Chapter 6-Inhalation Rates*.

US EPA. (2011c). *Exposure Factors Handbook- Chapter 7-Dermal Exposure Factors*.

US EPA. (2018). *Hazardous Waste Test Methods / SW-846* |. https://www.epa.gov/hw-sw846

US EPA. (2022). Conducting a Human Health Risk Assessment. In *United State Environmental Protection Agency*. https://www.epa.gov/risk/conducting-human-health-risk-assessment

US EPA. (2024a). *Polychlorinated Biphenyls (PCBs)*. United States Environmental Protection Agency. https://www.epa.gov/pcbs?utm_source=chatgpt.com

US EPA. (2024b). *Volatile Organic Compounds' Impact on Indoor Air Quality*. United State Environmental Protection Agency. https://www.epa.gov/indoor-air-quality-iaq/volatile-organic-compounds-impact-indoor-air-quality

US EPA. (2024c, October 11). *Abandoned Mine Lands*. United States Environmental Protection Agency. https://www.epa.gov/superfund/abandoned-mine-lands

US EPA. (2025, November 5). *Basic Information about Nonpoint Source (NPS) Pollution*. United States Environmental Protection Agency. https://www.epa.gov/nps/basic-information-about-nonpoint-source-nps-pollution?utm_source=chatgpt.com

USGS. (2017). Zirconium and Hafnium. *U.S. Department of the Interior, U.S. Geological Survey*. https://doi.org/10.3133/pp1802V

Ushakova, E., Menshikova, E., Blinov, S., Osovetsky, B., & Belkin, P. (2022). Environmental Assessment Impact of Acid Mine Drainage from Kizel Coal Basin on the Kosva Bay of the Kama Reservoir (Perm Krai, Russia). *Water (Switzerland)*, *14*(5). https://doi.org/10.3390/w14050727

Van Zyl, D., Sassoon, M., Digby, C., Fleury, A. M., & Kyeyune, S. (2002). Mining For The Furure. In *International Institute for Environment and Development (IIED)* (Vol. 68, Number April).

Vanguard. (2017). Reclamation of abandoned mining sites to cost $5bn–Official. In *Vanguard News*. https://www.vanguardngr.com/2017/01/reclamation-abandoned-mining-sites-cost-5bn-official/

Vanguard. (2018). FG begins probe of mining activities in Nigeria - Vanguard News. In *Vanguard News*. https://www.vanguardngr.com/2018/11/fg-begins-probe-of-mining-activities-in-nigeria/

Venditti, B. (2023, November 15). *All the Metals We Mined in One Visualization*. Visual Capitalist Elements. https://elements.visualcapitalist.com/all-the-metals-we-mined-in-one-visualization-2/

Venkateswarlu, K., Nirola, R., Kuppusamy, S., Thavamani, P., Naidu, R., & Megharaj, M. (2016). Abandoned metalliferous mines: ecological impacts and potential approaches for reclamation. *Reviews in Environmental Science and Biotechnology*, *15*(2), 327–354. https://doi.org/10.1007/s11157-016-9398-6

Venkatraman, G., Giribabu, N., Mohan, P. S., Muttiah, B., Govindarajan, V. K., Alagiri, M., Abdul Rahman, P. S., & Karsani, S. A. (2024). Environmental impact and human health effects of polycyclic aromatic hydrocarbons and remedial strategies: A detailed review. *Chemosphere*, *351*, 141227. https://doi.org/10.1016/J.CHEMOSPHERE.2024.141227

Vlasov, A. (2023, February 1). *Five Interesting Facts to Know About Zirconium*. IAEA Office of Public Information and Communication. https://www.iaea.org/newscenter/news/five-interesting-facts-to-know-about-zirconium

Waida, J., Ismail W. Olanyi, Rilwan, U., Yusuf, I. M., & Sunday, B. I. (2022). Pollution Load Index of Heavy Metals Resulting from Mining Activities in Plateau State, Nigeria. *Journal of Radiation and Nuclear Applications*, *7*(3), 75–81. https://doi.org/10.18576/jrna/070310

Wang, F., Li, W., Wang, H., Hu, Y., & Cheng, H. (2024). The leaching behavior of heavy metal from contaminated mining soil: The effect of rainfall conditions and the impact on surrounding agricultural lands. *Science of the Total Environment*, *914*. https://doi.org/10.1016/j.scitotenv.2024.169877

Wang, W., Yang, L., Gao, D., Yu, M., Jiang, S., Li, J., Zhang, J., Feng, X., Tan, W., Liu, F., Yin, M., & Yin, H. (2024). Characteristics of iron (hydr)oxides and Cr(VI) retention mechanisms in soils from tropical and subtropical areas of China. *Journal of Hazardous Materials*, *465*, 133107. https://doi.org/10.1016/J.JHAZMAT.2023.133107

Wang, Z., Xu, Y., Zhang, Z., & Zhang, Y. (2021). Review: Acid mine drainage (AMD) in abandoned coal mines of Shanxi, China. *Water (Switzerland)*, *13*(1), 1–21. https://doi.org/10.3390/w13010008

Wani, A. L., Hammad Ahmad Shadab, G. G., & Afzal, M. (2021). Lead and zinc interactions – An influence of zinc over lead related toxic manifestations. In *Journal of Trace Elements in Medicine and Biology* (Vol. 64). Elsevier GmbH. https://doi.org/10.1016/j.jtemb.2020.126702

WFD-UKTAG. (2014). *Rivers & Lakes - Metal Bioavailability Assessment Tool (M-BAT) | wfd uktag*. Water Framework Directive – United Kingdom Technical Advisory Group. https://www.wfduk.org/resources/rivers-lakes-metal-bioavailability-assessment-tool-m-bat

Whaley, P., Aiassa, E., Beausoleil, C., Beronius, A., Bilotta, G., Boobis, A., de Vries, R., Hanberg, A., Hoffmann, S., Hunt, N., Kwiatkowski, C. F., Lam, J., Lipworth, S., Martin, O., Randall, N., Rhomberg, L., Rooney, A. A., Schünemann, H. J., Wikoff, D., … Halsall, C. (2020). Recommendations for the conduct of systematic reviews in toxicology and environmental health research (COSTER). *Environment International*, *143*, 105926. https://doi.org/10.1016/J.ENVINT.2020.105926

WHO. (2003). *Polynuclear aromatic hydrocarbons in Drinking-water Background document for development of WHO Guidelines for Drinking-water Quality*.

WHO. (2010). *WHO human health risk assessment toolkit: chemical hazards*. World Health Organization.

WHO. (2011). *Guidelines for Drinking-water Quality*. http://www.who.int

WHO. (2021). *WHO Human Health Risk Assessment Toolkit: Chemical Hazards, second edition*. https://www.who.int/publications/i/item/9789240035720

Wietse Bandstra. (2024). Volatile organic compounds Solutions | JOA Air Solutions. *Https://Joaairsolutions.Com/*. https://joaairsolutions.com/blog/solving-the-challenge-with-volatile-organic-compounds/

Wikipedia. (2014a). Cadmium. In *https://en.wikipedia.org/wiki/Cadmium*. https://en.wikipedia.org/wiki/Cadmium

Wikipedia. (2014b). Copper. In *https://en.wikipedia.org/wiki/Copper*. https://en.wikipedia.org/wiki/Copper

Wikipedia. (2014c). Mercury. In *https://en.wikipedia.org/wiki/Mercury_(element)*. https://en.wikipedia.org/wiki/Mercury_(element)

Wikipedia. (2014d). Uranium. In *https://en.wikipedia.org/wiki/Uranium*. https://en.wikipedia.org/wiki/Uranium

Wilson, I., Peters, A., Merrington, G., & Baken, S. (2023). Following the evidence and using the appropriate regulatory tools: A European-wide risk assessment of copper in freshwaters. *Integrated Environmental Assessment and Management*, *19*(6), 1570–1580. https://doi.org/10.1002/IEAM.4768

Wolffe, T. A. M., Vidler, J., Halsall, C., Hunt, N., & Whaley, P. (2020). A Survey of Systematic Evidence Mapping Practice and the Case for Knowledge Graphs in Environmental Health and Toxicology. *Toxicological Sciences*, *175*(1), 35–49. https://doi.org/10.1093/TOXSCI/KFAA025

Wolkersdorfer, C., & Mugova, E. (2022). Effects of Mining on Surface Water. In *Encyclopedia of Inland Waters, Second Edition* (Vol. 4, pp. 170–188). Elsevier. https://doi.org/10.1016/B978-0-12-819166-8.00036-0

Wood, J. (2020, February 11). *Prospecting for Pollution: The Need for Better Incentives to Clean Up Abandoned Mines*. Property and Environment Research Center (PERC). https://www.perc.org/2020/02/11/prospecting-for-pollution-the-need-for-better-incentives-to-clean-up-abandoned-mines/

Worlanyo, A. S., & Jiangfeng, L. (2021). Evaluating the environmental and economic impact of mining for post-mined land restoration and land-use: A review. *Journal of Environmental Management*, *279*. https://doi.org/10.1016/j.jenvman.2020.111623

Xu, Q., Liu, Z., Chen, Y., Qin, L., Zhao, M., Tang, W., Chen, S., Zhang, Y., & Zhong, Q. (2024). Serum metabolic changes link metal mixture exposures to vascular endothelial inflammation in residents living surrounding rivers near abandoned lead–zinc mines. *Environmental Pollution*, *358*. https://doi.org/10.1016/j.envpol.2024.124493

Xu, W., Meng, K., Du, W., Cai, Z., Li, Y., Chen, X., & Zhang, Y. (2025). Cadmium dominance in heavy metal pollution: ecological risks and human health implications in the Guan River Estuary, China. *Frontiers in Marine Science*, *12*, 1554838. https://doi.org/10.3389/FMARS.2025.1554838/TEXT

Yabe, J., Nakayama, S. M. M., Ikenaka, Y., Yohannes, Y. B., Bortey-Sam, N., Oroszlany, B., Muzandu, K., Choongo, K., Kabalo, A. N., Ntapisha, J., Mweene, A., Umemura, T., & Ishizuka, M. (2015). Lead poisoning in children from townships in the vicinity of a lead–zinc mine in Kabwe, Zambia. *Chemosphere*, *119*, 941–947. https://doi.org/10.1016/J.CHEMOSPHERE.2014.09.028

Yahyaoui, A., & Ben Amor, R. (2024). Environmental Contamination and Health Risk Assessment of Heavy Metals in the Stream Sediments of Oued Kasseb (Northerwest of Tunisia) in the Vicinity

of Abandoned Pb–Zn Mine. *Water, Air, and Soil Pollution*, *235*(4). https://doi.org/10.1007/s11270-024-07039-y

Yang, J., Kim, E. C., Shin, D. C., Jo, S. J., & Lim, Y. W. (2015). Human exposure and risk assessment of cadmium for residents of abandoned metal mine areas in Korea. *Environmental Geochemistry and Health*, *37*(2), 321–332. https://doi.org/10.1007/s10653-014-9650-3

Yang, T., Shen, Y., Qin, Y., Zhang, Y., Lu, L., Jin, J., Zhao, Y., Zhu, Y., & Zhang, Y. (2021). Genetic Mechanism and Environment Implications of Siderites in the Lopingian Coal-Bearing Series, Western Guizhou of China: Constrained by Whole-Rock and In Situ Geochemistry. *Frontiers in Earth Science*, *9*, 779991. https://doi.org/10.3389/FEART.2021.779991/BIBTEX

Yang, Y., Bao, H., Chai, Q., Wang, Z., Sun, Z., Fu, C., Liu, Z., Liu, Z., Meng, X., & Liu, T. (2019). Toxicity, biodistribution and oxidative damage caused by zirconia nanoparticles after intravenous injection. *International Journal of Nanomedicine*, *14*, 5175. https://doi.org/10.2147/IJN.S197565

Yohannes, Y. B., Nakayama, S. M. M., Yabe, J., Toyomaki, H., Kataba, A., Nakata, H., Muzandu, K., Ikenaka, Y., Choongo, K., & Ishizuka, M. (2021). Delta-aminolevulinic acid dehydratase (ALAD) and vitamin D receptor (VDR) genes polymorphisms in children residing in an abandoned lead-zinc mine area in Kabwe, Zambia. *Meta Gene*, *27*. https://doi.org/10.1016/j.mgene.2020.100838

Younger, P. L. (1997). The longevity of minewater pollution: a basis for decision-making. *Science of The Total Environment*, *194–195*, 457–466. https://doi.org/10.1016/S0048-9697(96)05383-1

Younger, P. L. (2000). *The Adoption and Adaptation of Passive Treatment Technologies for Mine Waters in The United Kingdom*. www.IMWA.info

Younger, P. L., Banwart, S., & Hedin, R. (2002). *Mine water : hydrology, pollution, remediation* (S. A. Banwart & R. S. Hedin, Eds.; Vol. 198) [Book]. Kluwer Academic Publishers.

Younger, P. L., & Robins, N. S. (2002). Challenges in the characterization and prediction of the hydrogeology and geochemistry of mined ground. *Geological Society Special Publication*, *198*, 1–16. https://doi.org/10.1144/GSL.SP.2002.198.01.01;SERIALTOPIC:TOPIC:SERIES-TYPE

Yu, Z., Li, X., Wu, P., Han, Z., Zhu, J., Chen, M., & Chen, Z. (2025). Effect of lead zinc mineralization area on heavy metals accumulation and geochemical fractions of agricultural soils in Southwest China. *Scientific Reports*, *15*(1), 1–16. https://doi.org/10.1038/S41598-025-04993-3;SUBJMETA=172,2151,47,704;KWRD=BIOGEOCHEMISTRY,ENVIRONMENTAL+SCIENCES,SOLID+EARTH+SCIENCES

Yusuf, S. N., Faruk, M. U., Imagbe, L. O., Yohanna, O. M., Yusuf, I., Onoshagbegbe, A., Kamal, M., & Jacob, T. T. (2022). Integrated geophysical investigation for lead and zinc mineralization in Wase, middle Benue Trough, Nigeria. *Heliyon*, *8*(12). https://doi.org/10.1016/j.heliyon.2022.e12541

Zapico, I., Laronne, J. B., Martín-Moreno, C., Martín-Duque, J. F., Ortega, A., & Sánchez-Castillo, L. (2017). Baseline to Evaluate Off-Site Suspended Sediment-Related Mining Effects in the Alto Tajo Natural Park, Spain. *Land Degradation and Development*, *28*(1), 232–242. https://doi.org/10.1002/LDR.2605

Zhang, K., Chang, S., Fu, Q., Sun, X., Fan, Y., Zhang, M., Tu, X., & Qadeer, A. (2021). Occurrence and risk assessment of volatile organic compounds in multiple drinking water sources in the Yangtze River Delta region, China. *Ecotoxicology and Environmental Safety*, *225*, 112741. https://doi.org/10.1016/J.ECOENV.2021.112741

Zhang, Z., Shen, N., Wang, Y., Li, Y., Song, Y., & He, T. (2011). Geological environment problems and countermeasures of Shijiaying mine in western Beijing. *Procedia Environmental Sciences*, *11*(PART C), 1245–1252. https://doi.org/10.1016/J.PROENV.2011.12.187

Zhu, M., Li, B., & Liu, G. (2022). Groundwater risk assessment of abandoned mines based on pressure-state-response—The example of an abandoned mine in southwest China. *Energy Reports*, *8*, 10728–10740. https://doi.org/10.1016/J.EGYR.2022.08.171

Ziemkiewicz, P. F., Skousen, J., White, K. D., Erdc, U., Leavitt, B., & Stiles, J. (2021). *Guidelines for the Design of Abandoned Mine Land Remediation and Water Treatment*.

Zineb, M., Abdelhak, B., Bilal, B., & Fadila, A. (2024). Characterization and Pollution Assessment of Potentially Toxic Metals (PTMs) in the Sulfide Tailings from Boudoukha Abandoned Mine (Zn–Pb–Cu), NE Algeria. *International Journal of Environmental Research*, *18*(4). https://doi.org/10.1007/s41742-024-00620-7

Zoveidadianpour, Z., Doustshenas, B., Alava, J. J., Savari, A., & Karimi Organi, F. (2023). Environmental and human health risk assessment of polycyclic aromatic hydrocarbons in the Musa estuary (northwest of Persian Gulf), Iran. *Journal of Sea Research*, *191*, 102335. https://doi.org/10.1016/J.SEARES.2023.102335

Appendices

Appendix 4.1: Different risk assessment methods and references as extracted from each reviewed article. Some studies used multiple methods when different sources were considered.

Risk Assessment Methods	References
Background values	Wang et al., 2018
Background values	Environmental Monitoring Station in China, 1990; Tian, 2016
Background values of soil elements in China	CNEMC, 1990
Cancer Risks	USEPA, 1989
Carcinogenic Health Risk	Zhao et al., 2014; Duan., 2016
	Zhou et al., 2019; Zhao et al., 2014
Carcinogenic Risk (CR)	ASTM, 1995; ASTM, 2015; USEPA, 2002 and APAT-ISPRA, 2008
	Luo & Jia, 2021
	USEPA, 1997, 1999
	USEPA, 2002
	USEPA, 1989, 2011a, 2011b, 2009, 2013
	Basta et al., 2001
China Standards for Drinking Water Quality	GB 14848-2017
Chinese Environmental Quality Standards for Soils (CESQ) and Background values	CEPA, 1995 and CNEMC, 1990
Biological Exposure Indices	ACGIH, 2006
Contamination factor (Cf)	Hakanson, 1980
	Rakotondrabe et al., 2018
Contamination index (CI)	Alberruche del Campo et al., 2014
Crustal Enrichment Factors (EFc)	Krachler et al., 2005
Degree of contamination (Cd)	Hakanson, 1980 and Abrahim and Parker, 2008.
Drinking Water Guideline	WHO, 2011
Enrichment factor (EF)	Buat-Menard and Chesselet, 1979
	Varol, 2011 and Williams and Block, 2015
	Feng et al., 2004; Ghrefat et al., 2011
	Zoller et al., 1974
	Zoller et al., 1974; Müller, 1979; Buat-Ménerand and Chesselet, 1979; Barbieri et al., 2018
	Covelli and Fontolan, 1997
	Buat-Ménard and Chesselet, 1979; Sutherland, 2000; Acevedo-Figueroa et al., 2006
Environmental standards for water quality	KMOE, 2018 and KMOE 2017b
EU drinking water guidelines	EU Directive, 1998
Evaluation criteria limits	Not specified
Reference values from control sites	Not specified
Geoaccumulation Index (Igeo)	Muller, 1969
	Müller, 1979; Zoller et al., 1974; Buat-M´enard and Chesselet, 1979; Barbieri et al., 2018
	Ruiz, 2001
Geochemical background values	Loukil, 1994
Guidelines for drinking water quality	WHO, 2004 and N.M. 2015
Hazard Average Quotient (HAQ)	Alberruche del Campo et al., 2014
Hazard Quotient (HQ)	ASTM, 1995; ASTM, 2015; U.S. EPA, 2002 and APAT-ISPRA, 2008
	Luo & Jia, 2021

	OEHHA, 2009; USEPA, 1998, 2018b
	USEPA, 2009
	USEPA, 2001
	USEPA, 2001
	USEPA IRIS, 1997
	USEPA, 1989, 2011a, 2011b, 2009, 2013
	USEPA, 1997; ASTM 1998
	USEPA
	USEPA, 2006
	Smith, 1996
	USEPA, 1995, 2007; Isvilanonda, S 1995
Heavy metal Evaluation Index (HEI)	Mohan et al., 1996; Siegel, 2002
Heavy metal pollution index (HPI)	Mohan et al., 1996
Incremental Lifetime Carcinogenic Risk (ILCR)	OEHHA, 2009; USEPA, 1998, 2018b
Integrated Risk	Jensen and Mesman, 2006
Logistic regression models and linear regression models	Bobb et al., 2018
Maximum Allowable Concentration (MAC)	Lui et al., 2005; CEC, 1993
Maximum Allowable Limit	SEMARNAT, 2009
Maximum Tolerable Value in Irrigation Water	WHO, 1998
Mean ERM Quotient (M-ERM-Q)	Gao and Chen, 2012
National background	Wei et al. 1992; NEPA 1990, 1995
National Food Safety Standard of China and General Standard for Contaminants in Food	NHC, 2017 and JECFA, 2019
Noncarcinogenic Health Risk	Zhao et al., 2014; Duan., 2016
	Zhou et al., 2019; Zhao et al., 2014
Potential Ecological Risk (Er)	Chapman, 1995; Hakanson, 1980
	Hakanson, 1980
	Luo & Jia, 2021
	Guo et al., 2010
Potential leaching risk	Bao et al., 2016
Sediment Pollution Index (SPI)	Shin and Lam, 2001
Sediment Quality Guidelines (SQGs)	CCME, 1999, 2002
	MacDonald et al., 2000
	MacDonald et al., 2000
	MacDonald et al., 2000 and Bojakowska, 2001
	Long and MacDonald, 1998
	Mac-Donald et al., 2000
Single-Factor Pollution Index (PI)	Song et al., 2018
	Cheng et al., 2007; Brandy et al., 2015; Mazurek et al., 2015
Single-factor pollution index (Wi)	Fu et al., 2023
Soil environmental quality- standard	GB15618-2018
Soil Environmental Quality Standards	MEP, 2018
Soil Threshold and Guideline values	MEF, 2007; SEMARNAT, 2004
Translocation factor (Tf)	Bose and Bhattacharyya, 2008
USEPA Ecological soil screening levels (Eco-SSLs)	USEPA, 1996
USEPA Human health benchmarks soil screening levels (HHB- SSLs)	USEPA, 1996
World Average Natural Soils	Bowen H. J. M., 1979
Worrisome levels of soil contamination in Korea	KMOE, 2016
Benchmark Dose Levels (BMDLs)	EFSA, 2010

Appendix 4:2: Mixture risk assessment (MRA) methods with corresponding references as extracted from the reviewed studies.

MRA Method	Reference
Bayesian Kernel Machine Regression (BKMR)	Bobb et al., 2018
Cancer Risk (CRtotal)	ASTM, 1995; ASTM, 2015; U.S. EPA, 2002 and the APAT-ISPRA, 2008
Comprehensive Pollution Index (Wn)	Fu et al., 2023
Cumulative probability distribution of HI of toxic metal(loid)s	OEHHA, 2009; USEPA, 1998, 2018b
Cumulative probability distribution of ILCR of Pb and i-As	OEHHA, 2009; USEPA, 1998, 2018b
Degree of contamination (Cd)	Rakotondrabe et al., 2018
Hazard Index (HI)	Luo & Jia, 2021
	USEPA
	USEPA, 1989, 2011a, 2011b, 2009, 2013
	USEPA, 1997; ASTM 1998
	USEPA, 2006
	USEPA, 2009
Health Index (HI)	ASTM, 1995; ASTM, 2015; U.S. EPA, 2002 and the APAT-ISPRA, 2008
	USEPA, 2001
	USEPA, 2001
Heavy Metal Evaluation Index (HEI)	Mohan et al., 1996; Siegel, 2002
Heavy metal Pollution Index (HPI)	WHO, 2011
Modified Contamination degree (MCd)	Hakanson, 1980
Nemerow Comprehensive Pollution Index (PC)	Cheng et al., 2007; Brandy et al., 2015; Mazurek et al., 2015
Nemerow Comprehensive Pollution Index (Pn)	Song et al., 2018
Pollution load Index (PLI)	Hakanson, 1980
Potential Ecological Risk Index (RI)	Hakanson, 1980
	Chapman, 1995; Hakanson, 1980
	Guo et al., 2010
	Luo & Jia, 2021
	Varol, 2011 and Williams and Block, 2015
Total Cancer Risk (TCR)	Luo & Jia, 2021
Total Carcinogenic Risk (TCR)	USEPA, 1989, 2011a, 2011b, 2009, 2013
	USEPA, 2002
Total health Risk (RZ)	Zhou et al., 2019; Zhao et al., 2014.; Duan., 2016

The variables below were also used in some studies to characterise contaminant uptake and internal transfer within biotic receptors. These indices are not standalone risk assessment methods or exposure models; instead, they serve as quantitative parameters within the exposure assessment phase. Specifically, BAF represents the ratio of contaminant concentration in an organism to that in the

surrounding medium. At the same time, TF indicates the transfer efficiency of contaminants from roots to aerial plant parts. Together, these metrics inform the evaluation of contaminant bioavailability, trophic transfer, and potential exposure risks. BAF is also known as the bioconcentration factor (BCF)

Other Variables	References
Bioaccumulation factor (BAF)	Rezvani and Zaefarian, 2011 Nannoni et al., 2011
Bioconcentration Factor (BCF)	Islam et al., 2020; Wang et al., 2020
Translocation factor (Tf)	Bose and Bhattacharyya, 2008

Appendix 4.3: International Regulatory Agencies and Frameworks Relevant to Chemical Risk Assessment

Agency / Organisation	Jurisdiction & Focus	Framework / Tools	Alignment with USEPA Principles	Key Reference
United States Environmental Protection Agency (USEPA)	United States — environmental and human health protection	RAGS; IRIS; Ecological Risk Assessment Guidelines (1998)	Core risk framework: exposure pathways, toxicity, risk characterisation	USEPA (1989, 1998, 2004)
Canadian Council of Ministers of the Environment (CCME)	Canada — national environmental quality guidelines	Soil/Sediment/Water Quality Guidelines (SQGs, WQGs); ERA Framework	Tiered ERA; risk quotients; site-specific trigger values	CCME (2006, 2007, 2020)
European Chemicals Agency (ECHA)	European Union — chemical safety regulation	REACH CSA; PNEC; DNEL; PEC/PNEC	PEC/PNEC ratio approach; probabilistic risk modelling	ECHA (2012, 2016)
World Health Organisation (WHO)	Global — health-based exposure standards	Drinking Water Guidelines; ADI; TDI	Toxicological basis; dose-response; conservative thresholds	WHO (2010, 2017, 2022)
Australian and New Zealand Guidelines (ANZG)	Australia & New Zealand — soil, sediment, water quality	ANZG WQGs (2018); Sediment Quality Assessment Guidelines	Tiered framework; trigger values; ecosystem protection	ANZG (2018)

Agency / Organisation	Jurisdiction & Focus	Framework / Tools	Alignment with USEPA Principles	Key Reference
German Environment Agency (UBA)	Germany — soil and chemical environmental management	BBodSchV; Soil Screening Values; EQS	Soil quality screening; ecotoxicological endpoints	UBA (2004)
UK Environment Agency (EA)	United Kingdom — contaminated land regulation	CLEA Model; Soil Guideline Values (SGVs)	Multimedia exposure modelling; land-use specific guidance	EA (2009, 2010)
Dutch National Institute for Public Health and the Environment (RIVM)	Netherlands — soil and sediment risk policy	Dutch Target and Intervention Values; Soil Risk Framework	Mixture toxicity; intervention values; probabilistic ERA	RIVM (2001, 2008)
Chinese Ministry of Ecology and Environment (MEE)	China — industrial and mining site risk regulation	GB 36600–2018; Soil Risk Control Standards	Exposure-based screening values; emerging harmonisation	MEE (2018)

Appendix 5.1: pXRF Coordinates points at Abakaliki Lead/zinc Abandoned mine

Sample No	Sample ID	Longitudes (E)	Latitudes (N)	Altitude (m)
1	TS1	8°04´34.5"	6°18´06.00"	73
2	TS2	8°04´33.9"	6°18´06.0"	74
3	TS3	8°04´33.6"	6°18´06.9"	78
4	TS4	8°4'35.55"	6°18'5.76"	71
5	TS5	8°4'35.54"	6°18'5.73"	69
6	TS6	8°4'35.69"	6°18'5.76"	67
7	TS7	8°4'35.64"	6°18'5.77"	69
8	TS8	8°4'35.71"	6°18'5.74"	71
9	TS9	8°4'34.58"	6°18'5.71"	68
10	TS10	8°4'35.17"	6°18'5.64"	77
11	TS11	8°4'33.36"	6°18'6.44"	75
12	TS12	8°4'33.36"	6°18'6.44"	71
13	TS13	8°4'33.36"	6°18'6.44"	70
14	TS14	8°4'33.36"	6°18'6.44"	71
17	RS	8°04´33.6"	06°18´6.3"	74
18	SS1	8°04´30.4"	6°18´14.0"	71
19	SS2	8°04´31.3"	6°18´12.9"	69
20	SS3	8°04´35"	6°18´14.7"	81
21	SS4	8°04´37.4´´	6°18´09.5"	78
22	SS5	8°04´39.8"	6°18´03.8"	79
22	SS6	8°04´33.9"	6°18´03.6"	79

TS - Tailing sample, SS - Soil sample, RS - Rock sample

Appendix 5.2: Sample coordinates points at Abakaliki Lead/zinc Abandoned mine

Sample No	Sample ID	Longitudes (E)	Latitudes (N)	Altitude (m)
1	TS1	8°04´34.5"	6°18´06.00"	73
2	TS2	8°04´33.9"	6°18´06.0"	74
3	TS3	8°04´33.6"	6°18´06.9"	78
4	TS4	8°4'35.55"	6°18'5.76"	71
5	TS5	8°4'35.54"	6°18'5.73"	69
6	TS6	8°4'35.69"	6°18'5.76"	67
7	TS7	8°4'35.64"	6°18'5.77"	69
8	TS8	8°4'35.71"	6°18'5.74"	71
9	TS9	8°4'34.58"	6°18'5.71"	68
10	TS10	8°4'35.17"	6°18'5.64"	77
11	TS11	8°4'33.36"	6°18'6.44"	75
12	TS12	8°4'33.36"	6°18'6.44"	71
13	TS13	8°4'33.36"	6°18'6.44"	70
14	TS14	8°4'33.36"	6°18'6.44"	71
15	TS15	8°4'33.09"	6°18'7.27"	71
16	TS16	8°4'33.37"	6°18'7.75"	70
17	RS	8°04´33.6"	06°18´6.3"	74

18	SS1	8°04′30.4"	6°18′14.0"	71
19	SS2	8°04′31.3"	6°18′12.9"	69
20	SS3	8°04′35"	6°18′14.7"	81
21	SS4	8°04′37.4′′	6°18′09.5"	78
22	SS5	8°04′39.8"	6°18′03.8"	79
23	SS6	8°04′33.9"	6°18′03.6"	79
24	SS7	8°4'33.53"	6°18'9.27"	71
25	SS8	8°4'33.53"	6°18'9.27"	69
26	SS9	8°4'33.53"	6°18'9.27"	69
27	SS10	8°4'33.53"	6°18'9.27"	66
28	SS11	8°4'33.53"	6°18'9.27"	69
29	SS12	8°4'33.53"	6°18'9.27"	69
30	RSS1	8°4'33.53"	6°18'9.27"	59
31	RSS2	8°4'33.53"	6°18'9.27"	59
32	WS1	8°04′34.6"	6°18′06.2"	71
33	WS2	8°04′33.9"	6°18′09.9"	75
34	WS3	8°04′36.7′′	6°18′12.2"	85
35	SD1	8°04′34.8"	6°18′06.3"	74
36	SD2	8°04′33.9"	6°18′09.9"	75
37	SD3	8°04′36.7"	6°18′12.2"	85

TS - Tailing sample, SS - Soil sample, RS - Rock sample, RSS - Reference Soil Sample, WS - Water sample and SD - Sediment sample

Appendix 5.3: Sample coordinates points at Wase-Gimbi Abandoned Lead/zinc mine

Sample No	Sample ID	Longitudes (E)	Latitudes (N)	Altitude (m)
1	PWS 1A	10°13′45.68"	08°57′11.75"	143
2	PSD 1A	10°13′46.28"	08°57′12.71"	132
3	PWS1B	10°13′46.73"	08°56′56.02"	155
4	PSD1B	10°13′46.73"	08°56′56.02"	155
5	PWS2B	10°13′39.38"	08°56′34.88"	176
6	PSD2B	10°13′39.38"	08°56′34.88"	176
7	PWS2A	10°13′35.71"	08°56′33.19"	166
8	PSD2A	10°13′35.71"	08°56′33.19"	166
9	PWS3	10°13′24.37"	08°56′43.64"	168
10	TS1	10°13′44.83"	08°57′13.23"	129
11	TS2	10°13′34.55"	08°56′33.85"	171
12	TS3	10°13′30.80"	08°56′35.31"	175
13	TS4	10°13′30.29"	08°56′38.92"	182
14	SS1	10°13′45.40"	08°56′42.20"	179
15	SS2	10°13′43.25"	08°56′44.55"	173
16	SS3	10°13′42.33"	08°56′45.10"	177
17	SS4	10°13′17.63"	08°57′05.63"	169
18	SS5	10°13′19.17"	08°56′52.50"	174
22	SS6	10°13′11.26"	08°56′40.39"	163
23	SS7	10°13′16.78"	08°56′42.75"	164
24	SS8	10°13′37.65"	08°57′30.50"	176

25	SS9	10°13′40.93"	08°57′55.02"	169
26	SS10	10°13′36.30"	08°56′31.04"	168
27	SS11	10°13′40.33"	08°56′31.78"	169
28	SS12	10°13′44.68"	08°56′33.73"	173
29	CSS1	10°12′43.72"	08°57′55.67"	182
30	BHW1	10°15′58.48"	08°57′12.74"	173
31	BHW2	10°15′44.90"	08°57′14.62"	169
32	BHW3	10°15′52.85"	08°57′27.04"	165
33	BHW4	10°15′50.06"	08°57′27.16"	162
34	RW1	10°15′28.53"	08°57′17.99"	160
35	SD3	10°15′28.53"	08°57′17.99"	160
36	RW2	10°15′26.28"	08°57′19.57"	158
37	RW3	10°15′25.03"	08°57′19.78"	159
38	SD4	10°15′25.03"	08°57′19.78"	159
39	PWS4A	10°13′41.12"	08°58′01.57"	175
40	PSD4A	10°13′41.12"	08°58′01.57"	175
41	PWS4B	10°13′41.91"	08°58′03.48"	173
42	PSD4B	10°13′41.91"	08°58′03.48"	173
43	PWS5A	10°13′42.14"	08°57′59.28"	173
44	PSD5A	10°13′42.14"	08°57′59.28"	173
45	PWS5B	10°13′42.62"	08°57′54.93"	169
46	PSD5B	10°13′42.62"	08°57′54.93"	169
47	RS	10°13'49.7"	8°56'52.0"	133
48	SSS	10°13'48.2"	8°57'13.4"	133
49	SS13	10°13'34.9"	8°56'26.1"	173
50	SS14	10°13'31.1"	8°56'25.0"	174
51	SS15	10°13'26.2"	8°56'24.3"	169
52	SS16	10°13'20.9"	8°56'28.7"	168
53	SS17	10°13'52.8"	8°56'53.7"	178
54	SS18	10°14'0.6"	8°57'1.3"	170
55	SD5	10°15'28.2"	8°57'19.4"	168
56	SD6	10°15'27.2"	8°57'20.0"	167
57	TS5	10°13'33.5"	8°56'35.0"	181
58	TS6	10°13'33.5"	8°56'34.4"	184
59	TS7	10°13'27.4"	8°56'31.2"	172
60	TS8	10°13'31.8"	8°56'34.8"	194.5
61	TS9	10°13'27.12"	8°56'31.92"	192.7
62	TS10	10°13'24.6"	8°56'29.4"	190.6
63	TS11	10°13'20.64"	8°56'30.84"	191.6
64	TS12	10°13'16.68"	8°56'34.08"	184.7
65	TS13	10°13'19.56"	8°56'38.4"	191.4
66	TS14	10°13'22.44"	8°56'38.04"	192
67	TS15	10°13'27.12"	8°56'37.32"	191.7
68	TS16	10°13'24.6"	8°56'35.16"	191.5
69	TS17	10°13'34.8"	8°56'35.8"	180

PWS - Pond Water sample, PSD - Pond Sediment Sample, RW - River Water sample, SD - Sediment sample, SS - Soil Sample, BHW - Borehole water sample, RS - Rock Sample, SSS - Salt effervescent soil sample, CSS - Control soil sample and TS - Tailing sample

Appendix 5.4: Sample coordinates points at Wase-Gimbi-Rikaya Abandoned Lead/zinc mine

Sample No	Sample ID	Longitudes (E)	Latitudes (N)	Altitude (m)
1	PWS1 R	10°09′01.64"	08°59′26.41"	199
2	SD1 R	10°09′01.64"	08°59′26.41"	199
3	PWS2 R	10°09′09.81"	08°59′26.96"	180
4	SD2 R	10°09′09.81"	08°59′26.96"	180
5	TS1 R	10°08′53.33"	08°59′33.07"	229
6	SS1 R	10°08′54.50"	08°59′33.49"	222
7	SS2 R	10°08′57.11"	08°59′22.32"	210
8	SS3 R	10°08′57.11"	08°59′22.32"	205
9	SS4 R	10°09′05.02"	08°59′24.59"	209
10	SS5 R	10°09′06.62"	08°59′30.04"	216
11	SS6 R	10°08′58.25"	08°59′36.11"	222
12	CSS2 R	10°08′55.98"	09°00′74.00"	228
13	SD3 R	10°08′45.89"	09°00′23.12"	188
14	SS7 R	10°08′43.94"	09°00′27.30"	208
15	SS8 R	10°08′47.50"	09°00′26.32"	210
16	SS9 R	10°08′50.00"	09°00′21.04"	215
17	SS10 R	10°08′46.18"	09°00′18.25"	213
18	SD4 R	10°08′45.56"	09°00′19.51"	210
22	SS11 R	10°08′40.08"	09°00′20.20"	211
23	TS2 R	10°08′43.80"	09°00′23.68"	211
24	CSS3 R	10°08′24.88"	09°00′46.81"	204
25	CW1	10°08′18.95"	09°00′52.63"	202
26	SD1-Control	10°08′18.95"	09°00′52.63"	202
27	CW2	10°08′11.89"	09°01′07.42"	192
28	SD2-Control	10°08′11.89"	09°01′07.42"	192

PWS - Pond Water sample, PSD - Pond Sediment Sample, CSS - Control soil sample, SD - Sediment sample, CW - Control water Sample, SS - Soil Sample and TS - Tailing sample

Appendix 5.5: TOC Method validation table

TC/IC Conc. (mg/L)	Measured Conc. 1 (mg/L)	Measured Conc. 2 (mg/L)	Mean	Recovery %
1	0.8305	0.8305	0.8305	83
10	9.241	9.554	9.3975	94
20	18.29	17.87	18.08	90
50	49.99	47.46	48.725	97
100	93.79	95.23	94.51	95
250	318.1	363	340.55	136

TC – Total carbon and IC - Inorganic Carbon Concentration

Appendix 5.6: Method validation parameters for soil (mg/kg)

Analyte	Regression Equation	R^2	LOD	Accuracy %	Precision (%)
As	y = 1714.6x -470.23	0.9997	1.0	70-71	3-4
Zn	y = 15938x + 2403.9	0.9982	1.4	73-74	4-5
Pb	y = 4122.4x + 429.35	0.9993	0.1	68-70	1-4
Cd	y = 23070x + 3638.4	0.9981	1.0	69-71	0.4-2
Ni	y = 20340x + 2503	0.9990	1.5	75-76	1-2
Ba	y = 17248x + 1635.9	0.9995	1.5	76-79	3
Hg	y = 2883.9x + 100.52	0.9999	1.1	71-74	1.18-1.24
Mn	y = 140600x + 12402	0.9995	1.6	78-82	2-4
Cr	y = 68453x + 7093.6	0.9994	1.9	78-83	2-4
Fe	y = 41151x + 4745.2	0.9991	1.0	86-87	1-2
Cu	y = 140099x + 11552	0.9997	0.5	85-93	2-5
Ti	y = 300656x + 28229	0.9994	1.8	83-87	1-4
Zr	y = 271280x + 24443	0.9995	0.2	80-88	1-4
Al	y = 32046x + 974.07	1	0.5	72-80	3-5
Ce	y = 49830x + 4911.8	0.9995	1.7	79-86	0.4-4
Sr	y = 173470x + 13148	0.9985	1.1	58-60	3.1-3.3

Appendix 5.7: Method validation parameters for water (mg/L)

Analyte	Regression Equation	R^2	LOD	Accuracy %	Precision (%)
As	y = 1714.6x -470.23	0.9997	0.061	106-109	1-2
Zn	y = 15938x + 2403.9	0.9982	0.046	105-115	2-3

Pb	y = 4122.4x + 429.35	0.9993	0.004	105-107	1-2
Cd	y = 23070x + 3638.4	0.9981	0.033	103-105	1-2
Ni	y = 20340x + 2503	0.9990	0.051	102-106	1-6
Ba	y = 17248x + 1635.9	0.9995	0.051	103-105	2-3
Hg	y = 2883.9x + 100.52	0.9999	0.038	107-108	1-3
Mn	y = 140600x + 12402	0.9995	0.053	102-105	1-2
Fe	y = 41151x + 4745.2	0.9991	0.034	102-104	1-2
Cr	y = 68453x + 7093.6	0.9994	0.065	103-104	1-3
Cu	y = 140099x + 11552	0.9997	0.017	101-101	1-3
Ti	y = 300656x + 28229	0.9994	0.000	103-104	1-2
Zr	y = 271280x + 24443	0.9995	0.007	102-102	2-4
Al	y = 32046x + 974.07	1	0.016	104-104	1-4
Ce	y = 49830x + 4911.8	0.9995	0.057	103-104	2-3
Sr	y = 173470x + 13148	0.9985	0.037	112-113	1-4

Appendix 5.8: pXRF - Results (mg/kg) for Soil (SS), Tailings (TS) and Rock (RS) samples at Abakaliki Abandoned Lead-zinc mine

Analyte/sample id	SS1	SS2	SS3	SS4	SS5	SS6	TS1	TS2	TS3	TS4	TS5	TS6	TS7	TS8
Mg	< LOD	< LOD	< LOD	332.9	288.0	176.4	262.3	386.6	337.7	< LOD	< LOD	< LOD	< LOD	< LOD
Al	50.7	29	78.6	23.2	< LOD	135.4	17.0	< LOD	< LOD	68.6	178.5	54.1	62.8	47.1
Si	1301.7	728.9	1784.4	741.2	360.2	1571	721.6	524.3	261.3	706.2	1249.9	792.5	655.2	647.7
K	64.1	42.1	76.5	62.5	45.9	87.4	136.1	119.1	50.2	166.1	264.4	218.1	212.2	197.6
Ca	80.0	< LOD	352.0	265.0	< LOD	238.0	< LOD	< LOD	< LOD	< LOD	< LOD	< LOD	< LOD	< LOD
Ti	5257.0	2912.0	5131.0	1604.0	< LOD	6775.0	< LOD	< LOD	< LOD	1066.0	3565.0	1970.0	2539.0	2423.0
Cr	123.0	208.0	238.0	482.0	< LOD	130.0	61.0	80.0	108.0	< LOD	170.0	56.0	144.0	121.0
Mn	996.0	837.0	978.0	1491.0	839.0	1254.0	271.0	336.0	772.0	554.0	506.0	500.0	616.0	389.0
Fe	86908.0	116599.0	87825.0	76147.0	28318.0	80040.0	22481.0	29378.0	32244.0	53201.0	69592.0	54454.0	58984.0	50461.0
Ni	17.0	< LOD	27.0	26.0	< LOD	53.0	< LOD	< LOD	< LOD	47.0	36.0	24.0	25.0	50.0
Cu	34.0	16.0	30.0	12.0	< LOD	20.0	< LOD	28.0	< LOD	< LOD	30.0	24.0	< LOD	< LOD
Zn	236.0	137.0	478.0	922.0	572.0	555.0	568.0	2182.0	12858.0	1420.0	424.0	2303.0	1405.0	1647.0
As	38.0	< LOD	39.0	< LOD	88.0	116.0	54.0	148.0	56.0	< LOD	< LOD	< LOD	38.0	< LOD
Rb	45.0	65.0	53.0	87.0	114.0	60.0	133.0	137.0	104.0	156.0	170.0	156.0	147.0	158.0
Sr	61.0	29.0	54.0	51.0	30.0	53.0	43.0	63.0	22.0	136.0	176.0	146.0	147.0	147.0
Zr	1922.0	862.0	1886.0	522.0	108.0	1488.0	40.0	116.0	59.0	367.0	381.0	300.0	313.0	277.0
Cd	< LOD	< LOD	< LOD	17.0	< LOD	< LOD	< LOD	18.0	65.0	12.0	< LOD	17.0	< LOD	13.0
Sn	< LOD	211.0	< LOD	142.0	426.0	< LOD	166.0	116.0	250.0	< LOD	< LOD	46.0	< LOD	47.0
Ba	691.0	< LOD	345.0	647.0	610.0	315.0	1119.0	1011.0	886.0	1018.0	1001.0	997.0	753.0	919.0
La	173.0	< LOD	133.0	201.0	< LOD	< LOD	< LOD	< LOD	426.0	136.0	163.0	189.0	133.0	< LOD
Ce	439.0	358.0	246.0	504.0	< LOD	205.0	381.0	< LOD	< LOD	271.0	245.0	361.0	288.0	235.0
Pb	594.0	417.0	1811.0	201.0	1207.0	1637.0	415.0	2404.0	762.0	1319.0	626.0	1675.0	796.0	2645.0
Y	60.0	30.0	69.0	34.0	13.0	45.0	16.0	27.0	5.0	63.0	78.0	50.0	69.0	54.0
Ga	15.0	< LOD	< LOD	12.0	< LOD	< LOD	20.0	29.0	62.0	18.0	22.0	21.0	30.0	20.0
Th	< LOD	20.0	19.0	< LOD	< LOD	33.0	< LOD	< LOD	< LOD	31.0	22.0	52.0	21.0	40.0

U	< LOD	25.0	< LOD	22.0	< LOD	< LOD	< LOD	< LOD	< LOD	55.0	39.0	52.0	50.0	39.0

Table 1 (continued)

Analyte/sample id	TS9	TS10	TS11	TS12	TS13	TS14	RS1
Mg	171.2	252.8	< LOD	189.9	225.4	303.4	263.8
Al	81.7	68.7	167.7	88.7	133.2	31.1	< LOD
Si	782.3	661.6	1250.3	826.8	1126.8	509.3	158.4
K	238.0	140.9	268.1	199.7	263.5	104.4	15.2
Ca	< LOD	< LOD	< LOD	< LOD	< LOD	< LOD	< LOD
Ti	3409.0	1524.0	3905.0	2285.0	3787.0	< LOD	< LOD
Cr	140.0	61.0	85.0	128.0	306.0	99.0	52.0
Mn	651.0	395.0	479.0	405.0	435.0	454.0	972.0
Fe	69858.0	55457.0	65094.0	53954.0	106054.0	36337.0	19659.0
Ni	30.0	30.0	22.0	15.0	37.0	< LOD	16.0
Cu	< LOD	< LOD	< LOD	28.0	21.0	9.0	10.0
Zn	1619.0	1869.0	4631.0	274.0	875.0	687.0	669.0
As	61.0	86.0	< LOD	< LOD	< LOD	< LOD	< LOD
Rb	159.0	130.0	148.0	151.0	128.0	144.0	125.0
Sr	148.0	90.0	124.0	128.0	117.0	103.0	34.0
Zr	340.0	184.0	328.0	306.0	270.0	43.0	41.0
Cd	< LOD	32.0	< LOD	< LOD	< LOD	14.0	< LOD
Sn	< LOD	< LOD	< LOD	< LOD	< LOD	79.0	344.0
Ba	999.0	655.0	848.0	786.0	727.0	906.0	1761.0
La	177.0	< LOD	149.0	< LOD	< LOD	< LOD	< LOD
Ce	381.0	< LOD	139.0	< LOD	276.0	247.0	476.0
Pb	1816.0	1900.0	1646.0	375.0	116.0	194.0	476.0
Y	31.0	30.0	41.0	22.0	28.0	13.0	15.0
Ga	67.0	39.0	52.0	62.0	49.0	39.0	20.0

Th	42.0	< LOD	41.0	30.0	26.0	22.0	< LOD
U	< LOD	33.0	< LOD	50.0	22.0	50.0	< LOD

Appendix 5.9: ICP-OES - Total metal concentration results (mg/kg) of Soil (SS), Reference Soil (RSS), Rock (RS), Tailings (TS), and Sediment (SD) samples at Abakaliki Abandoned Lead-zinc mine

Sample ID Analyte	SS1	SS2	SS3	SS4	SS5	SS6	SS7	SS8	SS9	SS10	SS11	SS12	RSS1	RSS2
As	<LOD	<LOD	<LOD	<LOD	<LOD	<LOD	<LOD	<LOD	<LOD	<LOD	<LOD	<LOD	<LOD	<LOD
Zn	136.8	116.7	271.2	664.5	888.0	438.5	235.1	639.4	232.9	583.1	945.6	439.4	94.6	62.4
Pb	519.3	308.8	580.5	187.5	1516.9	1359.3	197.3	1322.2	569.2	490.8	1848.5	687.4	67.5	27.2
Cd	<LOD	<LOD	2.4	4.7	5.0	3.2	<LOD	1.8	<LOD	<LOD	2.8	2.1	<LOD	<LOD
Ni	4.9	5.7	5.4	15.4	29.5	11.7	9.1	17.6	16.0	8.9	19.5	15.8	18.7	14.2
Cr	142.5	115.4	226.0	154.4	56.7	207.7	140.4	77.2	108.3	132.0	82.5	114.8	66.6	43.0
Cu	15.1	13.6	21.5	25.6	56.4	41.7	16.7	43.0	24.3	16.8	37.4	17.6	22.8	16.3
Ti	26.8	38.6	51.8	23.8	10.5	33.3	21.9	12.6	23.1	34.2	24.3	29.3	17.8	11.4
Zr	0.9	1.6	0.2	<LOD	<LOD	2.2	8.4	5.4	7.3	11.6	7.7	11.6	8.7	10.8
Ce	20.0	27.7	23.5	46.6	29.8	46.0	39.9	33.2	49.2	35.6	35.6	56.2	29.0	33.8
Sr	12.0	10.8	12.2	15.6	17.9	17.6	13.7	14.0	13.8	9.5	13.6	12.7	39.3	19.6
Ba	17.8	15.7	15.9	36.0	49.5	25.5	28.4	37.8	46.5	22.1	30.2	49.8	74.0	43.9
Mn	575.9	700.5	872.9	1044.3	485.0	746.5	822.5	777.1	931.6	835.1	1619.4	2185.0	530.6	461.6
Al	13199.0	14304.4	14524.9	15884.0	24466.4	24802.0	11431.1	14869.6	14040.2	19068.5	17965.4	15710.5	17608.8	17402.5
Hg	<LOD	<LOD	<LOD	<LOD	<LOD	<LOD	<LOD	<LOD	<LOD	<LOD	<LOD	<LOD	<LOD	<LOD
Fe	45335.8	44222.1	45271.7	44041.7	37506.3	45466.8	40615.1	36192.5	36609.7	38258.4	34622.6	37926.9	37568.7	35341.7
Mg	950.5	1300.7	2007.8	8333.4	17585.8	4086.7	2008.9	9393.9	3018.3	1815.5	10675.0	3452.8	5744.9	1956.4
Ca	2160.9	1361.5	2418.7	5205.1	2959.4	2985.9	5210.6	4462.1	2583.3	1073.9	1725.4	1734.1	21076.1	7690.9
Na	1306.2	619.7	516.2	588.8	911.3	1190.8	836.9	452.0	512.7	581.5	590.1	462.0	833.6	1039.8
K	3704.6	2832.7	2404.8	3707.7	5256.4	6034.8	3192.6	2959.1	2791.3	2517.1	2705.3	2137.0	3884.8	5279.9

Appendix 5.9 (continued)

Sample ID Analyte	RS	TS1	TS2	TS3	TS4	TS5	TS6	TS7	TS8	TS9	TS10	TS11	TS12	TS13
As	<LOD	<LOD	<LOD	<LOD	<LOD	<LOD	<LOD	<LOD	<LOD	<LOD	<LOD	<LOD	<LOD	<LOD
Zn	429.5	1817.5	6084.5	9494.1	7520.7	2616.6	1735.5	1025.6	7704.5	5412.4	1830.0	14059.1	6144.8	5348.8
Pb	905.3	1032.2	2549.1	1022.0	847.4	287.0	739.2	226.8	660.3	3291.2	462.6	1496.2	812.2	2165.1
Cd	2.8	6.3	33.9	48.0	41.4	7.9	4.2	1.6	38.9	21.7	8.6	76.9	23.8	17.1
Ni	4.3	32.5	27.4	24.6	40.3	30.7	29.6	28.1	21.9	28.3	28.6	26.2	28.2	35.2
Cr	16.9	45.0	41.8	37.5	44.3	38.8	37.8	34.7	29.4	35.9	37.0	37.0	37.2	38.9
Cu	22.1	74.3	129.9	147.8	29.5	33.0	33.7	16.5	50.8	30.5	31.3	83.9	74.6	48.6
Ti	7.7	5.7	6.4	5.6	5.6	5.6	4.8	5.8	5.5	6.3	7.5	5.6	6.1	7.8
Zr	<LOD	<LOD	<LOD	<LOD	5.6	2.7	2.6	2.4	2.2	4.6	2.6	2.7	2.6	2.6
Ce	38.9	8.4	9.8	8.9	10.0	7.0	7.0	8.6	6.3	9.0	8.3	7.8	8.7	9.8
Sr	6.3	14.9	18.5	15.7	17.7	10.6	12.2	16.2	10.0	11.7	10.5	11.7	12.7	11.9
Ba	9.2	43.2	26.9	23.4	27.9	34.0	44.6	38.2	21.7	29.1	25.6	23.4	26.8	28.6
Mn	1030.4	279.3	240.2	203.6	479.9	272.7	280.1	309.3	205.6	290.6	277.2	220.4	245.1	270.0
Al	6964.9	28220.8	25780.8	23587.2	<LOD	<LOD	22976.7	22228.5	17948.8	22350.1	22136.3	21910.6	22680.4	23644.6
Hg	<LOD	<LOD	<LOD	<LOD	<LOD	<LOD	<LOD	<LOD	<LOD	<LOD	<LOD	<LOD	<LOD	<LOD
Fe	23203.7	35317.6	35714.2	34299.4	32245.0	37149.8	33184.7	28280.2	27278.2	28763.8	29627.1	29064.6	27791.6	28908.2
Mg	1932.4	31776.4	29513.8	27645.4	34781.6	34652.8	28453.7	27676.7	22748.1	26459.4	28699.1	25288.0	25317.5	28130.2
Ca	1880.5	3241.5	6109.5	2690.9	5732.7	3805.9	5801.0	5231.3	2598.1	3653.7	2298.0	1852.4	1973.0	1983.0
Na	1861.5	1215.0	1012.1	898.7	870.5	850.5	512.6	1004.1	1097.3	1358.6	434.7	481.8	575.4	828.5
K	4307.0	7695.7	7466.5	7146.4	5300.9	5556.7	4147.3	5026.7	5460.8	6489.6	3549.4	4553.0	4844.3	4896.7

Appendix 5.9 (continued)

Sample ID Analyte	TS14	TS15	TS16	TS17	TS18	SD1	SD2	SD3
As	<LOD	<LOD	<LOD	<LOD	<LOD	<LOD	<LOD	<LOD
Zn	6127.6	1656.4	345.7	346.4	1044.9	705.6	1473.1	1640.0
Pb	2447.1	1099.9	217.4	107.0	391.9	265.9	1330.6	1472.6

Sample ID Analyte	TS14	TS15	TS16	TS17	TS18	SD1	SD2	SD3
Cd	27.4	4.1	<LOD	<LOD	2.0	2.2	4.3	4.8
Ni	42.6	29.0	32.8	22.6	38.2	20.4	35.2	38.0
Cr	47.3	39.1	38.9	44.8	45.9	29.5	43.6	45.9
Cu	47.8	57.1	28.1	23.9	37.2	21.6	46.6	51.2
Ti	8.7	5.4	6.8	8.1	6.9	4.9	7.2	8.1
Zr	5.1	2.8	2.9	4.0	3.4	<LOD	<LOD	<LOD
Ce	12.4	6.9	11.0	14.7	14.1	5.9	10.6	12.1
Sr	13.5	9.9	10.1	9.4	13.0	12.6	16.5	18.6
Ba	39.5	37.2	36.9	29.1	57.7	28.1	38.5	41.2
Mn	324.2	245.5	320.5	245.2	373.0	255.2	326.3	339.3
Al	<LOD	20303.0	22493.8	19037.3	<LOD	23420.7	<LOD	<LOD
Hg	<LOD	<LOD	<LOD	<LOD	<LOD	<LOD	<LOD	<LOD
Fe	31525.3	29179.6	30190.9	30883.9	31752.7	32897.7	36899.1	37449.1
Mg	30418.2	21790.2	23530.9	13618.0	24131.0	29987.4	37872.7	39673.1
Ca	2018.3	1412.9	2381.1	881.4	2078.5	3783.0	3910.3	4234.2
Na	937.6	563.9	937.8	459.2	1150.5	630.3	1084.2	997.5
K	5057.1	3386.7	4758.2	4260.0	6439.3	4171.0	6150.6	6828.2

Appendix 5.10: Sequential analysis results F1-F3 (mg/kg) of Soil (SS), Reference Soil (RSS), Rock (RS), Tailings (TS), and Sediment (SD) samples at Abakaliki Abandoned Lead-zinc mine

Analyte	Sample Id/ F1- F3	SS1	SS2	SS3	SS4	SS5	SS6	SS7	SS8	SS9	SS10	SS11	SS12	RSS1	RSS2	RS
	F1	1.4	2.1	1.1	1.5	1.7	1.8	<LOD	<LOD	<LOD	<LOD	<LOD	<LOD	<LOD	<LOD	1.3
As	F2	<LOD	<LOD	<LOD	<LOD	<LOD	<LOD	1.0	1.4	1.2	1.2	1.5	1.6	1.3	1.2	<LOD
	F3	<LOD	<LOD	<LOD	<LOD	<LOD	<LOD	<LOD	<LOD	<LOD	<LOD	<LOD	<LOD	<LOD	<LOD	<LOD
Zn	F1	40.2	8.6	70.8	651.2	250.5	64.5	78.2	137.2	28.2	20.9	140.8	48.9	17.3	4.5	534.7
	F2	9.1	4.1	29.7	330.4	124.7	26.9	66.1	98.3	20.8	18.1	70.1	27.2	17.5	6.7	253.5

	F3	33.3	16.1	31.8	132.4	178.5	41.0	57.2	102.7	50.4	119.5	123.5	36.8	21.4	16.2	65.7
	F1	50.5	22.2	25.3	3.5	5580.8	205.0	2.9	82.0	45.8	40.0	260.1	14.8	1.0	0.7	360.7
Pb	F2	164.5	149.9	322.9	86.0	4130.3	696.3	93.3	779.1	335.8	308.3	1093.2	377.1	16.1	8.7	3578.3
	F3	67.9	79.5	135.6	92.9	894.8	447.5	105.3	305.8	218.8	208.0	479.9	103.6	17.9	9.8	348.5
	F1	1.9	1.4	4.1	5.8	6.3	4.9	<LOD	<LOD	<LOD	<LOD	2.3	1.1	<LOD	<LOD	8.6
Cd	F2	<LOD	<LOD	<LOD	2.4	<LOD	<LOD	<LOD	<LOD	<LOD	<LOD	<LOD	<LOD	<LOD	<LOD	1.6
	F3	<LOD	<LOD	<LOD	<LOD	<LOD	<LOD	<LOD	<LOD	<LOD	<LOD	<LOD	<LOD	<LOD	<LOD	<LOD
	F1	1.6	<LOD	1.8	4.5	3.4	1.5	<LOD	<LOD	<LOD	<LOD	<LOD	<LOD	<LOD	<LOD	3.8
Ni	F2	<LOD	<LOD	<LOD	3.0	<LOD	<LOD	<LOD	<LOD	<LOD	<LOD	<LOD	<LOD	<LOD	<LOD	<LOD
	F3	<LOD	<LOD	<LOD	2.6	4.0	1.8	1.9	1.6	<LOD	<LOD	2.8	<LOD	<LOD	2.0	1.6
	F1	43.6	8.2	6.3	30.3	19.2	11.4	2.8	3.7	2.7	5.9	1.9	4.7	5.4	1.9	4.4
Fe	F2	350.9	416.1	503.3	596.6	393.7	423.8	1083.5	351.3	381.6	437.5	505.0	535.8	1507.5	498.4	1352.7
	F3	1450.7	1862.1	4295.1	4325.6	4084.1	2399.2	5834.5	704.0	939.5	737.8	3085.5	2024.0	2455.1	1157.4	1694.7
	F1	<LOD	<LOD	<LOD	<LOD	<LOD	<LOD	<LOD	<LOD	<LOD	<LOD	<LOD	<LOD	<LOD	<LOD	<LOD
Cr	F2	<LOD	<LOD	<LOD	<LOD	<LOD	<LOD	2.3	<LOD	<LOD	<LOD	<LOD	<LOD	<LOD	<LOD	<LOD
	F3	5.5	6.2	11.0	9.5	6.1	12.4	21.4	5.0	6.1	4.2	13.2	4.3	6.0	2.9	3.1
	F1	0.5	<LOD	<LOD	0.8	3.1	0.5	1.1	1.3	1.2	1.2	1.7	1.2	1.8	1.1	1.4
Cu	F2	0.7	0.6	0.7	0.7	3.4	1.3	1.0	1.5	1.2	1.2	1.8	1.2	2.0	1.3	4.5
	F3	1.4	1.2	2.7	4.8	6.7	3.6	3.5	4.6	4.7	3.9	5.8	2.5	4.5	3.7	3.4
	F1	4.1	4.1	4.1	4.2	4.1	4.2	<LOD	<LOD	<LOD	<LOD	<LOD	<LOD	<LOD	<LOD	4.1
Ti	F2	<LOD	<LOD	<LOD	<LOD	<LOD	<LOD	<LOD	<LOD	<LOD	<LOD	<LOD	<LOD	<LOD	<LOD	<LOD
	F3	34.3	24.9	21.9	13.6	13.4	58.1	10.2	4.4	16.5	13.5	16.7	15.3	23.3	37.0	21.9
	F1	2.1	1.6	1.7	1.6	1.6	2.0	1.7	0.6	0.4	0.4	0.4	1.9	0.7	0.4	1.7
Zr	F2	0.5	<LOD	<LOD	<LOD	<LOD	0.2	1.1	0.6	0.6	0.5	0.5	1.0	0.7	0.6	<LOD
	F3	<LOD	<LOD	<LOD	<LOD	<LOD	<LOD	1.1	0.6	0.6	0.6	0.8	1.3	0.8	0.7	<LOD
	F1	2.4	2.2	1.8	2.1	2.6	3.4	<LOD	<LOD	<LOD	1.9	<LOD	<LOD	<LOD	<LOD	2.7
Ce	F2	3.0	3.2	3.8	2.8	7.2	9.2	2.1	5.2	6.5	8.2	8.3	10.8	6.3	9.4	65.4
	F3	2.6	3.9	6.7	15.8	13.9	13.0	8.5	<LOD	14.8	12.5	12.9	9.2	10.0	14.1	54.9
	F1	4.6	5.3	6.7	8.8	6.8	6.3	6.7	5.9	6.0	2.7	4.5	4.5	19.0	10.4	5.8
Sr	F2	0.8	0.8	1.2	2.8	2.6	1.0	2.9	2.8	1.9	1.2	1.7	1.6	4.6	3.1	1.7
	F3	1.2	1.1	1.5	1.9	1.5	1.3	1.9	1.6	1.7	1.5	1.6	1.6	2.5	2.1	1.1
Ba	F1	5.3	6.2	6.6	8.9	19.8	6.5	7.5	10.1	15.0	4.4	8.7	6.9	15.6	9.1	15.8

	F2	8.6	36.7	6.6	24.4	4.5	4.2	15.7	17.4	17.7	8.7	8.9	19.1	29.0	16.1	15.9
	F3	2.3	2.7	3.5	10.5	11.6	8.3	5.8	5.2	11.9	5.2	4.0	4.9	10.8	7.9	2.2
	F1	<LOD	<LOD	<LOD	<LOD	<LOD	<LOD	<LOD	<LOD	<LOD	<LOD	<LOD	<LOD	<LOD	<LOD	<LOD
Hg	F2	<LOD	<LOD	<LOD	<LOD	<LOD	<LOD	<LOD	<LOD	<LOD	<LOD	<LOD	<LOD	<LOD	<LOD	<LOD
	F3	<LOD	<LOD	<LOD	<LOD	<LOD	<LOD	<LOD	<LOD	<LOD	<LOD	<LOD	<LOD	<LOD	<LOD	<LOD
	F1	91.4	92.0	88.7	220.6	78.1	61.3	48.1	39.4	92.3	58.8	47.6	36.2	111.9	19.2	72.6
Mn	F2	368.1	673.3	786.2	1096.8	542.4	688.6	528.6	596.5	756.2	651.9	1482.4	1497.0	227.0	187.8	3541.0
	F3	32.4	75.9	100.8	134.1	79.6	101.9	100.9	68.4	117.4	211.7	182.2	107.9	36.1	43.2	222.3
	F1	251.7	223.8	96.6	69.5	55.6	318.1	28.1	26.0	95.8	344.6	62.8	121.8	63.2	47.5	48.8
Al	F2	449.5	533.0	477.9	598.5	476.6	808.2	377.3	437.4	534.3	691.0	633.1	651.6	550.1	475.6	775.5
	F3	525.6	685.3	942.5	1396.8	2001.9	1598.9	1092.6	774.4	1077.8	1098.2	1388.1	800.0	1014.5	1227.4	1679.1

Appendix 5.10 (continued)

Analyte	Sample Id/ F1- F3	TS1	TS2	TS3	TS4	TS5	TS6	TS7	TS8	TS9	TS10	TS11	TS12	TS13
	F1	1.2	1.6	1.6	<LOD	<LOD	<LOD	<LOD	<LOD	<LOD	<LOD	<LOD	<LOD	<LOD
As	F2	<LOD	<LOD	<LOD	1.2	1.4	1.0	1.3	<LOD	1.5	1.2	<LOD	<LOD	<LOD
	F3	<LOD	<LOD	<LOD	<LOD	<LOD	<LOD	<LOD	<LOD	<LOD	<LOD	<LOD	<LOD	<LOD
	F1	429.0	2057.6	2408.5	2008.2	230.5	236.7	449.1	478.1	449.4	311.1	882.0	833.9	626.5
Zn	F2	305.6	668.6	1129.1	337.3	166.7	172.9	335.3	240.7	341.0	221.8	368.5	381.9	493.6
	F3	613.0	1354.5	5622.3	1651.2	1185.0	725.9	562.5	4540.4	1570.7	1457.5	3336.2	1777.6	1483.6
	F1	8.9	201.2	113.6	86.5	1.3	194.8	0.6	75.5	120.5	110.0	47.3	0.5	100.4
Pb	F2	128.7	826.6	352.5	165.7	17.8	298.4	14.3	164.1	257.6	144.5	137.0	29.9	397.9
	F3	33.2	536.0	1139.3	1559.3	18.5	93.6	21.4	182.3	178.6	83.1	194.3	93.6	185.2
	F1	3.9	12.9	14.3	19.4	0.9	0.4	0.4	2.2	1.4	4.4	4.1	3.9	4.2
Cd	F2	<LOD	2.0	3.9	1.8	<LOD	<LOD	<LOD	<LOD	<LOD	1.0	1.0	1.1	2.7
	F3	2.3	4.9	28.6	6.0	4.0	1.4	1.2	23.8	4.3	5.5	16.1	6.2	4.3
	F1	2.4	3.8	3.1	7.0	<LOD	<LOD	<LOD	<LOD	<LOD	<LOD	<LOD	<LOD	<LOD
Ni	F2	<LOD	<LOD	<LOD	<LOD	<LOD	<LOD	<LOD	<LOD	<LOD	<LOD	<LOD	<LOD	<LOD
	F3	4.0	4.0	6.3	3.1	3.1	4.5	4.4	3.5	3.6	3.4	2.9	3.9	3.8

	F1	22.0	21.7	33.5	37.7	24.8	13.1	12.8	22.6	13.0	24.8	27.5	11.3	3.8
Fe	F2	857.8	976.3	1302.4	514.5	728.8	502.3	686.3	739.3	542.7	777.5	670.5	533.2	476.2
	F3	3034.8	3282.7	8469.4	2876.2	2674.7	2909.4	2741.5	3808.6	1774.7	3726.5	1982.5	4317.1	1818.1
	F1	<LOD	<LOD	<LOD	<LOD	<LOD	<LOD	<LOD	<LOD	<LOD	<LOD	<LOD	<LOD	<LOD
Cr	F2	<LOD	<LOD	<LOD	<LOD	<LOD	<LOD	<LOD	<LOD	<LOD	<LOD	<LOD	<LOD	<LOD
	F3	3.8	4.0	7.5	3.0	2.9	3.3	3.3	4.2	3.2	4.3	3.2	4.9	3.4
	F1	6.2	13.4	22.7	8.2	5.3	3.3	2.7	7.8	3.8	3.4	7.5	13.7	3.1
Cu	F2	6.1	8.8	17.4	2.6	3.8	3.3	2.9	5.6	3.6	4.9	5.7	9.7	3.8
	F3	6.9	13.1	67.4	4.8	21.5	6.1	4.8	12.7	5.8	9.1	17.3	11.3	6.2
	F1	4.1	4.1	4.1	<LOD	<LOD	<LOD	<LOD	<LOD	<LOD	<LOD	<LOD	<LOD	<LOD
Ti	F2	<LOD	<LOD	<LOD	<LOD	<LOD	<LOD	<LOD	<LOD	<LOD	<LOD	<LOD	<LOD	<LOD
	F3	3.5	3.0	7.5	3.7	3.1	3.2	3.0	3.8	1.7	4.5	1.8	5.5	1.8
	F1	2.0	1.6	1.6	0.4	0.4	0.4	0.4	0.3	0.5	0.3	0.4	0.3	0.3
Zr	F2	<LOD	<LOD	<LOD	1.1	1.0	0.6	0.6	0.5	1.3	0.6	0.6	0.6	0.5
	F3	<LOD	<LOD	<LOD	1.4	0.7	0.6	0.6	0.7	1.3	0.8	0.6	0.7	0.6
	F1	1.7	2.2	1.9	<LOD	<LOD	<LOD	<LOD	<LOD	<LOD	<LOD	<LOD	<LOD	<LOD
Ce	F2	<LOD	<LOD	<LOD	<LOD	<LOD	<LOD	1.9	<LOD	2.8	1.8	<LOD	<LOD	<LOD
	F3	<LOD	2.1	2.6	<LOD	<LOD	<LOD	2.2	<LOD	1.8	<LOD	<LOD	<LOD	1.8
	F1	4.2	7.4	4.7	3.1	2.9	3.6	4.1	2.8	3.5	3.4	2.6	2.8	3.8
Sr	F2	1.3	3.0	1.8	2.4	1.7	2.8	3.1	1.9	2.6	2.2	1.6	1.6	2.8
	F3	1.4	1.8	2.5	2.3	1.6	2.2	3.6	1.9	1.7	1.9	1.7	2.0	1.6
	F1	6.2	3.4	4.1	<LOD	3.6	5.3	0.9	2.4	3.2	3.3	0.8	0.4	8.2
Ba	F2	18.3	7.3	13.6	6.9	10.2	25.2	26.9	13.1	20.5	13.4	5.1	13.1	14.6
	F3	4.3	7.5	6.8	2.3	1.5	6.2	36.4	3.2	2.4	13.8	1.7	15.6	2.5
	F1	<LOD	<LOD	<LOD	<LOD	<LOD	<LOD	<LOD	<LOD	<LOD	<LOD	<LOD	<LOD	<LOD
Hg	F2	<LOD	<LOD	<LOD	<LOD	<LOD	<LOD	<LOD	<LOD	<LOD	<LOD	<LOD	<LOD	<LOD
	F3	<LOD	<LOD	<LOD	<LOD	<LOD	<LOD	<LOD	<LOD	<LOD	<LOD	<LOD	<LOD	<LOD
	F1	15.9	74.9	36.1	158.5	17.0	12.4	61.9	18.0	37.5	27.9	12.6	36.9	17.9
Mn	F2	111.7	50.0	53.9	22.7	9.4	23.9	81.1	36.6	109.0	145.2	10.7	15.9	127.1
	F3	28.3	20.4	35.4	19.5	17.7	19.8	30.7	22.1	26.3	19.3	13.7	23.7	26.2

	F1	72.0	173.5	126.2	258.0	83.7	33.3	57.6	61.8	56.2	71.0	84.9	49.2	23.0
Al	F2	905.8	1124.5	1184.8	710.9	856.3	611.9	460.5	840.0	715.3	755.4	862.5	597.0	449.9
	F3	2615.4	2230.7	3911.3	1882.1	1903.7	1984.6	2077.4	2027.0	1672.1	2205.7	1682.1	2640.1	1793.3

Appendix 5.10 (continued)

Analyte	Sample Id/ F1-F3	TS14	TS15	TS16	TS17	TS18	SD1	SD2	SD3
	F1	<LOD	<LOD	<LOD	<LOD	<LOD	1.3	1.4	1.4
As	F2	1.3	<LOD	1.1	1.1	<LOD	<LOD	<LOD	<LOD
	F3	<LOD	<LOD	<LOD	<LOD	<LOD	<LOD	<LOD	<LOD
	F1	618.7	270.3	75.9	148.6	252.4	540.5	641.0	432.5
Zn	F2	481.6	160.0	37.6	53.8	184.0	355.0	484.6	221.0
	F3	1258.4	211.1	103.9	123.2	278.7	501.8	860.5	174.4
	F1	25.3	38.6	2.2	2.7	9.5	2.9	159.6	5.1
Pb	F2	254.8	121.1	31.6	29.2	80.7	46.2	430.2	45.5
	F3	128.0	64.8	12.8	16.4	35.4	52.3	119.4	21.4
	F1	5.2	1.3	<LOD	<LOD	<LOD	3.9	5.9	4.3
Cd	F2	3.5	<LOD	<LOD	<LOD	<LOD	<LOD	1.6	<LOD
	F3	4.5	<LOD	<LOD	<LOD	<LOD	1.7	2.2	<LOD
	F1	<LOD	<LOD	<LOD	<LOD	<LOD	2.5	2.8	3.5
Ni	F2	<LOD	<LOD	<LOD	<LOD	<LOD	<LOD	<LOD	<LOD
	F3	4.4	2.4	2.6	2.2	4.4	4.3	6.9	5.0
	F1	3.2	3.7	3.7	3.6	2.0	60.3	25.4	44.5
Fe	F2	518.0	445.3	308.8	433.9	396.6	1046.8	959.1	942.5
	F3	2300.6	1757.4	2303.9	1392.7	3491.6	4022.0	3823.8	3085.2
	F1	<LOD	<LOD	<LOD	<LOD	<LOD	<LOD	<LOD	<LOD
Cr	F2	<LOD	<LOD	<LOD	<LOD	<LOD	<LOD	<LOD	<LOD
	F3	4.2	3.1	3.1	3.7	4.3	5.1	5.0	4.1
	F1	3.4	3.3	3.4	2.4	3.4	2.1	2.0	2.7
Cu	F2	4.2	3.7	2.9	2.4	5.5	2.9	3.7	3.3
	F3	7.0	9.4	2.9	4.2	8.8	8.3	6.1	5.3

Analyte	Sample Id/ F1-F3	TS14	TS15	TS16	TS17	TS18	SD1	SD2	SD3
	F1	<LOD	<LOD	<LOD	<LOD	<LOD	4.2	4.1	4.2
Ti	F2	<LOD	<LOD	<LOD	<LOD	<LOD	<LOD	<LOD	<LOD
	F3	2.3	1.8	3.1	2.9	3.5	4.7	6.4	4.2
	F1	1.9	0.6	0.4	0.3	0.3	1.6	1.6	1.6
Zr	F2	1.2	0.6	0.6	0.5	0.6	0.4	<LOD	<LOD
	F3	1.3	0.7	0.7	0.7	0.7	0.3	<LOD	<LOD
	F1	<LOD	<LOD	<LOD	<LOD	<LOD	1.8	1.7	1.8
Ce	F2	<LOD	<LOD	1.8	3.2	2.4	<LOD	<LOD	2.0
	F3	2.3	<LOD	1.8	3.9	3.4	3.1	3.2	3.2
	F1	3.4	3.1	3.1	2.8	3.2	5.5	5.9	5.5
Sr	F2	2.2	1.9	1.6	1.3	2.1	2.3	3.3	2.3
	F3	1.6	1.6	1.5	1.5	1.7	1.9	2.2	1.5
	F1	6.6	9.1	4.9	5.0	13.1	3.1	7.2	5.1
Ba	F2	25.8	20.0	13.9	10.7	41.3	21.7	26.4	28.6
	F3	3.4	5.6	2.6	3.6	11.7	17.0	25.5	5.3
	F1	<LOD	<LOD	<LOD	<LOD	<LOD	<LOD	<LOD	<LOD
Hg	F2	<LOD	<LOD	<LOD	<LOD	<LOD	<LOD	<LOD	<LOD
	F3	<LOD	<LOD	<LOD	<LOD	<LOD	<LOD	<LOD	<LOD
	F1	23.4	20.7	32.8	22.9	26.9	55.6	71.5	90.2
Mn	F2	235.8	26.2	82.3	60.8	216.9	64.1	128.6	46.3
	F3	32.5	14.8	23.0	23.2	54.7	45.4	44.2	24.7
	F1	24.3	39.3	47.5	67.5	32.8	109.8	58.3	116.7
Al	F2	486.9	603.5	481.7	583.2	642.9	766.9	815.9	1023.2
	F3	1976.9	1692.8	1605.9	1733.7	2302.9	2418.1	3378.9	2798.3

Appendix 5.11: Minimum, mean, and maximum percentage partitioning (%) of trace elements across sequential extraction fractions in soils, sediments, and tailings from Abakaliki abandoned lead-zinc mine

Abakaliki	**Mn**	**Zn**	**Pb**	**Ni**	**Cr**	**Cu**	**Ti**	**Zr**	**Ce**	**Sr**	**Ba**	**Cd**	**Al**	**Fe**	**Hg**	**As**
F1 (Exchangeable/carbonate fraction) Percentage (%) Partition (n=33)																
Mean	12.3	24.3	17.4	8.1	0.0	8.8	17.4	93.2	7.0	33.9	18.9	134.8	0.4	0.1	0.0	0.0
Min	1.7	3.6	0.1	0.0	0.0	0.4	0.8	0.0	1.1	17.4	0.0	0.0	0.0	0.0	0.0	0.0
Max	33.0	98.0	367.9	33.3	0.2	27.7	85.1	1645.2	30.1	56.4	41.3	2401.7	1.9	0.4	0.0	0.0
F2 (Reducible fraction) Percentage (%) Partition (n=33)																
Mean (n=33)	48.1	13.7	37.3	3.2	0.9	8.4	4.7	13.2	16.6	15.4	53.2	8.2	2.7	2.9	0.0	0.0
Min	3.5	2.6	3.1	0.0	0.2	2.6	-0.1	20.8	5.2	5.8	9.1	0.0	0.0	1.2	0.0	0.0
Max	111.8	50.3	272.3	19.6	1.6	17.6	10.8	55.5	31.3	23.1	233.1	51.4	5.0	7.5	0.0	0.0
F3 (Oxidisable fraction) Percentage (%) Partition (n=33)																
Mean (n=33)	10.5	30.2	27.4	13.4	9.2	19.2	64.2	13.4	23.3	13.5	23.8	20.3	6.7	13.6	0.0	0.0
Min	4.1	8.4	1.5	3.2	3.2	8.7	22.8	0.0	9.9	7.2	4.5	0.0	0.0	2.3	0.0	0.0
Max	25.4	79.6	184.0	25.6	19.9	65.0	174.6	30.8	53.2	22.4	95.1	77.4	16.6	48.3	0.0	0.0

Appendix 5.12: ICP-OES - Total metal concentration results (mg/kg) of Soil (SS), Control Soil (CSS), Rock (RS), Tailings (TS), and Sediment (SD) samples at Gimbi Abandoned Lead-zinc mine

Sample Id/Analyte	SS1	SS2	SS3	SS4	SS5	SS6	SS7	SS8	SS9	SS10	SS11	SS12	SSS	SS13	SS14	SS15	SS16
As	<LOD	<LOD	<LOD	<LOD	<LOD	<LOD	<LOD	<LOD	<LOD	<LOD	<LOD	<LOD	<LOD	<LOD	<LOD	<LOD	<LOD
Zn	26.8	55.5	25.7	54.1	35.3	850.0	448.2	249.3	911.7	24.9	30.1	32.7	6239.2	23.1	49.1	59.8	21.5
Pb	34.5	48.7	24.8	32.0	32.9	40.1	706.9	23.3	42.4	13.0	26.5	28.7	37.3	7.4	27.9	15.9	7.8
Cd	<LOD	<LOD	<LOD	<LOD	<LOD	1.6	<LOD	<LOD	1.9	<LOD	<LOD	<LOD	9.5	<LOD	<LOD	<LOD	<LOD
Ni	6.8	5.8	10.8	4.2	10.4	6.3	8.7	5.4	7.6	4.8	12.7	8.6	10.7	2.7	6.6	2.9	3.0
Cr	53.4	81.7	79.4	28.4	61.5	28.0	39.7	24.4	26.8	27.7	137.8	101.3	3.4	22.4	84.6	33.1	37.0

Sample Id/Analyte	SS1	SS2	SS3	SS4	SS5	SS6	SS7	SS8	SS9	SS10	SS11	SS12	SSS	SS13	SS14	SS15	SS16
Cu	9.4	10.3	16.4	7.4	10.5	13.7	39.6	10.9	15.9	5.9	16.8	9.9	10.7	5.5	9.0	5.4	5.1
Ti	73.1	116.0	34.0	65.5	24.7	9.7	36.3	18.8	18.4	73.7	139.5	76.9	1.2	27.2	37.3	18.7	23.4
Zr	5.2	8.7	11.6	4.9	6.4	3.2	4.5	2.5	3.4	5.2	15.9	7.9	2.3	4.4	7.1	4.9	8.6
Ce	36.8	27.4	46.9	26.2	52.5	33.3	45.7	30.3	37.2	27.6	44.8	32.6	3.3	16.8	22.6	19.0	21.7
Sr	20.5	26.8	25.7	14.8	18.6	21.0	22.6	16.0	25.7	16.6	25.5	23.9	39.1	5.5	11.1	13.0	13.1
Ba	135.5	77.6	113.5	84.9	149.3	99.3	113.4	77.0	107.0	110.6	101.5	67.7	19.5	30.1	55.1	58.3	57.3
Hg	<LOD	<LOD	<LOD	<LOD	<LOD	<LOD	<LOD	<LOD	<LOD	<LOD	<LOD	<LOD	<LOD	<LOD	<LOD	<LOD	<LOD
Mn	948.0	530.5	582.1	675.4	1004.7	818.8	903.8	371.2	774.1	848.6	745.9	594.7	1791.3	31.9	342.3	152.1	128.0
Al	7374.2	9311.1	17647.3	5299.9	10006.7	4777.4	6952.6	6821.8	7741.2	5221.5	13711.8	4845.9	2249.8	3953.5	6523.2	3504.2	4470.8
Fe	32596.4	37815.2	39051.4	15507.8	28073.1	17813.8	21833.6	20070.2	18829.2	16622.1	41548.4	40801.5	21001.7	8691.1	29048.3	8389.8	11729.6
Mg	2055.8	2266.9	3747.2	2577.3	2235.7	2541.6	4064.4	1604.1	3080.4	2811.5	4154.5	1983.2	58720.1	734.0	1004.5	1464.8	1368.0
Ca	10996.9	15444.6	12427.6	5812.4	6655.2	10983.5	13006.3	3975.4	12864.7	7554.1	9898.0	11348.7	8573.8	3325.8	6054.3	7458.0	5462.4
Na	768.6	597.1	1025.2	626.1	661.4	447.4	450.0	934.6	628.8	383.3	700.2	836.1	8680.8	1209.5	1348.0	1261.4	1067.3
K	4046.0	3865.6	7842.9	2667.1	4331.2	2590.3	3771.8	2654.9	3917.0	3019.5	8760.8	4257.0	5342.5	3150.2	4073.8	3899.9	3231.6

Appendix 5.12 (Continued)

Sample Id/Analyte	SS17	SS18	CSS	RS	TS1	TS2	TS3	TS4	TS05	TS06	TS07	TS08	TS09	TS10	TS11	TS12	TS13
As	<LOD	<LOD	<LOD	<LOD	<LOD	<LOD	<LOD	<LOD	<LOD	<LOD	<LOD	<LOD	<LOD	<LOD	<LOD	<LOD	<LOD
Zn	50.2	40.0	7.2	6258.1	552.4	111.2	12022.9	11982.4	14572.7	9440.1	574.9	3981.6	8596.2	10679.4	9220.2	1250.4	6394.7
Pb	25.6	21.3	8.3	939.9	21.6	22.5	1214.7	1408.7	807.8	2544.3	96.8	240.4	954.1	1065.0	1264.3	91.6	1749.8
Cd	<LOD	<LOD	<LOD	20.4	<LOD	<LOD	31.6	32.1	33.4	18.5	<LOD	4.3	18.1	22.6	20.2	4.8	25.1
Ni	3.4	3.6	2.6	22.6	20.4	39.1	22.8	26.4	31.5	28.4	32.7	15.3	23.0	22.1	21.8	18.8	17.2
Cr	23.7	28.3	33.1	20.5	3.8	14.5	9.4	17.5	19.6	5.8	23.6	14.4	12.9	12.7	16.7	9.9	15.1
Cu	6.0	5.5	7.3	1517.9	27.1	31.3	181.8	49.1	143.0	121.0	30.0	49.2	89.5	72.7	93.5	24.7	96.6
Ti	23.9	18.1	26.6	3.6	3.0	5.1	5.2	12.6	3.6	1.6	2.7	0.4	1.8	2.9	1.9	1.8	2.4

Sample Id/Analyte	SS17	SS18	CSS	RS	TS1	TS2	TS3	TS4	TS05	TS06	TS07	TS08	TS09	TS10	TS11	TS12	TS13
Zr	3.8	3.5	5.4	8.9	0.0	0.9	0.0	6.3	4.7	9.5	4.7	3.5	4.0	6.0	4.0	3.2	3.9
Ce	16.5	20.8	34.6	9.3	4.7	25.8	11.6	22.8	14.7	19.1	26.1	7.9	12.9	12.0	12.7	9.5	15.1
Sr	8.6	9.6	7.9	22.0	35.6	50.4	28.9	215.7	44.0	27.2	35.1	38.6	37.9	34.3	33.2	24.3	57.9
Ba	59.2	50.4	52.3	0.0	57.0	314.3	26.8	172.6	66.9	115.0	206.8	23.7	82.0	72.4	52.8	90.3	61.8
Hg	<LOD	<LOD	<LOD	<LOD	<LOD	<LOD	<LOD	<LOD	<LOD	<LOD	<LOD	<LOD	<LOD	<LOD	<LOD	<LOD	<LOD
Mn	351.9	250.0	195.5	8987.5	1068.3	1554.6	6894.5	1795.4	6282.7	7533.0	1333.8	5494.8	4951.4	4925.9	4183.0	787.3	2236.5
Al	2873.1	2858.8	5916.3	75.1	5838.4	9053.5	1756.3	9261.4	4327.6	792.1	9060.3	2720.6	4335.7	2980.5	3598.8	7059.1	4613.4
Fe	11167.4	9500.2	12597.9	36426.5	24317.8	23039.3	35107.4	23986.9	35066.5	38305.0	28154.0	32837.6	33037.6	34435.6	31549.8	20720.4	22878.0
Mg	1085.7	904.1	1025.3	1688.4	19342.0	9008.4	22770.9	14302.9	26541.1	16715.7	8715.1	22318.6	17285.9	19042.7	20591.2	8903.8	13749.2
Ca	4551.6	4682.5	3657.8	1705.5	15376.8	8639.2	14679.8	46649.3	29967.6	10966.4	11253.9	19593.5	19258.3	19165.8	17422.4	19868.6	26162.1
Na	923.1	902.7	891.2	2657.7	1759.7	2853.4	1270.7	1412.8	1805.4	818.0	1516.9	1418.3	1624.8	1190.0	2343.9	1985.7	2088.8
K	3138.2	2602.3	2639.6	5295.4	5828.2	8122.8	3567.3	5836.7	6359.2	2182.4	4964.2	4573.9	5371.4	4236.9	5812.1	5886.8	5487.4

Appendix 5.12 (Continued)

Sample Id/Analyte	TS14	TS15	TS16	TS17	PSD1A	PSD1B	PSD2A	PSD2B	PSD4A	PSD4B	PSD5A	PSD5B	SD3	SD4	SD05	SD06
As	<LOD	<LOD	<LOD	<LOD	<LOD	<LOD	<LOD	<LOD	1.3	<LOD	<LOD	<LOD	<LOD	<LOD	<LOD	<LOD
Zn	7588.2	17769.1	10184.0	6330.0	371.6	2634.7	680.6	206.5	92.4	1087.5	443.7	596.5	424.1	9.6	153.0	17.9
Pb	2450.2	622.5	1540.5	1423.8	275.2	374.2	134.6	48.6	26.4	448.1	250.2	110.1	76.8	21.0	116.8	16.8
Cd	16.2	31.4	22.2	28.5	<LOD	3.3	<LOD	<LOD	<LOD	2.8	<LOD	<LOD	<LOD	<LOD	<LOD	<LOD
Ni	16.6	23.9	22.6	17.6	22.1	15.3	39.5	12.4	2.7	33.7	13.4	15.0	39.5	3.8	13.5	6.9
Cr	14.1	4.3	11.8	15.4	7.1	11.0	33.9	81.3	5.1	62.8	16.8	26.0	19.5	15.8	25.5	14.7
Cu	76.8	78.8	82.7	91.9	18.8	21.4	57.3	33.3	20.2	99.1	24.5	47.8	31.5	6.2	16.2	8.7
Ti	2.9	1.5	2.2	4.6	7.3	5.5	3.8	13.2	5.3	10.9	9.6	8.6	7.9	15.4	27.4	11.6
Zr	3.6	9.5	4.0	3.9	1.6	0.5	0.7	4.3	0.4	4.3	4.8	6.8	1.5	2.8	8.5	5.7
Ce	11.4	14.1	11.3	18.2	11.1	7.8	53.7	26.3	8.3	64.3	29.3	56.8	74.4	40.9	57.0	38.1

Sample Id/Analyte	TS14	TS15	TS16	TS17	PSD1A	PSD1B	PSD2A	PSD2B	PSD4A	PSD4B	PSD5A	PSD5B	SD3	SD4	SD05	SD06
Sr	27.3	17.8	31.1	71.5	260.9	78.3	40.0	18.2	41.3	58.9	24.4	41.6	26.1	6.8	20.7	15.5
Ba	50.3	78.0	58.6	83.1	65.3	61.3	262.4	77.7	34.1	377.4	119.2	253.6	352.2	69.4	148.1	77.2
Hg	<LOD	<LOD	<LOD	<LOD	<LOD	<LOD	<LOD	<LOD	<LOD	<LOD	<LOD	<LOD	<LOD	<LOD	<LOD	<LOD
Mn	3170.2	6639.0	4231.7	2016.6	1010.7	1277.7	1173.2	506.0	245.8	2201.9	1161.1	2155.6	3850.1	467.8	548.3	280.0
Al	3177.3	624.6	2942.0	6971.7	5379.2	5114.8	11253.0	10531.2	1294.8	29793.0	14295.0	23798.5	11865.5	3405.1	15872.8	8085.8
Fe	28657.3	40403.1	32557.8	22993.6	27695.9	26472.8	32440.1	37181.3	33363.6	12909.7	6227.1	40401.5	21165.6	28976.2	18099.2	11943.7
Mg	12963.7	1346.3	18432.8	14729.8	30731.3	14144.6	10074.7	5438.6	5949.4	1270.0	6069.6	15003.0	4338.9	7874.3	6887.0	4383.2
Ca	13477.1	5815.1	16075.9	19777.5	188458.4	20481.9	11820.1	7663.7	8134.9	3763.4	96683.9	17554.4	6716.1	11929.3	9991.0	8389.0
Na	1541.4	1053.3	1884.9	3031.3	2619.8	2090.4	1609.5	864.5	1366.1	568.1	1972.3	2890.8	2137.0	1940.0	1830.5	1346.2
K	4710.5	3036.0	5342.3	7398.6	7873.6	6200.1	6134.1	3030.4	5232.8	1663.5	3632.8	13949.0	10083.4	11217.4	8651.1	5733.9

Appendix 5.13: Sequential analysis results F1-F3 (mg/kg) of Soil (SS), Control Soil (CSS), Rock (RS), Tailings (TS), and Sediment (SD) samples at Gimbi Abandoned Lead-zinc mine

Sample Id/F1- F3		SS1	SS2	SS3	SS4	SS5	SS6	SS7	SS8	SS9	SS10	SS11	SS12	SSS	SS13	SS14	SS15	SS16
	F1	1.4	1.4	1.4	1.7	1.0	1.6	1.5	1.8	1.5	1.7	1.5	1.2	1.0	<LOD	<LOD	1.2	1.0
As	F2	<LOD	<LOD	<LOD	<LOD	<LOD	<LOD	<LOD	<LOD	<LOD	<LOD	<LOD	<LOD	<LOD	1.0	<LOD	<LOD	<LOD
	F3	<LOD	<LOD	<LOD	<LOD	<LOD	<LOD	<LOD	<LOD	<LOD	<LOD	<LOD	<LOD	<LOD	<LOD	<LOD	<LOD	1.0
	F1	6.4	29.5	5.1	27.3	13.2	600.0	135.2	29.9	688.7	8.4	8.0	8.5	1526.9	8.6	21.4	20.7	9.4
Zn	F2	7.4	31.5	10.2	29.3	15.7	494.3	171.7	91.4	634.7	15.0	9.0	17.1	2371.8	4.2	10.3	14.2	6.1
	F3	8.6	17.5	9.0	17.0	35.4	163.0	134.3	65.5	225.0	8.6	6.1	15.1	2051.8	12.5	16.5	13.9	9.4
	F1	<LOD	<LOD	<LOD	<LOD	<LOD	0.1	76.1	<LOD	0.3	<LOD	0.2	<LOD	6.2	4.7	3.5	2.9	2.8
Pb	F2	8.8	22.6	14.9	22.5	14.6	17.1	635.7	14.1	25.9	5.7	8.7	9.8	5.6	6.1	15.2	6.8	4.9
	F3	23.4	31.8	24.7	29.1	21.8	28.4	286.0	12.3	45.7	15.1	17.3	24.2	28.6	15.6	16.7	8.6	6.6
	F1	1.2	1.3	1.2	1.3	1.3	2.8	1.6	1.4	2.9	1.3	1.3	<LOD	5.2	<LOD	<LOD	<LOD	<LOD
Cd	F2	<LOD	<LOD	<LOD	<LOD	<LOD	<LOD	<LOD	<LOD	1.0	<LOD	<LOD	<LOD	<LOD	<LOD	<LOD	<LOD	<LOD
	F3	<LOD	<LOD	<LOD	<LOD	<LOD	<LOD	<LOD	<LOD	<LOD	<LOD	<LOD	<LOD	2.2	<LOD	<LOD	<LOD	<LOD

Sample Id/F1- F3		SS1	SS2	SS3	SS4	SS5	SS6	SS7	SS8	SS9	SS10	SS11	SS12	SSS	SS13	SS14	SS15	SS16
	F1	1.5	<LOD	1.6	1.5	1.9	2.6	1.9	<LOD	2.8	1.6	1.5	<LOD	2.7	<LOD	<LOD	<LOD	<LOD
Ni	F2	1.7	<LOD	<LOD	<LOD	<LOD	1.8	<LOD	<LOD	2.3	2.4	<LOD	1.9	<LOD	<LOD	<LOD	<LOD	<LOD
	F3	2.3	<LOD	3.4	2.4	2.9	2.1	2.3	1.5	2.6	2.3	1.8	2.8	4.5	<LOD	<LOD	<LOD	<LOD
	F1	6.1	5.2	7.4	5.9	8.3	50.5	4.9	10.7	48.0	13.1	9.2	5.2	561.4	13.8	4.2	5.7	19.4
Fe	F2	553.8	284.2	358.7	519.7	581.1	1373.0	345.7	967.5	1530.9	914.3	591.7	502.3	5024.1	367.5	426.9	461.3	480.3
	F3	3048.3	1560.0	3072.1	746.3	1264.3	2567.3	665.0	1868.7	3079.6	1689.0	1665.8	2929.7	6134.9	57.8	1175.1	57.3	64.9
	F1	<LOD	<LOD	<LOD	<LOD	<LOD	<LOD	<LOD	<LOD	<LOD	<LOD	<LOD	<LOD	2.3	1.9	1.9	1.9	1.9
Cr	F2	<LOD	<LOD	<LOD	<LOD	<LOD	<LOD	<LOD	<LOD	<LOD	<LOD	<LOD	<LOD	<LOD	<LOD	<LOD	<LOD	<LOD
	F3	9.4	4.6	21.9	4.2	7.7	4.5	2.5	5.2	5.8	5.0	4.7	14.3	<LOD	3.5	9.4	2.8	3.3
	F1	<LOD	<LOD	0.6	<LOD	0.9	0.7	0.9	<LOD	1.6	<LOD	0.7	1.8	3.0	2.2	2.0	2.0	2.1
Cu	F2	0.5	2.8	2.7	0.7	<LOD	0.5	1.9	1.0	0.7	<LOD	1.3	<LOD	<LOD	<LOD	<LOD	0.7	<LOD
	F3	2.1	2.2	2.7	2.4	2.2	7.3	12.4	2.3	6.9	2.3	3.4	1.9	4.0	2.6	2.7	2.0	1.8
	F1	4.1	4.2	4.1	4.1	4.1	4.2	4.1	4.1	4.1	4.2	4.2	3.6	<LOD	<LOD	<LOD	<LOD	<LOD
Ti	F2	<LOD	<LOD	<LOD	<LOD	<LOD	<LOD	<LOD	<LOD	<LOD	<LOD	<LOD	<LOD	<LOD	<LOD	<LOD	<LOD	<LOD
	F3	34.7	25.1	145.8	18.9	26.1	7.9	12.3	16.9	10.3	23.3	52.1	25.1	<LOD	2.6	11.0	1.8	2.0
	F1	2.2	1.7	1.6	1.6	1.6	1.9	1.6	1.6	1.6	1.6	2.4	0.7	1.4	1.3	1.3	1.3	2.1
Zr	F2	<LOD	<LOD	0.3	<LOD	<LOD	<LOD	<LOD	0.5	<LOD	<LOD	<LOD	0.3	0.5	0.3	0.3	0.3	0.8
	F3	<LOD	<LOD	1.1	<LOD	<LOD	<LOD	<LOD	<LOD	<LOD	<LOD	<LOD	1.0	0.7	0.6	0.7	0.6	0.9
	F1	1.9	1.9	1.9	1.6	1.9	2.2	1.8	1.6	2.2	1.9	2.0	<LOD	2.0	2.6	2.0	2.1	2.3
Ce	F2	<LOD	<LOD	6.7	2.6	6.7	4.2	2.7	9.9	4.7	2.6	3.9	1.7	<LOD	4.9	2.4	1.7	4.2
	F3	28.1	14.8	47.1	23.5	35.5	27.3	20.1	21.3	35.0	29.6	28.3	25.6	<LOD	5.9	7.3	4.0	8.2
	F1	22.5	27.6	23.1	15.3	15.0	19.8	18.8	4.6	23.3	19.6	17.9	23.4	31.0	5.9	9.5	10.5	14.9
Sr	F2	9.1	6.2	12.1	6.3	6.4	9.7	7.9	5.0	12.8	10.1	6.3	9.9	2.5	<LOD	1.8	3.0	4.3
	F3	3.3	1.6	4.3	1.8	2.5	2.6	1.9	1.7	3.5	2.4	1.9	2.8	2.3	1.5	1.6	1.6	1.7
	F1	38.4	31.1	36.5	25.3	29.6	32.3	27.9	4.2	35.4	35.1	30.3	33.3	2.8	19.7	27.1	22.6	32.9
Ba	F2	150.2	59.8	192.1	106.6	79.4	80.3	76.9	42.1	113.9	148.8	89.7	109.6	13.6	12.5	29.3	23.3	35.7
	F3	32.2	8.9	36.6	15.9	22.9	17.8	16.4	11.0	25.9	29.5	15.7	21.2	<LOD	5.9	5.1	4.9	7.5
Hg	F1	<LOD	<LOD	<LOD	<LOD	<LOD	<LOD	<LOD	<LOD	<LOD	<LOD	<LOD	<LOD	<LOD	<LOD	<LOD	<LOD	<LOD

Sample Id/F1- F3		SS1	SS2	SS3	SS4	SS5	SS6	SS7	SS8	SS9	SS10	SS11	SS12	SSS	SS13	SS14	SS15	SS16
	F2	<LOD	<LOD	<LOD	<LOD	<LOD	<LOD	<LOD	<LOD	<LOD	<LOD	<LOD	<LOD	<LOD	<LOD	<LOD	<LOD	<LOD
	F3	0.0	0.0	0.0	0.0	0.0	0.0	0.0	0.0	0.0	0.0	0.0	0.0	0.0	0.0	0.0	0.0	0.0
	F1	196.8	129.2	148.8	130.1	79.8	276.1	184.9	17.1	305.7	167.5	143.9	187.9	368.9	11.3	54.8	55.0	47.8
Mn	F2	1090.9	440.1	921.7	864.5	569.8	727.8	732.9	288.7	951.2	1348.1	720.9	751.3	557.6	8.5	190.0	45.3	76.3
	F3	105.6	41.0	126.9	94.7	131.5	83.0	114.0	32.1	144.8	105.9	71.2	84.3	757.7	3.0	30.2	12.5	9.4
	F1	24.5	45.7	45.4	19.0	37.9	46.1	39.0	19.8	23.9	28.6	27.9	23.3	165.4	86.4	40.1	16.3	23.4
Al	F2	414.3	476.5	601.7	318.3	443.1	227.8	271.5	294.9	251.4	302.0	489.0	371.9	24.8	251.1	236.5	144.3	197.0
	F3	1008.2	794.2	1901.4	591.1	1294.4	450.7	682.1	589.9	635.4	667.2	1196.5	722.2	242.8	367.9	582.2	167.5	325.9

Appendix 5.13 (Continued)

Sample Id/F1- F3		SS17	SS18	CSS	RS	TS1	TS2	TS3	TS4	TS05	TS06	TS07	TS08	TS09	TS10	TS11	TS12	TS13
	F1	<LOD	<LOD	<LOD	1.0	<LOD	<LOD	1.2	<LOD	<LOD	<LOD	1.5	<LOD	<LOD	<LOD	1.1	1.0	1.1
As	F2	<LOD	<LOD	<LOD	5.2	<LOD	<LOD	<LOD	<LOD	<LOD	<LOD	<LOD	<LOD	<LOD	<LOD	<LOD	<LOD	<LOD
	F3	<LOD	<LOD	<LOD	<LOD	<LOD	<LOD	<LOD	<LOD	<LOD	<LOD	<LOD	<LOD	<LOD	<LOD	<LOD	<LOD	<LOD
	F1	19.3	11.9	2.2	162.9	145.9	1.9	10324.8	7195.7	6120.8	1626.1	129.1	1524.8	3830.1	3924.3	3488.8	688.1	3132.0
Zn	F2	12.1	4.9	1.5	640.7	28.2	19.2	9157.8	6446.6	3966.2	1225.6	205.4	2068.1	2929.3	4418.9	3639.3	562.2	2522.0
	F3	14.4	86.6	2.4	1025.8	19.0	20.3	11953.5	7050.3	8539.0	3752.1	100.3	753.8	3144.1	3019.3	1513.6	159.0	1075.7
	F1	2.8	2.5	0.6	24686.0	0.3	<LOD	4355.4	247.2	283.8	812.3	3.7	18.2	116.9	47.8	94.6	3.4	371.6
Pb	F2	16.9	11.5	5.5	4700.6	0.9	16.3	963.6	2173.0	1132.4	189.1	49.7	61.4	226.6	179.1	340.7	79.6	1090.0
	F3	11.4	16.4	3.2	26485.4	2.0	5.1	1628.8	631.0	174.2	1064.9	26.8	53.3	339.0	415.6	271.9	31.3	228.1
	F1	<LOD	<LOD	<LOD	<LOD	<LOD	<LOD	30.7	37.1	21.4	4.1	<LOD	3.6	9.9	11.7	12.6	3.5	20.5
Cd	F2	<LOD	<LOD	<LOD	9.8	<LOD	<LOD	14.4	8.1	5.7	2.1	<LOD	1.0	5.0	8.2	5.1	2.2	7.3
	F3	<LOD	<LOD	<LOD	1.2	<LOD	<LOD	14.1	4.8	14.5	5.9	<LOD	<LOD	4.8	4.2	1.7	<LOD	2.5
	F1	<LOD	1.8	<LOD	<LOD	5.9	<LOD	7.2	15.4	7.2	2.8	<LOD	4.0	5.0	4.7	4.6	3.3	5.9
Ni	F2	<LOD	<LOD	<LOD	7.1	<LOD	17.1	3.8	7.1	2.8	2.3	4.0	<LOD	3.1	4.5	3.2	5.1	3.2
	F3	<LOD	<LOD	<LOD	1.6	<LOD	33.8	20.4	9.2	9.8	10.1	12.4	4.5	6.7	6.5	5.2	7.2	5.3
Fe	F1	9.0	8.5	84.3	8.8	498.4	0.4	1082.3	1396.1	637.4	15.5	3.3	122.1	342.5	267.7	211.7	3.8	39.3

Sample Id/F1- F3		SS17	SS18	CSS	RS	TS1	TS2	TS3	TS4	TS05	TS06	TS07	TS08	TS09	TS10	TS11	TS12	TS13
	F2	445.5	482.0	2193.0	725.3	494.6	144.0	4444.2	3340.6	4125.0	5382.3	650.9	4462.7	4627.7	3915.3	4352.6	299.8	3161.7
	F3	36.9	598.8	1640.8	1810.5	1304.9	640.2	17161.1	4127.5	941.0	13926.5	2713.8	14180.7	9022.6	9138.4	5938.9	1635.3	3389.8
	F1	1.9	1.9	<LOD	2.4	<LOD	<LOD	<LOD	<LOD	3.2	2.5	1.9	2.5	2.7	2.5	2.5	1.9	2.6
Cr	F2	<LOD	<LOD	<LOD	17.5	<LOD	<LOD	1.1	<LOD	<LOD	<LOD	<LOD	<LOD	<LOD	<LOD	<LOD	<LOD	<LOD
	F3	<LOD	2.4	6.0	2.1	<LOD	<LOD	3.3	2.0	<LOD	2.0	3.6	2.1	2.2	2.3	2.6	2.7	2.9
	F1	2.0	2.0	2.0	16.6	2.4	0.6	33.6	16.9	17.6	4.6	2.7	6.7	12.5	11.4	18.9	3.2	35.1
Cu	F2	1.1	<LOD	1.4	8.7	1.5	1.3	2.6	6.8	16.7	<LOD	2.0	3.9	4.0	4.7	11.4	2.8	25.2
	F3	2.2	3.5	1.5	103.7	0.9	1.0	57.9	21.4	72.9	18.8	3.9	5.3	19.3	12.2	13.0	4.1	11.4
	F1	<LOD	<LOD	3.6	<LOD	3.6	3.5	3.6	3.6	<LOD	<LOD	<LOD	<LOD	<LOD	<LOD	<LOD	<LOD	<LOD
Ti	F2	<LOD	<LOD	<LOD	<LOD	<LOD	<LOD	<LOD	<LOD	<LOD	<LOD	<LOD	<LOD	<LOD	<LOD	<LOD	<LOD	<LOD
	F3	2.1	8.7	6.0	<LOD	<LOD	5.1	<LOD	4.7	<LOD	<LOD	5.6	<LOD	<LOD	<LOD	1.6	3.7	1.7
	F1	1.4	1.3	0.7	2.1	0.7	0.7	0.7	0.7	2.5	1.5	1.4	1.5	1.3	1.5	1.4	1.3	1.4
Zr	F2	0.3	0.3	<LOD	0.3	<LOD	0.8	<LOD	<LOD	0.9	0.3	0.2	0.4	0.3	1.1	0.4	0.2	0.4
	F3	0.6	0.6	<LOD	0.7	0.2	<LOD	<LOD	<LOD	1.0	1.0	0.8	1.1	0.8	1.6	0.9	0.8	0.7
	F1	2.1	2.2	2.0	2.0	<LOD	<LOD	<LOD	2.4	2.9	2.4	2.1	2.1	2.2	2.1	2.2	1.9	2.2
Ce	F2	2.5	3.5	13.8	<LOD	<LOD	<LOD	<LOD	<LOD	<LOD	2.0	2.1	<LOD	1.7	<LOD	<LOD	<LOD	<LOD
	F3	3.9	9.3	13.6	<LOD	<LOD	13.8	8.2	6.4	<LOD	<LOD	14.1	<LOD	2.1	1.9	1.8	3.8	2.8
	F1	9.1	9.0	7.2	4.0	21.7	9.5	11.0	52.8	20.0	9.0	13.5	14.5	18.7	13.4	11.2	12.7	25.0
Sr	F2	1.9	1.9	1.7	4.2	1.6	30.5	8.7	46.4	7.0	6.4	12.6	7.8	8.1	7.9	6.6	9.0	12.0
	F3	1.6	2.6	<LOD	2.3	1.2	8.3	12.1	19.5	3.6	2.5	3.8	4.1	4.5	4.9	3.4	3.4	3.5
	F1	23.9	22.5	32.4	1.3	20.7	11.0	9.0	<LOD	27.2	222.0	18.0	4.7	36.6	20.1	5.2	8.9	1.7
Ba	F2	37.9	23.6	18.2	<LOD	5.1	260.9	59.8	21.6	37.5	277.0	165.8	17.6	73.0	59.7	33.3	87.2	34.9
	F3	5.9	4.4	7.3	5.5	4.5	86.6	12.0	117.5	10.3	2.3	31.7	5.1	13.5	12.3	13.5	19.6	15.4
	F1	<LOD	<LOD	<LOD	1.7	<LOD	<LOD	<LOD	<LOD	<LOD	<LOD	<LOD	<LOD	<LOD	<LOD	<LOD	<LOD	<LOD
Hg	F2	<LOD	<LOD	<LOD	<LOD	<LOD	<LOD	<LOD	<LOD	<LOD	<LOD	<LOD	<LOD	<LOD	<LOD	<LOD	<LOD	<LOD
	F3	0.0	0.0	0.0	0.0	0.0	0.0	0.0	0.0	0.0	0.0	0.0	0.0	0.0	0.0	0.0	0.0	0.0
Mn	F1	90.3	69.9	89.3	1644.0	572.8	11.2	1540.6	914.2	1272.0	1392.3	41.5	1412.1	1200.5	943.4	866.9	54.7	504.8
	F2	281.8	153.4	121.4	9628.2	44.7	1341.6	2508.0	346.0	1485.1	4088.8	891.3	1435.9	2466.8	3011.6	1883.1	713.4	1297.4

Sample Id/F1- F3		SS17	SS18	CSS	RS	TS1	TS2	TS3	TS4	TS05	TS06	TS07	TS08	TS09	TS10	TS11	TS12	TS13
	F3	21.4	25.9	11.0	3234.1	29.5	733.4	5714.0	908.6	1613.0	3976.8	326.4	2763.3	2315.7	1984.9	1003.7	175.0	566.7
	F1	26.0	25.6	33.4	16.3	14.2	3.3	50.3	158.3	58.4	10.5	8.9	22.7	72.3	51.8	44.0	25.7	85.2
Al	F2	159.5	163.8	235.0	1.5	36.8	83.1	32.4	226.0	137.5	19.8	131.0	106.8	157.1	103.1	111.8	194.1	162.6
	F3	137.3	585.2	587.5	41.1	135.0	1876.4	115.3	843.4	115.0	43.0	1855.4	97.6	292.2	172.8	263.5	2458.5	373.5

Appendix 5.13 (Continued)

Sample Id/F1- F3		TS14	TS15	TS16	TS17	PSD1A	PSD1B	PSD2A	PSD2B	PSD4A	PSD4B	PSD5A	PSD5B	SD3	SD4	SD05	SD06	SD06
	F1	1.0	1.1	<LOD	<LOD	1.2	<LOD	1.1	<LOD	<LOD	<LOD	<LOD	<LOD	<LOD	<LOD	1.1	<LOD	<LOD
As	F2	<LOD	<LOD	<LOD	<LOD	<LOD	<LOD	1.1	1.1	1.1	<LOD	1.3	<LOD	<LOD	<LOD	<LOD	<LOD	<LOD
	F3	<LOD	<LOD	<LOD	<LOD	<LOD	<LOD	<LOD	<LOD	<LOD	<LOD	<LOD	<LOD	<LOD	<LOD	1.1	<LOD	<LOD
	F1	3401.1	4007.0	4808.2	3533.5	87.0	413.4	123.7	45.3	8.6	469.5	138.0	771.4	22.7	<LOD	37.7	2.0	2.0
Zn	F2	3856.2	1150.9	5193.9	2205.4	61.6	211.1	436.4	156.5	46.5	586.4	224.7	849.3	164.7	6.4	49.5	2.3	2.3
	F3	1987.2	16409.3	3393.2	1050.7	110.0	1599.1	250.6	66.6	188.6	649.4	267.4	3844.6	181.3	3.2	40.5	5.4	5.4
	F1	1505.0	81.3	377.4	227.8	69.1	36.6	4.2	3.0	0.8	158.1	3.8	2574.0	0.2	0.6	12.3	2.6	2.6
Pb	F2	146.3	199.7	458.7	690.1	30.6	116.2	105.4	56.9	33.9	599.7	144.1	1946.1	94.9	11.8	86.1	12.3	12.3
	F3	504.9	125.2	392.2	246.4	361.9	294.7	58.8	23.3	27.9	183.8	57.9	2741.3	42.5	4.0	53.5	6.8	6.8
	F1	12.9	11.2	18.9	22.2	<LOD	<LOD	<LOD	<LOD	<LOD	4.0	<LOD	<LOD	<LOD	<LOD	<LOD	<LOD	<LOD
Cd	F2	4.2	<LOD	6.9	7.5	<LOD	<LOD	<LOD	<LOD	<LOD	4.5	<LOD	<LOD	<LOD	<LOD	<LOD	<LOD	<LOD
	F3	1.7	27.3	4.7	3.4	<LOD	1.7	<LOD	<LOD	<LOD	<LOD	<LOD	5.0	<LOD	<LOD	<LOD	<LOD	<LOD
	F1	4.9	2.7	6.9	6.4	4.3	4.5	<LOD	<LOD	<LOD	<LOD	<LOD	4.7	<LOD	<LOD	2.9	<LOD	<LOD
Ni	F2	1.8	<LOD	3.9	2.8	1.9	2.9	3.7	2.9	4.0	2.7	7.6	7.0	12.3	0.8	1.7	<LOD	<LOD
	F3	5.9	10.7	7.2	5.5	7.6	6.6	9.4	14.0	4.9	2.0	3.4	5.1	23.3	<LOD	2.1	<LOD	<LOD
	F1	301.8	108.5	581.6	17.5	617.9	1582.0	3.1	5.4	9.5	53.5	14.6	40.1	1.5	13.9	39.5	12.6	12.6
Fe	F2	3367.5	2452.0	4513.8	2620.6	2440.5	2508.5	592.4	485.4	584.0	5219.9	2390.5	2852.7	1273.3	234.7	2140.9	812.6	812.6
	F3	6343.9	4363.0	817.5	3553.6	8818.4	5823.2	2587.9	4188.7	5664.0	3030.0	3205.5	6931.1	5835.5	635.9	1238.3	45.0	45.0
Cr	F1	2.8	2.3	2.9	2.6	<LOD	<LOD	<LOD	<LOD	<LOD	<LOD	<LOD	2.1	<LOD	<LOD	1.9	1.9	1.9
	F2	<LOD	<LOD	<LOD	<LOD	<LOD	<LOD	<LOD	<LOD	<LOD	<LOD	<LOD	3.7	<LOD	<LOD	<LOD	<LOD	<LOD

Sample Id/F1- F3		TS14	TS15	TS16	TS17	PSD1A	PSD1B	PSD2A	PSD2B	PSD4A	PSD4B	PSD5A	PSD5B	SD3	SD4	SD05	SD06	SD06
	F3	3.0	2.7	<LOD	3.5	<LOD	2.3	19.4	20.7	16.5	4.5	5.1	28.5	8.7	3.2	4.4	1.9	1.9
	F1	25.3	3.5	21.0	29.5	2.2	0.7	2.5	3.1	<LOD	12.6	4.3	50.2	0.7	<LOD	2.8	2.3	2.3
Cu	F2	6.6	1.6	8.2	21.2	<LOD	4.8	7.7	3.5	5.8	22.3	13.7	71.2	4.9	0.5	1.4	0.9	0.9
	F3	15.5	25.8	16.2	11.8	11.4	10.6	9.7	4.7	6.1	28.3	9.4	54.7	5.6	0.8	3.7	2.1	2.1
	F1	<LOD	<LOD	<LOD	<LOD	3.5	3.6	3.6	<LOD	3.1	3.1	3.0	3.0	<LOD	<LOD	<LOD	<LOD	<LOD
Ti	F2	<LOD	<LOD	<LOD	<LOD	<LOD	<LOD	<LOD	<LOD	<LOD	<LOD	<LOD	<LOD	<LOD	<LOD	<LOD	<LOD	<LOD
	F3	2.2	<LOD	<LOD	2.2	1.6	2.0	1.9	9.7	10.9	6.2	6.7	14.5	13.0	8.8	9.7	1.7	1.7
	F1	1.4	1.6	1.6	1.3	0.8	0.6	0.7	<LOD	<LOD	<LOD	<LOD	<LOD	<LOD	<LOD	1.3	1.3	1.3
Zr	F2	0.4	0.9	0.7	0.4	<LOD	<LOD	<LOD	0.8	<LOD	<LOD	0.7	<LOD	<LOD	<LOD	0.3	0.2	0.2
	F3	0.8	1.2	0.7	0.8	<LOD	<LOD	<LOD	<LOD	<LOD	<LOD	<LOD	<LOD	<LOD	<LOD	0.7	0.5	0.5
	F1	2.0	3.4	2.2	2.1	4.2	1.2	<LOD	<LOD	<LOD	<LOD	<LOD	26.5	<LOD	<LOD	2.4	2.3	2.3
Ce	F2	1.9	<LOD	<LOD	<LOD	1.9	<LOD	4.3	7.0	3.7	14.9	14.9	81.4	9.6	11.8	11.0	8.7	8.7
	F3	1.7	<LOD	1.7	3.3	7.2	5.7	37.0	40.9	21.1	35.2	38.0	59.3	66.0	7.7	31.5	15.5	15.5
	F1	11.0	6.2	13.3	19.0	315.4	102.4	7.1	2.9	6.5	18.3	17.1	21.7	7.3	2.7	12.9	12.0	12.0
Sr	F2	7.9	1.8	8.6	10.0	49.8	34.8	23.4	11.3	22.6	17.8	18.5	7.3	29.6	1.6	8.4	6.5	6.5
	F3	3.9	1.9	4.1	3.6	21.1	10.5	7.0	1.9	5.0	2.3	2.5	2.1	4.2	<LOD	2.2	2.0	2.0
	F1	4.8	3.6	6.7	4.0	34.8	41.2	8.3	8.4	16.8	68.8	109.6	227.7	10.2	11.7	58.5	35.2	35.2
Ba	F2	52.3	32.0	46.5	40.3	82.2	39.8	182.1	169.7	270.0	118.7	239.5	352.4	218.7	20.4	92.0	42.4	42.4
	F3	11.8	5.9	14.3	19.2	62.2	7.7	82.7	71.5	64.9	24.0	45.1	36.4	75.0	8.5	14.5	10.1	10.1
	F1	<LOD	<LOD	<LOD	<LOD	<LOD	<LOD	<LOD	<LOD	<LOD	<LOD	<LOD	<LOD	<LOD	<LOD	<LOD	<LOD	<LOD
Hg	F2	<LOD	<LOD	<LOD	<LOD	<LOD	<LOD	<LOD	<LOD	<LOD	<LOD	<LOD	<LOD	<LOD	<LOD	<LOD	<LOD	<LOD
	F3	0.0	0.0	0.0	0.0	0.0	0.0	0.0	0.0	0.0	0.0	0.0	0.0	0.0	0.0	0.0	0.0	0.0
	F1	577.0	1073.4	1070.5	565.0	712.2	556.7	22.1	73.7	27.0	305.5	178.0	2265.2	16.5	16.5	156.5	69.9	69.9
Mn	F2	1006.1	609.1	1955.5	1011.6	218.1	261.0	697.6	843.5	1505.5	478.9	2898.9	3124.7	2336.1	165.9	432.1	233.4	233.4
	F3	1051.7	1592.2	610.4	543.1	521.3	733.3	265.9	849.1	381.4	93.8	331.3	638.9	1439.3	30.4	52.7	21.1	21.1
	F1	160.4	55.2	91.4	74.1	29.7	16.3	3.4	66.4	8.3	20.1	23.4	150.0	12.0	15.2	14.9	12.9	12.9
Al	F2	128.6	53.5	109.3	184.2	58.4	122.1	137.2	122.6	218.5	537.6	454.4	437.3	220.1	109.0	286.3	248.8	248.8
	F3	267.6	109.9	213.8	820.8	326.3	551.0	1645.0	1701.4	2285.7	2031.2	1866.1	908.5	3017.6	454.4	1239.8	590.5	590.5

Appendix 5.14: Minimum, mean, and maximum percentage partitioning (%) of trace elements across sequential extraction fractions in soils, sediments, and tailings from Gimbi abandoned lead-zinc mine.

Gimbi	**Mn**	**Zn**	**Pb**	**Ni**	**Cr**	**Cu**	**Ti**	**Zr**	**Ce**	**Sr**	**Ba**	**Cd**	**Al**	**Fe**	**Hg**	**As**
F1 (Exchangeable/carbonate fraction) Percentage (%) Partition (n=49)																
Mean	24.5	36.3	67.8	22.9	9.5	17.0	37.3	30.4	11.9	63.7	33.7	117.6	1.2	1.0	0.0	0.0
Min	0.4	1.7	0.0	0.0	0.0	1.5	0.0	0.0	0.0	15.7	0.2	0.0	0.0	0.0	0.0	0.0
Max	105.1	129.3	2338.5	58.3	65.5	105.0	271.6	117.4	60.3	130.9	193.1	1252.1	8.8	10.2	0.0	0.0
F2 (Reducible fraction) Percentage (%) Partition (n=49)																
Mean	82.3	41.0	94.0	32.0	3.2	13.6	0.2	8.1	16.3	33.6	102.1	56.8	3.8	10.1	0.0	0.0
Min	4.2	5.1	4.4	0.0	0.0	0.3	0.0	6.6	0.0	4.5	9.0	0.0	0.6	0.9	0.0	0.0
Max	612.6	142.4	1768.0	314.7	23.6	149.1	2.8	83.4	143.2	113.6	792.2	1985.6	16.9	27.6	0.0	0.0
F3 (Oxidisable fraction) Percentage (%) Partition (n=49)																
Mean	29.6	56.6	108.5	36.8	28.0	29.1	68.9	8.7	55.4	12.4	25.9	265.9	14.1	21.0	0.0	0.0
Min	2.8	3.4	9.4	0.0	3.4	3.3	0.0	0.0	7.6	2.0	2.0	0.9	2.3	0.4	0.0	0.0
Max	167.8	644.6	2490.5	180.6	326.6	114.6	429.3	32.2	254.6	41.9	190.5	12357.4	176.5	108.2	0.0	0.0

Appendix 5.15: ICP-OES - Total metal concentration results (mg/kg) of Soil (SS), Control Soil (CSS), Rock (RS), Tailings (TS), and Sediment (SD) samples at Gimbi-Rikaya Abandoned Lead-zinc mine

Sample Id/Analyte	SS1	SS2	SS3	SS4	SS5	SS6	SS7	SS8	SS9	SS10	SS11	CSS1	CSS2	TS1	TS2
As	<LOD	<LOD	<LOD	<LOD	<LOD	<LOD	<LOD	<LOD	<LOD	<LOD	<LOD	<LOD	<LOD	<LOD	<LOD
Zn	21.3	23.2	198.2	50.9	13.4	60.2	44.6	30.4	28.5	37.3	29.5	17.4	190.4	421.7	452.5
Pb	5.7	4.7	5.9	36.1	4.3	40.2	118.8	37.3	34.3	66.1	13.8	15.2	24.1	10.9	546.8
Cd	<LOD	<LOD	<LOD	<LOD	<LOD	<LOD	<LOD	<LOD	<LOD	<LOD	<LOD	<LOD	<LOD	<LOD	<LOD

Sample Id/Analyte	SS1	SS2	SS3	SS4	SS5	SS6	SS7	SS8	SS9	SS10	SS11	CSS1	CSS2	TS1	TS2
Ni	2.9	2.0	3.7	11.7	2.4	11.3	4.4	10.3	12.2	19.5	4.9	4.8	4.9	15.6	11.8
Cr	9.9	8.7	11.3	22.3	5.9	7.8	31.4	37.1	38.0	66.5	21.9	21.6	9.9	3.5	22.8
Cu	3.5	3.7	16.7	15.4	3.7	10.4	12.3	7.7	10.2	18.2	10.4	8.7	14.7	13.8	109.7
Ti	38.9	30.5	14.9	15.4	11.0	19.7	53.6	46.9	45.1	45.2	49.7	74.8	28.3	4.0	17.0
Zr	2.0	2.6	2.0	2.4	1.5	1.4	3.9	5.5	4.6	6.8	3.7	4.0	0.9	1.1	4.2
Ce	28.2	27.6	30.5	41.4	28.7	23.9	42.1	64.8	70.7	119.2	44.1	27.2	35.5	9.4	65.0
Sr	9.2	8.4	10.7	31.0	6.7	14.9	11.4	9.2	21.0	19.7	13.8	26.4	55.4	20.5	18.5
Ba	25.5	34.5	45.5	91.8	34.7	118.2	84.7	151.3	205.4	202.1	64.2	88.9	59.0	20.5	116.6
Hg	<LOD	<LOD	<LOD	<LOD	<LOD	<LOD	<LOD	<LOD	<LOD	<LOD	<LOD	<LOD	<LOD	<LOD	<LOD
Mn	368.5	301.8	294.9	1291.4	154.6	1699.0	816.3	1338.6	1461.8	1898.7	319.8	640.0	763.5	809.4	1206.8
Al	2065.3	2608.5	4943.3	8971.5	2525.5	4268.2	4163.8	5019.0	6299.9	7421.4	5993.5	6483.7	4097.8	6921.9	9842.4
Fe	6799.0	3997.6	8994.1	16380.6	4438.9	12343.2	10598.1	15409.8	14929.9	17846.1	9375.3	10082.7	12421.5	11363.1	16392.0
Fe	11608.8	6416.0	16401.8	31646.8	6705.8	23455.5	21228.1	26206.5	25957.8	33994.7	14603.8	15583.9	21848.5	14798.4	25680.7
Mg	1469.6	1058.3	1635.8	4012.0	633.3	1925.7	1115.5	1213.8	2162.5	1684.4	1519.3	2817.6	2458.2	7105.4	2084.7
Ca	3770.2	3547.8	3465.2	12922.9	1988.1	5908.4	5761.9	4197.3	9883.3	7609.0	5900.2	15593.5	33426.9	4991.0	4852.9
Na	363.8	473.1	837.7	493.0	511.9	325.5	356.1	1071.3	1488.7	687.8	1929.0	1228.1	817.0	934.9	1475.6
K	2762.0	2017.0	3107.1	3774.5	1490.6	2033.8	1680.8	3745.7	5385.2	3160.1	5239.4	5764.0	4315.2	3597.4	4891.2

Appendix 5.15 (Continued)

Sample Id/Analyte	SD1	SD2	SD3-Pond Pit	SD4-Dry Pond	CSD1	CSD2
As	<LOD	<LOD	<LOD	<LOD	<LOD	<LOD
Zn	271.2	1438.8	4270.0	85.5	12.3	7.6
Pb	7.8	26.0	588.1	105.2	24.7	9.0
Cd	<LOD	5.4	8.4	<LOD	<LOD	<LOD

Ni	16.8	19.8	7.8	11.3	10.3	5.8
Cr	3.7	<LOD	3.2	27.2	95.4	23.4
Cu	31.7	32.1	70.2	23.7	13.6	6.2
Ti	4.5	3.6	7.7	21.4	44.7	70.1
Zr	0.6	<LOD	0.9	4.3	2.6	7.3
Ce	6.7	7.7	9.9	73.9	47.9	39.6
Sr	25.1	39.9	13.7	15.8	9.0	11.1
Ba	30.9	43.3	48.4	178.4	60.7	80.6
Hg	<LOD	<LOD	<LOD	<LOD	<LOD	<LOD
Mn	1437.6	2574.9	1147.1	959.2	621.3	252.3
Al	5630.1	3740.7	3057.5	8258.9	6969.2	12200.7
Fe	13516.4	17251.7	13853.6	17257.8	18984.9	7956.3
Fe	23907.0	36711.4	26146.9	32822.9	39787.8	11064.1
Mg	6336.2	5559.9	1965.6	1998.5	795.0	2626.7
Ca	7066.8	9090.0	6058.3	6692.0	3202.8	3449.3
Na	1293.2	1612.7	864.1	1254.6	1763.8	1643.8
K	5688.3	5893.3	2644.9	4913.9	4874.6	7380.8

Appendix 5.16: Sequential analysis results F1-F3 (mg/kg) of Soil (SS), Control Soil (CSS), Rock (RS), Tailings (TS), and Sediment (SD) samples at Gimbi-Rikaya Abandoned Lead-zinc mine

Sample ID/F1- F3		SS1	SS2	SS3	SS4	SS5	SS6	SS7	SS8	SS9	SS10	SS11	CSS2	CSS3	TS1	TS2	SD1
As	F1	1.6	1.1	1.7	1.2	1.2	<LOD	1.1	<LOD	1.0	<LOD	1.1	1.4	<LOD	0.9	1.2	<LOD
	F2	<LOD	<LOD	<LOD	<LOD	<LOD	<LOD	<LOD	<LOD	<LOD	<LOD	<LOD	<LOD	<LOD	<LOD	1.1	<LOD
	F3	<LOD	<LOD	<LOD	<LOD	<LOD	<LOD	<LOD	<LOD	<LOD	<LOD	<LOD	<LOD	<LOD	<LOD	<LOD	<LOD
Zn	F1	7.1	5.6	61.5	6.9	7.4	13.1	15.1	1.6	2.6	3.3	5.8	2.1	22.2	22.7	35.3	45.4
	F2	<LOD	5.3	40.0	11.2	3.4	16.6	17.7	14.8	6.3	5.0	7.2	3.6	28.6	22.1	115.1	42.1

Sample ID/F1- F3		SS1	SS2	SS3	SS4	SS5	SS6	SS7	SS8	SS9	SS10	SS11	CSS2	CSS3	TS1	TS2	SD1
	F3	6.2	6.0	33.3	8.7	6.2	15.5	10.4	5.0	5.4	5.3	5.7	3.2	19.9	73.2	46.9	66.8
	F1	<LOD	<LOD	<LOD	<LOD	0.1	0.1	2.0	<LOD	<LOD	<LOD	<LOD	0.3	<LOD	<LOD	37.9	1.8
Pb	F2	6.9	1.8	2.0	3.2	3.3	17.5	162.8	30.2	23.8	28.6	6.3	7.0	4.0	2.5	734.8	13.0
	F3	5.4	1.6	3.0	15.9	4.9	29.9	83.2	16.9	37.8	25.4	8.3	13.1	10.3	2.2	140.8	4.2
	F1	<LOD	<LOD	<LOD	<LOD	<LOD	<LOD	<LOD	<LOD	<LOD	<LOD	<LOD	<LOD	<LOD	<LOD	<LOD	-1.4
Cd	F2	<LOD	<LOD	<LOD	<LOD	<LOD	<LOD	<LOD	<LOD	<LOD	<LOD	<LOD	<LOD	<LOD	<LOD	<LOD	<LOD
	F3	<LOD	<LOD	<LOD	<LOD	<LOD	<LOD	<LOD	<LOD	<LOD	<LOD	<LOD	<LOD	<LOD	<LOD	<LOD	<LOD
	F1	<LOD	<LOD	<LOD	<LOD	2.2	<LOD	<LOD	<LOD	<LOD	<LOD	1.5	<LOD	<LOD	<LOD	<LOD	<LOD
Ni	F2	<LOD	<LOD	<LOD	1.7	<LOD	2.2	<LOD	<LOD	1.7	4.4	<LOD	<LOD	<LOD	<LOD	2.7	3.7
	F3	3.3	<LOD	<LOD	3.3	<LOD	4.3	2.2	3.2	3.9	5.7	1.5	1.8	<LOD	2.2	3.5	3.0
	F1	5.6	6.6	15.3	7.8	68.7	6.2	4.1	11.8	9.1	3.3	25.5	8.6	21.0	6.3	<LOD	14.5
Fe	F2	454.4	446.8	615.5	522.0	1453.3	539.8	481.6	383.8	430.5	517.4	867.3	416.0	225.5	100.2	573.7	2752.6
	F3	504.2	642.9	1164.1	1901.6	2167.4	1047.5	1881.3	1315.7	1788.6	984.2	1136.0	784.4	1012.7	1800.7	2209.0	1576.3
	F1	<LOD	<LOD	<LOD	<LOD	<LOD	<LOD	<LOD	<LOD	<LOD	<LOD	<LOD	<LOD	<LOD	<LOD	<LOD	<LOD
Cr	F2	<LOD	<LOD	<LOD	<LOD	<LOD	<LOD	<LOD	<LOD	<LOD	<LOD	<LOD	<LOD	<LOD	<LOD	<LOD	<LOD
	F3	2.4	1.9	2.6	4.0	3.0	2.9	6.2	5.9	7.9	10.1	4.0	3.0	<LOD	<LOD	2.3	<LOD
	F1	0.5	0.5	1.6	1.7	1.9	1.1	1.4	0.9	1.2	1.5	1.1	1.2	2.2	1.0	5.2	11.0
Cu	F2	<LOD	<LOD	1.9	<LOD	0.5	<LOD	0.7	<LOD	<LOD	<LOD	1.5	<LOD	<LOD	0.5	17.0	16.0
	F3	1.2	1.1	4.4	2.6	1.7	2.1	3.1	1.9	3.9	1.5	2.8	2.7	2.8	2.6	11.7	4.9
	F1	3.6	3.6	3.6	3.6	3.6	3.6	3.6	3.7	3.6	3.6	3.6	3.6	3.6	3.6	3.6	3.0
Ti	F2	<LOD	<LOD	<LOD	<LOD	<LOD	<LOD	<LOD	<LOD	<LOD	<LOD	<LOD	<LOD	<LOD	<LOD	<LOD	<LOD
	F3	8.7	9.0	7.9	17.2	11.7	14.8	12.7	19.5	25.4	29.2	8.7	13.3	9.5	0.5	16.2	<LOD
	F1	0.8	0.7	0.7	0.7	0.7	1.2	0.8	0.7	0.7	0.7	0.7	0.7	0.7	0.7	0.7	<LOD
Zr	F2	<LOD	<LOD	<LOD	<LOD	<LOD	0.7	<LOD	<LOD	<LOD	<LOD	0.7	<LOD	<LOD	1.1	0.2	<LOD
	F3	<LOD	<LOD	<LOD	<LOD	<LOD	1.1	<LOD	<LOD	<LOD	<LOD	<LOD	<LOD	<LOD	<LOD	<LOD	<LOD

Sample ID/F1- F3		SS1	SS2	SS3	SS4	SS5	SS6	SS7	SS8	SS9	SS10	SS11	CSS2	CSS3	TS1	TS2	SD1
Ce	F1	<LOD	<LOD	<LOD	<LOD	<LOD	<LOD	<LOD	<LOD	<LOD	<LOD	<LOD	<LOD	<LOD	<LOD	<LOD	<LOD
	F2	2.2	2.2	3.3	<LOD	4.6	<LOD	3.6	6.5	3.1	6.1	7.8	<LOD	<LOD	<LOD	16.7	<LOD
	F3	8.9	7.4	7.7	14.3	8.7	15.7	18.8	23.0	46.7	32.4	18.9	13.6	8.4	<LOD	46.1	<LOD
Sr	F1	9.9	8.2	8.2	21.7	8.0	14.4	12.5	8.5	17.5	14.9	11.6	17.7	46.0	8.5	9.2	11.0
	F2	3.7	2.5	2.8	14.3	1.7	7.7	4.7	2.5	7.7	5.8	3.4	7.7	9.5	4.7	6.8	9.6
	F3	1.3	1.1	1.2	3.7	1.3	3.0	1.4	1.3	2.2	2.0	1.3	1.8	1.9	1.6	1.5	1.2
Ba	F1	12.2	12.5	16.8	14.5	20.9	13.1	26.6	33.4	37.8	24.8	25.0	20.2	16.4	<LOD	22.0	14.0
	F2	55.2	23.0	26.9	67.3	25.8	131.3	150.4	139.9	277.6	210.9	27.4	61.8	28.8	4.4	180.8	26.9
	F3	9.8	6.5	5.7	17.7	7.4	18.1	15.0	16.2	39.0	23.1	9.9	13.5	5.6	<LOD	25.0	8.4
Hg	F1	<LOD	<LOD	<LOD	<LOD	<LOD	<LOD	<LOD	<LOD	<LOD	<LOD	<LOD	<LOD	<LOD	<LOD	<LOD	<LOD
	F2	<LOD	<LOD	<LOD	<LOD	<LOD	<LOD	<LOD	<LOD	<LOD	<LOD	<LOD	<LOD	<LOD	<LOD	<LOD	<LOD
	F3	<LOD	<LOD	<LOD	<LOD	<LOD	<LOD	<LOD	<LOD	<LOD	<LOD	<LOD	<LOD	<LOD	<LOD	<LOD	<LOD
Mn	F1	148.8	74.0	30.6	230.2	88.8	251.8	160.0	127.3	207.1	111.1	122.5	207.4	205.2	52.9	24.5	466.3
	F2	958.0	256.9	239.1	753.1	107.0	1811.6	1403.6	1210.4	1673.1	1441.7	160.3	405.4	353.3	198.1	1689.2	1468.3
	F3	181.4	27.1	31.0	111.4	22.4	303.9	112.7	99.7	219.0	185.1	23.8	56.3	36.8	46.7	309.5	153.4
Al	F1	24.0	14.2	26.3	37.6	66.8	32.0	17.0	47.4	20.0	25.6	28.5	16.4	29.8	25.4	27.7	20.8
	F2	210.8	160.8	218.0	608.7	310.9	570.9	320.5	402.0	434.4	479.0	261.5	167.9	200.0	86.7	268.4	266.5
	F3	313.0	290.3	316.2	1111.8	312.5	667.7	489.3	665.9	995.4	613.5	411.7	404.0	380.2	595.5	969.1	574.9

Appendix 5.16 (Continued)

Sample ID/F1- F3		SD2	SD3-Pond Pit	SD4-Dry Pond	CSD1	CSD2
As	F1	<LOD	<LOD	<LOD	<LOD	<LOD
	F2	<LOD	<LOD	<LOD	<LOD	<LOD
	F3	<LOD	<LOD	<LOD	<LOD	<LOD

Sample ID/F1- F3		SD2	SD3-Pond Pit	SD4-Dry Pond	CSD1	CSD2
	F1	147.5	8261.6	14.2	<LOD	<LOD
Zn	F2	290.9	4641.3	18.6	3.2	3.1
	F3	355.0	743.5	33.6	25.3	89.5
	F1	<LOD	135.2	10.1	3.4	0.6
Pb	F2	8.9	758.7	85.1	18.0	7.9
	F3	7.5	196.3	44.5	8.9	4.8
	F1	<LOD	18.6	<LOD	<LOD	<LOD
Cd	F2	3.3	9.5	<LOD	<LOD	<LOD
	F3	<LOD	<LOD	<LOD	<LOD	<LOD
	F1	<LOD	2.6	1.7	<LOD	<LOD
Ni	F2	6.1	3.3	2.1	1.9	1.6
	F3	3.4	<LOD	1.6	5.5	<LOD
	F1	12.4	2.9	76.0	30.7	21.4
Fe	F2	2060.7	259.1	4640.3	1532.8	1631.5
	F3	3551.1	1988.9	4531.3	3024.7	2017.5
	F1	<LOD	<LOD	<LOD	<LOD	<LOD
Cr	F2	<LOD	<LOD	<LOD	<LOD	<LOD
	F3	<LOD	<LOD	6.1	26.5	4.6
	F1	3.8	15.3	3.3	1.5	0.9
Cu	F2	10.5	15.4	10.7	1.6	1.0
	F3	11.3	12.4	14.2	2.8	2.9
	F1	<LOD	<LOD	<LOD	<LOD	<LOD
Ti	F2	<LOD	<LOD	<LOD	<LOD	<LOD
	F3	1.9	5.3	6.0	23.2	8.9
	F1	<LOD	<LOD	<LOD	<LOD	<LOD
Zr	F2	<LOD	<LOD	<LOD	<LOD	0.4
	F3	<LOD	<LOD	<LOD	<LOD	<LOD
Ce	F1	<LOD	<LOD	2.1	4.3	<LOD

Sample ID/F1- F3		SD2	SD3-Pond Pit	SD4-Dry Pond	CSD1	CSD2
	F2	<LOD	2.2	32.3	17.6	20.9
	F3	2.4	7.3	36.4	14.6	26.7
	F1	11.8	11.2	9.8	4.8	4.9
Sr	F2	39.4	4.4	3.1	1.8	4.4
	F3	5.9	0.9	0.7	0.9	1.2
	F1	8.8	27.0	165.2	57.5	56.8
Ba	F2	44.1	62.3	71.8	33.3	63.5
	F3	14.2	14.2	14.5	16.4	12.9
	F1	<LOD	<LOD	<LOD	<LOD	<LOD
Hg	F2	<LOD	<LOD	<LOD	<LOD	<LOD
	F3	<LOD	<LOD	<LOD	<LOD	<LOD
	F1	446.1	102.4	477.7	378.6	152.0
Mn	F2	4373.1	1788.6	866.6	278.1	275.6
	F3	543.0	239.3	70.1	76.9	27.0
	F1	44.4	56.6	49.0	121.3	13.9
Al	F2	194.3	100.6	393.4	328.2	283.2
	F3	450.2	966.4	1647.3	601.6	1041.4

Appendix 5.17: Minimum, mean, and maximum percentage partitioning (%) of trace elements across sequential extraction fractions in soils, sediments, and tailings from Gimbi-Rikaya abandoned lead-zinc mine.

Rikaya	**Mn**	**Zn**	**Pb**	**Ni**	**Cr**	**Cu**	**Ti**	**Zr**	**Ce**	**Sr**	**Ba**	**Cd**	**Al**	**Fe**	**Hg**	**As**
F1 (Exchangeable/carbonate fraction) Percentage (%) Partition (n=17)																
Mean	21.8	29.8	4.1	21.1	1.0	15.2	19.6	25.1	2.4	77.6	33.5	0.0	0.8	0.2	0.0	0.0
Min	2.0	5.2	0.0	1.4	0.4	4.7	0.0	0.0	0.0	29.5	5.1	0.0	0.3	0.0	0.0	0.0
Max	57.4	193.5	23.4	92.1	8.1	52.1	88.6	85.2	7.6	119.5	92.6	0.0	2.6	1.5	0.0	0.0
F2 (Reducible fraction) Percentage (%) Partition (n=17)																

Mean	108.6	29.4	74.5	20.2	10.2	15.0	0.3	11.0	13.1	36.9	99.3	0.0	6.4	9.0	0.0	0.0
Min	24.5	5.2	8.9	6.8	0.9	1.7	0.0	0.0	1.5	19.9	21.6	0.0	1.3	0.9	0.0	0.0
Max	260.0	108.7	167.5	48.8	105.3	50.6	1.1	95.4	43.6	98.6	216.2	0.0	13.4	32.7	0.0	0.0
F3 (Oxidisable fraction) Percentage (%) Partition (n=17)																
Mean	15.0	22.7	55.3	34.3	26.6	26.7	51.8	5.3	39.5	11.3	19.1	0.0	13.0	15.5	0.0	0.0
Min	5.8	10.4	20.2	4.1	10.3	8.1	12.1	0.0	4.2	4.4	6.2	0.0	6.4	5.5	0.0	0.0
Max	49.2	46.2	114.7	112.4	70.8	59.8	111.1	77.0	73.7	20.0	38.2	0.0	31.6	48.8	0.0	0.0

Appendix 5.18: Dissolved and Total metal concentration results for water samples collected at Abakaliki Abandoned Lead-zinc mine pond

Sample Id	As	Zn	Pb	Cd	Ni	Cr	Cu	Ti	Zr	Ce	Sr	Ba	Mn	Al	Mg	Ca	Na	K
Dissolved (ug/L) n = 3																		
WS1-F	13.1	115050.3	991.7	666.1	378.5	10.9	172.6	<LOD	19.9	51.6	487.9	440.3	12811.7	9296.8	415922.0	734142.7	55223.3	21300.1
WS2-F	19.9	114487.1	981.6	669.0	383.9	20.6	189.8	<LOD	34.4	60.3	483.5	575.1	14511.5	10039.6	411051.7	672272.0	52787.3	21661.5
WS3-F	20.1	88028.4	1013.8	518.9	264.5	6.6	121.0	<LOD	20.4	50.5	451.1	556.3	10632.2	7377.0	314373.2	625123.6	34660.1	15001.8
Total (ug/L) n = 3																		
WS1-UF	14.6	109019.3	985.1	629.5	346.6	16.2	172.4	<LOD	20.13	50.47	436.3	576.5	15008.1	10355.6	398150.0	612346.7	43510.7	18917.0
WS2-UF	<LOD	121727.6	1065.4	604.8	325.4	15.6	169.4	<LOD	<LOD	17.71	414.6	580.2	10705.2	7299.1	430454.6	667239.3	46330.4	20913.3
WS3-UF	<LOD	89592.2	992.3	442.2	210.2	5.1	111.6	<LOD	<LOD	7.81	375.6	349.1	11648.2	8390.2	320546.1	632503.1	34774.2	15176.8

Appendix 5.19: Dissolved and Total metal concentration results for water samples collected at Gimbi Abandoned Lead-zinc mine pond, river, borehole and Isolated ponds around the mine.

Sample Id	As	Zn	Pb	Cd	Ni	Fe	Cr	Cu	Ti	Zr	Ce	Sr	Ba
Dissolved (ug/L) n = 19													
BHW1-F	7.4	410.5	<LOD	1.7	<LOD	7.4	7.8	26.3	<LOD	28.7	10.2	3000.4	742.4
BHW2-F	15.4	543.6	3.6	<LOD	<LOD	<LOD	4.1	16.7	<LOD	20.0	8.0	2170.3	713.0
BHW3-F	9.3	456.3	7.6	<LOD	<LOD	61.7	3.7	16.6	<LOD	18.6	6.4	2082.2	713.8
BHW4-F	12.4	416.8	1.3	<LOD	<LOD	50.6	3.4	10.1	<LOD	18.2	7.6	1770.5	673.0

RW1-F	11.9	375.1	<LOD	<LOD	<LOD	<LOD	2.6	8.0	<LOD	17.9	12.8	697.0	805.0
RW2-F	16.4	489.0	7.0	3.6	0.5	126.1	8.0	23.1	<LOD	30.7	13.4	182.5	677.2
RW3-F	10.4	844.1	171.9	0.9	2.8	3050.5	7.2	29.2	<LOD	22.3	16.4	264.7	774.9
Control Water Sample1-F	11.7	429.8	4.5	<LOD	1.7	264.2	3.7	24.2	<LOD	19.6	9.2	361.5	912.6
Control Water Sample2-F	9.6	398.9	0.0	<LOD	<LOD	503.8	3.3	12.2	<LOD	18.9	7.7	166.2	584.8
PWS1A-F	14.4	996.0	1.4	<LOD	2.1	<LOD	5.5	8.6	<LOD	32.8	10.6	2217.3	642.4
PWS1B-F	15.3	557.5	0.7	<LOD	0.1	<LOD	4.0	7.1	<LOD	20.2	8.1	2113.6	609.8
PWS2A-F	23.9	26393.1	461.6	69.0	39.9	149.5	3.9	48.3	<LOD	19.1	17.1	887.3	606.0
PWS2B-F	10.8	25729.1	425.6	67.7	39.2	<LOD	3.5	49.6	<LOD	18.8	17.5	809.5	578.9
PWS3-F	13.6	6805.6	184.8	141.5	<LOD	<LOD	1.5	8.0	<LOD	18.3	10.9	783.4	631.2
PWS4B-F	18.8	176.8	2.9	<LOD	<LOD	<LOD	2.6	12.4	<LOD	26.1	9.6	181.3	644.2
PWS5A-F	<LOD	416.8	32.8	<LOD	<LOD	174.2	6.3	16.7	<LOD	<LOD	<LOD	459.3	1088.1
PWS5B-F	<LOD	453.9	9.4	<LOD	<LOD	109.8	2.6	13.6	<LOD	<LOD	<LOD	457.8	1034.7
PWS1-R-F	<LOD	335.4	0.7	<LOD	<LOD	<LOD	1.0	1.4	<LOD	<LOD	<LOD	219.3	602.2
PWS2-R-F	<LOD	335.7	<LOD	<LOD	<LOD	<LOD	1.9	6.8	<LOD	<LOD	<LOD	384.4	568.7

Total (ug/L) n = 19

Sample Id	As	Zn	Pb	Cd	Ni	Fe	Cr	Cu	Ti	Zr	Ce	Sr	Ba
BHW1-UF	19.0	364.6	<LOD	1.9	<LOD	35.0	5.5	16.7	<LOD	29.0	12.7	3146.0	678.5
BHW2-UF	12.0	424.6	6.2	<LOD	<LOD	<LOD	4.5	14.3	<LOD	19.8	9.6	2354.3	520.0
BHW3-UF	14.6	405.2	<LOD	<LOD	<LOD	<LOD	3.3	26.1	<LOD	18.9	7.7	2150.5	626.9
BHW4-UF	6.8	454.2	<LOD	<LOD	<LOD	115.0	2.6	19.3	<LOD	18.6	7.0	1741.3	657.4
RW1-UF	13.8	562.0	16.8	<LOD	<LOD	1208.3	5.0	15.7	<LOD	18.9	22.5	748.7	833.9
RW2-UF	9.9	458.3	5.6	3.5	0.7	267.7	8.0	28.3	<LOD	32.9	17.2	180.9	641.9
RW3-UF	12.2	1989.4	1298.0	7.4	19.6	22452.0	23.1	101.1	<LOD	24.3	75.4	330.8	908.1
Control Water Sample1-UF	11.4	501.8	20.0	<LOD	4.9	4136.1	6.0	41.5	<LOD	20.7	19.4	378.9	970.1
Control Water Sample2-UF	17.1	429.6	18.0	<LOD	2.0	7337.7	9.0	28.4	<LOD	18.9	92.3	232.6	956.3
PWS1A-UF	<LOD	871.3	<LOD	<LOD	<LOD	<LOD	4.8	3.9	<LOD	<LOD	<LOD	1974.1	632.9
PWS1B-UF	<LOD	470.0	<LOD	<LOD	<LOD	<LOD	4.1	4.5	<LOD	<LOD	<LOD	1949.9	584.8
PWS2A-UF	<LOD	25767.3	454.0	8.2	<LOD	<LOD	3.3	40.2	<LOD	<LOD	<LOD	756.1	549.6
PWS2B-UF	<LOD	26622.0	436.9	10.1	<LOD	<LOD	3.6	39.6	<LOD	<LOD	<LOD	782.9	572.2
PWS3-UF	<LOD	6921.4	190.2	79.6	<LOD	<LOD	1.6	4.9	<LOD	<LOD	<LOD	691.9	630.9
PWS4B-UF	<LOD	353.9	<LOD	<LOD	<LOD	<LOD	3.2	18.6	<LOD	<LOD	<LOD	161.7	654.0
PWS5A-UF	<LOD	319.4	<LOD	<LOD	<LOD	<LOD	2.1	12.4	<LOD	<LOD	<LOD	418.7	946.2

PWS5B-UF	<LOD	356.3	9.6	<LOD	<LOD	486.7	2.6	10.6	<LOD	<LOD	<LOD	431.3	1026.1
PWS1-R-UF	<LOD	345.4	<LOD	<LOD	<LOD	<LOD	1.6	3.8	<LOD	<LOD	<LOD	227.2	628.3
PWS2-R-UF	<LOD	311.3	<LOD	<LOD	<LOD	<LOD	1.8	4.0	<LOD	<LOD	<LOD	383.7	568.6

Appendix 5.16 (Continued)

Sample Id	Hg	Mn	Al	Mg	Ca	Na	K
Dissolved (ug/L) n = 19							
BHW1-F	138.5	0.0	129.6	335690.6	275159.6	546064.2	19251.4
BHW2-F	63.7	29.2	183.3	321942.5	212173.5	822347.6	19183.4
BHW3-F	18.8	<LOD	254.0	230275.9	193936.7	0.0	27252.0
BHW4-F	<LOD	<LOD	232.7	106708.2	90331.9	0.0	19630.9
RW1-F	6.2	<LOD	174.1	88991.5	370636.9	86180.1	33550.6
RW2-F	10.1	2473.6	194.3	4811.7	82594.7	70183.4	13646.4
RW3-F	<LOD	1678.6	2819.5	16997.5	76781.4	181542.3	35320.5
Control Water Sample1-F	<LOD	513.8	320.7	42642.8	109243.0	254990.6	151090.1
Control Water Sample2-F	<LOD	212.0	1091.1	0.0	20716.6	84811.5	20297.4
PWS1A-F	<LOD	734.3	174.5	829000.1	674749.3	250801.5	34631.5
PWS1B-F	2.5	144.3	156.9	821693.4	647091.0	251841.2	33677.5
PWS2A-F	<LOD	5493.1	206.3	339519.4	628579.0	123603.9	27071.2
PWS2B-F	5.7	5750.9	184.4	301941.2	476171.2	117201.9	24909.8
PWS3-F	6.9	400.1	139.0	230564.0	422679.1	219039.5	30539.5
PWS4B-F	13.6	<LOD	164.4	18269.0	63094.9	28212.1	19810.8
PWS5A-F	13.6	<LOD	190.4	71227.8	175756.7	130962.8	88278.4
PWS5B-F	8.8	<LOD	175.9	68799.4	172264.5	127976.1	85790.0
PWS1-R-F	16.4	<LOD	158.7	70624.5	114942.1	43609.5	39300.6
PWS2-R-F	4.8	<LOD	169.5	154927.0	286038.7	59607.5	27604.3
Total (ug/L) n = 19							
Sample Id	Hg	Mn	Al	Mg	Ca	Na	K
BHW1-UF	33.0	<LOD	165.1	351848.5	289387.0	572046.7	19169.0
BHW2-UF	0.2	44.1	163.6	345082.7	233522.6	0.0	19599.9
BHW3-UF	<LOD	<LOD	170.0	236951.1	198928.4	0.0	25914.7

Sample Id	Hg	Mn	Al	Mg	Ca	Na	K
Dissolved (ug/L) n = 19							
BHW4-UF	<LOD	<LOD	224.9	104567.6	91477.8	0.0	20444.9
RW1-UF	<LOD	1834.2	1569.0	100118.5	395705.5	98871.7	36567.3
RW2-UF	108.9	2364.1	377.3	5287.9	86074.5	74804.5	16567.9
RW3-UF	<LOD	2631.5	16659.2	30983.5	109198.9	198540.0	45326.1
Control Water Sample1-UF	<LOD	1602.8	1768.3	50202.3	128330.7	276412.5	159550.1
Control Water Sample2-UF	<LOD	1608.5	8449.6	7981.0	48890.7	92631.0	21969.8
PWS1A-UF	29.7	760.9	186.1	816530.9	665341.1	243623.3	32707.3
PWS1B-UF	13.7	183.4	159.7	831495.3	656898.2	254656.2	34200.5
PWS2A-UF	6.8	5937.7	188.9	325966.9	516504.6	125489.3	26651.8
PWS2B-UF	15.0	5924.1	160.6	324119.5	511087.1	124447.7	26212.6
PWS3-UF	9.2	391.9	140.0	231571.1	426170.5	221513.9	30538.0
PWS4B-UF	6.3	<LOD	155.7	18043.9	65557.7	28882.6	22216.7
PWS5A-UF	23.3	<LOD	175.5	70268.5	174713.2	127436.7	85205.9
PWS5B-UF	<LOD	259.8	845.0	71881.2	180961.9	133553.6	88051.6
PWS1-R-UF	19.2	<LOD	154.8	68888.6	112913.5	41961.5	37759.2
PWS2-R-UF	1.2	<LOD	163.3	152948.6	281037.4	58938.2	26934.0

Appendix 6.1: pXRF measurement details for each sample point

Sample No	Sample ID	Longitudes (E)	Latitudes (N)	Altitude (m)
1	CS1	7°26′44.7"	6°28′19.7"	288
2	CSS1	7°26′45.1"	6°28′20.4"	236
3	CSS2	7°26′38.6"	6°28′20.3"	248
4	CSS3	7°26′45.4"	6°28′23.0"	243
5	CSS4	7°26′43.1"	6°28′23.5"	247
6	CSS5	7°26′44.1"	6°28′23.3"	250
7	CSS6	7°26′46.6"	6°28′22.0"	245
8	CSS7	7°26′46.3"	6°28′22.1"	245
9	CSS8	7°26′47.6"	6°28′21.0"	243
10	CSS9	7°26′47.3"	6°28′19.8"	240
11	CSS10	7°26′49.1"	6°28′20.4"	242
12	CSS11	7°26′50.2"	6°28′18.5"	240
13	CTS1	7°26′51.9"	6°28′16.9"	240
14	CTS2	7°26′51.9"	6°28′14.1"	244
15	CTS3	7°26′55.5"	6°28′14.2"	241

CS - Coal Sample; CSS - Coal Soil Sample; CTS - Coal Tailing Sample

Appendix 6.2: Sample coordinates for each sample point/type

Sample No	Sample ID	Longitudes (E)	Latitudes (N)	Altitude (m)
1	CSS	7°27′09.9"	6°28′08.4"	237
2	CS1	7°26′44.7"	6°28′19.7"	288
3	CSS1	7°26′45.1"	6°28′20.4"	236
4	CSS2	7°26′38.6"	6°28′20.3"	248
5	CSS3	7°26′45.4"	6°28′23.0"	243
6	CSS4	7°26′43.1"	6°28′23.5"	247
7	CSS6	7°26′46.6"	6°28′22.0"	245
8	CSS8	7°26′47.6"	6°28′21.0"	243
9	CSS9	7°26′47.3"	6°28′19.8"	240
10	CSS10	7°26′49.1"	6°28′20.4"	242
11	CSS11	7°26′50.2"	6°28′18.5"	240
12	CTS1	7°26′51.9"	6°28′16.9"	240
13	CTS2	7°26′51.9"	6°28′14.1"	244
14	CTS3	7°26′55.5"	6°28′14.2"	241
15	CTS4	7°26′51.4"	6°28′14.9"	296
16	CTS5	7°26′51.2"	6°28′15.5"	232
17	CTS6	7°28′51.0"	6°28′15.0"	232
18	CTS7	7°28′50.5"	6°28′15.6"	232
19	CTS8	7°28′50.7"	6°28′15.9"	232
20	CWS1	7°26′36.3"	6°28′18.1"	238
22	SD1	7°26′36.3"	6°28′18.1"	238
23	CWS2	7°26′41.6"	6°28′20.0"	233
24	SD2	7°26′41.6"	6°28′20.0"	233
25	CWS3	7°26′47.7"	6°28′21.8"	231
26	SD3	7°26′47.7"	6°28′21.8"	231
27	CWS4	7°26′46.7"	6°28′22.4"	231
28	SD4	7°26′46.7"	6°28′22.4"	231
29	CWS5	7°26′47.2"	6°28′19.8"	236
30	CWS6	7°26′47.8"	6°28′19.0"	235
31	CWS7	7°26′47.8"	6°28′19.5"	232
32	SD5	7°26′47.8"	6°28′19.5"	232
33	Channel Water, collapsed area	7°26′52.5"	6°28′15.7"	234
34	CWS8	7°26′59.8"	6°28′12.4"	221
35	SD6	7°26′59.8"	6°28′12.4"	221
36	CWS9	7°27′14.2"	6°28′8.20"	214
37	SD7	7°27′14.2"	6°28′8.20"	214
38	CSD	7°27′18.5"	6°28′7.6"	226
39	WWS	7°27′18.9"	6°27′57.9"	222

CS - Coal sample; CSS - Coal Site Sample; CWS - Coal Water Sample; CSD - Coal Sediment sample; CTS - Coal Tailing Sample; WWS - Well Water Sample

Appendix 6.3: Method validation parameters for soil (ug/Kg)

Analyte	Regression Equation	R^2	LOD	$t_{R(min)}$	Accuracy %	Precision (%)
Napthalene	y = 0.944992 x + 0.028262	0.9999	4.5	4.6	92-101	2-9
Acenapthylene	y = 0.898087 x + 0.001655	0.9999	1.3	6.2	102-107	1-9
Acenapthene	y = 0.582359 x + 0.002290	0.9999	1.4	6.4	97-101	1-8
Fluorene	y = 1.036954 x + 0.006711	0.9999	1.9	7	95-100	0-8
Phenanthrene	y = 1.007587 x + 0.007535	0.9999	2.3	8.3	98-102	0-9
Anthracene	y = 2.355150 x - 0.001498	0.9995	3.6	8.4	95-99	0-9
Fluoranthene	y = 1.009038 x + 0.003970	0.9999	2.3	10.6	95-100	0-10
Pyrene	y = 1.023342 x - 0.001586	0.9999	0.3	11.1	94-99	1-10
Benzo(a)anthracene	y = 0.880600 x - 0.013512	0.9995	1.2	14.2	91-99	1-10
Chrysene	y = 0.880551 x - 0.013434	0.9995	1.2	14.2	91-99	1-10
Benzo(b)fluoranthrene	y = 0.861399 x - 0.027241	0.9971	0.8	16.9	85-92	2-10
Benzo(k)fluoranthrene	y = 0.836572 x - 0.024766	0.9976	0.9	17	91-111	2-9
Benzo(a)pyrene	y = 0.691797 x - 0.024293	0.9967	0.5	17.8	89-107	1-10
Indeno(1,2,3,-cd)pyrene	y = 0.494063 x - 0.022515	0.9939	4	21.5	68-105	2-11
Dibenz(a,h)anthracene	y = 0.470115 x - 0.021751	0.9939	3	21.7	77-116	2-9
Benzo(ghi)perylene	y = 0.588915 x - 0.022657	0.9959	1.1	22.6	64-99	2-19

Appendix 6.4: Method Validation parameters for water (ng/mL)

Analyte	Regression Equation	R^2	LOD	$t_{R(min)}$	Accuracy %	Precision (%)
Napthalene	y = 1.018756 x + 0.018306	0.9999	129	4.6	104.4-128	9-10
Acenapthylene	y = 0.911821 x - 0.009767	0.9996	3	6.2	12-Dec	9-13
Acenapthene	y = 0.593165 x - 0.001851	0.9999	34	6.4	97-101	9.0-9.3
Fluorene	y = 1.096555 x - 5.467318	0.9999	19	7	96-113	6-4
Phenanthrene	y = 1.093108 x + 0.001001	0.9999	6	8.3	94-110	3-5
Anthracene	y = 2.564827 x - 0.001812	0.9999	12	8.4	98-114	5-6
Fluoranthene	y = 1.100658 x - 0.003876	0.9999	2	10.7	88-105	4-5
Pyrene	y = 1.095460 x - 0.010335	0.9997	3	11.2	93.11	4-5
Benzo(a)anthracene	y = 0.935945 x - 0.015121	0.9993	6	14.3	75-95	5-6
Chrysene	y = 0.935945 x - 0.015121	0.9993	8	14.3	75-95	5-6
Benzo(b)fluoranthrene	y = 0.821531 x - 0.015365	0.999	12	16.9	70-88	8-11
Benzo(k)fluoranthrene	y = 0.821531 x - 0.015365	0.999	11	16.9	70-88	8-11
Benzo(a)pyrene	y = 0.688739 x - 0.017509	0.998	2	17.8	31-42	8-20
Indeno(1,2,3,-cd)pyrene	y = 0.626877 x - 0.022981	0.9958	1	21.5	43-57	18-18
Dibenz(a,h)anthracene	y = 0.662464 x - 0.025178	0.9957	2	21.7	Sep-32	6-11
Benzo(ghi)perylene	y = 0.733950 x - 0.019495	0.998	0.3	22.6	17-43	4-9

Appendix 6.5: Dataset of PAH concentrations (µg/kg) in soil samples collected at the Onyeama AML site.

Analyte /Sample ID	Nap	Acy	Ace	Fl	Phe	Ant	Flu	Pyr	BaA	Chr	BbF	BkF	BaP	IND	DBA	BghiP
CSS 01	3108.2	52.9	8.3	16.2	80.0	39.5	534.9	542.2	461.7	461.7	511.2	392.6	423.8	401.8	219.0	350.1
CSS 02	1516.6	47.8	2.7	<LOD	75.5	15.6	132.5	130.3	109.3	109.3	199.2	196.1	143.3	159.3	139.4	138.9
CSS 03	1988.0	38.2	3.1	16.1	112.4	36.8	150.2	161.7	113.3	113.3	178.1	177.7	135.8	158.6	137.7	141.5
CSS 04	435.5	30.6	<LOD	<LOD	4.3	3.8	20.6	33.8	45.4	45.4	77.1	89.5	91.2	122.5	123.4	105.0
CSS 05	1435.9	44.7	<LOD	<LOD	24.5	4.6	75.0	95.4	81.7	81.7	125.8	132.1	106.5	137.8	134.4	127.8
CSS 06	276.2	30.9	<LOD	<LOD	<LOD	<LOD	5.6	17.1	37.1	37.1	68.8	82.4	88.6	119.6	122.2	102.8
CSS 07	1265.1	30.9	<LOD	<LOD	84.8	102.4	55.0	84.6	78.8	78.8	103.1	112.3	98.9	136.9	127.4	123.1
CSS 08	924.0	33.5	<LOD	5.4	31.5	7.7	22.5	35.9	44.9	44.9	76.3	88.9	89.3	121.9	123.1	104.8
CSS 09	4980.8	26.7	<LOD	3.9	99.2	10.7	248.4	246.2	174.9	174.9	230.5	223.4	130.0	173.3	141.4	157.1
CSS	3841.7	21.6	<LOD	<LOD	174.8	12.2	244.7	190.8	149.0	149.0	157.2	159.5	105.2	151.4	132.3	141.2
CTS1	4064.0	34.4	<LOD	3.9	161.0	16.0	146.4	136.8	175.2	175.2	186.1	184.7	117.0	157.5	134.3	182.9
CTS2	788.6	77.7	<LOD	<LOD	26.2	6.5	29.9	49.4	64.2	64.2	101.3	110.7	93.4	123.8	124.2	112.4
CTS3	4168.6	40.9	9.5	4.5	112.8	16.8	121.1	138.7	139.6	139.6	212.2	207.5	119.7	147.1	137.4	168.2
CTS4	2535.5	42.8	6.9	8.6	109.9	131.1	93.1	112.4	115.7	115.7	171.9	172.3	114.1	147.5	129.4	154.4
CTS5	742.8	43.8	<LOD	<LOD	33.8	5.7	36.0	48.7	63.1	63.1	98.0	107.8	97.3	128.3	124.7	119.6
CTS6	596.6	48.4	<LOD	<LOD	50.6	5.8	43.8	56.6	69.6	69.6	99.7	109.3	97.7	126.1	123.7	118.0
CTS7	499.8	21.9	<LOD	<LOD	31.4	47.3	32.6	46.4	61.4	61.4	96.8	106.7	94.6	122.8	124.2	113.9
CTS8	2489.3	64.6	<LOD	5.4	266.4	302.8	174.1	187.0	155.0	155.0	154.8	157.3	105.8	135.1	128.9	130.0

Appendix 6.6: Dataset of PAH concentrations (µg/kg) in sediment samples collected at the Onyeama AML site.

Analyte /Sample ID	Nap	Acy	Ace	Fl	Phe	Ant	Flu	Pyr	BaA	Chr	BbF	BkF	BaP	IND	DBA	BghiP

CSD 01	<LOD	26.3	<LOD	<LOD	<LOD	<LOD	<LOD	9.1	30.6	30.6	59.2	73.9	87.8	118.0	122.7	99.1
CSD 02	<LOD	21.8	<LOD	<LOD	<LOD	<LOD	<LOD	13.9	34.2	34.2	64.3	78.4	88.7	119.2	121.5	102.1
CSD 03	<LOD	34.3	<LOD	<LOD	<LOD	<LOD	<LOD	9.5	30.8	30.8	60.0	74.7	87.6	116.9	128.5	99.5
CSD 04	<LOD	64.4	123.1	<LOD	<LOD	9.7	<LOD	10.3	31.2	31.2	59.8	74.5	85.7	116.8	122.9	99.4
CSD 05	<LOD	33.6	<LOD	<LOD	<LOD	5.9	<LOD	9.7	30.4	30.4	59.2	73.9	86.5	117.4	122.1	99.3
CSD 06	153.7	25.7	<LOD	<LOD	<LOD	<LOD	5.5	18.3	35.7	35.7	65.7	79.6	88.0	118.6	121.6	103.5
CSD 07	<LOD	60.7	<LOD	<LOD	<LOD	8.5	<LOD	7.2	31.4	31.4	59.3	74.0	85.8	117.1	123.9	99.5
CSD 08	<LOD	32.2	<LOD	<LOD	<LOD	8.4	<LOD	10.7	31.4	31.4	60.2	74.9	87.9	117.0	124.0	99.6

Appendix 6.7: Dataset of PAH concentrations (µg/kg) in water samples collected at the Onyeama AML site.

Analyte /Sample ID	Nap	Acy	Ace	Fl	Phe	Ant	Flu	Pyr	BaA	Chr	BbF	BkF	BaP	IND	DBA	BghiP
CWS1A	558.7	15.1	81.7	21.2	66.0	14.5	8.7	12.3	16.0	16.2	<LOD	<LOD	11.0	19.5	19.1	16.1
CWS2A	572.0	35.0	106.4	<LOD	58.9	<LOD	6.9	8.8	8.6	11.3	<LOD	11.7	12.7	16.1	15.5	13.2
CWS3A	887.8	58.7	108.3	264.2	226.7	43.2	47.6	50.6	1816.8	1816.5	492.2	492.2	80.7	41.0	58.6	253.8
CWS4A	818.4	201.9	265.6	327.5	38.9	44.5	47.0	46.0	29.8	29.9	656.4	656.4	66.8	26.4	40.2	21.0
CWS5A	680.4	8.7	<LOD	45.9	60.7	<LOD	13.3	13.7	16.7	19.3	21.4	21.4	20.6	22.4	20.6	17.4
CWS6A	718.5	29.1	45.3	32.9	65.4	12.7	10.8	11.4	12.8	13.0	15.5	15.5	11.0	20.7	18.6	15.2
CWS7A	696.1	12.7	43.0	34.7	61.6	13.5	14.1	14.7	22.4	22.6	28.6	28.6	21.6	25.5	20.9	17.3
CWS8A	601.9	15.6	<LOD	38.9	59.2	<LOD	11.7	12.3	23.5	23.6	26.4	26.4	20.9	21.8	19.8	17.4
CWS9A	546.3	13.0	51.7	<LOD	62.0	<LOD	11.0	11.6	10.8	11.0	<LOD	11.6	12.2	18.4	18.3	14.9
WWS10A	472.5	29.5	34.8	82.3	55.4	19.3	<LOD	18.1	39.0	39.1	50.9	50.9	37.2	32.7	18.2	14.8

Analyte /Sample ID	Nap	Acy	Ace	Fl	Phe	Ant	Flu	Pyr	BaA	Chr	BbF	BkF	BaP	IND	DBA	BghiP
CWS1B	516.8	13.7	33.8	49.4	61.8	<LOD	9.3	13.5	13.9	14.1	16.9	16.9	10.5	22.0	20.3	17.4
CWS2B	397.8	10.2	28.9	15.2	57.1	<LOD	6.2	7.7	8.7	8.9	<LOD	<LOD	11.4	17.3	18.3	14.2
CWS3B	445.0	6.4	34.2	21.3	56.3	12.9	8.8	9.3	11.5	11.7	15.3	15.3	13.6	19.4	19.1	16.2
CWS4B	420.3	15.0	<LOD	28.7	54.8	<LOD	9.0	9.5	11.2	11.4	12.4	12.4	9.6	18.6	19.0	14.4
CWS5B	567.8	4.0	<LOD	52.3	58.4	<LOD	8.8	9.6	6.7	<LOD	<LOD	<LOD	10.0	17.5	18.4	14.2

CWS6B	476.9	6.0	54.9	39.5	370.1	172.2	100.1	73.3	26.7	26.9	<LOD	<LOD	11.2	17.3	18.2	14.2
CWS7B	491.6	9.4	37.9	24.4	64.6	17.1	11.8	12.6	18.1	18.3	21.6	21.6	15.5	20.7	19.0	15.9
CWS8B	450.6	11.3	<LOD	38.4	59.5	12.6	10.6	10.7	10.3	10.5	12.3	12.3	11.8	18.5	18.8	14.5
CWS9B	442.2	39.9	126.1	<LOD	62.5	<LOD	9.8	11.6	13.3	13.5	<LOD	18.9	15.5	21.0	21.9	17.2
WWS10B	424.7	44.2	195.0	<LOD	72.3	45.0	20.4	18.6	13.6	13.8	<LOD	<LOD	10.2	17.0	18.2	14.7

Appendix 6.8: pXRF - Results (mg/Kg) for Soil (CSS), Tailings (CTS) and Rock (CS) samples at Onyeama (Enugu) Abandoned Coal Mine

Sample Id/Analyte	Mg	Al	Si	K	Ca	Ti	Cr	Cd	Ni	Mn	Fe	Cu	Zn	As	Rb	Sr	Y	Zr	Ba	Ce	Au	Pb	Th
CSS1	173.3	62.1	1208.6	40.5	<LOD	4929	80	<LOD	<LOD	206	15697	19	22	<LOD	33	106	97	3409	794	<LOD	12	<LOD	29
CSS2	191.1	<LOD	1086.5	22.3	<LOD	2129	39	<LOD	<LOD	142	8520	<LOD	18	<LOD	13	43	39	2475	358	<LOD	11	<LOD	<LOD
CSS3	<LOD	91.1	1481.2	14	571	5788	130	<LOD	<LOD	266	28063	59	131	17	6	38	25	1675	250	145	20	83	18
CSS4	<LOD	58.6	1225.8	20.6	1999	5125	103	<LOD	<LOD	152	32224	45	46	<LOD	12	81	61	2658	328	<LOD	17	46	26
CSS5	<LOD	37.1	1435.1	6.7	1333	4072	106	<LOD	<LOD	148	16632	14	39	<LOD	5	39	32	2122	155	<LOD	28	10	12
CSS6	<LOD	54.2	1858.5	10.4	96	2808	81	<LOD	<LOD	106	7556	6	33	<LOD	7	34	32	1895	123	<LOD	14	<LOD	<LOD
CSS7	<LOD	61.2	2065.3	8.7	300	2616	76	<LOD	<LOD	179	18041	31	15	<LOD	3	24	18	1333	<LOD	<LOD	19	23	<LOD
CSS8	<LOD	19.8	1672.3	2.2	312	1098	67	<LOD	<LOD	197	7073	45	26	<LOD	3	23	16	1592	<LOD	<LOD	12	28	<LOD
CSS9	<LOD	12.6	1235	1.1	399	681	129	<LOD	<LOD	168	31359	19	50	<LOD	<LOD	21	<LOD	884	109	<LOD	16	26	<LOD
CSS10	<LOD	37.3	1792.4	5	151	2239	35	<LOD	<LOD	98	8423	10	15	<LOD	5	28	80	1440	<LOD	<LOD	14	<LOD	16
CSS11	<LOD	11.3	1758.8	1.1	56	1467	108	<LOD	<LOD	74	5443	15	10	<LOD	<LOD	20	11	1420	140	<LOD	19	<LOD	<LOD
CTS1	<LOD	57.5	874.6	21.8	1133	5202	88	<LOD	<LOD	280	30596	39	61	7	21	102	77	2841	391	165	<LOD	61	23
CTS2	204.3	69.2	1320.1	38.4	<LOD	5441	177	<LOD	<LOD	143	12653	7	24	<LOD	26	104	105	3642	607	<LOD	14	<LOD	37
CTS3	0	93.1	2130.9	29.3	<LOD	6639	105	<LOD	18	393	33300	18	49	<LOD	16	69	62	3051	418	161	22	1624	<LOD
CS	317.6	0	314.8	6.1	<LOD	540	55	<LOD	<LOD	127	178	20	10	<LOD	<LOD	11	12	<LOD	<LOD	<LOD	21	<LOD	<LOD
Control Sample	0	90.5	1448.7	38.2	1996	8597	143	<LOD	<LOD	276	18071	20	54	<LOD	28	135	127	4159	510	234	0	18	23

Appendix 6.9: ICP-OES - Results (mg/Kg) for Soil (CSS), Tailings (CTS), Sediment (CSD) and Rock (CS) samples at Onyeama (Enugu) Abandoned Coal Mine

Sample Id/Analyte	As	Zn	Pb	Cd	Ni	Cr	Cu	Ti	Zr	Ce	Sr	Ba	Hg	Mn	Al	Fe	Mg	Ca	Na	K
CSS01	<LOD	15.4	30.7	<LOD	3.3	18.5	17.5	110.1	9.9	17.1	5.1	17.8	<LOD	10.9	2515.3	7873.9	0.0	1343.1	761.2	1369.0
CSS02	1.2	119.0	22.6	<LOD	10.2	19.7	54.8	296.1	13.2	28.0	9.0	37.6	<LOD	59.3	14544.7	10690.8	290.9	2945.7	944.1	2415.8
CSS03	<LOD	56.4	87.7	<LOD	6.7	11.0	22.0	39.1	3.6	18.5	6.3	20.9	<LOD	74.1	1783.5	13386.6	2.2	1710.3	792.9	1788.6
CSS04	<LOD	12.2	14.7	<LOD	2.5	6.3	44.4	26.3	2.0	5.7	3.6	4.3	<LOD	23.6	1006.0	5238.4	0.0	790.6	569.3	1084.1
CSS05	<LOD	28.8	8.6	<LOD	3.8	9.2	13.3	45.2	3.2	13.2	5.4	14.6	<LOD	44.2	1130.7	7726.1	0.0	2024.7	845.3	1739.6
CSS06	<LOD	12.9	33.2	<LOD	1.9	5.8	6.3	30.4	3.6	9.3	4.1	7.7	<LOD	24.6	1202.9	4102.5	5.6	1460.0	737.8	1606.2
CSS07	<LOD	19.9	72.7	<LOD	3.0	7.4	23.4	34.2	2.2	9.5	4.7	12.0	<LOD	34.4	1212.4	5747.3	0.0	1444.9	956.5	1832.2
CSS08	<LOD	15.1	6.1	<LOD	2.4	6.8	8.0	25.5	5.1	9.4	4.3	8.7	<LOD	35.1	1786.7	6104.6	144.0	1238.3	608.9	1238.1
CSS09	<LOD	36.6	54.4	<LOD	9.3	13.1	40.4	83.9	7.4	50.7	8.7	53.1	<LOD	59.2	2010.9	15821.0	10.9	928.9	872.6	2824.6
CSS10	<LOD	56.0	12.1	<LOD	10.2	17.3	11.6	91.5	8.0	48.3	15.3	44.2	<LOD	191.4	3692.1	14101.0	1241.7	4373.7	1952.3	5000.9
CTS01	<LOD	17.9	14.5	<LOD	4.6	8.4	13.4	58.5	8.8	89.7	14.2	107.1	<LOD	17.4	2704.9	3838.8	335.9	868.6	707.1	3083.5
CTS02	<LOD	16.7	9.0	<LOD	4.5	7.9	10.9	27.2	10.2	59.3	7.8	86.7	<LOD	55.6	2616.6	9085.0	201.7	1021.0	624.4	1898.4
CTS03	<LOD	17.4	10.7	<LOD	4.7	8.3	13.5	67.7	7.3	56.3	9.1	48.9	<LOD	34.2	2326.6	5057.5	245.1	990.2	1094.5	3095.1
CTS04	<LOD	13.9	8.3	<LOD	3.2	5.9	11.7	35.4	6.2	40.4	6.1	28.7	<LOD	23.9	1444.2	5286.1	145.5	911.4	755.6	2087.6
CTS05	<LOD	69.9	5.7	<LOD	2.6	6.4	7.9	18.6	3.8	24.6	4.5	16.9	<LOD	16.6	1684.0	4205.7	0.0	871.1	830.7	1948.7
CTS06	<LOD	11.8	8.3	<LOD	2.8	7.8	10.8	27.1	10.9	45.1	7.1	48.1	<LOD	29.7	2340.5	8928.2	103.5	1078.3	944.3	2307.1
CTS07	<LOD	10.9	9.1	<LOD	4.3	9.3	13.0	31.1	9.9	51.5	7.2	53.1	<LOD	66.7	2978.9	8327.9	634.0	847.6	715.2	1853.4
CTS08	<LOD	9.3	10.7	<LOD	2.7	7.9	12.1	44.5	9.8	31.4	6.7	62.6	<LOD	125.0	2076.4	9958.0	109.1	588.1	630.4	1867.6
CSD01	<LOD	1.6	0.4	<LOD	<LOD	2.8	1.6	12.0	2.1	1.6	2.8	<LOD	<LOD	3.7	187.3	758.3	0.0	529.0	601.7	959.4
CSD02	<LOD	4.7	1.7	<LOD	<LOD	4.4	2.3	27.9	3.8	4.6	3.1	2.8	<LOD	12.4	850.4	3037.6	0.0	559.4	503.7	971.7
CSD03	<LOD	5.3	1.7	<LOD	<LOD	4.5	2.4	27.9	4.8	4.7	3.1	2.9	<LOD	12.4	830.8	2015.0	0.0	311.1	414.3	702.4
CSD04	<LOD	4.1	1.3	<LOD	<LOD	3.7	2.1	18.7	2.9	2.7	2.8	2.6	<LOD	8.5	373.7	2400.6	0.0	1162.1	925.3	1597.7
CSD05	<LOD	4.8	3.0	<LOD	<LOD	3.4	2.9	30.7	2.7	11.5	4.9	2.9	<LOD	9.9	760.5	1407.9	0.0	649.3	586.9	1067.8
CSD06	<LOD	2.6	0.9	<LOD	<LOD	2.0	2.3	20.7	1.4	2.9	3.0	<LOD	<LOD	4.2	536.5	23251.5	296.4	1748.8	611.1	945.5

CSD07	<LOD	35.8	7.5	<LOD	2.4	12.4	6.4	100.0	3.8	7.5	9.2	8.9	<LOD	57.5	1821.3	2087.4	0.0	1074.7	780.3	1457.6
CCSD08	<LOD	2.6	1.4	<LOD	<LOD	2.6	2.5	23.9	1.6	7.4	3.5	2.6	<LOD	7.7	669.9	3933.0	0.0	699.5	456.3	719.0
CS EG	<LOD	4.2	3.3	<LOD	1.1	4.8	285.7	2.8	2.8	4.0	4.7	<LOD	3.6	293.8	190.7	190.7	0.0	2522.1	3150.7	5801.4

Appendix 6.10: Sequential analysis results F1-F3 (mg/Kg) of Soil (CSS), Tailings (CTS), Sediment (CSD) and Rock (CS) samples at Enugu (Onyeama) Abandoned Coal Mine

Sample	As			Zn			Pb			Cd			Ni			Fe		
Id/F1- F3	F1	F2	F3	F1	F2	F3	F1	F2	F3	F1	F2	F3	F1	F2	F3	F1	F2	F3
CSS1	<LOD	<LOD	<LOD	5.0	4.0	4.2	0.5	2.0	3.9	<LOD	<LOD	<LOD	<LOD	<LOD	<LOD	1.3	386.8	1345.5
CSS2	<LOD	<LOD	<LOD	<LOD	2.7	1.6	0.5	1.0	1.4	<LOD	<LOD	<LOD	<LOD	<LOD	<LOD	25.2	320.3	613.7
CSS3	<LOD	<LOD	<LOD	23.7	33.2	37.0	0.2	2.0	36.0	<LOD	<LOD	<LOD	<LOD	<LOD	1.8	4.2	181.9	1184.7
CSS4	<LOD	<LOD	<LOD	13.9	11.4	8.6	0.4	3.8	10.4	<LOD	<LOD	<LOD	<LOD	<LOD	<LOD	160.7	2095.2	3744.3
CSS5	<LOD	<LOD	<LOD	5.0	6.5	5.3	0.3	1.8	3.0	<LOD	<LOD	<LOD	<LOD	<LOD	<LOD	13.5	271.8	652.0
CSS6	<LOD	<LOD	<LOD	18.4	8.9	19.9	4.3	12.5	11.8	<LOD	<LOD	<LOD	<LOD	<LOD	<LOD	10.0	260.3	1100.6
CSS7	<LOD	<LOD	<LOD	15.5	16.5	36.4	2.6	14.4	18.2	<LOD	<LOD	<LOD	<LOD	<LOD	<LOD	5.3	451.7	3627.5
CSS8	<LOD	<LOD	<LOD	4.4	6.5	6.2	0.1	1.7	2.0	<LOD	<LOD	<LOD	<LOD	<LOD	<LOD	1.8	204.9	657.2
CSS9	<LOD	<LOD	<LOD	<LOD	2.6	5.7	0.3	3.3	4.4	<LOD	<LOD	<LOD	<LOD	<LOD	<LOD	3.8	228.6	690.2
CCSS	<LOD	<LOD	<LOD	28.5	30.2	14.1	0.2	2.6	4.9	<LOD	<LOD	<LOD	<LOD	1.6	<LOD	<LOD	248.1	1161.1
CS EG	<LOD	<LOD	<LOD	3.9	46.0	4.6	1.2	1.6	3.8	<LOD	<LOD	<LOD	<LOD	<LOD	3.4	19.8	47.0	571.5
CTS1	<LOD	<LOD	<LOD	11.1	9.6	12.4	0.5	4.6	12.5	<LOD	<LOD	<LOD	<LOD	1.6	<LOD	37.1	1493.3	3526.4
CTS2	<LOD	<LOD	<LOD	2.6	2.6	6.1	0.2	1.4	2.6	<LOD	<LOD	<LOD	<LOD	<LOD	<LOD	7.6	223.9	709.9
CTS3	<LOD	<LOD	<LOD	10.5	5.9	17.4	362.5	2238.4	1458.2	<LOD	<LOD	<LOD	3.4	2.3	7.5	5.5	242.0	7106.6
CTS04	<LOD	1.1	<LOD	9.6	5.3	14.2	1.7	2.5	4.9	<LOD	<LOD	<LOD	2.4	<LOD	2.2	5.1	229.9	752.0
CTS05	<LOD	<LOD	<LOD	5.9	9.1	30.5	0.2	3.5	6.4	<LOD	<LOD	<LOD	<LOD	<LOD	<LOD	2.5	335.8	320.3
CTS06	<LOD	<LOD	<LOD	4.5	<LOD	7.28	0.4	1.5	3.40	<LOD	<LOD	<LOD	<LOD	<LOD	<LOD	8.1	354.0	20.06
CTS07	<LOD	<LOD	<LOD	1.7	<LOD	10.42	0.2	1.2	5.36	<LOD	<LOD	<LOD	<LOD	<LOD	<LOD	6.1	291.4	57.24
CTS08	<LOD	<LOD	<LOD	<LOD	<LOD	5.56	0.5	1.4	3.42	<LOD	<LOD	<LOD	<LOD	<LOD	<LOD	6.0	212.7	28.65
CTS09	<LOD	<LOD	<LOD	<LOD	<LOD	16.29	0.5	1.1	4.01	<LOD	<LOD	<LOD	<LOD	<LOD	<LOD	7.6	499.8	56.69
CTS10	<LOD	<LOD	<LOD	2.0	<LOD	4.65	0.4	1.4	4.19	<LOD	<LOD	<LOD	<LOD	<LOD	<LOD	11.8	505.4	53.67
CTS11	<LOD	<LOD	<LOD	<LOD	2.5	5.77	0.1	0.8	4.06	<LOD	<LOD	<LOD	<LOD	<LOD	<LOD	38.7	1323.7	58.81
CDS1	<LOD	<LOD	<LOD	<LOD	<LOD	<LOD	0.5	0.9	0.4	<LOD	<LOD	<LOD	<LOD	<LOD	<LOD	50.2	53.3	183.4
CDS2	<LOD	<LOD	<LOD	<LOD	2.0	<LOD	0.3	0.5	0.1	<LOD	<LOD	<LOD	<LOD	<LOD	<LOD	12.6	94.9	237.7
CDS3	<LOD	<LOD	<LOD	3.0	<LOD	<LOD	0.8	0.5	<LOD	<LOD	<LOD	<LOD	<LOD	<LOD	<LOD	34.8	262.5	82.8
CDS4	<LOD	<LOD	<LOD	4.5	3.1	2.0	0.7	0.7	0.2	<LOD	<LOD	<LOD	<LOD	<LOD	<LOD	73.5	288.9	204.0
CDS5	<LOD	<LOD	<LOD	<LOD	3.2	3.1	0.6	0.6	0.7	<LOD	<LOD	<LOD	<LOD	<LOD	<LOD	81.8	309.7	991.2
CDS6	<LOD	<LOD	<LOD	3.3	3.7	4.7	0.6	1.0	1.1	<LOD	<LOD	<LOD	<LOD	<LOD	<LOD	210.3	1166.4	3086.5

CDS7	<LOD	<LOD	<LOD	<LOD	1.5	1.6	0.4	0.2	<LOD	<LOD	<LOD	<LOD	<LOD	<LOD	<LOD	12.8	37.5	166.1
CCSD08	<LOD	<LOD	<LOD	<LOD	8.1	5.76	0.2	0.7	2.17	<LOD	<LOD	<LOD	<LOD	<LOD	<LOD	2.8	249.4	99.10

Appendix 6:10 (continued)

Sample	Cr			Cu			Ti			Zr			Ce			Sr		
Id/F1- F3	F1	F2	F3	F1	F2	F3	F1	F2	F3	F1	F2	F3	F1	F2	F3	F1	F2	F3
CSS1	<LOD	<LOD	4.1	<LOD	0.5	4.0	2.8	<LOD	27.6	1.0	<LOD	<LOD	2.5	20.0	25.2	2.4	<LOD	<LOD
CSS2	<LOD	<LOD	1.8	<LOD	<LOD	0.7	2.6	<LOD	22.0	<LOD	<LOD	<LOD	3.8	6.1	<LOD	1.6	<LOD	<LOD
CSS3	<LOD	<LOD	12.3	0.7	1.8	25.0	2.9	<LOD	114.1	<LOD	0.7	<LOD	<LOD	<LOD	4.0	3.5	2.4	1.4
CSS4	<LOD	<LOD	8.8	0.5	0.9	12.3	3.1	<LOD	100.9	<LOD	<LOD	<LOD	<LOD	2.8	4.9	4.2	1.8	1.1
CSS5	<LOD	<LOD	3.1	<LOD	0.5	3.1	2.7	<LOD	38.3	<LOD	<LOD	<LOD	<LOD	<LOD	<LOD	1.7	<LOD	<LOD
CS	<LOD	<LOD	3.4	8.6	10.8	26.6	2.9	<LOD	22.8	0.8	<LOD	<LOD	<LOD	<LOD	<LOD	2.2	<LOD	<LOD
CSS7	<LOD	<LOD	3.6	1.0	2.8	9.3	2.6	<LOD	27.6	<LOD	<LOD	<LOD	<LOD	2.0	<LOD	2.9	1.4	<LOD
CSS8	<LOD	<LOD	2.0	<LOD	0.7	5.3	2.6	<LOD	24.8	<LOD	0.5	<LOD	<LOD	<LOD	<LOD	1.8	<LOD	<LOD
CSS9	<LOD	<LOD	2.6	<LOD	0.5	8.1	2.6	<LOD	41.3	<LOD	<LOD	<LOD	<LOD	<LOD	<LOD	1.6	<LOD	<LOD
CCSS	<LOD	<LOD	2.5	<LOD	<LOD	2.8	2.6	<LOD	23.7	<LOD	<LOD	<LOD	<LOD	<LOD	2.2	6.9	3.6	<LOD
CS EG	<LOD	<LOD	7.5	1.0	<LOD	5.8	0.7	2.0	690.1	<LOD	<LOD	<LOD	<LOD	<LOD	<LOD	1.7	1.4	3.1
CTS1	<LOD	<LOD	5.9	0.6	1.4	15.3	2.7	<LOD	51.1	0.7	<LOD	<LOD	<LOD	<LOD	2.8	2.9	1.5	1.1
CTS2	<LOD	<LOD	<LOD	0.6	0.6	2.1	2.6	<LOD	18.7	<LOD	0.8	<LOD	<LOD	<LOD	<LOD	1.6	<LOD	<LOD
CTS3	<LOD	<LOD	5.7	<LOD	<LOD	4.1	2.6	<LOD	69.2	<LOD	0.2	<LOD	<LOD	<LOD	<LOD	2.1	1.8	1.5
CTS04	<LOD	<LOD	2.6	2.3	2.2	3.6	<LOD	<LOD	34.5	1.3	0.5	0.7	3.1	<LOD	2.0	4.0	1.2	2.0
CTS05	<LOD	<LOD	2.0	1.3	0.6	4.4	<LOD	<LOD	26.4	1.0	0.2	0.8	<LOD	9.1	12.7	2.6	<LOD	2.1
CTS06	<LOD	<LOD	1.80	1.1	0.7	1.75	<LOD	<LOD	5.98	0.3	0.3	0.56	<LOD	<LOD	<LOD	1.4	<LOD	1.19
CTS07	<LOD	<LOD	<LOD	0.9	1.0	3.46	<LOD	<LOD	6.96	0.3	0.3	0.37	<LOD	<LOD	<LOD	1.2	<LOD	1.40
CTS08	<LOD	<LOD	1.56	0.7	0.8	1.78	<LOD	<LOD	7.38	0.3	0.8	0.32	<LOD	3.1	<LOD	<LOD	<LOD	<LOD
CTS09	<LOD	<LOD	<LOD	0.9	0.7	3.74	<LOD	<LOD	4.99	0.3	0.4	0.31	1.7	8.6	3.16	1.1	1.1	1.16
CTS10	<LOD	<LOD	<LOD	1.2	0.7	2.97	<LOD	<LOD	4.14	0.3	0.4	0.81	2.4	8.7	3.52	1.6	1.1	<LOD
CTS11	<LOD	<LOD	<LOD	0.6	2.0	3.25	<LOD	<LOD	6.69	0.7	0.3	0.45	<LOD	<LOD	<LOD	<LOD	1.2	1.19
CDS1	<LOD	<LOD	<LOD	<LOD	<LOD	0.7	3.1	<LOD	8.0	<LOD	<LOD	<LOD	<LOD	<LOD	<LOD	<LOD	<LOD	<LOD
CDS2	<LOD	<LOD	7.3	<LOD	<LOD	0.7	2.7	<LOD	5.0	<LOD	<LOD	<LOD	<LOD	<LOD	<LOD	<LOD	<LOD	<LOD
CDS3	<LOD	<LOD	4.3	0.5	<LOD	2.3	3.2	2.2	2.7	0.6	<LOD	<LOD	<LOD	<LOD	<LOD	<LOD	<LOD	<LOD
CDS4	<LOD	<LOD	<LOD	0.9	<LOD	36.6	3.2	<LOD	3.6	<LOD	0.9	<LOD	<LOD	<LOD	<LOD	<LOD	<LOD	<LOD
CDS5	<LOD	<LOD	<LOD	1.3	0.7	1.3	3.1	<LOD	6.8	<LOD	<LOD	<LOD	<LOD	<LOD	<LOD	<LOD	<LOD	<LOD

CDS6	<LOD	<LOD	<LOD	1.9	0.6	1.3	3.1	<LOD	11.8	<LOD	<LOD	<LOD	<LOD	<LOD	<LOD	<LOD	<LOD
CDS7	<LOD	<LOD	<LOD	0.6	<LOD	2.2	3.3	<LOD	5.0	<LOD	<LOD	<LOD	<LOD	<LOD	<LOD	<LOD	<LOD
CCSD	<LOD	<LOD	<LOD	1.0	2.3	3.77	<LOD	<LOD	1.63	0.4	0.3	0.33	<LOD	<LOD	<LOD	<LOD	<LOD

Table 6:10 (continued)

Sample Id/F1- F3	Ba			Hg			Mn			Al		
	F1	F2	F3	F1	F2	F3	F1	F2	F3	F1	F2	F3
CSS1	52.9	142.2	211.5	<LOD	<LOD	<LOD	5.2	<LOD	3.0	137.4	410.5	504.9
CSS2	<LOD	<LOD	<LOD	<LOD	<LOD	<LOD	1.9	<LOD	<LOD	70.7	100.9	320.1
CSS3	4.1	10.3	23.1	<LOD	<LOD	<LOD	3.7	19.5	10.0	723.3	2053.7	4679.9
CSS4	5.0	4.7	10.6	<LOD	<LOD	<LOD	10.3	4.7	3.9	259.9	616.0	1066.2
CSS5	<LOD	<LOD	4.0	<LOD	<LOD	<LOD	1.6	<LOD	<LOD	61.7	144.5	193.4
CSS6	<LOD	<LOD	<LOD	<LOD	<LOD	<LOD	27.3	7.3	4.7	45.3	125.6	208.4
CSS7	2.3	<LOD	7.5	<LOD	<LOD	<LOD	13.3	3.5	4.0	39.1	112.4	391.7
CSS8	<LOD	3.5	4.2	<LOD	<LOD	<LOD	2.5	5.4	2.3	55.7	140.4	262.2
CSS9	<LOD	<LOD	5.2	<LOD	<LOD	<LOD	<LOD	<LOD	2.0	75.8	125.6	275.0
CCSS	11.8	17.5	12.0	<LOD	<LOD	<LOD	29.2	21.1	5.2	14.6	87.6	296.4
CS EG	3.7	56.4	18.6	<LOD	<LOD	<LOD	1.8	<LOD	2.7	19.4	39.4	336.6
CTS1	4.0	4.1	6.6	<LOD	<LOD	<LOD	16.6	7.1	10.3	257.1	626.5	984.2
CTS2	4.6	4.1	4.1	<LOD	<LOD	<LOD	5.4	<LOD	0.9	67.9	116.5	248.9
CTS3	3.1	16.4	17.2	<LOD	<LOD	<LOD	99.2	10.7	33.2	602.3	378.5	711.1
CTS04	17.2	15.3	6.3	<LOD	<LOD	<LOD	29.9	<LOD	<LOD	124.8	198.8	325.0
CTS05	16.4	35.6	12.0	<LOD	<LOD	<LOD	27.9	16.2	3.9	120.7	359.1	978.5
CTS06	9.1	13.0	1.84	<LOD	<LOD	<LOD	20.1	2.9	<LOD	77.9	153.7	138.27

CTS07	5.8	8.1	1.85	<LOD	<LOD	<LOD	15.3	<LOD	<LOD	46.6	160.5	505.50
CTS08	6.8	22.0	8.59	<LOD	<LOD	<LOD	<LOD	<LOD	<LOD	115.5	187.3	189.39
CTS09	9.3	11.8	<LOD	<LOD	<LOD	<LOD	7.5	3.1	<LOD	135.1	301.6	518.97
CTS10	3.9	12.1	<LOD	<LOD	<LOD	<LOD	55.0	3.1	<LOD	199.9	302.0	301.33
CTS11	6.7	18.1	2.93	<LOD	<LOD	<LOD	16.3	<LOD	<LOD	55.1	149.8	484.68
CDS1	<LOD	<LOD	<LOD	<LOD	<LOD	<LOD	<LOD	<LOD	<LOD	62.9	29.2	80.0
CDS2	<LOD	2.3	2.2	<LOD	<LOD	<LOD	<LOD	<LOD	<LOD	39.9	51.3	98.0
CDS3	<LOD	<LOD	<LOD	<LOD	<LOD	<LOD	<LOD	<LOD	<LOD	34.8	64.8	54.5
CDS4	<LOD	<LOD	1.7	<LOD	<LOD	<LOD	2.1	<LOD	<LOD	35.0	28.2	122.4
CDS5	5.8	<LOD	3.3	<LOD	<LOD	<LOD	5.3	<LOD	<LOD	53.5	93.6	192.1
CDS6	5.8	<LOD	0.6	<LOD	<LOD	<LOD	14.7	2.2	3.1	41.4	53.0	198.3
CDS7	1.7	<LOD	2.7	<LOD	<LOD	<LOD	4.1	<LOD	<LOD	83.2	37.1	114.5
CCSD	3.9	2.1	<LOD	<LOD	<LOD	<LOD	3.7	<LOD	<LOD	25.7	28.3	98.49

Appendix 6.11: Mean Enrichment factor across soil and tailings samples at Onyeama AML

Media/Pollutant	*Mn*	*Pb*	*Zn*	*Cr*	*Cu*	*Ba*	*Ce*	*Ti*	*Sr*	*Ni*	*Zr*	*Cd*	*Al*	*Fe*
Geoaccumulation Index (Igeo)														
Tailing (n =8)	-3.4	-1.3	-1.8	-2.8	-1.1	-3.5	-0.9	-6.4	-4.5	-2.7	-5.1	1.1	-5.0	-2.0
Soil (n =9)	-3.6	0.6	-1.0	-2.3	0.0	-5.1	-2.4	-5.4	-5.0	-2.3	-5.7	1.0	-4.5	-1.7
Sediment (n =8)	-5.5	-4.3	-2.9	-2.7	-3.7	0.7	-4.3	-6.7	-4.1	0.0	-6.8	-2.6	-2.4	-2.5
Control Soil (1)	-1.4	1.2	-2.6	-2.4	-0.6	-5.8	-0.1	-8.7	-1.9	-0.3	-2.7	0.0	-4.3	-0.9

Appendix 6.12: Mean Geo-accumulation Index across soil and tailings samples at Onyeama AML

Media/Pollutant	*Mn*	*Pb*	*Zn*	*Cr*	*Cu*	*Ba*	*Ce*	*Ti*	*Sr*	*Ni*	*Zr*	*Cd*	*Al*
Enrichment Factor (EF)													
Tailing (n =8)	0.4	1.6	1.2	0.6	1.8	0.3	2.0	0.0	0.2	0.6	0.1	0.0	0.1
Soil (n =9)	0.3	4.8	1.5	0.7	3.2	0.1	0.0	0.0	0.1	0.7	0.0	0.0	0.1
Sediment (n =8)	0.1	0.3	0.7	0.8	0.4	8.8	0.0	0.0	0.3	0.0	0.0	0.0	1.0
Control Soil (2)	1.5	9.2	0.7	0.8	2.7	0.1	3.8	0.0	1.1	3.1	0.0	0.6	0.2

Appendix 6.13: Mean Contamination Factor and Degree of Contamination across soil and tailings samples at Onyeama AML

Media/Pollutant	*Mn*	*Pb*	*Zn*	*Cr*	*Cu*	*Ba*	*Ce*	*Ti*	*Sr*	*Ni*	*Zr*	*Cd*	*Al*	*Fe*	Cd=∑CFi
Enugu Contamination Factor (Cf) and Degree of Contamination (Cd)															
Tailing (n =8)	0.1	0.6	0.4	0.2	0.7	0.1	0.8	0.0	0.1	0.2	0.0	1.9	0.0	0.4	**5.6**
Soil (n =9)	0.1	2.3	0.7	0.3	1.5	0.0	0.3	0.0	0.0	0.3	0.0	3.0	0.1	0.5	**9.2**
Sediment (n =8)	0.0	0.1	0.2	0.2	0.1	2.4	0.0	0.0	0.1	0.0	0.0	0.3	0.3	0.3	**3.9**
Control Soil (n=1)	0.6	3.5	0.3	0.3	1.0	0.0	1.4	0.0	0.4	1.2	0.2	0.0	0.1	0.8	**9.8**